PROCEEDINGS

ORAL PRESENTATIONS

TOPIC 4:
MODELLING AND REGIONALISATION OF FLOODS

PAPERS:
COLLECTED AND ARRANGED BY JUDITH DOBMANN AND SIMONE HUNZIKER.
PLEASE NOTE THAT AUTHORS ARE RESPONSIBLE FOR CONSISTENCY IN SPELLING.

REGIONAL FLOOD DATA ANALYSIS USING PEAKS OVER THRESHOLD

Nassir El-Jabi[1], Fahim Ashkar[2]

[1] Department of Civil Engineering, Université de Moncton, Moncton N.B. E1A 3E9, Canada,
eljabin@umoncton.ca

[2] Department of Mathematics and Statistics, Université de Moncton, Moncton N.B. E1A 3E9, Canada,
ashkarf@umoncton.ca

SUMMARY

Financial pressures on governments have resulted in a reduction in the number of hydrometric stations that are available for estimating flood risk. In order to be able to analyze ungauged basins, data from neighbouring flood sites need to be utilized. This paper deals with regionalization procedures as an instrument to facilitate the transfer of information from sites where records exist, to other sites where data is required but is not available (or is too short). A detailed analysis of several stations has been done in order to estimate the recurrence of floods for various return periods. The method of peaks over threshold (P.O.T.) was used for these analyses. Verification was carried out to check whether the Poisson process may represent the number of stream-flow exceedances, and if a generalized Pareto law may represent the magnitude of these exceedances. The method of "region of influence" has been used for the regional analysis, so that the values of the flood quantiles obtained by the individual and the regional analyses could be compared. The results for the province of New Brunswick show that the region of influence methodology using P.O.T. is a useful tool for calculating flood values at ungauged sites.

Keywords: Flood Regionalization, Extreme Value, Generalized Pareto.

1 INTRODUCTION

Hydrometric networks, long considered the basis of all studies of hydrology, are in an ever increasingly precarious state. The main reason is financial pressure, which has reduced the size of hydrometric networks, thus leading to flood sites where data is required but is nonexistent or insufficient. In such a state of weakened hydrometric networks, regionalization methods have been used as an instrument to facilitate the transfer and/or extrapolation of information from sites where records exist, to others where data is required but is not available (or is too short). One of the pioneers of regionalization is Dalrymple (1960), who developed the "index-flood" method, still in use today. The procedure of regionalization is becoming a standard prerequisite for adequate solutions to innumerable problems related to the management of hydrometric networks.
The procedure of regionalization must explain how the characteristics of the basin affect the flood process, and should be capable of furnishing an error estimate for calculated flood values at ungauged sites (Riggs, 1990). The procedure must also be simple, and be based on the observed data, taking into consideration regional differences. Due to the complexity of flood systems, the steps used in the regionalization process must be rationalized and placed in a logical and systematic perspective (Simmers, 1984).

2 BACKGROUND

Referring to Figure 2-1, denote by Q(t), $t \geq 0$ a hydrograph which represents the discharge rate of river flow at a given site. We select a certain base level, Q_B, and consider the flows which exceed Q_B ("exceedances"). Denote by τ_1, τ_2, τ_3, ... the times of local maxima of water levels during these exceedances. Define also by

$$\xi_0 = 0 \text{ , and } \xi_k = Q(\tau_k) - Q_B \text{ , for } k = 1, 2, \ldots \quad (1)$$

the exceedance series, or the "*peaks-over-threshold" (P.O.T.)* series. This series (ξ_k) is also called "*partial duration series"*. The exceedances ξ_k can be assumed to be *independent* and identically distributed, or *dependent* and identically distributed, within a homogeneous time interval such as the year or the "season".

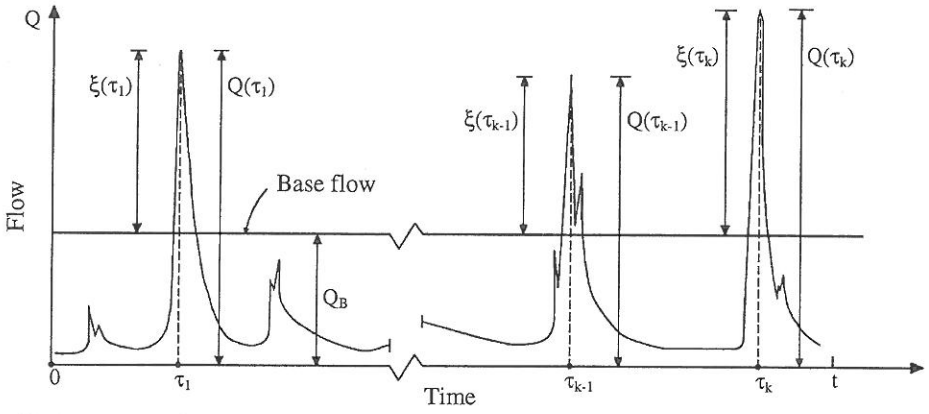

Figure 2-1: Hydrograph of instantaneous flow of a river at a given stations.

In this paper, we suppose that the exceedances ξ_k are independent and identically distributed. We define also flood counts or number of exceedances within a fixed time interval (0, t) by

(2) $$\eta(t) = \sup \{k | \tau_k \leq t\}$$

In this article, the time interval will be considered exclusively as one year; however, if there are significant seasonal variations in the river-flow process, the time interval can with no loss of generality be taken to be one season. Hence in the sequel, we shall omit the index t and write the random variable (r.v.) $\eta(t)$ in (2) as η, which is the number of *annual* exceedances. This r.v. has often been shown to follow a Poisson distribution of parameter λ [$\eta \sim$Poisson(λ)]; see for instance Borgman (1963), Shane and Lynn (1964) and Bernier (1967):

(3) $$P(\eta = k) = e^{-\lambda}\lambda^k/k! \text{ for } k = 0, 1, 2, \ldots$$

The r.v. exceedance ξ in (1), and the r.v. flood duration, T, often follow exponential distributions; see for instance Todorovic (1978); Cunnane (1979); North (1980); Ashkar and Rousselle (1981). In general, however, this use of the exponential distribution is a crude approximation. Davison and Smith (1990) and Madsen et al. (1997), among others, use the more flexible generalized Pareto distribution (Pickands, 1975), whose cumulative distribution function (cdf) is given by

(4) $$H(x) = P(\xi \leq x) = 1 - (1 - k\frac{x}{\alpha})^{1/k} \quad k \neq 0$$

and the probability density function (pdf) is

(5) $$h(x) = \begin{cases} \alpha^{-1}(1 - \frac{kx}{\alpha})^{1/k-1} & k \neq 0 \\ \alpha^{-1}\exp(-\frac{x}{\alpha}) & k = 0 \end{cases}$$

where $\alpha > 0$ is a parameter of scale, k is a shape parameter, and the domain of variation of ξ is such that $0 \leq x < \infty$ for $k \leq 0$ and $0 \leq x \leq \alpha/k$ for $k > 0$.
The mean, variance and skew coefficient of the generalized Pareto r.v. are respectively:

(6) $$\mu = E[\xi] = \frac{\alpha}{1+k}$$

(7) $$\sigma^2 = \text{var}[\xi] = \frac{\alpha^2}{(1+k)^2(1+2k)}$$

(8) $$C_s = 2(1-k)(1+2k)^{1/2}/(1+3k)$$

The coefficient of variation of ξ is therefore given by:

(9) $$C_v = \frac{\sigma}{\mu} = \{\alpha/(1+k)\sqrt{1+2k}]\}/[\alpha/(1+k)] = \frac{1}{\sqrt{1+2k}}$$

Two important results following from a generalized Pareto modeling of exceedances are considered. The first stipulates that if the maximum exceedance (χ) in the time interval (0,t} of one year is considered:

(10) $$\chi(t) = \frac{\sup \xi_v}{\tau(v) \le t}$$

where the ξ are always considered independent and follow a generalized Pareto pdf (5), and if exceedances arrive according to a Poisson process, then $\chi(t)$ follows a generalized extreme value (GEV) distribution with the distribution function (Rosbjerg et al., 1992):

$$F_t(x) = P[\chi(t) \le x]$$

(11) $$F_t(x) = \exp\left\{-\lambda[1-\frac{kx}{\alpha}]^{1/k}\right\} \quad k \neq 0$$

(12) $$= \exp[-\lambda e^{-x/\alpha}] \qquad k = 0$$

where λ is the Poisson parameter (Equation 3), which represents the average number of exceedances per year. Note that the shape parameter k of the generalized Pareto distribution is the same as that of the generalized extreme value distribution.
The second property of the distribution stipulates that if the random variable ξ follows a generalized Pareto distribution, then the conditional distribution of ξ - t, knowing that ξ > t, also follows a generalized Pareto distribution with the same shape parameter k. This property will be used in the next section. In hydrologic applications, the values of interest of the parameter k range between -0.5 and 0.5 (Hosking and Wallis, 1987).
From a sample of flood exceedances with mean $\bar{x}$ and variance s^2, the parameters α and k of the generalized Pareto distribution are estimated via to the method of moments by the equations:

(13) $$\bar{x} = \alpha/(1+k)$$

(14) $$s^2 = \alpha^2/(1+k)^2(1+2k)$$

The parameter estimators are therefore:

(15) $$\hat{\alpha} = \frac{1}{2}\bar{x}(\frac{\bar{x}^2}{s^2+1})$$

(16) $$\hat{k} = \frac{1}{2}(\frac{\bar{x}^2}{s^2}-1)$$

and for k > -0.25, Hosking and Wallis (1987) have shown that $\hat{\alpha}$ and $\hat{k}$ are asymptotically normally distributed with:

$$\text{var}\begin{bmatrix}\hat{\alpha}\\ \hat{k}\end{bmatrix} \sim \frac{1}{N}\frac{(1+k)^2}{(1+2k)(1+3k)(1+4k)} \times \begin{bmatrix} 2\alpha(1+6k+12k^2) & \alpha(1+2k)(1+4k+12k^2)\\ \alpha(1+2k)(1+4k+12k)^2 & (1+2k)^2(1+k+6k^2)\end{bmatrix} \quad (17)$$

Finally, the estimation of any flood quantile Q_T (discharge of return period T) can be obtained as $Q_T = Q_B + x$ by solving for x as a function of T in the equation $T = 1/(1-F_t(x))$, where $F_t(x)$ is given by Equation (11). This gives:

$$Q_T = Q_B + \frac{\hat{\alpha}}{\hat{k}}\left[1-\left(\frac{1}{\hat{\lambda}}\ln\frac{T}{T-1}\right)^{\hat{k}}\right] \quad k \neq 0 \quad (18)$$

$$= Q_B + \hat{\alpha}(\ln\hat{\lambda} + C) \qquad k = 0 \quad (19)$$

where $\hat{\alpha}, \hat{k}, \hat{\lambda}$ are the estimates of α, k, and λ, respectively, and C = -ln(T/T-1).

2.1 Analysis of Base Flow Q_B

Wang (1991) showed the effect of the choice of base flow on the estimation of various quantiles. In a partial duration series, he found that the base flow Q_B could be increased up to a certain level, without affecting the efficiency of the estimation of the quantiles. For this study, the base flow has been chosen to satisfy certain conditions and mathematical properties. In effect, if the arrival of exceedances follows a Poisson process, equality of the mean and variance is a characteristic of the Poisson law. Even if this property is necessary but not sufficient to guarantee a Poisson distribution, it may still be used as a first step to eliminate the base flows for which this condition is not satisfied. It is equally necessary to try to satisfy statistical tests of goodness-of-fit such as the chi-square test for the number of exceedances, or the Kolmogorov-Smirnov test concerning the distribution of exceedances and annual-maximum exceedances. The base flow was also chosen such that there would be at least one exceedance on the average per year.

2.2 Fitting the Generalized Pareto Law to the Exceedances

This study uses a simple graphical procedure as a first step to check the suitability of the generalized Pareto law as a model to fit the exceedances. The procedure is based on the property that when the generalized Pareto density function is truncated from below, the part above the truncation level always follows the same type of law, and the shape parameter k remains constant. Therefore, for several truncations, Equation (9) is used to calculate the coefficient of variation, that is:

$$C_v = \frac{1}{\sqrt{1+2k}} \quad (20)$$

This coefficient therefore remains constant if the exceedances follow a generalized Pareto distribution, and for k = 0 the coefficient of variation equals one, signifying that the distribution is exponential. An approximate confidence interval on C_v may be calculated, at a 95% confidence level, by taking the estimated value of $C_v \pm$ twice the standard error:

$$I = \hat{C}_v \pm 2\sigma(\hat{C}_v) = \hat{C}_v \pm 2\sqrt{Var(\hat{C}_v)} \quad (21)$$

where for large sample sizes we have

(22) $$Var(\hat{C}_v) \cong \left(\frac{dC_v}{dk} \right)^2_{k=\hat{k}} Var(\hat{k})$$

(23) $$\frac{dC_v}{dk} = \frac{d}{dk}\left(\frac{1}{\sqrt{1+2k}} \right) = -\frac{1}{(1+2k)^{3/2}}$$

and from Equation (17), one may write

(24) $$Var(\hat{k}) \cong \left[\frac{1}{N} \frac{(1+k)^2}{(1+2k)(1+3k)(1+4k)} (1+2k)^2 (1+k+6k^2) \right]_{k=\hat{k}}$$

so that:

(25) $$I \cong \hat{C}_v \pm 2\left[\frac{1}{(1+2k)^3} \frac{1}{N} \frac{(1+k)^2(1+k+6k^2)}{(1+3k)(1+4k)} \right]^{1/2}_{k=\hat{k}}$$
$$\cong \hat{C}_v \pm \frac{2(1+k)}{(1+2k)} \left[\frac{(1+k+6k^2}{N(1+3k)(1+4k)} \right]^{1/2}_{k=\hat{k}}$$

3 NUMERICAL APPLICATION

To provide an example, we shall consider 53 hydrometric stations located in the province of New Brunswick, Canada. A detailed analysis was performed on each station to estimate the recurrence of floods for various return periods. This analysis was used to verify that the number of exceedances may be represented by a Poisson process, and that the magnitude of these exceedances may be represented by a generalized Pareto law. The base flow is first chosen in order to fit the generalized Pareto distribution to the exceedances, by estimating its scale and shape parameters. The goodness-of-fit tests are then carried out, and the quantiles for various return periods are estimated. In this study, in order to preserve a certain degree of independence between two consecutive floods, and without having to be too restrictive, the following procedure was adopted (as proposed by WRC, 1976):

1. the exceedances of the base flow had to be separated by at least five days;
2. the intermediate flows between two floods had to descend to less than 75% of the least important flood in order for both flood events to be retained in the model.

In this type of study, it is very important to verify the reliability and the exactitude of the data that often exists in the form of a temporal series. As indicated by Bobée and Ashkar (1991), for the results of the frequency analysis to be theoretically valid, it is necessary that the flood series satisfy the criteria of homogeneity, stationarity, and independence. To verify these criteria, tests such as *Mann-Whitney* and *Wald-Wolfowitz* can be used. On the other hand, to test the linear dependence among the successive values of a given series, the analysis of autocorrelation may be employed. The autocorrelation coefficient at various lags is calculated, and for an independent series, the correlogram must be equal to zero for all positive lags. A confidence interval about the correlogram helps in deciding if it significantly deviates from zero. The confidence interval is given by Yevjevich (1972):

(26) $$R_k(95\%) = \frac{-1 \pm 1.645\sqrt{N-K-1}}{N-K}$$

(27) $$R_k(99\%) = \frac{-1 \pm 2.326\sqrt{N-K-1}}{N-K}$$

where R_k: autocorrelation coefficient at lag K
N: number of years of record

In this study, in order to respect as close as possible the criteria of homogeneity, the analysis has been restricted to Spring floods, i.e., those occurring between the 60th and the 180th day of the calendar year. This choice comes from the fact that in New Brunswick, according to Acres (1977), the most important floods of the century have occurred during Spring. These floods are generally caused by rain and melting snow with the presence of ice increasing the damage.
The period of study spans over seventy years. The collection of data has not been previously released in its entirety; although certain stations have been extensively studied. The median number of years of record is twenty-three. Specific years may have been excluded from the analysis in the event of insufficient data. The data used are provided by Environment Canada.

3.1 Distribution of Flood Exceedances

The estimation of events of return period T is sensitive to the choice of distribution used to model the exceedances. Therefore, before proceeding with the calculations, it is pertinent to choose the law that is most applicable. A simple graphical method is introduced to visualize the value of coefficient of variation (C_v) of exceedances at various truncation levels, which is intended (along with a goodness-of-fit test) to help check the suitability of the generalized Pareto law as a model to fit the exceedances. For each truncation, the sample C_v is calculated and used to construct an approximate 95% confidence interval for the population C_v (Equation 25). If the generalized Pareto law is appropriate, it is necessary that this coefficient remain constant for various truncation levels. Thus, if the coefficient of variation is constant and different from unity, the Pareto law might be appropriate. In the case where the coefficient is constant and equal to one, the exponential law might be more plausible. Finally, in the event that this coefficient changes with truncation level, it is preferable to fit exceedances using a law other than the generalized Pareto. This graphical procedure has been applied to the fifty-three stations in the data base, and has been later supported by a goodness-of-fit test (Kolmogorov-Smirnov). According to the procedure just outlined, forty-two stations in the Province of New-Brunswick showed the generalized Pareto law to be appropriate for modeling the exceedance values.

3.2 Specific Choice of Base Flow, Q_B

As has been mentioned, the partial duration series are used to model exceedances above a certain threshold. The determination of this threshold, commonly referred to as the *base flow*, requires careful thought. In this study, the determination of this threshold was based on several criteria and a compromise between several tendencies. First, the methodology suggested by El-Jabi et al. (1986) was applied, which employs a property of the Poisson distribution that the ratio (r) of the mean to the variance is theoretically equal to unity. For various base flows, the stability of this ratio about unity was checked for the various stations.
Figure 3-1 shows an example of a graph of this ratio r. Furthermore, the base flow had to be chosen high enough to satisfy the two conditions of: (1) a low autocorrelation between exceedances, and (2) an adequate fit of the hypothesized distribution to the exceedances (e.g., generalized Pareto).

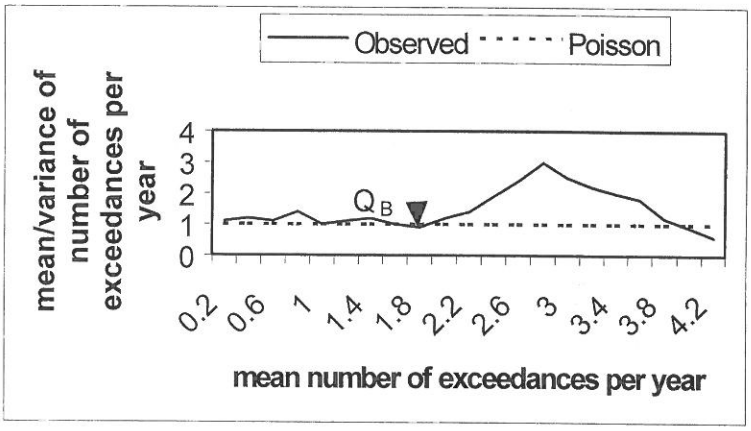

Figure 3-1: Determination of the base flow with the ratio of the mean to the variance of the number of exceedances per year.

3.3 Regionalization

Flood quantiles were first estimated for different return periods from *local* (*at-site*) analysis of the flood records. However, to improve the estimation of the quantiles, a *regional* study was also performed. Homogenous regions were formed, using the method of "region of influence" (Burn, 1990). This took into consideration the regionally recorded flood flows and physiographic characteristics of the basins. Of particular interest was the regional estimation of the *100-year* flood by the *P.O.T.* method. This regional estimate was calculated from a regionalization of a shape descriptor of the generalized Pareto density. The shape descriptor used was the coefficient of skewness, C_s, which is a dimensionless function of the shape parameter k [Equation (8)]. After defining the regions of influence, I_i , for each target station i, the coefficient of skewness is calculated for each station $j \in I_i$, using Equations (16) and (8). The regional coefficient of skewness ($C_s^*{}_i$) is then calculated for each target station, i, using the methodology described by Burn (1990) . Finally, a regional k (k^*_i) is determined in order to permit the calculation of the regional *100-year* flow X^*_{Ti} for the given target site [Equation (18)]. The relationship between the regional and at-site k values is shown in Figure 3-2. The relationship between the regional and the at-site *100-year* flood estimates for the various sites is shown in Figure 3-3.

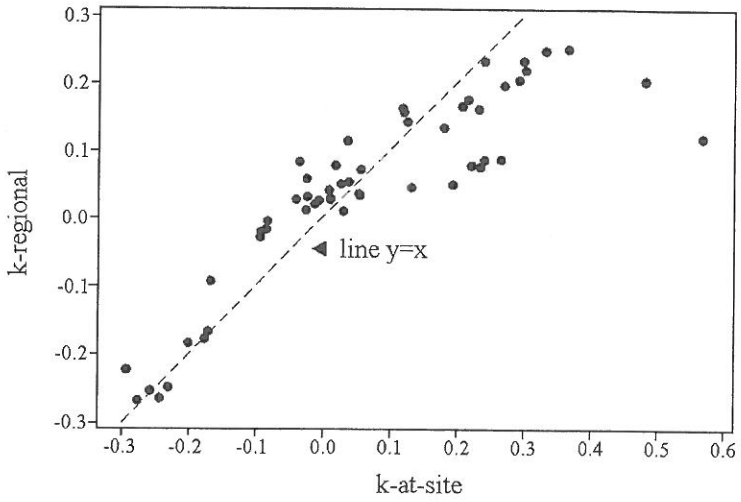

Figure 3-2: Relationship between the regional and at-site k values.

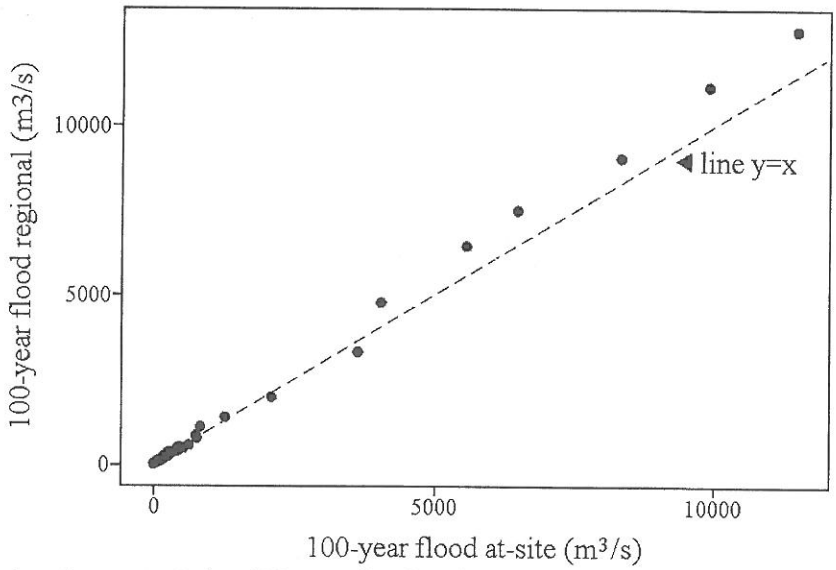

Figure 3-3: Regional versus at-site 100-year flood estimates.

4 CONCLUSION

The method of peaks over threshold (P.O.T.) was used to perform a flood frequency analysis and to estimate flood quantiles for 53 hydrometric stations in the province of New Brunswick, Canada. It was observed that the choice of truncation level (base discharge) remains a significant variable to be carefully handled in this type of approach. It is important that this threshold level be neither too low so as not to violate certain statistical criteria such as the independence between successive exceedances, nor too high so as not to lose information that may be pertinent to the analysis.
The data series that was used represents the daily average instantaneous discharge during the Spring season. During this season some of the most important floods of the century in New Brunswick have occurred. It was also important to restrict the analysis to a time period (season) within which flow data are more or less homogeneous. This homogeneity assumption can be checked by a statistical test such as the Mann-Whitney.
The base flow was then determined to satisfy the Poisson arrival process for the exceedances. In fact, only six of the fifty-three stations were rejected by the chi-square test based on the fit of the Poisson law to the number of exceedances per year. The details of the method used to determine the base discharge have already been presented by El-Jabi et al. (1986). This method suggests choosing a base discharge so that the ratio of average number of exceedances per year to the variance stabilized around one, and at the same time obtaining: (1) a low autocorrelation between exceedances based on a correlogram analysis, and (2) an adequate fit of a hypothesized distribution (e.g., generalized Pareto) to the exceedances based on the C_v test and a goodness-of-fit test. For the base discharges chosen, the average number of exceedances per year (λ) was generally quite low (predominantly between 1 and 2), since only the Spring season was considered. However, about 20% of the hydrometric stations presented a λ value greater than two.
In the regional analysis, the generalized Pareto law was systematically used to fit the exceedance values, even though the C_v test showed that for a small number of stations, the application of this law was probably not totally adequate. To estimate the parameters of this law, the method of moments was preferred to the methods of maximum likelihood and of probability weighted moments, based on a study by Hosking and Wallis (1987). Only one station displayed a shape parameter estimate greater than 0.5, which is considered an extreme case. As for the regional analysis, the method of "region of influence" was found to be quite easy to apply (Burn, 1990).

ACKNOWLEDGEMENTS

The financial support of the Natural Sciences and Engineering Research Council of Canada is gratefully acknowledged.

REFERENCES

Acres consulting services ltd. (1977): Regional Flood Frequency Analysis. Canada/New Brunswick Flood Damage Reduction Program. Fredericton, N.B. Canada, 141 p.

Ashkar, F., Rousselle, J. (1981): Design discharge as a random variable: A risk study. Water Resources Research. U.S.A. 17(3), 577-591.

Bernier, J. (1967): Sur la théorie de renouvellement et son application en hydrologie. HYD. 67(10). Electricité de France.

Bobée, B., Ashkar, F. (1991): The Gamma Family and Derived Distributions Applied in Hydrology. Water Resources Publications. Littleton, Colorado. 203 p.

Borgman, L.E. (1963): Risk criteria. J. Water ways Harbors Div. U.S.A. 80, 1-35.

Burn, D.H. (1990): Evaluation of regional flood frequency analysis with a region of influence approach. Water Resources Research. U.S.A. 26(10), 2257-2265.

Cunnane, C. (1979): A note on the Poisson assumption in partial duration series models. Water Resources Research. U.S.A. 15, 489-494.

Dalrymple, T. (1960): Flood Frequency Analysis. Manual of Hydrology: Part 3, Flood-Flow Tech., U.S. Geol. Surv. Water Supply Paper 1543 A. U.S.A. 11-51.

Davison, A.C., Smith, R.L. (1990): Models for exceedances over high thresholds. Journal of the Royal Statistical Society, G.B. 52(3): 393-442.

El-Jabi, N. et al. (1986): Etude stochastique des crues au Québec. Ministère de l'Environnement, Québec, Direction des relevés aquatiques. Canada. 91 p.

Hosking, J., Wallis, J.R. (1987): Parameter and quantile estimation of the generalized Pareto distribution. Technometrics. U.S.A. 29(3), 339-349.

Madsen, H. et al. (1997): Comparison of annual maximum series and partial duration series methods for modeling extreme hydrologic events. Water Resources Research. U.S.A. 33(4), 747-757.

North, M. (1980): Time-dependent stochastic model of floods. J. Hyd. Div. U.S.A. 106, 649-665.

Pickands, J. (1975): Statistical inference using extreme order statistics. Ann. Stat. U.S.A. 3, 119-131.

Riggs, H.C. (1990): Estimating Flood Characteristics at Ungauged Sites. Regionalization in Hydrology, IAHS Publication No. 191, Wallingford, GB, 159-169.

Rosbjerg, D. et al. (1992): Prediction in partial duration series with generalized Pareto-distributed exceedances. Water Resources Research. U.S.A. 28, 3001-3010.

Shane, R.M., Lynn, W.R. (1964): Mathematical model for flood risk evaluation. J. Hyd. Div. U.S.A. 90, 1-20.

Simmers (1984): A systematic problem-oriented approach to regionalization. Journal of Hydrology, The Netherlands. 73, 71-87.

Todorovic, P. (1978): Stochastic models of floods. Water Resources Research. U.S.A. 14, 345-356.

Wang, A.J. (1991): The POT model described by the generalized Pareto distribution with Poisson arrival rate. Journal of Hydrology. The Netherlands. 129, 263-280.

Water resources council (1976): Hydrology Committee, Guidelines for Determining Flood Flow Frequency. Bulletin No 17. Washington, D.C.

Yevjevich, V. (1972): Probability and Statistics in Hydrology. Water Resources Publications, Littleton, Colorado. 302 p.

MAXIMUM FLOODS AND THEIR REGIONALISATION ON THE ALBANIAN HYDROGRAPHIC RIVER NETWORK

Niko Pano, Bardhyl Avdyli

Hydrometeorological Institute, Hydrology Department, Rr."Durresit", 219, Tirana, Albania,
nikopano 56@hotmail.com; kgjo@inima.al

SUMMARY

Evaluation of maximum floods and their computation is one of the main and most complicated problems for the natural specific condition of the Albanian hydrographical network (mountaineous regions, lake system presence, intensive precipitation, snowmelt flood, etc.)
Flood studies on the Albanian hydrographic river network are performed by estimating maximum discharge with different probability, computing flood characteristics, evalutating rainfall regime and morphological factors that influence on the process of flood formation. Determination of regional formulas for the maximum discharge of medium catchment area (250 - 2000 km^2) and small catchment area (50 - 250 km^2), and classification of the homogeneous physiographical regions are an important part of the study.
In Albania many hydrological studies were performed to evaluate the maximum discharge of the river system (Pano, 1984 and 1982; Avdyli, 1983, 1980 and 2000; Selenica, 1982; etc.). In this paper, from the existing partial studies it is attempted to present a general evaluation of the maximum floods in the Albanian river system, including the maximum discharge regionalization.

Keywords: Floodwaves determination, annual maximum discharges, regionalisation

1 DESCRIPTION OF REGION AND DATA USED

The catchment area (F) of the Albanian hydrographical network is 43 305km^2, where 28 500 km^2 is inside the Albanian state territory and rest outside it.
In the Albanian hydrographical network, there are 11 principal rivers together with their numerous branches, such as Buna river with the catchment area of F=19 582 km^2, Vjosa F=6706 km^2, Semani F=5649 km^2, etc.There are 125 other rivers with small catchment areas (F>50 km^2).
The catchment area of the Albanian hydrographical network has particular natural conditions (the average altitude 785 m above sea level, presence of lake system Prespa-Ohri-Shkodra lakes of surface 270-365 km are among the biggest and most important lakes in the Balkan), the Mediterranean typical climatic regime (the annual precipitation up to 3500 mm), the intensive snow melt, etc.
Maximum floods evaluation was carried out based on the many years archival data of the Albanian hydrometeorological Institute. Albanian monitoring network consists of more than 175 hydrometric stations with observed periods of 20-50 years, 125 pluviometric stations and 35 pluviographic stations with 15-45 years observed period. These stations are located on all over the territory.
National topographical maps of 1:25 000 scale used to estimate the catchment characteristics.

2 FLOOD WAVES FORMATION AND MAXIMUM DISCHARGE

Floods formed in the catchment area of the Albanian hydrographical network are more of rainfall origin and less of melange origin (snowmelt-rainfall). Rainfall floods are formed during the first part of the wet period of the year (from X to XII). While melange floods are formed during the second part (from I to III).
In general, in the Albanian hydrographical rivers network have four distinct types of flood hydrograph (Figure 2-1).
In the Table 2-1 is presented the maximum peak discharge with different probabilities (p%) for the main Albanian rivers (Q_0^M, C_V, C_S).
The relationship: $Q_{ni}=f(h)$,where Q_{ni} is discharge in m^3/s and h respectively level in the hydrometer, is used to compute the volume (Wo^M) of the flood wave in the Albanian river system.

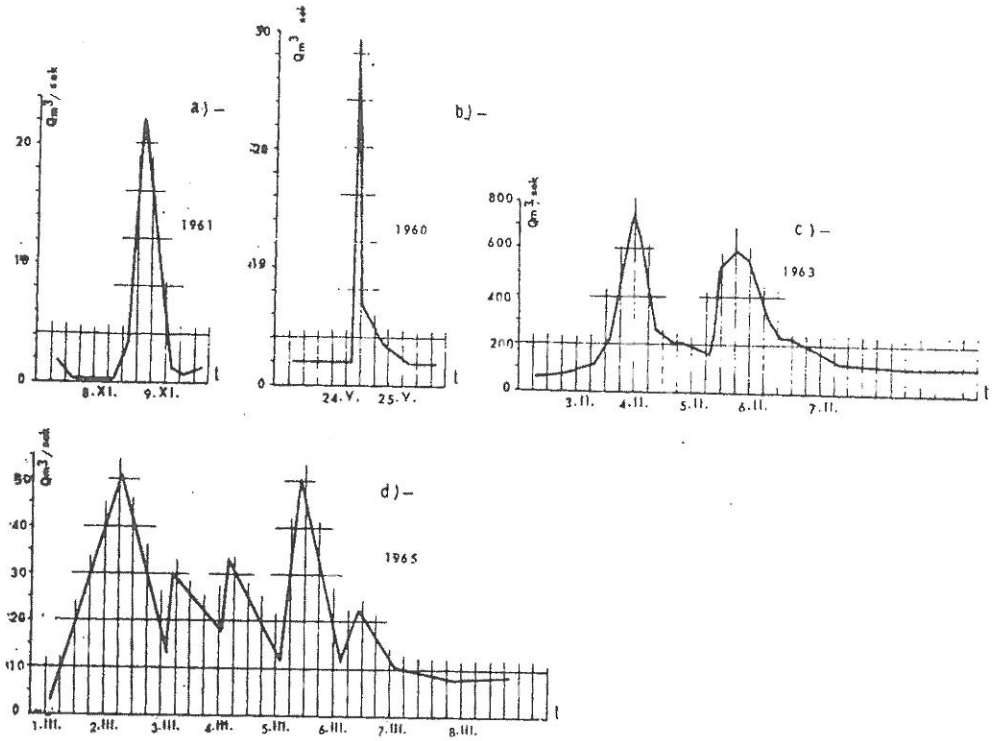

Figure 2-1: Flood types in Albania hydrographic river network
(a,b - one-peak flood c - two-peak flood d - multi-peak floods).

Table 2-1: Maximum discharge with different probability P %, for the main rivers of the Albania Hydrographical Network.

Nr.	River	Basin Surface Area F [km^2]	Mean Altitude of basin h [m]	Statistical parameters			Probabilities p %				
				Q_0^M [m^3/sec]	Cv	Cs	01	02	05	10	20
1	Drini i Zi - Kukes	5885	1132	640	0.48	1.42	1680	1480	1240	1060	860
2	Drini I Bardhe - Kukes	4965	862	700	0.56	1.72	2150	1830	1190	1220	960
3	Drini - Vau Deje	1365	988	2680	0.41	1.8	6530	5870	4850	4120	3400
4	Mati - Shoshaj	646	963	309	0.39	1.56	750	685	564	452	411
5	Fani - Rubik	1010	696	822	0.42	0.84	1833	1677	1420	1200	1085
6	Erzeni - Sallmonaj	755	438	587	0.47	1.88	1560	1380	1130	950	763
7	Ishmi - Sukth	651	367	625	0.67	1.34	1980	1740	1420	1180	925
8	Devolli - Kozare	3120	962	631	0.47	1.38	1600	1440	1210	1030	842
9	Osumi - Ura Vajgurore	2070	852	489	0.54	1.38	1370	1220	1010	843	673
10	Vjosa - Pocem	5570	947	1820	0.42	1.68	4860	4420	3630	3130	2620

Parameters of flood-wave volume probability distribution (Wo^M, Cv, Cs) for two different river types of the Albanian hydrographic river network are calculated (Drini river, F=13650 km^2 in the North of the drainage area and Vjosa river, F=6680 km^2 in the South). For these rivers grapho-analytic relations are also compiled as follows: $Q_{1\%}^M=f(F)$; $W_{1\%}^M=f(F)$ and $W_{1\%}=f(Q_{1\%}^M)$. Equations describing flood volume relation for a given probability ($W_{p\%}$) with its maximum discharge ($Q_{p\%}^M$) are as follows:

a) for Drini river, $W_{p\%}^M = 0.180\ Q_{p\%}^M + 207.8$, $R^2=0.95$, Er=±5,2% (where R is the coefficient of correlation and Er is relative deviations)
b) for Vjosa river, $W_{p\%}^M = 0.145\ Q_{p\%}^M - 92.0$, $R^2=0.84$, Er= ±5,6%

Equations describing maximum discharge relation for a probability to 1% ($Q_{1\%}^M$) with catchment area (F) for the main hydrometric principal axes are as follows:

a) For Drini river, $Q_{1\%}^M = 0.0075F^{1.4231}$, $R^2=0.88$, Er=±7,1%
b) For Vjosa river, $Q_{1\%}^M = 0.00006F^{1,1982}$, $R^2=0.99$, Er=±5,7%

Equations describing maximum volume relation for a probability 1% ($W_{p\%}^M$) with catchment area (F) for the main hydrometric principal axes are as follows:

a) For Drini river, $W_{1\%}^M = 0.0000F^{2.0673}$, $R^2=0.99$, Er=±8,3%
b) For Vjosa river, $W_{1\%}^M = 0.00266F^{1,4325}$, $R^2=0.98$, Er=±6,2%

3 REGIONALISATION OF THE TERRITORY

In this paper the division scheme of the Albanian territory in homogeneous regions, based on evalutation and determination of the natural factors influencing the flood flow process formation are presented. Many studies, treating maximum discharge of the river systems in correlation with catchment area characteristics are published (Rodda,1971; Kennedy, 1971; Stanescu, 2000).

One of the important representative indicators to estimate the integral impact of the flood flow formation process is the maximum discharge module ($q_{1\%}^M$). Apart from, flood flow coefficient ($\varphi_{1\%}^M$) is also important.

In the general scheme of flood flow formation process, natural conditions of the catchment area of the hydrographical network of Albania are grouped as the follows:

a) $H/\sqrt{F}$ – morphometric parameters.
b) $\varphi_{1\%}\ H_{1\%}^{24}$ – hydrometeorological parameters, where $H_{1\%}^{24}$ is the maximal 24 hours precipitation of p=1% propability in mm.
c) B/L - hydrographic parameters, where B is the width of river basin and B is length of basin.

Analysing and dividing the Albanian territory in homogeneous areas, region is accepted as the smallest tacsionometric unit.

Classification is carried out for the following flood categories: high, low and mean.

Because of the physiographical conditions of the Albanian territory, especially the Mediterranian typical climatic regime and mountainous relief, the principal natural factors that influence on the flood flow process formation are:

a) Climatic regime, especially atmospheric rainfall intensity
b) Morphological factors of the territory

Climate in the Albanian territory is Mediterranian typical . The mean annual precipitation on the plains varies from 650-1100 mm and on the mountains is about 3000-3600mm. The archival pluviographical data are used to estimate the intensity – magnitude - frequent relation of the rainfall.

Evaluation of atmospheric rainfall intensity is based on the construction of regional curves of the rainfall reduction calculated by means of Smirnova's method, (Smirnova, 1971). This calculating manner is considered more conform to regionalisation aims. Three different types of reduction curves of rainfall with increasing time interval -τ, which are the same with them of regions of maximum discharge module could also be identified in the Albanian territory (Figure 3-1).

Morphological factors are determined by the topohydrographical characteristics of the catchment area. The main considered parameters are:

F - basin area, h - mean height of basin, L - length of river reach, B - width of basin, I - the slope of bottom, Isl – the slope of mountains.

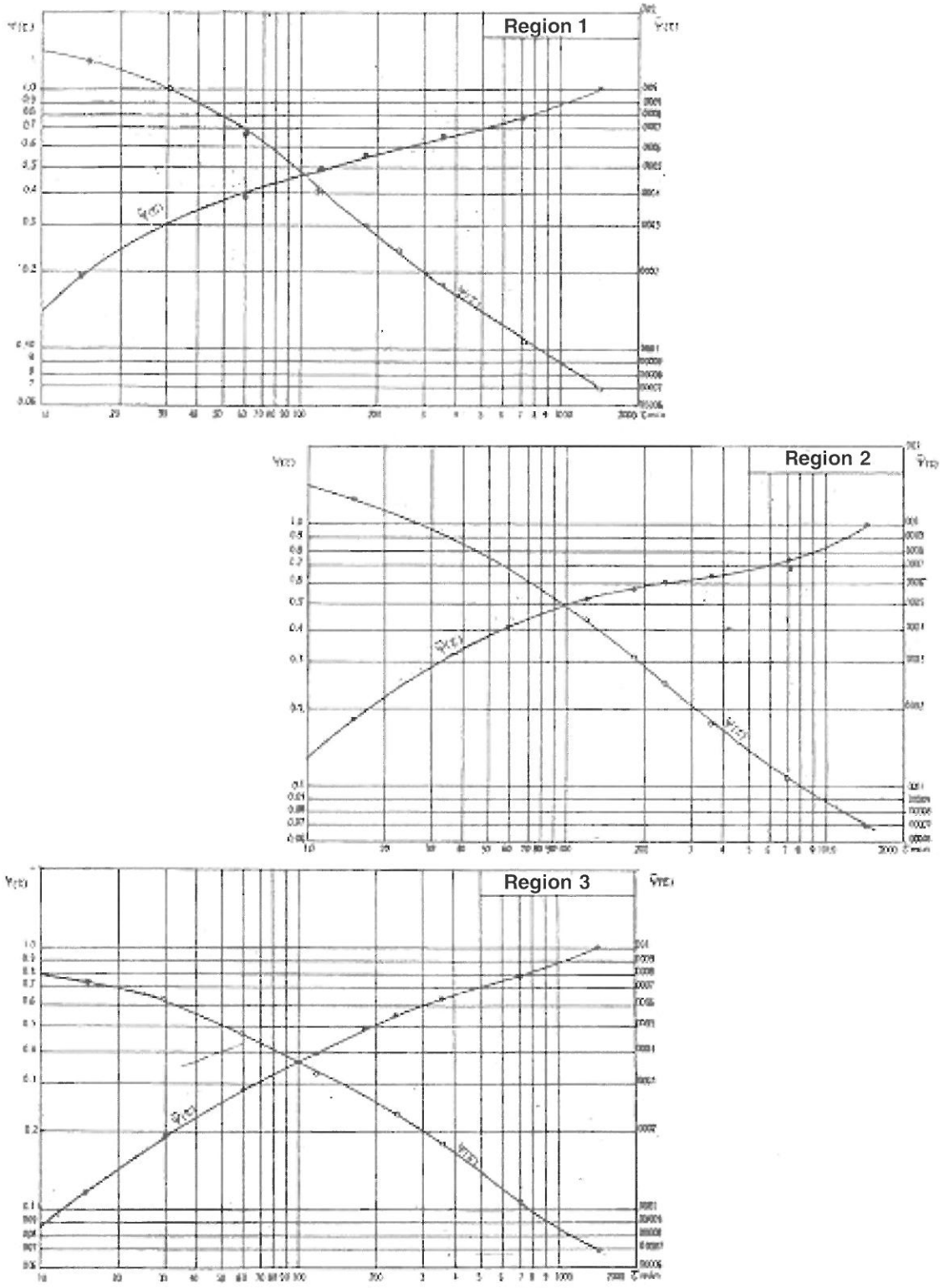

Figure 3-1: Reduction curves of the rainfall layer and their intensity.

4 PROCEDURE OF REGIONALISATION

This procedure consists of determination of the relationships between the maximum discharge module and a set of basin characteristic $q_{1\%}^{M} = f(F, h, B, L, \varphi_{1\%}, H_{1\%}^{24})$

a) Computation of maximum 24 hours precipitation with 1% probability H(p,24) for the representative meteorological stations.
Subroutine COMP(QM, αM,YM,i, j, p)

- Albanian territory classification by gradients PM = $H^{24}_{1\%}$ / h
- Composition of geographical distribution map for 24 hours precipitation with p =1% probability according to respective values of the gradient PM (Figure 4-1).

b) Input data of maximum discharges, flood volumes, etc.: Q_V, $\alpha V(i)$, i =1,...,N, H(j), F(j), j =1,...,M, pk
- Main parameters computation of the maximum discharges for representative axes such as maximum discharges $Q^M_{p\%}$, flood flow coefficient $\varphi^M_{p\%}$, flood flow layer $y^M_{p\%}$, interval of travel time $\tau_{p\%}$, etc.

  Subroutine COMP(QM, αM,YM,i, j, p)
- Computation of the specific maximum discharge module with 1% propability ($B_{1\%}$) for hydrometric representative axes, $B=q^M_{1\%} F^{1/2}$, where $q^M_{1\%}$ is maximum discharge module with 1% propability.

(1) $$QK(i,j,p) = QM(i,j,p);\ B(i,j,p) = QK(i,j,p)*\sqrt{F(j)}$$

- Evaluation of the territory based on the gradient

(2) $$R(i,j,p) = B(i,j,p)/h(j)$$

- Regionalisation of the territory based on values of the parameter B(i,j,p) (Figure 4-2).

c) Calculation of $\varphi_v(p,m)$ with p% probability for the representative hydrometric axes.
- Calculation of gradient P = $\varphi_v(p,m)$ /h, which together with $\varphi_v(p,m)$ serves for the territory regionalisation.
- Output of all results for all calculated parameters of this algorithm.

d) Computation for the reginalisation of territory by means of :

(3) $$q^M_{1\%} = f(F, h, B, L, \varphi_{1\%}, H_{1\%})$$

- Input data $q_v(p,m)$ preliminary obtained from algorithm 2.
- Computation of parabolic approximate $B(p) = q_v(p,m)(F+1)^n$
- From relation

(4) $$\Psi = \Omega / H(p,24) = qv(p,m)(F+1)^n (B/L) / (hv^n \cdot H(p,24)),$$

are calculated values of B parameter.
- Determination of calculated formula for regions with surface F>250km²:

(5) $$q_v(p,m) = (a\, h^n \cdot \varphi(p) \cdot H(p,24)) / (1000 \cdot (F+1)^n \cdot (B/L))$$

e) Computation of the atmospheric rainfalls intensity and regionalisation parameters (Table 4-1).
- The integral curves of atmospheric rainfalls reduction:

(6) $$\Psi\tau = H\tau p/Hp = f(p, \tau)/f_1(p) = \Psi p(\tau) = \Psi Hp,\tau$$

- The integral curves of mean intensity of the heavy rainfalls: $I=H\Psi p/\tau = Hp\ \Psi p(\tau)/\tau = Hp\ \Psi(\tau)$
- The integral curves of minimal intensity of heavy rainfalls: $I\tau p=dH\tau p/d\tau=d[Hp\ \Psi p(\tau)]/ d\tau= Hp\ \Psi(\tau\}$
- The integral reduction curve of the rainfall layer
- Reduction coefficient of the rainfall $\eta= \Psi p(\tau)/ \Psi(\tau)$
- The empirical subsidiary curves $S_\tau = 16{,}67\psi_\tau$ and $E_\tau=\tau\sqrt{}\ S(\tau)=\tau\sqrt{16.67\psi(\tau)}$

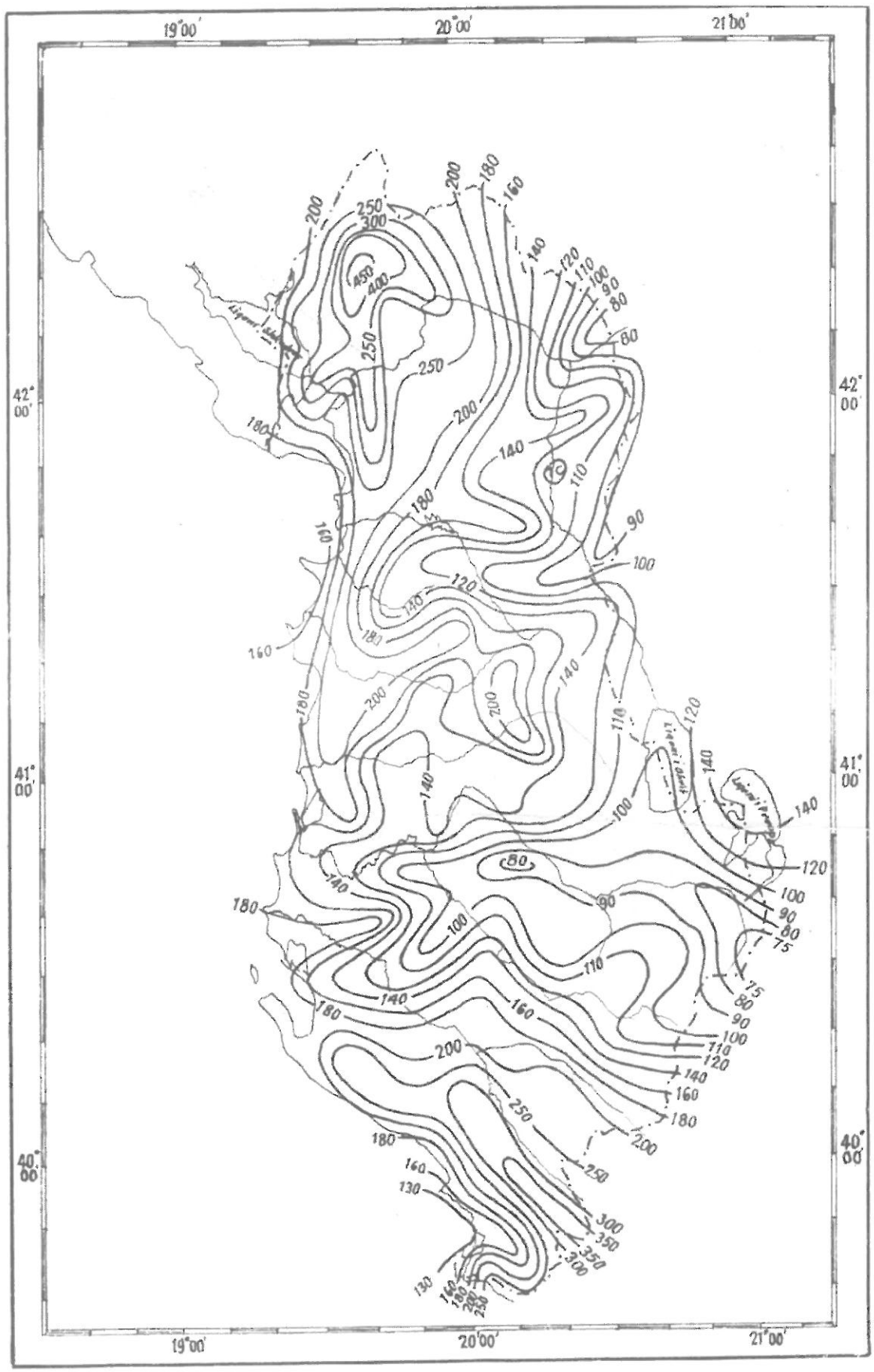

- Figure 4-1: 24 hours geographycal distribution rainfall map with p=1 % probability.

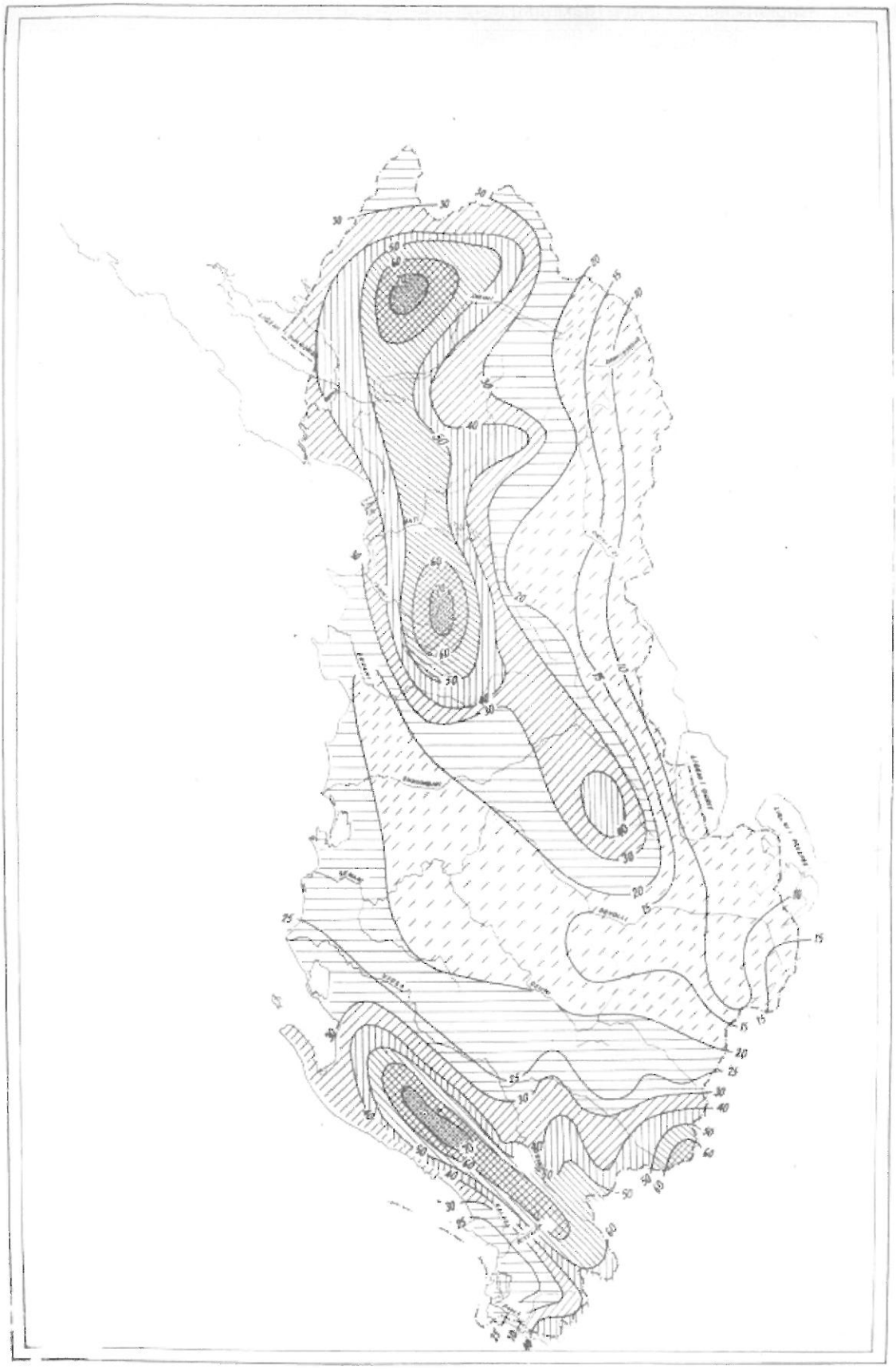

Figure 4-2: Maximum specific discharge module geographical distribution with p = 1 % probability ($B_{1\%}$).

Table 4-1: Regionalisation of the maximum discharge module on Albania.

NR	ELEMENTS	REGION 1 (Low module)					
1	24 hours maximum precipitation $H^{24}_{1\%}$	$H^{24}_{1\%}$ =75 - 120 mm					
2	Specific module of the maximum discharge $B_{1\%} \sim (q^{M}_{1\%} \cdot \sqrt{F})$	$B_{1\%}$ = 10 - 30					
3	Maximum runoff coefficient $\varphi^{M}_{1\%}$	$\varphi^{M}_{1\%}$ = 0.30 - 0.40					
4	Rainfall Intensity:	τ = 15'	30'	60'	120'	180'	240'
a)	Reduction of the rainfall depth $\Psi_p(\tau)$	0.195	0.310	0.399	0.493	0.555	0.607
b)	Mean intensity of rainfalls $\Psi(\tau)$	0.013	0.010	0.0066	0.004	0.0031	0.0025
c)	Coordinates mean of rainfalls intens. $I\tau_p$	1.14	0.834	0.328	0.196	0.134	0.095
d)	The coord. of the subsidiary curves S(τ)	21.67	17.17	11.00	6.83	5.17	4.17
e)	The coord. of the subsidiary curves E(τ)	32.25	61.20	108.4	193.2	270	340
f)	Coefficient of precipitation reduction η	0.59	0.54	0.33	0.32	0.30	0.26
5 a)	Maximum discharge module Calculation of the maximum module for F>250km^2: $q^{M}_{1\%} = f(F,h, \varphi_{1\%}, H^{24}_{1\%}, B, L)$	$q^{M}_{1\%} = \dfrac{3 \cdot h^{1.18} \varphi_{1\%} H^{24}_{1\%}}{1000(F+1)^{0.25} B/L}$					
b)	Calculation of the maximum module for F<250km^2: $q^{M}_{1\%} = f(h, \sqrt{F})$	$q^{M}_{1\%} = 0.0783 \left(\dfrac{h}{\sqrt{F}}\right)^{0.6993}$					
NR	**ELEMENTS**	**REGION 2** (Average module)					
1	24 hours maximum precipitation $H^{24}_{1\%}$	$H^{24}_{1\%}$ =121 - 200mm					
2	Specific module of the maximum discharge $B_{1\%} \sim (q^{M}_{1\%} \cdot \sqrt{F})$	$B_{1\%}$ = 31 - 50					
3	Maximum runoff coefficient $\varphi^{M}_{1\%}$	$\varphi^{M}_{1\%}$ = 0.41 - 0.50					
4	Rainfall Intensity:	τ = 15'	30'	60'	120'	180'	240'
a)	Reduction of the rainfall depth $\Psi_p(\tau)$	0.183	0.297	0.408	0.520	0.563	0.601
b)	Mean intensity of rainfalls $\Psi(\tau)$	0.012	0.010	0.007	0.004	0.003	0.0025
c)	Coordinates mean of rainfalls intens. $I\tau_p$	1.56	1.23	0.52	0.208	0.141	0.098
d)	The coord. of the subsidiary curves S(τ)	20.50	16.50	11.34	7.17	5.17	4.17
e)	The coord. of the subsidiary curves E(τ)	31.80	60.3	109.8	195.6	270	341
f)	Coefficient of precipitation reduction η	0.61	0.59	0.37	0.23	0.22	0.19
5 a)	Maximum discharge module Calculation of the maximum module for F>250km^2: $q^{M}_{1\%} = f(F,h, \varphi_{1\%}, H^{24}_{1\%}, B, L)$	$q^{M}_{1\%} = \dfrac{1.66 \, h^{0.44} \varphi_{1\%} H^{24}_{1\%}}{1000(F+1)^{0.40} B/L}$					
b)	Calculation of the maximum module for F<250km^2: $q^{M}_{1\%} = f(h, \sqrt{F})$	$q^{M}_{1\%} = 0.032 \left(\dfrac{h}{\sqrt{F}}\right)^{1.0534}$					
NR	**ELEMENTS**	**REGION 3** (High module)					
1	24 hours maximum precipitation $H^{24}_{1\%}$	$H^{24}_{1\%}$ = 201 - 450mm					
2	Specific module of the maximum discharge $B_{1\%} \sim (q^{M}_{1\%} \cdot \sqrt{F})$	$B_{1\%}$ = 51 - 70					
3	Maximum runoff coefficient $\varphi^{M}_{1\%}$	$\varphi^{M}_{1\%}$ = 0.51 - 0,70					
4	Rainfall Intensity:	τ = 15'	30'	60'	120'	180'	240'
a)	Reduction of the rainfall depth $\Psi_p(\tau)$	0.113	0.189	0.284	0.390	0.491	0.543
b)	Mean intensity of rainfalls $\Psi(\tau)$	0.008	0.006	0.003	0.003	0.003	0.002
c)	Coordinates mean of rainfalls intens. $I\tau_p$	1.83	1.48	1.02	0.38	0.397	0.295
d)	The coord. of the subsidiary curves S(τ)	12.67	10.66	7.83	5.50	4.50	3.83
e)	The coord. of the subsidiary curves E(τ)	28.2	53.7	101	185	260	335
f)	Coefficient of precipitation reduction η	0.67	0.64	0.62	0.57	0.41	0.36
5 a)	Maximum discharge module Calculation of the maximum module for F>250km^2: $q^{M}_{1\%} = f(F,h, \varphi_{1\%}, H^{24}_{1\%}, B, L)$	$q^{M}_{1\%} = \dfrac{0.997 \, h^{0.71} \varphi_{1\%} H^{24}_{1\%}}{1000(F+1)^{0.50} B/L}$					
b)	Calculation of the maximum module for F<250km^2: $q^{M}_{1\%} = f(h, \sqrt{F})$	$q^{M}_{1\%} = 0.4784 \left(\dfrac{h}{\sqrt{F}}\right)^{0.6023}$					

5 ESTIMATION OF THE CALCULATION ACCURACY

The relationship between calculated maximum discharge module $q_{1\%}^{M'}$ with formulas for F>250 km^2 and observed module $q_{1\%}^{M}$ is expressed by means of equation:

(7) $$q_{1\%}^{M'}=1,049q_{1\%}^{M}-28;\ R^2=0,98;\ Er=\pm 13.0\%.$$

In the meantime for the calculation of maximum discharge module for F<250 km^2, the relationship between calculated maximum discharge module $q_{1\%}^{M}$ and observed module $q_{1\%}^{M}$ is expressed by means of equation:

(8) $$q_{1\%}^{M'}=1,035\ q_{1\%}^{M}-25;\ R^2=0,85;\ Er=\pm 14.3\%$$

6 CONCLUSION

Maximum flood is an important and representative element of the hydrological regime of the Albanian river system for the natural specific conditions.

a) - Floods formed in the Albanian catchment area are more of rainfall and less of melange (snow-melt - rainfall). Beside this, generally are distinguished mainly 4 types of flood hydrograph.
b) - The principal results of the maximum flood regionalisation of the Albanian catchment are:
- The scheme of basin classification and division into homogeneous sectors based on evaluation and determination of the natural factors participating in the flood process formation.
- Region is accepted as the smallest tacsinometric unit.
- The principal natural factors that influence on the flood formation are: morphometric $h/\sqrt{F}$, hydrometeorological $\varphi_{1\%}^{M}$,$H_{1\%}^{M}$ and hydrographic B/L.

c) - Classification was carried out for the following parameters: low, mean and high.

I. The region with relatively low module values:

- 24 hours precipitation with p=1% probability $H_{1\%}^{24}$=75-120mm.
- Specific maximum discharge module with p=1% probability $B_{1\%}=q_{1\%}^{M}\sqrt{F}$=10-30.
- Maximum flood flow coefficient with p=1%probability $\varphi_{1\%}^{M}$=0,30-0,40
- Maximum discharge, modules respectively for:

a) Medium catchment area (F>250 km^2)

(9) $$q^{M}_{1\%}=(h^{1.18}\varphi_{1\%}H^{24}_{1\%})/1000(F+1)^{0.25}\ B/L$$

b) Small catchment area (F<250 km^2)

(10) $$q^{M}_{1\%}=0.0783(h/\sqrt{F})^{0.6993}$$

II. The region with relatively mean module values:

- 24 hours precipitation with p=1% probability $H_{1\%}^{24}$=121-200mm
- Specific maximum discharge module with p=1% probability $B_{1\%}=q_{1\%}^{M}\sqrt{F}$=31-50
- Maximum flood flow coefficient with p=1%probability $\varphi_{1\%}^{M}$=0,41-0,50
- Maximum discharge, modules respectively for:

a) Medium catchment area (F>250 km^2)

(11) $$q^{M}_{1\%}=(1.66\ h^{0.44}\varphi_{1\%}H^{24}_{1\%})/(1000(F+1)^{0.40}\ B/L)$$

b) Small catchment area (F<250 km^2)

(12) $$q^{M}_{1\%}=0.032(h/\sqrt{F})^{1.0534}$$

III. The region with relatively high module values:

- 24 hours precipitation with p=1% probability $H_{1\%}^{24}$=201-450mm
- Specific maximum discharge module with p=1% probability $B_{1\%}=q_{1\%}^{M}\sqrt{F}$=51-70
- Maximum flood flow coefficient with p=1%probability $\varphi_{1\%}^{M}$=0,51-0,70
- Maximum discharge, modules respectively for :

a) Medium catchment area (F>250 km^2)

(13) $$q^{M}_{1\%} = (0.997\, h^{0.71}\, \varphi_{1\%}\, H^{24}_{1\%})/(1000(F+1)^{0.50}\, B/L)$$

b) Small catchment area (F<250 km^2)

(14) $$q^{M}_{1\%} = 0.4784(H/\sqrt{F})^{0.6023}$$

REFERENCES

Avdyli, B. (1980): Construction of design curves for hydrological elements, Bulletin of Natural Sciences, No. 2, Tirana University

Avdyli, B. (1983): Determination of the maximum discharge in the basin of Seman river basin, IHM, No. 9

Avdyli, B., Bukli, M. (2000): XXth Conference of the Danubian countries on the Hydrological Forecasting and Hydrological Bases of Water Management, Bratislava, Slovakia, 4-8 September

Kennedy, R. J., Watt, W. E. (1971): The relationship between lag time and physical characteristics of dranage basins in Southern Ontario. "Floods and their computation. Studies and reports in hydrology". Proc. of the Leningrad symposium, Vol. 2, UNESCO-WMO

Pano, N. (1982): Maximal Discharges in Albania., IHM No. 8, Tirana

Pano, N. et al. (1984): Albanian Hydrology. Monography, IHM , Academy of Sciences, Tirana

Rodda, J. C. (1971): The significance of characteristics of basin rainfall and morphometry in a study at floods in the United Kingdom. Floods and their computation, L., Vol. 2, UNESCO-WMO

Selenica, A. (1982): Maximum discharge with different probability in Vjosa river. IHM, No. 8, Tirana

Smirnova, E. A. (1971): Design rainfall characteristics of the USSR territory. Tome 1. Studies and reports in hydrology, No. 3, IASH-UNESCO-WMO

Stanescu, V. (2000): Regional analysis of annual flood discharges in the Danub basin. XX –th conference of the Danubian countries, Bratislava, Slovakia

FLOOD MODELLING AND PREVENTION IN THE RHONE BASIN UPSTREAM OF LAKE GENEVA

Jean-Louis Boillat[1], Jérôme Dubois[2], Anton Schleiss[1], Frédéric Jordan[1]

[1] Laboratory of Hydraulic Constructions, LCH, Swiss Federal Institute of Technology, EPFL, 1015 Lausanne, Switzerland, secretariat.lch@epfl.ch

[2] HydroCosmos SA, Rue de l'Industrie 35, 1030 Bussigny, Switzerland, info@hydrocosmos.ch

SUMMARY

Today, the possibilities of numerical simulation allow a fully deterministic and physically oriented approach of hydrological phenomena based on hydraulic equations to compute the flood generation and routing in catchment areas. In alpine regions like in the Rhone Valley of the Canton of Valais, the influence of the numerous hydroelectric schemes and reservoirs on the hydraulic regime of rivers is significant and has to be considered as an additional parameter. In order to investigate the hydraulic behaviour of such complex natural and artificial networks during floods, the computer program "Routing System" was developed at the Laboratory of Hydraulic Construction of the Swiss Federal Institute of Technology in Lausanne. Its performance was tested and applied on the watershed of the Rhone River Valley, upstream of Lake Geneva over a total surface of about 3750 km^2.
Based on several meteorological scenarios, this numerical model allows to determine the natural run-off in the catchment area taking into account the water diverted by river intakes as well as flood routing in reservoirs for different operation rules of the hydropower and pumped storage schemes. Snow fall and snow smelt are modelled with functions related to the atmospheric temperature. By dividing the total area of the watershed into 83 sub-regions, a spatial rainfall distribution can also be considered in the fully transient calculation.
After calibration with several recent flood events, the hydraulic response of the whole complex catchment area was analysed in view of the flood formation and routing for various meteorological scenarios and possible operation cases of the hydraulic schemes. The results obtained revealed a significant routing effect of the reservoirs on the flood peaks, even in the case of initial high filling rates at the beginning of the flood season.
Nevertheless, the influence of the initial water levels in the reservoir clearly showed the potential of optimising the operation rules of the gated dam spillways and powerhouses during floods. Furthermore the management of flood plains could reduce the flood peaks. For this reason, the project is presently extended towards a real time flood simulation tool with a direct link to meteorological forecasting and hydraulic schemes. The aim is to elaborate an expert system, which can be used to manage successfully severe floods in the Rhone Valley. The real time simulation tool will also be linked to rainfall measurement and discharge gauging stations in order to control and to correct it continuously.

Keywords: numerical modelling of floods, flood routing in reservoirs, flood prevention, meteorological forecasting simulation, complex catchment areas

1 INTRODUCTION

Over a little more than 10 years, four important flood events have been observed (August 1987, September 1993, September 1994 and October 2000) in the watershed area of the Rhone River in Switzerland upstream of Lake Geneva. In 1993, disastrous floods took place in the Upper Valais region, in particular in the town of Brigue. In 2000, the disaster area was extended to the Lower Valais (Figure 1-1).
Following the 1993 flood, the Canton of Valais set up an interdepartmental work group, mainly composed of representatives of the Swiss Federal Office for Water and Geology as well as cantonal services. This work group was responsible for managing the CONSECRU project (safety concept against flood risks), the main objective being to make concrete propositions in order to reduce flood hazards in the future, including the possibilities offered by hydropower schemes and their storage reservoirs.
This project was an opportunity to highlight the importance of large hydropower plants with their reservoirs and waterway systems for flood routing as well as the reduction of peak discharges downstream. Promising analysis results have urged the Canton of Valais to improve flood prediction models and to

acquire a tool permitting to couple meteorological and hydrological information. Some components of this type of modelling are already operational on some watersheds.
The next step was to undertake the flood routing modelling over the total catchment area. This project named MINERVE was initiated jointly by the Laboratory of Hydraulic Constructions and the Institute of Soil and Water Management at the Swiss Federal Institute of Technology in Lausanne and the engineering office HydroNat, under the coordination of the cantonal services for hydropower and water courses of the Canton of Valais.
The motivations to develop the flood modelling were essentially to:

- gather all basic information – collected in the Valais watersheds concerning meteorology, hydrology and hydraulics – for flood situations which could endanger people and properties;
- process these basic data into a dynamic model permitting to simulate temporal evolution of discharges over the entire Valais territory, with the help of which the right decisions can be taken during floods;
- dispose of a flexible model which will allow to integrate in real time the most useful and most reliable information in order to feed the simulation model, whether it be hydro-meteorological forecasts supplied by MeteoSwiss or discharge measurements by means of remote-transmission by the Swiss Feeral Office for Water and Geology or other entities.

The present document describes the conceptual modelling approach adopted for that purpose.

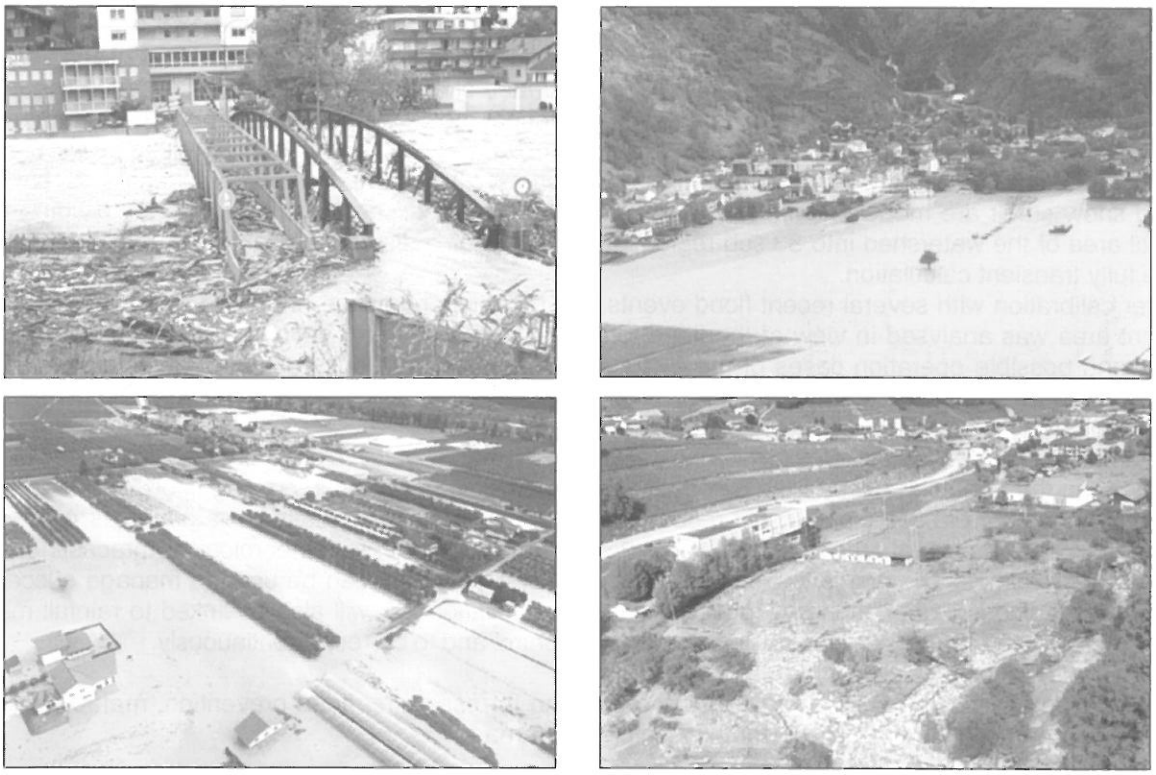

Figure 1-1: Flooding pictures during the flood event of October 2000 in Valais (source: *Nouvelliste Journal, October 2000).*

2 MODELLING CONCEPTS

In Switzerland, the major part of the hydro-electric potential is already equipped resulting in a large number of hydraulic schemes on the Swiss plateau and in the Alps. Each one regroups numerous structures which influence the natural flow of the water through its watershed. The possibility of modelling the behaviour of the whole set of equipped catchment areas allows a better management of hydraulic schemes under normal operation or during floods. Furthermore, the security of the hydraulic schemes can be evaluated more appropriately in analysing the entire hydraulic system with a global approach.
The hydraulic system of the catchment area becomes rapidly complex, with several inputs, several outputs and a set of regulation and operation rules. The modification of one element of this system can have repercussions on the entire system, which importance is difficult to evaluate at first sight.

Instead of tackling this complexity in full-face, the modelling numerical tool called "Routing System" (Dubois & Boillat 2000) proposes an approach based on the flux generation and routing. According to this concept, six hydraulic basic functions are sufficient to describe a hydraulic network:

- Flow generation. All the methods and hydrologic models are regrouped under this general name.
- Discharge splitting. This tool is able to represent likewise a simple orifice placed in a reservoir as well as a complex intake structure comprising a dam, a reservoir, a spillway, a sand trap or even a side weir in a flood protection system, which diverts a part of the discharge.
- Flood transport. Beside the routing of a flow discharge from one point to another in the river, this tool modifies the hydrographs, when it is considered with a non-stationary behaviour.
- Discharge summation. This tool simulates the junction of various fluxes in a hydraulic network.
- Flow storage. It allows flood routing calculation in a reservoir.
- Flow control. This particular tool allows to generate functional relations of various control works (spillways, orifices, ...) to convey them later into the other basic functions.

These basic tools are programmed in the LabVIEW graphical language and accessible in a library with the help of icons (Figure 2-1).

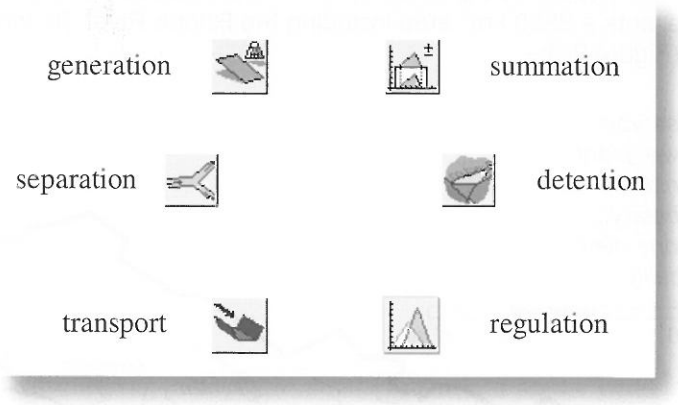

Figure 2-1: The 6 basic hydraulic tools of Routing System.

The modelling concept is presented in Figure 2-2 by a simple hydraulic system. The modelled system is the catchment area of the Turtman Valley in Upper Valais, whose outlet is the Rhone River. It is divided into lower-level watersheds and contains the storage reservoir of the Turtman dam, in which a directly connected watershed and two water intakes flow. Downstream of the dam, the main river and its tributaries can also be modelled from the dam to the Rhone river. The use of an adequate sub-division allows to model the system with the functional elements presented in Figure 2-1.

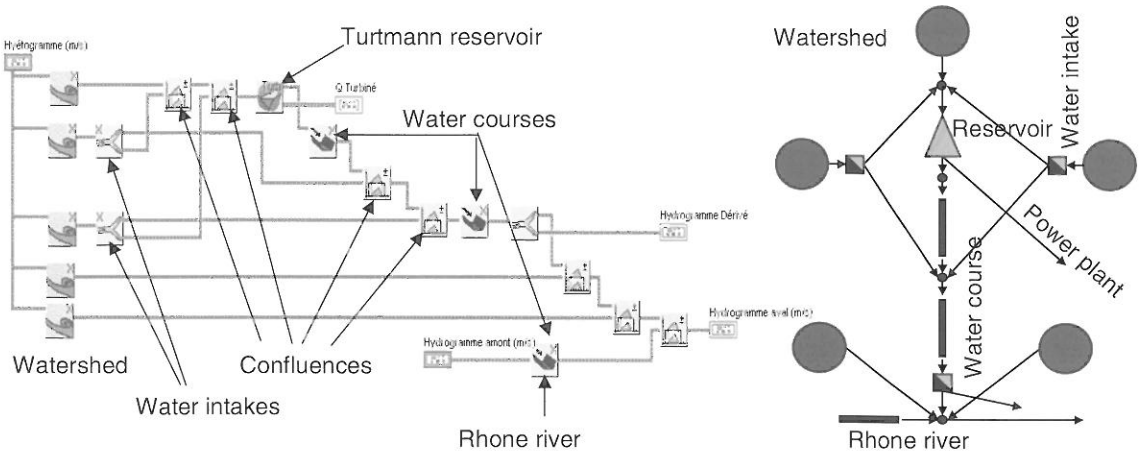

Figure 2-2: Turtman watershed and its hydro-power storage plant. Left: Routing System model. Right: hydraulic system scheme.

The input for every tool of Routing System can be characterized by variable or non-variable data.
Non-variable data are used to describe the system and are computed as constant values or as pre-defined relationships such as reservoir water surface - volume rating curves. They are stored in ASCII files and are read at every simulation.
Other types of non-variable data are the security constraints defined as operation rules for large dams. In fact, the operation rules of the spillways of every dam are defined in official and legal documents, established by the Federal Office for Water and Geology. In order to guarantee the safety of the dam during floods, the dam owner has to control the flow discharge through the outlet structures in function of the level of the water in the storage reservoir.
All these operation rules are considered in the model. For example, the water level - flow discharge relationship of a reservoir is chosen at every time step in function of the actual state of the system and security constraints, which are introduced in the model in the form of decision matrices stored in ASCII text files.
Unlike non-variable data, hydro-meteorological data and the operation of the hydro-power plant vary with time and represent the direct input of the model. The model then needs the variation in time of rain intensity for every modelled watershed before each run.
The modelling concept was applied to the whole Rhone River watershed from the source to the outlet in Branson, which represents a 3800 km^2 area including the Rhone River, its tributaries and the whole hydro-power schemes (Figure 2-3).

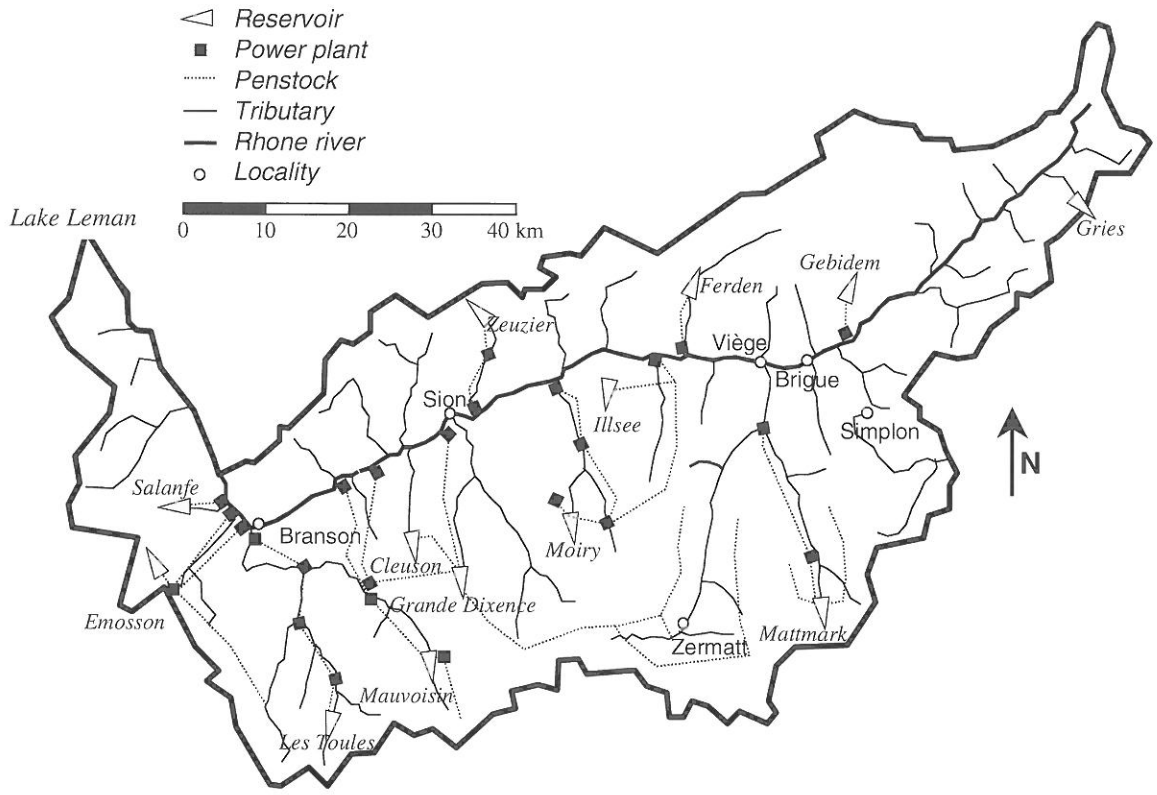

Figure 2-3: Catchment area of the Rhone River and major hydro-power plants and reservoirs.

For such a large scale modelling, the watershed had to be subdivided into 83 sub-catchment areas in 11 different zones shown in Figure 2-4. When computing different rain hydrographs at each watershed, corresponding hydrographs can be obtained at every node of the system.

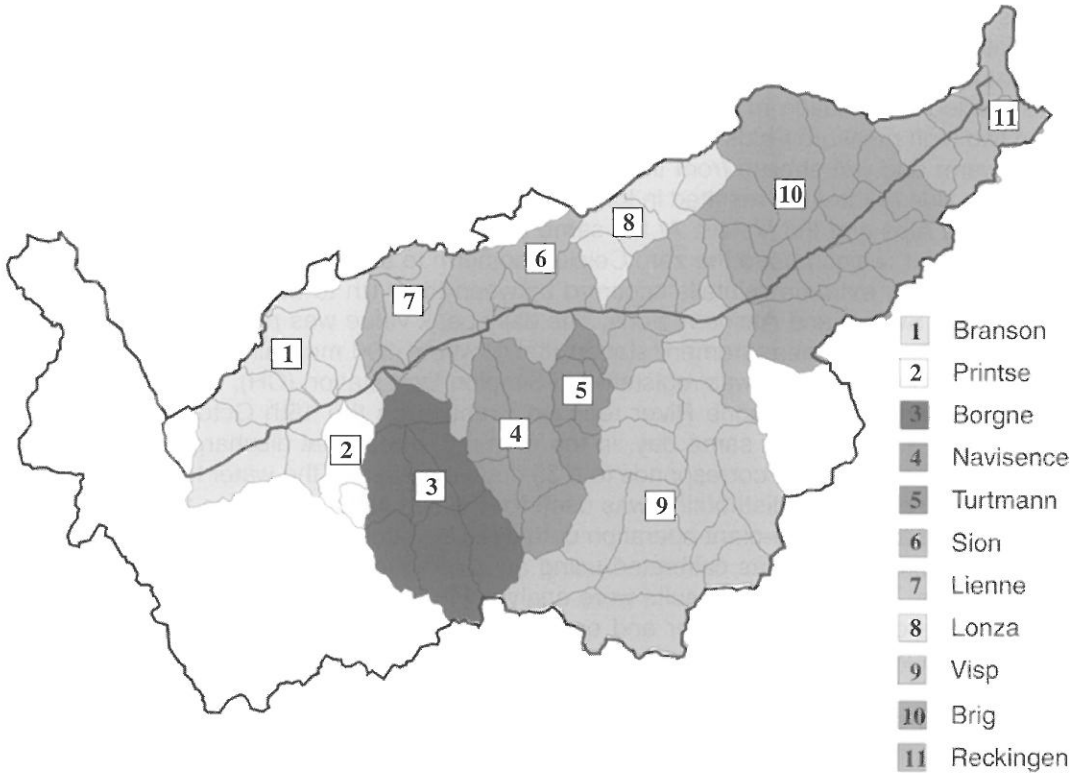

Figure 2-4: Hydrological subdivisions of the Rhone watershed in 11 regions and 83 smaller catchment areas.

3 THE FLOOD OF OCTOBER 2000

With the model described above, a first simulation focused on the sensitivity analysis of the influence of dams during flood events. The parameters studied were the initial rate of filling of the reservoirs and the start-up process of the turbines. The results obtained show clearly the important role of the dams during the flood event and in particular the effect of the initial filling rate of the reservoirs (Figure 3-1) (Dubois et al., 2000), (Raboud et al., 2001).

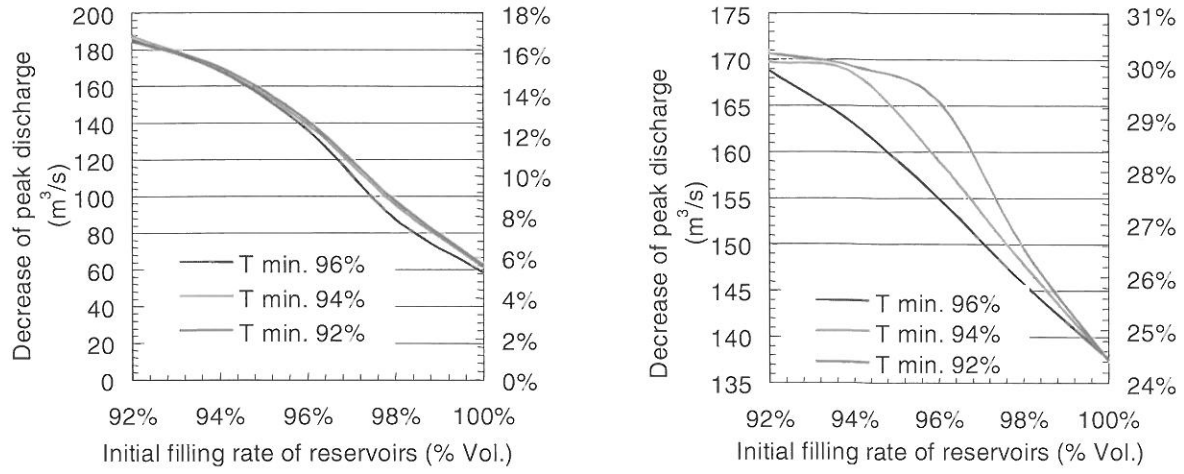

Figure 3-1: Influence of the initial filling rate of the reservoirs on the flood peak on the Rhone river at Branson (left) and on the Viège river at Viège (right), as a function of start-up of turbines (T_{min} indicates the filling rate at which the turbines are started).

In a second stage, the model was used to simulate historical events. The extreme flood event of October 2000 on the Rhone River in the Valais region is of special interest, since it was documented in detail in view of locally varying rain data, flow discharge measurements at several gauging stations

as well as data of hydro-power plant operations. Such data are obviously very useful for the calibration and validation of the model. Furthermore, this event was used to quantify the effect of dams and storage reservoirs on flood protection.
The meteorological situation in mid-October 2000 was as follows: A cyclonic depression was blocked between two high pressure fields located over the Atlantic Ocean and Russia. This situation generated a strong, warm and wet stream from the South over the Alps. The transportation and uplift of wet air on the South side of the Alps resulted in long precipitations with locally very high intensities, especially in the Ticinese Alps and the Valais. At the same time, the temperature in this region increased by the arrival of warm air, which raised the zero Celsius isotherm to an elevation of 3000 meters.
As a consequence, extreme rainfalls occurred between the 11th to the 15th and during the 30th and 31st October in Switzerland Alpine regions. The daily peak value was reached on the 13th October at the Bognanco-Pizzanco measurement station (Italy), where 396 mm rain in 24 hours was measured. On the 14th October, 250 mm was registered in Simplon-Dorf station (CH).
The peak discharge in the Rhone River reached Branson on the 15th October 2000 at 1 p.m., at a value of 980 m^3/s. During the same day, in the morning, a maximal discharge increase of + 67 m^3/s per hour was reached, which corresponds to a 35 cm/h increase of the water level in the Rhone River.
An interpolated spatial rain distribution was used for the simulation based on field rain measurements in the catchment area. Hydro-plant operation data were also collected from hydroelectric companies.
The comprehensive model was calibrated using an automatic procedure adjusting the main hydrological parameters. The computed results were analysed in five different locations corresponding to five gauging stations on the Rhone River and on the Viege River in the town of Viege. They showed a good agreement with the observed hydrographs. The flood rise, the peak discharges as well as wave speed were correctly reproduced (Jaberg, 2002).
The result of the simulation in Branson is presented in Figure 3-2 (left). The picture shows a sudden decrease of flow discharge occurring just after the flood peak which is the result of a failure of the river embankment dam located a few kilometres upstream near Chamoson. This unpredictable outflow from the Rhone in the flood plain was estimated at 3.5 mio m^3 and was not considered in the model, which was therefore calibrated with a corrected hydrograph.
In order to study the effect of hydropower plants storage reservoirs, two cases were compared. The first case was without considering the hydro-power plants and reservoirs. The second case was simulated using the measured reservoir filling rates and the prescribed operation rules. The results of this comparison in Branson are presented in Figure 3-2 (right) and show a peak discharge of 1120 m^3/s without hydropower plants compared to 980 m^3/s with these schemes. This is a 140 m^3/s reduction corresponding to a 75 cm water level decrease in the Rhone, which was a vital event in view of dam failure.

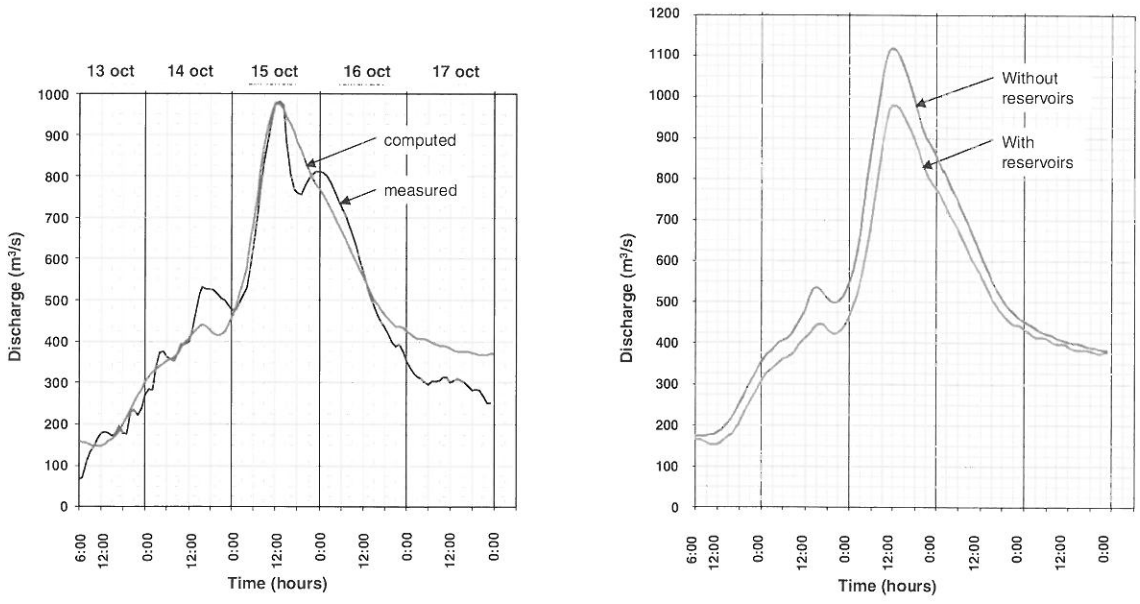

Figure 3-2: The flood event of October 2000 at the gauging station near Branson. Left: comparison between the measured and simulated hydrographs. Right: comparison of the hydrographs simulated with and without the hydro-electric power plants and reservoirs in the catchment area.

4 CONCLUSIONS AND OUTLOOK

Results obtained so far with the help of a powerful hydraulic model of the watershed of the Rhone River in the Valais allow to compare hydrographs in any location in the catchment area. The positive influence of hydro-electric power schemes on flood peaks in the Rhone River and its main tributaries could be clearly shown.
The importance, efficiency and precision of this model can be considerably increased by feeding it continuously with real time measured data (precipitation, discharge, etc.) and with meteorological forecast. This development will allow to follow flood evolution in real time and to suggest anticipated operation measures for hydro-power plants (lowering reservoir level, start-up of turbines, etc) at the location in the catchment area with the greatest benefit on flood peak reduction. The goals pursued can be summarized as follows:

- Develop a real time flood forecast tool on the basis of coupling of meteorological information with a hydrological model.
- Simulate flow through schemes and along rivers, for different meteorological scenarios.
- Follow in real time water flow through hydraulic schemes and rivers, with the help of the automatic acquisition of measured data.
- Optimise the operation rules of hydropower plants and dams in view of flood protection, for a certain meteorological scenario.
- Develop user-friendly screen menus for the simulation tool by control panels and window technique.
- Transfer this tool to a task force which can prepare decisions and action plans for the local government (such as lowering water level in storage reservoirs, of accumulation basins, decision to start or stop operation of powerhouses, closure or opening of intakes, information and preventive evacuation of the population, etc.)

ACKNOWLEDGEMENT

The research study was financed by the canton of Valais.

REFERENCES

Dubois, J., Boillat, J-L. (2000): «Routing System. Modélisation du routage des crues dans des systèmes hydrauliques à surface libre» Thèse 1890, Communication N° 9 du Laboratoire de constructions hydrauliques (LCH), École Polytechnique Fédérale. Lausanne.

Dubois, J., Boillat, J-L., Raboud, P-B., Costa, S., Pitteloud, P-Y. (2000): «Einfluss der Wasserkraftanlagen auf die Hochwasser der Rhone im Kanton Wallis (Schweiz)», Proceedings Wasserbau Symposium "Betrieb und Überwachung wasserbaulicher Anlagen", 19-21 Oktober. Graz, Austria, n°34, pp. 57-66.

Raboud, P-B., Dubois, J., Boillat, J-L., Costa, S., Pitteloud, P-Y. (2001): «Projet Minerve- Modélisation de la contribution des bassins d'accumulation lors des crues en Valais», Wasser-Energie-Luft, Heft 11/12. Baden, Schweiz, pp. 313-317.

Jaberg, P. (2002): «Modélisation des crues du Rhône en Valais. Approche numérique», Travail pratique de diplôme, EIVD. Yverdon, Suisse.

OPERATIONAL FLOOD FORECASTING IN MOUNTAINOUS AREAS – AN INTERDISCIPLINARY CHALLENGE

Therese Bürgi

Federal Office for Water and Geology, 3003 Berne-Ittigen, Switzerland, therese.buergi@bwg.admin.ch

SUMMARY

For over 15 years the Swiss National Hydrological Survey (SNHS), which is part of the Federal Office for Water and Geology (FOWG), has been using hydrological forecast models for the Alpine catchment of the River Rhine at Rheinfelden. Initially, statistical methods were used. Today the SNHS uses the conceptual HBV3-ETHZ rainfall runoff model linked with data from numerical weather forecast models. This rainfall runoff model is based on Bergström's HBV3 model (Bergström, 1976) which has been adapted to the hydrological and meteorological conditions prevailing in Switzerland by the Geographical Institute of the Federal Institute of Technology in Zurich (ETHZ). Furthermore, a new forecasting system is at present being developed in collaboration with the Institute for Inland Water Management and Waste Water Treatment (RIZA) in the Netherlands.
Because of its complexity, the Alps offer meteorologists and hydrologists interesting challenges in the way of developing forecast models. The locally varied and mountainous topography challenges meteorologists to develop numerical weather forecast models which encompass both large-scale weather patterns and extremely localised phenomena and which forecast the weather on both scales with geographical and temporal accuracy. For hydrologists engaged in developing models, and in particular in daily operations, the particular character of the Alps means that they have to take into consideration the fact that bodies of water in the small, steep catchments in the mountains are highly sensitive to precipitation, owing to the low storage capacity of the soil. The delay between rainfall and rising water levels is short. This means that both rapid rises in water level and maximum flood peaks must be forecasted with precision.
The winter months in the Central Lowlands constitute a further challenge for specialists in both disciplines. Under the influence of a warm front combined with heavy precipitation the snow cover can melt within a very short period. In order to be able to forecast such an event with hydrological precision it is essential to have exact forecasts for air temperature, 0°C-altitude and volume of rainfall. In view of this strong link between hydrology and meteorology it is necessary for the two disciplines to work closely together. Considerable progress is expected to be achieved by further developing the numerical weather forecast models and improving precipitation measurement (using radar).
A hydrological forecasting system for the Alpine region must include human influence, as well as natural factors. In this respect, water resource management and the regulation of the level in the Alpine peripheral lakes must be mentioned.
If it is possible, together with research, to combine all these characteristics of the Alpine region into an operational hydrological forecasting system for the Rhine catchment and thus to obtain satisfactory results, we shall also be able to develop such systems for the Swiss river systems on the southern side of the Alps.

Keywords: operational hydrological forecasting, model

1 INTRODUCTION

1.1 The basin of the River Rhine in Switzerland

The Rhine catchment as far as Basle covers an area of some 36,000 km^2, which is the larger part of northern Switzerland. From a topographical point of view this area can be divided into three zones. In the north are the Jura Mountains whose highest point is just over 1,600 m, in the south the Alps with several peaks at over 4,000 m, and between the two the Central Lowlands, which range from 200 m to 900 m in altitude. From a hydrological point of view the Rhine catchment can be divided into the catchments of its main tributaries, the River Aare (11,750 km^2), the River Reuss (3,380 km^2), the River Limmat (2,400 km^2) and the River Thur (1,700 km^2) (Figure 1-1).

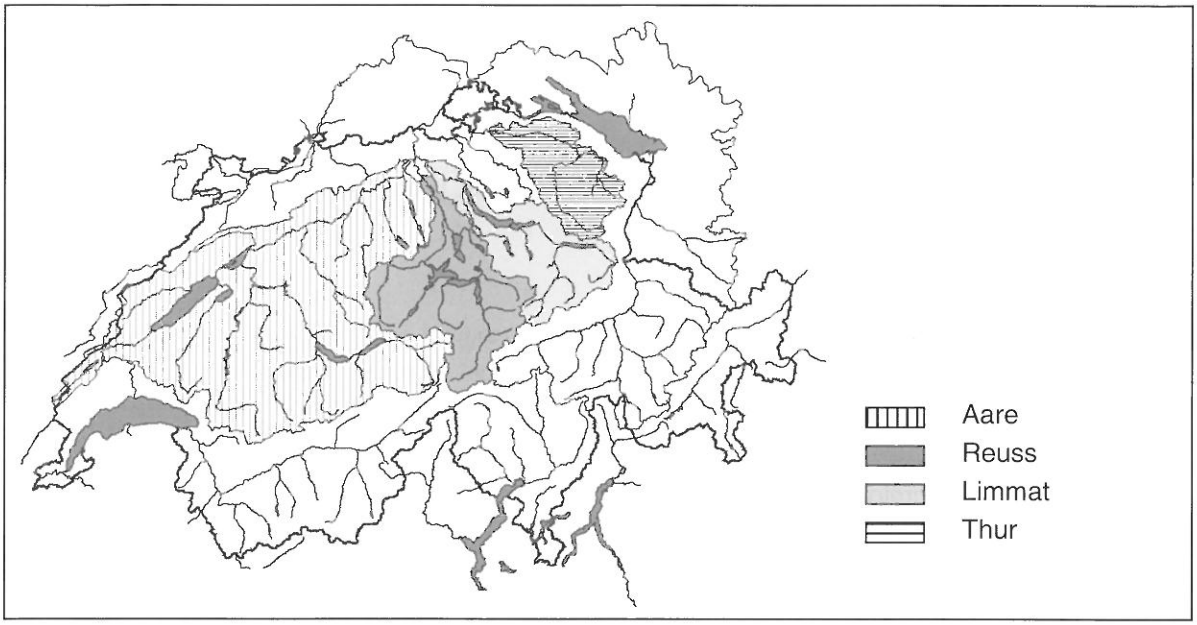

Figure 1-1: The River Rhine catchment in Switzerland.

From a climatic point of view northern Switzerland is strongly influenced by the prevailing weather patterns which arrive from the north and north-west. Here the Alps form a barrier which blocks and lifts the air masses which arrive in particular from the north-west. Consequently, the northern slopes of the Alps receive the most precipitation in the Rhine catchment. Mean annual precipitation in the Alpine area is around 3000 mm/a, in the pre-Alps 2000-2500 mm/a and in the Central Lowlands 1000-1500 mm/a, with approximately 1500 mm/a in the Jura Mountains. In all regions maximum rainfall is in the summer. There is no clear seasonal rainfall pattern, however, and long-lasting or heavy rainfall may occur at any time of the year. Owing to the differences in altitude, in winter the area can be divided into regions with a seasonal single build-up of snow and those with alternating snowfall and melt, depending on the weather pattern through the season.
The hydrology of the Rhine catchment reveals a differentiated picture, however. With the exception of the Thur, the seasonal runoff pattern of the tributaries of the Rhine is clearly defined. Under the influence of snow and glacier melt, peak discharge levels occur during the summer months and the lowest levels during the winter. A further characteristic can be seen in the Alpine peripheral lakes. Thanks to the retaining influence of these lakes flood runoff from the high Alps is attenuated, which in turn reduces the maximum discharge peaks. The Thur catchment is the only area which does not include any lakes, which means that a flood wave from this region flows down into the Rhine with little hindrance or loss of power.

1.2 The challenges for a forecasting system

In view of its natural and man-made characteristics, the challenges which a hydrological forecasting system for the Rhine catchment in Switzerland must meet can be summarised as follows:

1) The forecasting system must be able to predict with precision rapid increase and decrease in water level as well as the level and timing of extreme flood peaks (Figure 1-2). This is important because, owing to the steep slopes in the catchments, the rather small basins and short time lag (4-10 h), floods are rapid events.
2) The forecasting system must also give precise predictions of winter flooding in the Central Lowlands which occur as a result of a combination of melting snow and heavy rainfall. This is important because a continuous snow cover in the Central Lowlands can melt completely within a few hours under the influence of warm air advection and associated widespread heavy rainfall. This combination of widespread heavy rainfall and large volumes of water from snow-melt can lead to rapid and considerable rises in water levels.
3) Furthermore the forecasting system must take into account man-made influences in the catchments and their effect on discharge patterns of rivers and lakes. In particular the system must be aware of the rules for regulating the water level of Alpine peripheral lakes and calculate in a suitable way the volume of water retained by reservoirs and the delayed and controlled release into the drainage system over the following days and months.

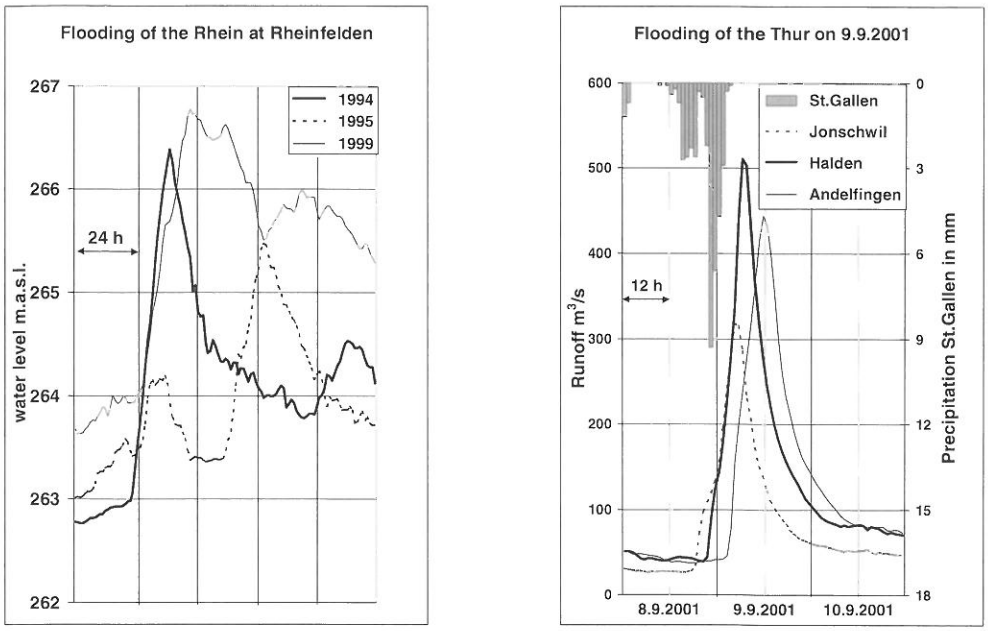

Figure 1-2: Flooding in Switzerland is an event of some few hours up to two days either for the whole river Rhine or for the tributaries. The peaks to forecast are very acute.

2 OPERATIONAL FORECASTING IN SWITZERLAND

2.1 Developing an operational service and a clientele

As early as the 1940s research and development was being carried out in Switzerland, namely at the Zurich Federal Institute of Technology (ETH), for a hydrological forecast model for the River Rhine catchment. Thanks to this research it was possible to develop operational short-term forecasting after 1960 (Schädler, 1993). In order for the ETH to be able to concentrate more on research and development, an agreement was drawn up in 1986 whereby operations concerning forecasting would be transferred to the Swiss National Hydrological Survey (SNHS) at the Federal Office for Water and Geology (FOWG). Since then the SNHS has been issuing hydrological forecasts from Monday to Friday for the Rhine at Rheinfelden. These forecasts cover the period from the time of issue until midnight on the next day but one. In the case of flooding, forecasts are also issued on Saturdays, Sundays and Bank Holidays, as well as several times daily. When water levels are high and extreme flooding is expected new forecasts are issued as frequently as every 2 hours.
The idea of hydrological forecasting originated in the business sector. It was the companies who operate hydroelectric power stations, shipping companies using the Rhine and the countries through which the Rhine flows which were and still are keen to receive forecasts for the Rhine. Hydrological forecasting is therefore still an important element today in planning the harnessing of the discharge to produce electricity, as well as in planning and organising the transport of basic commodities via the river. For the countries downstream the forecasts produced by Switzerland are important elements in their own forecast models.
Over the years the number of clients who use the Swiss forecasting system has grown. When water levels are high in particular, the recipients of our hydrological forecasts include crisis teams set up by regional authorities, private companies and the media. Thanks to the deregulation of the electricity industry, there has been growing interest in our daily forecasts in this sector over the past few years, with the result that brokers in the electricity market have recently joined our clientele. Today the FOWG's public services on Internet include a range of up-to-date figures and hydrological forecasts.

2.2 The statistical model

The SNHS's first operational system produced hydrological forecasts from the Swiss Alpine peripheral lakes downstream to the River Rhine in Rheinfelden (Lang et al., 1987). This area was divided into 11 sub-catchments. The system's database, which was in operation from 1986 until 1999 consisted of three elements: every 2 hours current water levels were transmitted from 18 SNHS measuring stations via the public telephone network. The SNHS received, by telex, hourly data for total precipitation and air temperature and, in winter, snow depth twice daily from around 70 stations within MeteoSwiss's automatic measuring network. In addition MeteoSwiss also sent, by telex, a precipitation and temperature forecast once a day which was tailored to the special requirements of SNHS. From the meteorological data and forecasts and the water level data converted into discharge values, the statistical model – a combination of various regressions – produced a forecast for the River Rhine at Rheinfelden.

2.3 The conceptual model

While the operational system was running a new procedure was being developed at the ETHZ, which replaced the old system at the end of 1999. The new system also produces forecasts for the area downstream from the Alpine peripheral lakes. It is only in the River Aare catchment that the area is extended to include the tributaries of Lake Biel, Lake Murten and Lake Neuchâtel. A new feature of the latest system is that the whole area is divided into around 50 sub-catchments. This division has been adapted to the SNHS's automatic measuring network which was set up in the 1990s. The database is made up of the mean hourly discharge measurements, the hourly temperature and precipitation measurements provided by MeteoSwiss's automatic measuring network and the hourly data for the forecast period from the high-resolution numerical weather forecast model. For the first time an operational runoff forecast model has been linked up with a numerical weather forecast model. In many ways the hydrological model involved, the HBV3-ETHZ, is based on the conceptual model HBV3 (Bergström, 1976). The adaptations concerned the interpolation of the meteorological data (see Section 3.1), the snow-melt model (see Section 3.2) and the change from daily to hourly time step. The same group at the ETHZ has taken care of the calibration of the 50 or so sub-catchments.

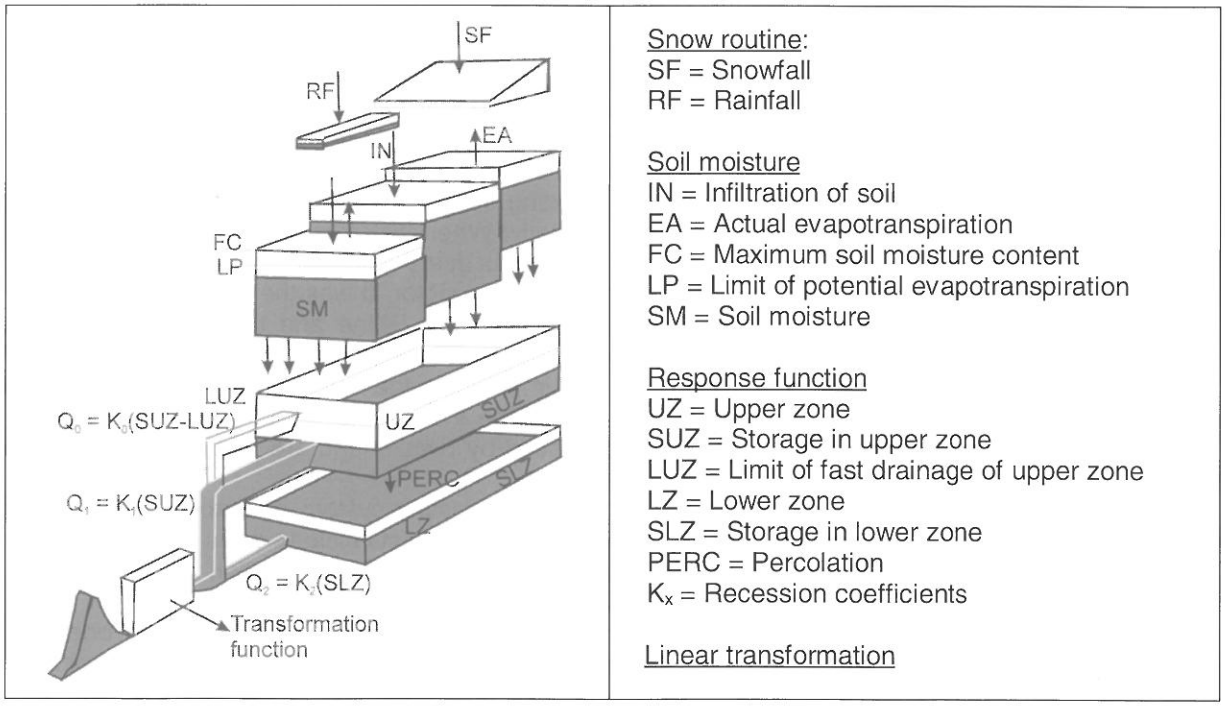

Figure 2-1: HBV-ETHZ model, adapted from Lindström et al. (1997).

The HBV model was chosen because the simple structure (Figure 2-1) of this conceptual model includes the most important elements of discharge formation. The model is based on homogenous catchments which are divided according to altitude. Using the "optimum interpolation" method (see Section 3.1), the system calculates precipitation for the area in question and temperatures for the different altitudes from meteorological point measurements. With the snow routine, the combined

energy balance and temperature index procedure (see Section 3.2), increase and decrease in snow cover is calculated for each altitude zone. The soil moisture routine is used to calculate actual evapotranspiration as a function of soil moisture in the model and potential evapotranspiration. Finally, the response function consists of a simple cascade system of two consecutive storage stages which represent the rapid and slow drainage of an area. The amount of water which drains off is converted into discharge using a filter. Finally, a statistically calculated linear transfer function produces the run-off for the individual areas as far as Rheinfelden. In view of the small catchments and the short time lag, no hydraulic method is needed for routing discharge within Swiss territory.

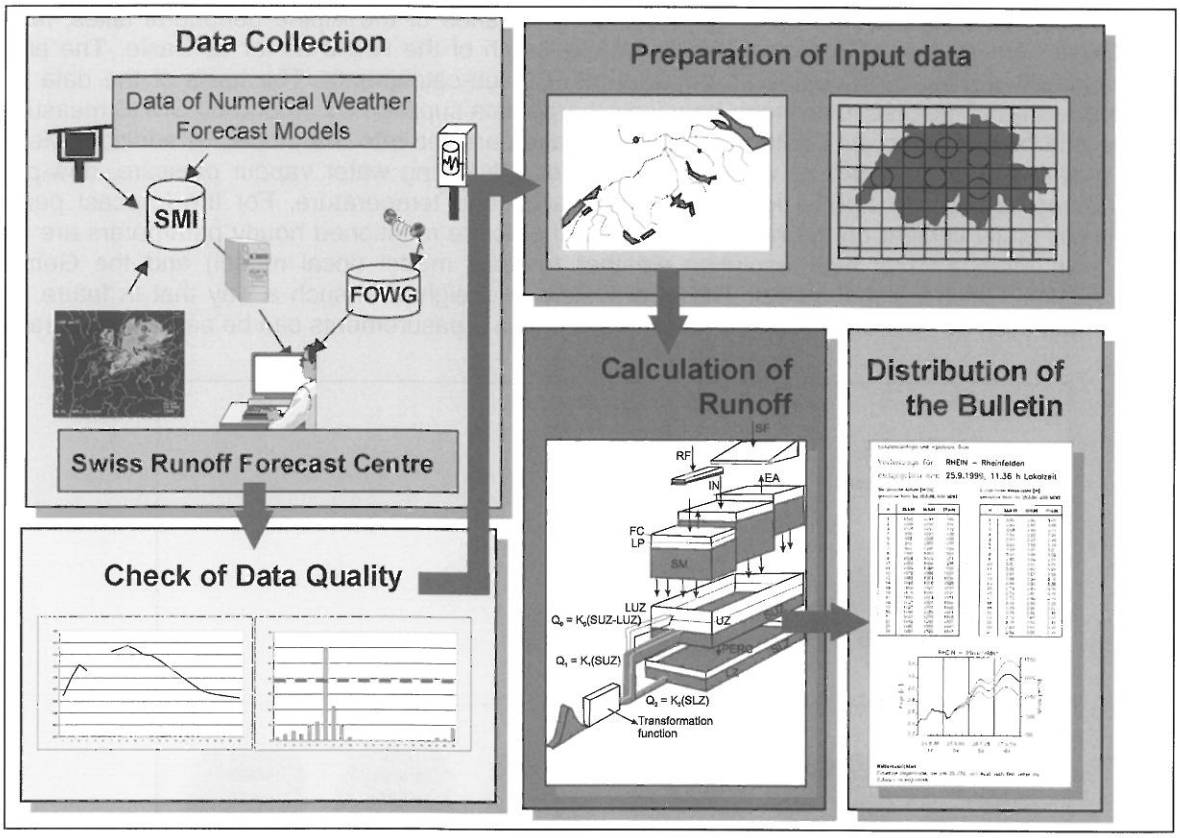

Figure 2-2: Operational data processing.

Figure 2-2 shows the individual steps needed to produce a forecast, from entering the data to preparing the forecast bulletin. Since automatically measured basic data is transmitted to the model electronically it is necessary to check the data for missing or inappropriate information. Furthermore, the data fed in must lie within statistically determined limits which are either more or less stringent (less stringent: highest and lowest value ever measured; more stringent: that +/- 20%). Dubious or missing figures must be corrected or completed by the user.
The current model takes into account the control of water levels in lakes only on a rudimentary basis. Such a method of regulation is only automatically incorporated for calculating discharge from Lake Biel. Since the area covered by the forecasting system in the other regions starts below the lakes, the system uses estimates of lake discharge rates, entered by hand, for the period covered by the forecast.

2.4 Development of the third generation forecasting system

Various floods which occurred in the 1990s along the whole length of the River Rhine showed that there is room for improvement in international collaboration with regard to forecasting during flood situations. The International Commission for Protection of the Rhine (ICPR-IKSR) drew up clear political aims as part of its Action Plan of Flood Defence (IKSR, 1998). These include among other things the improvement of forecast models, and urged that the periods covered by forecasts be extended. In order to achieve this aim the relevant institutions in the Netherlands (Institute for Inland Water Management and Waste Water Treatment, RIZA), Germany (German Federal Institute of Hydrology, BfG) and Switzerland (FOWG) decided to carry out the necessary studies in collaboration and to work

together to develop forecasting systems. Cooperation between these bodies has been facilitated by the fact that they are all using the HBV hydrological model. Accordingly, international collaboration on developing the flood early-warning system for the Rhine (FEWS-Rhine) was started in winter 1999, involving the FOWG and the RIZA as mandators and Delft Hydraulics (WL) and the Swedish Meteorological and Hydrological Institute (SMHI) as mandatees. Under the terms of the mandate WL is devising the forecasting tool – the FEWS system – and the SMHI is adapting the HBV-96 system to the current requirements of customers.
The new FEWS-Rhine Switzerland model has the following features. The area covered by the forecasting system includes the entire River Rhine catchment within Swiss territory, i.e. the present system has been extended to include in the south the tributaries of the Alpine peripheral lakes, in the north those from southern Germany, and the whole length of the Rhine as far as Basle. The entire area has been divided as regularly as possible into 60 sub-catchments. The basis of the data corresponds to that of the present system: hourly discharge data supplied by around 60 SNHS measuring stations and hourly water level data from some 10 lakes are fed into the model. In addition, MeteoSwiss provides measurements of wind-speed and, for calculating water vapour pressure, dew-point temperatures, apart from hourly figures for precipitation and temperature. For the forecast period, which is still until midnight on the next day but one, the above mentioned hourly parameters are also fed in from MeteoSwiss's high-resolution weather forecast model (local model) and the German Meteorological Office's global model. The new system is designed in such a way that in future new data formats such as data obtained from radar precipitation measurements can be easily incorporated.

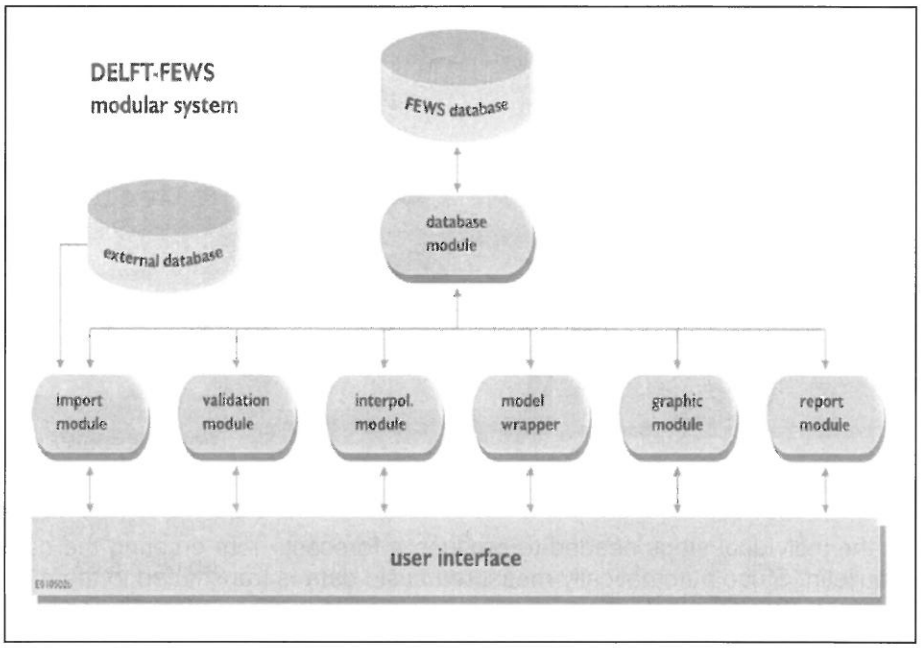

Figure 2-3: Modular structure of the FEWS system.

The many different types of data (both fed in and produced by the model) and the large volume of data demand a flexible, open and well structured data management system (WL | Delft Hydraulics, 2001). - Therefore, the FEWS database and the data management system are divided into individual modules (Figure 2-3) and are accessed via a deliberately simple interface which is invisible to the user. Furthermore, the user is guided through the process of drawing up a forecast by means of clearly defined steps and, in addition, at every stage of the process it is possible to obtain a graphic or tabular overview of the data, through an interactive map, or a list of stations or parameters (Figure 2-4).
Checking the data is also important in the FEWS system. It therefore includes a powerful editing tool for visualising the data, for automatic linear or spatial interpolation of missing measurements, for manual input or modifications and for checking extreme or unlikely figures. The interpolation method is adopted from the current system. The hydrological model is based on the HBV-96 (Holst et al., 1996). Wherein the data interval is modified (daily to hourly time step) as well as the snow routine (using the Anderson-Braun method, see Section 3.2). An ingenious updating procedure (see Section 3.5) guarantees that the forecast values obtained follow on from the last measurements with no gaps or jumps.
Thanks to the extension of the area covered by the forecasts to encompass drainage systems above the Alpine peripheral lakes, Alpine areas that are strongly influenced by human factors are included in the

model. The future model will focus mean daily runoff from these areas into the Alpine peripheral lakes, changes in their water level and runoff from these lakes. Most of them have controlled discharge.
The hydrological model will be calibrated with data for the period 1989-1999. The FEWS-Rhine Switzerland system will go into the testing stage during 2002.

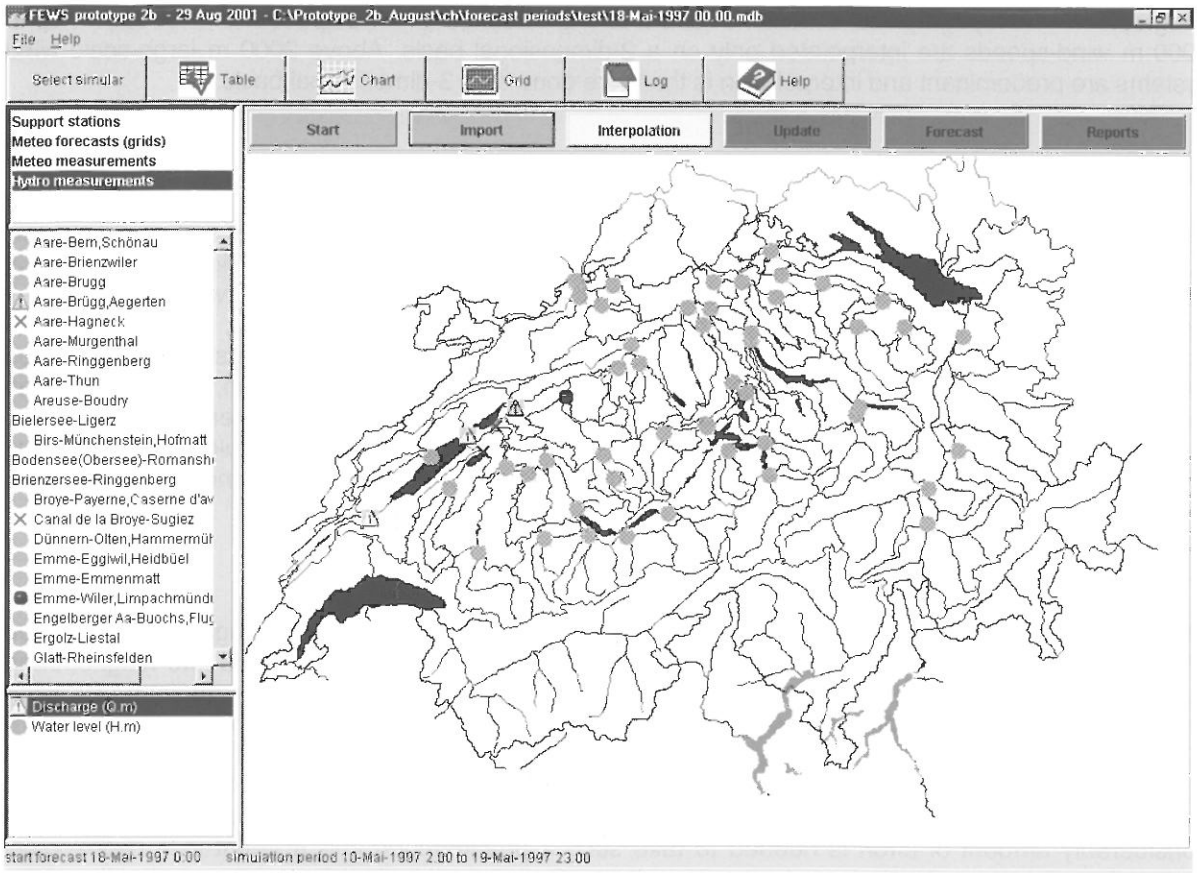

Figure 2-4: FEWS user interface.

Thanks to the development of this system, the entire extent and complexity of the catchment of the River Rhine within Swiss territory will be taken into account. Its natural Alpine aspect and its man-made characteristics are thus brought together in one system. If satisfactory results are obtained a hydrological model and a comprehensive forecasting tool will be available in the future which can be adapted for application to other Swiss Alpine river systems with relatively little effort.

3 SPECIAL FEATURES OF THE FEWS-RHINE SWITZERLAND HYDROLOGICAL RUNOFF PREDICTION MODEL

3.1 Interpolation of meteorological data and numerical weather forecasting

A rainfall runoff model is based on catchments and therefore on the computation of regional data. This means that meteorological data, normally point measurements, and data obtained using the numerical weather forecast model must be interpolated to obtain regional values according to the way the area is divided up. For this purpose the SNHS uses the "optimum interpolation" or Kriging method (Jensen, 1989). Assuming that precipitation varies only in the horizontal and not the vertical plane, precipitation figures are interpolated for the catchments according to the distance between the stations (measurements) and the points (weather forecasting model) in a 2-dimensional plane. It remains to be seen whether this approach can provide sufficiently accurate results for Alpine areas too, since it is difficult to differentiate with regard to rainfall distribution because of the unequal distribution of rainfall measurement stations. Therefore interpolation of measured rainfall will include an error which will be corrected in an appropriate way in the model.
As far as temperature is concerned, the usual approach of assuming a linear decrease in temperature of 0.6°C per 100 m increase in altitude will not be applied. Instead a 3-dimensional interpolation

method will be used, whereby the temperature at each altitude is interpolated taking into account the weighted distance between the stations. With this interpolation method temperature inversion, which often occurs in Switzerland in winter owing to persistent low cloud, can also be reproduced.
The same method is also used for interpolating water vapour pressure.
Two different approaches are used with regard to wind-speed. Below 2000 m it is assumed that the local geographical and topographical conditions have a strong influence on wind-speed. For this reason, up to 2000 m wind-speeds are interpolated only on a 2-dimensional basis. Above 2000 m large-scale wind systems are predominant and interpolation is therefore done on a 3-dimensional basis.

3.2 The snow-melt model

It has been seen (Braun, 1985) that the frequently used degree-day method is not sufficient for computing the rapid and complete melting of the snow cover, caused by weather conditions, in the Central Lowlands. Such melting occurs under the influence of a warm front, combined with widespread rainfall and strong winds. The turbulent energy exchange created by the wind is, however, not taken into account in the degree-day method. In order to include it the SNHS uses the Anderson-Braun method which combines an energy balance index and a temperature index method (Braun, 1985). When the weather is fine and dry the degree-day method is applied and when it is wet the energy-balance method is preferred. In the latter snow-melt is made up of the sum of radiant heat, sensible heat, latent heat and the warmth of the rain. Wind plays a decisive role in calculating both sensible and latent heat.

3.3 The influence of hydroelectric power stations

The natural discharge pattern has been disrupted in many Alpine river valleys through the construction of reservoirs, pumped storage stations and water diversion installations out of and into neighbouring river systems, as well as the associated harnessing of water to produce electricity. Instead of a clear difference between low discharge in winter and high discharge in summer, today the regime is more or less balanced all year round. This is aggravated on a daily basis by extreme short-term differences in discharge which result from the normal operation of reservoir installations. Since the daily running of these hydroelectric power stations is subject to the dictates of supply and demand of electricity, a considerably amount of effort is needed to take such a phenomenon into account in a hydrological forecasting system, and even then it cannot be done adequately. It is therefore not a priority aim of the FEWS-Rhine system to produce runoff forecasts on an hourly time step for the tributaries to the Alpine peripheral lakes. It is far more important to focus on the mean daily volume of water flowing into the lakes in order to obtain an adequate forecast of water levels and discharge from lakes.

3.4 Regulating discharge from lakes

Apart from Lake Constance and the Walensee, where no weirs have been installed, precisely defined regulatory schemes govern water levels in Swiss lakes. According to these regulatory schemes the accepted or required discharge at any time, depending on the season and the actual water level, is clearly defined. These schemes are in fact a political compromise between the interests of the various bodies representing flood protection, environmental protection, the hydroelectric power industry and shipping. Corresponding regulations pertaining to all the major, regulated Alpine peripheral lakes are taken into account in the FEWS-Rhine Switzerland system. While changes in the water level of individual lakes are computed on the basis of inflow, the model is capable, thanks to the implementation of the regulatory schemes, of calculating the acceptable discharge for each lake. In the case of important and extreme pan-regional flood levels the authorities can allow temporary breaches of these regulations. The forecasting system is so flexible that the user can interactively enter temporary, extraordinary regulations which the model will apply over a certain period of time.

3.5 Updating

Since a model cannot reflect the total complexity of the real situation it is not possible to calculate time series using the model which are congruent to the measurement series. It is important in an operational forecasting model, however, that the time series of calculated forecast values fit in perfectly with the

measurement series. In the FEWS-Rhine system this reconciliation of model data and measured data is achieved by adapting the initial values and using an autoregressive procedure. If the values obtained using the model diverge too strongly from the real measured values the first step is to vary the initial figures for precipitation and temperature according to strict rules. The remaining difference between the model and the real situation is then eliminated step-by-step using the autoregressive process.

4 CONCLUSION

The experience of the Swiss forecasting service since the 1980s shows that accurate hydrological forecasting is very much dependent on meteorological precipitation predictions. Owing to the small scale of the catchments, their topography and the rapid reaction time of rivers and lakes it is essential that precipitation can be forecasted as accurately as possible from a geographical and temporal point of view as well as in its intensity. Thanks to close cooperation between the SNHS and MeteoSwiss the hydrological models are regularly adapted to the latest developments in numerical weather forecast models.
The important local differences in precipitation in the Alpine regions are difficult to take account of. In particular, rain gauges which are distributed very irregularly provide an inadequate picture of regional precipitation. The SNHS is therefore placing great hopes in research into precipitation measurement by radar. If this method proves satisfactory in the Alpine regions it will be possible in the future to feed figures for high-resolution measured local precipitation into the models, as well as the high-resolution numerical forecast data for the period covered by the forecast. Joint projects on this approach involving hydrology and meteorology have already started (COST 717). This would open the way to integrating radar nowcasting into the models. These short-term rainfall predictions are based on radar measurements made over the previous few hours and are a temporal extrapolation of the rainfall belts identified and their direction of movement. The coupling of hydrological models with radar nowcasting would have the advantage of making it possible to integrate the intensity and direction of movement of rapidly changing or newly forming rainfall belts into hydrological forecasts immediately. This would provide a means of improving hydrological forecasts, especially in small catchments within the Alpine area.
Over the past few years, awareness of the existence of hydrological forecasting has increased considerably among the general population and the authorities. At the same time the need for accurate hydrological forecasts for the Alpine regions has grown, owing to recent flood disasters. It must therefore be expected that the demand for forecast systems for the two main catchments in southern Switzerland will grow. For this reason it is all the more important to develop today a comprehensive and flexible hydrological forecasting system with a modular structure which can later be easily adapted to other geographical areas. This is the SNHS's aim in developing the FEWS-Rhine system. On the one hand it should be user-friendly and meet the demands of operational use, and on the other it should reflect the most important hydrological elements of the Alpine region. Other aspects are the extension of the area covered by the forecast to include the entire Rhine catchment in Swiss territory, calculating local precipitation using the optimum interpolation method, calculating increase and decrease in snow cover using the Anderson-Braun method, and taking into account the regulations concerning water levels in the Alpine peripheral lakes plus the management of reservoirs in Alpine valleys.

5 REFERENCES

Bergström, S. (1976): Development and Application of a Conceptual Runoff Model for Scandinavian Catchments. Deptartment of Water Resources Engineering, Lund Institute of Technology, University of Lund, Bulletin Series A No.52, 134 p.

Braun, L. (1985): Simulation of snowmelt-runoff in lowland and lower Alpine regions of Switzerland. Zürcher Geographische Schriften no. 21, Zurich.

COST - European Cooperation in the field of Scientific and Technical Research: Use of radar observation in hydrological and NWP models. Action No. 717.

IKSR (1998): Aktionsplan Hochwasser. Internationale Kommission zum Schutze des Rheins, Koblenz.

Jensen, H. (1989): Räumliche Interpolation der Stundenwerte von Niederschlag, Temperatur und Schneehöhe. Zürcher Geographische Schriften no. 35, Zurich.

Holst, B. and Lindström, G. (1996): Development and verification of the distributed HBV-96 inflow forecasting model. Published at the Modelling, Testing & Monitoring for Hydro Powerplants Conference, July 1996, Lausanne, Switzerland.

Lang, H. et al. (1987): Short-range runoff forecasting for the River Rhine at Rheinfelden: experiences and present problems. Hydrological Sciences Journal 32, 3, 9.

Lindström, G. et al. (1997): Development and test of the distributed HBV-96 hydrological model. In: Journal of Hydrology 201, p 272-288, Elsevier.

Schädler, B. (1993): Operationelle Abflussvorhersage für Rhein-Rheinfelden - Grenzen und Möglichkeiten. In: D. Grebner (ed): Aktuelle Aspekte in der Hydrologie, Zürcher Geographische Schriften, Heft 53, pp. 213-222. Geographisches Institut ETH Zürich.

WL | Delft Hydraulics, (2001): Delft FEWS: Flood Early Warning System. Brochure, MH Delft.

PARSIMONIOUS AND SPATIALLY DISTRIBUTED MODELLING OF RUNOFF GENERATION IN MESOSCALE PREALPINE AND ALPINE CATCHMENTS

Richard Kuntner, Paolo Burlando

Institute of Hydromechanics and Water Resources Management, ETH Zurich, ETH Hönggerberg, CH8093 Zurich, Switzerland, paolo.burlando@ethz.ch

SUMMARY

Flood hydrology is still largely based on the use of empirical formulas and simple lumped models. As the accuracy of these methods has been often shown to be limited, the need for better performing modelling techniques arises. Process-oriented spatially distributed rainfall-runoff (R-R) models have recently become popular to overcome such limitations. However the structure and operation of these models is often affected by data availability and large computational requirements. Distributed conceptual models of flood runoff generation represent thus a good alternative, as they can rely on thematic maps, which are increasingly available. In this light, the present contribution analyses a world-wide diffused conceptual runoff generation approach, the *S*oil *C*onservation *S*ervice - *C*urve *N*umber (*SCS-CN*) method, evaluating its suitability in relation to the prealpine and alpine geographical environments. Some results of an on-going research work to achieve a modified version of the method are accordingly illustrated. Modifications are discussed and introduced on the basis of a qualitative and trial and error approach, which focuses at this stage on the CN assignment tables. A few validation tests carried out for a small mesoscale catchment by means of a distributed event-based model provided a preliminary feedback to assess the need for further refinements or additional and more substantial modifications.

Keywords: flood runoff, SCS-CN, distributed modelling, flood simulation

1 INTRODUCTION

The prediction of and prevention from flood hazard has been for long time a major task in both physical and engineering sciences. The demand for modelling techniques that are able to provide reliable predictions is still increasing because of the large social and economic impacts produced by flood events. Because of the erratic behavoiur of flash flood processes and of the lack of extended data with fine resolution in space and time, flashy streams in small and mesoscale basins are highly sensitive to the present methodological limitations and uncertainties in risk assessment. In the alpine regions of Europe flash-flood prone areas have experienced in the last decade more severe floods than those predicted on the basis of historical information, even based on long-term data series. Similarly, it happened that floods that were estimated as centennial occurred more frequently than expected.
Although there is an increased feeling that this may be due to man-induced climate changes, good arguments suggest as possible reason the large uncertainties, which characterise the methodologies used in practice to estimate peak flows for given return periods. On the one hand it is necessary to cope with the high complexity of processes, on the other hand sophisticated methodologies that account for such complexity often result into computationally heavy model applications, which frequently do not meet the need of operational hydrology. For this reason quick and straight procedures are generally preferred by practitionners. A considerable number of empirical formulas, dating back to the beginning of last century are still in use despite they have been worked out on the basis of limited data and knowledge. The traditional alternative to such formulas is represented by direct statistical estimates and statistical regionalisation. These techniques provide estimates characterised by a frequency information, but can account for process description only to a very limited extent. Methods based on rainfall-runoff (R-R) models are conversely the most appropriate technique to obtain realistic flood estimates, as they can account explicitely for climatic variability, catchment characteristics and process dynamics, both in the case of physically based approaches and in that of conceptual models. Thus, simulation techniques making use of R-R models are recognised to be the inevitable solution to accurate flood estimates (e.g. Burlando et al., 2001). A number of questions, however, remain open in this respect, thus suggesting that specific studies should address both the improvement of knowledge of the river basin system, and the search for rainfall-runoff modelling approaches that compromise between process representation and workable modelling applications.

Several methodological progresses have characterised the recent years (e.g., Rosso, 2001), but resistance to their introduction in operational hydrology is often encountered. A major obstacle is frequently represented by the limited resources allocated to operational hydrological studies as compared with the requirements imposed by advanced methods. The structure and operation of process-oriented spatially distributed rainfall-runoff models is indeed characterised by large data and computational requirements. Conceptually based rainfall-runoff models of flood runoff generation represent thus a workable alternative, as they are generally less data demanding or can rely on data available, e.g., from digital thematic maps, which are increasingly available. In addition their formulation represents a good compromise between process representativeness and operational requirements.
When modelling the rainfall-runoff transformation with the aim of flood estimation two questions are recognised to be key issues. These are respectively the space-time monitoring and modelling of storm rainfall and the correct representation of runoff generating mechanisms. With regard to the second aspect it can be recognised that several methods and models have been proposed throughout years of research to describe the infiltration process and to estimate the surface runoff. Nevertheless, no common agreement has been so far reached, about the selection of suitable models for different specific conditions. On the one hand many studies produced by the scientific community contributed to keep alive the debate, without being able to produce a consensus around a specific methodology. On the other hand, investigations at the elementary scale, looking for key factors that dominate the process of runoff generation (e.g. Markart, Kohl, 1995; Scherrer, 1997; Weiler, 2001), provided along the years a considerable amount of valuable knowledge, but did not offer a decisive argument in favour of a class of modelling approaches, and an operational approach worked out from such experiments is still lacking. It is therefore difficult to discriminate among flood runoff generation models, based on degree of resemblance of the physical processes as compared to their ability to reproduce the observed pattern of flood runoff generation.
An alternative route has been, and still is, the use of conceptual models, which can provide a good compromise between complexity of the representation and flexibility of use, by introducing a conceptualised representation of natural processes. In this respect the *S*oil *C*onservation *S*ervice - *C*urve *N*umber (*SCS-CN*) method proposed by the United States Department of Agriculture in the 70s (SCS-CN, 1972) has gained a world-wide diffusion due its engineering oriented formulation and easy parameterisation. As the method was developed with reference to North America agricultural catchments, a transfer to areas characterised by other climatic and geographic conditions must be carefully handled. Also, the parameterisation scheme is somewhat weak for natural basins. Accordingly, a straightforward application to catchments of any nature and climate requires further investigation. This is especially true for alpine and prealpine basins of the European Alps. Because of the suitability of the SCS-CN for distributed modelling and its capability to account for land use changes, the present contribution intends to report about an on-going research, which aims at improving the capability of the method to perform adequately in mountainous and perimountainous regions to model correctly flood runoff generation.
In the following a preliminary investigation to modify the SCS-CN method is introduced by means of a methodological framework that combines results from plot scale experiments available in the literature with upscaled applications at the scale of raster-based distributed rainfall-runoff models. An extensive digital database, covering most of the required information for parameterisation, has been used for the purpose. Some validation tests have been finally carried out for a few meso-scale catchments and subcatchments. The analysis of flood events at different scales has provided a preliminary feedback to assess the need for further refinements or additional and more substantial modifications.

2 MODELS OF RUNOFF GENERATION

Flood estimation by means of Rainfall-Runoff models requires to assemble a mathematical model that reproduce the response of the basin to rainfall (the input) by modelling the transformation of the input into runoff (the output) as function of the processes that take place within the basin. These are essentially the interception, the evaporation and evapotranspiration, the runoff generation (often denoted as infiltration) and its propagation over the hillslopes and throughout the river network. It is frequently assumed for mesoscale basins that interception and evaporation/evapotranspiration play a minor role during the evolution of the event, due the limited effectiveness of intercepted rainfall as compared to storm rainfall volumes, and to longer characteristic time scales of evapotranspiration processes. A key role with respect to the generation of flood runoff is therefore played by the infiltration module, which must be able to discriminate between generation of overland flow and infiltrating volumes, also reproducing the correct time evolution of the process.

For this reason, the scientific community developped along many years a large number of models, the suitability of which is often controversial. This stems mainly from the fact that overland flow can occur essentially as generated by two distinct mechanisms. The first, also known as *hortonian* (Horton, 1933), is observed when precipitation intensity exceeds the infiltration capacity of the soil (infiltration excess or saturated overland flow); the second, also denoted as *dunnian* (Dunne, 1978), is observed when the first soil layers are saturated due to the rising of the water table. Soil infiltration capacity can be limited by its texture, moisture content and structure, or by the fact that the soil is already saturated. Other mechanisms can be also observed due to some special conditions, such as in the case of return flows, which are generated by infiltrated water that returns to the soil surface when hillslopes are characterised by a close to the surface impermeable layer inhibiting the percolation (e.g., Faeh, 1997).
Recent investigations carried out by means of field experiments at small scales (Scherrer, 1997) tried to focus of exchange mechanisms between different soil structures, e.g. between the soil matrix and the macropores, highlighting how in some cases these can be the key for a correct modelling (Faeh, 1997). Along this line other contributions can be found in the literature (see, e.g., Beven, Clarke, 1985; Germann, 1990; Bruggeman, Mostaghimi, 1991; Zuidema, 1995). Major problems with these modelling approaches are yet the small scale of the analysis, the detailed survey of soil properties and the computational effort, which confine their use mainly to research purposes.
The formulation of a methodology, which complies with both the experimental evidence at the plot scale and the need for operational models for flood estimation at the basin scale, requires, however, the formulation of compromise solutions. These are offered by the many models that have been proposed in the literature, and that allow to estimate surface runoff at bigger scales which are compatible with traditional hydrologic analysis. A full set of models are in this respect available, ranging from the sophisticated and physically based Richards' equation (Richards, 1931), to its solution under simplified hypotheses (Philip, 1957); from the Horton equation (Horton, 1933), to other conceptual models, thereby including the Soil Conservation Service – Curve Number method (SCS, 1972). The use of these methods is nevertheless not always straightforward. For instance, conceptual models are often preferred to physically oriented models because of the high requirements of the latter in terms of parameterisation. On the other hand, conceptual models suffer of bad reputation due to their limited capability to describe thoroughly the complex dynamic of infiltration processes.
An efficient engineering oriented flood runoff generation scheme should obey a few requisites that are of importance in operational hydrological modelling. These are essentially the robustness and accuracy in reproducing the observed runoff generation pattern, the suitability for use in distributed models, an parameterisation scheme that can make use of catchment characteristics that are easily available, such as digital thematic maps, and last but not least an explicit land-use parameterisation, thus allowing its use in studies related to the effects of land-use changes on river flood regimes
The SCS-CN method looks interesting with respect to the objective of the present study, especially because of the large number of applications that are documented in the scientific and technical literature, and because of its parameterisation scheme, which can rely on data normally available. Many uncertainties arise indeed when the model must be parametrised for alpine and prealpine catchments, due to some peculiarities of the runoff generating mechanisms and to the poor literature relevant to parametrisation of these models for such type of basins. The present study investigates therefore the possibility to fill this gap, searching for a modified version of the SCS-CN method, which is suitable for the (swiss) alpine and prealpine environment, thus providing a runoff generation model component suitable for use with flood estimation R-R techniques used for design purposes in the hydrologic engineering practice.

2.1 The SCS-CN Method

In the present section a brief survey of the basic concept of the SCS-CN method, referring however the reader to specialised literature for a more comprehensive description (SCS, 1972; 1986).
The SCS-CN infiltration model was developed on the basis of a number of experiments carried out mainly on soils of North America. Its use has become nevertheless very popular worldwide, because of its straightforward and efficient application, mainly due to its monoparametric formulation and to the parametrisation based on a two-entry table that describes the Hydrologic Soil Type (henceforth referred to as HST, see Table 2-1) and the land use, as hereafetr briefly recalled.

The method is based on the assumption that the relation of effective soil retention, F, to the maximum soil potential retention, S, equals the relation of the actual accumulated surface runoff, Q, to the actual accumulated rainfall, P, subtracted of the initial losses due to interception and surface detention (initial abstraction), I_a. The method finally yields

$$(1) \qquad Q = \frac{(P - I_a)^2}{(P - I_a + S)} \quad \text{for} \quad P > I_a \;, \qquad Q = 0 \quad \text{for} \quad P \le I_a$$

where

$$(2) \qquad S = S_0\left(\frac{100}{CN} - 1\right),\ S_0 = 254, \text{ if } S \text{ is expressed in mm.}$$

and

$$(3) \qquad I_a = c \cdot S \;,$$

being c a coefficient that ranges between 0 and 1 (generally c≤*0.2), depending on the amount of sto*rage, which can be characterised as initial abstraction. The two unknowns of (1) are estimated by parametrising S by means of Curve Numbers (CN) ranging from 0 to 100, meaning 0 a theoretically unlimited storage capacity ($S = \infty$, in (2) for CN=0), and 100 a fully impermeable or totally saturated soil ($S = 0$, in (2) for CN = 100). The CN parameter is estimated from a two-entry table (see, for further details, *SCS*, 1972; 1986; Maidment, 1992) which provides the CN value on the basis of the geological/pedological features of the soil, which define the HST, and on the basis of the land cover and use. The value of CN depends additionally on the initial state of the system, i.e. the degree of saturation of the soil, expressed by the *Antecedent Moisture Condition* (henceforth AMC) index. This allows to convert the CN value corresponding to standard conditions (i.e. CN_{II}, corresponding to AMC class II), into higher values (CN_{III}), when the soil moisture content at the beginning of the storm event is estimated high from the index, and into smaller values (CN_I), when the soil moisture content is estimated low. The relationships which link the value of standard curve numbers, CN_{II}, to CNs corresponding to other AMC classes have been also derived from SCS experiment sets and are written as

$$(4) \qquad CN_I = \frac{CN_{II}}{2.3 - 0.013CN_{II}} \;, \text{ if } P_{5,ds}<12.7 \text{ mm or } P_{5,gs}<35.6 \text{ mm}$$

$$(5) \qquad CN_{III} = \frac{CN_{II}}{0.43 + 0.0057CN_{II}} \;, \text{ if } P_{5,ds}\ge 27.9 \text{ mm or } P_{5,gs}\ge 53.3 \text{ mm}$$

being $P_{5,ds}$ and $P_{5,gs}$ respectively the cumulative rainfall in the 5 days preceding the event in the dormant season and in the growing season.

Table 2-1: Hydrologic Soil Types according to the SCS method (shortened from SCS, 1986).

Hydrologic Soil Type	Description
A	These soils have low runoff potential and high infiltration rates even when thoroughly wetted (transmission rate greater than 0.76 cm/h).
B	These soils have moderate infiltration rates (silt loam and loam, transmission rate between 0.38 and 0.76 cm/h).
C	These soils have low infiltration rates (sandy clay loam, transmission rate between 0.13 and 0.38 cm/h).
D	These soils have high runoff potential. (clay loam, silty clay loam, sandy clay, silty clay, and clay, transmission rate between 0.0 and 0.13 cm/h).

3 METHODOLOGICAL FRAMEWORK

The methodology proposed in this study to assess the suitability of the SCS-CN method for alpine and prealpine regions aims at understanding three different aspects, which are mainly related to the effects of the considerable heterogeneities that are present in such regions and that may depend on the scale of observation and model application. Accordingly, three different steps (summarised in the flowchart reported in Figure 3-1), are proposed. These are:

- the comparison of the SCS-CN method data requirements with data available nationwide for Swiss alpine and prealpine environment, and parameterisation of its standard formulation (SCS, 1972; 1986) based on geological, pedological and land use characteristics of Swiss regions, especially alpine and prealpine;
- testing of the SCS-CN method with respect to literature data of plot scale experiments carried out in alpine and prealpine regions, with the purpose of validating the standard formulation of the method at the "elementary" scale, thus highlighting major limitations that must be accounted for to produce a revised and improved formulation;
- development of a revised formulation of the SCS-CN method, which is able to match runoff generation mechanisms across a number of scales, ranging from the plot to the small and meso- catchment scale.

The latter point should offer an evaluation of how scaling up the model by aggregation from the plot scale to larger scales influences the capability of the method to capture observed flood runoffs, eventually providing the necessary feedback to iteratively improve the modified formulation. This step of the analysis requires of course the use of a specific R-R modelling scheme that is able to describe the behaviour across a number of scales, and that is therefore, by necessity, distributed in space. A distributed R-R model based on the digital database of Switzerland for topographic and thematic maps is thus used to explore comprehensively the ability of the model to capture all of the identified SCS-CN soil categories. On this basis a preliminary evaluation of the suitability of the SCS-CN method for use in standard flood estimation methods is then formulated.

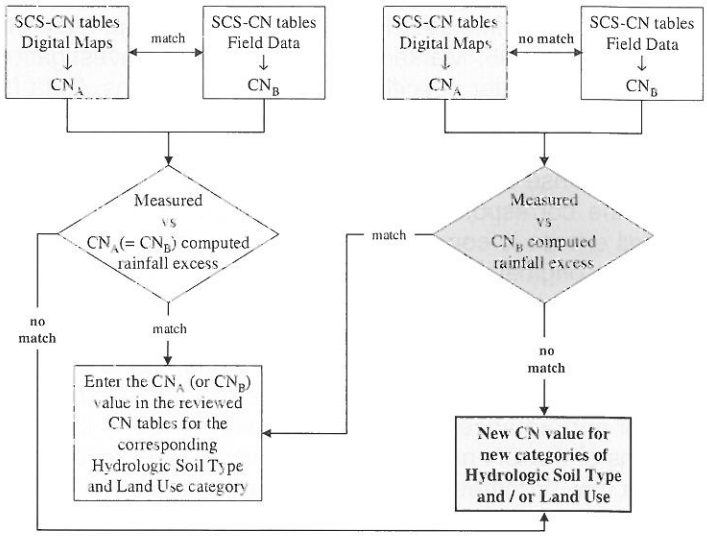

Figure 3-1: Summary outline of the review process for the SCS-CN methodology in alpine and prealpine regions .

3.1 SCS-CN Model Parametrisation Data Requirements

The first effort that must be therefore undertaken is concerned with the analysis of how the characteristics described in the database of Swiss soil properties and land use match with the two-entry table which defines the CN number for a given land use and a given soil hydrologic type. Keeping in mind the purpose of the overall project, that is the evaluation of nationwide suitability of flood estimation techniques, the digital database "GEOSTAT" is taken as a reference categorisation of Swiss soils and land uses. This is a geographical database operated by the Federal Office of Statistics (GEOSTAT, 1997), covering the whole area of Switzerland and containing – all in digital form, mainly raster based – data about land use and soil type in the form of

- land use raster maps with a grid size of 100×100 m, derived on the principle of "prevailing use" in the element (*Arealstatistik 72*, henceforth referred to as AK72), which includes 12 landuse categories derived from topographic maps;
- soil characteristics raster maps (*Bodeneignungskarte*, henceforth referred to as BEK, based on the 1:200.000 soil map of Switzerland), also characterised by a grid size of 100×100 m, containing 144 soil classification units, derived from the combination of typical landscape units and soil properties;
- a simplified geotechnical raster map (*Vereinfachte Geotechnische Karte*, henceforth referred to as VGK), which is based on the 1:200'000 simplified geotechnical map of Switzerland and contains 30 classes characterising the first geological layer under the soil.

Matching the SCS soil classification with the one provided by the GEOSTAT database requires some adjustments as detailed in the following sections. Essentially the four classes of hydrologic soil types defined by SCS (SCS, 1972; 1986) are preliminary extended by explicitely accounting for in between classes – as already foreseen by the original version of the CN method – in order to better compare the CN method with the more extended information available from GEOSTAT. A number of additional information included in GEOSTAT also provide the basis for a better description that could lead to a refined parametrisation for soil classes typical of the alpine and prealpine environment. In this light the soil layer thickness and the permeability offer a way to described in the soil type maps of GEOSTAT will be tentatively to build an enlarged classification of HSTs. The influence of slope angle and the saturated hydraulic conductivity reported in the BEK can be use in a similar way. The geotechnical map (VGK) is of help in properly identifying and classifying shallow soils, which are strongly influenced by the first underlying geologic layer.

3.2 Test of the CN Model at the Plot Scale

An extensive field campaign recently carried out at the Laboratory of Hydraulics, Hydrology and Glaciology of ETH Zurich investigated the runoff generating mechanisms over homogeneous experimental plots by means of a number of storm rainfall sprinkler experiments carried out throughout different soil and land use conditions in Switzerland (Scherrer, 1997). Similar experiments were carried out also in Austria (Markart and Kohl, 1995; Markart et al., 1996). Such investigations provide a valuable basis for testing infiltration models under specific experiment conditions. Data from the Swiss experiments published in the literature – and made available by courtesy of the Author (Scherrer, 1997) – have been the basis for a preliminary evaluation of the suitability of the CN method to reproduce alpine and prealpine runoff response characteristics. After proving that the information about the experimental site matches with the corresponding information reported in the GEOSTAT database, the computed cumulative rainfall excess is compared with the cumulative excess runoff observed at each considered plot, based on the original SCS classification (SCS, 1986). A visual interpretation is first carried out to identify cases that are correctly reproduced by the unmodified CN parameterisation, from cases that require a modified parameterisation to match the observed pattern. Cases are also observed, which are not captured at all by original method setup. Table 3-1 summarises qualitatively the overall performance, whereas Figure 3-2 illustrates three exemplary cases.
The cases that showed poor performances have not been addressed in this preliminary study by discussing theoretical limitations of the CN method, but they were rather investigated aiming at a further calibration. In this respect, a new parameterisation or a new land use and hydrologic soil type characterisation have been searched, as a first step, on the basis of the digital thematic maps available on a nationwide scale. Whenever the original parametrisation failed to capture the observed patterns of the surface runoff, a tuning of the CN value and of the I_a coefficient has been carried out, and the new value of CN has been used as initial value to correct the standard SCS classification for the corresponding LU and HST category or to define the parameterisation of the new land use categorisation.

3.3 Modification of the SCS-CN Assignment Table

In order to achieve a modified CN parameter table that can be used for testing at basin scale, the initial modifications stemming from calibration are complemented by additional physically oriented considerations based on soil properties and geotechnical and geological information, which are retrieved, in the specific case of Switzerland, respectively by the above mentioned BEK and VGK maps. Although they were not conceived for hydrologic purposes, these maps include information on soil characteristics and geological patterns that can be helpful in identifying the expected dominating runoff generation processes. In this respect soil depth and soil permeability are especially used in a

qualitative way to corroborate the modified CN parameterisation table, thus aiming at discriminating between soil covers that look similar but behave considerably different due to different soil properties. Accordingly, soils with high permeability and extreme thickness are considered to exihibit a high infiltration capacity and therefore fulfill the criteria of SCS hydrologic soil group A, whereas shallow soils with an extremely low permeability fulfill the criteria of hydrologic soil group D, thus having a low infiltration capacity. The other combinations of permeability and soil thickness are distributed in between those two extremes, as reported Table 3-2. If the soil is very shallow (i.e., all depth categories from < 10 cm to 30-60 cm), information on the first geological layer below the soil is primarily considered to assign the proper hydrologic soil group, and information on permeability of the shallow soil is used to refine this result and to achieve the final assignment of the hydrologic soil group. Table 3-3 shows the resulting values. This preliminary approach to categorisation as function of the geological structure should be improved, due to the high uncertainty that characterises some specific geologic structure, like, for instance, calcareous areas, which can be in turn highly permeable or nearly impermeable.

Table 3-1: Summary of SCS-CN model performance for controlled experimentscarried out by Scherrer (1997), based on the standard SCS-CN parameterisation. A light grey cell indicates a good performance (25.58%), a medium grey cell indicates a good performance after tuning (■37.21%) a black square cell indicates no fitting (■37.21%). Letters in the cells indicate the dominant runoff generation mechanism, namely: AH=absolute hortonian overland flow, DH= delayed hortonian o. f., TH= temporary hortonian o.f., SOF=saturation o.f., SSF=subsurface flow, DP=deep percolation.

SITE	EXPERIMENT						SITE CHARACTERISATION
	1	2	3	4	5	6	
Gotthardpass	AH						Podsol-Regosol / pasture / hydro-phobic vegetation dominates runoff
Sonvilier	AH	AH					Cambisol with high loam content / pasture / surface sealing
Willerzell Mulde	AH	AH	AH	AH			Gleysol / pasture / located in a sink
St. Imier	DP AH	DP AH					Cambisol / pasture / preferential flow path dominate runoff
Schnebelhorn	DH						Cambisol / pasture / wormholes dominate runoff
Bauma	DH						Cambisol / pasture / wormholes dominate runoff
Alpe San Gottardo	AH	AH	AH				Podsol-Cambisol / pasture / hydro-phobic vegetation dominates runoff
Bilten I	AH						Gleysol / forest / mouseholes
Bilten II	AH						Cambisol gleyic / forest / hindered infiltration
Ebersol	DP	DP	DP				Ranker-Cambisol / pasture / high permeability
Heitersberg	AH	AH	AH	AH			Cambisol with high loam content / pasture / hindered infiltration
Willerzell Hang	SSF	SSF	SSF	SSF	SSF		Cambisol with high sand content / pasture / high permeability
Hospental	DH	DH	DH	DH	DH	DH	Cambisol with high sand content / pasture / high permeability
Blauen	DH DP	DH DP					Rendzina / pasture / high permeability
Hittnau	DH						Regosol-Cambisol with high sand content / pasture /high permeability
Nenzlingen	DH	DH					Cambisol / pasture / macropores and fissures dominate runoff
Spreitenbach	SOF	SOF					Cambisol / forest / permeable soil
Therwil	DH	DH					Camibsol with high sand content / pasture / macropores

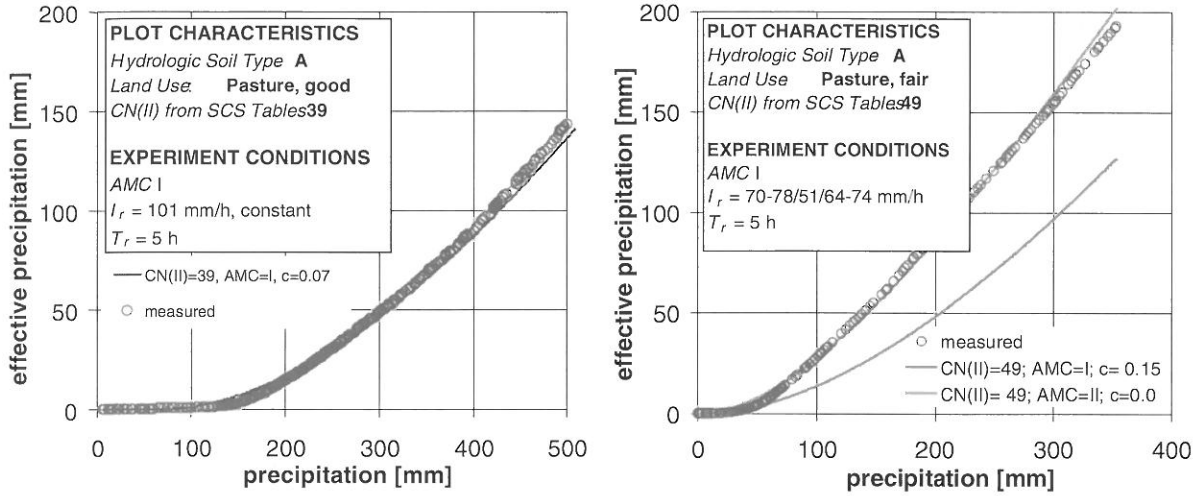

Figure 3-2: Example of SCS-CN model performance for three different experiments (data provided by courtesy of S. Scherrer, 1997).

Table 3-2: Equivalence criteria between SCS hydrologic soil groups and permeability and depth characteristics of the soil as observed from the GEOSTAT database.

	PERMEABILITY, K [cm/s]						
DEPTH [cm]	$K<10^{-6}$	$10^{-6}\leq K<10^{-5}$	$10^{-5}\leq K<10^{-4}$	$10^{-4}\leq K<10^{-3}$	$10^{-3}\leq K<10^{-2}$	$10^{-2}\leq K<10^{-1}$	$K\geq 10^{-1}$
>150	D	C-D	C	B-C	B	A	A
120-150	D	C-D	C	C	B-C	A-B	A
90 – 120	D	C-D	C	C	B-C	B	A-B
60 – 90	D	C-D	C-D	C-D	C	B-C	B
30 – 60	D	D	C-D	C-D	C	C	B-C
10 – 30	D	D	D	D	C-D	C-D	C
<10	D	D	D	D	D	D	C-D

Table 3-3: Hydrologic soil type for shallow soils (depth <60 cm) resulting from combined accounting of the VGK map and the influence of permeability.

PERMEABILITY, K [cm/s]	HYDROLOGIC SOIL GROUPS ASSIGNED FROM VGK						
unmodified hydrologic soil group	*A*	*AB*	*B*	*BC*	*C*	*CD*	*D*
$K\geq 10^{-1}$	A	A	AB	B	BC	C	CD
$10^{-2}\leq K<10^{-1}$	A	A	AB	B	BC	C	CD
$10^{-3}\leq K<10^{-2}$	B	B	B	BC	C	C	CD
$10^{-4}\leq K<10^{-3}$	BC	BC	BC	BC	C	C	CD
$10^{-5}\leq K<10^{-4}$	C	C	C	C	C	CD	D
$10^{-6}\leq K<10^{-5}$	CD	D	D	D	D	D	D
$K<10\text{-}6$	D	D	D	D	D	D	D
no soil	A	AB	B	BC	C	CD	D

In addition to refining the hydrologic soil type scheme, new land-use categories and the merge of others existing land-use groups have been considered, in order to account for some missing land-use groups in the original assignment table and to discriminate better among different hydrologic behaviours in the alpine and prealpine environments. The basis for introducing these new categories (shown in italic character in Table 3-4) is the information retrieved from thematic maps of GEOSTAT. The result of the above illustrated changes is finally reported in Table 3-4, where preliminary estimates of CN values are indicated for the adjusted classification scheme, accounting for qualitative considerations related to process dynamics and soil characteristics, thus reflecting the preliminary tuning to match the plot scale data.

Table 3-4: CN values for modified land use and hydrologic soil group classification. Shaded fields indicates modifications from the original SCS table. Figures in italic belong to a new soil group and to a new land use.

Class	CATEGORY	HYDROLOGIC SOIL GROUP							ORIGINAL SCS CATEGORY
		A	AB	B	BC	C	CD	D	
101	Snow and Ice	30	*30*	30	*30*	30	*30*	30	*No corresponding category*
102	Rocks	90	*90*	90	*90*	90	*90*	90	*No corresponding category*
103	Boulders	74	*79*	84	*86*	88	*89*	90	Streets and roads: mean of gravel and dirt
104	Swamps, Mulch and Peatlands	44	55	65	71	77	80	82	Open spaces etc: mean of good and fair condition
201	Rivers and Lakes	99	99	99	99	99	99	99	*No corresponding category*
401	Forest (dense)	30	*43*	55	*63*	70	*74*	77	Woods good condition
402	Forest (sparse), Shrubbery	36	*51*	65	*71*	76	*79*	82	Wood grass combination fair
403	Forest (sparse), Bushes	32	*45*	58	*60*	72	*76*	79	Wood grass combination good
602	Cereals and root crops (summer)	62	68	73	77	81	83	84	SCS CN ½ row crops + ½ small grain C and CR good
	Cereals and root crops (winter)	74	79	83	86	88	89	90	SCS CN crop residue cover good
603	Feed (s)	30	44	58	65	71	75	78	SCS-CN meadow
	Feed (w)	41	51	60	68	75	78	81	SCS-CN ¾ meadow + ¼ crop residue good
604	Cattle (summer)	49	59	69	74	79	82	84	SCS-CN pasture fair
	Cattle (winter)	49	59	69	74	79	82	84	SCS-CN pasture fair
605	Cattle and feed (s)	39	50	61	68	74	77	80	SCS-CN pasture good
	Cattle and feed (w)	44	52	59	66	72	76	79	SCS-CN pasture good - fair
606	Rotation (summer)	51	60	68	73	77	80	82	SCS-CN 2/3 cereals + 1/3 feed
	Rotation (winter)	63	69	75	79	83	85	87	SCS-CN 2/3 cereals + 1/3 feed
701	Vineyard	64	69	73	76	79	81	82	Row crops, mean of poor and good contoured and terraced
801	Areas with high settlement density	89	91	92	93	94	95	95	Commercial areas (85% impervious)
901	Areas with medium settlement density	77	81	85	88	90	91	92	Residential areas (65% impervious)
1001	Areas with low settlement density	54	62	70	75	80	83	85	Residential areas (25% impervious)
1101	Transportation infrastructures	98	98	98	98	98	98	98	Paved parking lots, roofs, driveways, etc.
1201	Industrial areas	81	85	88	90	91	92	93	Industrial district, (72% impervious)

4 PRELIMINARY BASIN SCALE VALIDATION TESTS

The modified parameterisation of the CN method based on its testing at the plot scale and on process oriented consideration provides only a partial test in relation to its performance at the catchment scale. Because the ultimate goal of SCS-CN method revision is the use as rainfall excess component of rainfall-runoff models, a preliminary investigation has been carried out, by using the modified CN parameterisation to simulate flood events in a small mesoscale catchment of the Swiss prealpine region. In principle, the CN method can be used as component of any kind of rainfall-runoff model, but given its suitability to account for variability of runoff generation at the plot scale, it has been tested in the context of this preliminary validation study as part of a distributed rainfall-runoff event-based model, which has been used to simulate selected events, ranging from low to very high return periods.The

choice of an event-based model stems from the need to minimise the number of process component that could contribute to add noise signals to simulations, thus limiting the capability of identifying major limitations related to the poor performance of the runoff generation component. The event-based model, named *FEST* (*F*lash– flood *E*vent–based *S*patially–distributed rainfall– runoff *T*ransformation) is consistent with the prototype of used by Mancini (1998), but is used in its modified version (see for details Burlando et al., 2001) and consists essentially of

- a distributed input represented by the observed storm rainfall field;
- the raster based CN model component, with parameters variable in space on 100×100 m grid;
- a surface transfer component to model overland flow, based on a Muskingum-Cunge representation of the flow propagation over the 100×100 m grid domain;
- a surface model component for channelised flow, also based on a Muskingum-Cunge scheme, and
- a sub-surface model component based on the linear reservoir conceptual scheme to account for runoff contribution due to the portion of the infiltrated rainfall that contributes to river discharge.

A preliminary set of simulations has been performed on a test basin located in the prealpine region of north-eastern Switzerland. The Murg basin is a mesoscale basin, largely rural, for which a set of flood event data is available at two different outlets representative of two nested catchments, respectively 8 (Fischingen) and 79 km^2 (Wängi) in size (see for details Burlando et al., 2001). The catalogue of flood events includes 19 events for which coupled hourly rainfall measured at a raingage close to the outlet and discharge data are available. Four event are used for the calibration of the model and the remaining events for the validation. By means of a trial and error procedure the calibration events allowed to adjust the parameterisation of the Muskingum-Cunge modules and as fine tuning of the CN values for agricultural and forest areas mainly in the Fischingen subcatchment, and for other land uses in the whole catchment. The adjustment necessary to allow a correct reproduction of the flood event are used as feedback in the final formulation of the assignment scheme of the CN method, mainly to test the adequacy of the conversion relationship to transform CN_{II} values into CN_{I} or CN_{III}, in order to account properly for the antecedent moisture conditions. An example of result for a calibration event is reported in Figure 4-1. Despite the large variability of the considered events, the validation carried out on the remaining 15 flood events, for both the considered basin outlets, put in evidence the ability of the model to capture in most of the cases the peak value, the time to peak, and, with a smaller rate of success, the flood volume. Figure 4-2 shows an exemplary result for the validation set of events.

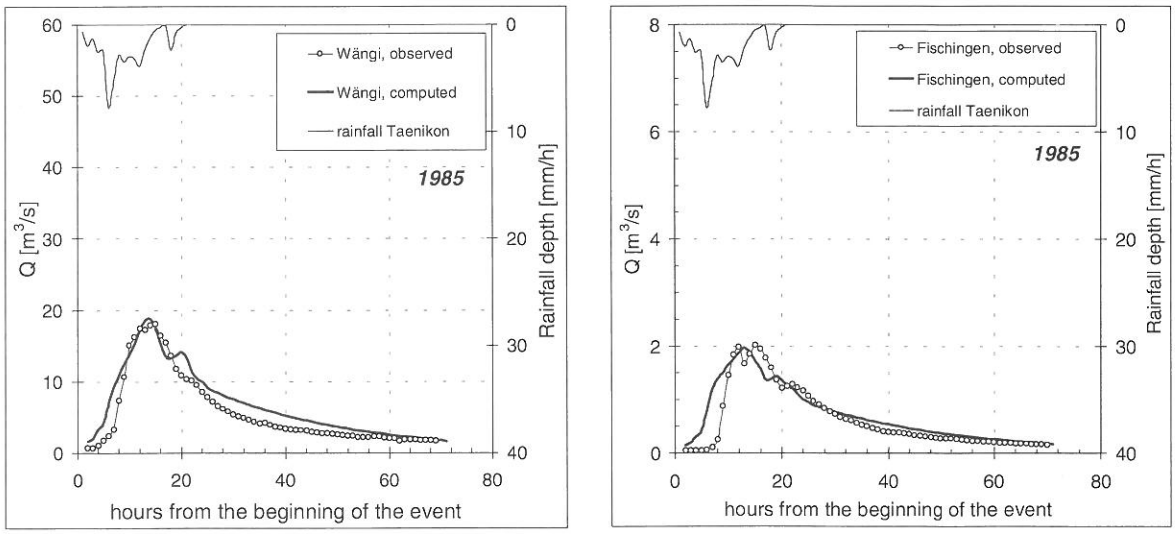

Figure 4-2: Example of simulation for a validation event at two different basin scales, Wängi (79 km^2), left side, Fischingen (8 km^2) right side.

In summary, the analysis of model performance has shown that the coupling of the CN method with a simple distributed rainfall-runoff scheme is enough robust to capture flood runoff at different basin scales over several and varied events. However, the timing of the hydrograph and the associated shift in the volume, especially evident at the small scale, suggest that, further to possible changes in the CN model structure, improvements of the CN parameterisation are anyway necessary in relation to the estimation of the initial abstraction and of the CN-dependence on the antecedent moisture condition. The latter has been computed with reference to the criteria defined by eq. (4), which has been shown to be often inadequate in capturing the effective wetness of the basin. In some cases it has been

indeed sufficient to use the parameterisation for the next AMC class in order to accommodate the insufficient fitting. The amount of experimental data that could be considered in this study did not, however, allow to investigate more comprehensively this aspect, which should account for the specific characteristics of the wetting and drying dynamics in prealpine and alpine regions.

5 CONCLUDING REMARKS

The purpose of the study was to explore the suitability of the popular SCS-CN method to reproduce correctly the flood runoff generation in alpine and prealpine regions. The results, although preliminar and based on a trial and error approach rather than on a theoretical basis, has highlighted the overall ability of the SCS-CN method to reproduce correctly a significant number of flood runoff occurrences when coupled with a simple rainfall-runoff distributed model. The revised parameter table (see Table 3-4) has been obtained by a qualitative and iterative process, which has made use of literature data from experimental plots and of an extensive thematic data sets in raster form. Some of the comparison between rainfall excess computed via CN method and observed from plot experiments highlighted that the presence of specific runoff mechanisms at the microscale can lead to poor performances. The performance is only slightly improved even when process oriented considerations are introduced on the basis of detailed soil information retrieved by the comprehensive raster data base. This would suggest the need for some structural changes of the model, in order to make it suitable for use at the individual plot scale. However, the validation of the modified CN assignment scheme carried out at the catchment scale indicate that microscale runoff generating mechanism have a limited propagation effect on flood runoff generation when catchment larger than a few km^2 are considered. The weaker performance at the plot scales could however suggest the presence of a break in the lower range of scales of application for this approach.
Although further quantitative testing of the model is required on an extended and comprehensive set of geographical locations and storm events to achieve a final parameterisation table, the results can be considered enough encouraging and may indicate that the model can perform satisfactorily despite its conceptual and simple nature, if properly used, within a range of scale which covers a large part of the scales of technical interest. The coupling of the CN method with the distributed representation of the runoff components of the rainfall-runoff transformation indicates especially a major deficit for those events, which are characterised by a strong influence of the soil saturation dynamics prior to the event itself. This suggests that the CN method is suitable in the prealpine and alpine for the estimation of values in the upper range of the flood frequency curve (i.e. rare events), which are characterised by a less pronounced influence of the soil saturation dynamics within the interstorm period. Further investigations are currently carried out, in order to improve this specific aspect, that is of great importance when storm events are characterised by a sequence of storm peaks spaced by short dry periods that allow a recovery of the soil retention capacity by temporary drainage.

ACKNOWLEDGEMENTS

This research work has been partially supported by Swiss Bundesamt für Bildung und Wissenschaft within the EU-project "FRAMEWORK" under the IV Framework Programme (contract n° ENV4-CT97-0529). The additional support of the Swiss Bundesamt für Wasser und Geologie through the grant FE/LHG/309-99-12 is also greatly acknowledged.

REFERENCES

Beven, K.J., Clarke, R.T. (1985): On the variation of infiltration into a homogeneous soil matrix, containing a population of macropores. Water Resour. Res. 22(3). 383-388.

Bruggeman, A.C., Mostaghimi, S. (1991): Simulation of preferential flow and solute transport using a efficient finite element model, in: Preferential Flow, ed. by T.J. Gish and A. Shirmohammadi, American Soc. of Agricultural Engineers, St. Joseph, Michigan, 244-255.

Burlando, P. et al. (2001): Intercomparison of methods and models. Ch. 6 in R. Rosso (ed.): FRAMEWORK – **F**lash-flood **R**isk **A**ssessment under the i**M**pacts of land use changes and river **E**ngineering **WORK**s. Final report. EU contract ENV4-CT97-0529. Politecnico di Milano, Italy. 30 pp.

Dunne, T. (1978): Field studies of hillslope flow processes. In: Hillslope Hydrology, ed. by M.J. Kirkby, J. Wiley & S., New York, USA.

Faeh, A. O. (1997): Understanding the Processes of Discharge Formation under Extreme Precipitation. A study based on the numerical simulation of hillslope experiments. Report of the Versuchsanstalt für Wasserbau, Hydrologie und Glaziologie, Nr. 150. ETH Zurich. Switzerland.

GEOSTAT (1997): Benutzerhandbuch. Bundesamt für Statistik. Bern, Switzerland.

Germann, P. (1990): Macropores and hydrological hillslope processes. In: Process Studies in Hillslope Hydrology, ed. by M.G. Anderson and T.P. Burt. J. Wiley & S. New York, USA.

Horton, R.E. (1933): The role of infiltration in the hydrologic cycle. Trans. AGU. 14. 446-460.

Maidment, D.R.(ed.) (1992): Handbook of Hydrology. McGraw-Hill. New York, USA.

Mancini, M. (1998): L'Evento alluvionale del 19 Giugno 1996 in Versilia: Dinamica dell'evento di piena. Chapter 4.1 in: 19 Giugno 1996: Alluvione in Versilia e Garfagnana, ed. by R. Rosso and L. Serva. Firenze, Italy. 145-166.

Markart, G., Kohl, B. (1995): Starkregenesimulation und bodenphysikalische Kennwerte als Grundlage der Abschätzung von Abfluss- und Infiltrationseigenschaften alpiner Boden-/Vegetationseinheiten. Report 89 of the Forstliche Bundesversuchsanstalt Wien. Vienna, Austria.

Markart, G. et al. (1996): Integralmelioration "Vorderes Zillertal". Einfluss von Boden, Vegetation und rezenter Bewirtschaftung auf den Abfluss bei Starkregen. Report of the Forstliche Bundesversuchsanstalt. Institut für Lawinen- und Wildbachforscung. Innsbruck, Austria.

Philip, J.R. (1957): The theory of infiltration. 1. The infiltration equation and its solution. Soil Sci.. 83. 345-357.

Rosso, R. (ed.) (2001): FRAMEWORK – **F**lash-flood **R**isk **A**ssessment under the i**M**pacts of land use changes and river **E**ngineering **WORK**s. Final report. EU contract ENV4-CT97-0529. Politecnico di Milano, Italy. 380 pp.

Richards, L.A. (1931): Capillary conduction of liquids through porous mediums. Physics. 1. 318-333.

Scherrer, S. (1997): Abflussbildung bei Starkniederschlägen, Identifikation von Abflussprozessen mittels künstlicher Niederschläge. Report of the Versuchsanstalt für Wasserbau, Hydrologie und Glaziologie. 147. ETH Zurich, Switzerland.

SCS – Soil Conservation Service (1972): National Engineering Handbook. Section 4, Hydrology. U.S. Department of Agriculture. Washington D.C., U.S.A.

SCS – Soil Conservation Service (1986): National Engineering Handbook. Section 4, Hydrology (Rev. ed.). U.S. Department of Agriculture. Washington D.C., U.S.A.

Zuidema, P.K. (1985): Hydraulik der Abflussbildung während Starkniederschlägen, eine Untersuchung mit Hilfe numerischer Modelle unter Verwendung plausibler Bodenkennwerte, Report of the Versuchsanstalt für Wasserbau, Hydrologie und Glaziologie. 145. ETH Zurich, Switzerland.

JOINT MODELLING OF MEAN AND DISPERSION WITH APPLICATION TO A RAINFALL-RUNOFF TRANSFER MODEL

Gorana Capkun[1], A. C. Davison[2], André Musy[1]

[1] Hydrology and Land Improvement Institute, Swiss Federal Institute of Technology Lausanne, 1015 Lausanne, Switzerland, gorana.capkun@epfl.ch, andre.musy@epfl.ch

[2] Department of Mathematics, Swiss Federal Institute of Technology Lausanne, 1015 Lausanne, Switzerland, anthony.davison@epfl.ch

SUMMARY

In this work we show how modern statistical tools can be useful in hydrology. We start by 'listening to what the data say' in order to elicit a flexible model for rainfall-runoff transfer. Our model respects the correlated structure of the runoff observations, and essentially models their conditional mean and variance. The conditional mean is taken to be a linear autoregressive combination of present and previous rainfall and previous runoff, while the variance also depends on rainfall history. Different algorithms for estimating model parameters are proposed. We also state some asymptotic results for the parameter estimators, needed to construct confidence and predictive bounds. We also underline the idea of model misspecification in order to construct robust `sandwich' confidence intervals. These ideas are illustrated on an example.

Keywords: confidence bounds, quasilikelihood, rainfall-runoff, variance model

1 INTRODUCTION

A comprehensive literature search would no doubt disclose the existence of several hundred rainfall-runoff models, and the number of unpublished models probably exceeds that of the published ones. During the last three decades, a substantial effort has been done in stochastic rainfall-runoff modelling, the majority of them based on time series modelling (Box, Jenkins, 1976). This approach has the major drawback that most standard linear time series models are intended to model variables lying in the real line; in fitting routines the white noise is generally taken to be normal, leading to symmetric distributions for runoff. Rainfall and runoff are non-negative and highly asymmetric, however, so transformations must be applied if the normal model is to fit. This makes the model parameters difficult to interpret even if their number is relatively small, and suggests that non-normal models may be more useful (Hipel, McLeod, 1994).

In rainfall-runoff modelling, the main objective is to model the mean behaviour of the runoff, while the variance structure is neglected and assumed constant. However, it is hard to believe that the variance does not change over time. One simple example is the difference in variances between the rainy and rainless periods.

When the distribution of the runoff data is to be chosen, as is usually the case in stochastic rainfall-runoff modelling, we say that the models are parametric. The obvious drawback is potential misspecification of the distribution. QuasiLikelihood (QL) theory (Wedderburn, 1974) gives the possibility to draw inferences when there is insufficient information about the data distribution.

In this work we propose a new methodology for rainfall-runoff modelling, which jointly models the mean and the variance structure and does not require a complete parametric distribution specification. The mean structure is taken to be a linear autoregressive combination of present and previous rainfall and previous runoff, while the variance also depends on rainfall history. Inference for our model is performed using classical likelihood methods, and also by the more robust technique of quasilikelihood, presupposing no particular distribution for runoff. The model has been developed on the Biorde catchment in Switzerland.

Data with its exploratory data analysis are presented in Section 2.1. Section 2.2 proposes the rainfall-runoff model for which the parameter estimation algorithms are given in Section 2.3. Some important asymptotic results are stated in Section 2.4. A data example in Section 3 illustrates our model.

2 RAINFALL-RUNOFF MODEL

2.1 Data and exploratory data analysis

Our data, two time series representing rainfall in mm and runoff in m^3/s, come from the Biorde catchment in the canton of Fribourg in Switzerland. Its area of 25.3 km^2 is composed of both rural and urban zones. Rainfall is measured at the Grange station and runoff at the Biorde outlet. Hourly values of the Biorde data from October 14, 1992 until December 28, 1993 are shown in Figure 2-1. Several things can be learned from this graph. First, both rainfall and runoff are positive valued. Comparing both series at the same time, we can conclude that a certain relation exists between them. However, our data set is quite large (10547 observations in each series) so the details cannot be seen. A closer look at one rainfall event and the corresponding catchment reaction represented by runoff shows a time lag between them.
One way to estimate the unit hydrograph is to fit a normal linear regression model taking the runoff at time t as response and rainfall at times t,t-1, ...,t-k as explanatory variables. Its residuals show that the model does not explain a recession curve structure that occurs during the rainless periods. This suggests separating the runoff data into rainy and rainless parts. Similar ideas can be found in Lu and Berliner (1999). We show some characteristics of rainy and rainless periods in Figure 2-2. In this initial analysis we examine the marginal distributions of the runoff even if the conditional ones are modelled (Section 2.2). Time plots for rainy and rainless runoff reflect the above-mentioned characteristics (increasing and pulsing phase for the rainy and decreasing phase for rainless data) and we should take account of these when modelling runoff. The raw runoff histograms may indicate that even if the rainy and rainless data belong to the same family of distributions, they probably do not have the same parameters. When comparing histograms for the runoff logarithms, we can hardly believe in the same distribution; the rainy data probably come from a bimodal distribution. The normal distribution is clearly not a suitable candidate. For simplicity, we suppose that both rainy and rainless data come from the same distribution, but with a different set of parameters. A similar analysis for the whole data series suggests a gamma distribution as a possible candidate. In the next section we use this information to construct our model.

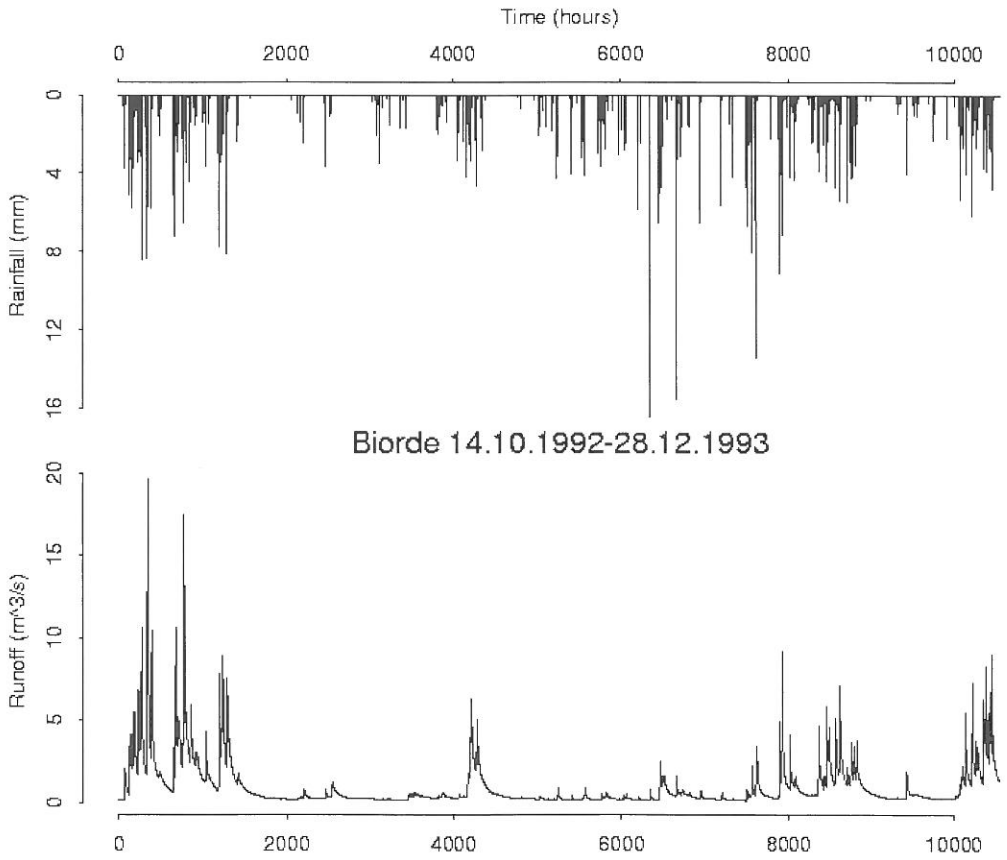

Figure 2-1: Hourly measurements of Biorde data. The top panel shows the rainfall data in mm measured at the rain-station Grange. The bottom panel shows the runoff data in m^3/s at the Biorde outlet.

2.2 Model

Let X_t and Y_t represent hourly rainfall and runoff at times t=1, ...,T. As our goal is to model runoff as a function of observed rainfall, we suppose that the runoff series Y_t is random and treat the rainfall series X_t as known. Let H_t denote the present and the past rainfall and past runoff at time t

$$H_t = (X_t,\ldots,X_{t-k},Y_{t-1},\ldots,Y_{t-l}); \tag{1}$$

we will call H_t the history. This is the information available to the modeler for prediction of the runoff Y_t at time t. In practice we only need a small subset of H_t, typically taking k and l to be small integers. The assumption that Y_t depends only on Y_{t-1}, ...,Y_{t-l} amounts to the l^{th} order Markov property. We suppose that the conditional distribution of Y_t given the history H_t is some unknown density $q(y_t|h_t;\theta)$, where y_t and h_t represent values of the random variables Y_t and H_t and the vector parameter θ summarizes their dependence structure.
Choosing any standard parametric distribution for q means choosing a wrong distribution (see Section 2.1). Therefore, we only specify the conditional mean and variance of Y_t

$$\mu_t = E(Y_t|H_t), \qquad \sigma_t^2 = \mathrm{var}(Y_t|H_t). \tag{2}$$

The mean runoff at time t is supposed to be a linear combination of present and previous rainfall and previous runoff,

$$\mu_t = \sum_{i=0}^{k}\beta_i x_{t-i} + \sum_{j=1}^{l}\gamma_j y_{t-j}, \qquad t = r+1,\ldots,T, \tag{3}$$

where r = max(k,l) and the values of k and l are determined by a model choice procedure. The advantage of a linear relationship is a quasi-physical interpretation of β_i and γ_j. The dimensionless parameters γ_j measure the association between expected current and past runoff, while the parameters β_i have the dimensions of runoff/rainfall and measure the effect of rainfall on expected current runoff, assumed to be linear. We expect all the β_i to be positive, though we do not impose this when fitting the model. We therefore suppose that a mean parameter of the conditional distribution keeps the same structure for all values of runoff.

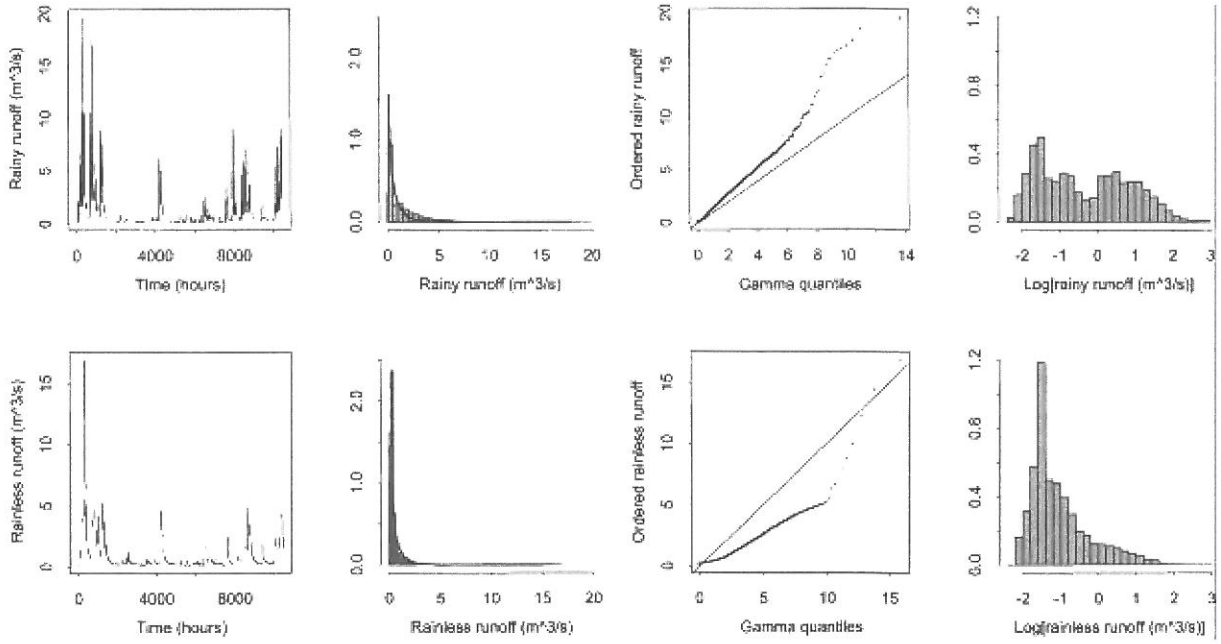

Figure 2-2: Characteristics of rainy (top) and rainless runoff (bottom). From left to right: a time plot, histogram with estimated gamma density (solid), gamma quantile-quantile plot (QQ-plot) and histogram of the log of data.

In the previous section, we outlined the necessity to model differently at least one parameter of the rainy and rainless distributions; see Figure 2-2. As these were defined as functions of the rainfall history that is a part of h_t for each y_t, we have found it useful to model changes in the conditional variance σ_t^2. Primary interest still attaches to how the mean response is affected by covariates, while the σ_t^2 parameters are regarded as a nuisance.
In the usual linear model there is no relation between the mean and variance of the response, and this is also the case for conventional time series models. This is rarely true for positive data like ours, for which the variance is often proportional to the mean squared. This property is shared by the exponential, gamma, lognormal and Weibull distributions; the 'usual' choices for the runoff. In our case it is useful to accommodate the possibility that the current variance of runoff depends on recent rainfall history, and to suppose that $\sigma_t^2 = \mu_t^2/\nu_t$, where the precision parameter $\nu_t = \exp(\lambda_1+\lambda_2 I_{t,k})$ depends on the indicator

$$I_{t,k} = \begin{cases} 0, & \text{if } x_{t-1} = \ldots = x_{t-k} = 0, \\ 1, & \text{otherwise,} \end{cases} \tag{4}$$

of rainfall in the preceding k days. Here we suppose that ν_t is a constant in both rainy and rainless periods. This is a very simple way to incorporate into a model our findings from Section 2.1.
In the data analysis below, we say that the period preceding time t is rainless if $x_{t-j} < 0.1$ mm for all $j = 1, \ldots, k$. Otherwise the period is considered to be rainy, with $I_{t,k} = 1$. During a rainy period runoff increases and can be rather variable, but in a rainless period it shows a slow essentially deterministic decline towards zero.
Our parameter vector $\theta = (\beta_0, \ldots, \beta_k, \gamma_1, \ldots, \gamma_l, \lambda_1, \lambda_2)^T$ contains terms for the dependence of $E(Y_t)$ on previous runoff and rainfall, and for dependence of its variance on the presence of recent rainfall. The next section discusses algorithms for estimating the model parameters.

2.3 Parameter estimation

Let $\psi = (\beta_0, \ldots, \beta_k, \gamma_1, \ldots, \gamma_l)^T$ and $\lambda = (\lambda_1, \lambda_2)^T$ represent parameters of the conditional mean μ_t and variance σ_t^2 models respectively. In this section we give several possibilities for the joint estimation of these parameters. We first distinguish between two main approaches: parametric and semiparametric. The parametric approach requires a full distribution specification for the conditional runoff Y_t. As proposed in Sections 2.1 and 2.2 the least inappropriate candidate would be the gamma distribution. Under the model described above, the runoff series form a Markov chain of order l, and the joint density for $Y_1, \ldots, Y_T$ given rainfall data $x_1, \ldots, x_T$ may be written as

$$f_Y(y|x,\theta) = f_{Y_1,\ldots,Y_r}(y_1,\ldots,y_r|x;\theta)\prod_{t=r+1}^{T} f_{Y_t|H_t}(y_t|h_t;\theta), \tag{5}$$

where $f_{Y_t|H_t}$ is gamma with mean μ_t and variance σ_t^2; $\theta = (\psi,\lambda)^T$. One difficulty is that the joint density $f_{Y_1,\ldots,Y_r}(y_1,\ldots,y_r|x;\theta)$ cannot be determined without additional assumptions, so we consider only the right part of equation (5). Regarded as a function of θ with y fixed, the right part of equation (5) is a conditional likelihood of $Y_{r+1}, \ldots, Y_T$ given $Y_1, \ldots, Y_r$. As r is usually small we do not lose much information. This conditional likelihood is then maximized at the maximum likelihood estimate $\hat{\theta} = (\hat{\psi},\hat{\lambda})^T$. We will call this method Gamma-Based Maximum Likelihood (GBML). Its main drawbacks are that it requires a full specification of the conditional runoff distribution and that it can be time consuming to fit (see Section 3).
In the text below, we discuss a semiparametric approach for estimating model parameters. The main idea is to parametrize aspects of model of primary importance such as dependence of the conditional mean and variance on previous rainfall and runoff minimizing the distributional aspects, which are regarded as secondary. One possibility is the use of the quasilikelihood method that constructs a quasiscore estimating function based only on the conditional mean and variance specifications (Wedderburn, 1974); the score function is defined as a derivative of the loglikelihood in vector parameter θ. The quasilikelihood estimator $\tilde{\theta} = (\tilde{\psi},\tilde{\lambda})^T$ is a solution of the quasiscore equations

(6) $$U_{Qt} = \frac{Y_t - E(Y_t|H_t)}{var(Y_t|H_t)} = 0, \quad t = r+1,\ldots,T.$$

The quasilikelihood method supposes $var(Y_t|H_t)$ to be constant, which is not satisfied in our model due to a time dependence of the precision parameter ν_t. Under the gamma-based model, the mean parameter ψ and the variance parameter λ are conditionally expected orthogonal (Cox, Reid, 1987). This result allows us to keep one orthogonal parameter fixed while estimating the other one. We then assign some initial fixed value to the parameter λ, estimate ψ, iterating between the ψ, λ estimation procedures until a suitable convergence criterion is satisfied. We assume that the algorithm has converged when $\|new.parameters - old.parameters\|_2 / \|old.parameters\|_2 < \varepsilon$, with $\varepsilon > 0$ usually fixed at 0.0001 and $\|a\|_2 = \sqrt{\sum_{i=1}^{n} a_i^2}$, where a is a n-dimensional real vector. It is simply an extension of the Iteratively Reweighted Least Squares procedure (Firth, 1991; Green, 1984).
For the fixed value of λ, the mean parameter ψ is estimated by solving for ψ

(7) $$\nu_t \frac{Y_t - \mu_t}{\mu_t^2} = 0, \quad t=r+1,\ldots,T,$$

where μ_t is defined in (3); $\tilde{\psi} = (\tilde{\beta}_0,\ldots,\tilde{\beta}_k,\tilde{\gamma}_1,\ldots,\tilde{\gamma}_l)^T$ is a maximum quasilikelihood estimator of ψ. We define

(8) $$\tilde{\mu}_t = \sum_{i=0}^{k} \tilde{\beta}_i x_{t-i} + \sum_{j=1}^{l} \tilde{\gamma}_j y_{t-j}, \quad t = r+1,\ldots,T.$$

We now describe two methods for estimating λ assuming ψ fixed. For the first, we use the fact that ν_t takes only two values: $\nu_r = \exp(\lambda_1+\lambda_2)$ for the rainy and $\nu_{nr} = \exp(\lambda_1)$ for the rainless periods, so these parameters can be consistently estimated by splitting the data into rainy and rainless parts by the method of moments

(9) $$\tilde{\lambda}_2 = \log T_r - \log\left\{\sum_{t_r} \frac{(y_t - \tilde{\mu}_t)^2}{\tilde{\mu}_t^2}\right\} - \tilde{\lambda}_1, \quad \tilde{\lambda}_1 = \log T_{nr} - \log\left\{\sum_{t_{nr}} \frac{(y_t - \tilde{\mu}_t)^2}{\tilde{\mu}_t^2}\right\}.$$

The second method takes

(10) $$\tilde{\nu}_t = \frac{\tilde{\mu}_t^2}{(y_t - \tilde{\mu}_t)^2},$$

to be the response of the quasilikelihood model $E(\tilde{\nu}_t|H_t) = \exp(\lambda_1 + \lambda_2 I_{t,k})$.
The conditional variance of $\tilde{\nu}_t$ is taken to be constant. The estimates of λ_1 and λ_2 are calculated by solving the quasilikelihood equation

(11) $$\sum_{t=r+1}^{T} \frac{\tilde{\nu}_t - \exp(\lambda_1 + \lambda_2 I_{t,k})}{\sigma_v^2} \frac{\partial \exp(\lambda_1 + \lambda_2 I_{t,k})}{\partial \lambda} = 0,$$

where σ_v^2 is the conditional variance. The fitted values of $\tilde{\nu}_t$, $\tilde{\tilde{\nu}}_t$ are calculated as $\tilde{\tilde{\nu}}_{nr} = \exp(\tilde{\lambda}_1)$ and $\tilde{\tilde{\nu}}_r = \exp(\tilde{\lambda}_1 + \tilde{\lambda}_2 I_{t,k})$, where $\tilde{\lambda}_i$ is the maximum quasilikelihood estimate of λ_i solving (7).
Starting from some initial values for ψ and λ, we iterate between (7) and (9) or (7) and (11) and obtain two additional quaslikelihood-based estimating methods: Method of Moments Estimators of Dispersion parameters (MMED) and QuasiLikelihood Dispersion Estimation (QLDE(I)) respectively. The latter allows for a straightforward extension of our model, replacing the binary variable $I_{t,k}$ with some continuous variable Z. A simple candidate for Z is a sum of the previous k observations

(12) $$Z_{t,k} = \sum_{i=1}^{k} X_{t-i},$$

which is related to the antecedent moisture conditions of the catchment. We estimate λ as in QLDE(I), except that we replace $I_{t,k}$ by $Z_{t,k}$. We will call this method of estimation QLDE(Z). Further extension of the basic model can be easily imagined changing both the mean and the variance model.

2.4 Asymptotic results

In this section we give the main results for the asymptotic (large sample) behaviour of the (quasi) likelihood estimator for the parameter of interest ψ, showing their use in constructing confidence and prediction intervals.
Under the model assumptions (2), respecting the Markov chain property for Y_t and under some regularity conditions, martingale limit results are used to show that the (quasi)likelihood estimator $(\tilde{\psi})\hat{\psi}$ is consistent and has the asymptotic normal distribution

(13) $$\tilde{\psi} \sim N\left\{\psi,(M^T\tilde{W}M)^{-1}\right\}, \qquad \hat{\psi} \sim N(\psi,I(\hat{\psi})^{-1}),$$

where $M = [x_t|x_{t-1}|\cdots|x_{t-k}|y_{t-1}|y_{t-2}|\cdots|y_{t-l}]$ is the (T-r) x (k+l+1) local design matrix, $\tilde{W}$ is a (T-r) x (T-r) diagonal matrix with t^{th} element $\tilde{v}_t/\tilde{\mu}_t^2$ and $I(\hat{\psi})$ is a form of conditional information that is in our example equal to $M^T\hat{W}M$. Hence (1-2α)% confidence bounds based on $\tilde{\psi}_j$ and $\hat{\psi}_j$ are

(14) $$\tilde{\psi}_j \pm z_\alpha \tilde{v}_{jj}^{-1/2}, \qquad \hat{\psi}_j \pm z_\alpha \hat{v}_{jj}^{-1/2}, \qquad j = 1,\ldots,k+l+1,$$

where $\tilde{v}_{jj}$ and $\hat{v}_{jj}$ are the j^{th} diagonal elements of $(M^T\tilde{W}M)^{-1}$ and $\{I(\hat{\psi})\}^{-1}$ respectively and z_α is the α quantile of the standard normal distribution.
This standard theory applies when the assumed model is the true one. If the variance model is misspecified, then considering the mean model as the true one, under mild conditions $\tilde{\psi}$ remains consistent and asymptotically normal, but $(M^T\tilde{W}M)^{-1}$ does not estimate its covariance well. The estimator for the covariance of $\tilde{\psi}$ under the misspecified variance model (2) is called a 'sandwich' estimator because of its form

(15) $$(M^T\tilde{W}M)^{-1}M^T\tilde{W}(y-\tilde{\mu})(y-\tilde{\mu})^T\tilde{W}M(M^T\tilde{W}M)^{-1}.$$

By similar arguments, if the error distribution is misspecified in the parametric approach (we know that gamma model is not the true one), but the other aspects of the model are correct, then under mild conditions the estimator $\hat{\psi}$ remains consistent and asymptotically normal with the 'sandwich' covariance estimator

(16) $$\left[M^T\hat{W}M + M^T\mathrm{diag}\left\{\frac{2\hat{v}_t(y_t-\hat{\mu}_t)}{\hat{\mu}_t^3}\right\}M\right]^{-1} M^T\hat{W}^2\mathrm{diag}\left\{y_t-\hat{\mu}_t^2\right\}M\left[M^T\hat{W}M + M^T\mathrm{diag}\left\{\frac{2\hat{v}_t(y_t-\hat{\mu}_t)}{\hat{\mu}_t^3}\right\}M\right]^{-1}.$$

These results can be then used to construct 'sandwich'-based confidence intervals for ψ. Using both model- and 'sandwich'-based confidence intervals for ψ, we may construct prediction intervals for future observations

(17) $$\left[\max\left\{\tilde{y}_t - z_\alpha \widehat{\mathrm{var}}(\tilde{y}_t)^{1/2},0\right\};\tilde{y}_t + z_\alpha \widehat{\mathrm{var}}(\tilde{y}_t)^{1/2}\right],$$

where $\text{var}(\tilde{y}_t) = \text{var}(\tilde{\mu}_t)(1+\frac{1}{\nu_t}) + \frac{\mu_t^2}{\nu_t}$, $\text{var}(\tilde{\mu}_t)=M\text{var}(\tilde{\psi})M^T$. The same theory holds for maximum likelihood estimators. More details can be found in Capkun (2001), Chapter 4.

3 MODEL CALIBRATION AND VALIDATION

In order to define the complexity of the model for Biorde data, we used the model choice algorithm developed in Capkun et al. (2001). That algorithm combines automatic information criteria with model diagnostics to define the smallest couple (k,l) that fits the data reasonably well. The GBML algorithm for parameter estimation was used on the first 2500 Biorde observations. The chosen model has a mean structure with four parameters, of which β_1, β_2 explian the direct impact of rainfall and γ_1, γ_2 the recession curve of the runoff. There are also two parameters λ_1, λ_2 that control the coefficient of variation of the model. The $\hat{\beta}_0$ is taken to be zero and it seems that one hour is enough for the Biorde catchment reaction, because $\hat{\beta}_1$ is significantly different from zero. Parameter estimates with the corresponding model- and 'sandwich'-based standard errors, calculated with four estimating methods from Section 3-2, for the parameters of interest $\psi=(\beta_1, \beta_2, \gamma_1, \gamma_2)^T$ are given in Table 3-1. The estimates of the direct rainfall parameters β_i are small compared to estimates of the autoregressive parameters γ_j. This is not surprising, because the autoregressive time series model (e.g. AR(p)) is a satisfactory description for the stationary runoff data (Delleur, 1991). The first three methods, GBML, MMED and QLDE(I), concern the basic model described in Section 2-1. Their estimates for the parameters of interest are very similar but QLDE(I) has rather different estimates for the dispersion parameters. The value of dispersion parameter estimates influences the model-based standard errors, while the 'sandwich'-ones remain robust. 'Sandwich'-based standard errors for the parameters of interest are about two times bigger than model-based ones and probably more plausible. The interpretation for QLDE(Z) estimates remains the same as for the other three method's, their values being different due to the different model for variance. It is worth noting that the 'sandwich'-based standard errors are comparable to these for other three methods of estimation, while the model-based ones are rather different.
In Figure 3-1 we compare the cumulative periodograms of the deviance residuals, time plots of the deviance residuals and the ratios of the observed and fitted values for the (2,2) model with the parameters estimated by GBML, MMED, QLDE(I) and QLDE(Z) algorithms. There is no significant difference between the cumulative periodogram plots and the ratios of the observed and fitted values. However, the larger value of the dispersion parameter estimates obtained with QLDE(I) or QLDE(Z) algorithms influences the deviance residuals, making them larger than those for GBML or MMED algorithm. We would therefore prefer the two latter. Note that in the right part of all time plots of the deviance residuals and ratios of the observed and fitted values, there are some periods of 'perfect fit'. These correspond to the longer rainless periods where either the recession curve or a horizontal line is observed for the runoff. We may include that information to a new nonlinear model that separates

Table 3-1: Parameter estimates with the model- and 'sandwich'-based standard errors (SE) for the (k,l)=(2,2) model fitted to the Biorde data using GBML, MMED, QLDE(I) and QLDE(Z) algorithms.

Parameter	Estimate (Model-based SE, 'Sandwich'-based SE)			
	GBML	MMED	QLDE(I)	QLDE(Z)
β_1	0.022 (0.004, 0.007)	0.022 (0.004, 0.007)	0.022 (0.001, 0.007)	0.019 (0.001, 0.003)
β_2	0.029 (0.005, 0.010)	0.029 (0.005, 0.009)	0.028 (0.002, 0.009)	0.017 (0.001, 0.005)
γ_1	1.556 (0.016, 0.035)	1.551 (0.016, 0.034)	1.580 (0.006, 0.033)	1.669 (0.006, 0.028)
γ_2	-0.561 (0.016, 0.034)	-0.557 (0.016, 0.033)	-0.585 (0.006, 0.032)	-0.672 (0.006, 0.027)
λ_1	7.998	8.012	9.849	9.757
λ_2	-2.890	-2.993	-2.440	-0.680

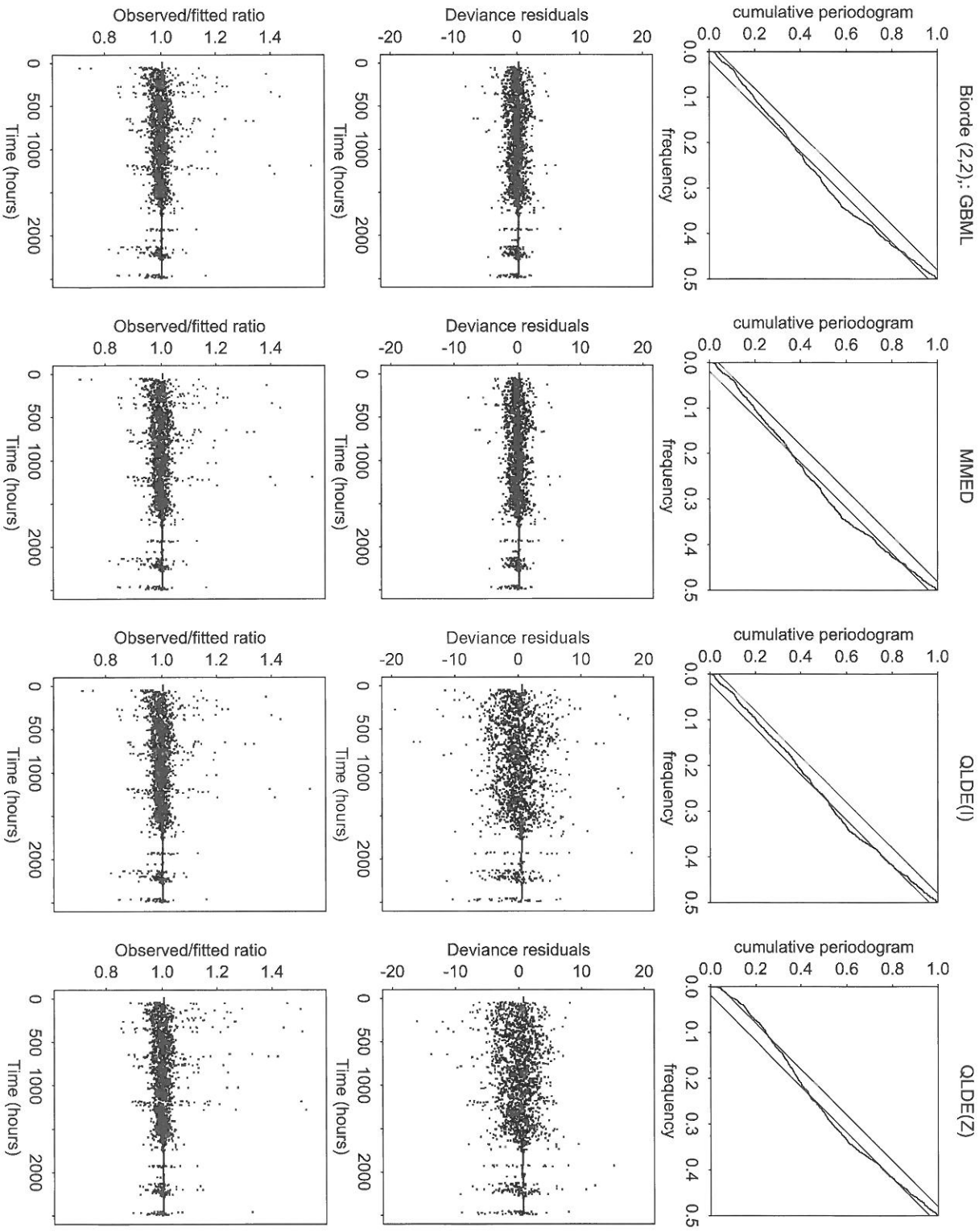

Figure 3-1: Observed versus fitted ratios (left), deviance residuals (middle) and cumulative periodograms of deviance residuals (right) for the Biorde (2,2) model fitted using GBML, MMED, QLDE(I) and QLDE(Z) algorithms. Diagonal lines in the top panel represent 95% confidence intervals.

deterministic form the stochastic behaviour of the runoff; the runoff values that are less than some y_{min} and for which the rainfall is less than some x_{min} belong to the deterministic part of data. We do not consider this here.
Calculating times for estimating the parameters of a (2,2) model for the first 2500 Biorde data 468.7, 2.3, 3.9 and 6.3 seconds for the GBML, MMED, QLDE(I) and QLDE(Z) respectively, using `S-plus` on a `Silicon Graphics` work station with the `IRIX64 1 195 MHZ IP28 Processor`. The interest of using iterative reweighted least squares algorithms is obvious because the fitting time is considerably diminished in all cases compared to GBML. Our preference though goes to the MMED algorithm.

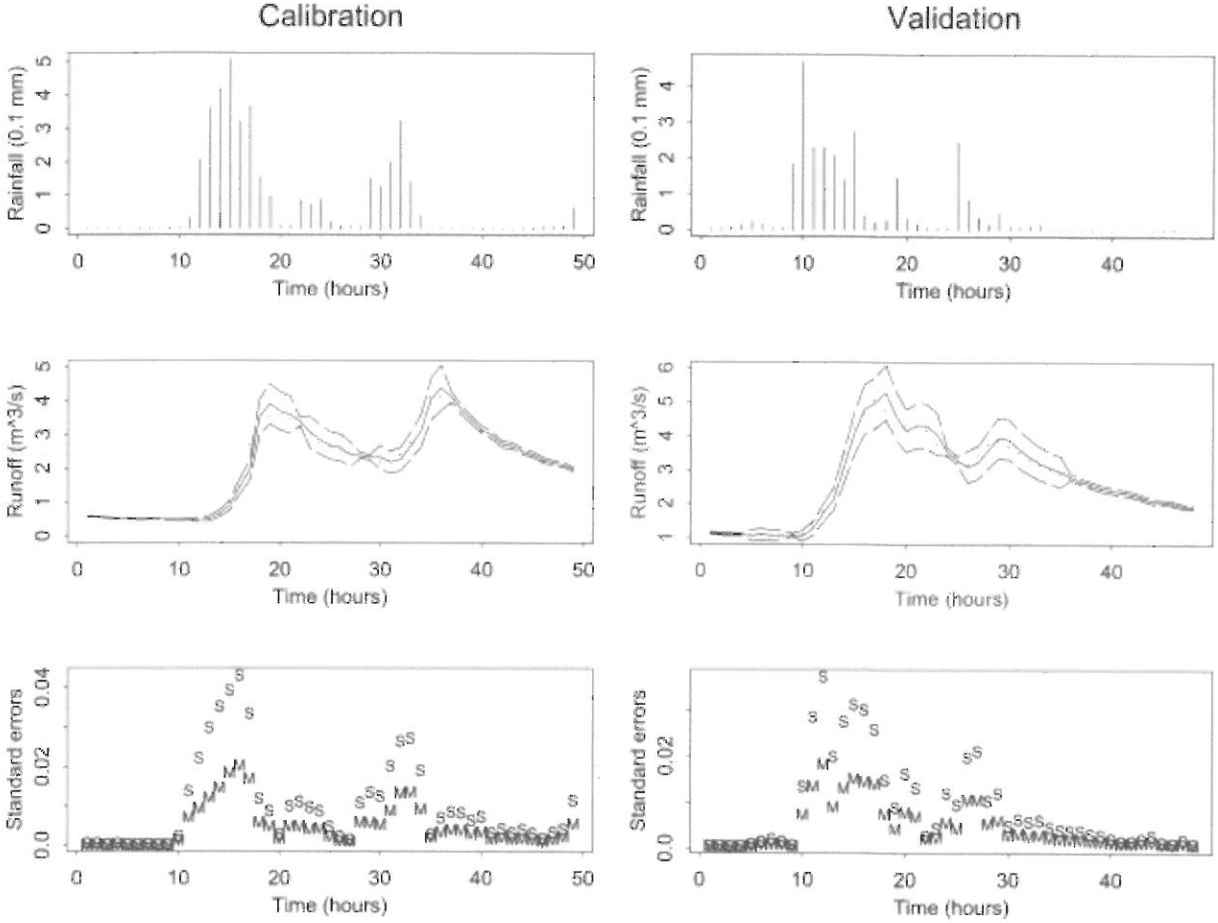

Figure 3-2: One-step predicted values, fitting and predictive confidence intervals. The left part shows results for 50 observations from the calibration period and the right part shows the results for 50 observations from validation period. The upper panels show the corresponding rainfall data and the bottom panels are model- (M) and 'sandwich'- (S) based standard errors for the mean estimator. The runoff observations (points), predicted values (solid line) and 95% prediction intervals (dashed lines) are shown in the central panel.

In order to examine the one-step prediction, the prediction and confidence intervals more closely, we chose intervals of 50 consecutive observations from the calibration (first 2500 Biorde data) and validation (the rest of the data) periods; see Figure 3-2. The upper panels show the corresponding rainfall and the bottom panels the model and 'sandwich' standard errors for the fitted means. The observed runoff values, the predicted values using MMED estimating method and the 95% prediction intervals are shown in the central panel. The variance $\mathrm{var}(\tilde{\mu}_t)$ is a negligible part of the predictive variance $\mathrm{var}(\tilde{y}_t)$ so the model and 'sandwich' prediction intervals coincide to within drawing accuracy.

4 CONCLUSIONS

Classical time series models for the rainfall-runoff transfer have two major drawbacks. One is the use of symmetric distributions rather than positively skewed ones for non-negative data such as runoff. The second is the constant variance assumption, which is inappropriate; at least two different parts of runoff exist: the rainy and rainless. None of the existing hydrological and statistical models satisfies exactly our needs, but a combination of them allows for different methods of estimation: Gamma Based Maximum Likelihood (GBML), Method of Moments Estimators of Dispersion parameters (MMED) and Quasi-likelihood Dispersion Estimation (QLDE). Classical likelihood theory combined with martingale limit laws gives an elegant proof of consistency and asymptotic normality for estimators of the parameters of interest; the orthogonality of mean and dispersion parameters is used. We also allow for the misspecified model structure in both parametric and and quasilikelihood cases. These results are then used to construct model- and 'sandwich'- confidence bounds for the model parameters and fitted values, as well as the prediction intervals for future observations. The necessity for these robust techniques is confirmed in practice where the 'sandwich'- confidence bounds remain stable under different methods for estimating dispersion. However, some additional work is needed in order to investigate into the limit properties of the estimators calculated with different methods mentioned above. In practice, we suggest the use of the MMED procedure. The main drawback of our approach is that it is not able to generate new data sets and is not appropriate for long-term prediction.

REFERENCES

Box, G. E. P., Jenkins, G. M. (1976): Time Series Analysis, Forecasting and Control. Revised edition. Holden-Day. San Francisco

Capkun, G. (2001): Stochastic Rainfall-Runoff transfer Modelling with Joint Estimation for Mean and Dispersion: Application to the Swiss Plateau Catchments. PhD thesis. Swiss Federal Institute of Technology. Lausanne

Capkun, G. et al. (2001): A robust rainfall-runoff transfer model. Water Resources Research, 37, 3207-3216

Cox, D. R., Reid, N. (1987): Parameter orthogonality and approximate conditional inference (with Discussion). Journal of the Royal Statistical Society, Series B, 49, 1-39

Delleur, J. W. (1991): Time Series Analysis Applied to Hydrology. V. U. B. – Hydrologie. Brussels

Firth, D. (1991): Generalized linear models. In D. V. Hinkley, N. Reid, and E. J. Snell (Eds.), Statistical Theory and Modelling, In Honour of Sir David Cox, Chapter 3. Chapman and Hall. London

Green, P. J. (1984): Iteratively reweighted least squares for maximum likelihood estimation, and some robust and resistant alternatives (with Discussion). Journal of the Royal Statistical Society, Series B, 46, 149-192

Hipel, K. W., McLeod, A. I. (1994): Time Series Modelling of Water Resources and Environmental Systems. Elsevier. Amsterdam

Lu, Z.-Q., Berliner, L. M. (1999): Markov switching time series models with application to a daily runoff series. Water Resources Research, 35, 523-534

Wedderburn, R. W. M. (1974): Quasi-likelihood functions, generalized linear models, and the Gauss-Newton method. Biometrika, 61, 439-447

DESCRIPTIVE CAPABILITY OF SEASONALITY INDICATORS FOR REGIONAL FREQUENCY ANALYSES OF FLOOD AND RAINFALL

Attilio Castellarin, Armando Brath

DISTART, University of Bologna, Viale del Risorgimento, 2, I-40136 Bologna, Italy,
attilio.castellarin@mail.ing.unibo.it, armando.brath@mail.ing.unibo.it

SUMMARY

The paper analyses the effectiveness of incorporating information about the timing and recurrence of hydrological extreme events in defining homogeneous groups of sites for regional frequency analysis of floods or rainstorms in a wide study area in Northern-Central Italy. Through a series of Monte Carlo experiments a recent study proved that the seasonality indicators have a high descriptive capability with respect to the regionalisation of floods. Therefore the analysis investigates the descriptive potential of these indicators concerning the regionalisation of rainstorms. Starting from an initial subdivision of the study area into homogeneous rainfall regions, based upon geographical criteria (e.g., altimetry, closeness to the sea, orography, etc.) the analysis explores the possibility to enhance this subdivision on the basis of the spatial variability of seasonality indicators. The degree of homogeneity of a series of alternative subdivision hypotheses is assessed by utilising a bootstrap resampling technique. Quite surprisingly, the study results do not seem to show any significant improvements when considering the seasonality of extreme rainfall in the delineation of homogeneous rainfall regions.

Keywords: Regional frequency analysis, seasonality, Monte Carlo, bootstrap, design flood and storm

1 INTRODUCTION

Regional flood frequency analysis techniques represent valuable tools to perform efficient and reliable estimations of the design flood when the required information is not available for the site of interest, or the short record length does not allow one to perform an at-site estimate without introducing unduly extrapolations. In these circumstances hydrologists and technicians may also adopt a different procedure. They could perform a statistical estimation of the design storm for the catchment of interest, and subsequently use this rainfall event as the input of a rainfall-runoff model to obtain an indirect estimation of the design flood as the model output (see for example Brath et al., 2001). If the application of this approach collided with the issue of rainfall data scarcity, the technician would probably choose to apply regional frequency analysis techniques in order to produce an effective estimate of the design storm. Either way, regional frequency analysis techniques are meaningful options in estimating the hydrological design events.

The *index flood* approach (Dalrymple,1960) is probably the first structured and formalised regionalisation procedure to appear in the scientific literature. Nevertheless, up-to-date versions of the procedure are still widely employed around the world. The approach is based on the subdivision of the study area into zones, called homogeneous regions, wherein the probability distribution of annual maximum peak flows is invariant save for a scale factor represented by the index flood.

Soon after the presentation of the index-flood approach, further research showed that in order to improve the reliability of the regional estimates of the design event it was necessary to base the zoning procedure upon physical and climatic criteria (Acreman, Sinclair, 1986) and objective techniques, such as the Region of Influence (ROI) approach (Burn, 1990).

The research for highly descriptive, and possibly simple, indexes of hydrological similarity on which to base the homogeneous region identification process is still a crucial task in hydrology (see for example, Bates et al., 1998; Castellarin et al., 2001).

This paper presents the results of an extensive analysis performed for a broad geographical region of Northern-Central Italy. The analysis employs Monte Carlo experiments and bootstrap resampling techniques to asses the descriptive capability of the seasonality indexes of extreme hydrological events proposed by Bayliss and Jones (1993). In particular the analysis tries to achieve a clearer understanding of whether these indexes may be effectively used in the study area to form homogeneous groups of sites for regional frequency analyses of floods or rainstorms.

The paper is structured as follows: the second section briefly recalls the seasonality indexes of hydrological extreme events, the third and fourth sections present the results of the analyses relative to the regionalisation of extreme flood and precipitation respectively.

2 SEASONALITY OF HYDROLOGICAL EXTREME EVENTS

Seasonality indexes of hydrological extreme events can be defined by means of directional statistics (Mardia, 1972). After Bayliss and Jones (1993), the date of occurrence of the event *i*, with *i* being either a flood or rainfall event, can be written as a directional statistic by converting the Julian date of occurrence into an angular measure through,

$$\theta_i = (\text{Julian Date})_i (2\pi/365) \tag{1}$$

Each date of occurrence for a series of *n* events, such as an Annual Maximum Series (AMS) or a Partial Duration Series (PDS), can be represented as a vector in polar coordinates with a unit magnitude and a direction given by Equation (1). The *x* and *y* coordinates of the mean of this sample of *n* dates of occurrence can be computed through,

$$x = (1/n)\sum_{i=1,n} \cos(\theta_i);\ y = (1/n)\sum_{i=1,n} \sin(\theta_i) \tag{2}$$

The direction, $\bar{\theta}$, along with the magnitude, *r*, of the vector representing this point in polar coordinates can then be obtained by,

$$\bar{\theta} = \arctan(y/x);\ r = \sqrt{x^2 + y^2} \tag{3}$$

The direction $\bar{\theta}$ represents a measure of the mean timing for the sample of *n* dates, and can be converted back to a mean date, *MD*, through,

$$MD = \bar{\theta}(365/2\pi) \tag{4}$$

The magnitude *r* provides a measure of the regularity of the phenomenon. Values of *r* close to one detect a strong seasonality, or regularity, in the dates of occurrence of the events. Values close to zero are symptomatic of a great dispersion in the dates of occurrence throughout the year (Figure 2-1).

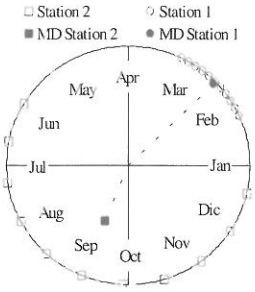

Figure 2-1: Representation of the mean date of occurrence (*MD*) for two series of events.

3 REGIONALISATION OF FLOODS USING SEASONALITY INDEXES

The seasonality indexes defined by Equations (2), or equivalently by Equations (3), and computed with respect to AMS of flood flows have been adopted in several recent regional flood frequency analyses as measures of hydrological similarity among catchments (Zrinji, Burn, 1996; Merz et al., 1999; Castellarin et al., 2001).
In particular Castellarin et al. (2001) evaluated the descriptive capability of several physical and climatic indexes to be used as indicators of hydrological similarity within a Region of Influence (ROI) approach (Burn, 1990). The authors considered a group of 36 unregulated catchments that are dislocated over a geographical area with a significant degree of homogeneity with respect to the flood regime (Figure 3-1). All 36 gauging stations have more than 15 years of observation and the average record length is 33 years.
Through a series of Monte Carlo experiments, the analysis proved that pooling the hydrometric information according to the similarities in the MDs of annual flood, as defined in Equations (2), could considerably improve the estimates of the design flood. Furthermore, the analysis seems to indicate that coupling the seasonality of annual flood with the seasonality of annual maximum daily rainfall for a given catchment into a single hydrological similarity measure could lead to additional improvements in the design flood estimation.
Some results of the Monte Carlo experiments are reported in Figures 3-2 and 3-3. The figures refer to three different estimators. WAS (Whole Area of Study) is a reference condition that uses under the index-flood hypothesis (Dalrymple, 1960) the hydrometric data collected over the entire area of study in estimating the design flood for each site in the region. MDF (Mean Date of Flood) estimates the design flood for a given location by pooling the hydrometric information with a Region of Influence

approach (Burn, 1990) from those sites with a *MD* of the annual flood that is similar to the *MD* of the site of interest. MDFR (Mean Dates of Flood and daily Rainfall) is analogous to MDF, but the pooling procedure simultaneously takes into account the *MD*s of the annual maximum flood and annual maximum daily rainfall (Castellarin et al., 2001).

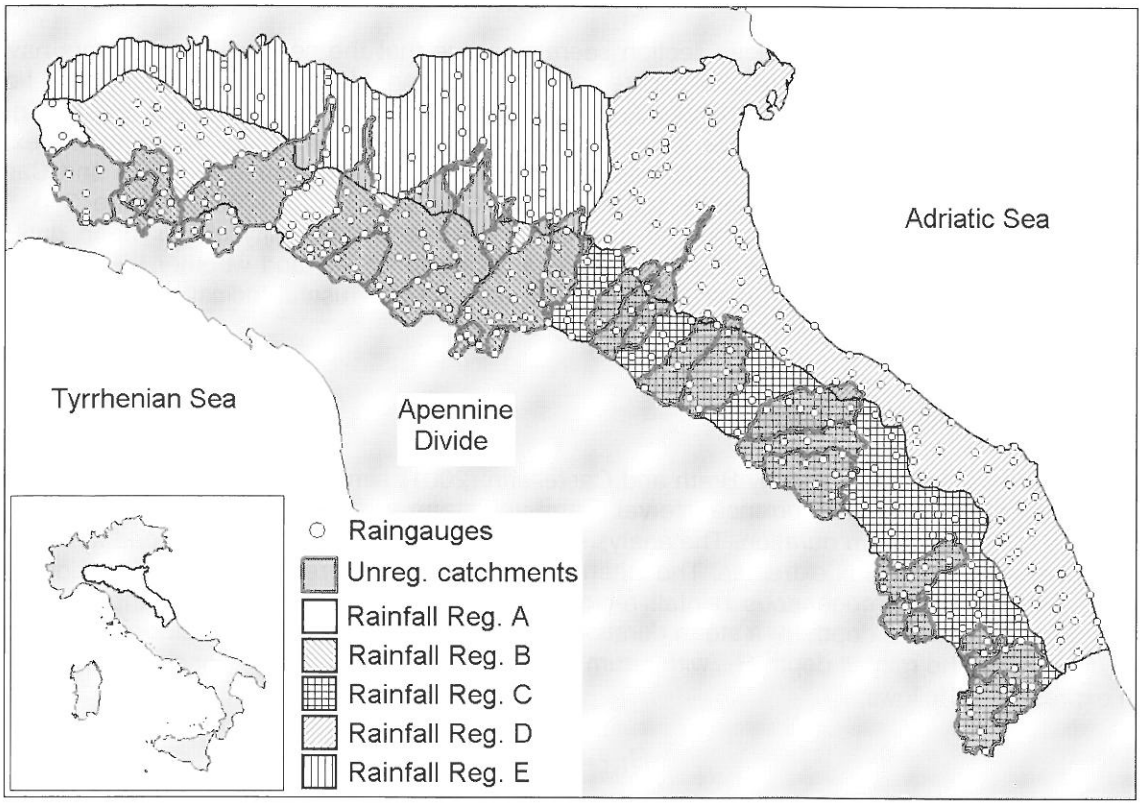

Figure 3-1: Area of study, 36 unregulated basins considered by Castellarin et al. (2001), raingauges measuring daily rainfall with at least 30 years of observed data; subdivision into rainfall regions.

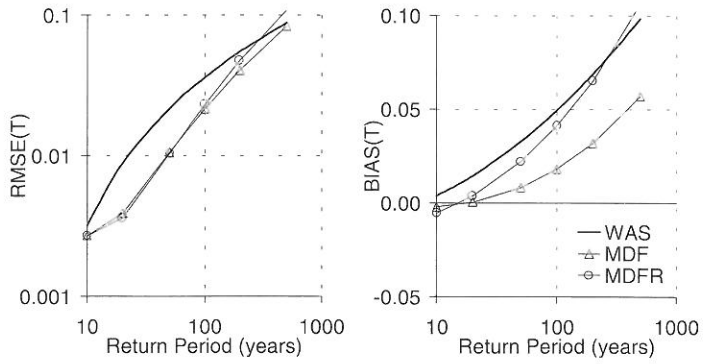

Figure 3-2: Average values over the study area of RMSE and BIAS as a function of the return period.

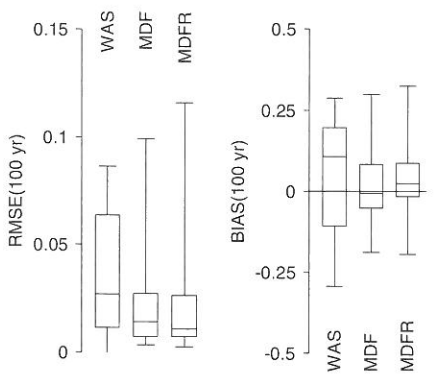

Figure 3-3: At-site values of the RMSE and BIAS for the 100-year design flood.

Figure 3-2 reports the average values over the entire study area of the relative mean squared error (RMSE) and BIAS for the design flood estimates as function of the recurrence interval. The diagrams of Figure 3-2 show quite evidently the superior overall performances of MDF and MDFR estimators with respect to the WAS estimator.

Figure 3-3 presents the distributions of the mean values of RMSE and BIAS obtained during the Monte Carlo experiments for the 36 considered sites by using the three different estimators of the 100-year design flood. The Box Plots of Figure 3-3 report the 25th, 50th and 75th percentiles, along with the minimum and maximum values. The better performances of MDF and MDFR with respect to the WAS estimator are highlighted by the box plot representation both in terms of RMSE and BIAS. Figure 3-3

shows for MDFR a higher median BIAS, but a lower median RMSE, and a lower dispersion in at-site performances than what is observed for MDF.

4 REGIONALISATION OF RAINSTORMS

The results presented in the previous section seem to prove that the seasonality indicators have a remarkable descriptive capability when they are used in the regional frequency analysis of flood flows. The result led to an examination of the possibility to efficiently employ the seasonality indexes in the regionalisation of precipitation extremes as well. This section of the paper briefly describes the extensive regional frequency analysis of rainfall depths that was recently performed by Brath and Castellarin (2001) for the same area of study considered by Castellarin et al. (2001) (Figure 3-1). The analysis' outcomes are then examined with respect to the spatial variability of the mean dates of occurrence of daily and hourly rainfall annual maxima, trying to understand whether the seasonality indicators defined by Equations (2), or Equations (3), may provide useful indications for the identification of homogeneous rainfall regions on the study area.

4.1 Regionalisation procedure

The regional analysis performed by Brath and Castellarin (2001) aims at providing reliable estimates of rainfall depth for a given recurrence interval T and any storm duration t ranging from 1 hour to 24 hours, and for a daily storm duration. The analysis adopts an extension of the index flood approach to the regionalisation of rainfall extremes. The extension of the approach relies on the subdivision of the area of interest into homogeneous rainfall regions, within which the probability distribution of the annual maximum rainfall depth for a storm duration t is invariant save for a scale factor represented by the index storm. The rainfall depth $R_{T,t}$ with return period T and storm duration t for a given location, is then expressed as follows,

$$R_{T,t} = m_t R'_{T,t} \tag{5}$$

where m_t is the scale factor of the examined site (the index storm), and $R'_{T,t}$ is the dimensionless growth factor, which has regional validity. A common choice for the index storm is the mean annual maximum rainfall depth with storm duration t.
The estimation of $R'_{T,t}$ requires the selection of an appropriate statistical model to be used as the parent frequency distribution, and the identification of a subdivision of the study area into homogeneous rainfall regions.
Concerning the selection of a suitable parent distribution, the regional frequency analyses developed for the Northern-Central Italy within the Research Project VAPI ("VAlutazione delle Piene"; Flood Estimation), activated by the NCR of Italy (see for instance Brath et al., 1998) have proven the Generalized Extreme Values (GEV; Jenkinson 1955) and the Two Components Extreme Value (TCEV; Rossi et al., 1984) distributions to produce reliable representations of the observed frequency distributions of annual rainfall extremes.
Regarding the identification of the homogeneous rainfall regions, the approach adopted consists of delineating contiguous and non-overlapping geographical areas according to morphological and climatic criteria, such as orography, valleys' orientation, closeness to the sea shoreline. The approach is hierarchically composed of two main steps (Gabriele, Arnell, 1991). The first step aims at identifying homogenous rainfall regions in which the skewness and kurtosis coefficients, or analogously their L-moment (Hosking, 1990) equivalents L-skewness and the L-kurtosis, can be assumed to have no spatial variability. The second step focuses on the subdivision of the study area into homogeneous rainfall sub-regions, within which also the coefficient of variation, or equivalently the L-CV, can be considered to be constant. The homogeneity testing of the hypothesized rainfall regions and sub-regions is based upon several statistical tests (see for example Brath et al. 1998), such as the Hosking and Wallis (1993) heterogeneity measure, or the χ^2 and *Kolmogorof-Smirnov* goodness-of-fit test among the observed frequency distribution of the coefficients of variation and skewness, or equivalently of L-CV and L-skewness, and the corresponding theoretical distributions obtained through Monte Carlo experiments.
Due to the high density of the Italian gauging network measuring daily rainfall, the procedure firstly identifies the homogeneous rainfall regions with respect to a storm duration t = 1 day. Afterward, the validity of this subdivision, as well as the applicability of $R'_{T,1day}$, is tested for the other storm durations

of interest. In case the validity of the assumptions defined for t = 1 day does not hold for some durations, the hierarchical approach is then performed again with respect to these storm durations.
The estimation of the scale factor m_t is straightforward for gauged sites having a sufficiently long observation record. In this case m_t can be easily evaluated as the average of the annual maximum rainfall depths with storm duration t. In case that the considered site is ungauged, one possible solution is to define an empirical indirect relation through multiregression analysis expressing m_t as a function of an appropriate set of geomorphoclimatic parameters. Due to the high spatial variability in the values of the index storm (Brath et al., 1998), this approach leads to significant fragmentation of the study area into small sub-regions, each one characterized by its own empirical relation. Because of this fragmentation, a more viable solution is to derive the index storm for the t and the location of interest from an isoline representation of m_t over the whole study area.

4.2 Case study

The study area, depicted in Figure 3.1, extends over 37,200 km^2. The boundaries are set by the Po River to the North, the Adriatic Sea to the East and the Apennine divide to the Southwest. The Northeastern portion of the study area is mainly flat, whereas the Southwestern and coastal part is predominantly hilly and mountainous. The Adriatic portion presents an elementary morphology where the main streams are primarily oriented perpendicularly to the shoreline and parallel to one another. The valleys of the Northwestern region run perpendicularly to the Apennine divide and the main rivers flow from the Southwest to the Northeast and are tributaries of the Po River.
The extreme Southwestern portion of the study area is very close to the Tyrrhenian shoreline and is characterized by altitudes inferior to 1000 m a.s.l., therefore lower than the surrounding Apennine relieves that have peaks around 1800-2000 meter a.s.l.. This natural window facilitates the surmounting of the Apennine Divide for the atmospheric disturbances originated over the Tyrrhenian Sea. Such disturbances can exert their meteorological influence upon a wide portion of the Southwestern extremity of the study area, thus affecting significantly the local regime of extreme rainfall events.
The observed rainfall data consist of the annual rainfall extremes with duration t = 1, 3, 6, 12, 24 hours and 1 day collected by the National Hydrographic Service of Italy (SIMN). Table 4-1 describes the number of raingauges and the corresponding station-year of data for different values of the minimum record length, whereas the location of the raingauges with more than 30 years of observation is depicted on Figure 3-1.

4.3 Analysis' results and indications inferable from seasonality indexes

4.3.1 Daily rainfall

The identification of rainfall regions was performed with respect to raingauges with more than 30 years of observation of daily rainfall (Table 4-1), and it produced the zoning reported in Figure 3-1. The results of the statistical tests mentioned in section 4.1 seem to indicate that the Regions A, D, E and the merger of Regions B and C can be regarded as homogeneous at the first hierarchical level (i.e., constant skewness, or L-skewness within the region), and all 5 regions can be separately considered to be homogeneous at the second hierarchical level (i.e., constant CV, or L-CV within the region).
The zoning presented in Figure 3-1 is only one of the several subdivision hypotheses that were tested during the analysis, and its delineation originates from the following considerations about physical and climatic patterns of the area. Regions A, B and C are predominantly hilly and mountainous regions, and they are separated from Regions D and E by a boundary that is coincident with the 200 m a.s.l isoline. Region A is an Apennine region, like Regions B and C, yet it was separated from Region B because of the strong influence exerted on its rainfall regime by the Tyrrhenian disturbances overpassing the Apennine divide. The lower altitudes that characterise Region A and its closeness to the shoreline can justify this assumption. The separation between Regions B and C at the second hierarchical level is likely to be a consequence of the effect of the Adriatic Sea on the extreme rainfall regime of Region C. Region D is mainly a coastal area, whereas Region E is an inland and largely flat area, whose annual rainfall regime is mainly conditioned by the disturbances coming from Northeast (Brath, Castellarin, 2001).
In order to get a clearer perception of the real differences existing among the annual maximum daily rainfall regimes of the five homogeneous rainfall regions, Figure 4-1a depicts the dimensionless regional growth factor, $R'_{T,t}$, as a function of the recurrence interval, the so-called dimensionless growth

curve. The growth curves of Figure 4-1a were identified for the different rainfall regions by considering the GEV distribution (Jenkinson, 1955) as a parent distribution (Brath, Castellarin, 2001).

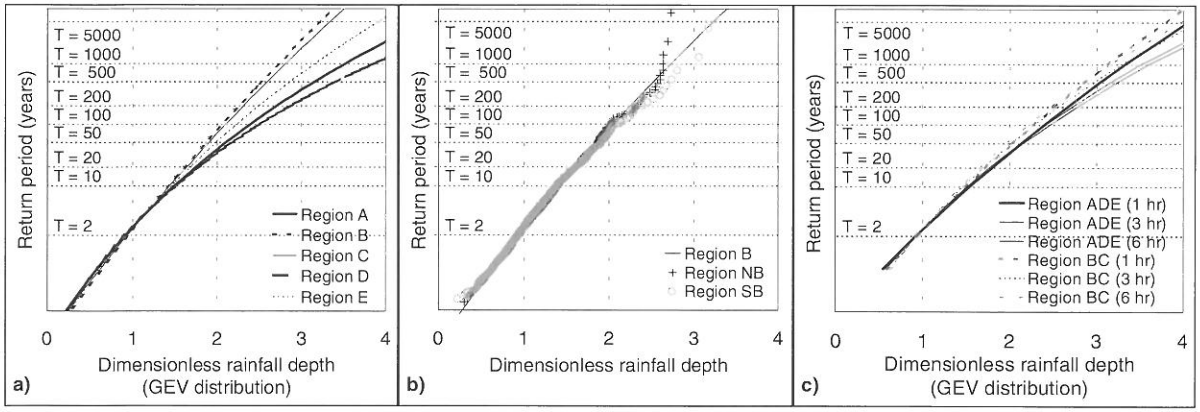

Figure 4-1: **a)** Dimensionless daily growth curves relative to the rainfall regions A, B, C, D and E;
b) sample frequency distributions of the AMS of dimensionless daily rainfall for Regions NB and SB;
c) dimensionless hourly growth curves relative to the macro-regions ADE and BC.

4.3.2 Seasonality of annual maximum daily rainfall

Figure 4-2a depicts the spatial variability of MDs, defined by Equations (3), over the study area. Each vector on Figure 4-2a represents the MD computed with respect to the AMS of daily rainfall depths for a given raingauge. The raingauges having a record length longer than 30 years were the only stations considered in the evaluation of the seasonality indexes. For any given vector of Figure 4-2a, the angle between the vector and the East represents the mean date of occurrence $\overline{\theta}$, whereas the vector magnitude is proportional to the measure of regularity *r*.

The analysis of Figure 4-2a does not show a clear pattern for the Northern portion of the study area (i.e., flat and hilly areas). The vectors present remarkably different directions and magnitudes, proving a weak homogeneity in the seasonality of the phenomenon. Considering the Northwestern portion of the Apennine divide (i.e., mountainous areas), the vectors show similar orientations and magnitudes, which indicates a higher degree of homogeneity in the seasonality of the phenomenon.

The identification of general patterns in the variability of seasonality indexes for the Southeastern portion of the study area is even more difficult.

The geographical variation of the MDs reported on Figure 4-2a does not justify nor support the zoning of Figure 3-1, that is also reported on Figure 4-2a. In fact, *1)* the mean values of MD for the five rainfall regions are quite close to one another; *2)* the distribution of MD values on Figure 4-2a does not account for the borderline between

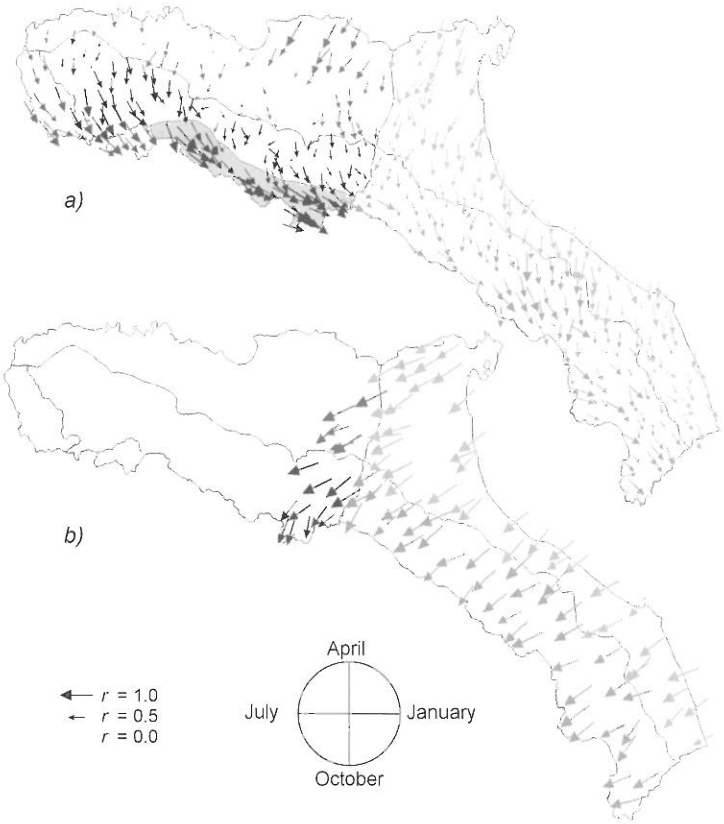

Figure 4-2: MDs for the AMS of rainfall depths with 1-day (a) and 1-hour (b) storm duration.

Regions B and E and Regions C and D. This borderline moves along the 200 m a.s.l. isoline and separates the mountainous portion of the study area from the hilly and flat lands. The annual maximum daily rainfall depths in these two zones have markedly different frequency distributions, as shown in Figure 4-1a. *3)* Figure 4-2a does not corroborate the location of the boundary between Regions A and B that arises from morphological and climatic considerations, and separates two zones with an evidently different regime of extreme daily precipitations as previously mentioned (Figure 4-1a).

Table 4-1: Rainfall gauging network information for different values of the minimum record length.

	min. rec. length: 15		*min. rec. length:* 30	
	raingauges	station-year	raingauges	station-year
Daily rainfall	619	25904	419	21616
Hourly rainfall	209	7905	132	6283

So far, the seasonality indexes do not seem to be particularly useful in the identification of areas with different regimes of rainfall extremes. In order to better investigate this point it was deemed useful to perform further analyses that were suggested by the presence within Region B of an area with a visible pattern in the seasonality indexes. Within a geographical belt located along the Southern border of Region B, close to the Apennine divide, the MDs of the AMS of daily rainfall present a rather high regularity (i.e., high vectors' magnitude) and the mean timings (i.e., vectors' directions) concentrated around the beginning of December (Figure 4-2a).
The analysis considered and tested several different hypotheses for partitioning Region B into two different sub-regions with different seasonality regimes, yet the remainder of the paragraph refers only to the hypothesis that resulted to be the most descriptive. This option splits Region B into a Southern (i.e., grey area on Figure 4-2a) and a Northern sub-region, hereafter referred to as Regions SB and NB respectively.
Figure 4-3 reports the MDs of Region B as points on a polar chart instead of vectors, highlighting which point belongs to the Region NB (+) or Region SB (o). The seasonality regimes for the two sub-regions are rather different. The clouds relative to each different sub-region are almost separated from one another, and the positions of the clouds' centroids, with markedly different timings (i.e., angle formed with the x axis) and regularities (i.e., distance from the polar chart origin), prove rather evidently that Region SB is characterised by a stronger seasonality of annual maximum daily rainfall with respect to Region NB.
Table 4-2 collects the number of raingauges, the station-year of data and the Hosking and Wallis (1993) measures of heterogeneity, H_1, H_2 and H_3, for the whole Region B and for the two sub-regions. It is useful to recall here that the measure H_i provides indications about the heterogeneity of a group of sites by measuring the dispersion of the sample L-moments around the regional L-moments values, and comparing it to the variation that would be expected in a homogeneous group because of sample variability. In particular, H_1 refers to dispersion of the sample L-CV, H_2 to the joint dispersion of L-CV and L-skewness and H_3 the joint dispersion of L-skewness and L-*kurtosis*. Hosking and Wallis suggest that a group of sites may be regarded as "acceptably homogeneous" if $H_i < 1$, "possibly heterogeneous" if $1 \leq H_i < 2$, and "definitely heterogeneous" if $H_i \geq 2$.
Table 4-2 shows that Region B and sub-region NB have similar values of H_i, whereas Region SB, characterised by a high homogeneity in the seasonality of daily rainfall annual maxima (see Figure 4-2a), exhibits a higher homogeneity degree in terms of H_1 but a lower one in terms of both H_2 and H_3.

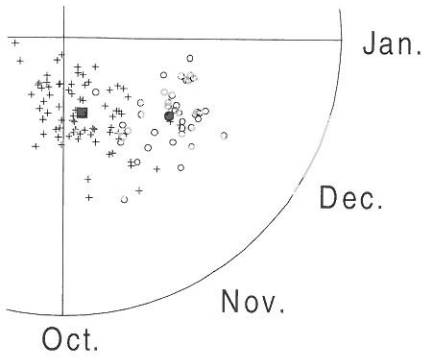

Figure 4-3: MDs for the AMS of daily rainfall depths of Region NB (+) and Region SB (o); regional MDs (•-Region NB, •-Region SB).

The lower value of H_1 obtained for Region SB might be a sign of the sub-region higher degree of homogeneity in terms of L-CV with respect to the whole Region B, but it also might be a consequence of the smaller size of the sub-region. Two bootstrap resampling experiments were designed and performed in the analysis in order to shed some light on this problem. Each experiment allowed us to randomly generate 1000 sub-regions of Region B with sample-size similar to Region SB, and to sub-

sequently measure the synthetic sub-regions' homogeneity degree by means of the Hosking and Wallis test.
The first experiment, bootstrap#1, randomly collected 38 raingauges within region B 1000 times, 38 being the number of sites included in Region SB (Table 4-2). The second experiment, bootstrap#2, randomly selected 1000 pooling groups from Region B with a variable number of raingauges and a station-year of rainfall data ranging between 1920 and 1930, where 1925 is the Region SB station-year of data (Table 4-2).

Table 4-2: Number of raingauges, station-year of data and Hosking and Wallis (1993) heterogeneity measures for Region B and sub-regions NB and SB.

	Raingauges	Station-year	H_1	H_2	H_3
Region B	112	5471	0.39	-0.83	-0.78
Region SB	38	1925	0.14	0.45	0.18
Region NB	74	3546	0.41	-0.15	-1.22

Table 4-3 reports the mean values of H_i obtained from the two bootstrap resampling experiments. These values seem to prove that randomly selecting pooling groups of raingauges within Region B generates, on average, sub-regions that are more homogeneous (H_2 and H_3) or as homogeneous as (H_1) Region SB, which was delineated through the exam of the seasonality characteristics. For each bootstrap experiment, the box-plots of Figure 4-4 present the distributions of the H_1, H_2 and H_3 values relative to the 1000 synthetic regions and allow a comparison of these distributions with the H_1, H_2 and H_3 values characteristic of Region SB (•). Each box-plot reports the minimum and the maximum values of H_i along with the 25th, 50th and 75th percentiles. One noticeable observation is that for both of the bootstrap experiments a random choice of raingauges within Region B produces pooling groups that have a higher homogeneity degree in terms of L-CV than Region SB in the 50% of the cases, and even more often for the higher order L-moments (i.e., around 90% of the cases for H_2 and 80% of the cases for H_3). Figure 4-1b shows the sample frequency distributions of the dimensionless annual

Table 4-3: Number of raingauges, station-year of data and Hosking and Wallis (1993) heterogeneity measures for two different bootstrap resampling experiments.

	Raingauges	Station-year	H_1	H_2	H_3
Bootstrap#1	38	variable	0.21	-0.51	-0.45
Bootstrap#2	variable	1925 ± 5	0.17	-0.46	-0.41

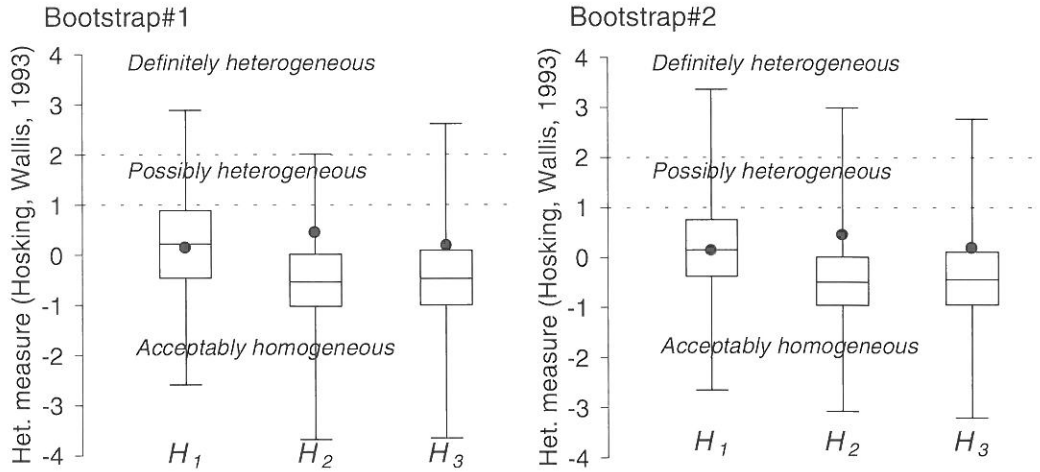

Figure 4-4: Heterogeneity measures for the AMS of daily rainfall observed within Region SB (•), and box-plot representations of the distributions of H_i values obtained through bootstrap experiments.

maximum daily rainfall depths observed within Regions NB (o) and SB (+), together with the dimensionless growth curve of Region B. Figure 4-1b illustrates without ambiguity the limited differences among the two sample frequency distributions, which become negligible for recurrence intervals lower than 200 years.

Quite surprisingly, the analysis seems to prove that seasonality indexes have a very little utility in the identification of homogeneous rainfall regions, if they have any utility at all, with respect to the study area and AMS of daily rainfall.

4.3.3 Hourly rainfall

The validity of the zoning identified for annual maximum daily rainfall and the applicability of $R'_{T,1day}$, were tested for the hourly storm duration of interest (i.e., 1, 3, 6, 12 and 24 hours). The test results indicate that the zoning hypothesis presented on Figure 3-1 and the growth curves depicted on Figure 4-1a still hold for storm durations higher than or equal to 12 hours (Brath, Castellarin, 2001).
On the contrary, the results of the statistical tests performed for the 1, 3 and 6 hr storm duration indicated the need to re-identify the regional growth curves. Given the need to re-identify the regional growth curves it was also deemed interesting to revise the subdivision into homogeneous rainfall region for shorter storm durations.
Several studies suggest that the dimensionless frequency distribution of annual rainfall extremes for short storm duration (i.e., $t \leq 60$ min) can be considered to be independent of geographical location (Alila, 2000). Supported by these considerations, the homogeneity degree of several mergers of the five rainfall regions depicted in Figure 3-1 was statistically tested for $t = 1 \div 6$ hr. This phase of the analysis produced two main results. First, the hypotheses of assuming the entire region of study to be homogeneous at the first hierarchical level for $t = 1$ hour, and for $t = 3 \div 6$ hours were found to be acceptable according to all tests performed. Second, two macro-regions consisting of the mergers of Regions A, D and E (Macro-region ADE) and Regions B and C (Macro-region BC) appeared to be homogeneous for each one of the considered hourly storm durations (i.e., $t = 1$, 3 and 6 hours). Figure 4-1c shows the dimensionless hourly growth curves identified for the macro-regions ADE and BC by considering the GEV distribution.

4.3.4 Seasonality of annual maximum hourly rainfall

Figure 4-2b presents the MDs of AMS of rainfall depth with 1-hour storm duration for the Eastern portion of the study area. Unfortunately during this study it was impossible to include in the database the dates of occurrence of hourly rainfall AMS for the Western portion. Nevertheless, the comparison between the Eastern portions of the study area on Figures 4-2a and 4-2b shows a remarkable difference in the timing and regularity of the two phenomena. Figure 4-2b reveals a high degree of homogeneity in the spatial variability of MDs. The vectors of Figure 4-2b have magnitude close to one, which is the theoretical case for events with all identical dates of occurrence, and they show a timing that ranges between the end of July and the beginning of August. This is consistent with the observation that in the study area the hourly rainfall extremes are almost invariantly summer showers generated by local convective cells.
The strong homogeneity of hourly rainfall MDs over the study area could be consistent with the assumption of a lower variability of the dimensionless frequency distributions of annual rainfall extremes for short storm durations. However, the conclusions of the analysis relative to daily rainfall extremes presented in the previous paragraph advise to be careful in founding considerations regarding the frequency regime of rainfall extremes upon the seasonality of the phenomenon.

5 CONCLUSIONS

This paper analyses the effectiveness of using simple seasonality indexes of hydrological extreme events in a regional frequency analysis framework to identify homogeneous pooling groups of gauging stations. The analysis was performed over a wide geographical area of Northern-Central Italy and considered both the regionalisation of flood flows and the regionalisation of rainstorms.
In particular, through a series of Monte Carlo experiments it was shown that the incorporation of information regarding the seasonality of annual flood in the homogeneous region identification process produces for the 36 unregulated catchments of the study area improved regional estimates of the design flood. Furthermore, combining together the seasonalities of annual flood and annual maximum rainfall depth seemed to have a positive effect on the identification of homogenous groups of hydrometric stations.

Subsequently the study focussed on the regional frequency analysis of rainstorms for the same study area, aiming at establishing whether the seasonality indexes of annual maximum series of rainfall depths may be effectively employed to identify homogeneous rainfall regions. The results of the analysis are quite surprising and seem to contrast with the findings relative to the regionalisation of flood flows. Considering the daily rainfall extremes the analysis showed that the patterns visible for the spatial variability of seasonality indexes do not appear be connected with the patterns in the regime of annual maximum daily rainfall. The results of a series of bootstrap resampling experiments seem to corroborate these considerations.
Due to an intrinsic high degree of homogeneity in the occurrence characteristics of the annual maxima of hourly precipitation, it was impossible to detect any pattern at all in the spatial variability of seasonality indexes when considering hourly storm duration. Therefore, the seasonality indexes offered very little indications in the identification of homogeneous rainfall regions also for hourly storm durations.

REFERENCES

Acreman, M.C., Sinclair, C.D. (1986): Classification of drainage basins according to their physical characteristics and application for flood frequency analysis in Scotland. J. Hydrol., vol.84(3). Elsevier. Amsterdam, NL

Alila, Y. (2000): Regional rainfall depth-duration-frequency equations for Canada. Wat. Resour. Res., vol.36(7). AGU. Washington, USA

Bates, B.A. et al. (1998): Climatic and physical factors that influence the homogeneity of regional floods in Southern Australia. Water Resour. Res., vol.34(12). AGU. Washington, USA

Bayliss, A.C., Jones, R. C. (1993): Peaks-over-threshold flood database: summary statistics and seasonality. Rep. 121. Inst. of Hydrology. Wallingford, UK

Brath, A. et al. (1998): Valutazione delle piogge intense nell'Italia centrosettentrionale (in Italian). L'Acqua, vol.4. All. Rome, Italy

Brath, A. et al. (2001): Estimating the index flood using indirect methods. Hydrol. Scienc. J., vol.43(6). IAHS Oxford, UK

Brath, A., Castellarin, A. (2001): Tecniche di affinamento delle previsioni regionali del rischio pluviometrico (in Italian). La progettazione della difesa idraulica. BIOS. Cosenza, Italy

Burn, D.H. (1990): Evaluation of regional flood frequency analysis with a region of influence approach. Wat. Resour. Res., vol.26. AGU. Washington, USA

Castellarin, A. et al. (2001): Assessing the effectiveness of hydrological similarity measures for regional flood frequency analysis. J. Hydrology, vol.241(3-4). Elsevier. Amsterdam, NL

Dalrymple, T. (1960): Flood frequency analyses. Wat. Supply Paper 1543-A, USGS, Reston, VA USA

Gabriele, S., Arnell, N. (1991): A hierarchical approach to regional flood frequency analysis. Wat. Resour. Res., vol.27(6). AGU. Washington, USA

Hosking, J.R.M. (1990): L-moments: analysis and estimation of distributions using linear combination of order statistics. J. Royal Statistical Soc. Series B., vol.52(1). RSS. London, UK

Hosking, J.R.M., Wallis, J.R. (1993): Some statistics useful in regional frequency analysis. Wat. Resour. Res., vol. 29(2). AGU. Washington, USA

Jenkinson, A.F. (1955): The frequency distribution of the annual maximum (or minimum) of meteorological elements. Quarterly J. of the Royal Met. Society, vol.81. RMS. London, UK

Mardia, K.V. (1972): Statistics of directional data. Academic Press. New York, NY USA

Merz, R. U. (1999): Seasonality of flood processes in Austria. Proc. '99 Symp. IAHS. Birmingham, UK

Rossi, F. et al. (1984): Two component extreme value distribution for flood frequency analysis. Wat. Resour. Res., vol.20. AGU. Washington, USA

Zrinji, Z., Burn, D.H. (1996): Regional flood frequency with hierarchical region of influence, J. Water Resour. Plann. Manag., vol. 122(4). ASCE. New York, USA

USE OF MESOSCALE WEATHER FORECASTING FOR EARLY FLOOD WARNING ON EUROPEAN SCALE

A. de Roo, J. Thielen, B. Gouweleeuw and G. Schmuck

European Commission, DG Joint Research Centre, Institute for Environment and Sustainability, TP 261, 21020 ISPRA (VA), Italy, ad.de-roo@jrc.it

SUMMARY

The European Flood Forecasting System project (EFFS) aims at developing a prototype of an integrated European flood forecasting system. This Pan-European early flood warning system is to provide National Water Authorities, Civil Protection Authorities and international aid-organisations with a large lead-time to prepare for possible flood crises. The broad objectives of the still ongoing project are to use operationally available short and medium-range weather forecasts available from National Weather Authorities and the European Centre for Medium-Range Weather Forecasts (ECMWF) to increase the lead time for reliable flood warnings from a maximum of 3 days at present to 4-10 days and beyond in the future, to design a medium-range flood forecasting system for the whole of Europe, and to produce flood forecasts in regions where at present no flood forecasts are made on the basis of the newly developed system.
The two core elements of the EFFS are the state-of-the-art meteorological numerical weather predictions and the hydrological modelling system LISFLOOD. The constraints of the project are mostly with data availability at a European scale, such as cross sections. Other constraints are the within-grid variability and the downscaling problem of the weather forecasts.
First results of EFFS are very encouraging. Waterbalance simulations over a period of 10 years show that on a daily timestep the model performs very well for those catchments that are mostly affected by larger scale and synoptic rainfalls, while for those catchments that are often dominated by local rainfalls, e.g. in the mountainous terrain of the Alps and the Pyrenees, the agreement is less good. From the preliminary results obtained so far it appears that it is not with one single forecast that a flood warning can be issued, but with the total of the different meteorological predictions using different resolutions and initial conditions.

Keywords: Europe, Flood Forecasting, EFFS, LISFLOOD, medium-range forecasts, ensemble forecasts

1 INTRODUCTION

In the last decade Europe has experienced a number of unusually long-lasting rainfall events that produced severe floods, e.g. in Meuse and Rhine (1993, 1995), Oder (1997), several rivers in North Italy (1994, 2000) and in the UK (e.g. 1998, 2000). The trend seems to be continuing in the new millennium which started with severe and exceptional rainfalls: according to the WMO statement on the status of the global climate in 2001 (WMO, 2001), in England in Wales the 24-months period ending in March 2001 was the wettest in the 236-year time series of precipitation. October 2000 to March 2001 precipitation was also exceptional in the Bretagne region in France, where the normal annual rainfall was exceeded by 20 to 40% in parts of the region. In the East, a third consecutive year of severe flooding occurred in Hungary and parts of Eastern Europe in March - the Tisza river reached its highest level in more than 100 years, the previous record was set in 1888. The worst flooding in Poland since the 1997 floods occurred in July after two weeks of heavy rain caused flooding in the Vistula river. The summary of events seems to support projections of future climate indicating that further increase in severe floods in North and Northwest Europe are likely (e.g. IPCC, 1997). If the recent climate projections are correct, flood forecasting and flood prevention will become an import issue for the environment, civil protection, and also the economy in case of repeated damage through floods.
In Europe flood forecasting is done on national scale or regional scale and not on catchment scale. As a consequence, for most trans-national countries the National Water Authorities depend on measured discharge of the upstream country. This reduces the forecasting lead time to the travel time between the upstream measurement locations and the downstream area of interest. Any longer forecast would be unreliable, because integrated flood modelling that can also incorporate the hydrological processes in the upstream country is not possible.
Typically flood forecasting lead-times are of the order of 2 to 3 days. In many cases, however, an increased warning time could be beneficial to civil-protection Agencies and National Water Authorities,

e.g. for staff allocation before and during a crisis or increased data collection and preparation time. One way to increase the lead-time for flood forecasts is to use an integrated approach by simulating floods on catchment scale. The hydrological model system LISFLOOD (De Roo et al., 2000a) has been developed explicitly for the simulation of floods in large European drainage basins. It has been tested and validated for the 1995 Meuse and the 1997 Oder floods (De Roo et al., 2000c). Within the framework of the ongoing research project EFFS (European Flood Forecasting System) it is now studied if its application to the whole of Europe is feasible. The main advantage of working with very large integrated catchments is that it allows to make use of the comparatively coarse meteorological forecasting data. In particular the medium-range weather forecasts from the European Centre for Medium-Range Weather Forecasts (ECMWF) are still hardly used for practical flood forecasting because their spatial resolution of 40 km is too coarse compared with the size of an average European catchments. However, in combination with a flood forecasting model on a European scale, they can potentially increase the lead time for qualitative early flood warnings up to 10 days in advance.
Another new aspect of the EFFS project is the incorporation of so-called Ensemble Prediction System (EPS) into the flood forecasts. EPS has been part of the operational ECMWF forecasts since 1992. They are designed to simulate possible initial uncertainties by adding, to the unperturbed analysis, small perturbations within the limits of uncertainty of the analysis (Molteni et al., 1996). From these, at present 50 so-called ensembles are produced. One of the atmospheric situations in which uncertainty is often greatest is potentially severe weather events (Legg and Mylne, 2001) such as heavy or prolonged precipitation events and storms. It is, however, exactly these events that may cause flooding and that have to be considered.
In the following first the LISFLOOD model is described, followed by a description of the EFFS in Section 3. Several results are shown and discussed in Section 4, and the paper is concluded in Section 5 with a summary of the presented results.

2 THE HYDROLOGICAL LISFLOOD MODELLING SYSTEM

2.1 Background

LISFLOOD is a model that has been developed explicitly for the simulation of floods in large European drainage basins. Unlike most other hydrological models – such as MIKE-SHE (Abbott et al., 1986), TOPMODEL (Beven & Kirkby, 1979) or HBV (Lindstrom et al., 1997) -, it is capable of simulating large areas, while still maintaining a high resolution, proper flood routing methods and physical process descriptions. Since the physical process descriptions are universal, no or little additional calibration is needed if applied in a new catchment. LISFLOOD is also especially designed to simulate the effects of change in a easy and realistic way: land-use changes, modifications of the river geometry, water reservoirs, retention areas and effects of climate change. LISFLOOD is embedded in a GIS and is using readily available European datasets, such as Corine Land Cover, the European Soils Database, and the 1km resolution European Flow Network (De Roo et al., 2000b) and used as a basis for the pan-European Catchment Information System (CIS).

2.2 Set-up and simulated processes

LISFLOOD simulates the hydrological processes at the surface, in the soil, and in the river channel network on a regular horizontal grid (Figure 2-1), usually using a high resolution compared to the catchment size: LISFLOOD can easily handle 100,000 grids or more. In the vertical a total of 4 different layers are considered. For each grid point a value is calculated at every time step.
The theory of the model is described in detail in publications from De Roo et al. (2000a), De Roo et al. (2000c) and De Roo et al. (2001). In the following, only the basic processes are summarised

- At the surface, the predominant processes are the division of precipitation into rainfall and snow, snowmelt, glacier flow, interception by vegetation and evapotranspiration. Seasonal variations of the vegetation cover are also taken into account. The amount of effective precipitation is divided into overland flow and infiltrated water.
- In the soil, LISFLOOD calculates the vertical transport of water in two soil layers. The flow rate depends on soil parameters such as soil texture. The percolation to the groundwater and storage of groundwater is also simulated. Also, lateral subsurface flow is simulated.
- The routing of overland flow water and river water can be calculated with a kinematic wave or a dynamic wave, depending on data availability and channel bed gradient. LISFLOOD can also

simulate special structures such as water reservoirs and retention areas by giving their location, size and in- and outflow boundary conditions (maximum storage volume, minimum and maximum outflow, reservoir management parameters).

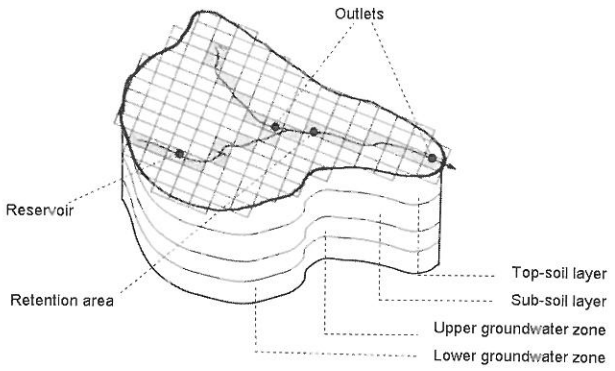

Figure 2-1: Schematic view of a catchment in LISFLOOD including two soil layers and two groundwater zones.

2.3 INPUT AND OUTPUT DATA

Meteorological input data can either be given as point data (from weather stations) or as gridded data (as from radar measurements or meteorological forecast models). Other input data are needed to define the surface (topography, slope gradient) and the canopy (land-use, leaf area index, rooting depth), the soil (soil texture, soil depth, Manning coefficient), and the channel network (dimensions of the channel and the floodplain such as width and depth, bedslope, Manning). The rule holds that the better the quality of the input data the better the model results. Inputs used are readily available European datasets such as Corine Land Cover, a 1km resolution DEM, a 1km resolution European Flow Network (De Roo et al., 2000b), the 1M and 250k scale European Soils Database (European Soils Bureau, 1998), the HYPRES soil hydraulic properties database, and the JRC-MARS meteorological database.
The LISFLOOD output can be any variable calculated by the model. The format can be hydrographs at user-defined locations in the catchment - usually those locations where also observations exist, time-series of for example evapotranspiration, soil moisture content or snow depth, and maps such as water source areas, discharge coefficient, total precipitation, total evapotranspiration, total groundwater recharge and soil moisture maps (Figure 2-2).

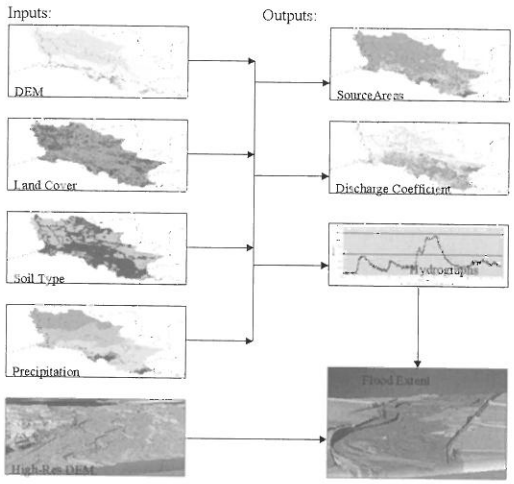

Figure 2-2: Examples of LISFLOOD input and output data.

LISFLOOD is programmed and embedded in the PCRaster GIS dynamic modelling language (Wesseling et al, 1996), which makes the model user-friendly and its results easy to export and to compare with other data sources. Depending on the time step, LISFLOOD can operate as a waterbalance model (daily time step, simulating time periods of the order of one to several years) and as a flood

simulation model (hourly time step, simulating time periods of the order of days to weeks). The waterbalance model can either stand alone or serve to provide the initial conditions for the flood model. Coupled to the flood simulation model LISFLOOD can also be a flood plain inundation model, which then calculates with a time step of the order of seconds how a floodplain may be inundated during a flood (time period of the order of 1 hour to days) (Bates & De Roo, 2000).

2.4 Model validation

LISFLOOD has been extensively tested for several transnational catchments – amongst them the Meuse and the Oder. Figure 2-3 illustrates with one example for the Ourthe sub-catchment of the Meuse how well the model performs as a waterbalance model with a daily timestep when it is initialised with high-resolution measured rainfall data. For a catchment size of 1618 km^2 data of 38 raingauges were available. For this case study the LISFLOOD model is set-up with a grid resolution of 300 m and run with a daily time step. Obviously the model captures very well the dynamics of the time series, and also represents the quantity of the discharge during the peak flow as well as the low flow. This is particularly true for the major flood events of December 1993 and January 1995. It is possible that some peaks that are not simulated by LISFLOOD, e.g. in January 94, result from local convective storms that are not captured by the meteorological network.

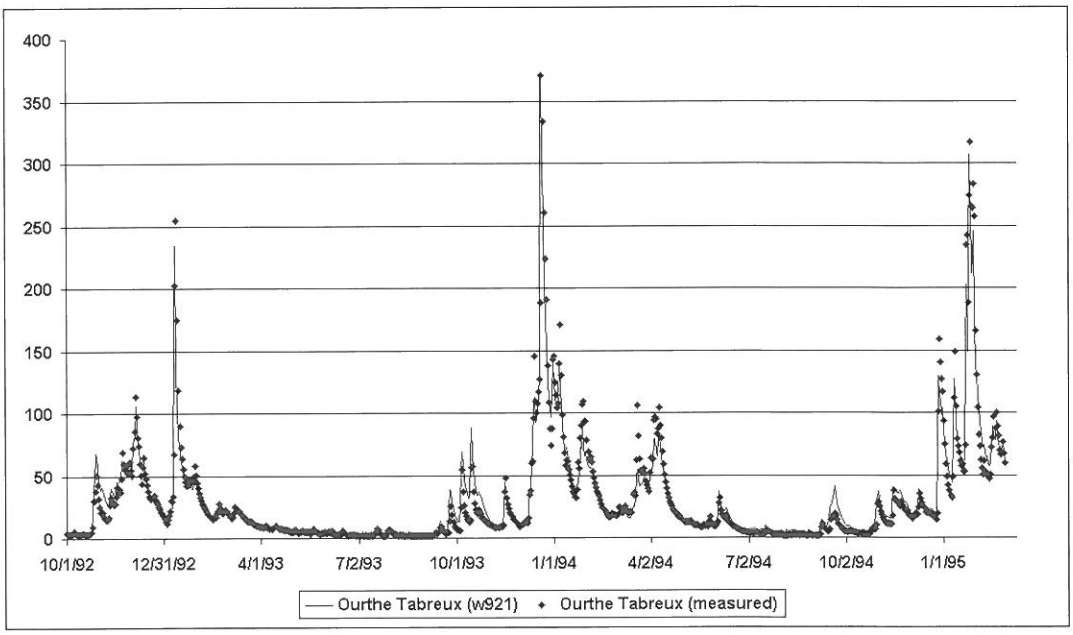

Figure 2-3: Comparison between measured discharge and simulation for the Ourthe sub-catchment of the Meuse at Tabreux for the time period October 1992 - February 1995. Measured discharge is shown as dots and LISFLOOD simulations as lines. (a) using high resolution rainfall data, and (b) using data from the synoptic network only.

3 THE CONCEPT OF A EUROPEAN FLOOD FORECASTING SYSTEM

3.1 Objectives and broad aims

The objective of the European Flood Forecasting System (EFFS) project (2000-2003) is to produce pre-warnings of possible flood events up to 10 days in advance for all medium to large size catchments in Europe (>5000 km^2). It is the first attempt to combine state-of-the-art expertise in meteorology and hydrology on European scale. One of the aims of the project is to assess the feasibility of such an approach and to determine to what extent the lead time for qualitatively and quantitatively satisfactory flood predictions can be increased in the major catchments.

3.2 Brief description of the set-up

The two core elements building the EFFS are the 10-day numerical weather forecasts from the European Centre of Medium-range Weather Forecasting (ECMWF) and the LISFLOOD model. The system is being developed in close collaboration with leading European meteorological services (ECMWF, DMI, DWD), water authorities (RIZA, SHMI, GRDC), and research institutes and organisations (Delft Hydraulics, JRC, University of Bologna, Bristol University, Lancaster University). Other local models can also be incorporated into the EFFS, for example results from the HBV model for the Rhine will be made available within the EFFS, but only LISFLOOD simulates floods on European scale.
In addition to the predicted discharge, information on the uncertainty of the prediction is incorporated. This uncertainty can arise from both the meteorological forecast and from the hydrological model. The uncertainty regarding the meteorological model data is captured by simulating the flood risk with the deterministic forecast (grid resolution 40 km), and the whole set or a selection of ensemble forecasts (total set of 50 ensembles or selected cluster representatives, grid resolution 80 km, slightly varying input conditions that are newly defined with every forecast day). The uncertainty from the hydrological model and the combined forecasting system is assessed using the GLUE approach (Binley & Beven, 1991).
For the EFFS project three historic flood events have been selected, the January 1995 Meuse and Rhine flood, the July 1997 Oder flood, and the October 2000 UK and Po flood. The meteorological services are rerunning their models for these past events, producing so called hindcasts. The Danish and German National Weather Authorities (DMI and DWD) are providing these hindcasts using their limited area models (LAM) with lead times up to 3 days ahead with a 11 and 7 km grid resolution respectively for the whole of Europe. The ECMWF hindcasts are provided on a 40 km grid for a forecasting period up to 10 days at intervals of 6, 12, and 24 hours depending on the forecasting lead time.

3.3 Problems with data availabitlity and quality

The system runs on 5 km for the whole of Europe and on 1km for two test catchments, the Meuse and the Oder. These have been chosen because high resolution and good quality input data such as topography, soil data, land use or channel parameters are available. This allows a detailed validation of the EFFS results and an estimation of its performance. For the 5 km grid the preparation of the input data is more problematic, first, because data such as channel dimensions are at this stage of the project not available within the project for all rivers, and second, because discharge data to compare the EFFS results with are also not made available for the project for all catchments or the whole time span. It is hoped that once the EFFS has shown positive results, that more data will be contributed for the system by the individual countries. The lacking input data is approximated using empirical functions derived from existing data. An example is channel width, which is calculated using the upstream contributing area. As yet, the approximations are applied to all catchments, thus also for the Meuse and the Oder catchment, and are not replaced with available higher quality data, allowing to test the sensitivity of the model results to some of the input parameters.
Another issue that cannot be dealt with at this stage is the influence of regulating measures, such as reservoirs or weirs. LISFLOOD can simulate both, but the necessary data – location, geometry, management rules - are lacking. It can be expected that for heavily controlled rivers the simulations will be overestimating the number of peaks because artificial lowering of the water levels are not considered.

4 MODEL RESULTS

4.1 The European Waterbalance

As mentioned in the description of the LISFLOOD model, the waterbalance simulations provide the input conditions for the flood model. Ideally the waterbalance runs at least one year before the flood event to provide initial conditons for the flood forecasting model. To do this within EFFS a coherent meteorological data set including precipitation, temperature, humidity and wind data for the whole of Europe over the period of 10 years, 1990 to 2000 is needed.
These data are extracted from the JRC-MARS meteorological data base, MARS being an acronym for *Monitoring Agriculture with Remote Sensing*. This data base contains agriculturally relevant data including also meteorological variables such as temperatures, humidity, and rainfall since 1974. The data base is constituted from the synoptic network. However, not all the stations are available in the data base and the number of stations varies per country and with time. This has an obvious impact on the

quality of the data. In particular in the years 1990 to 1995, the rainfall coverage in Scandinavia, Spain and the eastern European countries is not complete or sparse, making the rainfall data in these areas and for the years 1990-1995 unreliable. The JRC-MARS data base stores the individual station data as well their interpolation onto a 50x50 km grid. For this study the pre-processed interpolated grids have been used, except for Switzerland where higher resolution data are available.
Figures 4-1a/d show examples for water balance runs in the Meuse and the Rhine catchment for the period March 94 to March 95, and for the Oder and the Inn for the period March 96 to October 97. These periods include the floods in the Meuse and Rhine early 95, and the Oder flood in 97. The results in Figure 4-1 have to be understood as preliminary results. They are performed with no or little catchment specific calibrations, which will be undertaken in the near future. Nevertheless these first results are very encouraging. This is particularly true for the Meuse (b). Although the results are not as good as those in Figure 2-3 for the high-resolution case, the agreement between model and observations is very good. The discrepancy between the first 40 to 60 days is the time the model needs to start up and to adapt to realistic values. For the Rhine (a) and the Oder (c) the simulations are less accurate, however, the general agreement is good. The fact that the model does not predict the peak discharge in the Oder correctly is a combination of two reasons: First, the kinematic wave is applied throughout the simulation for the European runs, which is not able to resolve the flood wave correctly in the relatively flat Oder and on a daily time step. Second, during this event a number of dyke breaks occurred that have lowered the peak discharge. The result of the Inn is an example where the model only reproduce the measurements in a qualitative but not quantitative way.

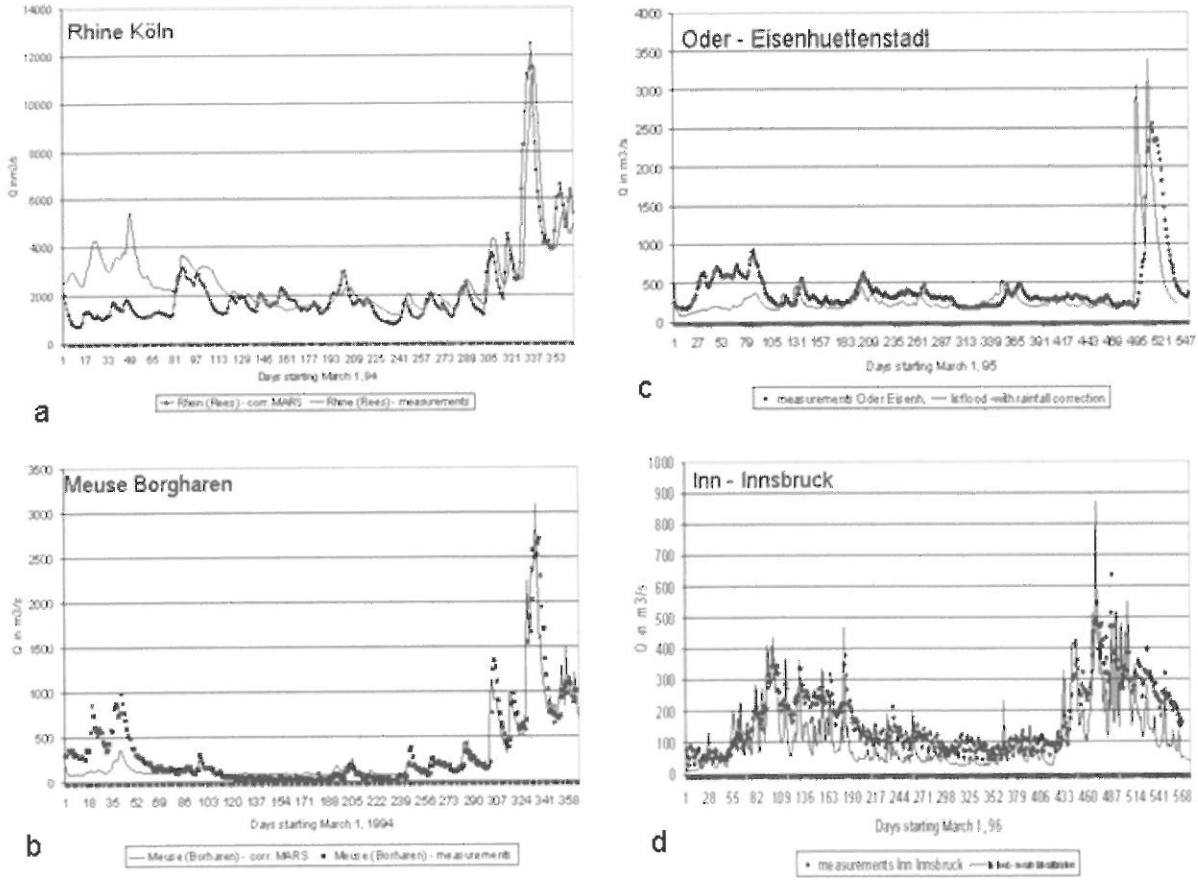

Figure 4-1: Results from the European waterbalance simulations performed with daily time step and on a 5 km grid using observed meterological data from the JRC-MARS data base as input. The simulations (red, thin line) are compared with observations at (a) Cologne, Rhine catchment (1.4.94-1.4.95), (b) Borgharen, Meuse catchment (1.4.94-1.4.95), (c) Eisenhuettenstadt, Oder catchment (1.3.96-1.10.97), and (d) Innsbruck, Inn catchment (1.3.96-1.10.97).

Over the 10 years there is a trend (not shown) that (i) the further to the East the less agreement is observed between the simulations and the measured discharge, and (ii) overall the simulations become much better from 1995 onwards. Both are a direct effect of the quality of the rainfall as described earlier. The better quality from 1995 onwards is also a direct result of the higher number of stations incorporated into the data base. It is to be reminded at this point that the channel geometry input into the model are not measured data but estimations based on variables such as upstream area. Sensitivity tests on these parameters are yet to be performed in detail.

4.2 PRELIMINARY EFFS-LISFLOOD RESULTS

4.2.1 On a 5 km grid

For the hourly flood forecast with the waterbalance data are output a few days before the onset of the flood. Figure 4-2a visualises the spatial distribution of the discharge including overland flow for the whole of Europe, including a zoom for the Meuse/Rhine area as calculated from the waterbalance model. This output represents the initial conditions for the floods model on Jan 21, 1995. The spatial representation is very helpful to identify flood hotspots. These discharge maps can also be animated to give temporal information on flood development. In the following the discussion focuses on the Rhine/Meuse flood towards the end of January 1995.

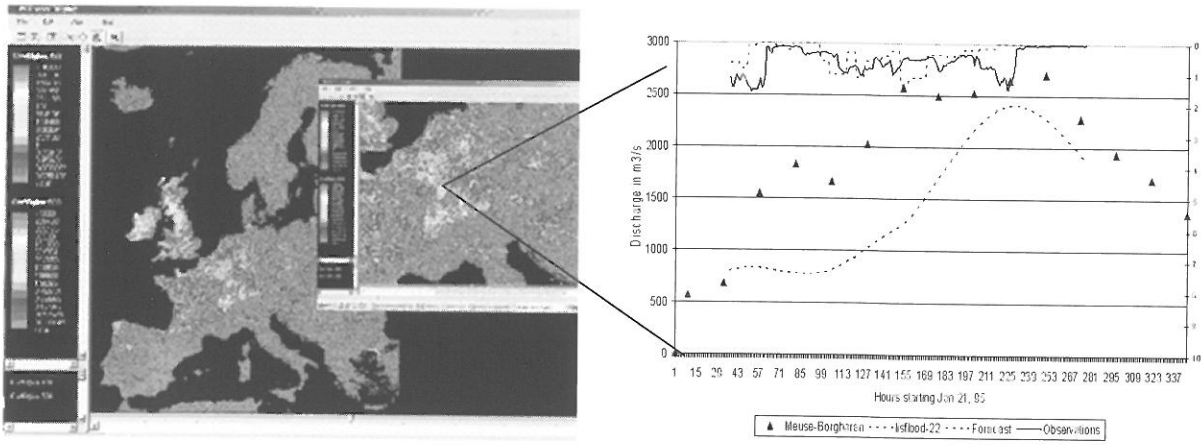

Figure 4-2: (a) Spatial distribution of surface flow per grid in m^3/s on Jan 22, 1995 as simulated with the LISFLOOD waterbalance model, including a zoom of the Meuse/Rhine area. Overland flow is visible by the lighter colours.
(b) Combined 10-day ECMWF-LISFLOOD flood forecast for Borgharen, Meuse, for Jan. 22, 1995 (solid line) and measurements (triangles). At the top axes also the measured rainfall per catchment is shown (thick) as well as the forecasted rainfall per catchment (thin). The curves show hourly data.

Figure 4-2b shows the discharge forecast using the combined ECMWF-LISFLOOD system on a 5 km grid. In this case the EFFS forecast delivers a satisfactory forecast for Borgharen: the peak discharge is predicted within 7-8 days from begin of the simulation of the order of 2500 m^3/s. Bearing in mind that EFFS aims only at a pre-warning, this is a very good result. Looking into detail, there are two basic observations. First, the simulated discharge does not contain the first secondary peak at around 80 h. This is at least partly explained by the lack of simulated rainfall within the ECMWF forecast. It is also possible that the initial conditions provided by the waterbalance model were not accurate enough. Second, the discharge tails off too quickly after the peak, which can again be explained by the fact that the ECMWF data predicts only 5.2 mm from 154 hours to 240 hours, while in fact a total of 31.5 mm were measured.
Figure 4-3 illustrates the performance of the EFFS over several days, starting at Jan 21 to Jan 24 for the Meuse catchment (Borgharen) and the Rhine (Rees), and using ECMWF forecasts only. It is surprising how the results can differ from one day to the other. However, although quantitatively quite different, all curves predict an oncoming flood within a time period beyond the 3 days that normally National Water Authorities would provide.

4.2.2 On a 1 km grid, with uncertainty

The final aim of the EFFS system is flood forecasting at 1 km grid-scale for entire Europe. Since with present resources only a 5km European system is feasible, we are comparing the 1 and 5 km results to examine the effect of grid-resolution for selected catchments (Meuse, Oder, Po). The same forecast data are used, but obviously other spatial input data are at higher resolution. Figure 4-4 shows the result of the 1km flood forecast in the Meuse catchment. Included are simulations using observed precipitation (150 stations), the deterministic ECMWF forecast at 40 km grid size, and 4 perturbed ensemble forecasts at 80 km grid size. From the entire set of 32 perturbed ensembles, the ones with maximum and minimum total precipitation after 240 hours and 120 hours have been selected. The idea is that these 4 should produce the extremes in discharge forecasts. One aim of the EFFS project is to define the optimum use of ensembles in hydrological modelling without having to simulate them all.

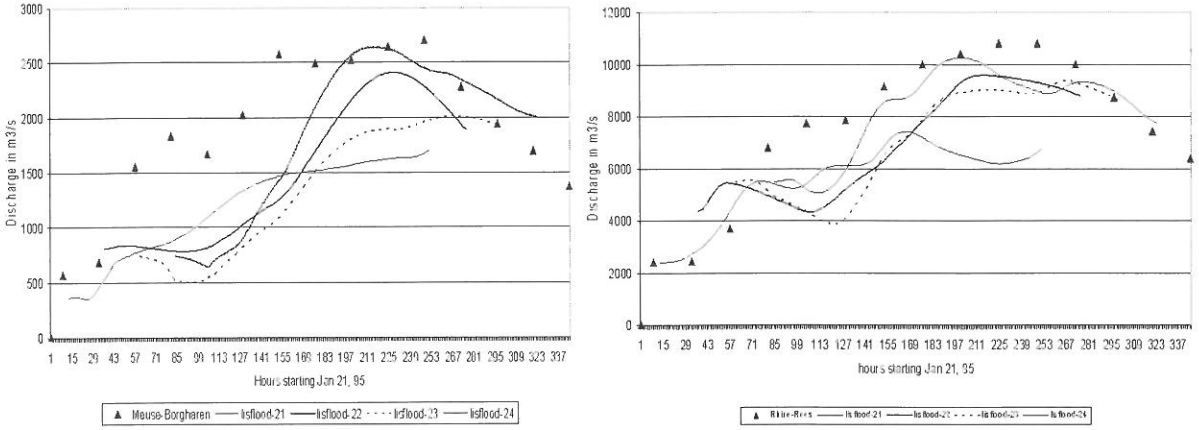

Figure 4-3: Discharge forecast using the combined ECMWF-LISFLOOD system on a 5 km grid for the Meuse (left) and the Rhine (right). Observations of discharge are shown as triangles. The EFFS simulations for Jan. 21(thin), Jan 22 (thick), Jan 23 (dots) and Jan 24 (triangles) are shown in solid lines. They can be identified by the order of starting points.

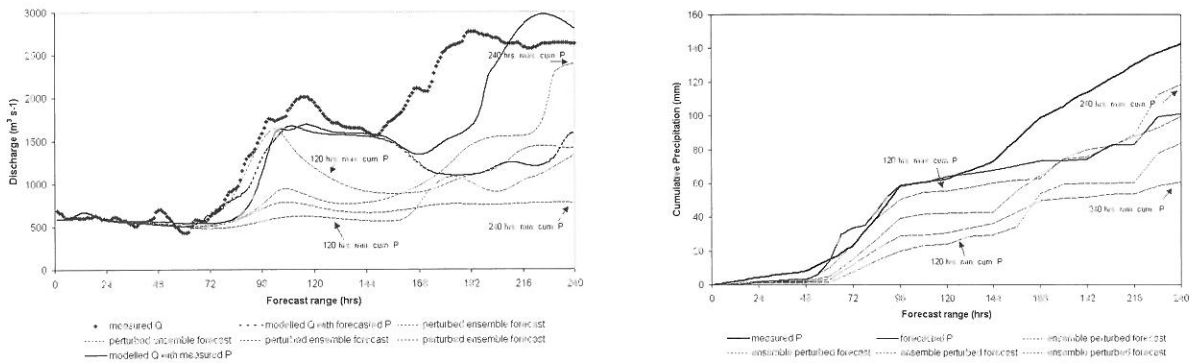

Figure 4-4: Discharge (left) and cumulative precipitation (right) forecast using the combined ECMWF-LISFLOOD system on a 1 km grid for the Meuse at Borgharen. Observed discharge is indicated with dots. The simulated discharge using observed precipitation is indicated with a thicker solid line. Observed cumulative precipitation is shown, together with the deterministic forecast and the 4 perturbed ensembles.

From figure 4-4 it is clear that until 7 days the deterministic forecast is closest to the observed precipitation, and as a consequence the discharge forecast until 7 days is good, which is 4-5 days beyond the current lead-time. At least one ensemble - the maximum 10 day precipitation perturbed ensemble - predicts the observed peak discharge almost correctly at day 10, although during the first days this ensemble is too low.

5 SUMMARY AND CONCLUSIONS

The EFFS (*European Flood Forecasting System)* project aims at developing a Pan-European early flood warning system to provide National Water Authorities and international aid-organisations with a large lead-times to prepare for a possible flood crisis. This will be achieved by using operationally available short-range (1 to 3 days) and medium-range (4 to 10 days) weather forecasts available from the National Weather Authorities and the European Centre for Medium-Range Weather Forecasts (ECMWF) respectively. It is hoped with this approach to increase the lead time for reliable flood warnings from a maximum of 3 days at present to 4-10 days and beyond in the future, to design a medium-range flood forecasting system for the whole of Europe, and to produce flood forecasts in regions where at present no flood forecasts are made on the basis of the newly developed system.
The EFFS project is still ongoing and only preliminary results can be shown. The first incoming results are positive and encouraging. For many catchments the EFFS would have correctly acted as a pre-warning system beyond the usual 3 days of flood forecast available to the National Water Authorities succeeded to give a pre-warning. First results using perturbed ensemble forecasts show the potential benefit of them in flood forecasting and giving a measure of uncertainty.

ACKNOWLEDGEMENTS

We thank all EFFS participants for the fruitful discussions on the work and for data support, for this paper especially Tony Hollingsworth of ECMWF, Jaap Kwadijk of Delft Hydraulics and Eric Sprokkereef of RIZA. GRDC Koblenz and the Dutch and German Water Authorities are acknowledged for the observed discharge data. We further would like to acknowledge the help of the IES staff, in particular G. Liberta, S. Peedell, A. de Jaeger and J.M. Terres. Parts of this research benefit from two European Commission funded projects: EFFS (EVG1-CT-1999-00011 EFFS) and DAUFIN (EVK1-CT1999-00022), coordinated by Wageningen University.

REFERENCES

Abbott, M.B. et al. (1986), An introduction to the European Hydrological System. Journal of Hydrology, Vol. 87, 45-59.

Bates, P., De Roo, A.P.J. (2000), A Simple Raster-Based Model For Flood Inundation Simulation. Journal of Hydrology, Vol.236, 54-77.

Beven, K., Kirkby, M. (1979), A physically-based, variable contributing area model of basin hydrology. Hydrological Sciences Bulletin, Vol. 24, 43-69.

Binley, A.M., Beven, K. (1991), Physically-based modelling of catchment hydrology: a likelihood approach to reducing predictive uncertainty. In: Farmer & Rycroft, Computer modelling in the environmental sciences, Clarendon Press.

De Roo, A.P.J. et al. (2000a), Physically-based river basin modelling within a GIS: The LISFLOOD model. Hydrological Processes, Vol.14, 1981-1992.

De Roo, A. et al. (2000b), European Flow Network at a 1 km grid. Internal Document. Joint Research Centre, Ispra, Italy.

De Roo. A. et al. (2000c) Using The Lisflood Model To Simulate Floods In The Oder And The Meuse Catchment. Proceedings of the European Conference on Advances in Flood Research, PIK-report No.65, Potsdam, 518-532.

De Roo, A. et al. (2001), Assessing The Effects Of Land Use Changes On Floods In The Meuse And Oder Catchment . Physics and Chemistry of the Earth, Part B, Vol. 26, No. 7/8, 593-599.

European Soils Bureau (1998), Georeferenced Soil Database for Europe. Manual of Procedures. Version 1.0 Joint Research Centre, European Commission. EUR 18092 EN

Legg, T.P. et al. (2001) The use of medium-range ensembles at the Met. Office. I: PREVIN - a system for the production of probabilistic forecast information from the ECMWF EPS. Submitted to Meteorological Applications.

Lindstrom, G. et al. (1997), Development and test of the distributed HBV-96 model. Journal of Hydrology, Vol. 201, 272-288.

Molteni, F. et al. (1996) The new ECMWF ensemble prediction system: metodology and validation. Q.J.R. Meteorol. Soc., 122, 73-119;

Wesseling, C.G. et al. (1996) Integrating dynamic environmental models in GIS: The development of a Dynamic Modelling Language. Transactions in GIS,1-1, 40-48.

FAITOU: A PHYSICALLY BASED AND SPATIALLY DISTRIBUTED NUMERICAL MODEL FOR EXTREME FLOOD SIMULATIONS

Jérôme Dubois[1], Jean-Louis Boillat[2], Anton Schleiss[2]

[1] HydroCosmos SA, Rue de l'Industrie 35, 1030 Bussigny, Switzerland, info@hydrocosmos.ch

[2] Laboratory of Hydraulic Constructions, LCH, Swiss Federal Institute of Technology, EPFL, 1015 Lausanne, Switzerland, secretariat.lch@epfl.ch

SUMMARY

The appropriate estimation of the discharge of extreme floods, with a return period higher than 1000 years, is a key issue for the safety assessment of dams and hydraulic structures. In the past, extreme floods were often estimated by the application of empirical formulae relating the specific discharge with the catchment area and some other descriptive parameters. More recently statistical approaches were used abundantly for the adjustment of observed peak discharges to various distribution laws. However, with such flood statistics, the problem of extrapolation to extreme values occurs because the confidence interval strongly increases with the return period. Another group of methods are the comprehensive hydrological models, like the unit hydrograph, which connects a flood event with the rainfall. The weakness of all these models is often the lack of the physical significance of the parameters. Furthermore, the adjusted values are normally maintained when extrapolating.
The latest generation of hydrological models are physic based and spatially distributed. With these models, the equations of the physical phenomena are fully implemented and a solution at any point of the catchment area is obtained. The kinematic wave approximation is generally used to compute the rainfall-discharge transfer, by modelling the topography by surface planes. In addition to infiltration, the only parameter concerning the runoff is the surface roughness coefficient. The early models using this concept simplified the catchment area by one or two surface planes only connected to the river. Sometimes the catchment area is modelled by a geomorphologic description. Normally the friction losses of the flow on the surface planes are estimated according to Manning-Strickler. The experience shows that the calibration of this type of model results in very low Strickler coefficients between 0.2 and 2 $m^{1/3}/s$, which are clearly beyond the range of application of this formula.
The present contribution emphasizes the drift of these models and proposes an alternative concept for a physically more appropriate modelling of flood events in catchment areas. A numerical model named "Faitou" is presented, which was developed to simulate the formation and routing of floods in steep river basins. Based on a new head loss equation particularly adapted to surface runoff, "Faitou" solves the 2D kinematic wave equation over the catchment topography with the finite volume method. Furthermore, the computation of surface flow is coupled with a hydrodynamic modelling of the river network. The definition of the watershed limits, the mesh of finite volumes and the river network are automatically generated from a digital topographic model. Examples of application on an alpine watershed demonstrate the potential and qualities of the numerical model.

Keywords: extreme floods, dam safety, surface run-off in catchment areas, numerical modelling, finite volume method, kinematic wave

1 INTRODUCTION

The problem residing in the quantification of a design discharge has, for a long time, retained the attention of hydraulic engineers, very aware of the importance of this point at the origin of all security concepts with regard to floods. The first tool the design engineer had at disposition consisted of empirical formulae relating the design discharge to the surface of the watershed and to the length developed of its hydrographical network. Unfortunately, the extreme discharge calculated with the help of a certain number of these empirical formulae for an identical scheme can vary with a ratio of 1 to 3 (Boillat, Schleiss, 2002).
The hydrological model which has been used most often is without doubt the adjustment and extrapolation statistics of a series of measured discharges. With this method, the reliability problem of the extrapolation still remains. In fact, when a series of discharge measurements over 5, 20 or 50 years is extrapolated to 1000 years or more, the discharge reliability interval calculated results in disconcerting

values. It has been demonstrated that on the basis of a 50 year long series, the ratio between maximum and minimum values of the reliability interval at 80% of Q_{1000} can be superior to 2.
The third approach used to determine the design flood is the one proposed by the global hydrological models. An important stage has been made with such models., It is possible to obtain a complete flood from a unique rainfall event. In other words, the discharge evolution is determined over a period of time and not only a peak discharge. Some hydrological models have known and still know a great success, as in particular the unitary hygrogram method. The principal default of these models resides in the signification of their parameters. Furthermore, the constancy of these parameters is always subject to question during the usage in extrapolation of this type of model.
The latest generation of hydrological models are models which are physically based and spatially distributed. A model is said to be "physically based" when it describes the physics of phenomena with the help of differential equations. And it is "spatially distributed" when the solution is known in all points in space, contrary to the global model which provides a result only at the output. The most common applied model in hydrology is the kinematic wave over a surface plane. This simplified solution of the St.-Venant equation is used to compute the rainfall-discharge transfer when modelling the topography by a number of surface planes. Concerning the runoff, the only adjustment parameter of the model is the roughness coefficient which obviously has a physical meaning.
The first models solving the kinematic wave equation over surface planes considered only one or two planes joining-up on a river (Hager, 1984) or using a geomorphologic description to build a model of the watershed (Bérod, 1995). These types of models used the Manning-Strickler equation for the head loss computation. The experience obtained with these models shows that the calibration process according to historical data leads to strange values of the Strickler coefficient beyond physical limits, usually comprised between 0.2 et 2 $m^{1/3}/s$. The present paper attempts to explain the drift of such models and proposes a new approach towards physically based flow modelling in catchment areas.

2 MODELING CONCEPTS

The topographic modelling of a watershed using only a smaller number of surface planes, is a gross simplification for the surface runoff. This scale effect has to be entirely compensated by the roughness coefficient, the only remaining parameter of the hydraulic model. This partially explains the forced drift of the roughness coefficient when applying kinematic wave models over surface planes in order to reproduce observed floods satisfyingly.
Nowadays, detailed topographic data are often available and easily accessible when using digital elevation models (DEM). DEM give a very detailed description of the surface geometry and allow in consequence a more accurate runoff modelling. This new technology has to be used whenever possible in order to reduce the drift of the roughness coefficient mentioned above.

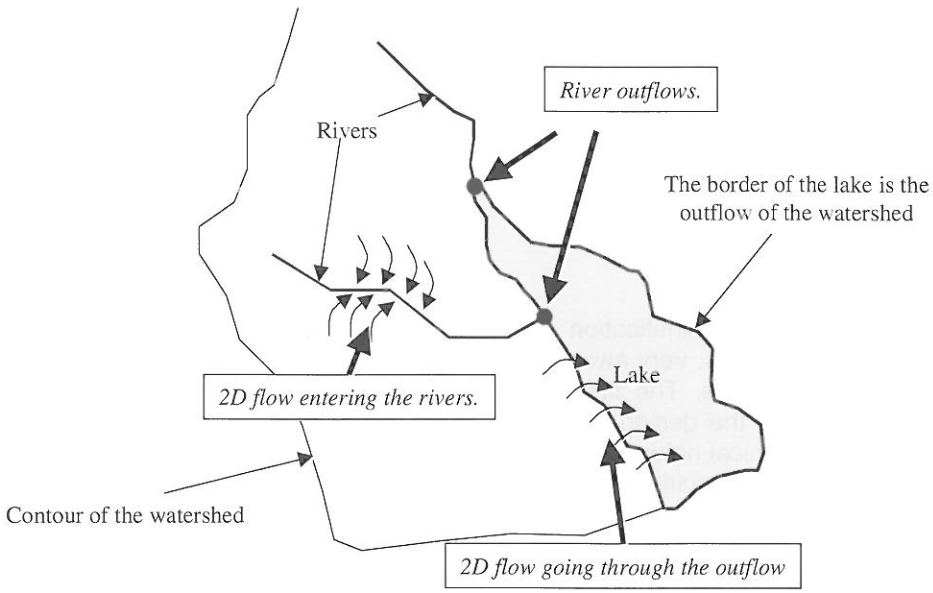

Figure 2-1: Scheme of the different flowing types considered by the model Faitou.

It is therefore necessary to develop hydrological numerical codes which are able to take into account the detailed topographic information with the aim of replacing the global models. The program "Faitou" (Dubois, Pirotton, 2002) which was developed in the frame of a research program on the topic of extreme floods, gives an answer to this target by considering the general flow conditions described in Figure 2-1.
First of all, this hydrodynamic model solves the two-dimensional (2D) equations of the kinematic wave over the topography as described by the digital elevation model, down slope to the border corresponding to a river or a reservoir. Then, a hydrodynamic 1D model computes the flood routing in the river network down to the output. In this way, Faitou carries out the coupled modelling between the surface runoff, commonly called hydrological flow, and the river hydraulic flow.

3 HYDRAULIC BEHAVIOR OF OVERLAND FLOW

The very detailed description of the flowing features when using a DEM undoubtedly constitutes a progress in comparison with the previous models based only on one or more surface planes. However, it is to be questioned whether the Manning-Strickler equation, commonly used for the head loss computation, is really adapted in the perspective of a higher level of precision. This equation doesn't take into account the Reynolds number value. In comparison with pressure flows, the Mannig-Strickler equation is applicable only in the case of rough turbulent flow conditions. However, small flow depths and velocities, characteristic of runoff processes, correspond mainly to laminar or weakly turbulent flows. Furthermore, the surface asperities are 100 to 1000 times smaller than the water depth of river flows, whereas they are in the same order of magnitude for surface flows. All these considerations lead to question the validity of the Mannig-Strickler law for its application in hydrological modelling.
A fundamental research was undertaken at the Laboratory of Hydraulic Structures of the Swiss Federal Institute of Technology in Lausanne in order to get a better insight on the hydraulic behaviour of low depth flows over macro roughness (Dubois, 1998). Two experimental set-ups were built for this purpose.
The first was used to study the relationship between the water depth and the velocity over a plate covered with a variable number of marbles, for uniform and steady flow conditions. The results obtained through 273 experimental series allowed to develop a new formula linking the water depth and the flow velocity applicable to this particular type of flow conditions.
The model of Dubois has the advantage that it covers the flow behaviour with a steady relationship from laminar to the turbulent conditions. The surface roughness is defined by an equivalent roughness produced by balls of a certain diameter D placed with a certain density ρ on the surface, similar to the common approach of equivalent sand roughness according Nikuradse.

Geometrical definitions

(1) $$\rho = \frac{nb_{balls} \cdot V_{1\,ball}}{Surface}$$ density of balls (m)

(2) $$\rho_{max} = 0.9069$$ maximum density (m)

(3) $$\cos(\theta/2) = 1 - 2 \cdot h/D$$ height of water (rad)

(4) (h < D) $$\eta = 1 - \sqrt{\rho/\rho_{max}} \cdot \frac{D}{8 \cdot h} \cdot [\theta - \sin(\theta)]$$ section porosity

(5) $$\Omega = 1 + \sqrt{\rho/\rho_{max}} \cdot \frac{\theta}{2}$$ wet perimeter of balls (m)

(6) (h ≥ D) $$\eta = 1 - \sqrt{\rho/\rho_{max}} \cdot \frac{\pi}{4} \cdot \frac{D}{h}$$ section porosity

(7) $$\Omega = 1 + \sqrt{\rho / \rho_{max}} \cdot \pi$$ wet perimeter of balls (m)

Velocities

(8) (h < D) $$S_f = \frac{3 \cdot (3 + \frac{\Omega^2}{\eta^3}) \cdot \nu}{4 \cdot g \cdot h^2} \cdot V + \frac{0.345 \cdot \rho^{0.545} \cdot \Omega}{8 \cdot g \cdot \eta^3 \cdot h} \cdot V^2$$

(9) (h ≥ D) $$V_0 = V_{(h=D)} \text{ in (8)}$$

(10) $$\sqrt{g \cdot S_0} \cdot (5.62 \cdot \log \frac{\Delta h}{D} + 3.13 \cdot \rho^{-0.613}) \cdot \sqrt{\Delta h} = V_0$$

(11) $$\sqrt{\frac{8}{f}} = 5.62 \cdot \log \frac{h - D + \Delta h}{D} + 3.13 \cdot \rho^{-0.613}$$

(12) $$V = V_0 \cdot \frac{D}{h} + \sqrt{\frac{8 \cdot g \cdot S_f}{f}} \cdot \sqrt{h - D + \Delta h} \cdot (1 - \frac{D}{h})$$

where V_{1ball}: volume of 1 ball (m^3); S_f : energy slope; S_o: geometric slope; h : height of water (m); f : friction coefficient; ν: kinematic viscosity (m^2/s); V, V_0: velocity (m/s); D: diameter of 1 ball (m); Δh: height parameter (m); g: earth acceleration (m/s^2).
The obtained formula was then tested for non uniform and unsteady flow conditions provided by a second installation placed under a rain simulator.
The new developed head loss relation is presented graphically in Figure 3-1. It covers laminar and turbulent flows and the transition domain in-between. It fits with the classical laws for free surface flows when the water depth becomes higher than the roughness elements as well as with the analytical solution for laminar flows over a surface plane when the water depth and the velocity are very low.

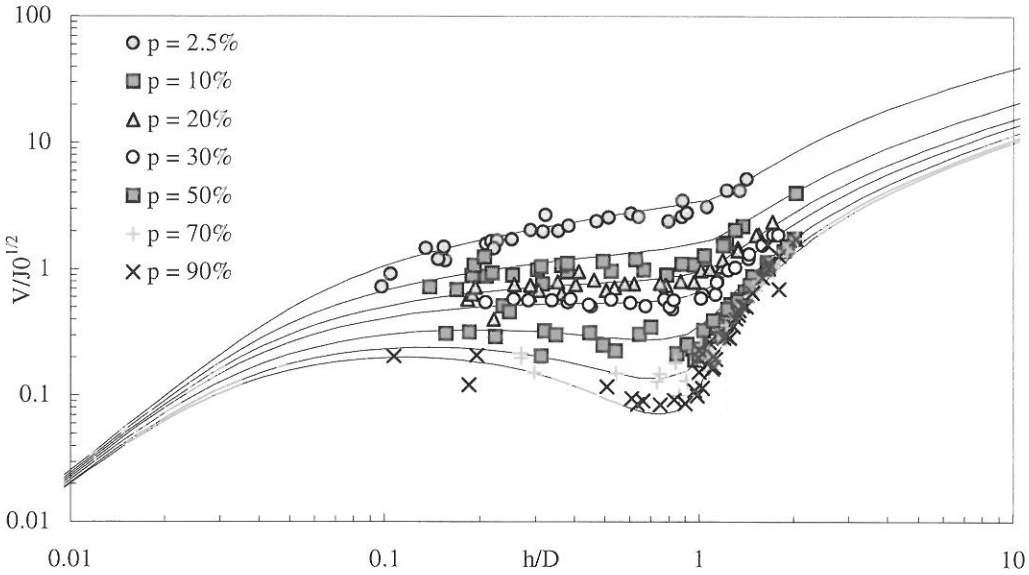

Figure 3-1: Comparison of the new head loss equation with the experimental results.

This experimental research revealed interesting behaviours of free overland flows. For example it could be observed that the velocity is independent of the water depth for an asperity size between one tenth and one times the water depth. Such a behaviour is comparable with the flows in porous media, which depend only on the hydraulic gradient. When the flow covers the asperities of the surface roughness, the velocity increases abruptly in function of the water depth, so as to make up with the lost time.

4 Example of application

The catchment area of the Mattmark reservoir located in the South-eastern part of Switzerland has been selected to carry out a detailed validity test of the model Faitou (Sander & Haefliger 2001). The data of the very well documented extreme flood which occurred in this region between 23rd and 25th September 1993, was used. This exceptional flood event produced the first spillway overtopping of Mattmark dam since it's commissioning in 1960. The watershed of the reservoir has a surface of 37 km^2, at altitudes comprised between 2200 et 3900 m s.l., with a 21% mean slope. It is mainly covered with moraines and rocks as well as glaciers on 22% of the surface. Figure 4-1 shows a zenithal view of Mattmark region as a shadow map produced by Faitou.

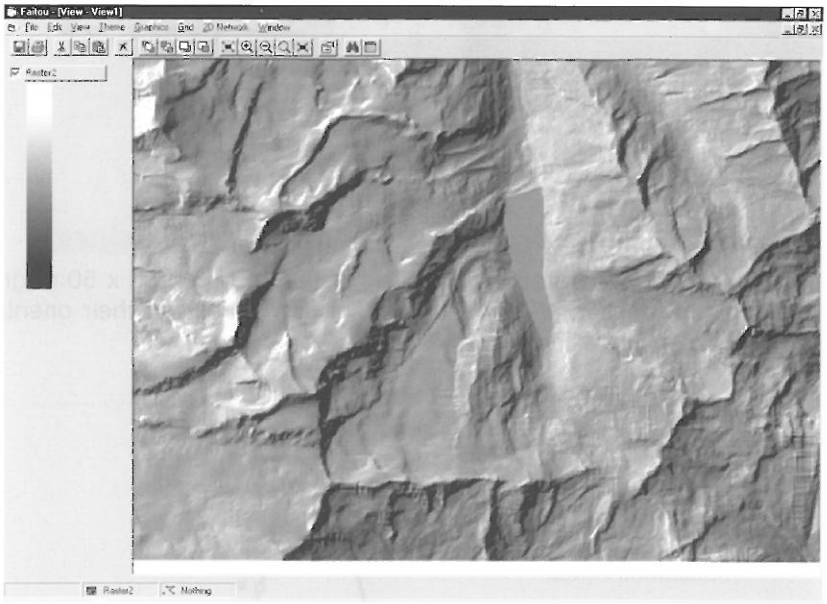

Figure 4-1: General view of Mattmark dam area. The dam is located in the centre, the reservoir extends towards the South.

The first step of simulation consists in establishing the finite volumes mesh of the watershed and in the definition of the river network. A DEM with a spatial resolution of 50 m was used for the generation of the computation model. The result of this automatic process is presented in Figure 4-2.
At this resolution level, the surface model as for the example of Mattmark contains 28'229 finite volumes and 46'472 borders. The river network model is made up of 4723 cross sections and 385 bifurcations.
The rainfall and discharge data of the flood event of September 1993 have been analysed in detail. As no measuring station exists on the watershed, the flood hydrograph was obtained from the reservoir water level records and the operating data of the power plant. Depending on the computation method, the peak discharge of the flood was estimated between 134 et 152 m^3/s. The reconstituted hydrographs are presented on Figure 4-3 and compared with the simulated one by Faitou.
Taking into account the uncertainties related to the reconstruction of the hydrograph as well as to the rainfall definition, it can be seen that the simulated flood and the observed event are in good agreement. This result could be obtained without any excessive calibration effort, meaning without optimisation of the main parameters as roughness coefficients of surface planes and rivers. This low sensitivity of the model regarding to the parameters underlines its quality and robustness. This behaviour is very important when the model is used for the simulation of extreme floods beyond measured events.

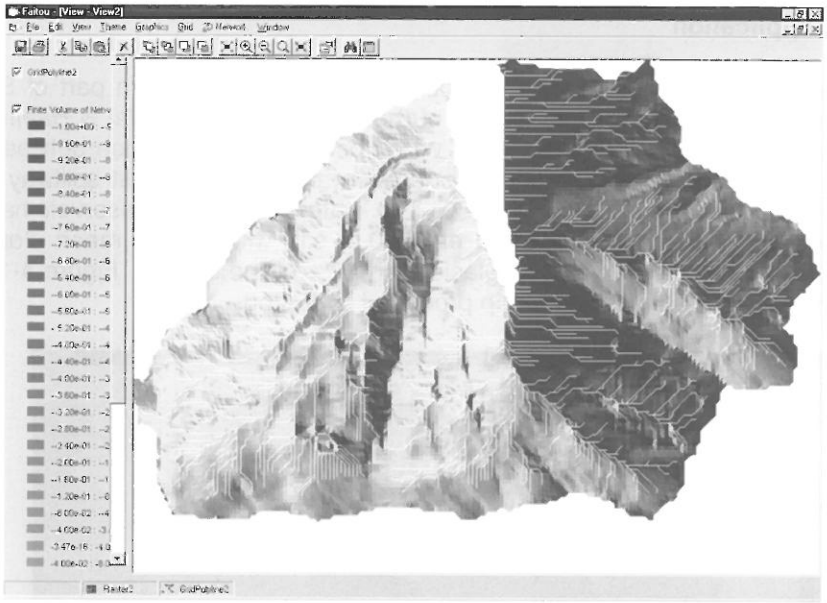

Figure 4-2: Computation model generated on the basis of the DEM 50 (50 x 50 m grid). Finite volumes are tinted in function of the x-component (East-West) of their orientation. The river network appears in white lines.

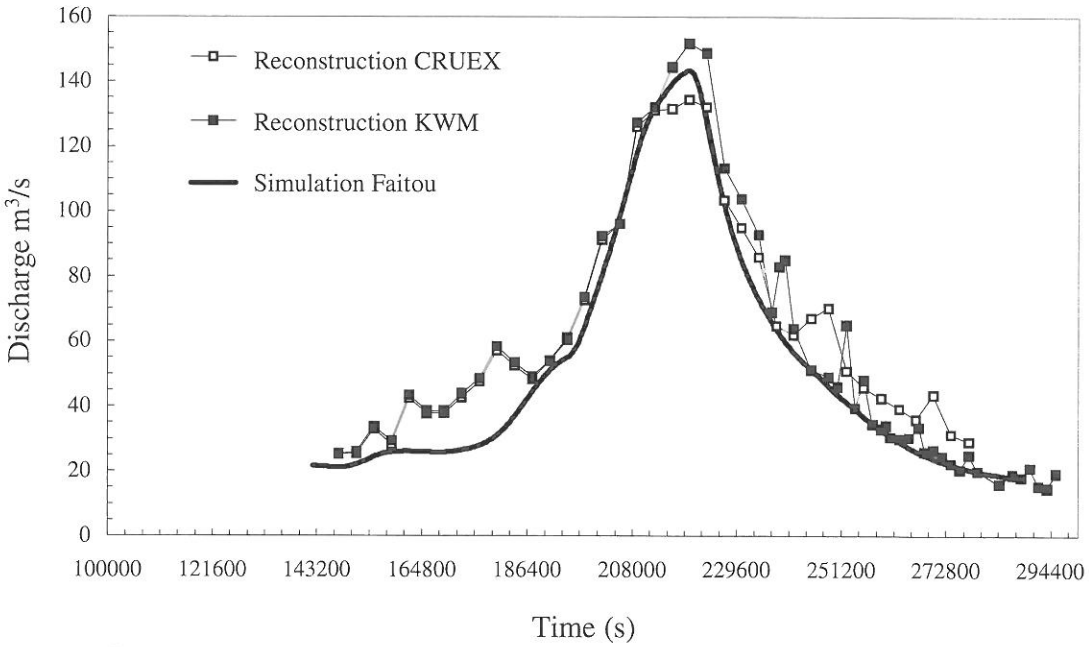

Figure 4-3: Comparison between the reconstructed hydrograph from the 1993 event in Mattmark's reservoir and the Faitou simulation.

5 CONCLUSIONS

To get reliable flood estimations, the richness of spatial reference information available today must be used and integrated in hydrological analysis. Nevertheless, only spatially distributed models are able to manage such information. Furthermore, they propose a result not only at the location of a chosen catchment outlet, but also at any other point of the watershed. Anthropogenic modification such as a growing urbanization, can be easily considered with the physically based parameters of the model in the concerned region allowing to estimate its effect at the scale of the catchment area.
Faitou does not only include all the typical functionalities of spatially distributed models, but it also considers an improved flow law of thin layer overland flow over macro roughness. This law, verified on the basis of tests performed under a rainfall simulator, takes into account the wide range going from laminar to turbulent fluvial flows. Faitou has proved to be a very reliable tool for alpine catchment areas for the extrapolation of observed flood events to extreme flood events as they are considered in the design of spillways of large dams.

ACKNOWLEDGEMENTS

The research study was financed by the Swiss Federal Office for Water and Geology and the Swiss Committee on Dams.

REFERENCES

Bérod, D. (1995): Contribution à l'estimation des crues rares à l'aide de méthodes déterministes. Apport de la description géomorphologique pour la simulation des processus d'écoulement., Thèse N^0 1319, Département de Génie Rural, École Polytechnique Fédérale, Lausanne.

Boillat, J-L., Schleiss, A., (2002): Détermination de la crue extrême pour les retenues alpines par une approche PMP-PMF. Submitted for publication in Wasser-Energie-Luft, Baden.

Dubois, J. (1998): Comportement hydraulique et modélisation des écoulements de surface. Thèse 1890, École Polytechnique Fédérale, Lausanne et Communication N° 8 du Laboratoire de constructions hydrauliques (LCH), Lausanne.

Dubois, J., Pirotton, M., (2002): Le modèle Faitou, Communication N° 10 du Laboratoire de constructions hydrauliques (LCH),École Polytechnique Fédérale Lausanne.

Hager, W. H., (1984): A Simplified Hydrological Rainfall-Runoff Model. Journal of Hydrology, 75, 151-170.

Sander, B., Haefliger, P., (2001): Hochwasserschutz durch das Speicherkraftwerk Mattmark, Wasser-Energie-Luft, Heft 7/8, 169-174, Baden.

ESTIMATION OF EXTREME FLOODS IN THE RIVER RHINE BASIN BY COMBINING PRECIPITATION-RUNOFF MODELLING AND A RAINFALL GENERATOR

Mailin Eberle[1], Hendrik Buiteveld[2], Jules Beersma[3], Peter Krahe[1], Klaus Wilke[1]

[1] Federal Institute of Hydrology (BfG), Kaiserin-Augusta-Anlagen 15-17, 56068 Koblenz, Germany, eberle@bafg.de / krahe@bafg.de / wilke@bafg.de

[2] Institute for Inland Water Management and Waste Water Treatment (RIZA), P.O. Box 9072, 6800 ED Arnhem, The Netherlands, h.buiteveld@riza.rws.minvenw.nl

[3] Royal Netherlands Meteorological Institute (KNMI), P.O. Box 201, 3730 AE De Bilt, The Netherlands, jules.beersma@knmi.nl

SUMMARY

The determination of design discharges from statistical analyses of peak discharges faces various problems. Here an alternative approach is investigated that makes use of precipitation as the source of discharge generation. A stochastic rainfall generator based on nearest neighbour resampling has been developed to produce the daily meteorological input of a hydrological/hydraulic modelling system. In two 1000-year simulations much larger multi-day precipitation amounts are found than in the historical record. With the exception of a slight underestimation of annual maximum peak flows, the HBV precipitation-runoff model satisfactorily reproduces the discharges of the main tributaries of the river Rhine. The methodology is tested further for the Moselle basin using one of the 1000-year precipitation simulations. The largest simulated flood event based on generated precipitation is 20% larger than the 1993 flood event.

Keywords: Flood estimation, rainfall generator, HBV, precipitation-runoff modelling, Rhine basin

1 INTRODUCTION

In the Netherlands, the design discharge for the river Rhine (and the other large rivers) is exceeded on average once every 1250 years (Parmet et al., 1999). Statistical approaches for estimating the design discharge have a number of weaknesses. First, the representativeness of the relatively short discharge record of about 100 years can be questioned. For a number of fitted extreme-value distributions it turned out that the 90% confidence interval is about 2500 m³/s around the estimated 1250-year event. Second, the discharge record is potentially non-homogeneous because of changes in the drainage basin, the river geometry and climate since 1901. A third point of uncertainty concerns the choice of frequency distributions. Furthermore, statistical methods provide no information about the volume and duration of the considered flood event.

Therefore, a new methodology is being developed to provide a better physical basis for the design discharge (Parmet et al., 1999). The development is co-ordinated by RIZA and is carried out so far in co-operation with KNMI and BfG. The first component of this new methodology is a stochastic multivariate weather generator, which generates long simultaneous records of daily rainfall and temperature over the basin. The second component consists of precipitation-runoff models for the major Rhine tributaries. The final component is a one-dimensional hydrodynamic model that routes the runoff from the hydrological models. In this way, the generated rainfall is transformed into a homogeneous discharge series thereby tackling the problem of the short, non-homogeneous historical discharge record. The coupling with the hydrodynamic model in order to simulate discharge of the whole river Rhine basin has not yet been realised.

An additional advantage is that the new methodology may give a better insight into the shape and duration of the design flood, because meteorological conditions and catchment responses are explicitly taken into account. Furthermore, it can potentially assess the effects of future developments like climate change and upstream interventions such as retention-basins and dike-relocations. The latter are incorporated in the hydrodynamic model (Lammersen et al., 2002).

In section 2 the rainfall generator for the complete Rhine basin is presented. Section 3 describes the HBV modelling for the major tributaries downstream of Basel and in section 4 both models are combined for the Moselle basin. The conclusions are given in section 5.

2 STOCHASTIC RAINFALL GENERATOR

Daily rainfall and temperature are simultaneously simulated at 36 stations in the Rhine basin using nearest-neighbour resampling. A major advantage of a non-parametric resampling technique is that it preserves both the spatial association of daily rainfall over the drainage basin and the dependence between daily rainfall and temperature without making assumptions about the underlying joint distributions.

2.1 Nearest-neighbour resampling

In the nearest-neighbour method weather variables like precipitation and temperature are sampled simultaneously with replacement from the historical data. To incorporate autocorrelation, one first searches the days in the historical record that have characteristics similar to those of the previously simulated day. One of these nearest neighbours is randomly selected and the observed values for the day subsequent to that nearest neighbour are adopted as the simulated values for the next day t. A feature vector $\mathbf{D}_t$ is used to find the nearest neighbours in the historical record. $\mathbf{D}_t$ is formed out of the standardised weather variables generated for day t-1. The nearest neighbours of $\mathbf{D}_t$ are selected in terms of a weighted Euclidean distance. In this study a decreasing kernel is used to select randomly one of five nearest neighbours.
For each day the simulated values (i.e. the observed data of the selected day) may also include the observed data of the selected day from stations that are not used in the feature vector or include the area-average precipitation data from subcatchments of the selected day. The simulation of such additional data is designated as *passive* simulation. More details about nearest-neighbour resampling can be found in Rajagopalan and Lall (1999), Wójcik et al. (2000) and Buishand and Brandsma (2001).

2.2 Data

Daily temperature and precipitation data for the 35-year period 1961-1995 were made available for 36 stations in the Rhine basin: 25 in Germany, 1 in Luxembourg, 4 in France and 6 in Switzerland. Because precipitation P and temperature T depend on the atmospheric flow, three daily circulation indices are also considered: (i) relative vorticity Z, (ii) strength of the westerly flow W and (iii) strength of the southerly flow S. These circulation indices were computed from daily mean sea-level pressure data on a regular 5° latitude and 10° longitude grid.
Before resampling the data were deseasonalised through standardisation. The effect of seasonal variation is reduced further by restricting the search for nearest neighbours to days within a moving window, centred on the calendar day of interest. The width of this window was 61 days. To keep the dimension of the feature vector low, a small number of summary statistics was calculated from the observed data at 34 of the 36 stations (two Swiss mountain stations were excluded). Both for P and T the arithmetic mean of the standardised daily values was used. In addition, the fraction F of stations with $P \geq 0.1$ mm was considered. F helps to distinguish between large-scale and convective precipitation.

2.3 Performance of the rainfall generator

The performance of the rainfall generator was mainly studied for the winter half-year (October-March) because most extreme river discharges in the lower part of the Rhine basin occur during that season. Twenty-eight runs of 35 years were generated to investigate the reproduction of standard deviations and autocorrelation coefficients. Both the standard deviations of the daily values and the monthly values (totals for precipitation and averages for temperature) were considered. Table 2-1 presents the differences between the standard deviations and the autocorrelation coefficients of the simulated and historical data for a model with a 3-dimensional feature vector and for a model with a 6-dimensional feature vector.
For the model that incorporates only the large-scale features of the P and T fields (model UE) the precipitation and temperature statistics are well reproduced. A slight, though statistically significant, bias is present in the lag 1 autocorrelation coefficients. Incorporation of the circulation indices into the feature vector (model UEc) generally worsens the reproduction of daily temperature statistics. For precipitation both models give similar results.

Table 2-1: Percentage differences between the mean standard deviations of monthly and daily values, $\bar{s}_M$ and $\bar{s}_D$ respectively, and absolute differences between the mean lag 1 and 2 autocorrelation coefficients $\bar{r}$ (1) and $\bar{r}$ (2) in the simulated time series (twenty-eight runs of 35 years) and the historical records (1961-1995) in winter (October-March), averaged over 34 stations. Bottom lines: average historical estimates (standard deviations in mm for precipitation and in °C for temperature). Values in bold refer to differences more than twice the standard error (se) from the historical estimate. The elements $\tilde{P}$ and $\tilde{T}$ in the feature vector $\mathbf{D}_t$ refer to the average standardised precipitation and temperature of 34 stations, F refers to the fraction of stations with precipitation and $\tilde{Z}$, $\tilde{W}$ and $\tilde{S}$ are standardised atmospheric circulation indices.

		$\Delta\bar{s}_M$ (%)		$\Delta\bar{s}_D$ (%)		$\Delta\bar{r}(1)$		$\Delta\bar{r}(2)$	
Model	Elements of $\mathbf{D}_t$	*P*	*T*	*P*	*T*	*P*	*T*	*P*	*T*
UE	$\tilde{P}_{t-1}, F_{t-1}, \tilde{T}_{t-1}$	0.3	-1.1	0.2	0.2	**-0.019**	**-0.032**	-0.001	0.006
UEc	$\tilde{Z}_{t-1}, \tilde{W}_{t-1}, \tilde{S}_{t-1}, \tilde{P}_{t-1}, F_{t-1}, \tilde{T}_{t-1}$	-1.7	-8.2	-1.2	-1.9	**-0.018**	**-0.036**	0.001	-0.020
Historical		35.7	2.1	4.2	4.2	**0.283**	**0.826**	0.144	0.639
se		4.5	6.2	2.5	2.5	**0.008**	**0.007**	0.009	0.015

2.4 Long-duration simulations

With the two models 1000-year simulations have been performed. Figure 2-1 shows Gumbel plots of the 10-day winter precipitation maxima for the area average precipitation of the 34 stations used in the feature vector.

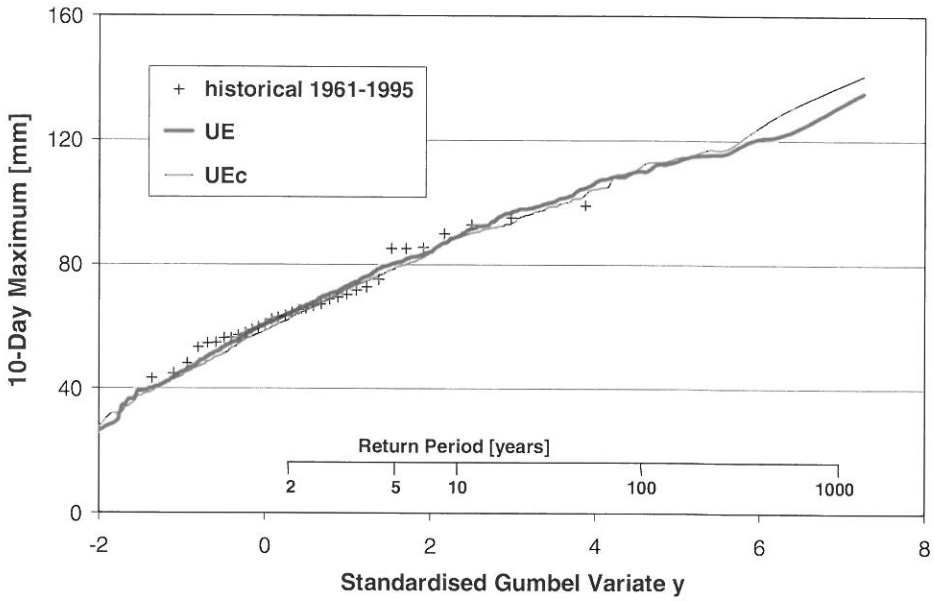

Figure 2-1: Gumbel plots of 10-day winter precipitation maxima for observed and simulated data (runs of 1000 years).

The figure shows that there is a good correspondence between the historical and simulated distributions. Realistic multi-day precipitation amounts much larger than the largest historical precipitation amounts are found in these simulations, which is particularly interesting from the viewpoint of precipitation-runoff modelling. Figure 2-1 shows e.g. that the largest 10-day precipitation amounts in the simulations are up to 40% larger than in the historical record. The 1000-year simulation with the UE model serves as input for precipitation-runoff modelling of the river Moselle. The simulated daily temperatures of 8 stations in the Moselle basin are used as well as passively simulated daily area average precipitation amounts of 42 subcatchments (see section 4).

3 PRECIPITATION-RUNOFF MODELLING OF THE RIVER RHINE BASIN

3.1 HBV modelling of the major river Rhine tributaries

The major tributaries of the river Rhine downstream of Basel (Figure 3-1) are modelled with the precipitation-runoff model HBV on a daily basis. Discharge formation of the remaining (white) areas along the river Rhine is less important concerning floods at Lobith - however, they will be considered in the future. In addition, it will be necessary to incorporate precipitation-runoff modelling for the Swiss part of the basin.
HBV is a conceptual semi-distributed precipitation-runoff model. It was developed at the Swedish Meteorological and Hydrological Institute (SMHI) in the early 1970s and has been applied in more than 30 countries with only small adjustments (Lindström et al., 1997 - e.g. Lidén, Harlin, 2000 and Eberle et al., 2001). HBV describes the most important runoff generating processes with simple and robust structures. In the "snow routine" storage of precipitation as snow and snow melt are determined according to the temperature. The "soil routine" controls which part of the rainfall and melt water forms excess water and how much is evaporated or stored in the soil. The "runoff generation routine" consists of one upper, non-linear reservoir representing fast runoff components and one lower, linear reservoir representing base flow. Flood routing processes are simulated with a simplified Muskingum approach.
Since HBV is a semi-distributed model, the basin of each tributary is subdivided into subbasins (see. Figure 3-1). Inside these subbasins some processes are simulated separately for different elevation zones and forested and non-forested areas. The subbasins are based on catchment boundaries defined for the International Commission for the Hydrology of the river Rhine basin (CHR). Another aspect concerning the delineation of subbasins is the availability of gauging stations that are necessary for calibration. Most of the subbasins cover between 500 and 2000 km^2. The elevation zones inside the subbasins as well as the area covered with forest within these zones are derived from grid based GIS data, i.e. a land use classification based on Landsat-TM satellite data and the digital elevation model of the U.S. Geological Survey.

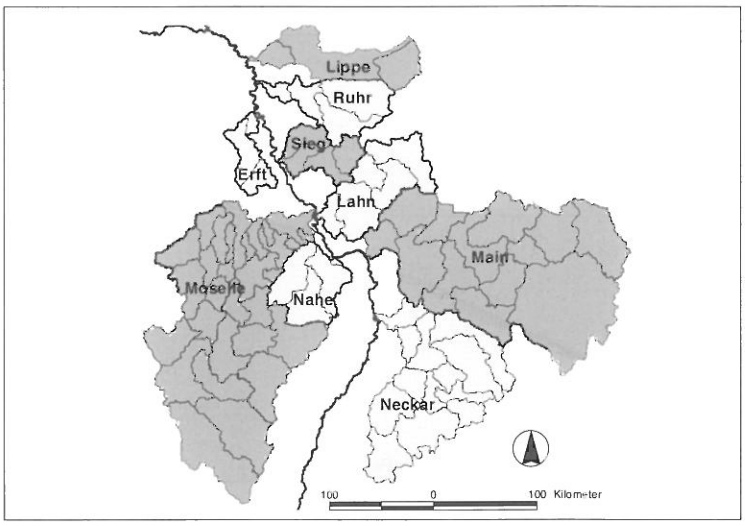

Figure 3-1: Subbasin structure for modelling the major river Rhine tributaries with HBV.

Precipitation data for the German part of the Rhine basin are available from the CHR as time series of subbasin average precipitation. For the Moselle basin, which partly belongs to France, Belgium and Luxembourg, daily gridded precipitation recently calculated at the University of Trier (White, 2001) is taken to calculate areal precipitation time series for the subbasins. Air temperature data from 36 stations are used. For the same stations daily values of reference evapotranspiration are computed from temperature and sunshine duration using the Penman/Wendling approach (Wendling, 1995). However, runoff simulations are also possible with long-term mean monthly values of reference evapotranspiration.
Calibration is done manually by comparison of observed and computed hydrographs and statistical criteria, i.e. the Nash/Sutcliffe criterion R^2 and the accumulated difference of observed and computed discharge. For some HBV parameters, for example the parameter representing the maximum water storage in the soil, values are estimated from the catchment characteristics (e.g. land use and field capacity). The calibration period is 1976 to 1985; it includes both dry and wet years.

Results are satisfactory. As Table 3-1 shows, the Nash/Sutcliffe criterion R^2 generally exceeds 0.85 both in the calibration period and in the validation periods (1986-1990 and 1991-1995). The only basin with poor results is that of the river Erft where discharge dynamics are dominated by technical measures related to brown coal mining. Results tend to be best for the rivers Ruhr, Moselle and Lahn; concerning the river Ruhr, this is rather surprising because the large reservoirs in the river Ruhr basin have not been taken into account explicitly. More information about daily HBV modelling in the river Rhine basin can be found in Mülders et al. (1999).

Table 3-1: Values of the Nash/Sutcliffe criterion R^2 for HBV modelling the river Rhine tributaries.

River	Gauging station	Catchment Area [km^2]	R^2 - Calibration 1976-1985	R^2 - Validation1 1986-1990	R^2 - Validation2 1991-1995
Neckar	Rockenau	14,000	0.86	0.88	0.79
Main	Frankfurt	24,764	0.88	0.87	0.86
Nahe	Grolsheim	4,060	0.87	0.86	0.85
Lahn	Kalkofen	6,000	0.90	0.91	0.94
Moselle	Cochem	27,088	0.92	0.90	0.94
Sieg	Menden	2,880	0.91	0.91	0.91
Erft	Neubrück	1,880	< 0	< 0	< 0
Ruhr	Hattingen	4,500	0.89	0.91	0.94
Lippe	Schermbeck	4,880	0.85	0.91	0.88

3.2 Validation with respect to peak simulation and representation of discharge statistics

Calibration based on the Nash/Sutcliffe criterion R^2 does not focus on peak discharges specifically. Therefore, the simulation of peak discharges and the representation of discharge statistics are examined subsequently.
Table 3-2 shows "peak errors", i.e. the relative deviation between the computed and the observed mean annual discharge maxima for the period with measured discharge data. It has to be kept in mind, that measured and simulated maxima may occur at different times.

Table 3-2: "Peak errors" of simulations for the major Rhine tributaries (relative deviation between computed and observed mean annual discharge maxima).

River	Gauging station	Catchment Area [km^2]	Period	Peak error [%]
Neckar	Rockenau	14,000	1970 - 1995	-3.6
Main	Frankfurt	24,764	1970 - 1995	7.8
Nahe	Grolsheim	4,060	1975 - 1995	-4.1
Lahn	Kalkofen	6,000	1970 - 1995	-11.4
Moselle	Cochem	27,088	1961 - 1998	-6.2
Sieg	Menden	2,880	1976 - 1995	-19.3
Erft	Neubrück	1,880	1970 - 1995	-
Ruhr	Hattingen	4,500	1970 - 1995	-5.9
Lippe	Schermbeck	4,880	1970 - 1995	-6.7

Most of the deviations are acceptable. Beside the river Erft, only the simulations for the rivers Sieg and Lahn show a "peak error" of more than 10%. Except for the river Main, there is a tendency for the underestimation of high peaks.
For the Moselle basin, where the new methodology for flood estimation is tested, the simulation of annual discharge maxima and the reproduction of discharge statistics is examined in more detail. Computed and observed annual discharge maxima are compared in Figure 3-2. In contrast to the general underestimation of the annual maxima, the largest two observed discharges are slightly overestimated. Table 3-3 presents standard statistics for measured and simulated discharge.

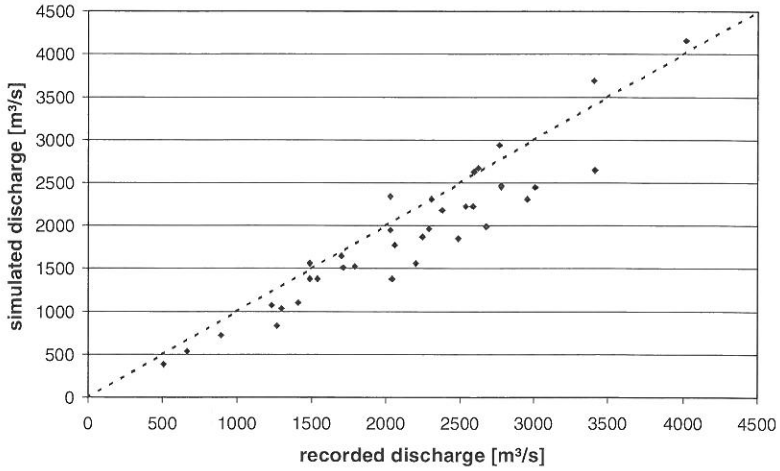

Figure 3-2: Scatter plot of recorded and simulated annual discharge maxima at gauging station Cochem/Moselle 1962-1997

Table 3-3: Standard statistics of recorded and simulated discharge at gauging station Cochem/Moselle (period 1962-1997).

	Mean [m^3/s]	median [m^3/s]	maximum [m^3/s]	minimum [m^3/s]	standard deviation of daily values [m^3/s]
recorded discharge Cochem	331	207	4020	10	361
HBV simulation Cochem	321	200	4159	19	354

Figure 3-3 shows the discharges for different return periods estimated from measured and simulated data assuming a log Pearson Type III distribution. This distribution is commonly used for calculating design discharge at federal waterways in Germany. Note, that for the recorded data, the computed discharges for certain recurrence periods may differ from the official values because they are based on daily average discharge values during a relatively short period (36 years). The HBV model overestimates the return periods of discharges smaller than ~3700 m^3/s and underestimates the return periods for larger discharges.

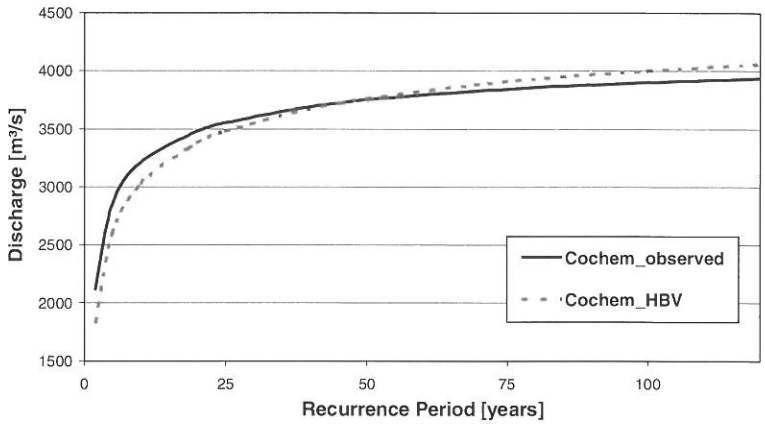

Figure 3-3: Log Pearson Type III distribution estimated with the maximum-likelihood method on the basis of measured and simulated annual peak discharges at gauge Cochem/Moselle 1962-1997.

4 APPLICATION OF THE METHODOLOGY FOR THE RIVER MOSELLE BASIN AND ITS COMPARISON WITH THE RESULTS OF STATISTICAL APPROACHES

A 1000-year simulation with the rainfall generator (model UE, see section 2) is taken as input for the HBV model of the river Moselle.
The input data set for the Moselle comprises daily values of temperature at 8 climate stations that are simulated with the rainfall generator and time series of 42 subbasin average precipitation amounts that are generated passively. Evapotranspiration is simulated in the HBV modelling system based on long-term mean monthly values.
Figure 4-1 shows the annual maxima of daily discharges of the simulated 1000 years. The simulated maximum values fit quite well into the range of observed annual maxima during the period from 1962 to 1997 and there is no visible trend. Since there are significantly larger 10-day precipitation amounts in the 1000 years generated precipitation than in the historical record, it is not surprising that some of the simulated floods are considerably higher than the 1993 flood, which marks the maximum of the recorded data. Hydrographs of the 1993 flood event, the maximum peak simulated with generated precipitation and the simulated flood event caused by the maximum generated 30-day precipitation sum are presented in Figure 4-2. The latter flood event is one of the simulated floods with maximal volume.

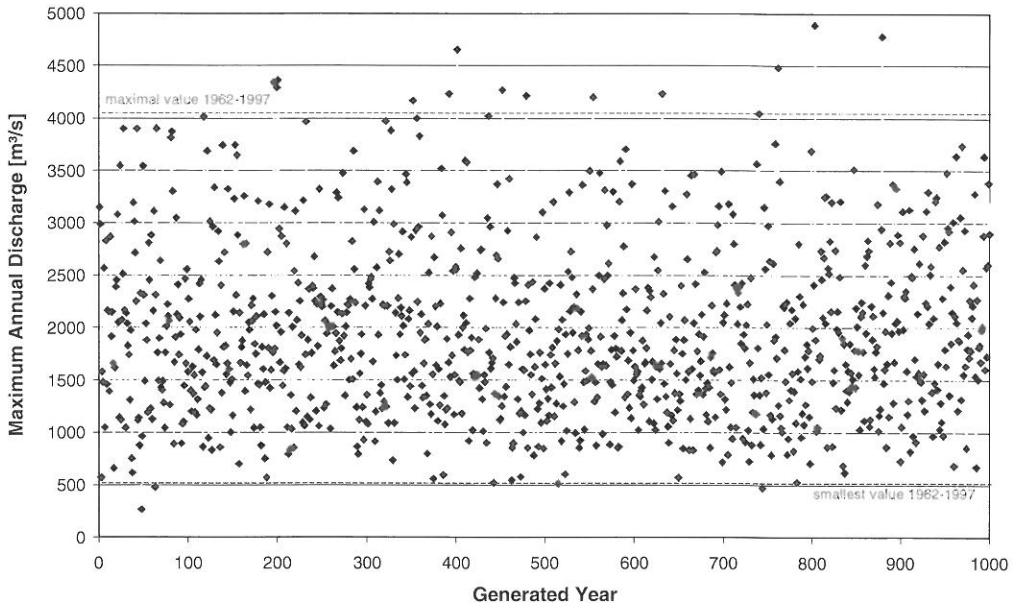

Figure 4-1: Annual maximum peaks of 1000 years of simulated discharge at gauging station Cochem/ Moselle based on generated precipitation.

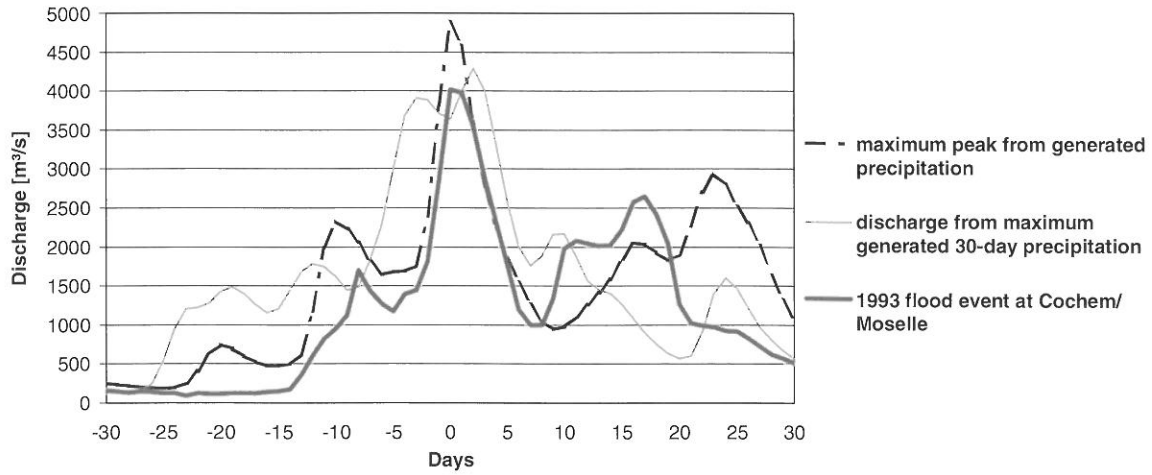

Figure 4-2: Hydrographs of the 1993 flood event and simulated floods based on generated precipitation at gauging station Cochem/Moselle.

Figure 4-3 compares the ranked recorded and simulated annual discharge maxima. Fitted log Pearson Type III distributions on the basis of the recorded and simulated discharge are added to facilitate a comparison.

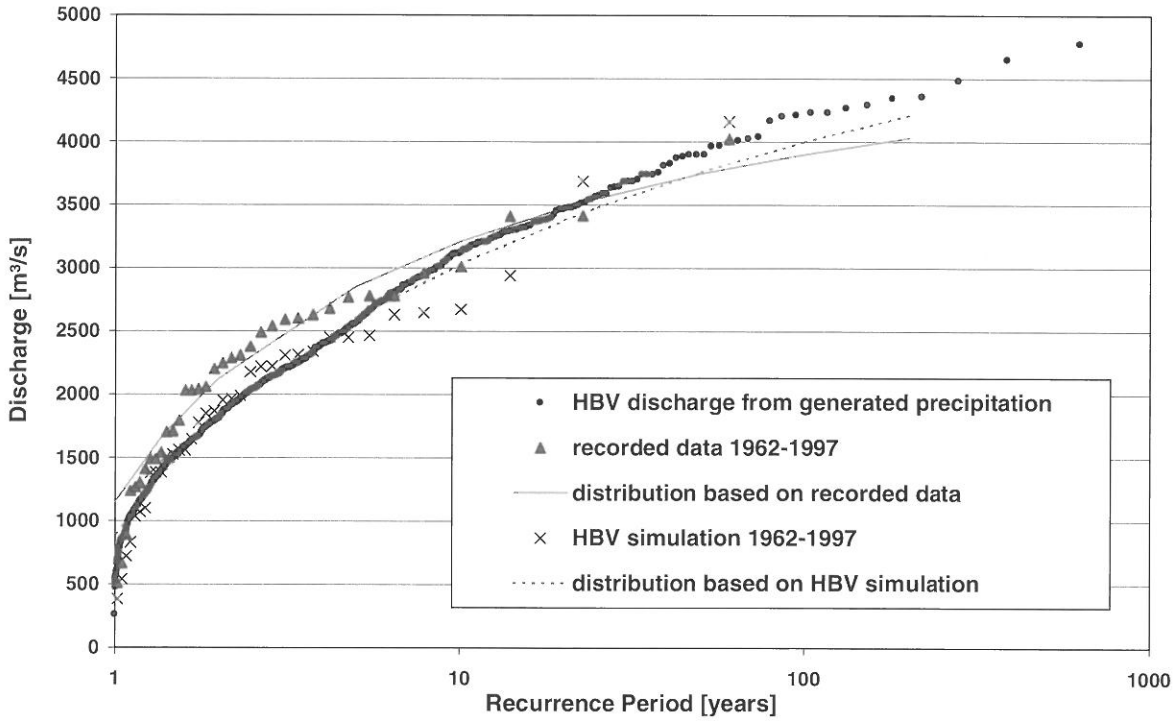

Figure 4-3: Frequency distributions of annual discharge maxima from a HBV simulation based on generated precipitation, a HBV simulation based on recorded precipitation and recorded discharge data.

The HBV simulation based on generated precipitation of 1000 years results in other design discharges than by using the statistical approach. However, the deviation is within the range that could be expected when applying different distributions as well. Especially concerning discharges of longer return periods there is a good agreement with the measured values. For smaller peaks the results of the 1000-year simulation show a similar underestimation as that for the HBV simulation with historic rainfall.

5 CONCLUSIONS AND DISCUSSION

In order to reduce the uncertainties in the estimation of the design discharge for the Rhine basin, a new methodology is being developed in which a stochastic rainfall generator and precipitation-runoff models are coupled. Promising results have been obtained for the Moselle basin, the largest tributary of the Rhine. The largest shortcoming is an underestimation of the annual maximum discharges by the HBV model. An underestimation of peak discharges is also found for most other subbasins of the Rhine. There is, therefore, some need to reconsider the calibration of the HBV model using other statistical criteria than the Nash/Sutcliffe criterion R^2. Another option for improving HBV results might be to simulate considered flood events on an hourly basis, hence, simulating the actual peak discharges instead of daily average discharges. Concerning the rainfall generator, the good correspondence between the HBV simulation based on observed precipitation data and the HBV simulation based on the precipitation input from the rainfall generator suggests that the effects of possible errors in the statistics of the simulated extreme precipitation are negligible. Nevertheless, it should be noticed that the nearest-neighbour resampling method does not simulate *daily* precipitation values higher than those in the historical precipitation record. Generally, uncertainty is introduced by the relatively short length of the observed precipitation record on which the rainfall generator is based (35 years) and by the limited period with data that is available for the calibration of the HBV model in the Rhine basin.
There are various options for using the long simulation runs of discharges. The design discharge can be derived with or without fitting a distribution to the simulated annual maxima. A first impression of the uncertainty can be obtained from an ensemble of 1000-year generated discharges.

A major advantage of the new method is that it provides information about the shape of the hydrograph, including volume and duration of the floods. A potentially useful application is that the simulated hydrographs can be used as model-floods in other studies.

ACKNOWLEDGEMENTS

The daily precipitation, temperature and sunshine duration data were made available by the following institutions: German Weather Service (DWD), Service de la météorologie et de l 'hydrologie de Luxembourg, Météo France and the Swiss Meteorological Institute through the International Commission for the Hydrology of the Rhine Basin (CHR/KHR). The pressure data were kindly provided by P.D. Jones (Climatic Research Unit, University of East Anglia, Norwich). Discharge time series were made available by the water authorities of the federal states Bavaria, Baden-Wurttemberg, Rhineland-Palatinate, Saarland, Hesse and North Rhine-Westphalia, by the Service de la météorologie et de l 'hydrologie de Luxembourg and by regional water authorities in France.

REFERENCES

Buishand, T.A., Brandsma, T. (2001): Multi-site simulation of daily precipitation and temperature in the Rhine basin by nearest-neighbor resampling. Water Resour. Res., 37: 2761-2776. American Geophysical Union (AGU). Washington.

Eberle, M., Sprokkereef, E., Wilke, K., Krahe, P. (2001): Hydrological Modelling in the River Rhine Basin, Part II. Report on Hourly Modelling. BfG - 1338. Bundesanstalt für Gewässerkunde. Koblenz.

Lammersen, R., Buiteveld, H., Ritter, N., Disse, M., Engel, H. (2002): Simulating the effect of flood reducing measures on the flood conditions of the river Rhine. Draft December 2001. To be published in the proceedings of the International Conference on Flood Estimation in Berne, March 6-8, 2002. CHR. Lelystad.

Lidén, R., Harlin, J. (2000): Analysis of conceptual rainfall-runoff modelling performance in different climates. Journal of Hydrology, 238, 231-247. Elsevier Science. Amsterdam.

Lindström, G., Johansson, B., Persson, M., Gardelin, M., Bergström, S. (1997): Development and test of the distributed HBV-96 hydrological model. Journal of Hydrology, 201, 272-288. Elsevier Science. Amsterdam.

Mülders, R., Parmet, B., Wilke, K. (1999): Hydrological Modelling in the River Rhine Basin. Final Report. BfG - 1215. Bundesanstalt für Gewässerkunde. Koblenz.

Parmet, B., Buishand, T.A., Brandsma, T., Mülders, R. (1999): Design discharge of the large rivers in The Netherlands - towards a new methodology. In: Hydrological Extremes: Understanding, Predicting, Mitigating. Proceedings of IUGG 99 Symposium HS1. L. Gottschalk, J.-C. Olivry, D. Reed and D. Rosbjerg (Eds.). IAHS Publ. No. 255. IAHS Press. Wallingford.

Rajagopalan, B., Lall, U. (1999): A k-nearest-neighbor simulator for daily precipitation and other variables. Water Resour. Res., 35: 3089-3101. American Geophysical Union (AGU). Washington.

Wendling, U. (1995): Berechnung der Gras-Referenzverdunstung mit der FAO Penman-Monteith-Beziehung. In: Wasserwirtschaft 85, H. 12. Friedr. Vieweg & Sohn Verlagsges. mbH. Wiesbaden.

White, W. (2001): Spatio-Temporal Structure of Precipitation in the Moselle Basin with Particular Regard to Flood Events. University of Trier. Trier.

Wójcik, R., Beersma, J.J., Buishand, T.A. (2000): Rainfall generator for the Rhine basin: Multi-site generation of weather variables for the entire drainage area. KNMI-publication 186-IV. KNMI. De Bilt.

THE FLOOD ESTIMATION PUZZLE

Andrew Faeh[1], Balz Cavelti[1], Benno Zarn[2], Hans Müller-Lemans[3]

[1] Ingenieurbureau Heierli AG, Culmannstrasse 56, Postfach, CH-8033 Zurich, Switzerland, inbox@heierli.ch

[2] Hunziker, Zarn & Partner AG, Ingenieurbüro für Fluss- und Wasserbau, Schachenallee 29, CH-5000 Aarau, Switzerland, info@hzp.ch

[3] Tergeso AG, Büro für Umweltfragen, Stadterwingert 4, CH-7320 Sargans, Switzerland, tergeso@pop.agri.ch

SUMMARY

Flood estimation is an extremely challenging endeavour, even more so in the light of the increasingly limited availability of financial resources. In order to obtain reliable flood estimates, particularly for large and heterogeneous catchments, considerable effort must be placed in ensuring that no clue to catchment behaviour goes unnoticed. Obtaining reliable estimates for flood discharges and their return periods could therefore also be referred to as solving the flood estimation puzzle. The available information on catchment behaviour thereby serves as the puzzle's pieces to be gathered and correctly assimilated.
Such a comprehensive methodology for flood estimation is discussed in this paper for the 6'100 km^2 mountainous Alpenrhein catchment, for which estimates of the 30-, 100- and 300-year floods as well as the so called "extreme flood" with an even larger return period were required. It is shown to what extent the holistic approach, in which all the obtainable information on catchment behaviour was collected, analysed and collated, was able to provide a better understanding of flood generation in this catchment. The diverse information sources such as historical flood records, discharge measurements and their statistical analysis, a study of the extreme meteorological conditions, the influence of anthropogenic activity in the catchment, and flood modelling are dealt with, showing what information could be gleaned from each of these sources. The extent to which the individual sources of information assist in flood estimation, depending on the return period of the flood in question, is shown. The information used to determine the 30-year flood, is for example, of little use for estimating floods with 300-year return periods and greater.
Although the holistic approach without doubt improves catchment understanding, it is not able to remove all the uncertainties associated with flood estimation. As is shown, this is to a large extent due to the problems associated with assigning return periods to the flood modelling results. Only with an improved understanding of the extreme meteorological characteristics of a catchment can the potential of flood modelling, being one of the pieces of the flood estimation puzzle, be fully harnessed.

Keywords: Flood estimation, flood frequency, historical flood records, meteorological factors, rainfall-runoff modelling, extreme flood scenarios

1 INTRODUCTION

The Alpenrhein is the uppermost Rhine reach extending from the confluence of its two uppermost tributaries Vorderhein and Hinterrhein to its mouth into Lake Constance (Figure 1-1). The total area of the mountainous Alpenrhein catchment lying in the territories of Switzerland, Austria and Liechtenstein is 6'100 km^2. For the planning of flood protection measures, estimates of the discharges at various locations were required for the 30-, 100- and 300- year floods as well as the even larger so called "extreme flood" with an unspecified return period. This paper describes the holistic approach which was applied in order to obtain reliable estimates for the required flood discharges. Thereby, in what might be referred to as solving the flood estimation puzzle, all available information on the flood hydrology of the Alpenrhein was gathered and assimilated in defining flood discharges and their return periods (Ingenieurbureau Heierli AG et al., 2000). The individual sources of information available and the clues these provided on the behaviour of the catchment are described. Thereafter it is shown how these puzzle pieces were ordered and to what extent flood frequency could be defined.

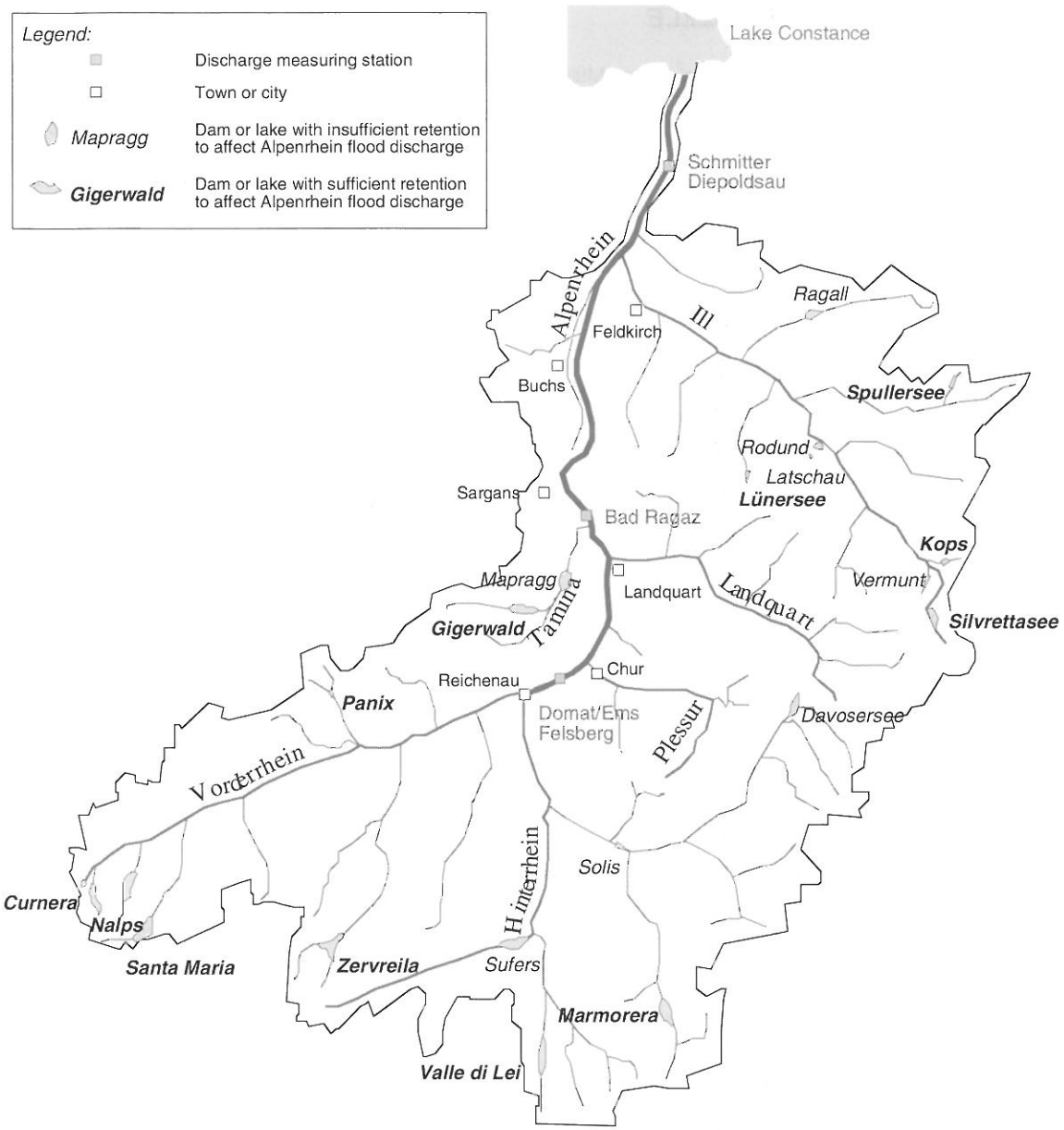

Figure 1-1: The 6100 km^2 Alpenrhein catchment showing the main tributaries and locations of discharge measuring stations. The dams and lakes are shown with respect to their retention capacities such that these are able to influence flood discharge magnitudes.

2 HISTORICAL FLOOD RECORDS

As summarised in Figure 2-1, extensive information on the historical flood records of the Alpenrhein was available from a preliminary study (ETH Zurich and Basler&Hofmann, 1998). Three catastrophic Alpenrhein floods occurred in the last 800 years, namely in the years 1343, 1566 and 1762. Beside the catastrophic floods, an additional twelve extremely large floods occurred in this period.
In the main study an attempt was made at obtaining quantitative estimates of the flood discharges for the known historical floods. The intention being to enable the database for statistical flood analysis to be lengthened, if not in absolute terms, then at least qualitatively. For this purpose, the available information on the maximum flood levels was gathered and used in conjunction with the available information on the reach geometry at that time. For those historical floods where the flood levels could not be ascertained or the reach geometry was unknown, no discharge estimates could be made. Generally sufficient information for flow estimation is only available for the more recent historical floods. In the case of the Alpenrhein the discharges for the floods of 1834, 1868 could be estimated. Together with

the discharge measurements of the 20th century this meant that maximum discharge values for the four largest flood events which occurred in the last 200 years were known or could be approximated.

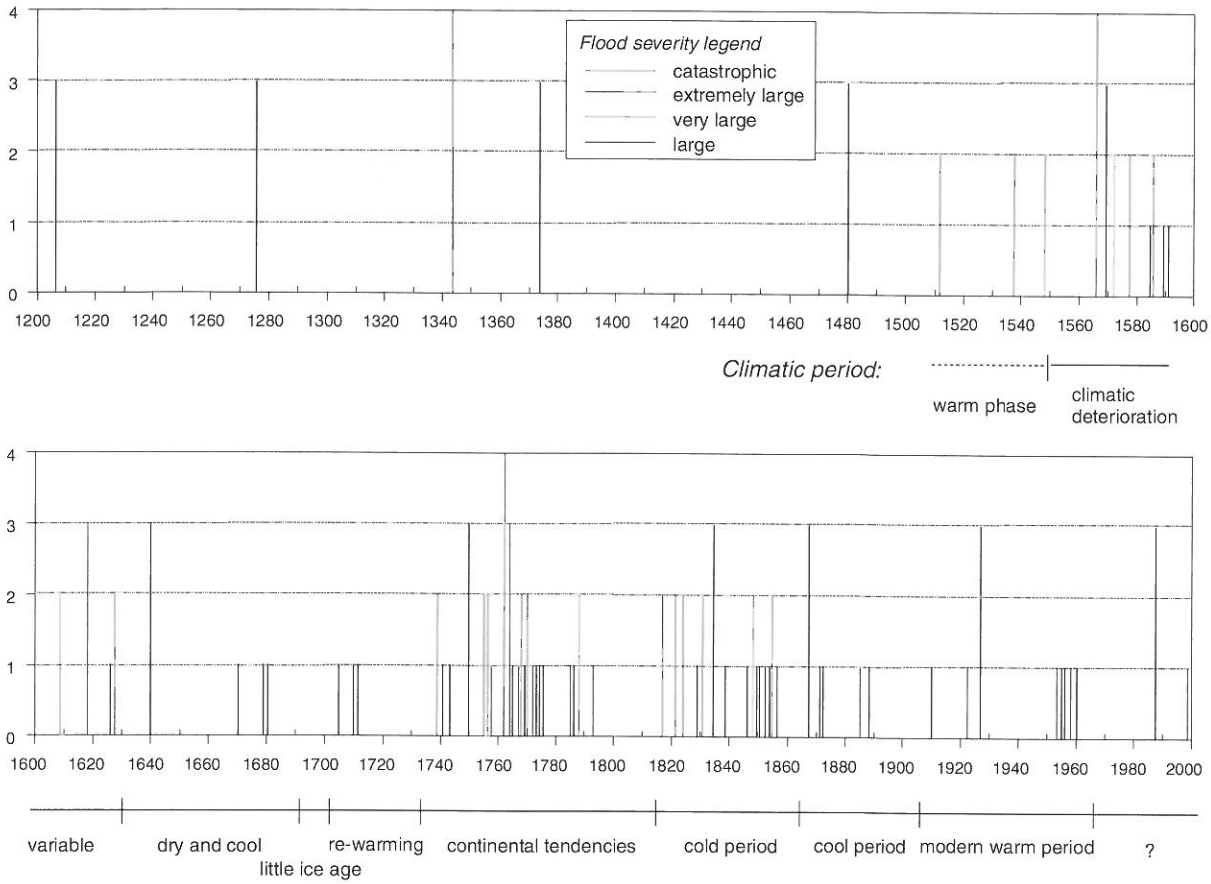

Figure 2-1: Historical flood record for the last 800 years showing approximate flood magnitude (1 = large, 4 = catastrophic) as could be determined on the basis of the available descriptions of the events. The prevailing climatic conditions since 1500 are also shown.

Historical floods for which no discharge estimates could be made still provided valuable clues on the behaviour of the catchment. Firstly, they enabled the seasonal susceptibility to flooding to be ascertained. The large floods of the Alpenrhein only occur between the months of July and September. Even for very old flood records some indication on the then prevailing weather could generally be found, the historical flood records furthermore provided an indication as to the meteorological conditions required for flood formation. For example, all of the catastrophic floods in the last 800 years were probably caused by continued heavy rainfall lasting several days alone without being significantly exacerbated by snowmelt.

3 METEOROLOGICAL ANALYSIS

A further piece of the puzzle was provided by knowledge of the meteorological conditions leading to flood formation. The weather patterns for the last century were analysed which led to the occurrence of floods. For the Alpenrhein, either of two distinct meteorological conditions, i.e. a precipitation field centred north or south of the Alps, were found to be responsible for flood formation. The difference between these types of events is apparent in Figure 7-1.
For the north centred events, the centre of the rainfall area lies somewhere in the northern region of the catchment. Its actual position can, however, vary considerably from event to event. This is not the case for south centred events, which generally show less variation in locality. Here the geographical catchment features have a controlling influence on the precipitation, which falls principally in the southernmost catchment regions when large scale precipitation fields spill over from the southern side of the alps. Of the six largest floods in the last 200 years, five were south centred events (1834, 1868, 1927, 1954 and 1987) and only one was north centred (1910). It would seem therefore, that Alpenrhein floods are more frequently induced by south centred events than by north centred events.

As very large floods of the Alpenrhein are mainly to be expected between the months of July and September, the influence of snow melt on flood formation could be regarded as being small. Based on the meteorology of previous flood events, three meteorological factors could however be identified to be requirements for flood formation of the Alpenrhein. Firstly, a large area discharge, i.e. large amounts of precipitation over the majority of the catchment. Secondly, a high snowfall level (0° altitude), which ensures that the precipitation falls almost exclusively as rain. Thirdly, considerable rainfall prior to the main precipitation event, especially in the days immediately preceding the main precipitation.
In order to facilitate the estimation of the magnitude and frequency of future flood events, the influence and extent of climate change on flood formation was of interest. No evidence of the effects of climate change could, however, be found from the meteorological data relating to Alpenrhein floods. Nevertheless, should climate change result in an increase of the 0° altitude for future precipitation events, then floods will probably occur more frequently. This, because that for several large precipitation events in the 20th century flooding did not occur purely as a result of these occurring in conjunction with low snowfall levels.

4 ANTHROPOGENIC INFLUENCES

Assessment of anthropogenic effects on flood generation provides another clue to be taken into account for flood estimation. Relative to the total catchment area only a very small percentage of the Alpenrhein catchment displays rural or urban development. The effects of soil compaction in rural areas or surface sealing in urban areas could thus be neglected. Due to the presence of extensive hydroelectric power installations however (Figure 1-1), artificial catchment retention was suspected to have a considerable effect on Alpenrhein flood generation.
Three distinct periods could be identified which are differently influenced by artificial catchment retention (Figure 4-1). Up until 1950 reservoirs sufficiently large to have an effect on flood generation did not exist in the catchment. Thereafter, in the period from 1950 to 1970, flood generation was increasingly influenced by the construction of reservoirs. Subsequent to 1970 the artificial catchment characteristics have remained practically unchanged. Comparison of flood records assessed for each of these periods provided an insight which alone was not sufficient to enable the effects of artificial catchment retention to be assessed. For this purpose, the yearly fluctuations in reservoir levels – being at their lowest from March to May and at their highest in September and October – also had to be taken into account.

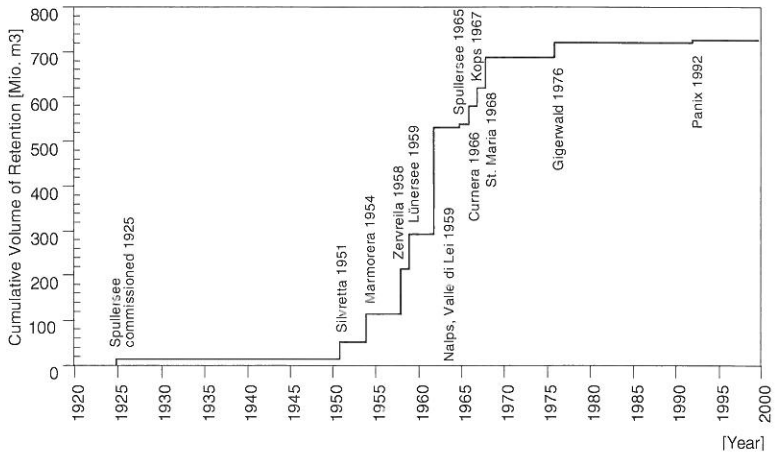

Figure 4-1: Cumulative retention volume of the reservoirs in the Alpenrhein catchment in the period 1920 to 2000. Date of commissioning of the individual dams and their influence on total retention volume is indicated.

Although it was apparent that the damping effect due to artificial catchment retention would be greatest for floods occurring in July, a means of quantifying the retention effect was required. Here the comprehensive rainfall-runoff model developed for the catchment taking the artificial retention basins and diversions into account (as described later) proved to be a valuable tool. By modelling the floods of September 1981 and July 1987 with and without artificial catchment retention, the damping effect on maximum discharge was determined to lie between 10% and 25% depending on reservoir filling.

5 DISCHARGE MEASUREMENTS

When available, discharge measurements provide an invaluable tool for flood estimation. Whereas measurements of the river in question offers the basis for a statistical flood analysis, measurements of the tributaries provide an insight into the differing behaviour of the various sub-basins.
As would be expected for such a large catchment, measurements were available for several locations. The measurements on the tributary streams and rivers indicated the differing behaviour of the various sub-basins in as much as they were used for the calibration and verification of the rainfall-runoff model. The measurements for the three stations along the Alpenrhein itself were statistically examined in the framework of a flood frequency analysis (Figure 5-1). These three stations also provided insight into the accuracy of the model for the Alpenrhein itself.

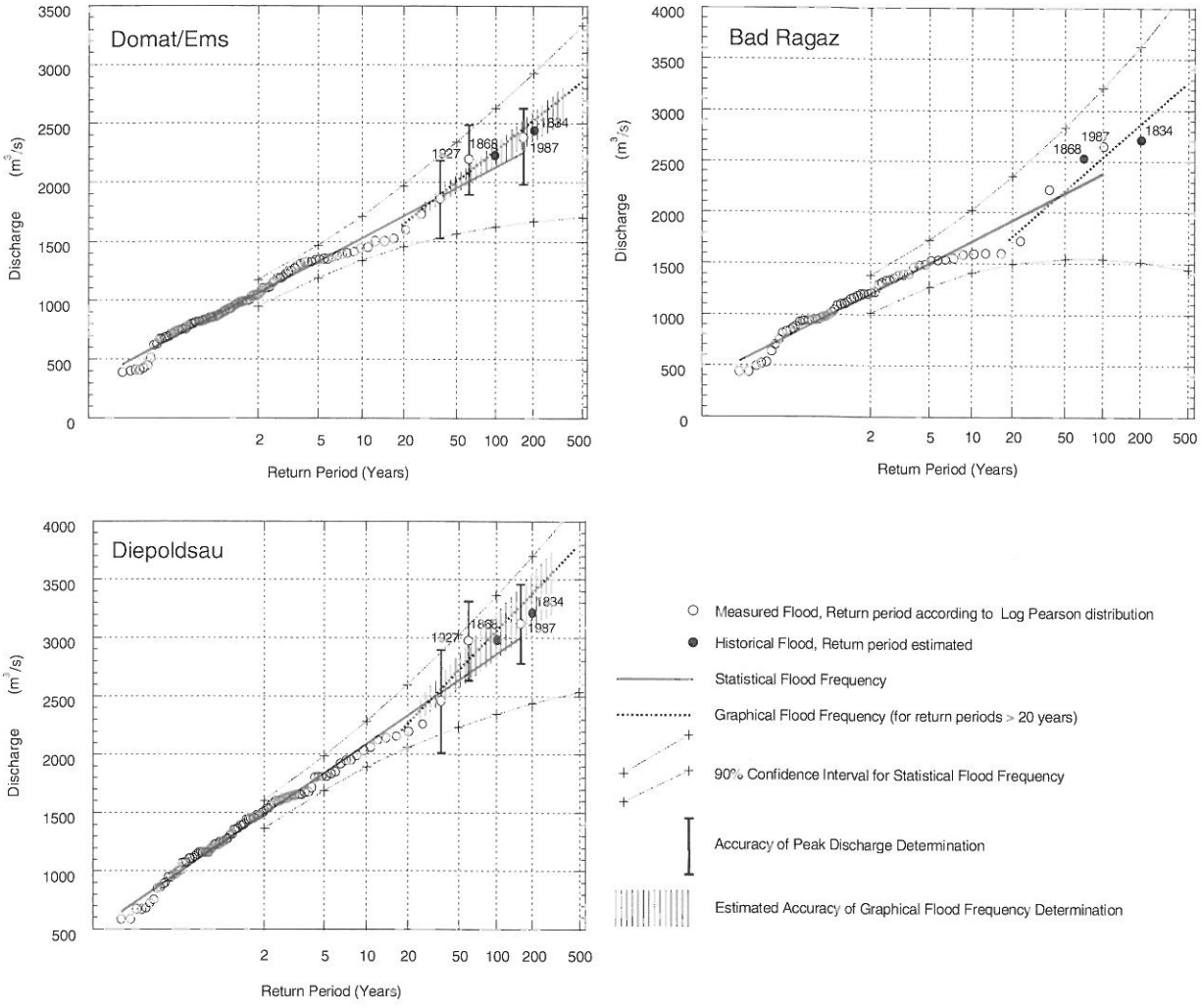

Figure 5-1: Statistical analysis according to Log Pearson using the homogenised flood records for the discharge measuring stations Domat/Ems, Bad Ragaz and Diepoldsau. The two largest floods in the 19th century for which the return periods were estimated are used for the graphical flood frequency analysis.

The value of a flood frequency analysis, for which the maximum discharge measurements of each year are usually used, depends not only on the length of the measurement records but to a large extent on the accuracy of the measurements. The measuring stations along the Alpenrhein were thus examined in order to assess the accuracy and possibly correct the measurements of flood discharges. For the uppermost (Felsberg, Domat/Ems) and lowermost (Diepoldsau, Schmitter) discharge measuring stations (see Figure 1-1), with measurements since 1899 and 1904, respectively, no major corrections to the published discharge values were found to be necessary. This, despite the fact that the level-discharge relationships at the lowermost location do take floodplain flows into account – the general magnitude of this problem was probably known to the relevant authorities and thus the inaccurate

level-discharge relationships were corrected by the use of fictitious water levels for discharge evaluation. At the middle location (Bad Ragaz) – in operation between 1930 and 1991 – the measurements were influenced by the effects of bed-load transport and alternate sand bars. Here, no statement as to the accuracy of the measurements could be made. Based on the measurements of the neighbouring stations, the maximum discharge values at this location could however still be sufficiently well ascertained to enable a flood frequency analysis to be performed.
For the flood of 1927, a dam breach occurred between the middle and lowermost measuring locations thus affecting the lowermost measurement. This measurement was thus reconstructed by transforming the flood wave measured upstream of the breach on the basis of unsteady discharge computations using the inflows from the sub-catchments lying between these locations as determined with the rainfall-runoff model.
Using the peak discharge values estimated for the two largest floods in the 19th century (1834, 1868), the existing record of measurements in the order of 100 years was effectively doubled for the statistical flood frequency analysis. Together with the discharge measurements, the flood discharges of 200 years could be brought into relation to one another, as shown in Figure 5-1. The flood of 1834 was thereby probably the greatest of the period 1800 to 2000, albeit by a small margin. In terms of peak discharge, the floods of 1834, 1868, 1927 and 1987 were thus all of comparable magnitude. Flood volumes displayed more variability. For the events of short duration of 1834 and 1927, the discharge volumes were considerably less than those for the floods of 1868 and 1987, which were longer in duration.

6 RAINFALL-RUNOFF MODEL

Even with the lengthened flood records of 200 years the statistical database was insufficient to enable predictions of floods with return periods of 300 years and more to be made. For this purpose, a detailed, physically based rainfall-runoff model was drawn up for the Alpenrhein catchment. The model used was able to take into account the spatial variability of precipitation and discharge generation, time of concentration and wave transformation as determined by the hydraulic catchment properties and the effects of retention and diversions due to the intensive hydroelectric infrastructure installed in the catchment. In this model, the catchment was subdivided into approximately 1800 area elements, each with specific discharge generation characteristics, these being linked on the basis of the hydraulic properties of the furrows, streams and rivers into which these drain.
Although the results of rainfall simulation experiments were used to define flood generation of the individual area elements (Faeh, 1997), the variability of natural flood generation will always dictate the necessity for model calibration. The model was therefore calibrated and verified on the basis of the measurements of the floods of the latter half of the 20th century for which sufficient measurements were available. E.g. having calibrated the model for the 1987 event, it was verified that the 1981 and other events were reproduced using the same unchanged parameter set. Due to the variability and size of the Alpenrhein catchment and the as yet unsolved hydrological problems associated with quantifying discharge generation and basin drainage, modelling imprecision could not be totally eliminated, especially in the sub-catchments. Two slightly different parameter sets were therefore found to be necessary for long duration and short duration events. When modelling extreme meteorological scenarios, as described in the next section, these two parameter sets were used to estimate the minimum and maximum response of the Alpenrhein to the assumed precipitation.
Another factor affecting the simulation results was the magnitude of the available database. For more recent events, sufficient data on rainfall distributions and intensities was available. Considerably less data was available for less recent events, with the result that simulation results were less accurate for these events. Despite the modelling inaccuracies of some sub-catchments and the inconsistencies of the available database, feasible simulation results were generally obtained for the Alpenrhein for all flood events examined. Typical modelling results for different events are shown in Figure 6-1.

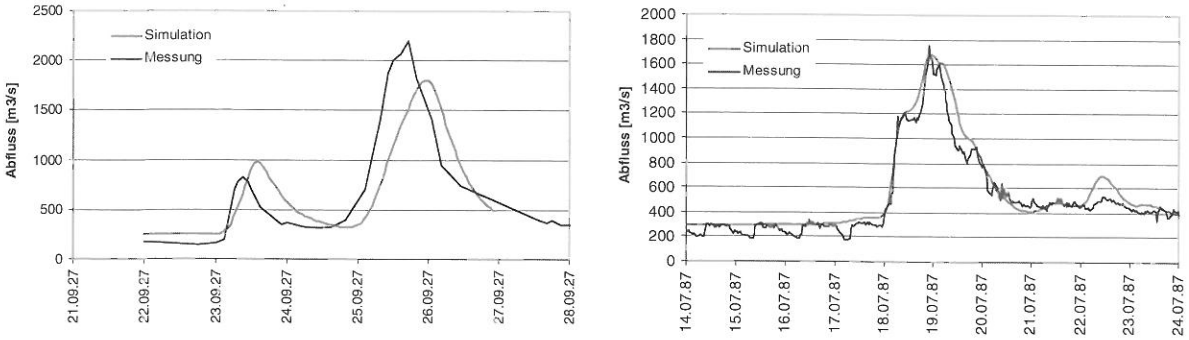

Figure 6-1: Typical results obtained with the rainfall-runoff model shown here at the location Domat/Ems for the 1927 (left graphic) and 1987 (right graphic) events. (Abfluss = Discharge, Messung = Measured Discharge). A time interval of one hour applied for all simulations. Depending on the event in question, up to ten days were simulated.

7 EXTREME METEOROLOGICAL SCENARIOS

To enable very large flood events with large return periods to be modelled, extreme meteorological scenarios were required. On the basis of the meteorological analysis, ten feasible scenarios were developed (five north and five south centred), which would be expected to lead to large Alpenrhein floods (see Figure 7-1 and Table 7-1). Actual measurements were used in the definition of the scenarios to ensure their plausibility. Furthermore, they could thereby be compared and brought into relation with the known Alpenrhein flood events.

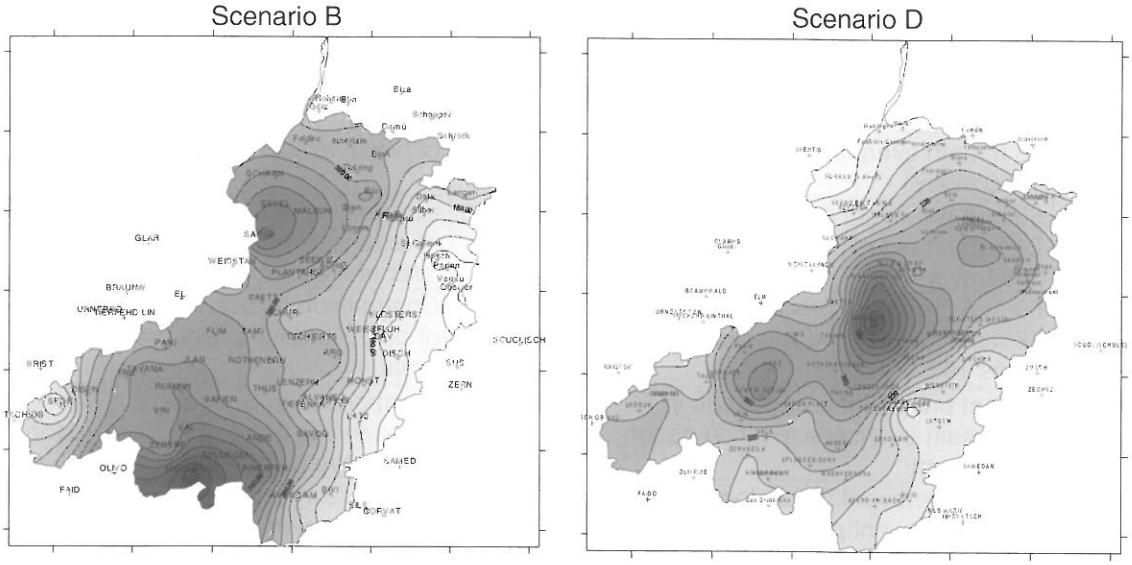

Figure 7-1: Rainfall distribution (as event total) for a typical south centred Scenario B, with precipitation centre in the Hinterrhein region, and a typical north centred Scenario D, with precipitation centre in the middle of the catchment. Whereas the south centred rainfall distributions A, B, E, F and I were based directly on measurements, the precipitation fields for the north centred scenarios C, D, G, H and J were shifted such that their centres came to lie in the middle of the catchment.

The north centred scenarios were based on the 1910 event, being the largest such event in the 20th century. Based on the variability of the north centred events, as discussed in Section 3, the precipitation fields of 1910 were shifted into the centre of the catchment to maximise the effect of the precipitation on the Alpenrhein for these scenarios. No shift in the precipitation field was to be expected for the south centred scenarios. These scenarios were therefore based directly on the measured precipitation for the 1984 event, for which the greatest precipitation was measured in the 20th century – this event did not lead to an Alpenrhein flood due to a low snowfall level (0° altitude). The individual scenarios varied with regard to the amount of precipitation assumed to occur before the main event or in terms of the intensity

and duration characteristics of the main precipitation. For all scenarios, snowfall levels were assumed to be sufficiently high such that the precipitation would fall exclusively as rainfall.
The scenarios resulted in flood discharges considerably larger than those which have been observed in the last 100 years. In order to enable these computed flood values to be compared with the historical and measured flood values in terms of their probability of occurrence, the return periods of the computed values needed to be estimated. Based on a comparison with the flood frequency analysis obtained using the historical and measured flood events and the meteorological assumptions made for the individual scenarios, their return periods were roughly estimated (see Table 7-1).

Table 7-1: The meteorological assumptions underlying the scenarios examined (A to J), and the rough estimates made for the return periods of the calculated flood values. The reasoning upon which the return period estimates are based is also given. The return periods for the floods of 1910 and 1987, upon which the estimated return periods are founded, were determined from the statistical flood frequency analysis.

Scenario		Return Period [Years]	
	Characteristics	Rough Estimate	Reasoning
A South Centred	96 h pre-event precipitation as for 1987 event 24 h main event precipitation as for 1984 event	150 - 250	Comparison to 100-year event of 1987: Greater return period due to greater precipitation
B South Centred	96 h pre-event precipitation as for 1987 event 48 h main event precipitation, (double 1984 event)	300 - 500	Comparison to Scenario A: Probability of twice 1984 precipitation smaller
C North Centred	No pre-event precipitation 24 h main event precipitation as for 1910 event	150 - 250	Comparison to 30-year event of 1910: Probability the centroid of rainfall will lie exactly in centre of catchment considerably smaller
D North Centred	No pre-event precipitation 48 h main event precipitation, (double 1910 event)	400 - 700	Comparison to Scenario C: Probability of twice 1910 precipitation smaller
E South Centred	60 mm pre-event precipitation in 72 h 24 h main event precipitation as for 1984 event	200 - 300	Comparison to Scenario A: Probability of extensive pre-event precipitation over entire catchment smaller
F South Centred	60 mm pre-event precipitation in 72 h 36 h main event precipitation, (1.5 times 1984 event)	250 - 400	Comparison to Scenario B: Probability of only 1.5 days event precipitation greater
G North Centred	60 mm pre-event precipitation in 72 h 24 h main event precipitation as for 1910 event	250 - 400	Comparison to Scenario C: Probability of extensive pre-event precipitation over entire catchment smaller
H North Centred	60 mm pre-event precipitation in 72 h 36 h main event precipitation, (1.5 times 1910 event)	400 - 700	Comparison to Scenario D: Probability of pre-event precipitation smaller, probability of main event precipitation larger
I South Centred	60 mm pre-event precipitation in 72 h 18 h main event precipitation (1984 event with increased intensity)	300 - 600	Comparison to Scenario E: Probability of greater precipitation intensity smaller
J North Centred	60 mm pre-event precipitation in 72 h 18 h main event precipitation (1910 event with increased intensity)	500 - 900	Comparison to Scenario G: Probability of greater precipitation intensity smaller

8 COMPLETING THE PUZZLE

In what may be referred to as completing the puzzle, the results of the previously described investigations were aggregated thereby obtaining estimates for the full range of flood discharges of the Alpenrhein and their return periods. Essentially, the results of the historical flood analysis, the investigation of the anthropogenic influences and the discharge measurements are reflected in the flood frequency

analysis of Figure 5-1. Similarly, the meteorological analysis and the rainfall-runoff modelling are reflected in the results of the extreme scenario investigation of the previous section. The Alpenrhein flood hydrology puzzle was therefore completed by aggregating the results of the flood frequency analysis with those of the extreme scenario investigation, as is shown in Figure 8-1. The flood estimates thereby obtained for events with large return periods are considerably larger than those which would have resulted on the basis of the flood frequency analysis alone. These larger flood estimates are however plausible when taking into account the fact that flood activity in the 20th century was generally low, and that small changes in the precipitation characteristics e.g. snowfall level or temporal and spatial rainfall distribution, can significantly increase flood severity.

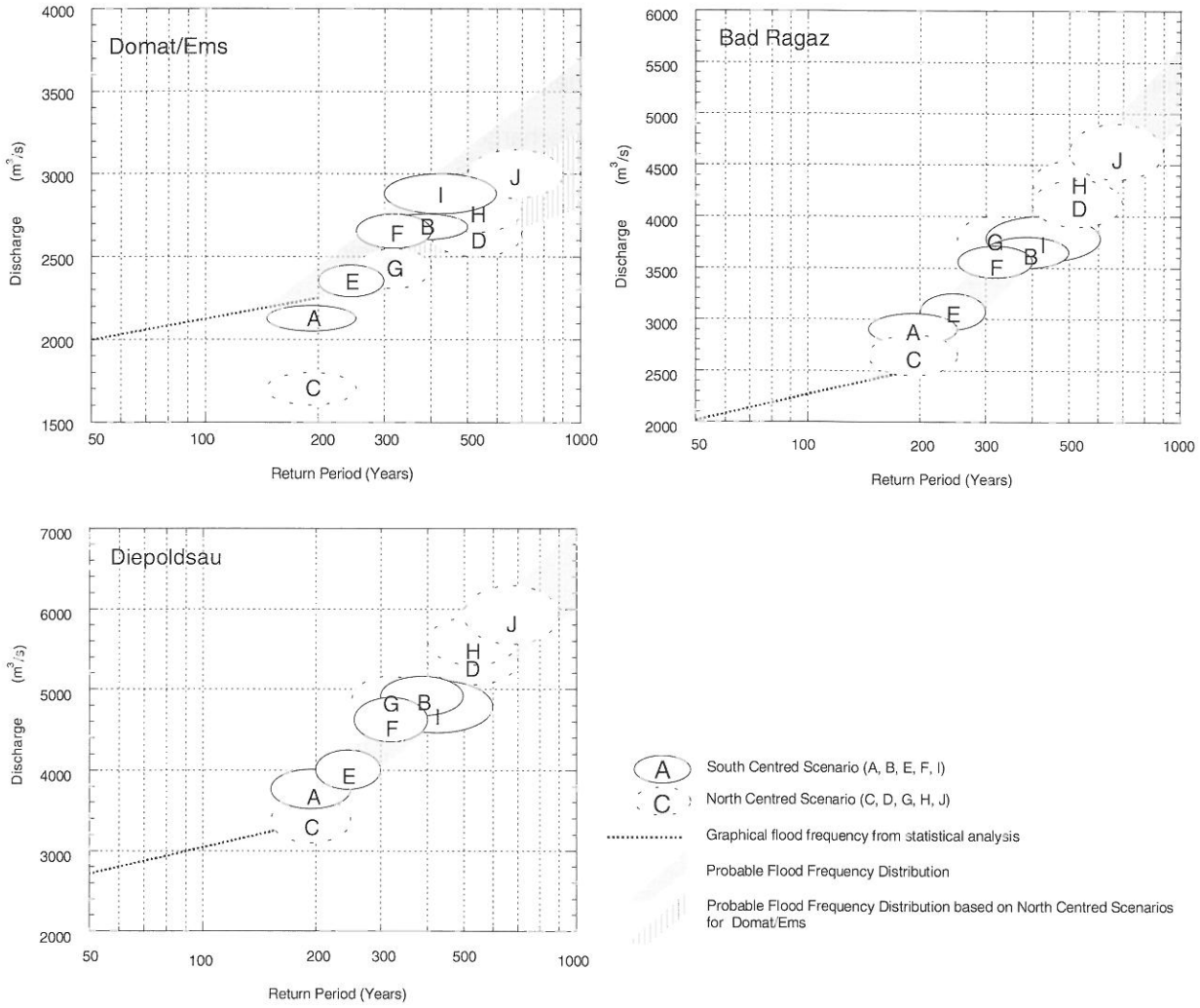

Figure 8-1: Results of the scenario computations shown on a flood frequency diagram based on their estimated return periods for the three locations Domat/Ems, Bad Ragaz and Diepoldsau. Also shown the flood frequency distributions as they result on the basis of the measured discharges and the historical flood values.

From the corrected discharge measurements alone, a statistical basis of 100 years was available. This record could be lengthened to 200 years by taking those historical floods into account. Based on the rainfall-runoff computations for the scenarios defined, the flood record was further lengthened by estimating the return periods for computed flood values. While the scenario computations provide a valuable tool for estimating the magnitude of large infrequent flood events, their use for the extrapolation of flood frequency analyses is heavily dependant on the estimates made with regard to their return periods. Although this problem remains, the gathering and collation of all available information in solving the flood estimation puzzle minimises the effects of this uncertainty, and ensures that reliable flood estimates can be made.

ACKNOWLEDGEMENTS

Thanks go to the Hydraulic Engineering Section of the International Government Committee Alpenrhein for entrusting us with this study. Dr Dietmar Grebner of the Swiss Federal Institute of Technology, for his assistance and advice with regard to the meteorological investigation. Dr Armin Petrascheck of the Federal Office for Water and Geology, for his constructive criticism on rainfall-runoff modelling issues.

REFERENCES

ETH Zurich, Basler&Hofmann (1998): Vorstudie Hydrologie Alpenrhein, preliminary study performed for the Internationale Regierungskommission Alpenrhein. Zurich. (not published)

Faeh, A.O. (1997): Understanding the processes of discharge formation under extreme precipitation. A study based on the numerical simulation of hillslope experiments. Mitteilung der VAW, Nr. 150. Zurich.

Ingenieurbureau Heierli AG, Hunziker, Zarn & Partner AG, Tergeso AG (2000): Hydrologie Alpenrhein, Study performed for the Internationale Regierungskommission Alpenrhein. Zurich. (not published)

EFFECTS OF GRID RESOLUTION AND PRECIPITATION INTERPOLATION ON A MESO-SCALE FLOOD FORECAST MODEL

Kai Gerlinger[1], Norbert Demuth[2], Karl Ludwig[1]

[1] Ingenieurbüro Dr.-Ing. K. Ludwig, Beratender Ingenieur, Herrenstrasse 14, D-76133 Karlsruhe, Germany, buero@ludwig-wawi.de

[2] Landesamt für Wasserwirtschaft Rheinland-Pfalz, Am Zollhafen 9, D-55118 Mainz, Germany, Norbert.Demuth@wwv.rpl.de

SUMMARY

Due to frequent flooding within the watershed of the Moselle River (A ≈ 28,000 km^2), the extension of flood forecast lead times to up to 48 hours represents one key measure of improved flood management. In order to reach this goal, a grid-based flood forecast model for the Moselle River was developed and refined by applying the program system LARSIM.
The first Moselle River model consists of 154 cells with an area of 14 km by 14 km for each cell. It is currently used as a real-time flood forecasting system for the German part of the Moselle River. Input data include hourly values of measured discharge (at 20 gauges), measured precipitation (at 50 rain gauges) and the 48-hour precipitation forecasts of the German Weather Service. In the event of a flood, measured data are automatically transmitted from France, Luxembourg, and Germany to the flood forecast center in Trier, Germany.
The second Moselle River model has a higher resolution with a grid cell size of only one square kilometer, resulting in about 28,000 grid cells. Additionally, the interpolation of precipitation has been improved by integrating information from historical precipitation events using geostatistical methods. Calculating 12-hour forecasts, the reliability of the new 1 km² grid model could be demonstrated.
A comparison of simulation results of the two models shows that the geostatistical interpolation procedure for measured precipitation does not improve results derived from the inverse-distance-method. Slightly improved results are obtained for the model with the denser grid, especially for smaller catchments and for the upstream regions. Furthermore, the model with the denser grid provides a vastly more flexible tool for flood management: it is capable of including spatial data with higher resolution (e.g., weather forecasts, radar) and has the potential for future flood warning for local flood events.

Keywords: flood forecasting model, geostatistical interpolation, grid size, LARSIM, Moselle

1 INTRODUCTION

The floods of 1993 and 1995 along the Rhine and the Maas rivers inundated entire cities and villages in France, Belgium, and Germany and led to the evacuation of several 100,000 people in the Netherlands. Due to the enormous damage, the secretaries of the environment of the respective countries signed a resolution with which the watershed commissions along the Rhine, the Moselle, the Saar, and the Maas River were assigned to plan integrated and internationally coordinated flood prevention measures.
In the watersheds of the Moselle and the Saar rivers, which cover parts of the countries France, Luxembourg and Germany (Figure 2-1(1)), transboundary co-operation started early, when the first international workgroup for flood prevention was founded in 1985. Two years later, an agreement was signed coordinating the information flow process during floods with the goal of installing a real-time transmission water level information system. In 1998, the International Commission for the Protection of the Moselle and Saar Rivers (IKSMS) set up the "Aktionsplan Hochwasser" ("Action Plan Floods") (IKSMS, 1999) with the following objectives:

- Short-term optimization of monitoring systems and measuring devices.
- Improvement of disaster prevention plans.
- Extension of the forecast times for the Lower Moselle River to up to 12 hours until the year 2000 and of up to 24 hours until the year 2005.

2 THE LARSIM MODEL

2.1 Overview

To extend forecast times up to 48 hours, a flood forecast model based on the program system LARSIM was established for the Moselle river basin (approx. 28,000 km^2) on behalf of the Rhineland-Palatinate (a federal state of Germany) water authorities.
LARSIM (Large Area Runoff Simulation Model) is based on the river basin model FGMOD (Ludwig, 1982), which was developed for the systematic modelling of runoff generation and flood-routing. LARSIM can be applied both as a water balance model for continuous simulation and as an event-based flood forecast model. It is successfully used for operational flood forecasts in several German flood forecast centers.
If LARSIM is applied as a water balance model, the processes of interception, evapotranspiration and water storage in soils and aquifers are included besides runoff generation in the area and translation and retention in river channels (Bremicker, 2000). It is currently tested for the operational use in such a mode for the low and mean flow forecast for the Neckar River (Bremicker, Gerlinger, 2000).
Snow accumulation and snow melt can be considered in both model versions as well as artificial influences (e.g. storage basins, diversions or water transfer between different basins).

2.2 Model components

The program system LARSIM offers alternative subroutines for most stages of the rainfall-runoff process. Due to data limitation, the number of free model parameters required for the Moselle flood forecast model had to be kept to a minimum. As an operational flood forecast model, it only uses comparatively simple model components which are satisfying for practical purposes and for individual flood periods due to the possibility of on-line parameter adaptation:

- Calculation of areal rainfall similar to the gridpoint-procedure of the NWSRFS model, an inverse-distance method (U.S. Department of Commerce, 1972).
- Parallel storage models for subareas consisting of two linear storages (a fast and a slower storage) and a distribution of effective runoff to these storages by a threshold value (interflow index rate).
- Transformation of runoff in the interflow zone is simulated by a single linear storage. For direct runoff, a modified Clark model (Clark, 1945) is used where the shape of the subarea is approximated by a rectangle. The result is a triangle or a trapezoidal shape of the time-area-diagram. Retention constants for interflow and direct runoff are assumed proportional to the lag-times in subareas.
- Runoff coefficient function: runoff-dependent description of runoff coefficients (Ludwig, 1988). Runoff of the slower storage in the parallel storage model for the runoff is used as a soil moisture index. Variable runoff coefficients are derived from this index using a parabolic function, which is limited on both ends (minimal and maximal runoff coefficient).
- Flood routing procedure which accounts for nonlinear storage processes, especially for differences in runoff character between runoff in the main bed and the floodplain. Retention in channel sub-reaches is described by storage components, whose constants depend on inflow and outflow (Williams, 1969).

The modules for runoff predictions using the precipitation forecasts include:

- Warning model: before the beginning of the flood, when the discharge has not increased yet, fixed parameter values of the runoff coefficient function are used. These parameter values are determined for each gauge separately by analyzing historic flood events.
- Forecasting model: If the measured discharge shows a significant increase, the parameter values of the runoff coefficient function are determined from the current rainfall and runoff data. Differences between calculated and measured runoff are minimized using an adaptive optimization of the parameters of the runoff coefficient function by the Gauss-Marquardt procedure (Marquardt, 1963).
- Discrepancies between calculated and measured hydrographs are determined and calculation results for subsequent forecasts are corrected according to the analyzed error distribution by autoregressive models (ARIMA-correction) (Box, Jenkins, 1970).

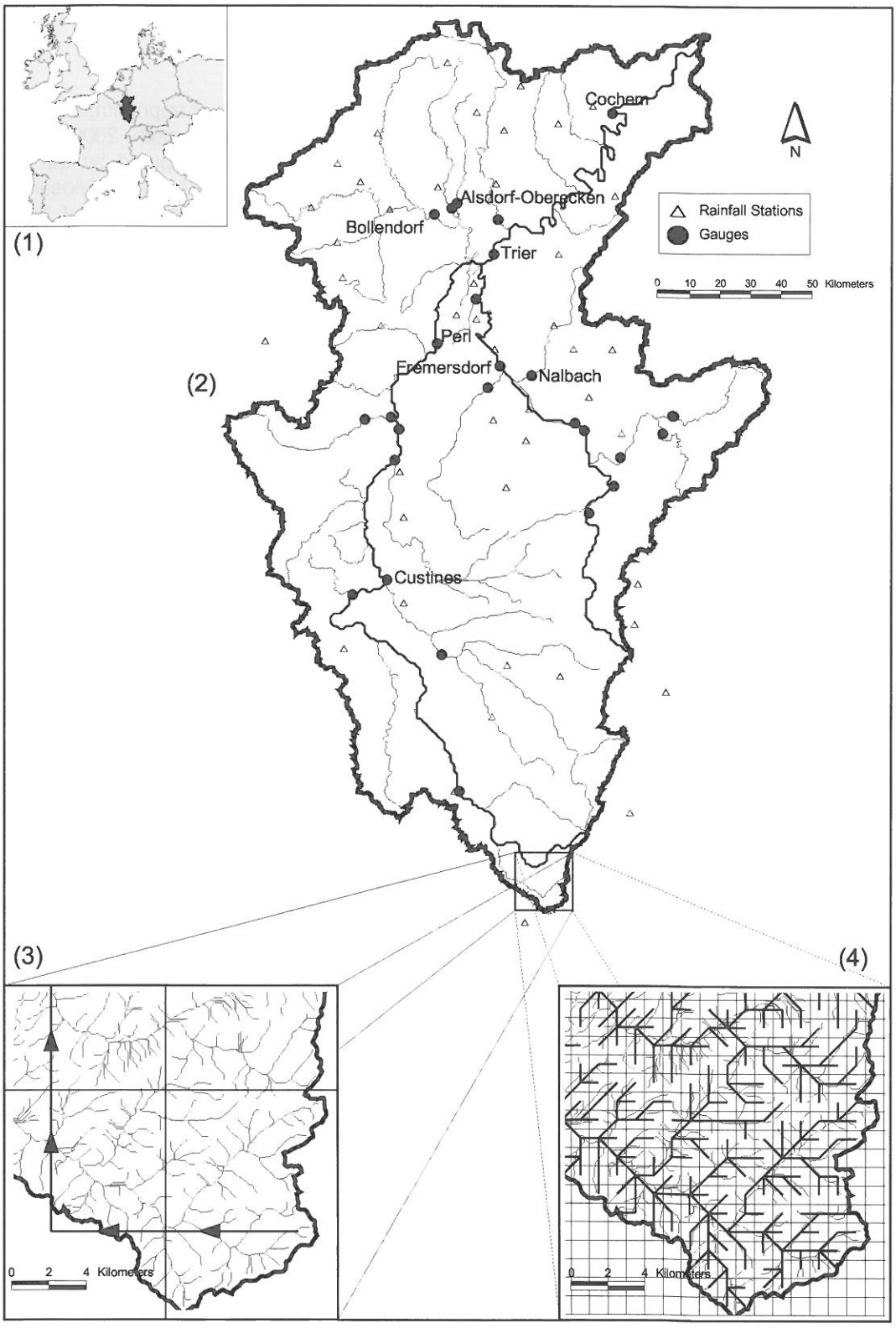

Figure 2-1: (1) Location of the Moselle basin in Europe
(2) Moselle basin and location of operationally used rainfall stations and water level gauges
(3) Example of 14 km by 14 km model grid and river network
(4) Example of the improved 1 km by 1 km model grid and river network

3 THE MOSELLE MODEL

3.1 The 14 km grid model of the Moselle river basin

In a first step, an event-based flood forecasting model with a coarse grid size of approximately 14 km by 14 km was established for the Moselle river basin (Figure 2-1(2)) (Gerlinger, Demuth, 2000). Input data for the runoff forecasts are the 48-hour precipitation forecasts which are computed by the German Weather Service (DWD) numerical weather prediction model (NWP) system for the whole Moselle basin. The grid structure of this model was designed according to the horizontal resolution of the NWP-"Deutschland Modell" ("Germany model" of the DWD) to use a direct reference of precipitation forecast results on NWP nodepoints and model subarea grid cells. 154 grid-based subareas are used. Figure 2-1(3) shows a section of the 14 km by 14 km grid structure with the schematic graph of the subarea sequence according to the existing river network.
As input data for channel reaches information on their width and depth is needed for calculating the flood propagation in the river channel network. Since these data are not available for large parts of the river basin, they were estimated using a "hydraulic-geometry" assumption based on a statistical discharge index (Allen et al., 1994). Lengths and gradients of the river subreaches for the Moselle catchment were determined from topographical maps. From an existing flood routing model, more detailed system data was available for some channel reaches (Moselle downstream gauge Custines and Saar rivers) which was integrated in the model to substitute the approximate river geometry values.
At time, the model is operationally used in a test mode as a real-time flood forecasting system at the flood forecast center in Trier (Germany). First applications of the LARSIM model in the Moselle river basin for 24 hours flood forecasts have been successful. The predicted and measured discharges correspond quite well for the Lower Moselle River downstreams Perl. Input data for the continuous adjustment of the model are hourly values of water levels of 20 gauges and the precipitation measurements of 50 rain gauges transmitted automatically from France, Germany and Luxembourg to Trier (Figure 2-1(2)).

3.2 The 1 km grid model of the Moselle river basin

Improvements in the model performance were expected from a more detailed 1 km by 1 km grid. The grid size was chosen to improve the forecasts especially for small basin parts and the Upper Moselle River.
A completely new model structure has been designed (Figure 2-1(4)) based on an analysis of a Digital Elevation Model (50 m grid). Length and gradients of the rivers were determined with the help of GIS tools. A recalibration of the model was done using six historical flood events. For the forecast of precipitation, a higher resolution grid is now used ("Lokal-Modell" of the German Weather Service, at time a 7.5 km by 7.5 km grid).

3.3 Forecast results

To show the quality of flood forecasts with the high resolution model, the runoff values for 12 hours forecasts are compared with the measured values on the example of historic flood events. To simulate the real-time forecast procedure, a time interval of 8 hours between forecast timepoints has been used. In this test, information on measured precipitation has been used for the forecasts to check the possible model performance without additional errors introduced through precipitation forecasts. For precipitation interpolation the geostatistical procedure was applied.
Figure 3-1 shows the 12-hour runoff forecast values in relation to the measured runoff values for the three largest historic flood events of this test. The upper diagram in Figure 3-1 displays results for a gauge with a small catchment and the lower diagram those for a gauge with a large catchment.
The quality of the forecasts for the large catchment is very high. Forecasts for the smaller catchment show greater differences between forecasted and measured runoff values. Nevertheless, the results for the smaller catchments represent a decisive improvement, mainly because simulations for catchments of this size could not be carried out with the 14 km by 14 km grid model.

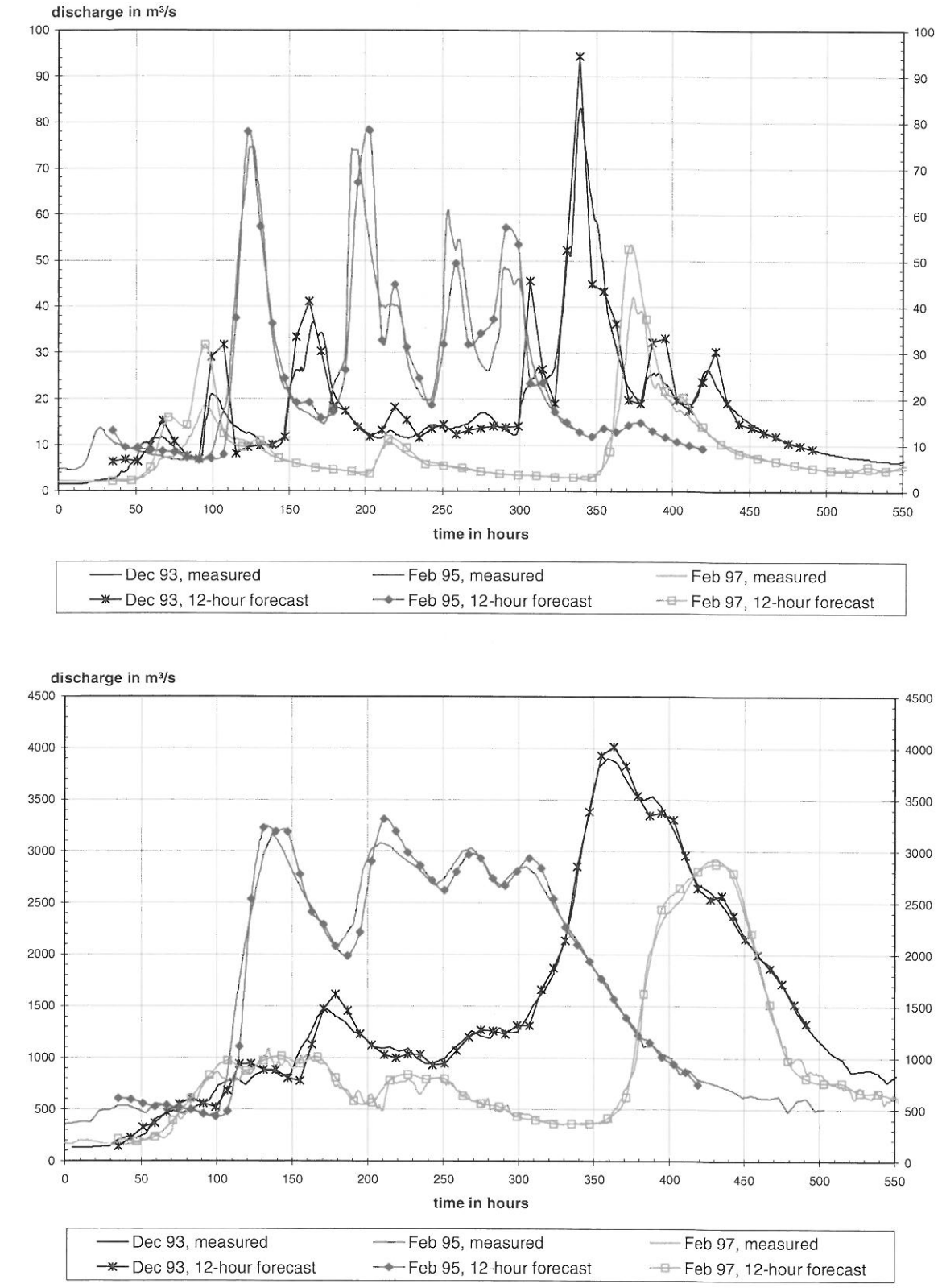

Figure 3-1: 12-hour forecast results for gauge Alsdorf/Nims (above; A = 264 km^2) and for gauge Trier/ Moselle (below; A = 23.857 km^2).

4 INFLUENCE OF PRECIPITATION INTERPOLATION AND GRID SIZE

4.1 Criteria for the comparison

To compare the model performance, measured and calculated discharges for the gauges are compared by statistical measures (i.e., goodness-of-fit test) and additionally by visual comparison. A meaningful combination of several techniques should be employed for the model validation as well as for a thorough model assessment (Janssen, Heuberger, 1995).
Also, one should be aware of the fact that the various statistical measures for deviation typically highlight specific features of the flood hydrographs and therefore are no objective stand-alone values. The coefficient of determination, for instance, evaluates the degree of coincidence between the forms of hydrographs and can reach the maximal value of 1.0. It also equals 1.0 if measured and simulated hydrograph have the exact same form but differ by a constant value.
A more informative measure for the simulation quality is the "model efficiency" (Table 4-1) (Nash, Sutcliffe, 1970). The model efficiency measure reaches a value of 1.0 if measured and simulated valued are identical. However, it is important to notice that large single-peaked deviations from the mean of runoff values tend to increase model efficiency values thereby biasing the result.
Another reasonable statistical measure for flood simulation is the "hydrologic deviation" (Table 4-1) (Schultz, 1967). Values of the hydrologic deviation range from 0 % - 5 % ("good" results) to more than 15 % (not usable), with 10 % representing usable results (Schultz, 1967). This parameter is influenced by the hydrograph's peak value.
None of the statistical measures can claim to be the absolute truth while judging the quality of a model. Modeling characteristics like the data density and distribution or the modeling period etc. all affect the statistical output. Nevertheless, the various statistical measures allow relative comparisons between results of different simulation models or model runs, making them a valuable asset in model judgement.

Table 4-1: Model simulation measures "model efficiency" and "hydrologic deviation".

Model efficiency	Hydrologic deviation
$\frac{\left[\sum_{i=1}^{N}(O_i-\overline{O})^2-\sum_{i=1}^{N}(P_i-O_i)^2\right]}{\left[\sum_{i=1}^{N}(O_i-\overline{O})^2\right]}$	$\frac{100}{Q_{max}^{\ 2}\cdot N}\sum_{i=1}^{N}2\cdot O_i\lvert O_i-P_i\rvert$
P_i and O_i denote the predicted value and observed value i; $\overline{O}$ the mean	

4.2 Influence of precipitation interpolation method on simulation results

Since the quality of flood forecasting models depends on the quality of their input parameters, the improvement of the interpolation of point measurements of precipitation (areal rainfall calculation) could lead to better simulation results, particularly as long as no radar data is available.
Due to the high variability of precipitation in space and time, modeling and interpolation of short-term precipitation is problematic and likely to be one of the largest sources for simulation errors. Essentially, the joint influence of atmospherical and orographical factors should be considered to estimate time-space distribution of precipitation adequately. Simple interpolation procedures as the Thiessen polygon or the inverse-distance method can produce errors (Goovaerts, 2000), which depend on the degree of precipitation heterogeneity during the actual flood.
Therefore an interpolation procedure for the hourly measured precipitation data was tested, which accounted for information from historical precipitation data and the relevant precipitation patterns (Hinterding, 2001).
In this interpolation procedure, a five-step procedure is performed to identify the typical precipitation patterns, yielding the so-called "background fields" necessary for the interpolation (Figure 4-1). A fuzzy set-type procedure based on a combination of geostatistical models has been chosen as mathematical basis for the interpolation.
For operational use, this interpolation procedure allows the estimation of the spatial distributions of precipitation with regard to the actual weather situation. It is installed at the flood forecast center in Trier for interpolating the measured and the predicted precipitation. It had also been applied to the catchment of the Nahe River and to the area of Rhineland-Palatinate.

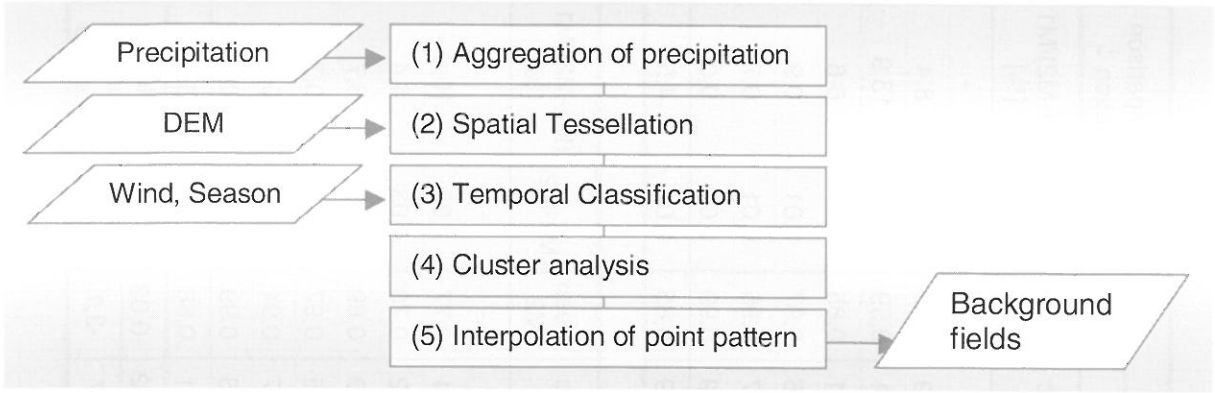

Figure 4-1: Identification of typical precipitation patterns (Hinterding, 2001).

To test the differences in runoff simulation quality, the geostatistical precipitation interpolation method and the inverse-distance-method were employed. The identical input data sets stemmed from six historical flood events. Simultaneously, the influences of different grid dimensions were examined (chapter 4.3). With regard to the interpolation of the precipitation data set for the higher resolution model, the remark should be made that the data was thinned by a factor of four (from ~ 28,000 data points to ~ 7000 data points) in order to save computing time.
To overlook the modeling results, Table 4-2 contains all values of the model efficiency parameter. Table 4-3 originates from a table similar to Table 4-2 but only summarizes the mean values of the hydrologic deviation parameter. For both tables, seven gauges with different orders of catchment size from different parts of the Moselle basin were selected (positions of the gauges see Figure 2-1(2)).
Runoff values for the gauge Alsdorf with the smallest catchment area cannot be simulated with the 14 km x 14 km model grid resolution. Model efficiency values and hydrologic deviation values for this gauge were consequently not incorporated for calculation of the mean values. This gauge was however used in Table 4-2 to demonstrate the possible high simulation quality with the 1 km x 1 km model.
Table 4-2 shows that the new interpolation method produces no improvements compared with the formerly used simpler method. In most cases, model efficiencies are approximately equal, in some cases even better with the simpler method. This tendency is independent of the chosen grid size dimension, but more marked in the simulation results of the model run with the coarser grid. The mean values of the hydrologic deviations (Table 4-3) display the same tendencies as the model efficiency values.

4.3 Influence of grid size on simulation results

The comparison of model simulation quality for the model runs with different grid sizes (Table 4-2) depicts that for gauges with small or intermediate catchment size (e.g., Nalbach, Bollendorf) and for gauges in the upper part of the Moselle River basin (e.g., Custines) the simulation quality increases when the high-resolution grid is used.
For gauges with intermediate and large catchment sizes in the lower parts of the Moselle River, only very small improvements result from the usage of the high-resolution model. This is not surprising since in these cases the low-resolution model already yielded very high model efficiency values.
The mean values for the hydrologic deviation parameter show the same tendency (Table 4-3). Especially for gauges with small to intermediate catchment size, lower values of the hydrologic deviation are reached. The mean values of the hydrologic deviation for results of the high-resolution model of about 7 % or less indicate "good" simulation results (Schultz, 1967). The coarser model leads to simulation results for these gauges with mean values of up to 10 %.

Table 4-2: Model efficiencies of the Moselle model with different grid resolutions and interpolation procedures for 7 gauges.

Grid resolution		1 km by 1 km grid							14 km by 14 km grid							Results comparison grid resolution ↓	
Interpolation procedure		Geostatistical interpolation															
Gauge	Area [km²]	Dec 93	Feb 95	Nov 96	Feb 97	Oct 98	Dec 99	Mean M1	Dec 93	Feb 95	Nov 96	Feb 97	Oct 98	Dec 99	Mean M2	M1-M2	(M1-M2)/M1 [%]
Alsdorf /Nims	264	0,94	0,94	0,68	0,94	-	0,60	0,82	-	-	-	-	-	-	-	-	-
Nalbach/Prims	712	0,95	0,92	0,77	0,88	0,79	0,83	0,86	0,88	0,83	0,71	0,72	0,78	0,79	0,79	0,07	8,4
Bollendorf/Sauer	3226	0,97	0,99	0,39	0,85	0,19	0,72	0,69	0,60	0,77	0,45	0,77	0,24	0,71	0,59	0,10	13,9
Custines/Mosel	6829	0,99	0,98	0,97	0,98	0,95	0,58	0,91	0,97	0,96	0,97	0,96	0,92	0,31	0,85	0,06	6,6
Fremersdorf/Saar	6983	0,98	0,98	0,97	0,98	0,96	0,97	0,97	0,97	0,98	0,96	0,98	0,94	0,96	0,97	0,01	0,9
Perl/Mosel	11522	0,99	0,99	0,84	0,98	0,94	0,97	0,95	0,98	0,98	0,87	0,97	0,90	0,97	0,95	0,01	0,7
Cochem/Mosel	27088	0,99	0,99	0,98	0,99	0,98	0,99	0,99	0,99	0,99	0,98	0,99	0,98	0,99	0,99	0,00	0,0
	Mean M3	0,98	0,98	0,82	0,94	0,80	0,84	0,89	0,90	0,92	0,82	0,90	0,79	0,79	0,85	0,04	4,5
Interpolation procedure		Inverse-Distance-Interpolation															
Gauge	Area [km²]	Dec 93	Feb 95	Nov 96	Feb 97	Oct 98	Dec 99	Mean M1	Dec 93	Feb 95	Nov 96	Feb 97	Oct 98	Dec 99	Mean M2	M1-M2	(M1-M2)/M1 [%]
Alsdorf /Nims	264	0,94	0,94	0,70	0,92	-	0,86	0,87	-	-	-	-	-	-	-	-	-
Nalbach/Prims	712	0,94	0,91	0,81	0,89	0,78	0,84	0,86	0,87	0,76	0,75	0,71	0,82	0,71	0,77	0,09	10,6
Bollendorf/Sauer	3226	0,98	0,98	0,58	0,91	0,36	0,77	0,76	0,75	0,90	0,66	0,94	0,41	0,72	0,73	0,03	4,4
Custines/Mosel	6829	0,99	0,98	0,97	0,98	0,96	0,76	0,94	0,97	0,96	0,96	0,96	0,94	0,53	0,89	0,05	5,7
Fremersdorf/Saar	6983	0,98	0,98	0,97	0,98	0,96	0,96	0,97	0,98	0,98	0,96	0,98	0,94	0,95	0,97	0,01	0,7
Perl/Mosel	11522	0,99	0,99	0,83	0,98	0,94	0,97	0,95	0,98	0,98	0,86	0,97	0,90	0,97	0,94	0,01	0,7
Cochem/Mosel	27088	0,99	0,99	0,98	0,99	0,98	0,98	0,99	0,99	0,99	0,98	0,99	0,98	0,98	0,99	0,00	0,0
	Mean M4	0,98	0,97	0,86	0,96	0,83	0,88	0,91	0,92	0,93	0,86	0,93	0,83	0,81	0,88	0,03	3,5
	M3-M4	0,00	0,00	-0,04	-0,01	-0,03	-0,04	-0,02	-0,02	-0,01	-0,04	-0,03	-0,04	-0,02	-0,03	← Results comparison inter-polation procedure	
	(M3-M4)/M3 [%]	0,0	0,3	-4,5	-1,2	-3,5	-4,3	-2,1	-2,8	-1,1	-4,7	-3,0	-4,8	-2,7	-3,1		

Table 4-3: Hydrologic deviation [%] of the Moselle model with different grid resolutions and interpolation procedures (means of 6 gauges according to Table 4-2).

	1 km by 1 km grid							14 km by 14 km grid							M1-M2	(M1-M2)/M1 [%]	Comparison model grid ↑
	Dec 93	Feb 95	Nov 96	Feb 97	Oct 98	Dec 99	M1	Dec 93	Feb 95	Nov 96	Feb 97	Oct 98	Dec 99	M2			
	Geostatistical interpolation																
M3	1,7	2,9	4,1	1,8	7,3	5,6	3,9	4,2	5,3	7,4	2,3	8,7	9,7	6,3	-2,3	-59,7	
	Inverse-Distance-Interpolation																
M4	1,6	3,1	3,9	1,6	6,8	5,3	3,7	3,7	4,4	7,7	1,9	7,7	9,0	5,6	-1,9	-50,5	
	0,1	-0,2	0,3	0,2	0,5	0,3	0,2	0,5	0,9	-0,3	0,4	0,1	0,7	0,7	M3-M4		
	5,1	-6,5	6,0	11,6	7,0	4,9	4,9	12,7	16,5	-3,7	17,0	11,5	6,7	10,4	(M3-M4)/M3 [%]		
	Comparison interpolation procedure ↑																
M (M1, M2, M3, M4): Means																	

5 CONCLUSION

The investigation shows that grid-type flood forecast models based on the program system LARSIM lead to valuable simulation and forecast results for gauges in the Moselle basin. Independent of the used precipitation interpolation method or the grid dimension, high values of model efficiency were obtained. Only a few simulations resulted in model efficiency values below 0.7. Analogously, values of hydrologic deviation are in most cases below 10 %. It is likely that data insufficiencies of measurements at the level gauges caused a major part of the few weak simulation results. The model simulations perform the best for gauges with large catchments. But also for relatively small catchments, reliable simulations and forecasts could be modeled using the high-resolution model.
On top of the improved simulation quality, the high-resolution model provides further advantages:

- Simulations for small catchments are possible as for instance at the gauge Nalbach/Prims, which could not be modeled using the coarser grid model structure.
- Additional points in the river network (gauges, catchments, or new forecast points) can now be incorporated easily and with great accuracy.
- Improvements through the use of the high-resolution model can further be expected by higher spatial resolution of precipitation measurements and next-generation precipitation forecast models.
- Perspectively, even short-term warnings with respect to local flood events as a consequence of convective storms seem possible.
- The 1 km x 1 km grid structure allows an adaptation of the model to a continuous water balance model which can be a realistic base for assessment of land use and/or climate changes as well as for large-scale high-resolution water quality modeling.

The geostatistical precipitation interpolation method did not result in a decisive improvement of simulation quality compared with the simpler inverse-distance-interpolation. However, more rainfall stations were available for the simulations compared to the operational use. And additionally, the loss of single stations in operational use has to be taken into consideration. Keeping this in mind, the geostatistical precipitation interpolation method might still be capable of outperforming the inverse-distance-interpolation and thereby increase the simulation quality in the operational use. Therefore, LARSIM is applied using the geostatistical interpolation method at the flood forecast center in Trier.

REFERENCES

Allen, P.M. et al. (1994): Downstream channel geometry for use in planning level models. Water Resources Bulletin, Vol. 30, No. 4, 663-671. Bethesda (USA)

Box, G.E.P., Jenkins, G.M. (1970): Time series analysis. Holden-Day. San Francisco (USA)

Bremicker, M., Gerlinger, K. (2000): Operational application of the water balance model LARSIM in the Neckar basin. In: Proc. of Intern. Workshop October 2000, Freiburger Schriften zur Hydrologie, Institut für Hydrologie der Universität Freiburg, Band 13. Freiburg i. Br. (Germany)

Bremicker, M. (2000): Das Wasserhaushaltsmodell LARSIM - Modellgrundlagen und Anwendungsbeispiele. Freiburger Schriften zur Hydrologie, Institut für Hydrologie der Universität Freiburg, Band 11. Freiburg i. Br. (Germany)

Clark, C.O. (1945): Storage and the unit hydrograph. Transactions of the ASCE, Vol. 110, 1419-1446. Reston (USA)

Gerlinger, K., Demuth, N. (2000): Operational flood forecasting for the Moselle river basin. In: Proc. Europ. Conf. Adv. in Flood Research, Potsdam, PIK Report No. 65, 546–556. Potsdam (Germany)

Goovaerts, P. (2000): Geostatistical approaches for incorporating elevation into the spatial interpolation of rainfall. Journal of Hydrology, 228, 113-129. Amsterdam (The Netherlands)

Hinterding, A. (2001): InterNied - A geostatistical interpolation procedure for hourly measured precipitation data. In: Krahe, P. and D. Herpertz (ed.): Generation of Hydrometeorological Reference Conditions for the Assessment of Flood Hazard in Large River Basins (Workshop papers). KHR-Report I-20 (in press). Lelystad (The Netherlands)

IKSMS (1999): Aktionsplan Hochwasser im Einzugsgebiet von Mosel und Saar. Sekretariat der Internationalen Kommissionen zum Schutze der Mosel und der Saar (IKSMS). Trier (Germany)

Janssen, P.H.M., Heuberger, P.S.C. (1995): Calibration of process-oriented models. Ecological Modelling 83, 55-66. Amsterdam (The Netherlands)

Marquardt, D.W. (1963): An algorithm for least-square estimation of nonlinear parameters. Journ. Soc. Indust. Appl. Math., Vol. 11, 431-441. Philadelphia (USA)

Nash, J.E., Sutcliffe, J.V. (1970): River flow forecasting through conceptual models. Part 1: a discussion of principles. Journal of Hydrology, 10, 282-290. Amsterdam (The Netherlands)

Ludwig, K. (1982): The program system FGMOD for calculation of runoff processes in river basins. Zeitschrift für Kulturtechnik und Flurbereinigung 23, 25-37. Berlin (Germany)

Ludwig, K. (1988): Hochwasservorhersagen für grosse, semiaride Einzugsgebiete am Beispiel des Gelben Flusses. Inst. für Wasserwirtschaft, Hydrologie und landwirtschaftlichen Wasserbau, Univ. Hannover. Hannover (Germany)

Schultz, G.A. (1967): Bestimmung theoretischer Abflußganglinien durch elektronische Berechnung von Niederschlagskonzentration und Retention (Hyreun-Verfahren). Bericht Nr. 11 der Versuchsanstalt für Wasserbau der TH München. München (Germany)

U.S. Department of Commerce (1972): National Weather Service River Forecast System (NWSRFS-Model). NOAA Technical Memorandum NWS-Hydro-14. Washington (USA)

Williams, J.R. (1969): Flood routing with variable travel time or variable storage coefficients. Transactions of the ASAE, p.100. St. Joseph (USA)

A SUGGESTION FOR THE ESTIMATION OF PEAK FLOOD DISCHARGES IN SMALL TORRENTIAL CATCHMENTS

Christoph Hegg, Felix Forster

WSL, Swiss Federal Research Institute, Natural Hazards Department, Zürcherstr. 111, CH-8903 Birmensdorf, hegg@wsl.ch

SUMMARY

The determination of peak flood discharges in small torrential catchments in many cases only relies on simple estimation formulas as no flood record data is available and simulation models are too expensive in their application. Many such estimation formulas have been proposed by different authors but a systematic testing in small catchments was not carried out up to now in Switzerland.
In the present paper the results of tests carried out for more than 12 such formulas are described. The tests have been carried out with runoff data from seven small torrential catchments with areas between 0.5 and 3.5 km^2 where time series between 25 and 95 years have been available.
More than 50 % of the tested formulas had to be classified as unsuitable for estimating peak flood discharges in small torrential catchments. As no single formula is reliable under all conditions an approach combining the five most reliable estimation formulas is described and proposed for future peak flood estimations.

Keywords: peak flood discharge estimation, estimation formulas, flood generation

1 INTRODUCTION

The estimation of peak flood discharges is essential for hazard mapping as well as for the design and planning of protective measures in torrents. For larger rivers, long time series of stream flow data provide a base from which peak flood values based on the statistics of extremes can be derived. In small torrential watersheds, such time series are generally not available. Therefore, the peak flood discharge needs to be estimated by a hydrologic model or by a simpler flood estimation formula. Kleindienst and Forster (2000) show that a carefully parametrised hydrological model does not necessarily produce much better results than a simple estimation formula, but that is much more time consuming in it's application. Therefore in common practice mostly simple estimation formulas are applied, that are easy to use and allow a quich estimation of peak flood values.
As WSL has a longterm tradition in advising engineers with regard to determine peak flood discharges in small torrential catchments, many of these formulas have been tested in the last years. In the present paper the results of the testing of about 12 formulas are described briefly. Most of the known estimation formulas have been developed to determine peak flood discharges only and cannot provide a flood hydrograph. As in many small torrential catchments sediment transport is an important factor, a flood hydrograph is essential for assessing sediment transport problems. For this purpose a new formula has been developed and included in the tests. It is the main purpose of this paper to propose a method to estimate peak flood discharges in small torrential catchments based on the experience gained during these tests and in many other projects.
For this purpose first the data base available for testing will be described. Then the result of a preliminary test excluding the most unreliable formulas is briefly described. The five remaining approaches are then described as basis for the presentation of the detailed analysis, resulting in the proposition of a method combining the five estimation formulas. Final discussion and evaluation of the results conclude the paper.

2 METHOD AND MATERIAL

2.1 Data set used for testing of estimation formulas

The tests have been carried out in seven catchments where discharge has been measured for 22 up to 95 years. They are all situated in the Swiss subalpine belt. Erlenbach and Vogelbach are part of the Alptal valley, while Rappengraben and Sperbelgraben belong to the Emmental region. These four catchments pertain to the central part of the subalpine belt. Rotenbach and Schwändlibach are close

to the Schwarzsee region and are part of the western belt, whereas Rietholzbach in the lower part of Toggenburg belongs to the eastern part of the Swiss subalpine belt. The main characteristics of these catchments are given in Table 2-1.

Table 2-1: Main characteristics of the test catchments-

	Test series	area	mean altitude	geology	water logging	forested
	[years]	[km^2]	[m.a.s.l.]			[%]
Erlenbach	22	0.75	1350	flysch	yes	40
Vogelbach	26	1.55	1360	flysch	yes	65
Rappengraben	95	0.6	1140	molasse	yes	35
Sperbelgraben	85	0.55	1060	molasse	no	95
Rappengraben	95	0.6	1140	molasse	yes	35
Rotenbach	45	1.65	1450	flysch	yes	15
Schwändlibach	45	1.4	1440	flysch	yes	30
Rietholzbach	23	3.2	800	molasse	yes	30

The evaluation of the quality of a flood estimation method for a chosen return period can only be achieved in catchments with longterm series of discharge measurements. The statistic extrapolation of the corresponding measured data served as reference values. In the catchments with times series of >25 years the annual maximum flood approach (AMF) was applied for flood frequency analysis. In the two other cases the peak over threshold method (POT) was used.

2.2 Results of preliminary testing

In earlier WSL projects different types of flood estimation formulas such as regression procedures, empiric and conceptual methods as well as approaches basing on the rational formula have been tested. Five of these methods were labelled as unsuitable for the reasons described in Table 2-2. The methods to be recommended to the practical engineer are to be parameterised by objectively determinable catchment characteristics. Corresponding to the demands of a new federal law, requiring a differentiation of the protection objectives, the methods have to give results for varying flood return periods. Out of the many tested empiric flood estimation formulas, the one that seemed most reliable was included in the set of five formulas described in chapter 2.3 that has been tested in more detail.

Table 2-2: The following flood estimation procedures are labelled as unsuitable for small catchments.

Method	**Type of method**	**Evaluation**	**Literature**
Sackl	regression	The Austrian method developed in the Steiermark region produces high flood values; for the two smallest catchments (0.5km^2) the estimated 100-year flood value exceeds the statistically, from measured data extrapolated value by a factor 2-3	Sackl, 1990
IfK	regression	This method produces the most varying results of all the studied approaches; the formula does not produce reliable results for small catchments	Sydler et al., 1982
Hager	conceptual	The procedure has too many parameters which are not objectively determinable, the results for the test catchments are very inconsistent	Hager, 1989
TM61	empiric	The procedure, developed in New Zealand could not be adopted to Swiss conditions without major changes	NWSCA, 1984
Unit-Hydrograph	Black-Box	The assumption of a linear precipitation / discharge process for small catchments is very problematic; the idea of regional unit-hydrographs is not realistic for small prealpine and alpine catchments	Weingartner, 1989

Preliminary tests furthermore showed that the tool developed by Barben (2001) for mesoscale catchments does not provide reliable results in small catchments. The reason for this is not to be found in the formulas included in this tool, but in the fact that all input data are derived from digital information. As such information is only available in small scale maps, it cannot take into account local variations that play a key role in small catchments. Up to now the necessary degree of detail can only be obtained with field assessments.

2.3 Description of the most reliable estimation formulas

The following description of the five most reliable estimation formulas evaluated by preliminary tests intends to give a short overview only. For the application of these formulas in small torrential catchments the mentioned references have to be considered.

2.3.1 The modified Müller formula

Empiric flood estimation formula mostly are based on relations between discharge [Q] and the area [A] of the catchment. This type of formula aims at the maximum flood without referring to a return period. As a representative of the numerous empiric approaches, the one by Müller (1943) seems to be the most reliable for small catchments:

(1) $$Q_{max} = 43 * \Psi * A^{2/3}$$

with:
Q_{max}: maximum flood [m^3/s]
ψ: runoff coefficient
A: area [km^2]
43: fitting factor determined by Müller (1943)

For this study the original approach by Müller (1943) was modified by estimating the runoff coefficient ψ based on a field survey according to the recommendations made in Rickli and Forster (1997). The approach is meant for catchment areas ≥ 1 km^2. For areas between 0.5 and 1 km^2 it provides conservative values, because $A^{2/3}$ stands for a numerical value, which exceeds the area A of the catchment. For catchments with areas smaller than 0.5 km^2 that approach is inapplicable.

2.3.2 The modified Rational Formula

The most common hydrologic method for computing peak discharge is the so-called rational formula. Originally it has been used for the design of drainage systems in urban areas (Chow, 1964). It is assumed that the maximum discharge rate is caused by a rainfall event of a duration equal to the time of concentration. The rational method, currently used by many engineers, is usually expressed in terms of the following equation (Kleindienst, Forster, 2000):

(2) $$Q(x) = 0.278 * i\,(T_c,x) * \Psi * A\ [m^3/s*km^2]$$

with:
Q(x): flood discharge with a return period of x years [m^3/s]
i: controlling rainfall intensity [mm/h]
Ψ: runoff coefficient [-]
A: area of the catchment [km^2]
T_c: time of concentration [min]
x: return period [years]
0.278: conversion factor due to the chosen units

The runoff coefficient is to be determined spatially distributed with field surveys according to Rickli and Forster (1997).
The time of concentration T_c defines the controlling rainfall intensity. The time of concentration T_c is calculated as the sum of travel time and wetting delay. The travel time T_{travel} is determined following the

approach of Kirpich (Chow, 1964), depending on the maximum flow length and the average channel slope. The wetting delay $T_{wetting}$ was suggested by Kölla (1986) and stands for the time needed to wet the unsaturated soils. At first, a wetting rainfall volume $P_{wetting}$ is determined based on the soil suitability map (EJPD, 1980) and field surveys. Starting from an estimated concetration time T_c, the effective value of T_c is determined with an iteration. For this purpose rainfall intensities are determined with the 'Hydrological Atlas of Switzerland' (HADES, 1992) as described by Forster and Baumgartner (1999).

2.3.3 The Taubmann/Thiess/Chow approach

The approach combining the rational formula with a procedure of the U.S. Soil Conservation Service (SCS) is based on a method, which was proposed by Chow (1962; 1964). The approach allows both, the determination of the flood discharge and the corresponding hydrograph. The procedure was adapted by Thiess (1975) for the situation in Baden-Württemberg and Taubmann (1984) tested the approach in several medium-sized catchments in Switzerland.
According to Taubmann/Thiess/Chow the rational formula is transformed as follows:

(3) $$Q(t,T) = X(t,T) * Y(t,T) * Z(t) * A$$

with:
Q: peak discharge with a return period of x years [m^3/s]
X: runoff factor corresponding to the intensity of the effective rainfall, depending on the SCS curve number [-]
Y: climatic factor representing the ratio of the relevant rainfall intensities in the considered catchment and in Urbana (Illinois,USA) (Chow, 1962) [-]
Z: peak reduction factor ($Z(t) = Q(t) / Q$) [-]
A: area of the catchment [km^2]
t: relevant rainfall duration (time of concentration) [h]
T: return period [years]

Chow (1962) developed the method for rural catchments up to 30 km^2. Taubmann (1986) used it for a catchment up to 300 km^2 and for the present study the method was applied to areas between 0.5 and 1 km^2, without causing any obvious trouble.

2.3.4 The Kölla approach

This method as well is based on the rational formula. As a result of a study on runoff production, the original rational formula was modified as follows (Kölla, 1986; 1987):
- the remote parts of the catchment do not contribute to the peak discharge; instead of the total area only the contributing area nearby the channels is considered.
- the time of concentration depends widely on a wetting rainfall volume, which is necessary to reach a predisposition for surface runoff on the contributing area to occur.

According to Kölla (1986) the rational formula is transformed as follows:

(4) $$Q(x) = C^* [i(T_c, x) - f(T_c, x)] * A_{eff} * k_G + Q_{GI},$$

(5) $$\text{with } T_c = T_{travel} + T_{wetting}$$

with
Q: peak discharge with a return period of x years [m^3/s]
i: controlling rainfall intensity [mm/h]
f: leakage to underground [mm/h]
A_{eff}: contributing area [km^2]
k_G: factor considering the discharge enhancing influence of a wet soil [-]
Q_{GI}: runoff from glaciated area [m^3/s]
T_c: time of concentration [h]
T_{travel}: total travel time from a remote part of the catchment [h]
$T_{wetting}$: wetting delay [h]

x: return period [years]
C: constant conversion factor due to the chosen units [-]

The method was developed for the 20-year flood event with a complement to convert the results for a 100-year event. The crucial parameters are the contributing area and the wetting rainfall volume. The contributing area can be determined based on the cumulative length of the channels in the map at the scale 1:25'000 or with GIS functions. The wetting rainfall volume is determined with the aid of the soil suitability map (EJPD, 1980; scale 1:200'000). In small catchments it is in many cases necessary to modify the contributing area and the wetting rainfall volume with information from field surveys.

2.3.5 The Clark-WSL approach

Within the scope of the WSL project 'Flood Estimation in Small Catchments' an estimation procedure was developed allowing to determine a peak flood discharge and the corresponding flood hydrograph for a given return period (Vogt et al., 2002).
The presented flood estimation approach is based on the conceptual model by Clark (Koehler, 1976) which describes the runoff process in catchments as a combination of a linear reservoir and a linear translation.
The linear reservoir is characterised by the storage constant and is supposed to be at the lower end of the catchment. The storage constant has the dimension of time and can be understood as the time difference between the centroid of the inflow and the one of the outflow of the reservoir.
The linear translation, which defines the input function to the linear reservoir, is assessed by a time-area diagram. Basically, the time-area diagram takes into account the temporal distribution of the rainfall, the part of the rainfall which is contributing to the flood and in what temporal sequence the water is fed into the linear reservoir.
The runoff production is based on the time-area diagram and on the zoning of the whole catchments in hydrologically homogenous subcatchments (Rickli, Forster, 1997). For the numerical computation of the flood output from the reservoir, Clark used discrete timesteps by applying the Muskingum procedure (Koehler, 1976).

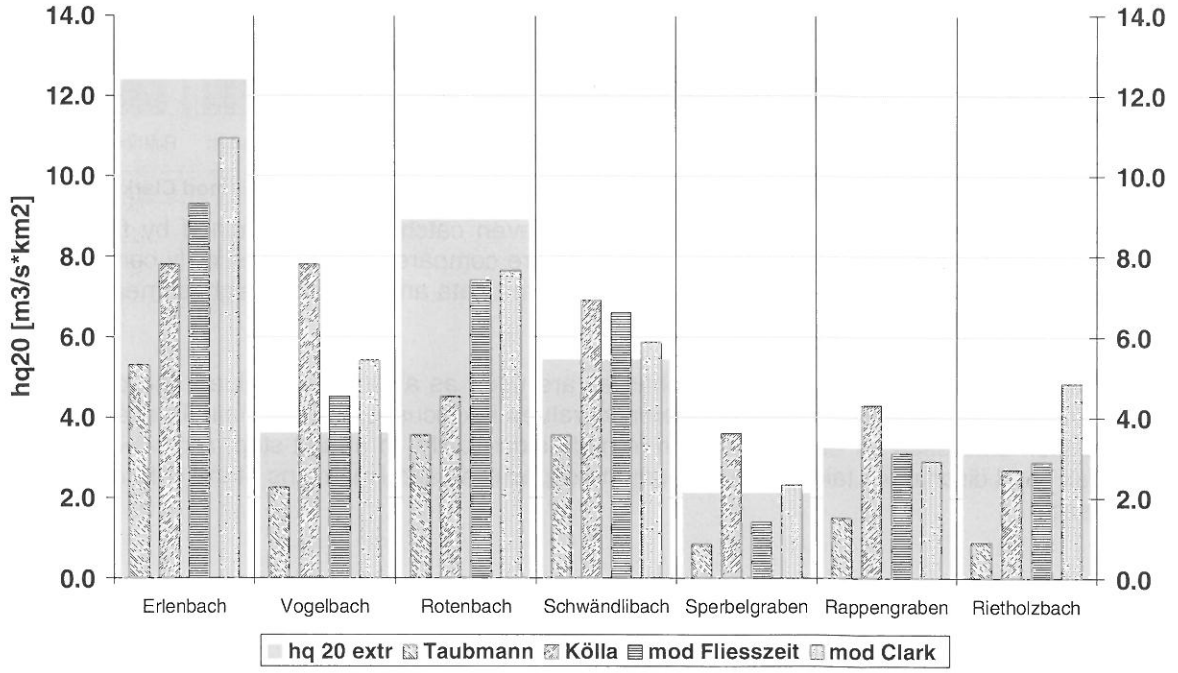

Figure 3-1: The 20-year peak flood discharge for seven catchments determined by four different flood estimation approaches. They are compared to the statistically computed 20-year flood ($hq20_{extr}$) resulting from measured data.

3 RESULTS

These five estimation formulas have been applied in the seven catchments described in chapter 2.1. For this purpose the necessary parameters have been determined as described by the respective authors. All important parameters have either been assessed directly in the field or at least a field verification has been carried out.
In a next step the peak flood discharges with a return period of 20 respectively 100 years have been calculated with the four estimation formulas allowing this. In Figure 3-1 the calculated 20 year peak flood discharges are plotted together with the corresponding value determined by statistical methods. As the modified Müller formula determines a maximum peak flood without reference to a return period, and as this value exceeds a 20 year flood by far, only the results of four formulas are considered.
Figure 3-2 depicts the results of all five flood estimation approaches for the 100-year flood event in the same catchments. In this case of the 100-year event the modified Müller approach is also included, even though it produces a maximum and not a 100-year flood. As a second reference value the so far highest measured peak discharge is plotted beside the statistically determined value for the 100-year event.

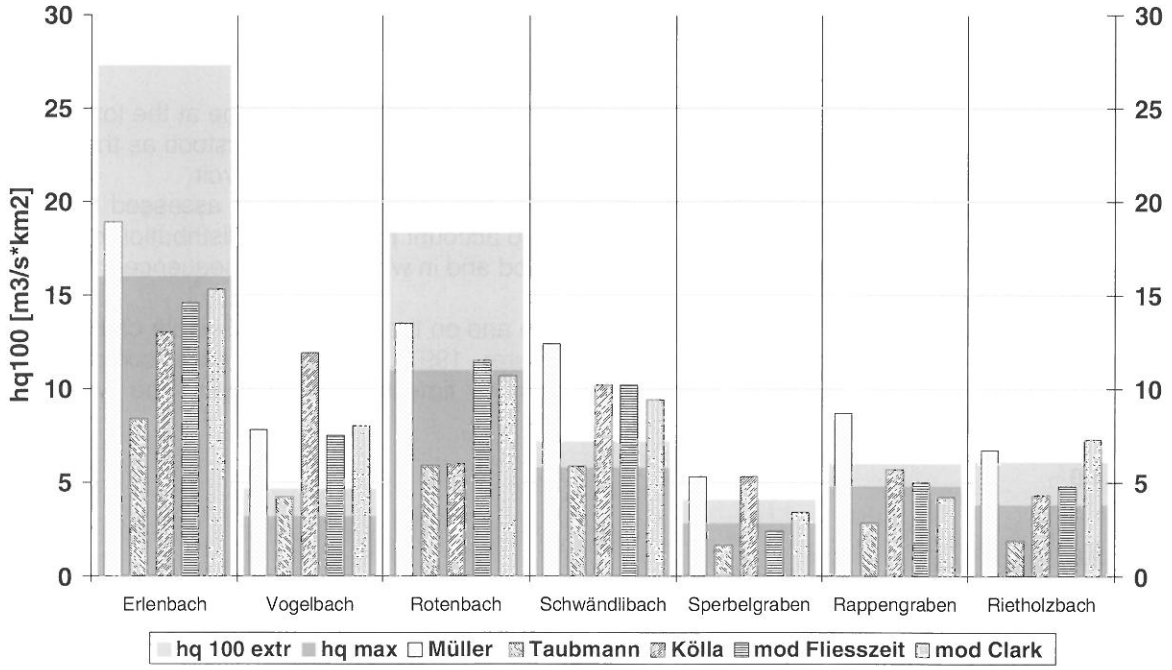

Figure 3-2: The 100-year peak flood discharge for seven catchments determined by five different flood estimation approaches. The values are compared to the statistically computed 100-year flood ($hq100_{extr}$) resulting from measured data and the so far highest measured peak discharge (hq_{max}).

As statistically extrapolated peak flood discharges are used as a basis to evaluate the quality of an estimation formula, the quality of these reference values is discussed below, first. The results of the tests are then discussed for each estimation formula individually. In a next step, a procedure to estimate peak flood discharges taking into account the capabilities and limitations of the different formulas is proposed.

4 DISCUSSION

4.1.1 How reliable are the statistical extrapolations?

Records of reliable hydrological observations are mostly short and data on corresponding extremes are very limited. Peak flood discharge estimation by statistical methods therefore requires the extrapolation beyond the range of observations. Therewith the choice of a distribution function, the consideration of the largest events within the measured time series, the method of parameter estimation and the length of the time series are open for discussion. Confidence intervals cannot help much in many cases, because the lower and the upper limit of such an interval are far below respectively above any reasonable value, determined by any of the mentioned formulas.

Therefore, beside the statistical arguments, a good knowledge of the catchments and their hydrological behaviour is essential for a reliable assessment of the statistical results. In this study, the statistically extrapolated peak flood discharges combined with hydrological knowledge are considered as important reference values. The two catchments Rotenbach and Schwändlibach exemplify the problem very well. Concluding from the hydrological knowledge the two neighbouring catchments show a far too big difference in the extrapolation results. A part of the difference may be explained by the two different distribution functions that have been chosen (log Gumbel for Rotenbach and Gumbel for the Schwändlibach). Nevertheless the difference remains too large or in other words, the extrapolated 100-year peak flood value for Rotenbach catchment is too high and the corresponding value for Schwändlibach is rather underestimated.
Even though the time series of the two Alptal catchments Erlenbach and Vogelbach are short, we conclude from the catchment knowledge that the extrapolated peak flood values for the Erlenbach catchment are overestimated, mainly because of two extreme events and in contrast underestimated for the Vogelbach, where big events are lacking.
In the following, the results of the different estimation approaches are discussed and compared with the hydrologically rated extrapolated peak flood values.

4.1.2 Discussion of the capabilities and limitations of the five estimation formulas evaluated in detail

The modified Müller formula
Considering that the approach does not aim at the 100-year event but at the maximum flood a rough evaluation can only be performed for the four catchments Sperbelgraben, Rappengraben, Rotenbach and Schwändlibach. Except for Rotenbach the modified approach by Müller produces reasonable results exceeding the statistically extrapolated value for a 100-year event. For the other time series which are rather short (see Table 2-1), we used the peak over threshold method (POT). Considering the above made comments on Rotenbach and the Alptal catchments, we conclude that for these cases also the modified Müller approach produces plausible results.

The Taubmann/Thiess/Chow approach
This procedure shows a remarkable consistency for the tested catchments: compared to the other methods the approach by Taubmann/Thiess/Chow provides consequently peak flood values at the lower end of the bandwidth generated by the different estimation approaches.
The hydrograph is rather a mathematical apportionment of the known discharge volume with a given peak flow, than a hydrologically justified run of the curve.
For small catchments, the approach produces very small peak flood values. The results could be rated as a lower limit of the corresponding peak flood discharge.

The Kölla approach
Taking into account the above made comments on the extrapolated peak flood values for Rotenbach, Schwändlibach, Erlenbach and Vogelbach, the Kölla approach produces only partially satisfying results for the small catchments. Whereas Kölla provides to some extent appropriate results for some few catchments, it overestimates peak flood discharge obviously in some other cases and underestimates them clearly in a last catchment. For small catchments the approach seems to provide rather variable results.

The modified rational formula
Both, the estimated 20-year and the estimated 100-year peak flood discharge behave in the same manner in comparison with the corresponding extrapolated values. For Rappengraben and Rietholzbach the estimated and the extrapolated value are in good agreement. For Vogelbach and Schwändlibach the modified rational formula seems to overestimate the extrapolated values. Considering the comments in chapter 4.1.1 however, the results for these two catchments may be accepted as good too. In the cases of Erlenbach and Rotenbach the underestimation can be explained with the too large extrapolation values discussed above. For the Sperbelgraben catchment this approach produces rather a lower limit.
As a whole, the modified rational formula approach produces reliable results for the tested small catchments.

The Clark-WSL approach
For five catchments, the estimated 20-year peak flood discharge differs less than 15% from the corresponding extrapolated value. For Vogelbach and Rietholzbach, the estimated 20-year peak flood discharge amounts to 150% of the extrapolated value. For the Vogelbach catchment, this result confirms the confidence in the Clark-WSL procedure, because the extrapolated value is supposed to be too small. An analysis of the measured precipitation data of the Rietholzbach shows that the underlying precipitation data from the 'Hydrological Atlas of Switzerland' (HADES, 1992) provide too high values for the Rietholzbach catchment (Vogt, 2001). The difference may be reduced to less than 20%.
For the higher return periods, the differences between the estimated and the extrapolated values increase but they remain explainable with all the above made comments on the different catchments. In general, the Clark-WSL approach provides satisfying results.

4.1.3 A combined approach for estimating peak flood discharges

The above discussion of the five estimation formulas shows that none of them is clearly more reliable than the others. The Müller and the Taubmann/Thiess/Chow formulas do not reproduce the statistically extrapolated values in most cases. But it looks like as if they had a similar behaviour in all catchments. Taubmann/Thiess/Chow is always underestimating the statistically extrapolated values, while Müller is overestimating them with the exception of the catchments of the Erlenbach and the Rotenbach discussed above.
The other three approaches generally reproduce the statistically extrapolated values. However, every formula produces in one or in the other case a result that is not completely satisfying, e.g. the result of the Kölla approach is rather high in the Vogelbach, the one of the modified rational formula comparatively low in the Sperbelgraben and the one of Clark-WSL is surprisingly high in the Rietholzbach. In many cases in the research catchments treated in this article, these outliers can be explained and corrected as described above for the result of the Clark-WSL approach in the Rietholzbach due to additional information.
As this is not the case in a practical application in a catchment without measurements, a combined approach is proposed to determine peak flood discharges in small torrential catchments.
Generally only the three estimation formulas reproducing the statistically extrapolated values are used (Kölla, modified rational formula, Clark-WSL). It is proposed to calculate the peak flood discharge in a catchment as the mean of the two highest values out of the three results. However, if one or the other of these three values is considerably higher respectively lower than the results of the Müller or Taubmann/Thiess/Chow formulas, it is probable that this value is an outlier. The peak flood discharge is then determined as the mean of the two remaining values. If two or more values out of the results of the three estimation formulas are considerably below or above the limits described above, a reliable peak flood value can only be determined with additional hydrological studies.
For the results presented above in Figure 3-2, this combined approach means that in the Vogelbach the result of the Kölla approach should not be considered as it exceeds the result of the Müller formula by far. The results of Kölla in the Sperbelgraben and of Clark-WSL in the Rietholzbach are considered, as they are only little above the value of the Müller formula. The respective results are shown with black bars in Figure 4-1.
As all parameter estimations allow a certain bandwidth it is in many cases not appropriate to present only one value as a peak flood estimation. To give an honest result it is in most cases more advisable to present a bandwidth of possible peak flood discharges. The upper and the lower limit of this bandwidth can be calculated in a similar way as the mean or most probable value described above. However, for all methods not mean parameters but parameters of the upper respectively of the lower limit of reasonable values are used. In this bandwidth a peak flood discharge can then be determined taking into account additional information e.g. on historic events or from neighbouring catchments.

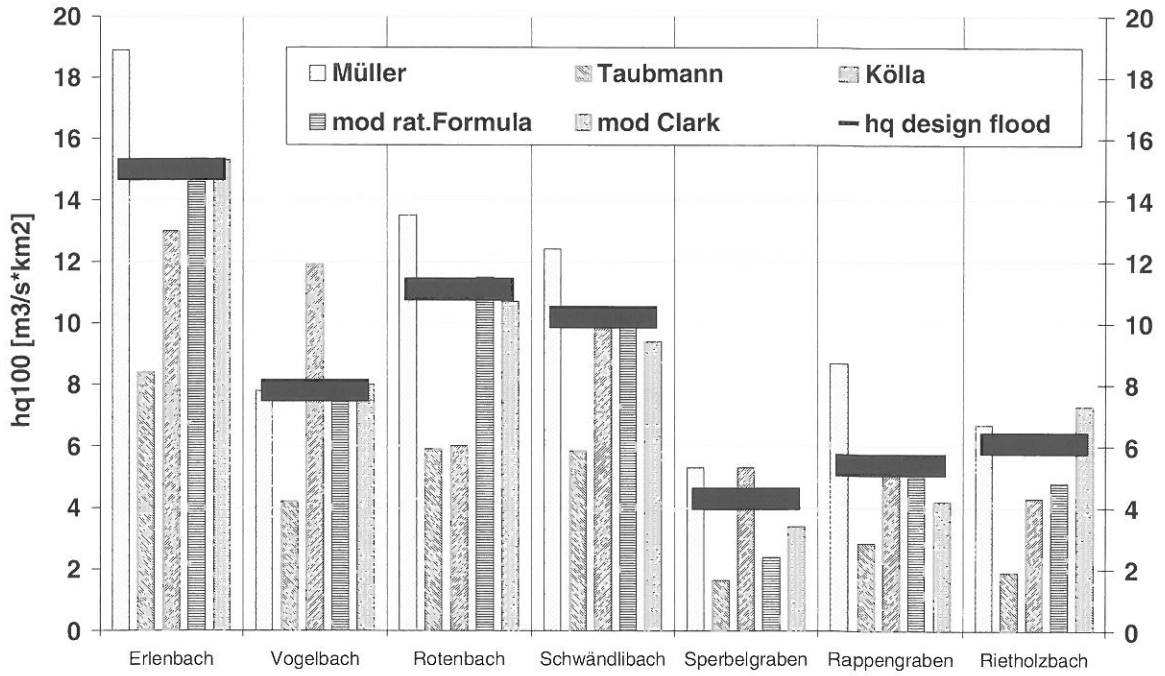

Figure 4-1: The suggested 100-year peak flood discharge for seven catchments as mean of the two highest values out of the Kölla, the Clark-WSL and the modified rational formula. None of these three values is allowed to exceed considerably the value which is provided by the modified Müller approach. The Taubmann/Thiess/Chow approach represents a lower boundary value for the peak flood discharge whereas the modified Müller approach gives an upper limit.

5 CONCLUSIONS AND OUTLOOK

The procedure to estimate peak flood discharges in small torrential catchments presented above seems to be able to produce reliable results. However, it has to be kept in mind that the procedure could only be developed and tested with a very limited data set. Therefore in the future additional tests and eventual modifications will be necessary. This may also include the incorporation of new methods that will be developed in the future.

ACKOWLEDGEMENTS

A part of the presented work in this paper was performed within the CHR-project on flood estimation in the Rhine basin and was financially supported by the Federal Office for Water and Geology, which also provided some of the needed hydrological data.
A special thank goes to Christian Rickli, who supported us in the parameter assessment of several catchments.

REFERENCES

Barben, M. (2001): Beurteilung von Verfahren zur Abschätzung seltener Hochwasserabflüsse in mesoskaligen Einzugsgebieten. Dissertation in der Gruppe für Hydrologie des Geografischen Instituts der Universität Bern. Bern.

Chow, V. T. (1962): Hydrologic determination of waterway areas for the design of drainage structures in small drainage basins. Bulletin No 462 University of Illinois. Illinois.

Chow, V.T. (1964): Handbook of applied hydrology. A compendium of water-resources technology. New York.

Forster, F., Baumgartner, W. (1999): Bestimmung seltener Starkniederschläge kurzer Dauer – Fallbeispiele im Vergleich mit den schweizerischen Starkniederschlagskarten. Schweizerische Zeitschrift für Forstwesen. 150, 6: 209-218. Zürich.

EJPD, Eidg. Justiz- u. Polizeidepartement, Eidg. Volkswirtschaftsdepartement, Eidg. Departement des Innern (1980): Bodeneignungskarte der Schweiz 1:200'000. EDMZ. Bern.

Hager, W.H. (1989): Abflussmaximum aus kleinen Einzugsgebieten. Schweiz. Ingenieur und Architekt, 1989, Nr.22, pp. 577-583. Zürich.

Hydrologischer Atlas der Schweiz (1992): Blatt 2.4: Extreme Punktregen unterschiedlicher Dauer und Wiederkehrperioden 1901-1970. Landeshydrologie und - geologie, Bundesamt für Umwelt, Wald und Landschaft. Bern.

Kleindienst, H., Forster, F. (2000): Bemessungshochwasser in kleinen Wildbacheinzugsgebieten - Was bringt ein hydrologisches Prozessmodell gegenüber einfachen Schätzformeln. Hydrologie und Wasserbewirtschaftung, 44, 1: 9-19. Koblenz.

Koehler, G. (1976): Niederschlag-Abfluss-Modelle für kleine Einzugsgebiete. Schriftenreihe des Kuratoriums für Wasser- und Kulturbauwesen, Heft 25. pp. 41 – 48. Hamburg – Berlin.

Kölla, E. (1986): Zur Abschätzung von Hochwassern in Fliessgewässern an Stellen ohne Direktmessungen. Mitteilung Nr.87 der Versuchsanstalt für Wasserbau, Hydrologie und Glaziologie der ETH Zürich. Zürich.

Kölla, E. (1987): Abschätzung von Spitzenabflüssen in kleinen natürlichen Einzugsgebieten der Schweiz. Schweizer Ingenieur und Architekt, 1987, Nr.33-34, S.965-972. Zürich.

Müller, R. (1943): Theoretische Grundlagen der Fluss- und Wildbachverbauungen. Mitteilung Nr.4 aus der Versuchsanstalt für Wasserbau der ETH Zürich. Zürich.

NWSCA, National Water and Soil Conservation Authority (1984): A method for estimating design peak discharge (Technical Memorandum No. 61), Water & Soil, Technical Services Report. Wellington.

Rickli, C., Forster, F. (1997): Einfluss verschiedeneder Standortseigenschaften auf die Schätzung von Hochwasserabflüsen in kleinen Einzugsgebieten. Schweiz. Zeitschr. Forstwesen, 148 Jg., Nr.5, pp. 367-385. Zürich.

Sackl, B. (1990): Influence of basin characteristics on flood hydrographs. In: White, W.R. (ed): International Conference on River Flood Hydraulics, sept 17-20: p 31-40. John Wiley & Sons Ltd. Chichester.

Sydler, P., Widmoser, P., Zollinger, F. (1982): Statistische Untersuchungen von Extremabflüssen in kleinen Einzugsgebieten, Institut für Kulturtechnik, ETH Zürich. Zürich.

Taubmann, K.-C.,Thiess, N. (1984): Ingenieurmässige Anwendung verschiedener Hochwasser-Abschätzmethoden auf kleine und zusammengesetzte Einzugsgebiete am Testbeispiel der Ergolz. Ingenieurschule beider Basel. Muttenz.

Taubmann, K.-C. (1986): Ingenieurhydrologische Hochwasserabschätzung. Wasser, Energie, Luft, Jg.78, Nr 10, S. 277-281. Baden.

Thiess, N. (1975): Ermittlung von Bemessungsganglinien für kleine Einzugsgebiete nach Ven Te Chow, Landesamt für Umweltschutz Baden-Württemberg. Karlsruhe.

Vogt, St. (2001): Zur Abschätzung von Hochwasser in kleinen Wildbacheinzugsgebieten, unveröffentlichte Diplomarbeit WSL / Institut für Klimaforschung ETH. Birmensdorf / Zürich, 90 p.

Vogt, St., Forster, F., Hegg, Ch. (2002): Clark-WSL - A method for the estimation of design flood hydrographs in small torrential catchments. (Same publication as the present article)

Weingartner, R. (1989): Das Unit-Hydrograph-Verfahren und seine Anwendung in schweizerischen Einzugsgebieten. Projektschlussbericht. Geograph. Inst. Univ. Bern, Publikation Gewässerkunde Nr.107, 103 S. Bern.

Widmoser, P. (1974): Extremabflüsse aus vierzig kleinen Einzugsgebieten der Schweiz. Schweizerische Bauzeitung, 92. Jg., Nr 32, 1974, S. 757-765. Zürich.

REGIONALISATION OF ANNUAL FLOODS – AN ADAPTIVE METHOD TO ERRORS AND DATA UNCERTAINTIES

Markus Niggli, Daniela Talamba, Benoît Hingray, André Musy

HYDRAM, Ecole Polytechnique Fédérale de Lausanne, 1015 Lausanne,
Markus.Niggli@epfl.ch, Daniela.Talamba@epfl.ch, Benoit.Hingray@epfl.ch, Andre.Musy@epfl.ch

SUMMARY

Instead of developing one "accurate" estimation method, we propose a methodology combining two already existing methods for flood discharge assessment. The basic idea of the combination is to define a weighted average of the proposed models, where the weight of each model is inversely proportional to the model error. The resulting combination can be considered as a linear empirical Bayes estimator of the flood quantiles. The model error is here defined as the variance of the residuals between the "true" quantile estimation and the model estimation (corrected by the bias). It depends on catchment properties, availability of data and can be determined using weighted least square regression analysis. By using this type of approach, it is also possible to provide confidence intervals for the "individual" models and for the resulting combination model. The objective is to define a general framework for flood estimation, which leads to a "best" flood estimate using all the available information (models, catchment properties, eventually discharge measurement, etc.). The methodology must also give a measure of the accuracy of the estimation, especially when only little information is available.
In order to show the potential of the combination method, this paper will present one example made with two different regional methods, adapted to western Switzerland. The first one is an "index flood" method, which performs well for bigger catchments (say more than 10-20 km^2) and the second one is a synthetic rational method, giving more accurate quantile estimates for smaller catchments. As mentioned above, drainage area plays an important role in the accuracy of quantile estimation with both methods. Therefore, it was assumed that the variance of the residuals is a power function of the catchment area, for which the parameters can be estimated using a weighted least square regression. The first results show that the resulting combination model is an interesting compromise that moves from the rational method for smaller catchments to the index flood method for bigger catchments. Moreover, it provides model errors that are generally as small as those of the "best" of each individual method.

Keywords: regionalisation of floods, empirical Bayes estimators, weighted least square regression, uncertainty, rational method, index flood method.

1 INTRODUCTION

This paper shows how some statistical tools like empirical Bayes estimators and weighted least square regression could be useful for flood estimation. This is illustrated with a simple combination methodology of two complementary regional methods applied to Western Switzerland. The first one (presented in section 3 of this paper) is the "index-flood" method, which performs well for bigger catchments (say more than 10-20 km^2) and the second one (section 3) is a synthetic rational method, giving more accurate quantile estimates for smaller catchments. An empirical bayesian approach (section 4 of this paper) allows for the computation of model errors for the "individual" models and a resulting combination model. It provides also a measure of the accuracy of the estimation, especially useful when only little information is available. The flood estimation improvement of the combination model versus both "individual" methods is also evaluated in this section. Finally some suggestions of improvement of the methodology are given in the concluding remarks.

2 AREA OF STUDY AND AVAILABLE DATA

The area of study includes 42 catchments located in the Western part of Switzerland, covering the Aare basin, the Swiss parts of the Rhone and Doubs basin as well as the Jura part of the Rhine basin (Figure 2-1). The catchments with a mean elevation higher than 1500 m (hydrologic regime influenced by glacier- and snowmelt) have not been considered. The hydrologic data include annual floods series which length varies between 5 and 80 years. Three specific geographical regions of Western Switzerland were distinguished. All available gauging sites where then affected to one of these three regions (Figure 2-1), with a simple rule presented in Niggli et al. (2001), based on geology and mean elevation.

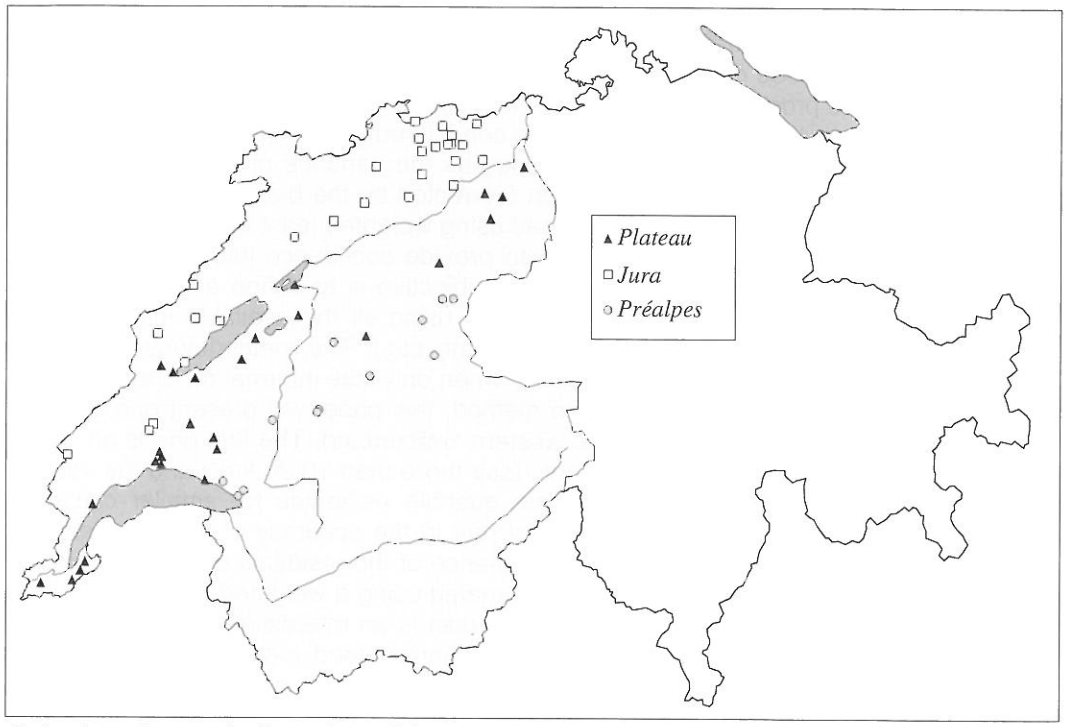

Figure 2-1: Location and affectation of the gauging sites to one of the three specific regions defined for Western Switzerland.

Within each region, floods are produced by different precipitation and runoff processes. The first region, called "Jura", is a mountainous non-glaciated area where catchments have an average elevation between 850 and 1500 m. Maximum annual floods occur generally during the winter season with west-frontal precipitations. They are strongly influenced by karst and slightly by snowmelt. The second region "Plateau" includes catchments of the Swiss Lowlands (mean elevation ranges from 500 to 850 m) where maximum annual floods are also produced in most cases by winter precipitation, but without influence of snow and karst. The third region, called "Préalpes", is typical of steep and impervious mountainous areas where maximum annual floods are often generated by intense thunderstorms, occurring during the summer season. As in the case of the "Jura" region, the mean elevation of catchments ranges from 850 m to 1500 m with no glacier-covered areas. Figure 2-2 shows that differences in flood generation processes for these regions can be highlighted using some statistical properties like the L-coefficients of variation and symmetry (respectively *L-CV* and *L-CS*) defined by Hosking (1990). The "Préalpes" catchments show high values of both *L-CV* and *L-CS* while the "Jura" ones are generally much lower. The values observed for the region "Jura" are sparse, probably because of the heterogeneity of the hydrological behavior induced by karst effects. The catchment of the "Plateau" region shows intermediate values. Note that the catchments with an area less than 10 km^2 have greater dispersion of the *L-CV* and *L-CS*. This can be explained by the much higher variability of the local specific characteristics at that scale. In that case, variation in flood statistics cannot be explained by the belonging to a geographical region only.

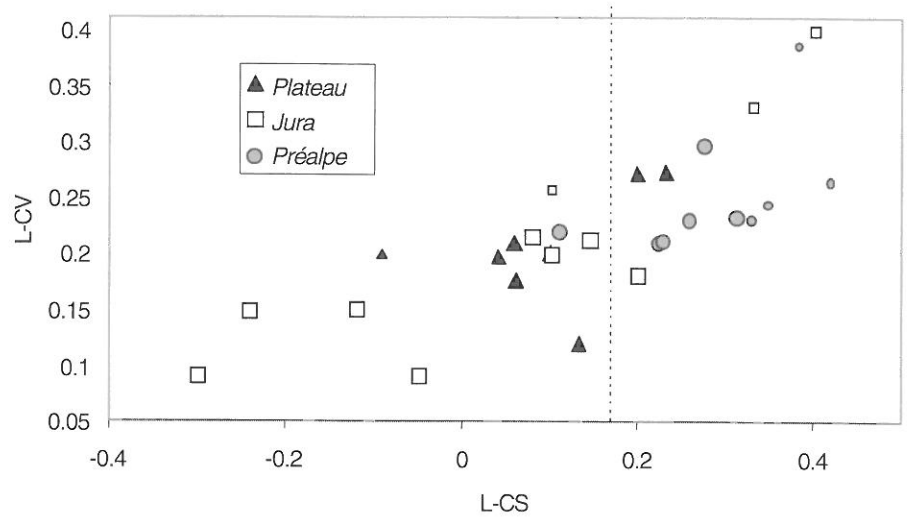

Figure 2-2: L-moments diagramme. Only catchments with at least 20 years of measurement are displayed in this graph. Smaller symbols indicate the catchments with an area less than 10 km^2.

3 THE INDEX-FLOOD METHOD (HYDRIF MODEL)

The first method used to produce a given discharge estimate (called HYDRIF model) is the index flood method proposed by Dalrymple (1960). The key assumption of an index flood procedure is that the frequency distributions (growth curve) of N sites within a region are equivalent and variations from one station to another can be represented by a scaling factor. The scaling factor is the mean annual maximum flood, which is estimated by multivariate analysis. It is required that the regions are homogeneous, i.e. the regional growth curves can be considered as representative for all the catchments within the region. Therefore, to obtain the flood estimate formulation for the HYDRIF model, the following steps have been successively achieved:

- Homogeneity assessment of the above defined geographical regions
- Determination of the regional growth curves by selecting and fitting an appropriate statistical distribution to the observations
- Determination of the mean annual maximal flood as a function of physiographic and climatic catchments characteristics

The homogeneity of each geographical region was tested with a L-moments test defined in Chowdhurry et al. (1991). The basic idea of this test is to check for the distance between the L-moments of each catchment and a "mean" regional value of the L-moments. If only the catchment with an area greater than 10 km^2 are considered, then the regions "Préalpes" and "Plateau" are found to be homogeneous at a 5% level, while the "Jura" is heterogeneous. The incorporation of catchments with an area less than 10 km^2 leads to increase the regional heterogeneity in all three cases. That means that the index flood must be preferably applied for bigger catchments and caution should be exercised for catchments within the "Jura" region.
Because of its robustness (Cunnane, 1988), the General Extreme Value (GEV) distribution was selected for determining the different regional growth curves. Parameters are estimated on the basis of probability weighted moments (Hosking et al., 1985). According to the results of the homogeneity test, only catchments with an area greater than 10 km^2 were considered for deriving the growth curves. Figure 3-1 compares the computed regional growth curves and shows significant differences between the 3 regions. For instance, the 100-year flood is almost three times the value of the mean annual flood in the "Préalpes" region while it is less than 2 in the "Jura" area. It is worth noting, that the growth curve for the region "Plateau" can be well described with a GEV type I distribution (i.e. a Gumbel distribution).
The relationship between the maximum annual flood and the catchment characteristics was then determined by stepwise regression. The relevant physical catchment characteristics highlighted by that procedure are the catchment area, the catchment mean altitude and a variable representing the effect of the drainage density.

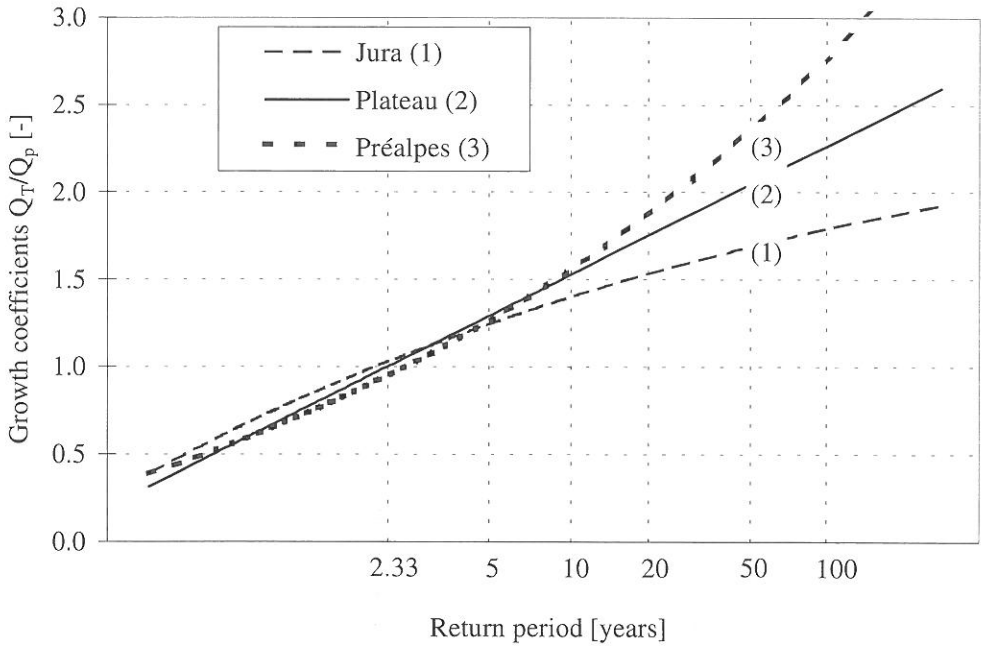

Figure 3-1: Growth curves for regions "Jura", "Plateau" and "Préalpes".

By combining the results of step 2 and 3 of the index flood procedure, one can define the specific flood $Hq_{x,HYDRIF}$ in [l/s/km^2] for a certain return period x and for a catchment belonging to a given region R:

(1) $$Hq_{x,HYDRIF} = 5.6 \cdot f_{(x,R)} \cdot EL^{-0.56} \cdot ALT^{0.63} \cdot A^{-0.34}$$

where $f_{(x,R)}$ is a growth coefficient depending on the region R and on the period return x (cf. Figure 3-1), A is the catchment area in [km^2], ALT is the mean elevation in [m] and EL is a factor which expresses the drainage density. The latter can be defined as follow:

(2) $$EL = 2 \cdot \frac{\sqrt{A/\pi}}{L}$$

where L is the length of the hydrographic network measured at a 1:25'000 scale. It is worth noting that L cannot be accurately measured for very small catchments (say less than 10 km^2), because of the subjectivity in the topographical interpretation of the river network at that scale. The maximum flood discharge estimates obtained for different return periods by the application of this method are presented in Niggli et al. (2001). The method shows good results for catchments with areas ranging between 10 and 500 km^2. Its applicability may however be inadequate for small catchments (less than 10 km^2) for which cases the method constantly underestimates the flood quantiles. Other limitations to the application of the method are encountered for catchments with significant karstic areas and for catchments outside the range of validity defined in the section 2 of this paper.

4 THE SYNTHETIC RATIONAL METHOD (HYDRAT MODEL)

In order to improve the flood quantiles estimation for small catchments, a synthetic expression of the rational formula is proposed (cf. Equation (5)). This classical approach was chosen because it is felt that empirical methods (as the rational formula) could provide a good alternative to statistical regional methods (as the index-flood), which are suited for region (or groups of catchments) where enough data are available. This is generally not the case for smaller catchments. Moreover, because of the lack of data and the greater local variability of the runoff process at that scale, statistical methods may fail to identify physiographic or climatic characteristics explaining the flood variability. It therefore proposed to introduce "what we know" about the flood generation process *a priori* in the model. Of course, the rational formula is the simplest alternative to statistical methods. Other more sophisticated models

could be applied in the future. Note that the assumptions, which are requested to apply the rational formula (spatial homogeneity of the rainfall, as well as the runoff coefficient), restrict its use to smaller catchments. The HYDRIF and HYDRAT models can therefore be considered as complementary.
The obtained expression, called HYDRAT model, is the result of the combination of two typical relationships reported in the literature for both the time of concentration and the rainfall Intensity-Duration-Frequency (IDF) curve. The details concerning the development of the model can be found in Niggli et al. (2001). The IDF curve is assumed to follow a Montana law with parameters $\varepsilon_1(x)$ and $\varepsilon_2(x)$:

(3) $$i(x,d) = \varepsilon_1(x) \cdot d^{\varepsilon_2(x)}$$

where $i(x,d)$ is the maximum mean rainfall intensity [mm/h] over the rainfall duration d [mn] for the return period x. $\varepsilon_1(x)$ and $\varepsilon_2(x)$ can be estimated using the information given in the Hydrological Atlas of Switzerland (Jensen et al., 1992) or in the catalogues of extreme rainfall for Switzerland (Röthlisberger et al., 1971,1981,1992). Many formulations of time of concentration found in the literature (Ventura, Passini, Bransby, Kirpich, NERC presented for instance in Maidment (1993)) can be simplified in one single expression, where the time of concentration is defined as a function of the drainage area A [km^2] and the mean slope p [m/m]:

(4) $$t_c = \beta \cdot \left(\frac{A}{P} \right)^{\alpha}$$

where α and β are regional parameters. We have chosen to set the parameter having the lowest variability (α) to 0.5. This value corresponds to the value generally adopted in the literature. By combining Equations (3) and (4) and the general expression of the rational formula, one can obtain the maximum specific flood $Hq_{x,HYDRAT}$ in [l/s/km^2] for a certain return period x:

(5) $$Hq_{x,HYDRAT} = u \cdot C_r \cdot \beta_R^{\varepsilon_2(x)} \cdot p^{-0.5 \cdot \varepsilon_2(x)} \cdot \varepsilon_1(x) \cdot A^{0.5 \cdot \varepsilon_2(x)}$$

where u is a factor depending on the units used in the equation (in this case u=280) and Cr [-] is the runoff coefficient. The latter is determined as a function of land-cover according to the Swiss norms SNV (presented for instance in Musy et Higy, 1998). β_R is an integrative parameter of all unaccounted-for physiographic and climatic factors which variability depends on the geographical region defined in the section 2 of this paper. The adopted value shown in Table 4-1 allows for a well reproduction of the annual flood distribution.

Table 4-1: Optimal β_R values for regions "Jura", "Plateau" and "Préalpes".

Region	β_R
Préalpes	20
Plateau	30
Jura	75

Unsurprisingly, the application of the HYDRAT model to the region of study shows that the synthetic rational formula performs better than the HYDRIF model for catchments with areas less than 10 km^2. For larger catchment areas, the model tends to underestimate the flood quantiles and performs much worse than the HYDRIF model. Note that there is a domain (between 10 km^2 and say 100 km^2) where it is difficult to chose between the two models. Both models perform as well (or as bad), justifying therefore a combination method. Moreover, the same limitations as the HYDRIF model, concerning the applicability of the model for catchments with significant karstic areas or outside the range of validity defined in section 2, must be mentioned. An extensive evaluation of the HYDRAT model is given in Niggli et al. (2001).

5 THE COMBINATION METHOD

Given the complementary performance of both presented methods, a combination of the two methods is proposed. This issue is addressed by the use of an empirical Bayes approach (EB) that combines the estimates given by the individual models. The HYDRIF estimate is used to construct the prior quantile distribution and the HYDRAT estimate is used to build the likelihood function. The EB approach was selected in order to avoid the need to choose between the two methods, while generally offering an additional gain in precision. If the prior and the likelihood distributions are normal, the posterior distribution will also be normal. The mean $E_{EB}(HQ_x)$ and the variance $V_{EB}(HQ_x)$ of the combined estimation is then:

(6) $$E_{EB}(HQ_x) = p \cdot E_{HYDRAT} + (1-p) \cdot E_{HYDRIF}$$

(7) $$V_{EB}(HQ_x) = \frac{V_{HYDRAT} \cdot V_{HYDRIF}}{V_{HYDRAT} + V_{HYDRIF}}$$

with:

(8) $$p = \frac{V_{HYDRIF}}{V_{HYDRAT} + V_{HYDRIF}}$$

E_{HYDRAT} and E_{HYDRIF} are the unbiased expected values of HQ_x given by respectively the HYDRIF and the HYDRAT models (cf. Equations (1) and (5)). Note that both HYDRIF and HYDRAT models provide not necessarily unbiased estimated for HQ_X. This is due to the fitting method that was chosen, as well as the data availability, at the moment when the models were parametrised. V_{HYDRAT} and V_{HYDRIF} are the variances of respectively the prior and the likelihood distributions. Note that the estimates obtained by the models must be obtained independently. The basic idea of this approach is to estimate the desired quantiles as a weighted combination of the two methods presented above and that the weights p and 1-p depends on the model error. The model error is here defined as the variance of the residuals between the "true" quantile estimation (the quantile value if at-site data would be available for a very long period) and the model estimation (corrected by the bias). According to the previous results regarding the domain of validity of the model, it is suggested that the variance of the residuals depends on the catchment area. In order to allow for bias correction and to take into account the effect of catchment area, the following expressions were therefore defined:

(9) $$E_{MODEL} = a_{0,MODEL} + a_{1,MODEL} \cdot HQ_{x,MODEL}$$

(10) $$V_{MODEL} = V_{0,MODEL} \cdot A^{n_{,MODEL}}$$

where $a_{0,MODEL}$ and $a_{1,MODEL}$ are related to the bias (absolute and relative, respectively) of the regional individual model (MODEL=HYDRIF or HYDRAT). V_{MODEL} is modelled as the product of a constant term $V_{0,MODEL}$ and a scale factor $A^{n_{,MODEL}}$ depending on the catchment area (A). To estimate $a_{0,MODEL}$, $a_{1,MODEL}$ $V_{0,MODEL}$ and $n_{,MODEL}$, resort is made to weighted least squares analysis (Stedinger et Tasker, 1996), which compares the calculated quantiles (with the model HYDRAT or the model HYDRIF) with the true ones. The latter are not known but can be estimated from at-site data, which are assumed to be unbiased. The variance of the at-site estimate must be determined in order to solve the regression model. This was achieved by considering that the observed annual floods follow a Gumbel distribution, so that the variance can be estimated by asymptotic theory (Meylan et Musy, 1999).
In order to assess the relative performance of the HYDRIF and the HYDRAT models, we determined two optimal sets for $a_{0,MODEL}$, $a_{1,MODEL}$ $V_{0,MODEL}$ and $n_{,MODEL}$ by weighted least square analysis for the 42 catchments of the area of study. The residual variance V_{MODEL} (depending on the catchment area) obtained with Equation (10) can then be compared between both methods. For a particular area, a high residual variance can be associated to a poor model performance and vice versa. Unfortunately the solutions given by the weighted least square analysis are not unique for both models and an additional criterion must be added. We chose to select the two optimal parameter sets where $a_{0,MODEL}$ is the closest to 0 (minimisation of the absolute bias). This option was selected because it ensures consis-

tent estimations and doesn't change the internal structure of the model. Figure 5-1 shows that V_{HYDRAT} is increasing with catchment area, while V_{HYDRIF} is decreasing. Moreover the relative performance of the HYDRAT model versus the HYDRIF model is higher when A is less than approximately 10-20 km^2 (lower value for V_{HYDRAT} than for V_{HYDRIF}) and lower for larger values of A.

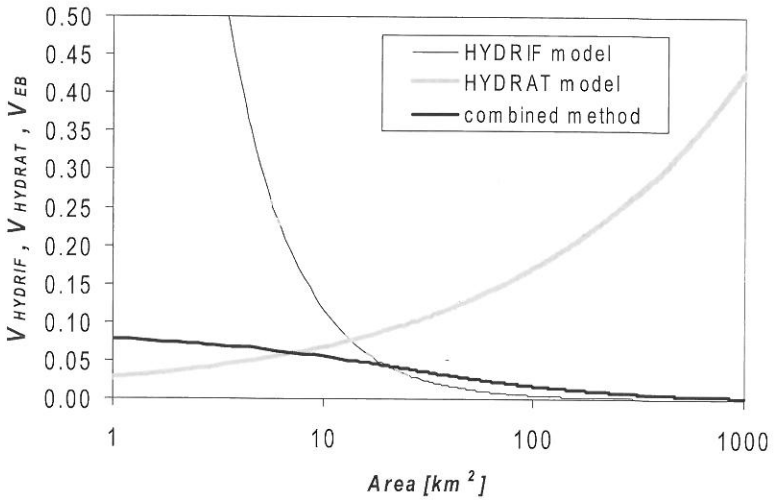

Figure 5-1: comparison of the residual variance for the HYDRIF, HYDRAT and combined model.

Figure 5-1 shows also that the combined method (using Equations (6) and (7)) is doing almost as well as the best of the two methods HYDRIF or HYDRIF for each value of A. In some cases (A between 8 and 20 km^2), the combined methods gives even better results than both individual models. However, the most important point to note is that the combined method always gives moderate value of V_{EB} while the V_{HYDRIF} and V_{HYDRAT} become unreasonably large for respectively small and big catchments. Note that in the case of the combined method the two optimal sets $a_{0,HYDRIF}$, $a_{1,HYDRIF}$ $V_{0,HYDRIF}$ and $n_{,HYDRIF}$ as well as $a_{0,HYDRAT}$, $a_{1,HYDRAT}$ $V_{0,HYDRAT}$ and $n_{,HYDRAT}$ were re-computed after dividing randomly the total sample of 42 catchments into two groups of 21 catchments. One group is used for estimating $a_{0,HYDRIF}$, $a_{1,HYDRIF}$ $V_{0,HYDRIF}$ and $n_{,HYDRIF}$, while the other group allows for estimation for the corresponding parameters for the HYDRAT estimate. This ensures that the parameters of Equations (9) and (10) are obtained independently, which is a necessary condition.
Figure 5-2 shows the evolution of p with the catchment area. Logically, it shows that the HYDRAT model has more weight in the combined method than the HYDRIF model for smaller catchments ($p > 0.5$ for $A <$ 20 km^2) and that the contribution of the HYDRIF model becomes more important for larger catchments.

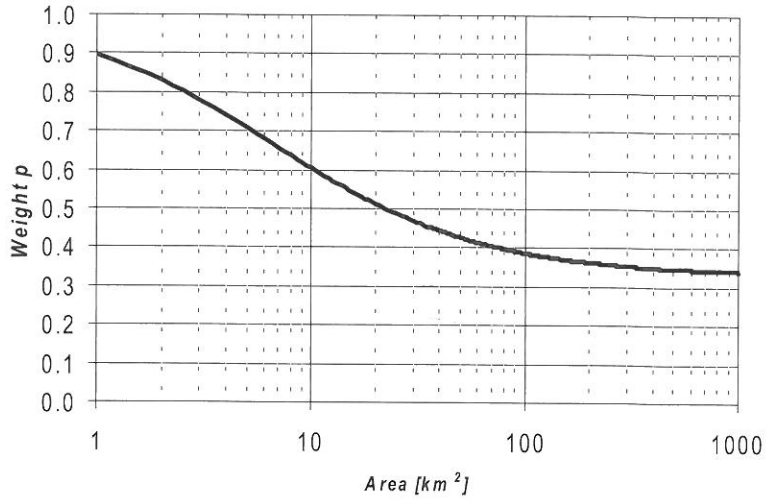

Figure 5-2: relation between p (see Equation (8)) and the catchment area

6 CONCLUSION

The first results of this empirical Bayesian methodology show that the combination model is an interesting compromise that moves from the rational method for smaller catchments to the index floods methods for bigger catchments. The combination model gives model errors (or residual variance) that are generally as small as those of the "best" of each individual method. Moreover, it always gives moderate value of model errors while the use of the "individual model", index flood method or rational formula, only, leads to unreasonably large errors for respectively very small or very large catchments. The methodology presented in this paper has not only the advantage to provide a combination model reliable for a large range of catchment areas. It also provides the necessary information to derive confidence intervals for the combined and the individual methods, which are very useful for engineering problems. The parameterisation of the models takes also into account the uncertainty of the observed flood quantiles, which depend on the preciseness of the available at-site data. For instance observed quantiles estimated from longer time series have more weight in the model evaluation than quantiles estimated from shorter time series.
Further developments will involve investigation into some assumptions made in this paper. For instance the normality of the residuals between the "true" quantiles and the modelled quantiles must be checked. A log-transformation of the flood quantiles may be applied instead of working with the quantiles directly. By applying this bayesian methodology, a further general frame of combining different models for flood estimation has to be considered. Other potential regional models as methods using simple conceptual models can also be taken into consideration

REFERENCES

Chowdhury, J.U. et al. (1991): Goodness-of-fit tests for regional generalized value flood distributions. Water Ressources Research, vol 27(7), pp. 1765-1776.

Cunnane, C. (1989): Statistical distributions for flood frequency analysis. World Meteorological Organization, Operational Hydrology Report N°33. Geneva.

Dalrymple, T. (1960): Flood frequency analysis. Manual of Hydrology, Pt 3, US Geological Survey.

Hosking, J.R. (1990): L-moments: analysis and estimation of distributions using linear combinations of order statistics. Journal of the Royal Statistic Society, serie B, vol. 52(1), pp. 105-124.

Hosking, J.R. et al. (1985): Estimation of the generalized extreme value distribution by the method of probability weighted moments. Technometrics, 27(3), pp. 251-261.

Jensen, H. et al. (1992): Extreme point rainfall of varying duration and return period 1901-1970. Hydrological Atlas of Switzerland, table 2.4[2]. Landeshydrologie und -geologie, Berne.

Maidment, D.R. (1993): Handbook of hydrology. MacGraw-Hill.

Meylan, P., Musy, A. (1998): Hydrologie fréquentielle. HYDRAM. EPFL. Lausanne.

Musy, A., Higy, C. (2000): Hydrologie appliquée. HYDRAM. EPFL. Lausanne.

Niggli, M. et al. (2001): Estimation des débits de pointe pour des bassins versants non jaugés: Application à la Suisse Occidentale. Wasser, Energie, Luft, 9-10.

Röthlisberger, G. et al. (1979, 1981, 1992): Starkniederschläge in der Schweiz, Band 4–9. Eidgenössiche Forschungsanstalt für Wald, Schnee und Landschaft. WSL. Birmensdorf.

Stedinger, J.R., Tasker, G.D. (1985): Regional hydrological analysis. 1.Ordinary, weighted and generalized least squares compared. Water Ressources Research, 21(9), pp. 1421-1432.

EVALUATION AND INTERCOMPARISON OF ATMOSPHERIC MODEL DRIVEN FLOOD RUNOFF SIMULATIONS IN THE LAGO MAGGIORE BASIN

Karsten Jasper, Joachim Gurtz, and Herbert Lang

Atmospheric and Climate Science, ETH, Winterthurerstr. 190, CH-8057 Zürich, Switzerland,
jasper@geo.umnw.ethz.ch

SUMMARY

To investigate the current use of flood runoff predictions in complex mountain watersheds by coupled atmospheric-hydrological modelling, the authors carried out a multitude of combined high-resolution one-way driven model experiments to reproduce the runoff hydrographs for seven extreme flood events which occurred in the Lago Maggiore basin between 1993 and 2000. For the Alpine Ticino-Verzasca-Maggia basin (2627 km^2), an area located directly to the south of the main Alpine ridge and draining from the north into the Lago Maggiore, the grid-based hydrological catchment model WaSiM-ETH was employed to calculate the runoff hydrographs using two different sets of meteorological input data: (1) surface observation data from station measurements and from weather radar, and (2) forecast data of five different high-resolution numerical weather prediction (NWP) models (cell sizes between 2 km and 14 km).
This paper presents and compares selected results of these flood runoff simulations with particular attention to the experimental design of the model coupling. The configuration and initialization of the hydrological model runs are outlined as well as the down-scale techniques which proved to provide an adequate spatial interpolation of the meteorological variables onto the 500 m x 500 m grid of the hydrological model. In order to evaluate the various hydrological model results as generated from the different outputs from the five NWP models, some coupled experiments with "non-standard" NWP model outputs have been carried out. In particular, the results of these sensitivity studies point to inherent limits of high-resolution flood runoff predictions in complex mountain terrain.

Keywords: Mountain hydrology, atmospheric-hydrological modelling, flood forecasting

1 INTRODUCTION

In the Lago Maggiore basin, an area located directly to the south of the main Alpine ridge, exceptional precipitation amounts and intensities lead to relatively frequent flood events with sometimes devastating results for life and property (Frei, Schär, 1998). In the very last years, several major Alpine flooding events occurred in this region, such as the "Brig flash flood" (September 1993), the "Piedmont flood" (November 1994), and the "Gondo flood" (October 2000), all together claiming over 100 victims and property damage amounting to about 30 billions of Swiss Francs (Binder, Schär, 1996, Kleinschroth, 2001).
With these heavy losses in mind, the general public is strongly interested in reliable flood predictions and warning systems. The traditional way of flood forecasting by hydrological simulations using observed precipitation data is not practical for most of the Alpine river catchments because of their dynamic runoff regimes with quite short response times on precipitation events (Petrascheck, 1996). To extend the lead time between warning and occurrence of a flood event, advanced methods for runoff and flood prediction are necessary, which make optimal use of the prediction potential of both the hydrological and atmospheric system.
With the aim to test such new methods in mesoscale mountain watersheds, the EU project RAPHAEL, a project initiated by the Mesoscale Alpine Programme (MAP) (Bougeault et al., 1998), has been started in 1998 to run over two years (Bacchi, Ranzi, 2000). Within this project, meteorologists and hydrologists worked closely together in order to investigate the current potential of flood forecasting by coupling high-resolution weather prediction models and distributed hydrological models in complex terrain.
Within RAPHAEL and its post-activities, seven relevant flood events, which occurred in the Lago Maggiore area between 1993 and 2000 (Table 1-1), were selected for being simulated by passively coupling high-resolution atmospheric and hydrological models. The first four cases have been intensively investigated within the RAPHAEL project, whereas cases 5 and 6 represent two events with heavy precipitation which occurred within the Special Observation Period (SOP) of MAP (Bougeault et al., 2001). Case 7 happened to become one of the most heavy and damaging rain-caused flood events that has been observed in the region around the Lago Maggiore during the last decade (Grebner et al., 2000).

Table 1-1: List of investigated events in the Ticino-Verzasca-Maggia basin.

Case No.	Flood event	Simulation periods		Area-averaged precipitation	Max. station-observed precipitation
1	Brig	22-24 Sep 1993	72 h	272 mm	541 mm (Camedo)
2	Locarno	12-14 Oct 1993	72 h	193 mm	315 mm (Maggia)
3	Piedmont	03-06 Nov 1994	72 h	152 mm	357 mm (Camedo)
4	Snowmelt	27-29 Jun 1997	72 h	137 mm	250 mm (Crana-T.)
5	IOP2b	19-21 Sep 1999	72 h	172 mm	399 mm (Camedo)
6	IOP3	25-27 Sep 1999	60 h	125 mm	246 mm (Brissago)
7	Gondo	11-16 Oct 2000	144 h	326 mm	695 mm (Simplon)

The coupled meteo-hydrological model experiments were focused on the Swiss Lago Maggiore basin including the river catchments of Ticino, Verzasca and Maggia (total area: 2627 km^2) (Figure 1-1). For this target area, the distributed catchment model WaSiM-ETH (Schulla, 1997, Jasper, 2001) was applied to calculate the runoff hydrographs based on different meteorological inputs:

(a) surface observations: (1) from station measurements, (2) from weather radar,

(b) simulation data of five different high-resolution numerical weather prediction (NWP) models: (1) SM (Swiss Model - Switzerland) (Majewski, 1991, DWD, 1995), (2) MESO-NH (MESOscale Non-Hydrostatic model - France) (Lafore et al., 1998, Stein et al., 2000), (3) BOLAM3 (Bologna Limited Area Model version 3 - Italy) (Buzzi et al., 1994, Buzzi, Malguzzi, 1997), (4) MC2 (Mesoscale Compressible Community model - Canada) (Tanguay et al., 1990, Laprise, 1995, Benoit et al., 1997), and (5) ALADIN (Aire Limitee Adaption DYNamique - joint international development) (Bubnova et al., 1995).

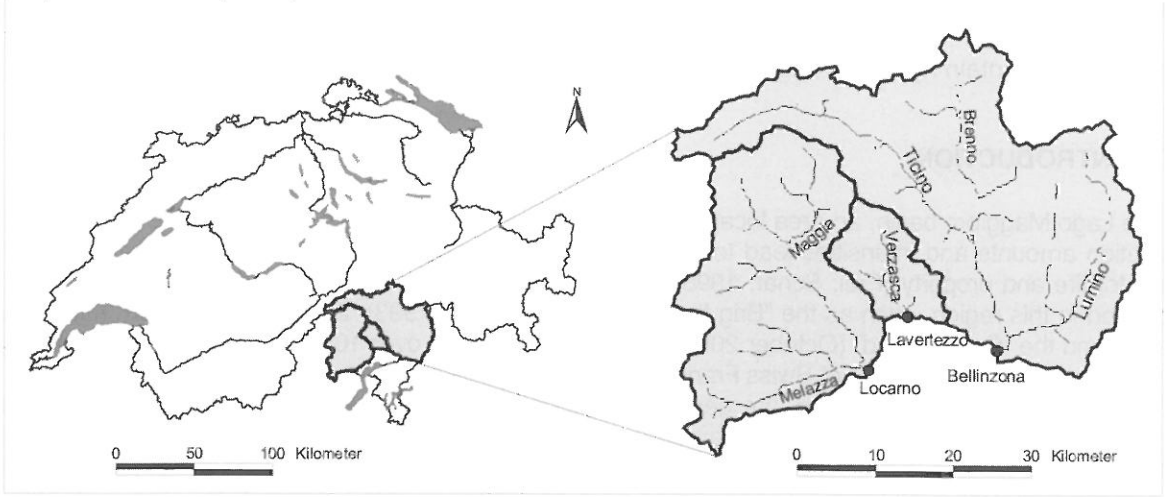

Figure 1-1: Ticino-Verzasca-Maggia basin showing the locations of the main river gauging stations.

The model experiments were carried out as one-way coupled simulations. For this purpose, atmospheric model outputs were directly taken as input for the hydrological model. The NWP models provided hourly time series of the following meteorological parameter fields: total precipitation, air temperature, wind speed, air humidity, and surface short wave total incoming radiation or net radiation.
In order to evaluate the efficiency and sensitivity of one-way coupled flood runoff simulations, some additional model experiments using "non-standard" NWP model outputs were investigated. The sensitivity analyses were focused on the following experiments:

- precipitation parameterization (SM, MESO-NH),
- increased vertical model resolution (SM),
- increased horizontal model resolutions (MC2, ALADIN, MESO-NH, BOLAM3),
- shifting of simulated precipitation patterns (SM),
- size of investigation area (SM, MC2),
- model initialization (SM).

2 STUDY AREA AND NUMERICAL MODELS

2.1 The Ticino-Verzasca-Maggia basin

The investigated basins of the rivers Ticino, Verzasca and Maggia cover a great part of the Swiss canton Ticino and draining from the north into the Lago Maggiore. Their total drainage area, which is controlled by river gauging stations, amounts to 2627 km^2. The area is subdivided as follows: Ticino basin up to the gauge Bellinzona 1515 km^2 (57.7 %), Maggia basin up to the gauge Locarno-Solduno 926 km^2 (35.3 %), and Verzasca basin up to the gauge Lavertezzo 186 km^2 (7 %).
The Ticino-Verzasca-Maggia basin is strongly determined by high mountain topography. The altitude ranges between 200 m and 3400 m a.s.l. and mean slopes amount to about 30°. Due to its particular location and orographic configuration in the overall alpine context, this basin is especially affected by exceptional precipitation amounts and intensities leading to relatively frequent flood events (Frei, Schär, 1998, Frei et al., 2001).

2.2 The high-resolution atmospheric models

It is not possible to explicitely discuss five different atmospheric models in this paper, hence a tabular model overview informs about some characteristic model features, such as individual time and mesh width strategies (Table 2-1).

Table 2-1: Nested NWP models in forecast mode. Listed are both the driving models providing the initial (INI) and lateral boundary (LB) conditions for the subsequent nesting stage and the final models. The "final" NWP models are characterized by the features "grid spacing" and "domain" including both the number of horizontal grid points (x-y) and the number of vertical levels (z).

NWP model	SM	MC2	Meso-NH	BOLAM	ALADIN
Driving model (INI & LB)	EM-ana [a] ~ 55 km every 6 hours	EM-ana (fc) [a] ~ 55 km every 6 (1) hs.	ECMWF [b] ~ 50 km every 6 hours	ECMWF [b] ~ 50 km every 6 hours	ARPEGE [c] ~ 50 km every 6 hours
Subsequent nesting stage (LB)	EM-fc [a] ~ 55 km every hour	SM ~ 14 km every hour	Meso-NH ~ 50 km every 3 hours	BOLAM ~ 35 km every 3 hours	ALADIN-L. [d] ~ 12 km every 3 hours
Final NWP model	SM ~ 14 km (145-145-20)	MC2 ~ 10 km (171-171-25)	Meso-NH ~ 10 km (100-100-45)	BOLAM ~ 10 km (130-120-36)	ALADIN-V. [d] ~ 10 km (133-117-31)
Operat. used?	Yes [e]	No	No	No	Yes
Further experimental configurations	40 z-levels, prec. param., model initializ.	~ 3 km (350-300-50)	~ 2 km (100-100-45)	~ 3.5 km (145-135-40)	~ 4 km (97-97-31)

[a] "Europa-Modell" of the German Weather Service (DWD) (ana: analysis mode, fc: forecast mode) (Majewski, 1991; DWD, 1995)
[b] global model system of the "European Centre for Medium-Range Weather Forecasts"
[c] global model system of the French climate community (Meteo-France): "Action de Recherche Petite Echelle Grande Echelle"
[d] ALADIN-LACE, ALADIN-VIENNA
[e] for the period 1994-2001

2.3 The hydrological model

The employed Water Flow and Balance Simulation Model (WaSiM-ETH) is a fully distributed catchment model using physically based algorithms for most of the process descriptions. For instance, the model uses a combination of an infiltration approach after Green and Ampt (1911) with estimation of saturation time after Peschke (1987), including the Richards equation (Richards, 1931, Philip, 1969) for the description of the soil water fluxes in layered soils.
Originally, WaSiM-ETH was designed for sensitivity studies regarding the effects of climatic changes on the water balance and runoff regime of pre-alpine and alpine river catchments (Grabs, 1997).

Various model applications covering catchment sizes from 3 km^2 to 145000 km^2 have demonstrated its capabilities in addressing different hydrological problems, such as the development of appropriate strategies for sustainable water management in arid and semi-arid regions (Schulla et al., 1999), the simulation of glacier melt and glacier runoff in partly and heavily glacierized high-alpine catchments (Klok et al., 2001), and the validation of runoff and its components in mountainous watersheds (Gurtz et al., 2002).
WaSiM-ETH can be employed for continuous as well as event-based simulations. Depending on the available input data and the type of hydrological situation, the model simulates the runoff regime of river catchments in virtually any spatial and temporal resolution. Since the quality and availability of model input data can vary strongly between river basins, WaSiM-ETH and most of its submodels offer various methods with different data requirements to calculate the requested outputs. The minimum amount of input data required to run the model are precipitation and temperature, as well as gridded information on soil properties, land-use and topography.

3 EXPERIMENTAL DESIGN

3.1 Calibration and validation of WaSiM-ETH

In order to calibrate and validate the hydrological catchment model WaSiM-ETH for the target area, extensive data of surface observations from 51 climatological and 12 hydrometric stations have been made available by MeteoSwiss and the Swiss National Hydrological and Geological Survey, respectively. Since the natural river flows in the catchments Ticino and Maggia are strongly affected by hydropower companies and river flow control structures, these impacts had additionally to be taken into account for the hydrological simulations. Unfortunately, only daily values of lake levels, lake volume changes, diverted water flows and redistributed inflows could be made available by the corresponding Swiss hydropower companies. Based on this data pool, continuous observation-driven runoff simulations were carried out in hourly time steps and in a horizontal grid resolution of 500 m x 500 m for the periods 1993 to 1996 (calibration period) and 1997 to 2000 (validation period), respectively. The analysis of the model results as achieved shows a generally good agreement between the observed and simulated runoff hydrographs, both in periods with low and in periods with high runoff dynamics. The calculated values for the catchment water balances as well corresponds to values and maps as given in the Hydrological Atlas of Switzerland (FOWG, 2001).

3.2 Coupling strategy

The atmospheric and hydrological models have been passively coupled without any feedback interactions. For this purpose, the atmospheric model provided its output data for the hydrological model with an updating interval of one hour. Both models used their own scheme of hydrological process description (Benoit et al., 2000).
The hydrological catchment model WaSiM-ETH generated the runoff simulations in the target area for each of the river basins Ticino, Verzasca and Maggia separately. In order to improve the basis of comparison between the model results as produced by the different experiments, the basin-specific output variables calculated by WaSiM-ETH were not separately analysed, but they were added up and accordingly assigned to the total Ticino-Verzasca-Maggia basin (2627 km^2). By means of this procedure, it was taken into account that a NWP model has an expected skill at horizontal wave lengths of about $4 \cdot \Delta x$, where Δx is the grid spacing. In case of a NWP model with Δx = 10 km, the area used for the validation of the passively coupled model runs should normally not be smaller than 1600 km^2.
Two different down-scaling techniques were selected which appeared to be of sufficient accuracy to spatially interpolate the meteorological variables onto the 500 m x 500 m grid of the hydrological model: A combined altitude-dependent and inverse distance weighting interpolation scheme was applied to interpolate the irregularly distributed surface observations, whereas the gridded parameter fields of the NWP models were down-scaled by using a bilinear interpolation technique.
It is worth noting that the parameter settings for WaSiM-ETH as derived from the model calibration and validation have not been changed for the coupled and uncoupled flood runoff simulations. The initial conditions for the last-mentioned model runs were always taken from the continuous observation-driven runoff simulations.

3.3 Observation data as validation tools

The quality of the simulation results can be evaluated by comparisons with observation data. According to the importance of precipitation for the generation of flood events, precipitation observations from surface stations and weather radar were compared with the results of NWP model simulations. These comparisons considered in particular the following precipitation characteristics: (1) spatial pattern, (2) temporal distribution, (3) intensity, and (4) amount. In addition to precipitation, runoff measurements at the outlets of the Ticino, Verzasca and Maggia river basins were used to validate the short-term model runs.
Radar-derived precipitation data: The Monte Lema radar, one of the operational Swiss weather radars, was used to provide high-resolution precipitation fields (cumulated rainfall over one hour, grid spacing 1 km x 1 km, differentiation of 15 rain rate levels) as input for the hydrological flood simulations in the investigated river basins. The doppler type radar is located on top of Monte Lema (1625 m a.s.l.) on the east side of Lago Maggiore and covers the nearby mountain region of Switzerland and Italy (Joss et al., 1998).

4 CASE STUDY EXAMPLES OF COUPLED FLOOD SIMULATIONS

In the following, some examples of flood forecast simulations are briefly presented and discussed. The examples reflect quite well the main features found in most of the model experiments. Hence, they can be assumed to be representative.

4.1 Piedmont flood episode (November 3-6, 1994)

Heavy precipitation occurred when a prefrontal low-level jet impinged upon the local orography and uplifted warm and moist air along the south Alpine slope. High-intensive rainfalls exceeding 200 mm/day could be recorded at several stations in the area around Lago Maggiore. Especially, in the region of Piedmont in northern Italy (located SW of Lago Maggiore), precipitation peaks of about 300 mm/day were recorded, e.g. 314 mm/day on the 5th of November 1994 at the Oropa rain-gauge station (Buzzi et al., 1998).
Figure 4-1 presents selected results of the „Piedmont" forecast experiments. The calculated graphs for average precipitation and corresponding runoff show a remarkable big spread over most of the time of the simulation. The BOLAM, MC2 and SM driven model runs produce similar results and achieve quite a good forecast of the main runoff peak. Even if the peak is predicted slightly too high and also a little late (time lag of about 2-6 hours), from the practical point of view, these flood forecast experiments can be rated as successful. However, evident deficiencies in the forecast occur during the first half of the episode, where the predicted totals of precipitation are too high.
Rather different from these model results are the results obtained by the Meso-NH forecast-driven model runs. Figure 4-1 reveals that the Meso-NH model produces much too little precipitation for the target area. Obviously, the location of the predicted precipitation centres was not accurate during the time before the runoff peak. This speculation is strongly supported by the spatial precipitation patterns presented in Figure 4-2. Due to underestimated precipitation amounts, the predicted Meso-NH runoff hydrograph shows a completely different shape as compared to the observed one and does not allow a successful flood prediction.
As expected, the radar-derived precipitation shows a better timing, but precipitation amounts are clearly underestimated for the time around the station-observed precipitation peak. Consequently, the predicted runoff peak is simulated too small. It is likely that the radar observations were affected by difficulties during the most important time of the episode.

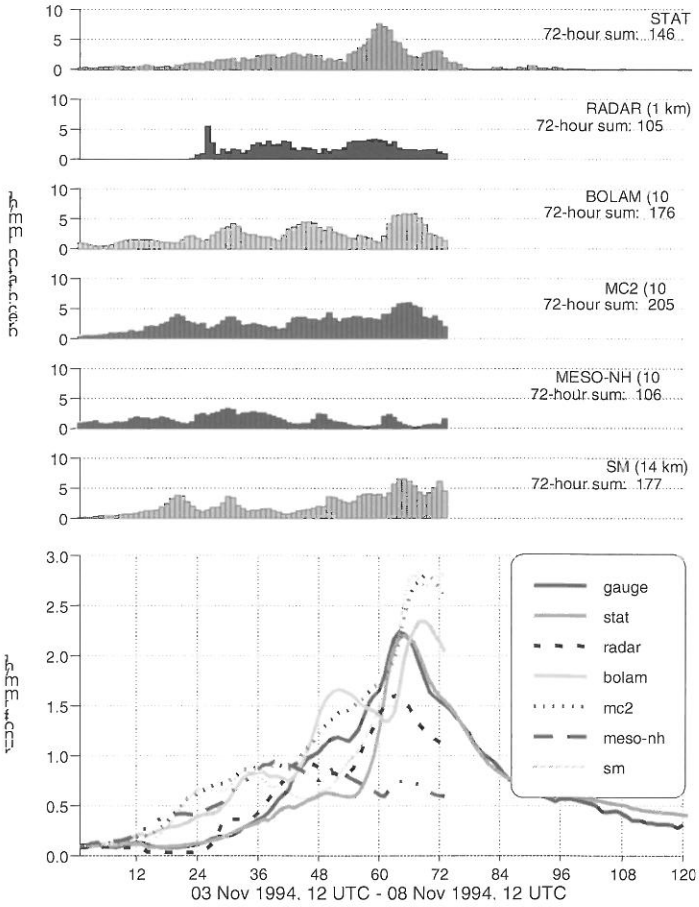

Figure 4-1: Piedmont flood episode. Area-averaged precipitation and resulting flood runoff for the Ticino-Verzasca-Maggia basin. Forecast mode.

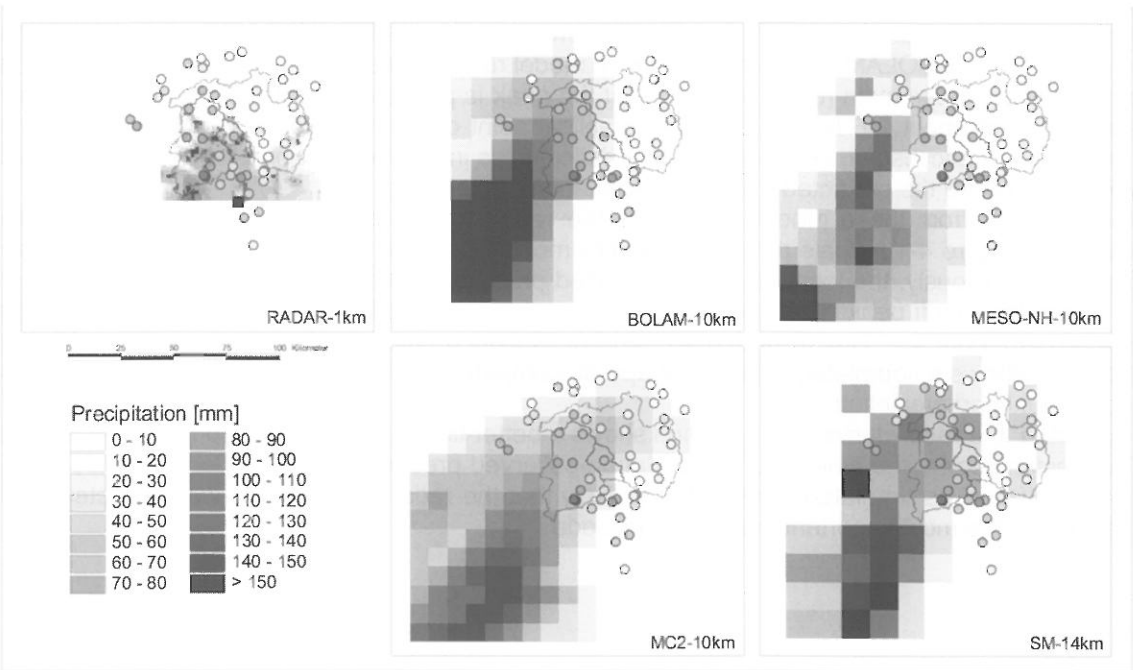

Figure 4-2: Spatial distribution of 12-hour precipitation totals of radar and forecasts (from 5 November 1994, 12 UTC to 6 November 1994, 00 UTC). Filled circles: 12-hour observations. Black symbol in radar panel: location of weather radar.

Figure 4-3 indicates that the spatial precipitation patterns are reflected quite well by all NWP models. The precipitation centres are mostly located in the Verzasca-Maggia area and approximately match the observations. Nevertheless, it becomes also obvious that the predicted precipitation patterns are too less structured.

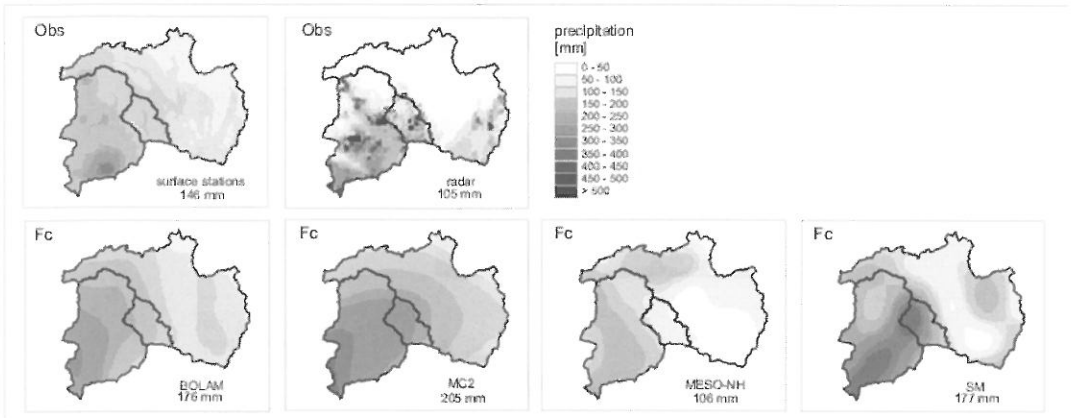

Figure 4-3: Piedmont flood episode. Comparison of 72-hour accumulated precipitation fields over the Ticino-Verzasca-Maggia basin (500 m x 500 m) resulting from downscaled precipitation observations (Obs) and simulations (forecast mode).

4.2 Geometric-ensemble SM forecasts

A sensitivity study with respect to the relative positioning of the simulated precipitation patterns was carried out for the Piedmont flood episode. For this purpose, the precipitation fields as predicted by the operational SM forecast were repeatedly shifted each time by one grid cell (14 km x 14 km) to north, east, south and west, respectively (Figure 4-4). The shifted patterns were then used as precipitation input for the WaSiM-ETH runoff simulations.
The results clearly indicate that the displacement of the precipitation patterns has considerable consequences on the development of flood runoff peaks in mesoscale areas like the Ticino-Verzasca-Maggia basin (Figure 4-5). North and east shifts lead to a slight increase in peak runoff of about 10%, whereas south and west shifts decrease precipitation amount and peak flow more clearly by about 30%. The general characteristics of the runoff hydrograph, however, remain the same for all cases of this experiment.

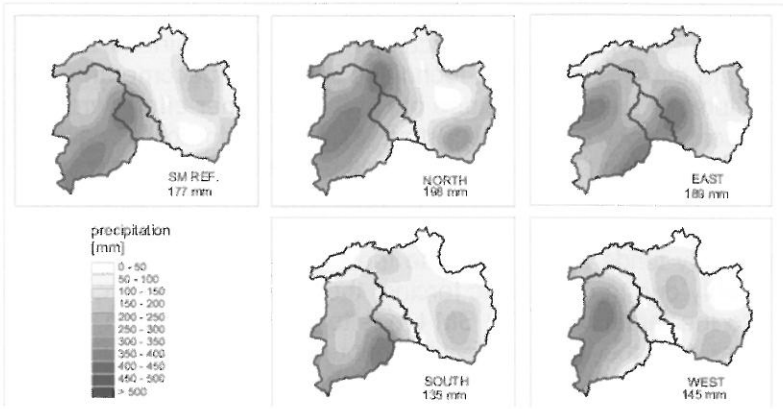

Figure 4-4: Piedmont flood episode. 72-hour precipitation sums of the SM ensemble forecasts for the Ticino-Verzasca-Maggia basin as spatially interpolated on the hydrological model grid.

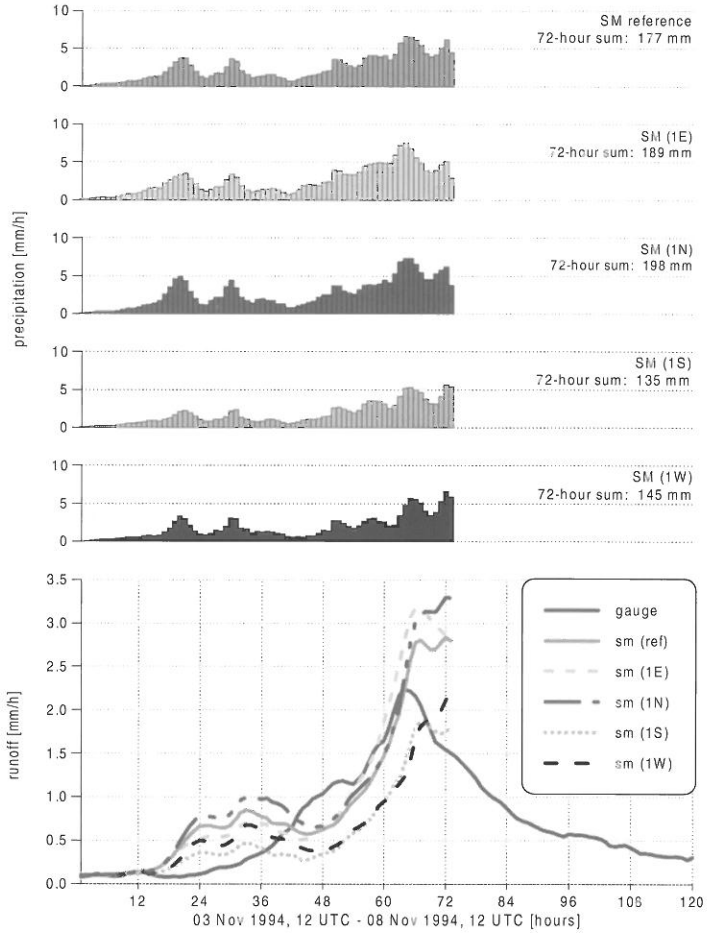

Figure 4-5: Piedmont flood episode. Area-averaged precipitation of geometric ensemble forecasts of the SM with repeated one grid cell shifts of the SM output to east (E), north (N), south (S), and west (W), and resulting flood runoff for the Ticino-Verzasca-Maggia basin.

5 DISCUSSION

One-way coupled atmospheric-hydrological flood runoff simulations have been carried out in complex mountain watersheds at the hydrological mesoscale. The results obtained from these experiments are encouraging and indicate that this modelling technique is likely to become an advanced flood forecasting tool in the near future. At the present stage of research, further efforts are necessary in particular towards an improved consistency of the forecasting results. The forecast quality sometimes considerably varies between selected flood episodes as well as between the different NWP models. The simulation results do not provide a clear indication whether any of the involved NWP models (standard mode) is definitely superior in predicting precipitation for the target area.
The SM forecast generally tends to overestimate the precipitation amount, especially with high precipitation peaks. Probably due to orographic forcing, these peaks often occur at one or at a few grid points. With respect to the target area, the SM tends to produce two such local precipitation centres ("grid point storms"), one over the Verzasca catchment and the other one over the eastern Ticino area. Nevertheless, the general positioning of the SM precipitation forecast is quite accurate in most of the investigated cases. Compared to the SM, the MESO-NH model apparently has more difficulties in correctly predicting precipitation patterns for the area of investigation. The BOLAM and MC2 model, which use a much more smoothed orography than the SM and MESO-NH model, produce quite similar precipitation forecasts with a tendency towards underestimating precipitation amounts.
In general, it is shown that the NWP models produce less intermittent precipitation sequences in comparison to the observed precipitation rates. They tend to simulate more "bulky" precipitation peaks which might be related to the precipitation parameterization schemes that are used in most of the considered NWP model configurations (convection process is parameterized and not explicitly resolved). This often leads to deviations in the simulated runoff hydrographs with respect to timing and amplitude in comparison to the measured runoff.

The experiments have revealed that precise quantitative precipitation forecasts are an absolute prerequisite to successful flood forecasting. This point becomes even more accentuated for alpine watersheds with their relatively short runoff response times on rainfall. The study results make clear that the NWP models must predict the precipitation as accurately as possible with respect to timing, intensity, amount, and spatial distribution. The results show that relatively small errors in rain storm tracks, in areal extent or in precipitation amounts can easily lead to large errors in the computed runoff hydrographs. In this context, the authors particularly refer to the results of sensitivity experiments (Jasper, 2001) and the inaccuracies introduced by downscaling of precipitation from NWP models. Moreover, it has to be recognised that successful flood forecasting in alpine and high-alpine watersheds is often closely linked to accurate predictions of the air temperature. Here minor deviations to reality can have strong effects on the snow/rain percentage of total precipitation and on snow melt during flood events. For the investigated flood episodes, a so-called "snowmelt-runoff-ratio" has been estimated to be between 2 % ("Brig event") and 40 % ("Gondo event") for the target area.
Like the coupled atmospheric-hydrological model experiments, the radar-driven flood runoff simulations show quite significant differences in quality from case to case which might be mainly caused by the extreme orographic situation in the target area. The investigated watersheds are located in very steep and rugged mountainous terrain which poses special difficulties to radar measurements (ground clutter, beam blockage, vertical reflectivity profile, etc.). The spatial structure of the radar-derived precipitation fields allows, of course, to indentify such problematic zones in the investigation area (Ticino catchment). Nevertheless, whenever possible, radar observations should be integrated into the process of flood forecast as a qualitative validation tool because of its comparatively great potential in describing the fine spatial and temporal structures of rainfall fields.
The simulation results of the passively coupled forecasting experiments illustrate that the future improvements mainly depend on the further development of the NWP models. Only if the atmospheric models can be significantly improved with regard to their process modelling at all scales of model nesting, especially during extreme storm periods, we could expect to produce more consistent and reliable flood runoff forecasts. However, the natural inherent limits to predictability of rainfall events should also be kept in mind. The weather is a chaotic dynamic system. Small differences in the initial conditions can lead to big differences in the predicted synoptic constellation. For this reason, it is evident that even a "perfect" high-resolution NWP model does not necessarily produce good precipitation forecasts, especially in high mountain terrain.

ACKNOWLEDGEMENTS

This study was part of the EU project RAPHAEL and funded by the Swiss Federal Office for Education and Science. The authors wish to thank the RAPHAEL colleagues for their data supply as well as for the fruitful and pleasant co-operation we had. We are much obliged to the Swiss water power companies (Tessin), the Swiss National Hydrological Survey and MeteoSwiss for their allowance to use recorded data.

REFERENCES

Bacchi, B., Ranzi, R., eds. (2000): The RAPHAEL Project. Final Report. EC, Directorate General XII, Programme Environment and Climate 1994-1998. Contract no ENV4-CT97-0552, Brussels.

Benoit, R. et al. (1997): A semi-Lagrangian, semi-implicit wide-band atmospheric model suited for finescale process studies and simulation. Mon. Wea. Rev. 125: 2382-2415.

Benoit, R. et al. (2000): Towards the use of coupled atmospheric and hydrologic models at regional scale. Mon. Wea. Rev. 128: 1681-1706.

Binder, P., Schär, C., eds. (1996): The Mesoscale Alpine Programme MAP: Design Proposal. 2nd Ed., pp. 77. [Available from MAP Programme Office, c/o MeteoSwiss, CH-8044 Zürich].

Bougeault, P. et al. (1998): The Mesoscale Alpine Programme MAP: Science Plan. [Available from MAP Programme Office, c/o MeteoSwiss, CH-8044 Zürich].

Bougeault, P. et al. (2001): The MAP Special Observing Period. Bull. Amer. Met. Soc. 82: 433-462.

Bubnovà, R. et al. (1995): Integration of the fully elastic equations cast in the hydrostatic pressure terrain-following coordinate in the framework of the ARPEGE / Aladin NWP system. Mon. Wea. Rev. 123: 515-535.

Buzzi, A. et al. (1994): Validation of a Limited Area Model in Cases of Mediterranean Cyclogenesis: Surface fields and Precipitation Score. Meteorol. Atmos. Phys. 53: 137-153.

Buzzi, A., Malguzzi, P. (1997): The Bolam III model: Recent improvements and results. MAP Newsletter 7: 98-99.

Buzzi, A. et al. (1998): Numerical simulation of the 1994 Piedmont flood: Role of orography and moist processes: Mon. Wea. Rev. 126: 2369-2383.

DWD (1995): Documentation of the EM-DM-System. Technical Report, Deutscher Wetterdienst, Research Department, Zentralamt, D-63004 Offenbach am Main.

Frei, C., Schär, C. (1998): A precipitation climatology of the Alps from high-resolution rain-gauge observations. Int. J. Climatol. 18: 873-900.

Frei, C. et al. (2001): Climate dynamics and extreme precipitation and flood events in Central Europe. Integrated Assessment, 1, 281-299.

FOWG (2001): Hydrological Atlas of Switzerland. Federal Office for Water and Geology, Swiss Hydrological Survey, Bern, Switzerland.

Grabs, W., ed. (1997): Impact of climate change on hydrological regimes and water resources management in the Rhine basin. CHR-Report I-16, International Commission for the Hydrology of Rhine Basin (CHR), Lelystad, 172 pp.

Grebner, D. et al. (2000): Charakteristik des Hochwassers vom 9. bis 16. Oktober 2000 auf der Alpensüdseite und im Wallis. In: "Wasser, energie, luft – eau, ènergie, air", 92. Jg, Heft 11/12: 369-377.

Green, W.H., Ampt, G.A. (1911): Studies of soil physics. Part 1. The flow of air and water through soils. Journal of the Agricultural Society 4: 1-24.

Gurtz, J. et al. (2002): A comparative study in modelling runoff and its components in two mountainous catchments. Hydrol. Processes (in press).

Jasper, K. (2001): Hydrological modelling of Alpine river catchments using output variables from atmospheric models. Diss. ETH No. 14385, Zürich.

Joss, J. et al. (1998): Operational use of radar for precipitation measurements in Switzerland. In NRP 31: Climate Change and Natural Disasters. ETH Zürich.

Kleinschroth, S. (2001): Überschwemmungen und Erdrutsche in Norditalien und in der Südschweiz. In: Exposure – Property & Engineering, No. 5, GE Frankona Rückversicherungs-AG.

Klok, E.J. et al. (2001): Distributed hydrological modelling of a glaciated Alpine river basin. Hydrol. Sciences Journal, 46 (4), 553-570.

Lafore, J.P. et al. (1998): The Meso-NH atmospheric simulation system. Part I: Adiabatic formulation and control simulations. Ann. Geophys. 16: 90-109.

Laprise, R. (1995): The formulation of André Robert`s MC2 (Mesoscale Compressible Community) model. Atmos.-Ocean 35: 195-200.

Majewski, D. (1991): The Europa Modell of the Deutscher Wetterdienst. Proc. ECMWF Seminar on numerical methods in atmospheric models, Vol. II, September 1991, 147-191.

Peschke, G. (1987): Soil Moisture and Runoff Components from a Physically Founded Approach. Acta hydrophysica 31 (3/4): 191-205.

Petrascheck, A. (1996): Hochwasserschutz in der Schweiz: Probleme, Anforderungen, Massnahmen. Zeitschrift für Kulturtechnik und Landesentwicklung 37 (5): 134-137.

Philip, J.R. (1969): The theory of infiltration. In: Advances in Hydrosciences. Ed. by Ven Te Chow, Academic Press, New York, 216-296.

Richards, L.A. (1931): Capillary conduction of liquids through porous mediums. Physics 1: 318-333.

Schulla, J. (1997): Hydrologische Modellierung von Flussgebieten zur Abschätzung der Folgen von Klimaänderungen. Zürcher Geographische Schriften, Heft 69, ETH Zürich, 187 pp.

Schulla, J. et al. (1999): Sustainable agriculture and water management in semi arid regions. 2nd Inter-Regional Conference on Environment-Water, September 1-3, 1999, Lausanne.

Stein, J. et al. (2000): High-resolution non-hydrostatic simulations of flash-flood episodes with grid-nesting and ice-phase parameterization. Meteorol. Atmos. Physics 72: 203-222.

Tanguay, M. et al. (1990): A semi-implicit semi-Lagrangian fully compressible regional forecast model. Mon. Wea. Rev. 118: 1970-1980.

FLOOD ESTIMATION BUENZ VALLEY, SWITZERLAND PRACTICAL USE OF RAINFALL-RUNOFF MODELS

Donat Job, Max Humbel, Dieter Müller and Jacques Sagna

Colenco Power Engineering Ltd., Mellingerstrasse 207, CH-5405 Baden, info@colenco.ch

SUMMARY

Between 1994 and 2000 Colenco Power Engineering Ltd. completed various flood studies for the Bünz Valley in the Canton Argovia, Switzerland. During the past decade several extreme floods occurred, leading to major damage at different key locations. The planning of various flood protection measures and their realisation in the Bünz Valley is currently entering the final stage. Therefore, the State Department has decided to enhance evaluations made for flood assessment prior to the completion of the flood protection works.
Within a general hydrologic, hydraulic and environmental assessment of the whole valley the main issues to be discussed here are the elaboration of flood hydrographs with various return periods at different key locations along the Bünz River and its tributaries. Furthermore, the performance of two planned flood retention basins, "Drachtenloch", final design stage, and "Nidermoos", feasibility phase, was evaluated.
To address the above issues, a rainfall-runoff model was established by using the U.S. Army Corps of Engineer's Hydrologic Modelling System (HEC1/HMS). For model calibration and validation, the flood events of 1987, 1991 and 1999 were used. Thereby, the flood occurring in 1999, was of particular importance. Since at that time the discharge of the Bünz River and its tributaries was measured at 6 key locations, a sound data basis for model calibration was available.
In addition to the HEC model, the new software Faitou, recently developed at the Laboratory of Hydraulic Constructions of the Swiss Federal Institute of Technology in Lausanne, was also applied to a portion of the watershed. In this model, flood generation is based on the 2D kinematic wave equations over the watershed topography, coupled with a hydrodynamic modelling of the river network.

Keywords: Practical Use of Rainfall-runoff Models for Flood Discharge Assessment, Model Calibration

1 INTRODUCTION

The Bünz valley is located in the Canton Argovia in the Midlands of Switzerland. After the confluence of the two creeks Rüeribach and Aspibach south of the village of Muri, the main river Bünz flows some 25 km in northern direction to join the Aabach just upstream of its confluence with the Aare River. On its western side, the Bünz valley is separated from the Seetal valley by the Lindenberg, whereas on the eastern side, a low ridge of moraines separates it from the Reuss valley. The watershed of the Bünz comprises a total area of some 123 km^2 at its confluence with the Aabach at Wildegg.
At the beginning of the 19^{th} century large portions of the swampy Bünz valley were canalised and drained. The main goal at that time was the amelioration of the agricultural land. At the same time, a mitigation of the flood situation of the frequently inundated valley could be achieved.
Since then, land use by agriculture, settlement and industries were intensified. At the same time, flood protection requirements became more urgent. Frequent inundation at bottlenecks along the river course called for protection measures. In the seventies, a number of larger and smaller measures were studied and partly implemented. The most prominent example was the construction of the Greuel flood retention basin upstream of the town of Muri in the early eighties, which was designed by Colenco and proved to be successful (Meier, Roggwiller, 1985; Roggwiller, 1985).
In the course of the past decade, environmental and ecological aspects became increasingly integrated in the realisation of flood protection works. Within this context, Colenco, commissioned by the State Department of Construction, has conducted extensive studies for the Bünz Valley between 1994 and 2000 (Colenco, 1994; 2000). The motive of the studies was primarily given by the occurrence of several extreme floods in 1994, 1995 and 1999, leading to major hazards at different key locations.
The main issues of the latest stage of the hydrology studies comprised an examination of flood hydrographs with various return periods at 8 different key locations along the Bünz River and its tributaries and the evaluation of design flows relating to the current flood protection works in the villages of

Othmarsingen and Möriken. Furthermore, the performance of two planned flood retention basins, "Drachtenloch", final design stage, and "Nidermoos", feasibility phase, was evaluated.
To address the above issues, a rainfall-runoff model was established with by using the U.S. Army Corps of Engineer's Hydrologic Modeling System (HEC1/HMS) (US Army Corps of Engineers, 1981; 2000). In addition to the HEC model, the new software Faitou, developed recently at the Laboratory of Hydraulic Constructions of the Swiss Federal Institute of Technology in Lausanne (Dubois et al., 2001), was also applied to a portion of the watershed.
In the following, this contribution presents the results of the study. Emphasis is put on the modelling procedure.

2 HYDROLOGIC CHARACTERISTICS OF THE CATCHMENT AREA

2.1 Main Characteristics

The highest elevation of the drainage area is the above mentioned Lindenberg with around 880 m a s l. whereas the lowest altitude at the confluence of the Bünz with the Aabach amounts to 350 m a s l. According to these conditions, even the highest areas are not covered permanently by snow during winter. Consequently, snow-melt is only playing a minor role for discharge formation. All the major tributaries of the Bünz origin from the western hill slopes (Figure 2-1).

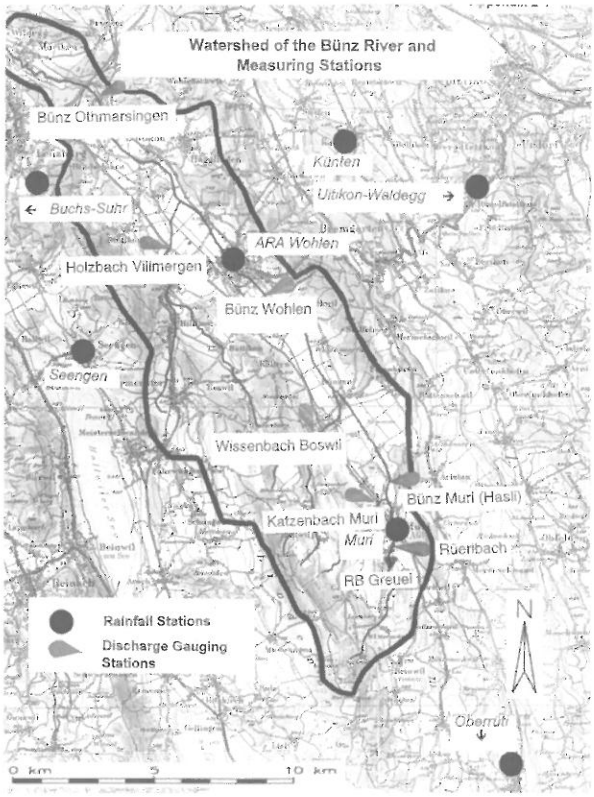

Figure 2-1: Watershed of the Buenz River. Rainfall and discharge gauging stations

Both sides of the valley are only gently sloped. They are covered either with forest or used for agriculture. The valley bottom is characterised by amelioration works. Therefore, the Bünz is mainly kept in a straight course with a trapezoidal cross section from Muri up to the river mouth at Wildegg. The agricultural areas are largely drained with the Bünz as the receiving water.
The long-term precipitation lies between 1000 and 1200 mm/y. Such values are typical for the Midlands of Switzerland along the Aare River. The mean specific discharge in the Bünz and its tributaries varies between 12 and 17 l/s/km^2, again typical values for such regions. The mean annual run-off coefficient is about 0.5.

2.2 Rainfall Data

One of the first steps in the modelling process involved the evaluation of rainfall data in view of model calibration. Thereby, hourly precipitation data at 6 nearby locations were collected. These stations are operated by the federal and local government.
The flood event occurring in May 1999 was of particular importance. An extremely heavy rain yielded the highest monthly total in the lower Bünz valley since 1901. At Buchs-Suhr, on May 12 1999, 115 l/m^2 were recorded within 24 hours. The return period of such intensities correspond to about a 100 year event. Furthermore, this rainfall followed a wet and rainy April. As a consequence of an already soaked soil left, distinct discharge peaks in the Bünz occurred immediately after each heavy pour of rain.

2.3 Discharge Data

The discharge of the Bünz River and its tributaries is measured at 6 gauging stations, operated by the local government. These are: Katzenbach at Muri (4.5 km^2), Bünz at Muri (14.8 km^2), Wissenbach at Boswil (11.7 km^2), Bünz at Wohlen (53.1 km^2), Holzbach at Villmergen (23.6 km^2) and Bünz at Othmarsingen (110.6 km^2). Since at all these stations data were available for the investigated flood events, a sound basis for model calibration was at disposition.
As can be expected, the heavy rainstorm on May 1999 resulted in corresponding large floods with an unusual long duration (around 2 days). In Othmarsingen, for example, a flood peak of 69.1 m^3/s was measured. It was the highest discharge ever recorded since the gauging station was installed in 1957. The flood in May 1999 was about a 100 year event, as it is the case with the related rainfall.

3 THE RAINFALL – RUNOFF MODEL HEC1/HMS

3.1 General

As pointed out in Section 2.3, a dense monitoring network is operational in the watershed. However, long term data were available only for one gauging station (Othmarsingen, 1957). All others stations became operational after 1980. As a consequence, such data do not allow for a reliable determination of floods with larger return periods (50 years, 100 years) on a purely statistical basis. This fact was one of the reasons, why a rainfall runoff model was developed.
Furthermore, a hydrologic model has the advantage to allow for the determination of flood hydrographs at any desired location according to the project needs. The final objective of the project was the elaboration of flood protection measures. For instance, the application of a model offers an efficient way of investigating the behaviour of flood retention basins.
Basically, the modelling procedure involved the following steps: First, estimated values for the hydrologic characteristics were applied to the mathematical model. An important second step was the model calibration, where an optimum set of model parameters is sought based on different measured flood events (known discharge and rainfall data, preferably at different locations representing different hydrologic conditions). A third step in this case involved the elaboration of hypothetical design storms and their model application in order to investigate different alternatives.

3.2 Choice of the Model

Watershed runoff processes are complex and comprise an important part in the field of engineering hydrology. Today, a large variety of mathematical models exist to simulate these processes with various degree of complexity. Rainfall runoff models are used for different purposes. On one hand, for example, there are continuous models, simulating a longer period and predicting watershed response both during and between precipitation events. On the other hand, an event model simulates a single storm only, where the duration of the storm may range from a few hours to a few days. For the Bünz study, the application of the latter class of models was appropriate.
For such reasons, the HEC1/HMS model was chosen. An advantage of this easy-to-use model is the fact that it can be applied with a relatively low effort, according to the needs of a project. Furthermore, this package, being updated continuously by the USCE, is used and verified world-wide by many users.

3.3 Model Description

The HEC model is designed to simulate the surface runoff response of a river basin to precipitation by representing the basin as an interconnected system of hydrologic and hydraulic components. A component may represent a surface runoff entity, a stream channel, or a reservoir. The representation of a component requires a set of parameters which specify the particular characteristics of the component and mathematical relations which describe the physical processes. The result of the modelling process is the computation of flow hydrographs at desired locations in the river basin.
The experience gained in the Bünz study showed that the computation of the runoff volumes is clearly the crucial step in the modelling process. The program package offers a variety of loss models to calculate the complexity of land surface interception, depression storage and infiltration processes. In the present study it was found that the exponential loss rate model gave the best calibration results. This is an empirical method which relates loss rate to rainfall intensity and accumulated losses, which are representative of the soil moisture storage.

4 MODEL CALIBRATION

4.1 Purpose

The application of rainfall-runoff models require a number of parameters which characterise the watershed. As a first step, the value of each parameter was estimated on experience records and hydraulic /hydrologic formulae to use the model for estimating runoff and routing hydrographs. However, in order to enhance the reliability of model results, a more exact determination of most of the parameters was necessary. This was achieved by calibration.
As described in Section 2, for several flood events quite a number of stream flow and rainfall data were available (1987, 1991, 1994, 1995, 1999). In the calibration procedure, this hydro-meteorological information was used in a systematic search for parameters which yield the best fit of the computed results to the corresponding observed runoff. Thereby, individual sub-areas were first considered separately and joined afterwards. The calibration process comprised the most laborious step of this hydrologic study.

4.2 Model Parameters

As mentioned in Section 3.3, the set-up of the model consists of a network of model components. The Bünz model consists of 10 runoff entities, 5 stream channels, and 1 existing reservoir (Figure 4-1). Thereby, most of the model parameters are associated with a runoff component. The runoff component basically involves three models. These are the loss model, direct runoff model and the base flow model.
Besides the known areas of the 10 sub-watersheds, the loss models contains 4 parameters to describe the exponential loss and an initial value of the loss rate, taking into account the soil moisture content at the beginning of the flood event. These parameters were all subject to calibration.
The direct runoff model simulates the direct runoff of excess precipitation on a watershed. For the Bünz study, the traditional unit hydrograph method was used. Thereby, the SCS UH model was selected. The SCS UH is a dimensionless unit hydrograph, described by only one parameter T_P, the time to UH peak.
The base-flow was simulated with the exponential recession model. The parameters of this model include the initial flow, the recession ratio and the threshold flow, where the recession constant was calibrated.
The 5 stream channel components in the Bünz model involve a routing model which computes a downstream hydrograph, given an upstream hydrograph as a boundary condition. In this case, the Muskingum method was used.

4.3 Measured Data

For calibration purpose, the modelling of the flood event of May 1999 was considered to be the most appropriate. Thereby, the whole flood duration from May 11, 12:00 to May 14, 00:00, comprising 60 hours, was taken into account. Of crucial importance was the selection of the decisive rainfall stations or, in other words, the assignment of reasonable weights according to their influence on different parts of the watershed. The weights were selected in order to allow for a realistic consideration of the temporal and local sequence of the rainfall event in the watershed.

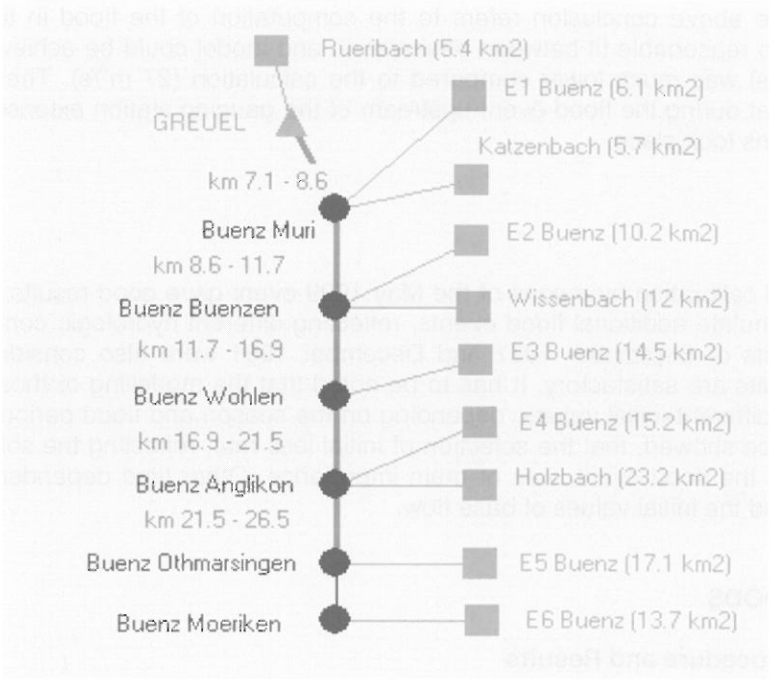

Figure 4-1: Hydrologic model of the Buenz River. HMS element network.

4.4 Calibration Results

Generally, the parameter optimisation resulted in a very good agreement between observation and simulation at 5 of the 6 available discharge gauging stations (Figure 4-2). This statement is valid not only for the peak values, but also for the volumes and the shape of the hydrographs. For example, in the upper part of the watershed, the flood hydrograph of May 1999 is characterised by 3 distinct flood peaks. They were all calculated more or less correctly. Furthermore, the temporal evolution of the water levels in the flood retention basin Greuel could also be reproduced. Consequently, it is concluded that the response of the watershed to the rainfall process was modelled essentially in a satisfactory way.

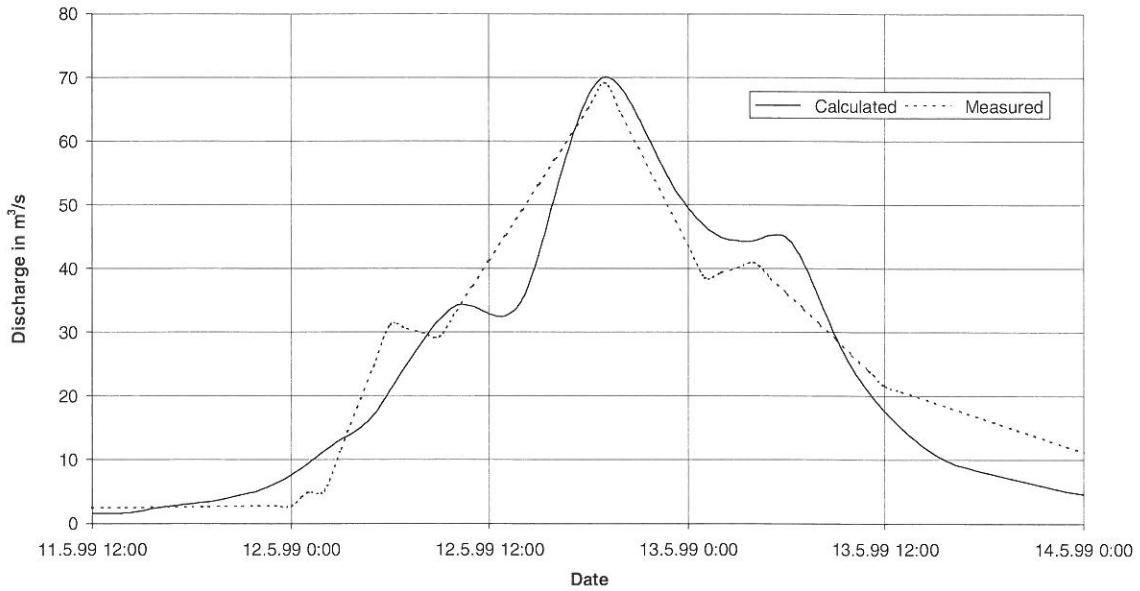

Figure 4-2: Flood event May 1999 at Othmarsingen. Measurement and calculation.

An exception to the above conclusion refers to the computation of the flood in the tributary of the Holzbach, where no reasonable fit between observation and model could be achieved: The observed flood peak (10 m^3/s) was much lower compared to the calculation (27 m^3/s). The reason for this is found in the fact that during the flood event upstream of the gauging station extensive inundation due to capacity limitations took place.

4.5 Validation

Although the model calibration by means of the May 1999 event gave good results, it was considered as necessary to simulate additional flood events, reflecting different hydrologic conditions. Therefore, the two flood events of September 1987 and December 1991 were also considered for validation purposes. The results are satisfactory. It has to be noted that the modelling of those events involved the introduction of different initial values, depending on the season and flood period respectively. The validation experience showed, that the selection of initial loss rate, reflecting the soil moisture content at the beginning of the flood event, was of main importance. Other time dependent values of minor significance included the initial values of base flow.

5 DESIGN FLOODS

5.1 Modelling Procedure and Results

A main task of the Bünz study comprised the determination of design floods with a return period of 10, 50 and 100 years respectively at different locations. For these calculations, corresponding rainfall events were required. Thereby it is common practice to assume that a rainfall with a certain return period leads to a corresponding flood event with the same probability of occurrence. The measured rainfall and discharges during the flood event of May 1999 demonstrate that this assumption applied very reasonably to the Bünz study. The selection of the design storm was based on the following:
Duration of rainfall: Basically, a rainfall event leads to the highest flows, if its duration corresponds to about the concentration time of the considered watershed area. At Othmarsingen (110 km^2), for example, an analysis of measured rainfall and flow data led to a concentration time between 5 and 6 hours. The decisive rainfall duration was also optimised with the model, where a result of 5 hours was obtained. This indicates that the model parameters were selected reasonably.
Size of watershed: At a rainfall station, point precipitation is measured. For the determination of the areal precipitation depth, reduction factors were introduced in the model. Thereby, the depth-area curves of Grebner and Richter, 1990 were applied. At Othmarsingen (110 km^2), for example a reduction factor of around 20% was selected. At other locations these factors were chosen accordingly.
Decisive rainfall station: In Switzerland, for many rainfall stations intensity-duration-frequency relationships are available (Zeller et al., 1976). For the Bünz study, the values at the three stations Muri, Buchs-Suhr and Seengen were used.
Rainfall distribution: For all computations a rainfall of constant intensity was assumed. Since heavy rain storms often occur within longer wet periods, for all simulations a base rain of some minor magnitude was inserted at the beginning and at the end of the actual event.
Figure 5-1 shows the computed hydrographs at Othmarsingen. In view of the flood protection measures in this town, the 100 year flood (70 m^3/s) was selected as the design flood.

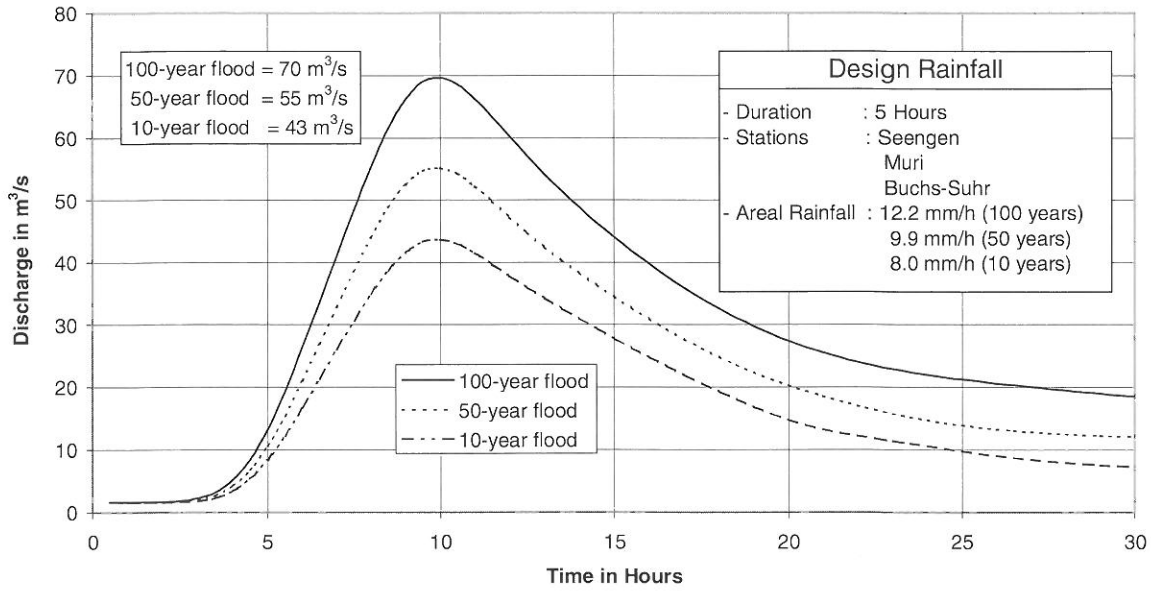

Figure 5-1: Flood simulation at Othmarsingen. Return periods of 10, 50 and 100 years respectively.

5.2 Comparison with Frequency Analysis

As mentioned in Section 2.2, the discharge in Othmarsingen has been measured continuously since 1957. Since instantaneous peak values were available, it was therefore obvious to determine flood peaks of various return periods additionally with the aid of a frequency analysis. The outcome for the 100 year flood was 72 m^3/s, which compares very well to the 70 m^3/s obtained with the rainfall runoff model. A similar good agreement was achieved for the 10 and 50 year flood peaks respectively. This result further indicates that the model parameters and the initial conditions were selected on a sound basis.

6 FLOOD PROTECTION MEASURES

6.1 Possibilities

In view of flood protection measures in the Bünz valley, additional studies were completed by Colenco since 1994. An outcome of these investigations included the identification of various endangered areas and propositions of appropriate protection measures. These were: capacity improvement works, flood plain retention, diversion tunnel, inundation ponds and flood retention basins.

6.2 Flood Retention Basins Drachtenloch and Nidermoos

Besides capacity improvement works, which are currently being completed at Othmarsingen, the latest protection measures at present include the flood retention basin "Drachtenloch" at Villmergen and the inundation pond "Nidermoos" near the village of Bünzen. The former, final design stage, is designed to protect the village of Villmergen whereas the latter, feasibility phase, serves as a retention basin combined with the release of controlled downstream discharges into the Bünz River. The efficiency of both projects and also their combination was optimised with the rainfall runoff model.
The flood retention basin "Drachtenloch" reduces the floods in the tributary Hinterbach (8.8 km^2). Since its volume is merely 150'000 m^3, it is considered to be only a local measure. The simulations confirmed the presumption that the basin has only little effect on the present protection works in Othmarsingen further downstream.
The effect of the inundation pond "Nidermoos" at the Bünz River (39.3 km^2) is studied by Colenco since 1996. It is considered as an alternative to various other measures. Since the establishment of this pond would offer a retention volume of several million cubic meters, floods of any size may be reduced to a limited downstream discharge. Thus, a considerable effect on the downstream villages can be achieved.

7 APPLICATION OF RAINFALL-RUNOFF MODEL FAITOU

7.1 Model Description

The model Faitou (Dubois et al., 2001) belongs to the physically based and spatially distributed category. The net rain runoff transfer is modelled by solving the 2D kinematic wave equation over the watershed topography with the finite volume method. The computation of surface runoff is coupled with a 1D hydrodynamic modelling of the river network in the watershed.
The determination of the watershed limits, the mesh of finite volumes and the river network are automatically generated from a digital elevation model (DEM). The main model parameters for the hydraulic computations include the surface roughness coefficients related to a new head loss law developed at the Federal Institute of Technology in Lausanne (Dubois et al., 2001).
Precipitation losses as a function of cumulative precipitation, soil cover, land use and antecedent moisture is calculated with the SCS curve number model.

7.2 Example Application to the watershed of the Holzbach

In view of the design of the flood retention basin Drachtenloch, Faitou was applied to the sub-watershed area of the tributary Holzbach (23.6 km^2). The application of this new mathematical model allowed a comparison with the corresponding HEC1/HMS simulations.
The DEM, was used with a resolution of 100 by 100 meters. The pre-processing involved the establishment of the watershed contour and the localisation of the hydro-graphical network based on the DEM. This automatic step for the generation of the watershed yielded a very good result.
Since at the outlet of the watershed at the village of Villmergen a discharge gauging station is located, an opportunity of model calibration was offered. Thereby, the flood event of February 1999 was used. The calibrated parameters included the roughness coefficients and the SCS curve number. The calibration result was very satisfactory in terms of peak value and volume. However, the study showed that it was difficult to adequately model the shape of the hydrograph, characterised by three distinct flood peaks. This is partly attributed to the fact that storage effects are not taken into account in the model.
Faitou was also applied to the flood event of May 1999. In addition, the 10, 50 and 100 year floods were simulated. The results are comparable with the HEC1/HMS simulations.
Experience showed that, besides calibration, a laborious step in the modelling procedure involved the grid optimisation of the supplied DEM. The reason for this lies partly in the fact that the model is rather designed for steep river basins (Dubois et al., 2001).

8 CONCLUSIONS

Main flood protection measures in the Bünz valley include the realisation and the planning of flood retention basins where besides peak flood values also the volume of the design hydrographs were required. The use of a rainfall runoff model offered an efficient way to address this issue. Furthermore, a hydrologic model has the advantage to allow for the determination of hydrographs at any desired location. Thus, with the same model, various present and future project alternatives can be studied.
The choice of the HEC1/HMS package was reasonable. The model is verified and applied world-wide by many users and it is updated continuously by the USCE. Since model calibration involves many computer runs, the little CPU time needed is also of great advantage.
The calibration was the most important and laborious step for the establishment of the Bünz model. If data are available, calibration is a must, since, of course, the quality of the simulations depends almost entirely on the quality of the model parameters.
The parameter optimisation resulted in a good agreement between observation and simulation at five of six discharge gauging stations. This statement is valid for the peak values, volumes and the shape of the hydrographs.
Regardless of the good calibration result, it has to be kept in mind that the real-world complexity of the rainfall runoff processes can be simulated only to a limited extent.

REFERENCES

Colenco Power Engineering Ltd. (1994): Gewässerstudie Bünztal, Hydrologie/Hydraulik. Baden

Colenco Power Engineering Ltd. (2000): Hochwasseranalyse Bünztal. Baden

Dubois, J. et al. (2001): Physically based and spatially distributed forecasting of extreme floods. Laboratory of Hydraulic Constructions, LCH, Swiss Federal Institute of Technology. Lausanne

Grebner, D., Richter, K.G. (1990): Gebietsniederschlag; Abschlussbericht. Flächen-Mengen-Dauer-Beziehungen für Starkniederschläge in der Schweiz. Zürich

Meier, H., Roggwiller, B. (1985): Hochwasserrückhaltebecken „Greuel", Muri, Wasser Energie Luft, Heft 3 /4, 1985. Baden

Roggwiller, B. (1985): Hochwasserrückhaltebecken Greuel bei Muri bewährt sich, Wasser Energie Luft, Heft 10, 1988. Baden

US Army Corps of Engineers (1981): HEC-1, Flood Hydrograph Package. Hydrologic Engineering Center. Davis, CA, USA

US Army Corps of Engineers (2001): Hydrologic Modeling System. Hydrologic Engineering Center. Davis, CA, USA

Zeller, J. et al. (1976): Starkniederschläge des schweizerischen Alpen- und Alpenrandgebietes. Eidg. Anstalt für das forstliche Versuchswesen. Birmensdorf

PRACTICAL APPLICABILITY OF REGIONAL METHODS FOR DESIGN FLOOD COMPUTATION IN SLOVAKIA

Silvia Kohnová, Ján Szolgay

Department of Land and Water Resources Management, Faculty of Civil Engineering, Slovak University of Technology, Radlinského 11, 813 68 Bratislava, Slovak Republic
kohnova@svf.stuba.sk, szolgay@svf.stuba.sk

SUMMARY

Regional empirical flood formulae based on the relationship between flood quantiles and physiographic catchment characteristics have usually been considered a safe solution for design discharge computation in ungauged basins for river engineering works and dam design in Slovakia. However they are not generally applicable to hydroecological design problems (e.g., restoration of rivers, wetland management etc.) since they were usually derived as envelope curves. In the study a different regional approach based on the Hosking and Wallis methodology was applied using annual maximum summer flood data from 251 basins in Slovakia. Several physiographic catchment characteristics were used to pool catchments into homogeneous pooling groups by cluster analysis. Regional flood frequency distributions were derived for the annual maximum summer floods using L moment statistics. Regional formula for the computation of the summer index flood was derived by multiple regression methods. A comparison of flood quantiles computed by the Hosking and Wallis regional approach was performed in selected homogenous pooling group with statistical reference values and values derived using traditional envelope curve approaches. The applicability of the compared methods for design purposes was discussed.

Keywords: Regional flood frequency analysis, summer floods, L-moments, flood formula

1 INTRODUCTION

The recent extreme floods in Central Europe have resulted in scientific and societal concerns about flood risks and the reliability of flood frequency estimates in Slovakia. As a consequence, the currently used flood frequency estimation methods are being re-evaluated. The design discharge calculation in small and medium-sized ungauged catchments had mainly been based on empirical regional flood formulae. Other methods, such as the rational method, the unit hydrograph analysis, the SCS model and other mathematical models were far less employed (e.g. Miklanek et al., 2000; Svoboda et al., 2000). Here, results achieved by the application of the Hosking and Wallis methodology (Hosking and Wallis, 1997), together with the index flood method using annual maximum summer flood data from 251 basins in Slovakia, are compared with the performance of traditional empirical approaches. The applicability of the tested methods for various hydraulic and hydro-ecological design tasks is also discussed.

2 DESIGN FLOOD COMPUTATION METHODS IN SLOVAKIA

Empirical regional methods in Slovakia are traditionally based on the computation of 100-year flood from the catchment size in subjectively delineated geographically continuous regions, which are considered to be homogeneous with respect to the flood regime:

$$q_{100} = \frac{A}{(F+1)^n}.(1+\sum_i o_i) \quad (1)$$

where q_{100} is the 100-year maximum specific discharge [$m^3 \cdot s^{-1} \cdot km^{-2}$], F is the catchment area [km^2], O_i are correction factors accounting for various catchment shapes, the percentage of forested land, climatic factors, etc., and A, n are regional parameters. For the most popular formulas of Dub, Halasi-Kun, the Czechoslovak Hydrometeorological Institute - HPIII method, the Slovak Hydrometeorological

Institute (SHMI) method; 8, 7, 26 and 60 regions were suggested, respectively. Flood quantiles for shorter return periods are computed by regional frequency factors from the 100-year discharges.
A comparison of 100-year floods (Q_{100}) computed by regional formulae with statistically derived values using new data from more than 250 gauging stations in small and mid-sized catchments in Kohnová, Szolgay (1995,1996) has shown that the most popular traditional formulae behave as envelope curves over the statistically determined values. The necessity to apply the envelope curve approach in the past was historically justifiable and was caused by the rare and short data series, by the necessity to mix measured data, historical data and floods estimated by hydraulic methods in the regional flood frequency analysis and probably also due to the fact, that usually floods with different genetic origin were employed. Consequently the resulting safety factor in the computation of the design values led to safer engineering design, which has proven its reliability in practice by the relatively small number of catastrophic accidents in the past decadesin small and mid-sized catchments. It is, however difficult to define the actual degree of risk of failure of hydraulic structures because of the (rather high and arbitrarily defined) safety factor: the traditional methods are not generally applicable to ecological river training and restoration, since they tend to overestimate the design discharges in almost all the basins of a particular region. Therefore, in following studies, regionalisation methods based on similarities in catchment geomorphology and including boundaries of the main catchments were tested with the use of the traditional form of the flood formula in Kohnová and Szolgay (1996). 18 and 28 regions were defined, respectively. To reduce the heterogeneity in data origin, summer and winter floods were separately treated. The results have shown that probably due to the high heterogeneity of runoff forming factors no acceptable regional formulae could have been defined without using envelope curves. Also the safety factor was reduced and its magnitude became comparable in different regions, it became apparent that other approaches based on different concepts must be also tested and subsequently introduced into the practice especially for hydroecological design problems, such as restoration of rivers, wetland design and management etc.
The growing number of gauging stations in small basins with longer records made it possible to test how some of the new concepts of homogeneity reported in the literature (e.g. Acreman, Sinclair, 1989, Zrinji, Burn, 1994, Meigh et al., 1997, Hosking, Wallis, 1997 and FEH, 1999) perform in the estimation of design discharges in the specific physiographic conditions of Slovakia. In these methods the concept of regions does not refer only to contiguous zones identified by geographical boundaries, but also to a group of catchments with similar properties with respect to the analysed phenomena. To distinguish between these to concepts, Reed et al. (1999) introduced the term pooling group for the latter; here the term regional type will be also used alternatively. Some of the new approaches were developed under specific conditions, and modifications to them may be necessary under the rather heterogeneous geological and geomorphological conditions. These methods are being consecutively tested for practical applicability and compared with the traditional approaches. The idea of using geographically continuous regions was abandoned, and physiographic properties of basins and flood runoff characteristics were used as variables in cluster analysis to define homogeneous pooling groups. Detailed summaries of the recent results of these efforts were published in Čunderlík (1999), Kohnová and Szolgay (1999, 2000). From an engineering point of view, none of the tested methods was found exclusively advantageous over the others, nor was up to now recommended for practical use.

3 DATA ANALYSIS

Seasonality analysis of flood occurrence in Kohnova (1997) and Čunderlik (1999) suggested, that for small and mid-sized catchments the frequency occurrence of rainfall-induced floods and snowmelt floods is comparable and they could be treated separately. For this study annual maximum summer floods were chosen as input data into the analysis. That also reduced the heterogeneity in the data due to the diverse genetic origin of flood events, when compared to an analysis based on annual maximum floods. Data from 251 small and mid-sized catchments with no significant impoundments or abstractions with the catchment area in a range from 10 to 360 km^2 from the whole territory of Slovakia and with observation periods ranging from 15 years to 67 years were collected from the database of the Slovak Hydrometeorological Institute. The site characteristics selected for this study were similar to those used in the previous ones. Site characteristics included: the catchment area (F,km^2), the gauge datum (NV, m.a.B.), the length of the river network (DL, km), the mean catchment slope (SL,%), the slope of the mean stream (IU,%), the catchment shape coefficient ($ALFA$), the mean aspect of the slopes (ASP, degrees), the mean catchment elevation (HPR, m a.s.l.), the percentage of forested area (LES, %), the long-term mean annual runoff (ODT,l.s^{-1}.km^{-2}) the an index of infiltration capacity of the soils (IFI) and the time of concentration (TC,h) according to Kirpich ($KIRP$), Hradek

(*HRAD*) and Nash (*NASH*). To involve the characteristics of the spatial distribution of extreme precipitation into the regional flood frequency analysis, grid maps of the absolute maximum daily precipitation amounts and of the maximum daily precipitation amounts with return periods of 2, 50 and 100 years were derived using geostatistical analysis. From these maps the areal averages of the maximum daily precipitation amounts from the period 1901-1980 (*ABSMAX*, mm), and the maximum daily precipitation amounts with return periods of 2, 50 and 100 years (*NTn 2, NTn50, NTn100*, mm) for all the catchments were computed in a GIS and added to the site characteristics (Kohnová et al., 2000).

4 IDENTIFICATION OF HOMOGENOUS POOLING GROUPS (REGIONAL TYPES)

Numerous techniques have been used to identify homogeneous pooling groups for regional flood frequency analysis. Hosking and Wallis (1997) recommended using methods that rely on site characteristics only when identifying homogeneous groups of catchments. Here, physiographic properties of basins and climatic characteristics were used as variables in the cluster analysis to pool catchments into homogeneous groups (K-means clustering with Euclidean metrics after Hartigan (1975) with the same weight assigned to each characteristic in the clustering process). Subsequently, at-site flood characteristics were used to independently test the homogeneity of the pooled catchments. The measure proposed by Hosking and Wallis (1997) based on L-moment ratios for testing the homogeneity of proposed pooling groups, which compare the between site variation in sample *L-Cv* (coefficient of variation) values with the expected variation for a homogeneous pooling group, was applied here. The method fits a four-parameter kappa distribution to the regional average *L-Cv* ratios. The estimated kappa distribution is used to generate 500 homogeneous pooling groups with population parameters equal to the regional average sample *L-Cv* ratios. The properties of the simulated homogeneous pooling group are compared to the sample *L-Cv* ratios as

$$H = \frac{(V - \mu_V)}{\sigma_V} \tag{2}$$

where μ_V is the mean of the simulated V values, and σ_V is the standard deviation of the simulated *V* values. For the sample and simulated pooling groups, respectively, *V* is calculated as

$$V = \left\{ \frac{\sum_{i=1}^{N} n_i (t^{(i)} - t^R)^2}{\sum_{i=1}^{N} n_i} \right\}^{1/2} \tag{3}$$

where *N* is the number of sites, n_i is the record length at the site *i*, $t^{(i)}$ is the sample L-Cv at site *i*, and t^R is the regional average sample *L-Cv*.

About 70 different combinations of physiographic catchment characteristic were tested for pooling the catchments into homogenous pooling groups. Since no estimate about the "correct" number of clusters can be given, a balance was sought between using pooling groups that were too small or too large. Pooling groups with few sites are likely to achieve little improvement in the reliability of a quantile estimates over at-site analysis; too large pooling groups are likely to fail the homogeneity test, and this can cause bias in the quantile estimate at some sites (Hosking and Wallis (1997) recommend the value of 20 sites as an approximate threshold). Only combinations with little correlation between the selected catchment characteristics were used. No unique combination of acceptable characteristics was found. With the following groups of physiographic catchment characteristics, acceptable measures of homogeneity were achieved:

1. DL, ASP, ABMAX, IFI
2. ALFA, TC NASH, IFI, NTn 100
3. F, IFI, SL, ALFA, NTn 100

All include some description of the measure of extremity of the daily rainfall (*ABMAX* or *NTn 100*), the index value of the infiltration capacity of the upper soil layer *IFI*, a measure of the catchment size (*DL*, *F*, or *TCNASH*); two of them contain a descriptor of the catchment shape. From a heuristic point of

view except for the mean aspect of the catchment slopes *ASP*, all the selected parameters should have a direct effect on the rainfall-runoff process; thus, their inclusion as pooling group descriptor seems to be justifiable. The inclusion of *ASP* can be heuristically underpinned by the argument that looking at the direction of the main mountain ranges in Slovakia, it can be argued, that north and northwest looking slopes are likely to receive higher amounts of precipitation due to the prevailingly western circulation patterns and southern slopes have higher evapotranspiration rates. Table 4-1 shows the values of the Hosking-Wallis homogeneity measure for combination of characteristics No1. Following Hosking and Wallis, catchment groups were classified as acceptable homogeneous (*H<1*), possibly homogeneous (*1<H<2*) and heterogeneous (*2<H*). The homogeneity of the pooling groups was also subjectively tested using the cluster profile plots. An analysis of the cluster profile plots revealed that in some pooling groups it was not possible to avoid that the site characteristics overlap between the clusters.

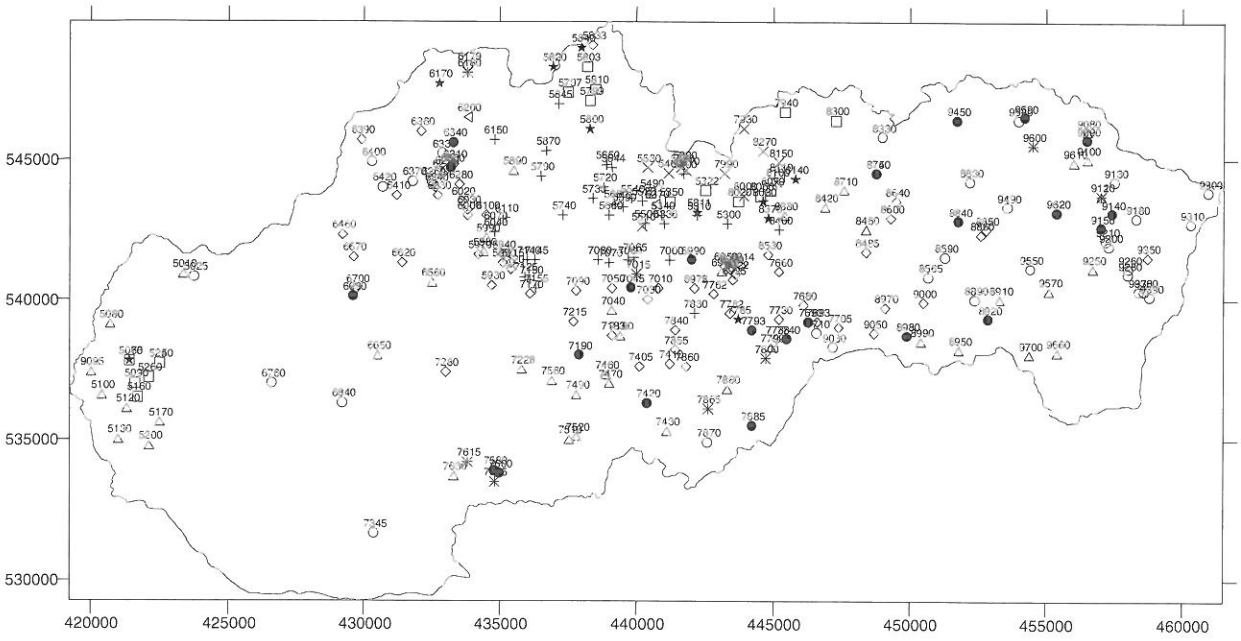

Figure 4-1: Location of catchments in the pooling groups for the combination of characteristics No.1.

Table 4-1: Values of the Hosking-Wallis homogeneity measure for the combination of characteristics No. 1.

Pooling group	No. of basins	H	Degree of homogeneity
1	30	1.62	possibly homogeneous
2	15	1.43	possibly homogeneous
3	21	1.58	possibly homogeneous
4	15	0.18	homogeneous
5	25	1.81	possibly homogeneous
6	15	2.03	possibly heterogeneous
7	31	1.76	possibly homogeneous
8	29	0.78	homogeneous
9	12	0.42	homogeneous
10	25	1.12	possibly homogeneous

For the purpose of the comparison of the design discharge computation methods in this study and the discussion about their respective practical applicability, the achieved degrees of homogeneity were regarded as satisfactory and comparable to those achieved by a similar approach in Čunderlik (1999). For practical applicability of the approach further refinements would be necessary. The question as to whether it is possible to successfully use the proposed methodology for practical engineering purposes remains on the whole territory of Slovakia unanswered so far.

5 SELECTION OF THE REGIONAL FLOOD FREQUENCY DISTRIBUTION AND THE ESTIMATION OF THE INDEX FLOOD

Catchments from the pooling group 8 were selected here for the purpose of the comparison of the design discharge computation methods. To select the appropriate regional distribution function, the Z^{DIST} goodness of fit test (Hosking and Wallis (1997)) and L-moment ratio diagrams for all pooling groups were used. The L-moment ratio diagram is a widely used tool for graphic interpretation and comparison of sample L-moment ratios *L-Cs* (skewness) and *L-Ck* (kurtosis) of various probability distributions. The goodness-of-fit test described by Hosking and Wallis (1997) is based on a comparison between sample *L-Ck* and population *L-Ck* for different distributions. The test statistic is termed Z^{DIST} and given as:

(4) $$Z^{DIST} = \frac{(\tau_4^{DIST} - \tau_4^R + B_4)}{\sigma_4}$$

where *DIST* refers to a candidate distribution. τ_4^{DIST} is the population *L-Ck* of the selected distribution, τ_4^R is the regional average sample *L-Ck*, B_4 is the bias of the regional average sample *L-Ck*, and σ_4 is the standard deviation of the regional average sample *L-Ck*. In Figure 6-1 the L- moment ratio diagram showing the regional average values of *L-Cs* and *L-Ck* of the pooling group weighted proportionally to the site record length of observations and their at-site estimates are presented. The general extreme value distribution, which was closest to the regional average value was chosen.
For a site with no flow records within the selected homogeneous pooling group, it has been expected that the mean annual maximum summer flood – the index flood *(XL)* – could be estimated by a regional regression equation in the form:

(5) $$XL = k \cdot A^a \cdot B^b \cdot C^c \ldots$$

where *k, a, b, c...* are regional parameters, and *A, B, C ...* are climatic and physiographic catchment characteristics.
A stepwise multiple regression was used to determine the relationship between the climatic and physiographic basin characteristics and the index flood values in the pooling group. In order to minimize the effect of multicollinearity, attention was paid to the choice of predictors with a low mutual dependence. Several subjectively chosen and hydrologically reasonable starting combinations of the independent variables were used as seeds in the discrimination process. For computational reasons the number of predictors was restricted between 2 and 4. The values of the multiple correlation coefficients ranged between 0.6 and 0.95 for the resulting combinations of predictors. It was not possible to determine which particular set of variables exclusively controls the index flood computation. Different combinations of independent variables gave statistically comparable results. The resulting equation for the pooling group 8 was selected in following form:

(6) $$X_L = e^{-8.210} \cdot F^{0.83} \cdot HPR^{0.99} \cdot LES^{-0.286}$$

6 COMPARISON OF METHODS

No independent data set was available to test the performance of the proposed approach and compare it with the traditional methods. The following heuristic scenario was therefore adopted to demonstrate the capabilities of the different approaches. It was assumed that in a number of sites with sufficient discharge data a design flood has to be estimated for flood protection requiring a high de-

gree of safety. In most cases in Slovakia the 100-year discharge would be chosen for such a scenario, and statistical methods would be preferred over regional ones. 12 such sites were selected from the analysed homogeneous pooling group with record length of more than approx. 30 years, which is usually considered to be sufficient for statistical analysis in Slovakia. These sites were also classified into regions according to the following often used regional methods:

- the method of Dub (1957)
- the method of the Czechoslovak Hydrometeorological Institute- the HPIII method (1970)
- the method of the Slovak Hydrometeorological Institute – the SHMI method
- the geomorphological regionalisation method of Kohnová (1997)

The last one was derived using annual maximum summer floods; the first three are based on annual maximum floods, but in the selected catchments late spring and early summer floods dominate the flood regime (Cunderlik, 1999).

The Hosking and Wallis heterogeneity measure was also used to test the homogeneity of the regions in to which the catchments were classified. Interestingly, only about one third of them could be considered as homogeneous. Than the optimal at-site frequency distribution was chosen and the 100-year design flood Q_{100} was estimated using L-moment statistics. Q_{100} was computed by the regional approaches at each site, as well. The relative differences *(X-Y)/Y* between the values of Q_{100} computed using the regional approaches *(X)* and statistically *(Y)* at-site for each site were computed and compared (see table 6-1 and figure 6-3).

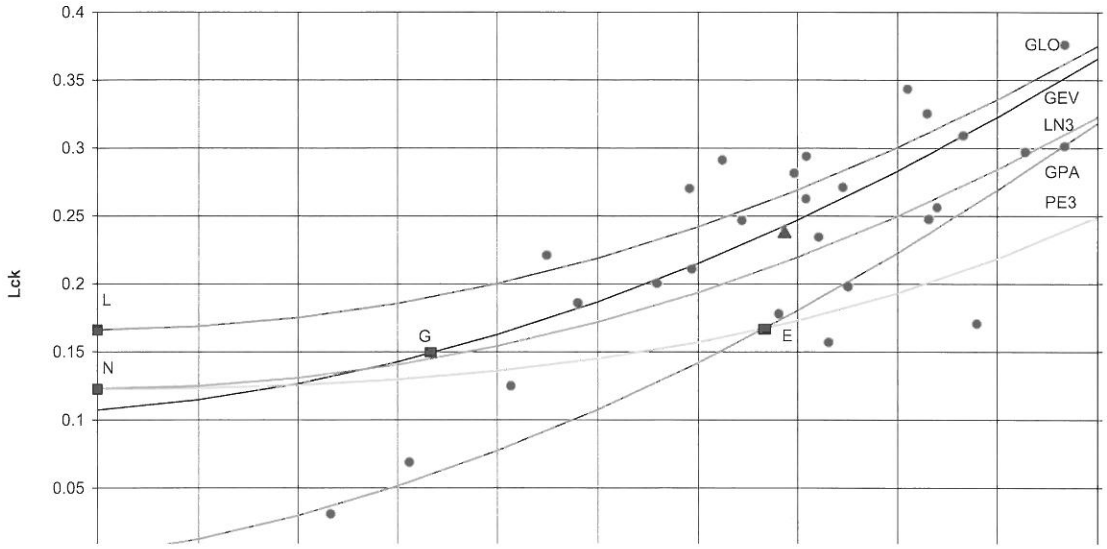

Figure 6-1: L-moment ratio diagram for the pooling group 8, regional average is marked as black triangle
(legend of distributions functions: GLO: Generalized logistic, LN3: Lognormal, GEV: Generalized extrem value, GPA: Generalized Pareto, PE3: Pearson III, L: Logistic, N: normal, E- exponencial, G: Gumbel).

Table 6-1: The relative differences *(X-Y)/Y* between the values of Q_{100} computed using the regional approaches *(X)* and statistically at-site *(Y)* for the selected catchments from the pooling group 8.

Site	F [km^2]	No of observ.	Hosking-Wallis method	Dub method	HPIII method	SHMI method	Kohnova method
5130	7.5	38	-0.068	4.023	N/A	3.807	1.024
5930	44.7	32	0.137	2.920	N/A	1.566	1.420
6950	79.28	68	0.155	0.363	0.362	0.411	0.379
6990	285.63	27	-0.054	-0.354	N/A	0.037	-0.172
7010	59.04	36	0.148	0.404	N/A	0.370	0.157
7030	64.61	31	-0.607	0.087	0.078	0.118	0.000
7060	36.01	52	0.499	0.910	0.198	0.198	0.504
7065	47.1	69	0.087	0.385	N/A	-0.101	0.089
7070	53.02	69	0.678	0.810	0.773	0.478	1.029
7080	82.1	69	1.142	1.019	1.358	0.965	1.420
7180	51.99	38	0.024	3.440	3.210	2.660	1.896
7830	73.95	35	-0.350	1.366	0.336	0.604	0.686

It can be seen that the traditional methods tend to overestimate the statistical values in most cases. When compared with the statistically based design values, the safe design criterion is met in almost each case (without taking into account the uncertainties associated with the statistical values); the degree of safety is, however, arbitrarily defined, and it changes from site to site and method to method. Moreover, it makes return period based risk analysis virtually impossible, since the "actual return period" remains unknown.

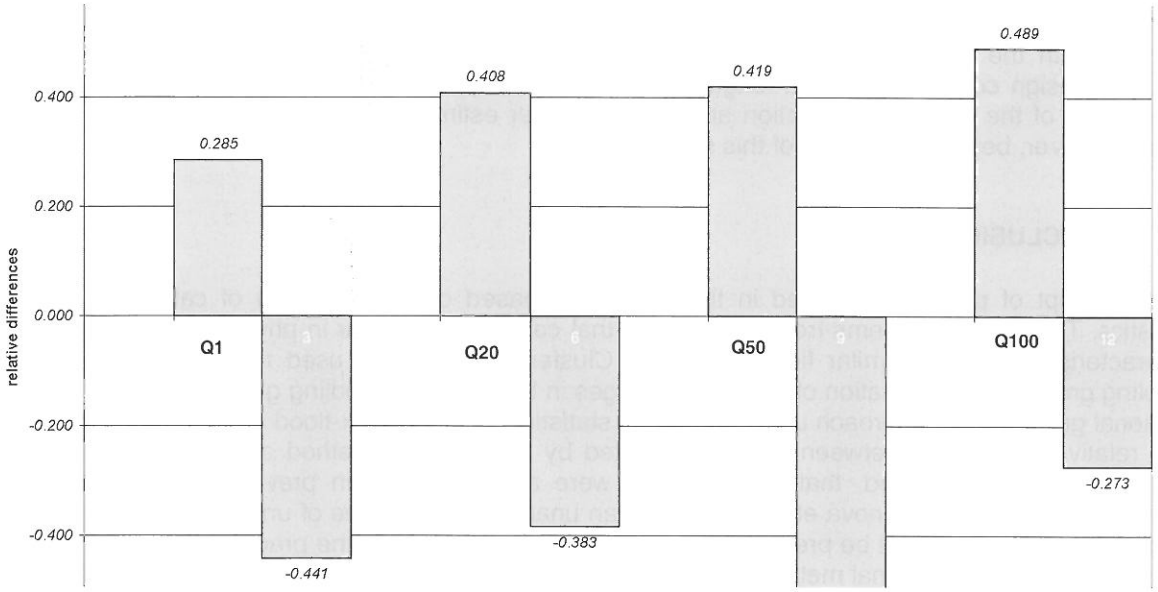

Figure 6–2: The mean positive and negative relative differences *(X-Y)/Y* between the values of Q_N for N=1, 20, 50, 100 computed using the regional approaches *(X)* and statistically at-site *(Y)* at each site in the pooling group 8.

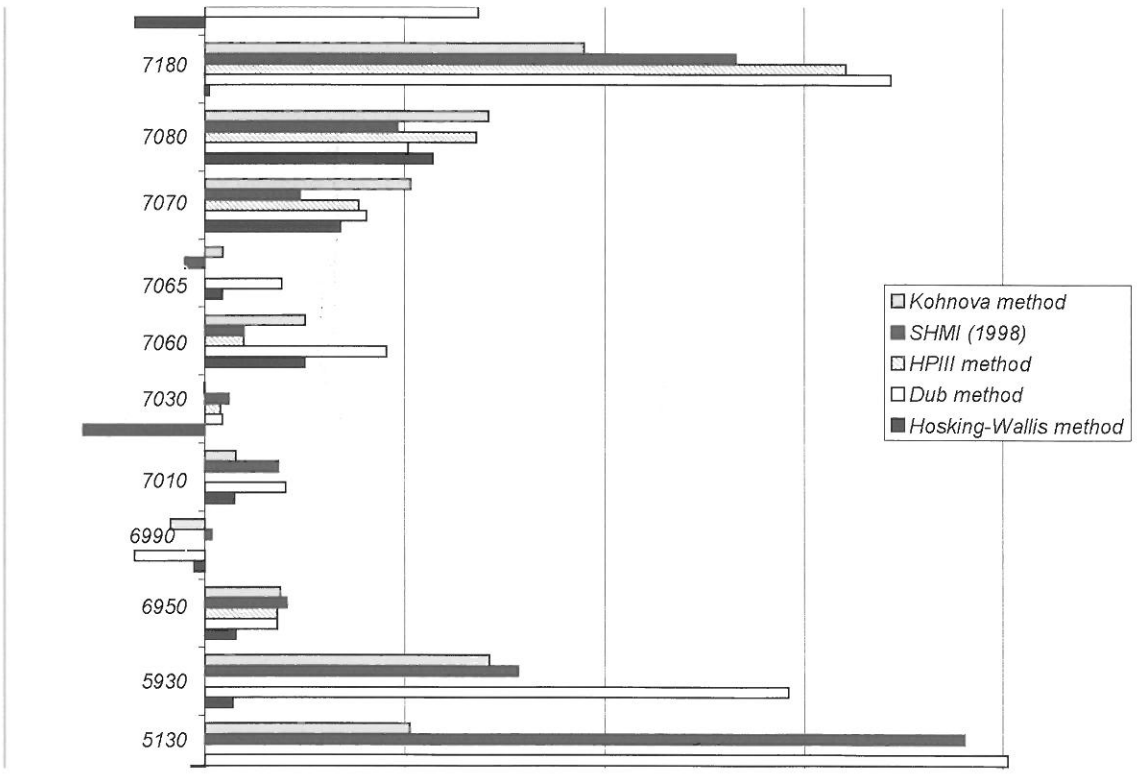

Figure 6-3: The relative differences *(X-Y)/Y* between the values of Q_{100} computed using the regional approaches *(X)* and statistically *(Y)* at-site for each site in the test cachtment group.

On the other hand the methodology tested in this study overestimates the "proper" values in approximately one half of the cases and underestimates them in the other half in the pooling group as whole, as it can be seen in Figure 6-2. This tendency is naturally present in the group of basins selected for the comparison also; thus, the criterion of safe design may not be met on the whole, since "underdesign" cannot be compensated for by "overdesign". This fact makes return-period based risk analysis difficult, since the "actual return-periods" remain again uncertain. The degree of design safety associated with this (and similar) methods could be acceptable, if using a large independent flood dataset (or simulation) it could be shown, that some measure of over and underestimation is comparable with the uncertainty associated with statistical methods, when used under average engineering design conditions (record length, data homogeneity, data quality, uncertainty resulting from the choice of the distribution function and the parameter estimation method, etc.). Such an analysis was, however, beyond the scope of this study.

7 CONCLUSIONS

The concept of pooling presented in the study was based on the similarity of catchment characteristics. This approach stems from the concept that catchments similar in physiographic and climatic characteristics have a similar flood response. Cluster analysis was used to define homogeneous pooling groups. The estimation of design discharges in homogenous pooling groups was based on the regional growth curve approach using L-moment statistics and the index-flood method. The analysis of the relative differences between values estimated by the regional method and those computed by statistical analysis showed, that better results were achieved than in previous studies (Kohnová, Szolgay, 1999, 2000; Kohnová et al., 2000), but an unacceptable degree of under and over-estimation of design values could not be prevented by the approach. Concerning the practical applicability of this method and of the traditional methods in engineering design in Slovakia, the following suggestions can be made: the traditional methods are not generally applicable to ecological river training and restoration, since they tend to overestimate the design discharges in almost all the basins of a particular pooling group. For these tasks, the regional method tested in this study, which does not include the regional safety principle (introduced by the envelope curve concept in the previous methods), but allows for site specific over and under-estimation resulting from the regional average concept, seems to be more appropriate. For hydroecological engineering design, pooling approaches with the lowest variability over the regional reference values should be preferred in a practical application. For flood protection and hydraulic engineering design where a high degree of safety is required, the traditional methods should be used, since under-design cannot be compensated for by over-design.
Several questions remain to be investigated, such as the preference for a particular pooling approach under specific physiographic conditions, quantification of statistical uncertainty under which the concept of regional homogeneity can be used for design purposes, etc. Regional frequency analysis following the principles of Hosking and Wallis could possibly lead to the selection of more appropriate pooling groups with different climatic and physiographic catchment parameters than used in this study. Inclusion of other variables controlling the variability of flood formation, and describing the intensity of overland flow formation, upper layer permeability, catchment storage, etc., should be further investigated in order to test the practical applicability of the concept of regional homogeneity based on physiographical characteristics.

ACKNOWLEDGEMENT

The Slovak Grant Agency supported the research presented in this paper under VEGA Projects Nos.1/8250/01 and 1/9363/02. The support is gratefully acknowledged.

REFERENCES

Acreman, M. C., Sinclair, C. D. (1986): Classification of drainage basins according to their physical characteristic - an application of flood frequency analysis in Scotland. J.of Hydrol., 84, 365-380.

Čunderlík, J. (1999): Regional estimation of N-year maximum floods in selected catchments in Slovakia. PhD. thesis, Svf STU Bratislava, 144 p. (in Slovak)

Burn, D. H. (1990): Cluster Analysis as applied to regional flood frequency, J.of Wat. Res. Plan. and Manag., 115, 5, 567-582.

Dalrymple, T. (1960): Flood frequency methods, U. S. Geolog. Survey, 1543-A, 11-51.

Dub, O. (1957) : Hydrology, hydrography, hydrometry. SVTL Bratislava, 488 p. (in Slovak)

FEH (1999): Flood Estimation Handbook. Part 3. Statistical procedures for flood frequency estimation, IH Wallingford, 325 p.

Hartigan, J. A. (1975): Clustering Algorithms. John Wiley and Sons. New York.

Hosking, J.R.M., Wallis, J.R. (1997): Regional Frequency Analysis: An Approach Based on L-moments. Cambridge University Press.

HYDROLOGICKÉ pomery ČSSR (1970): Diel III., Praha, 87-104. (in Slovak)

Kohnová, S. (1997): Regional analysis of maximum specific discharges on small catchments in Slovakia. PhD. thesis, SvF STU Bratislava, 159 p. (in Slovak)

Kohnová, S., Szolgay, J. (1995): On the use of the Dub regional formulae on the territory of Slovakia, J. Hydrol. Hydromech., 43, 28-56 (in Slovak)

Kohnová, S., Szolgay, J. (1996): The regional estimation of maximum specific discharges in small catchments of Slovakia. (in German) Zeitsch. für Kulturtechnik und Landentwicklung. 28, 116-121.

Kohnová, S., Szolgay, J. (1999): Regional estimation of design summer flood discharge in small catchments of northern Slovakia. In: Gottschalk, L. – Olivry, C. – Reed, D. – Rosbjerg, D. eds.: Hydrological extremes: Understanding, Predicting, Mitigating. IAHS publ. No. 255, IAHS Press Wallingford, 265-268.

Kohnová, S., Szolgay, J. (2000): Regional estimation of design flood discharges for river restoration in mountainous basins of northern Slovakia. In: Marsalek, et al. (eds.), Flood Issues in Contemporary Water Management, NATO Science Series, Vol 71. Kluwer Academic Publishers, 41-47. ISBN 0-7923-6452X

Kohnová, S. et al. (2000b): Untersuchungen zur Anwendbarkeit des Konzeptes der regionalen Homogenität für die Bestimmung von Bemessungshochwassern in der Slowakei. In: Moehlmann, Ch. et al.: Berichte 11, TU Kaiserslautern, BRD. ISSN 1433-4860, 67-83.

Kohnová, S. et al. (2000b): Analyse der raumlichen Variabilitaet von Starkniederschlaegen in der Slowakei fuer die regionale Hochwasseranalyse. In:Szolgay et a.l eds.: XX. Konferenz der Donaulaender, Bratislava, 8 p., CD

Meigh, J.R et al. (1997) A wordwide comparison of regional flood estimation methods and climate. Hydrological Science Journal, 42, 2, 2225-2244.

Miklánek, P., Halmová, D., Pekárová, P. (2000): Extreme runoff simulation in Mala Svinka Basin. Conference on Monitoring and Modeling Catchment Water Quality and Quantity, Laboratory of Hydrology and Water Management, Ghent University, Belgium, 49-52.

Reed, D. (1999): Regional flood frequency analysis: a new vocabulary. In: Gottschalk, L. – Olivry, C. – Reed, D. – Rosbjerg, D. eds.: Hydrological extremes: Understanding, Predicting, Mitigating. IAHS publ. No. 255, IAHS Press Wallingford, 237-243.

Svoboda, A., Pekárová, P., Miklánek, P. (2000): Flood Hydrology of Danube between Devín and Nagymaros. Publication of the Slovak Committee for Hydrology, Bratislava, No.5, SVH a ÚH SAV,97

Szolgay, J., Kohnová, S. (1999): Vergleich der Methoden fuer die Abschaetzung von Bemessungsabfluessen in kleinen und mittleren Flussgebieten der Slovakei. (in German) In: Berichte 9, ed. Koehler, G.: Bemessungsabfluesse fuer kleine Einzugsgebiete. Fachgebiet Wasserbau und Wasserwirtschaft,TU Kaiserslautern, 93-105

Zrinji, Z., Burn, D. H. (1994): Flood frequency analysis for ungauged sites using a region of influence approach. J. Hydrol., 153, 1-21

REGIONAL FORECASTING OF RIVER FLOWS USING A HIGH RESOLUTION NUMERICAL WEATHER MODEL COUPLED TO A HYDROLOGICAL MODEL

Nicholas Kouwen[1], Robert Benoit[2]

[1] Department of Civil Engineering, University of Waterloo, Waterloo, ON, Canada, N2L 3G1
kouwen@uwaterloo.ca

[2] Recherche en Prévision Numérique, Environment Canada, Dorval, Quebec, Canada, H9P 1J3
Robert.Benoit@ec.gc.ca

SUMMARY

This paper reports on the use of meteorological data generated by the MC2 Numerical Weather Model (NWM) for a domain that included the Rhine above Lake Constance, the Rhone above Lake Geneva, parts of the Po river including the Toce-Ticino, and parts of the Danube River including the Isar, Inn and Enns rivers to drive the WATFLOOD hydrological model for the Mesoscale Alpine Program (MAP) Special Observing Period (SOP), lasting from September 7 to November 15, 2000. (http://www.map2.ethz.ch/, 2001)

Keywords: Numerical Weather model, Hydrological Model, Flood Forecasting

1 INTRODUCTION

The objective of this study was to determine if river flows can be predicted by linking an NWM with an hydrological model. The headwaters of the Danube, Rhine, Rhone, and Po rivers lie within the MAP domain and presented an opportunity make this determination. Observed flow data for 33 gauging stations in four countries were available to compare forecasted with observed flows. Ten of these stations were selected for presentation in this paper.
For this study, the NWM used is the Mesoscale Compressible Community Model (MC2) (Benoit et al. 1997), and the hydrological model is the WATFLOOD model (Kouwen et al., 1993). A one-way coupling technique is applied to link two models. The objective of this study is to examine the performance of MC2 model with respect to predicting rainfall at an areal and temporal resolution adequate for flood forecasting. This can be done in two ways. First, the MC2 output data, such as temperature and precipitation data, are used to drive WATFLOOD. The simulated flows are then compared with the observed flows. If the time and magnitude of the peak flows at various locations are coincident, the forecast is successful. Thus an evaluation can be made if MC2 produces rainfall events that are temporally and spatially correct. Second, if the forecasted flows are grossly in error, the MC2 precipitation forecast can be qualitatively compared to radar data to determine the reason for the error.

1.1 Weather Model – MC2

The MC2 model was developed over the last seven years at Recherche en Prévision Numérique (PRN), Environment Canada (Benoit et al., 1997, Benoit et al. 2000, Wen et al. 2000). The model uses the full-unified PRN physics package, which is also used in for the operational models at the Canadian Meteorological Centre (CMC). It is a nonhydrostatic limited-area model (Benoit et al., 1997, Benoit et al., 2000) that uses a semi-implicit semi-Lagrangian (SISL) time scheme and a generalized terrain-following coordinate system. It is a 3D fully compressible model that is able to solve the Euler equations at a fine spatial scale (Benoit et al., 2000). The force-restore method is a simple but widely used land surface scheme. The model uses a one-way nesting strategy, where a coarse-grid forecast provides initial and boundary conditions for a fine-grid forecast without feedback (Kouwen, Innes, 2001). A detailed description of MC2 can be found in Benoit et al., (1997).
For the MAP, MC2 was run as the last stage in a chain of models, where each consecutive model uses data from previously run models. First the new globe GME model of the German Weather Service (DWD) was run at a resolution of 125km around the entire globe. Then DWD ran the Europa-Model at a resolution of 56km covering the whole of Europe. Second, the German/Swiss high-resolution model (HM) ran at the resolution of 14km by the Swiss Meteorological Institute (SMI) over central

Europe. Finally, the MC2 was run at a resolution of 3km covering the alpine region of Europe, which included the areas under study.

1.2 Hydrological Model - WATFLOOD

WATFLOOD is an integrated set of computer programs to compute flows for watersheds having response times ranging from one hour to several weeks. Continuous simulation of hydrologic response can be carried out by chaining up to a maximum of 100 events. Each event can be up to one year in length. (Kouwen, 2000). WATFLOOD makes optimal use of remotely sensed land cover data and digital elevation data. Radar rainfall data, LANDSAT or SPOT land cover data can be directly incorporated into hydrological modeling. The use of Grouped Response Units (GRU's) allows WATFLOOD to preserve the distributed nature of a watershed's hydrologic and meteorological variability while maintaining computational efficiency.
The GRU technique models the land surface processes separately for each land cover within a computational grid element when all individual areas within that element are subject to the same meteorological condition. The hydrological responses from all GRUs in a grid are summed to give its total response. Identical hydrologic parameters are employed for the same land cover throughout the domain (Kouwen et al., 1993). This allows the same set of parameters to be applied over large regions with many watersheds. Water is routed from one grid to the next until the outflow at the outlet of watersheds is obtained.
The hydrological processes incorporated in WATFLOOD include: interception, infiltration, evapo-transpiration, snow melt, interflow, baseflow, overland routing, and channel routing. The routing of water through the channel system is accomplished using a storage routing technique, which involves a straightforward application of the continuity equation. The flow is related to the storage through the Manning formula. A comprehensive description of WATFLOOD can be found in Kouwen et al. (1993) or at http://www.watflood.ca (2001).
The WATFLOOD model was calibrated on the Columbia River watershed in Canada as part of a dam safety study. The parameters obtained were applied directly to the current domain without further adjustment except that the river roughness was reduced to account for the type of rivers found in Europe.

1.3 Linked Model: Coupling MC2 and WATFLOOD

MC2 was run at a resolution of 3km over the Alpine region of Europe, including the headwaters of the Danube, Rhine, Po and Rhone rivers. The hydrological model WATFLOOD uses the one-hour precipitation accumulation and temperature from MC2 at each hour of simulation. Both models use their own simplified land surface physical process (Benoit et al. 2000). The hydrological model uses a water balance calculation as opposed to a water and energy balance calculation in MC2. During the MAP Special Observation Period (SOP), the hydrological model WATFLOOD was used in real-time to validate the daily MC2 forecast of precipitation for a small portion of the MC2 model domain.

2 LITERATURE REVIEW

Many atmospheric and hydrological processes are so intertwined that these cannot be considered separately. To successfully model global energy and water cycles, the linkage of the hydrologic model and atmospheric model is required. The linking of hydrological and atmospheric models is often based on a one-way coupling approach. The hydrological models are linked to atmospheric models through simple forcing method by only using the atmospheric model output. Kim et al. (1998) present a well-designed numerical modeling system, which coupled atmospheric, land surface, and hydrologic models to integrate regional climate prediction and assessments of atmospheric, land surface, and hydrologic processes over the mountainous area in California. Benoit et al. (2000) presented a one-way coupling to validate and interpret the output from the atmospheric model. Other examples of one-way coupling are reported by Hamlet et al. (1999), Leung et al. (1999), Ji et al. (1994), Giorgi et al. (1989), and Wen et al. (2000).
One-way linking can be misleading since the land-surface is treated independently in each model, resulting in inconsistent basin state variables. This can be avoided if the two models share the same land-surface scheme. The experience gained in such one-way off-line coupling of atmospheric and

hydrological models will be useful in developing numerical weather models of the full hydrological cycle with full coupling of atmospheric, oceanic and hydrological models.

3 CASE STUDY - MAP PROJECT

The Mesoscale Alpine Programme (MAP) is an international research initiative devoted to the study of atmospheric and hydrological processes over mountainous terrain. It aims towards expanding the knowledge of weather and climate over complex topography, and thereby to improve current forecasting capabilities. The project includes numerous activities, ranging from high-resolution numerical modelling to a major field campaign in the Alpine area. A primary objective of MAP is to improve the understanding and short-term numerical prediction of Alpine precipitation, and particularly of the heavy precipitation and flooding events. As part of the MAP project, this study is focused on linking atmospheric-hydrologic models to simulate runoff for flood alerts to validate the precipitation forecast from MC2 and to perform a field test of the linkage of atmospheric and hydrological models.

3.1 Study Area

The MC2 domain is 43° 40' N - 50° 20' N by 4° E - 16° E. This covers eastern France, northern Italy, southern Germany, most of Austria, and the whole of Switzerland. The major watersheds included are the headwaters of the Danube, Rhine, Po, and Rhone rivers.

3.2 Watershed Data Collection

A considerable amount of information relating to the watershed is required by WATFLOOD to produce accurate results. These data include elevation, land use, drainage direction, streamflow, temperature, and precipitation for the period being studied. All the input data should be converted to WATFLOOD format in order to run the software properly.

3.2.1 Elevation

The characteristics of the drainage layer database came from the gridded Digital Elevation Model (DEM) called the Defense Land Mass System (DLMS) (Volkert, 1990). They consist of an ordered array of gridded elevations at regularly spaced intervals with 3″ resolution (i.e. 1200 data points per degree). The geometric resolution is about 185 m. Each file consists of elevation data units expressed in meters relative to mean sea level. The elevation data were used for the storage routing scheme. For illustration only, Figure 3-1 shows the DEM for the study area based on GTOPO30 (http://edcdaac.usgs.gov/gtopo30/gtopo30.html, 2001).

3.2.2 Land Use Data Acquisition

The land-cover data were derived from the Distributed Active Archive Center from USGS Eros Data Center, the Global Land Cover Characteristics Data Base. They were generated at a resolution of 1-km for use in a wide range of environmental research and modeling applications, and were developed on a continent-by-continent basis. All continental databases share the same map projections (Interrupted Goode Homolosine and Lambert Azimuthal Equal Area), have 1-km nominal spatial resolution, and are based on 1-km Advanced Very High Resolution Radiometer (AVHRR) data. A core set of derived thematic maps produced through the aggregation of seasonal land cover regions are included in each continental database to provide flexibility for a variety of applications. In the data set, there are seven different cover types across the Alps area. The cover types were: Coniferous Forest, Deciduous Forest, Water, Agriculture, Barren land, Urban, and Glacial.

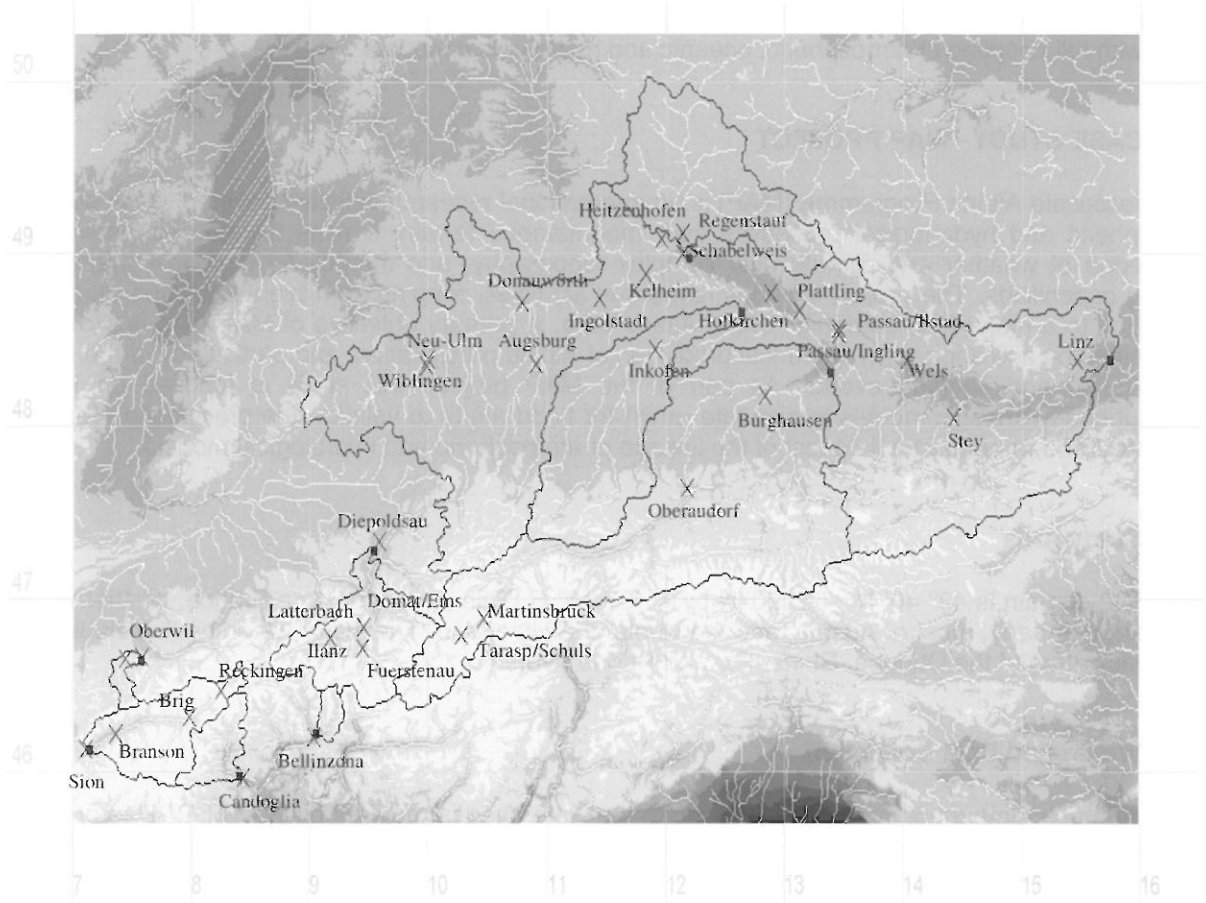

Figure 3-1: Model domain showing streamflow stations.

3.3 Streamflow Data Acquisition

Observed streamflow data are required in WATFLOOD to allow for validation of the simulated flow from WATFLOOD model. The purpose of this study is to examine if MC2 predicted precipitation events agreed with observations both spatially and temporally. The WATFLOOD model converted the MC2 data to streamflow so that the precipitation data could be validated with streamflow. A total of 33 stream gauge stations are used for this project, i.e. 13 stations in Switzerland, 3 in Austria, 1 in Italy, and 16 from Germany. Plots of the flow data show that many stations are very highly regulated. Unfortunately, reservoir data were not available for this study. Table 1 lists the station information for 10 of the 33 stations used. These 10 stations were selected to be representative of all 33 stations.

3.4 Precipitation and Temperature Data Acquisition

Distributed precipitation and temperature data were generated hourly by the MC2 numerical weather model. The data were processed once a day to produce 24-hour forecasts of precipitation and temperature. Data were transformed into the WATFLOOD latitude-longitude grid with hourly time steps for processing for the MAP SOP.

3.5 Drainage Layer Creation

For the study area, the drainage layer databases were created automatically using the program MapMaker. This program uses output from the image processor EASI/PACE produced by PCI Industries. EASI/PACE (PCI Geomatics, 1998) uses the DEM to calculate such fields as flow direction and flow accumulation, and delineates watersheds. From these fields, MapMaker then calculates the flow characteristics of the drainage layer database. Then the program processes the land cover information so that it can be used by WATFLOOD. During each step of the drainage layer database setup, the

data were visually inspected to ensure that they were correct. Meanwhile, the programs perform their own validation procedures to make sure that the flow networks are logical, i.e. ensuring water flows to a lower elevation and avoiding dead ends in the flow networks (Kouwen et al., 2000).

4 RESULTS AND DISCUSSION

This section presents the results of the comparison between the observed streamflow and the forecasted streamflow using the MC2-WATFLOOD linked models. When the MC2 based flows appeared to be in error, the real-time radar precipitation images were compared to MC2 precipitation maps to determine the cause of the discrepancy. The performance of MC2 can be evaluated in terms of the four situations:

1. The resulting hydrograph matches the observed flow data
2. The MC2 derived hydrograph appears in the wrong location and/or the wrong time
3. MC2 produced hydrographs at one or more locations where there is no observed hydrograph
4. MC2 computes no hydrograph while observed data shows increased flows

The comparison for this study is on a station-by-station basis to check the implementation of MC2. The predicted magnitude of the storm is also of interest, but was not the focus of this study. More emphasis is placed on the ability of the MC2/WATFLOOD linkage to point to areas where a potential for flooding exists. For large domains, real-time flow forecasting can be updated using radar and/or flow observations. The value in modelling such a large domain is to provide a first alert and an awareness of what may occur. Table 3-1 lists 10 of the 33 streamflow stations used in this study. The 10 selected stations are representative of the 33 and are also the ones that appear to be least affected by regulation. Their locations, actual and modelled drainage area as well as the percent difference between the actual and modelled drainage area is shown. Figure 3-1 shows the model domain and streamflow gauge locations.

Table 3-1: Station Information For Model Domain.

Streamflow Station	Description	Latitude	Longitude	Drainage Area	Simulated Drainage Area	Difference
		(°N)	(°E)	(km^2)	(km^2)	(%)
Ilanz	Vorderrhein	46.7771	9.1741	776	752	-3.09278
Tarasp/Schuls	Inn	46.7891	10.2786	1584	1574	-0.63131
Wels	Traun	48.3853	14.0275	78190	76894	-1.65750
Linz	Danube	48.3833	15.4622	95970	94322	-1.71720
Neu-Ulm	Donau	48.3887	10.0014	7578	7553	-0.32990
Kelheim	Donau	48.8861	11.8232	22950	23040	0.39216
Hofkirchen	Donau	48.6723	13.1262	47496	47150	-0.72848
Brig	Rhone	46.3174	7.975	913	901	-0.836070
Bellinzona	Ticino	46.2000	9.033	1515	1526	-0.836070
Candoglia	Toce	45.9667	8.433	1532	1525	-0.836070

4.1 Simulated Results versus Observed Streamflow Data

In general, the MC2/WATFLOOD model underestimated the total runoff during the MAP SOP. Figure 4-1 shows the percent error for all 33 stations used in the study. The error for larger drainage areas is reduced because much of the flow is base flow which is initialized at the start of the simulation and is not subject to much random error. The point above the 100% line is for a highly regulated site. But this figure shows an underestimation for most of the intermediate basins.
Figures 4-2 to 4-3 show the observed and computed hydrographs for the stations listed in Table 3-1. Figure 4-2 shows the results for the head waters for the four major rivers modelled. Figure 4-3 shows the results for stations along the Danube river which range in drainage area from 7578 km^2 at Neu-Ulm to 94322 km^2 at Linz. The time step of the model and the plotted hydrographs is one hour.

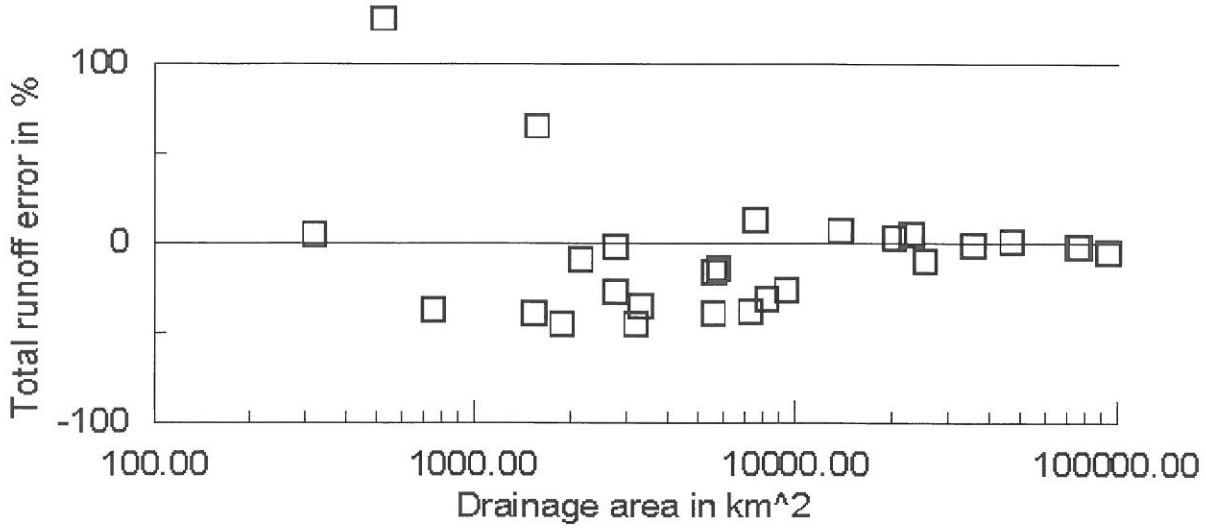

Figure 4-1: Error in runoff for the MAP SOP (for all 33 stations).

In general, considering that the input data is derived from a meteorological model, the four events during September 21 through October 5 are reproduced very well in the headwaters of the Rhone, Ticino, Rhine, Inn and Danube rivers. This area straddles the Swiss-Austrian border. The computed flows for the Danube at Neu-Ulm and Donauworth match the observed flows very well for this period. However, the watersheds to the east, namely the Lech at Augsburg (not shown), the Amper at Inkofen (not shown) do not show any substantial hydrographs for this period. This deficiency is evident on the flow plots for the Danube below these rivers at Hofkirchen, Weis and Linz (Figure 4.3). In comparing the MC2 forecast with the Alpine Composite Radar on the MAP website for September 28 (http:// www.map2.ethz.ch/sop-doc/catalog/products/, 2001), radar shows a substantial amount of rain fell on the Austrian Alps but MC2 did not forecast this rain. On September 30, radar shows a widespread rain over Bavaria and the Austrian Alps but MC2 forecasted rain only in a small area in the headwaters of the Danube. This is reflected in the computed hydrographs for the Danube at Neu-Ulm and Donauworth. On October 3 and 4, another event with widespread rainfall was recorded by the MAP Alpine Composite Radar. MC2 forecasted rain for the same area but with much lower intensities than indicated by the radar. This deficiency in the MC2 forecasted rain is clearly evident in the under predicted flows in the Danube at Hofkirchen, Wels and Linz.

Three measurable events (not flood events) occurred during October 22-24 on the Ticino and Rhine above Chur. Hydrographs were computed at all stations in the domain. At Brig, Ilanz, Bellinzona and Candoglia, small hydrographs were properly modelled. From October 23-24, MC2 predicted rain for the Danube above Neu-Ulm, the Iler above Wiblingen (not shown) and the Inn at Tarsasp. For this same period, radar showed some widespread spotty rain on October 23 and a band of rain that remained to the west of the modelled watersheds. This resulted in overestimated hydrographs for the upper reaches of the Inn and Danube which converged when routed downstream to produce the hydrographs beginning October 30 for the Danube at Linz.

On November 2-3, 1999 MC2 forecasted an event centered in the Liechtenstein area. Hydrographs were incorrectly predicted for the Simme above Oberwil (not shown) and the Danube at Neu-Ulm. As with the earlier events, the hydrograph is routed downstream and shows up approximately one week later at Linz, where it blends in with another event that was properly predicted. This last event during the MAP SOP was centered in the upper reaches of the Danube Watershed and is modelled very well at Neu-Ulm. This hydrograph is routed down the Danube past the various flow stations and matches the flows at Weis and Linz.

Overall, the simulated flows of the Danube at Linz match the observed flow quite well except for the period from September 28 to October 9. The deficit in the Danube flows can be traced back to the missed events in central Austria during this period.

The observed hydrograph at Linz shows 90 mm runoff from the whole watershed for the MAP SOP while the computed hydrograph is 87 mm. More than 50% of this is base flow, but still the overall predictions are close to the observed flows.

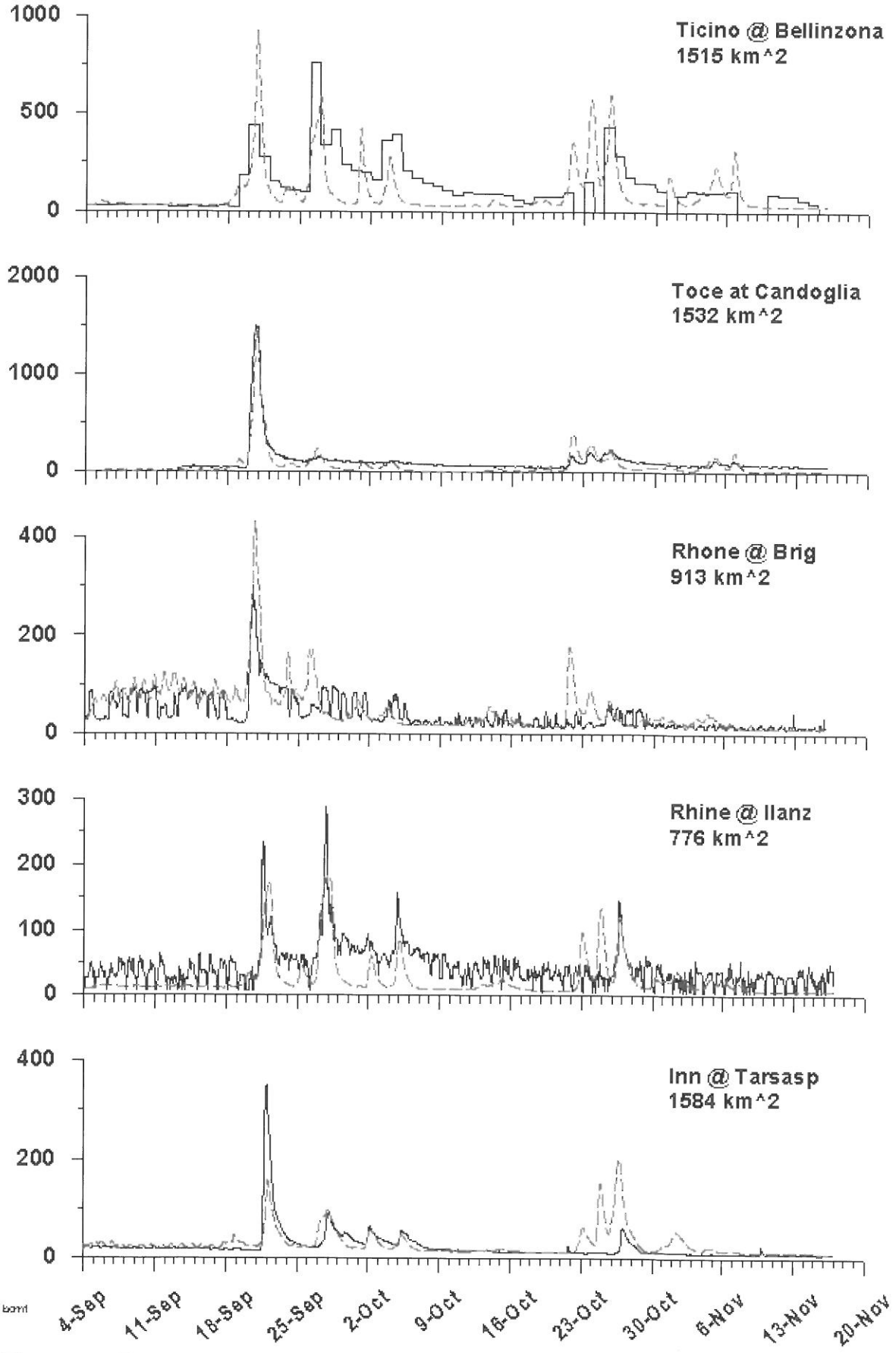

Figure 4-2: Forecasted flows using MC2/WATFLOOD (Solid = observed, broken = computed).

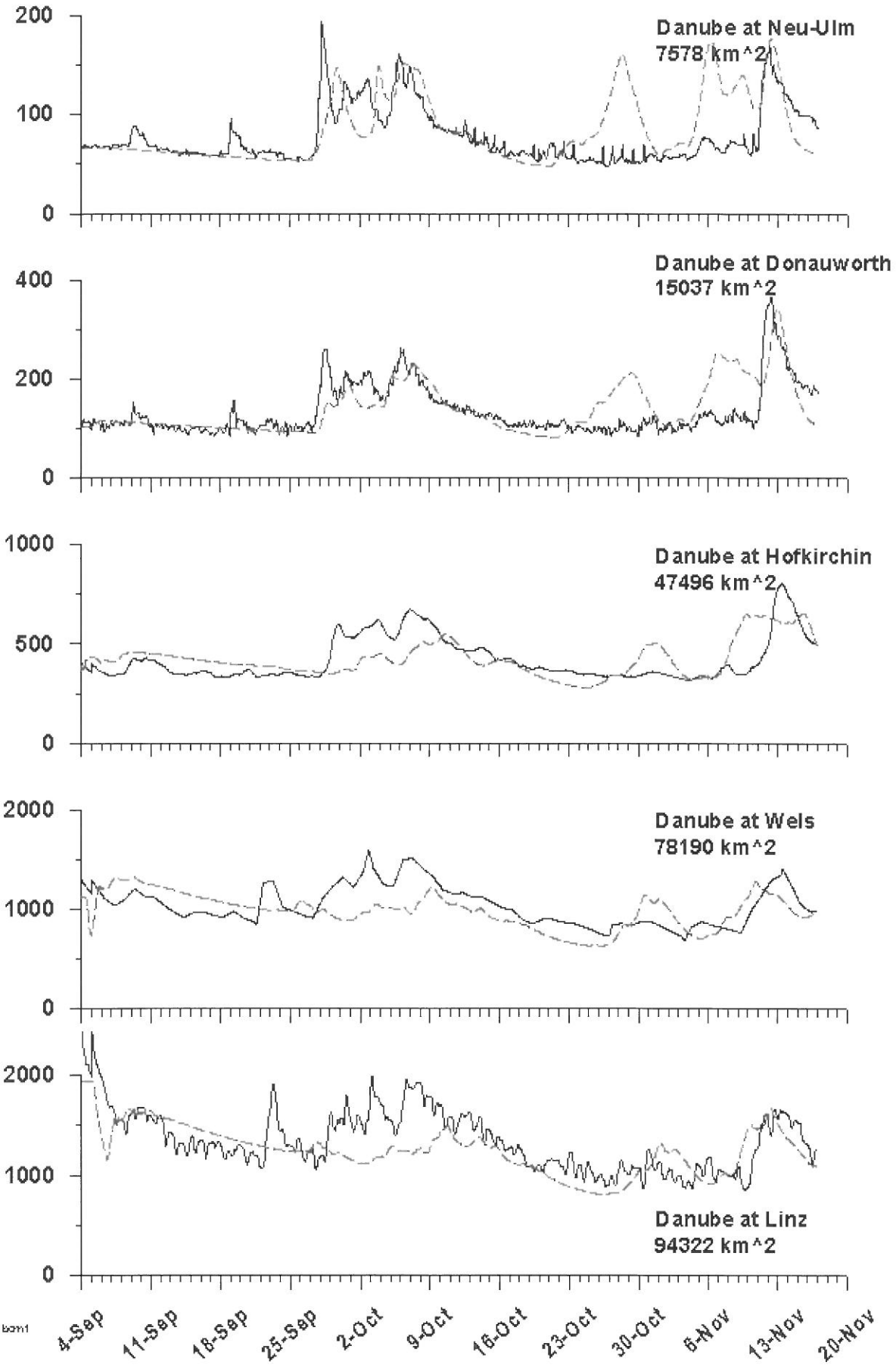

Figure 4-3: Forecasted flows using MC2/WATFLOOD (Solid = observed, broken = computed).

In a more detailed analysis Liu (2001) summarizes the overall performance of MC2 using all 33 flow stations. Within the MAP-SOP, 11 events were simulated and generated 97 hydrographs at various locations. Of the recorded hydrographs, 84 were predicted by MC2 and 13 were missed by MC2. In addition, 21 hydrographs were predicted by MC2 that did not occur. As a result, using MC2 for flood alert and early warning, there is an 87% chance that it can predict an increase in flow correctly while there is a 13% chance that it will miss an event. There is also a 22% possibility it will produce a false alarm. From the overall point of view, this confirms that MC2 is able to predict storms for large domains although there is a concern with the uncertainty in terms of the prediction for individual rivers. These figures are based on using only MC2 forecast data and flows were not nudged with recorded data. Flow forecasts on larger basins obviously would be improved if recorded flows were used up to the time of the forecast. The use of MC2 can usefully extend the forecast by the length of it's forecast, in this case, 24 hours.
In general, the MC2/WATFLOOD model underestimated the total runoff during MAP SOP. This is consistent with study of Benoit et al. (2002): the precipitation was under-predicted by MC2 by a factor of 2 during MAP SOP. After the field experiment, a coding error in the precipitation parameterization of MC2 was found, which explains, to a large extent, this underestimation.
This study shows that in addition to the possibility of increased lead times for flood forecasts, a hydrological model can be used as a performance check on a meteorological model. Although a comparison of the MC2 generated precipitation maps with radar images and precipitation gauge data indicated an under-prediction of precipitation, the hydrological model more clearly showed quantitatively the areal extent of the problem as well as the implications of the problem on flood forecasting.

5 CONCLUSIONS

This paper examined the effectiveness of a Numerical Weather Model for flood alerts on a regional basis. The MC2 atmospheric model used in this study, is a 3D fully compressible model, which uses semi-implicit semi-Lagrangian time scheme to solve the Euler equation. MC2 was run at a resolution of 3 km covering the alpine region of Europe, which including the study area of this project, namely, the headwaters of the Po, Rhine, Rhone and Danube rivers.
The hydrologic model WATFLOOD was employed to achieve the evaluation of MC2. It is a distributed flood-forecasting model that can incorporate remotely sensed data and digital elevation data into hydrological modelling. The storage routing technique involving the continuity equation and the Manning Formula is applied in WATFLOOD to model the physical process.
The one-way coupling technique of linking atmospheric and hydrologic models is applied for the Alpine study areas. Precipitation and temperature data produced by MC2 are incorporated into WATFLOOD model for simulating runoff. The results from WATFLOOD are compared with the observed flow data. Where the MC2/WATFLOOD flow predictions did not match the observed flows, the MC2 precipitation forecast and Alpine Composite Radar data were used to explain the deficiencies in the hydrographs. For each unsuccessful flow forecast, it was possible to qualitatively determine that the MC2 precipitation forecast was in error. However, there were a sufficiently large number of cases where hydrographs were predicted to show that a flow forecast from linked weather and hydrological models can serve as a useful first alert and quantitative forecast. Only one event of flood magnitude occurred in one location during the MAP SOP. For this event, on the Toce River at Candoglia, the hydrograph was very well predicted.
The simulated runoffs match the regionally observed flow quite well although a coding error found after the field experiment resulted in under-predicted precipitation. This information could be valuable in predicting and forecasting the occurrence of high flows at specific times and locations for Alpine regions. It seems especially appropriate to produce an initial alert, to be followed up by more detailed modelling for specific problem areas using radar and other real-time observations. In addition, the study shows the value of linking a hydrological model to a meteorological model as a way of checking the performance of the precipitation forecast.

ACKNOWLEDGEMETS

This hydrological study was carried out by Maggie X. Liu in partial fulfillment of her M.A.Sc. degree requirements at the University of Waterloo. Her efforts are deeply appreciated and acknowledged by the writers. The work of Pierre Pellerin and Stephane Chaimberlain to produce the daily MC2 precipitation forecasts during the MAP SOP is also acknowledged. The German flow data were kindly

provided by Dr Alfons Vogelbacher from the Bavarian Water Survey, the Candoglia gauge data were made available by CNR-Istituto Idrobiologico di Pallanza through Regione Piemonte and the Swiss data were provided by Bundesamt Für Wasser und Geologie. This study was financed by Environment Canada, the National Science and Engineering Research Council of Canada and the University of Waterloo. This support is appreciated by the writers.

REFERENCES

Benoit, R. et al. (1997): "The Canadian MC2: A semi-Lagrangian, semi-implicit wideband atmospheric model suited for finescale process studied and simulations", Monthly Weather Review, 125, 2382-2415.

Benoit, R. et al. (2000): "Toward the use of Coupled Atmospheric and Hydrologic Models at Regional Scale", Monthly Weather Review. 128(6). 2000. 1681-1706.

Giorgi, F., Bates, G. T. (1989). " The Climatological Skill of a Regional Model Over Complex Terrain". Mon. Wea. Rev., 117, 2325-2347.

Gurtz, J. K. et al. (2000) Application of Hydrologic Models for RAPHAEL. Runoff and Atmospheric Processes for Flood Hazard Forecasting and Control: Final Report. June 2000. Section 2.4 "Runoff and Atmospheric Processes for flood HAzard forEcasting and controL", RAPHAEL Final Report, EU Contract ENV 4-CT97-0552. Kouwen, N. and J. Innes contributors. Ed. By B. Bacchi and R. Ranzi. June 2000. 344 pages.

Hamlet, A. F., Lettenmaier, D. P. (1999): "Effects of Climate Change on the hydrology and Water Resources in the Columbia River Basin. J. American Water Resources Assoc., 35(6): 1597-1623.

Ji, M., Kumar, A., Leetmaa, A. (1994). "A Multiseason Climate Forecast System at the National Meteorological Center". Bull. Amer. Meteor. Soc., 75, 569-577.

Kim, J. et al. (1998). "River Flow Response to Precipitation and Snow Budget in California during the 1994/95 Winter", Journal of Climate, Vol. 11, 1998, 2376-2386.

Kouwen, N. et al. (1993): "Grouping Response Unit for Distributed Hydrologic Modelling", ASCE Journal of Water Resources Management and Planning, 119(3), May/June: 289-305.

Kouwen, N. (2000): " WATFLOOD Users Manual". Department of Civil Engineering, University of Waterloo. (Available at http://www.watflood.ca, 2001)

Kouwen, N., Innes, J. (2001) Coupled MC2-WATFLOOD Flood Forecasting. Hydrological Aspects in the Mesoscale Alpine Programme-SOP Experiment, Edited by R. Ranzi and B. Bacchi. University of Brescia, Department of Civil Engineering, Technical Report Number 10.

Kouwen, N. et al. (2000): "The Creation of the Drainage Layer Database of the WATFLOOD Distributed Hydrologic Model over the Trent-Severn Waterway". Department of Civil Engineering, University of Waterloo.

Leung, L. R. et al. (1999): "Simulations of the ENSO Hydroclimate Signals in the Pacific Northwest Columbia River Basin". Bull. American Meteoologicals Soc., 80(11): 2313-2330.

Liu, M. L. (2001): "Flood Alert Based on Linked Numerical Weather and Hydrological Models", MASc. Project Report, Department of Civil Engineering, University of Waterloo, Waterloo, ON., Canada.

PCI Geomatics, (1998). EASI/PACE Users Manual, Version 6.3. PCI Geomatics, Ontario, Canada.

Volkert, H., 1990: "An Alpine Orography Resolving Major Valleys and Massifs", Meteorol. Atmos. Phys. 43:231-234.

Wen, L. et al. (2000). "The Role of Land Surface Schemes in Short-Range, High Spatial Resolution Forecasts", Monthly Weather Review, Jan., 49-61.

FLOOD RISK ZONING AND LOSS ACCUMULATION ANALYSIS FOR GERMANY

Wolfgang Kron[1], Winfried Willems[2]

[1] Geo Risks Research Dept., Munich Reinsurance Company, Königinstrasse 107, 80791 Munich, Germany, wkron@munichre.com

[2] Institute for Applied Water Resources and Geoinformatics (IAWG), Alte Landstrasse 12-14, 85521 Ottobrunn, Germany, willems@iawg.de

SUMMARY

Worldwide, flood is the number one cause of losses from natural events. Besides public and individual measures, insurance is a key factor in reducing the flood risk of individuals, enterprises and even whole societies. In recent years, flood insurance has become an important topic and the increasing demand for cover is forcing the insurance industry to develop solutions. At the same time it is vital for the insurers to know the probable maximum losses that they might face as the result of an extreme event.
In contrast to natural hazards such as windstorm, flooding typically affects certain areas with a higher frequency than others. Therefore the specific flood risk of different areas has to be assessed. Three risk zones were chosen corresponding to a low, moderate and high exposure. To identify the zones, the discharges in rivers for given recurrence intervals are determined and then transformed into flooded areas by using stochastic hydrologic regionalization, a digital elevation model and a simple, one-dimensional hydraulic model.
For accumulation control, probable maximum losses during extreme floods must be computed. This is done by superimposing land-use data and liability information on flooded areas using a Geographic Information System (GIS) and applying average loss ratios. Five flood recurrence intervals are considered. As it is extremely unlikely that a flood event will hit all or most of Germany at one and the same time, eight independent regional loss accumulation zones have been defined. The accumulation analysis is carried out separately for each of these zones.

Keywords: Flood types, flood disasters, flood losses, flood insurance, flood zonation, probable maximum losses

1 INTRODUCTION

In most parts of the world, flooding is the leading cause of losses from natural phenomena and is responsible for a greater number of damaging events than any other type of natural hazard. Roughly half of all losses due to nature's forces can be attributed to flooding. Flood damage has been extremely severe in recent decades and it is evident that both the frequency and intensity of floods are increasing. In the past ten years losses amounting to more than US$ 250bn have had to be born by societies all over the world to compensate for the consequences of floods. There are countries, such as China, in which flooding is a frequent, at least annual event, and others, such as Saudi Arabia, where inundation is rare but its impact sometimes no less severe. No populated area in the world is safe from being flooded. However, the range of vulnerability to the flood hazard is very wide, in fact wider than for most other hazards. Some societies (communities, states, regions) have learnt to live with floods. They are prepared. Others are sometimes completely taken by surprise when a river stage (or the sea) rises to a level neighbouring residents have never experienced before in their lives.
The dramatic increase in the world's population and in particular in certain regions creates the necessity to settle in areas that are dangerous (Kron, 1999a). Additionally the movement of political, social and other refugees, increased mobility and the attractiveness of areas that have a beautiful natural environment and a mild climate lead to people settling at places whose natural features they do not know. They are not aware of what can happen and they have no idea how to behave if nature strikes.
During the last few decades many flood plains have been occupied by residential areas and industrial parks. These areas are usually flat and not necessarily good for agricultural use. The nearby rivers have been tamed and confined in narrow strips by dikes, and cheap and attractive land has been reclaimed. Towns and villages declared these areas residential areas and, therefore, many potential buyers of property counted on there being no flood hazard to be feared. These are the underlying reasons why flood catastrophes are becoming more and more frequent and severe, although protection and preparedness measures have been improving. Besides public and individual measures,

insurance is an important factor in reducing the risk of individuals, enterprises and even whole societies from natural hazards. Proper insurance can considerably mitigate the effects of extreme events on them and avoid their being ruined.

2 TYPES OF FLOOD

In insurance contracts, flooding is defined as a temporary covering of land by water as a result of surface waters escaping from their normal confines or as a result of heavy precipitation. When it comes to insurance cover it is very important to distinguish between the different causes for flooding. There are three main types of flood and a number of special cases (Munich Re, 1997). The main types are: storm surges, river floods, and flash floods; special cases include tsunami, waterlogging, backwater (e.g. caused by a landslide that blocks a water-course), dam break floods, glacial lake outbursts, groundwater rise, debris flow events and others.
Storm surges can occur along the coasts of seas and big lakes. They bear the highest loss potential of water-related natural events, both for lives and for property. Improved coastal defence works have prevented huge losses in developed regions during the recent past, but the loss potential of storm surges remains very high.
River floods are the result of intense and/or persistent rain for several days or even weeks over large areas sometimes combined with snowmelt. The ground becomes fully saturated and the soil's capacity to store water is exceeded. It behaves as if it were sealed and the precipitation runs off directly into creeks and rivers. The same effect is produced by frozen ground, which also prevents the water from infiltrating the soil. River floods build up gradually, though sometimes within a short time. The area affected can be very large in the case of flat valleys with wide flood plains. In narrow valleys the inundated area is restricted to a small strip along the river, but water depths are great and flow velocities tend to become high, with the result that mechanical forces and sediment transport play a major role as a cause of damage. Although inundation due to river floods starts from a water-course and is somewhat confined to its valley, the areas affected can be far greater than those hit by storm surges.
Flash floods sometimes mark the beginning of a river flood, but mostly they are local events relatively independent of each other and scattered in time and space. They are produced by intense rainfall over a small area. The ground is not usually saturated, but the infiltration rate is much lower than the rainfall rate. Typically, flash floods have an extremely sudden onset. A surge may rush down a valley that does not even have a creek at its bottom. Such a flood wave can propagate very quickly to locations some tens of kilometres away, where the rainstorm is not even noticeable. From this fact comes the – probably true – saying that "in a desert more people drown than die of thirst". Forecasting flash floods is almost impossible, with lead times for early warnings in the order of minutes. Although flash floods usually occur in a relatively small area and last only a few hours (sometimes minutes), they have an incredible potential for destruction.

3 STATISTICS OF FLOOD DISASTERS

Reinsurance companies, due to their worldwide activities, are among the best sources for natural disaster statistics (Kron, 2000). Their analyses focus on three aspects: the number of people affected (fatalities, injured, homeless), the overall economic damage to the country hit, and the losses covered by the insurance industry.
Natural disasters with thousands of deaths almost always hit poor countries and are mainly caused by earthquakes. The poverty aspect is related to the higher vulnerability in less developed countries (poorer quality of structures, more people), the cause (earthquakes) to the sudden onset of such events, which strike without warning. In the past (more than 10 years ago), floods were responsible for a huge number of deaths. This is not so anymore today, because early warning methods have become more operational, more reliable and hence more effective.
In the statistics of economic losses floods take a leading position. While two earthquakes (Kobe: US$ 100bn; Northridge: US$ 44bn) still have been the costliest natural disasters so far, floods, which usually affect much larger areas than earthquakes and occur much more frequently, have at least the same importance. Not only the great disasters, but also the vast number of small and medium-sized events cause tens of billions of dollars of losses every year for economies and severe distress to people. Probably, floods are responsible for more damage than all other destructive natural events together. Additionally, the financial means societies all over the world spend on flood control (sea dikes, levees, reservoirs, etc.) is a multiple of the costs they devote to protection against other impacts from nature.

Table 3-1 shows the greatest flood losses in recent years. It is apparent that China is the country who's economy suffers most and most regularly from such disasters, although it must be admitted that the numbers for China listed in the table are subject to high uncertainty and are aggregate values for the whole country, i.e. summarized for floods in different regions. It also becomes clear that great flood losses can occur in practically any region of the world.

Table 3-1: The costliest floods of the past 10 years (original values, not adjusted for inflation).

rank	*year*	*country/-ies (mainly affected regions)*	*economic losses US$ bn*	*insured [%]*
1	1998	China (Yangtze, Songhua)	31	3
2	1996	China (Yangtze)	24	2
3	1993	USA (Mississippi)	21	6
4	1995	North Korea	15	0
5	1993	China (Yangtze, Huai)	11	0
6	1994	Italy (North)	9.3	<1
7	1993	Bangladesh, India, Nepal	8.5	0
8	2000	Italy (North), Switzerland (South)	8.5	6
9	1999	China (Yangtze)	8	0
10	1994	China (Southeast)	7.8	0
11	1995	China (Yangtze)	6.7	1
12	2001	USA (Texas)	6.0	58
13	1997	Czech Rep., Poland, Germany (Odra)	5.9	13

The insured share of flood losses from these big events is relatively small. For the insurance industry windstorms are clearly the most critical loss events, simply because the insurance density is highest for this type of peril. However, a tendency to higher insurance density for flood is observed worldwide and, in particular, a tendency to extreme losses due to water. As an example may serve tropical storm Allison that drenched the Houston/Texas area with over 750mm of rain in just five days in June 2001 and caused insured losses of US$ 3.5bn. With economic losses of US$ 6bn this event ranks 12 in Table 3-1 and has an insured share of almost 60%.

Recent large flood events in Europe reveal some factors that influence the extent of flood losses. In December 1993 and in January 1995 the Rhine River – and some of its tributaries – experienced two extreme floods with recurrence intervals of more than 50 years in its middle and lower reaches. The economic losses from the second event (US$ 320m) were only about half as big as those from the first (US$ 600m), although the two events were of comparable size. One of the main reasons for this difference was the fact that the previous flood was still in people's minds, i.e. they knew what to do when the water rose, and some lessons had been learnt and put into action (e.g. replacing oil burners and tanks by gas heating).

Practically no lessons were learnt in Italy from the 1994 event. Like before 1994, settlement behaviour in Italy is far from being surveyed and controlled effectively. Many houses are built very close to torrent-type creeks and rivers. They were destroyed by the raging waters, in 1994 and again in 2000. Besides flooding many areas, the torrential rainfall in October 2000 – up to 740 mm in four days at some locations – also triggered numerous disastrous landslides and debris flows.

Italy is not an atypical example though. The situation in other countries concerning land-use is not good either. The floods in the United Kingdom in fall 2000 led to various political initiatives with the aim of stricter land-use regulations, and the very same aspects were discussed in Germany after the May flood of 1999 in southern Bavaria.

4 INSURANCE PROBLEMS ASSOCIATED WITH FLOODS

The basic problem in flood insurance is the difference in the demand for cover from potential clients who are exposed to flooding and the offer made by the insurance sector (Kron, 1999b). Most people have a certain – and they think good – perception of the flood hazard they are exposed to. The ones who have already experienced flooding on their property are aware of the threat, others – even if they live close to a river – ignore the danger or just do not believe that they can be affected at all. Often their perspective is wrong though. About half of all losses from floods occur far away from major rivers and outside major events that hit large areas and whole river systems. Instead, these loss events

(flash floods) occur in relatively small areas, but with potentially extreme intensity and with high frequency (although not at the same site). Even property on the slopes high above the valley floor may be damaged by excessive rainfall that runs off on the surface and right into the houses. If this is made known to the majority of the people, the conditions for effective flood insurance are good.
To river floods, only a relatively small proportion of the cover for buildings and contents in any given insurance market is exposed. However, the areas affected are always the same and flooding on a specific river occurs at almost regular intervals and cannot be regarded as an unforeseeable event. Only people in these flood-prone areas seek insurance. On the other hand, those whom the insurance companies are willing to give cover are not interested, because they feel their exposure is low. Hence, if an insurance company wished to sell individual policies on a voluntary basis, the insurance premiums would have to be so high that policyholders would normally find them prohibitive. This phenomenon is called *adverse selection* or *antiselection*.
In the case of the storm surge hazard the effect of adverse selection is even more severe. Furthermore, the extremely high loss potential during a single event in connection with a very low probability that it happens, makes the calculation of premiums difficult (this is the problem of multiplying a very low and a very high number or "zero" times "infinity"). Therefore storm surges are, in general, not insurable.
In contrast to this, flash floods have a relatively uniform probability in time and space. The necessary geographical spread of risks is given and the community of insureds is large, i.e. the frequency of someone being hit by an extreme event is low. As a consequence, the premiums can be kept low, too. Consumer demand for insurance protection could be developed on a broad front, and adequate premiums can be calculated with a relatively high degree of reliability. Hence, flood damage caused by flash floods is insurable without any problem.
There is no reasonable insurance solution that can possibly make insurance companies settle all the losses that may be incurred. Instead, a certain amount has to be borne by the insureds before the insurance becomes effective, i.e. deductibles must be introduced. Such a structure has advantages for both the insurer and the insured. On the one hand, the insurer does not have to settle masses of small losses and saves – besides loss compensation money – a lot of administrative costs. On the other hand, the client may only become insurable at all if he pays a share of the losses.

5 FLOOD ZONATION

Premiums for flood insurance must reflect the individual exposure. It would be unfair and inexplicable to clients if each member of an insured community had to pay the same premium not taking into account the individual risk his property is exposed to. In mass business – i.e. for private homes and small businesses plus their contents – the effort required to assess the exposure of a certain building must be seen in the context of the annual premium income for one such object, which is in the range of perhaps US$ 50–100. Therefore, an individual assessment of the risk and the calculation of an individual premium for these objects are impossible, so that the premium must be fixed on the basis of a flat-rate assumption. For this, zones with a similar flood risk must be identified and/or defined, within which the premiums are constant.
The German insurance industry recently established a rating system that defines the exposure of all areas of the country to river floods according to three exposure classes:

I	small exposure	Areas that are affected less that once per 50 years on average; objects there are insurable without restriction.
II	moderate exposure	Areas that are affected by floods in the recurrence interval range of 10 to 50 years. Objects in these areas are basically insurable.
III	high exposure	Areas on flood plains that are affected by floods with recurrence intervals of up to 10 years; objects in these areas are in general not insurable, but under certain conditions they may become so.

This zonation does not consider the storm surge and flash flood hazards. The first type of flooding is not associated with rainfall and restricted to a relatively small area along the coasts. The risk from the latter is assumed to be uniform all over Germany, because the spatially varying extreme rainfall intensities are thought to be more or less compensated by the required design assumptions for storm water systems and river works, and natural water-courses have also usually adapted a regime that reflects the local hydrologic situation. As a consequence, in regions with higher rainfall intensities the discharge capacities of the drainage systems and channels are also higher.
Flood zonation is a tedious and difficult task. In order to come up with a zonation system that covers the whole of Germany, the areas along all significant water-courses had to be considered. These were defined by the so called "ArcDeutschland" river network (scale 1:500,000; total length of the rivers

included: 35,110 km), which was digitally available for the whole area of Germany. The required task was to (a) provide different T-year discharges in and (b) compute the corresponding water levels and flooded areas at any cross-section of each of the chosen water-courses. The hydrological and hydraulic computations were carried out by the Institute for Applied Water Resources and Geoinformatics (IAWG) with the help of a Geographic Information System (GIS).

5.1 Hydrology: discharges

Basically, frequency analysis of discharge values can only be performed for gauged locations. As extreme discharges have to be known for every cross-section of each German river, a regionalization procedure had to be developed. First, series of annual discharge maxima for 322 selected gauges of three German regions (248 Bavaria, 29 Rhineland-Palatinate, 45 Lower Saxony) were fitted by the five-parameter Wakeby or the three-parameter Pearson distributions (Kleeberg et al., 1998). Parameters were estimated using L-moments. The model chosen consisted of two steps: the first part connected the drainage area A_E at a given river cross-section to the cumulative length L_c of all water-courses upstream of the regarded point, where L_c could be determined with the GIS using the digital river network. In a second step the actual regression for the discharge quantiles was executed, in which the independent variable was A_E (derived in the first part of the regression from L_c). The simple model used linear regression with T-year discharge $Q_T = 0$ for $A_E = 0$. The samples for determining the coefficients were weighted by their size. The obtained coefficient of determination for $A_E=f(L_C)$ was r^2 = 0,9566 at a significance level of 99.9%. Including other variables such as mean annual rainfall and parameters describing topographical features did not improve the goodness of fit and were therefore discarded. With this regression relationship quantiles could be obtained for any given point along the river network corresponding to the return periods of $T = 10$ and 50 years.

5.2 Hydraulics: flooded areas

On the basis of the discharge values thus derived the corresponding flood stages and the flooded areas could be calculated. As data and computing time were limiting factors, simplifying assumptions concerning the underlying physics had to be made. Channel cross-sections and local slopes were extracted from a digital elevation model of Germany (DHM-M745, scale 1:50,000, horizontal resolution 30 m). Profiles were taken at about every 100 m orthogonally to the flow direction; in this way more than half a million cross-sections had to be considered. Existing flood control measures (e.g. dikes) were not taken into account.
The hydraulic calculations were performed with a simple, one-dimensional, stationary hydraulic model based on the Manning-Strickler relationship. Manning's n was assumed to be constant for all rivers with values of $n = 0.04$ for the 10-year scenario and $n = 0.067$ for the 50-year scenario. Flooded areas along the rivers were obtained by interpolating between the flow-widths at the profile locations considered. Once this step had been completed, the flooded areas were known for the different flood scenarios all over Germany. The accumulated area of the 50-year flood zones amounted to 16,437 km^2, which was 4.5% of Germany's total area of 356,974 km^2.
In cooperation with the German State Water Authorities, the model results were corrected according to locally available better knowledge. For example, flood control measures such as dikes and retention basins were taken into account. The final result was two digital maps of Germany displaying all 10-year and all 50-year flood areas.

5.3 Flood exposure zones

The insurance industry of Germany represented by the German Insurance Association (GDV) took these areas and superimposed on them administrative information on the location of objects to be insured. The original coarse approach using post code areas was successively refined to a quite sophisticated system of address groups corresponding to reaches of streets. The average length of these reaches was in the order of 200 m. With this system called ZÜRS (Zonation System for Flood, Backwater and Intense Rainfall) any given address can now be attributed to one of the three flood exposure zones. Stored in a table on his laptop, it allows the insurance representative to immediately identify the exposure of his client to flooding.

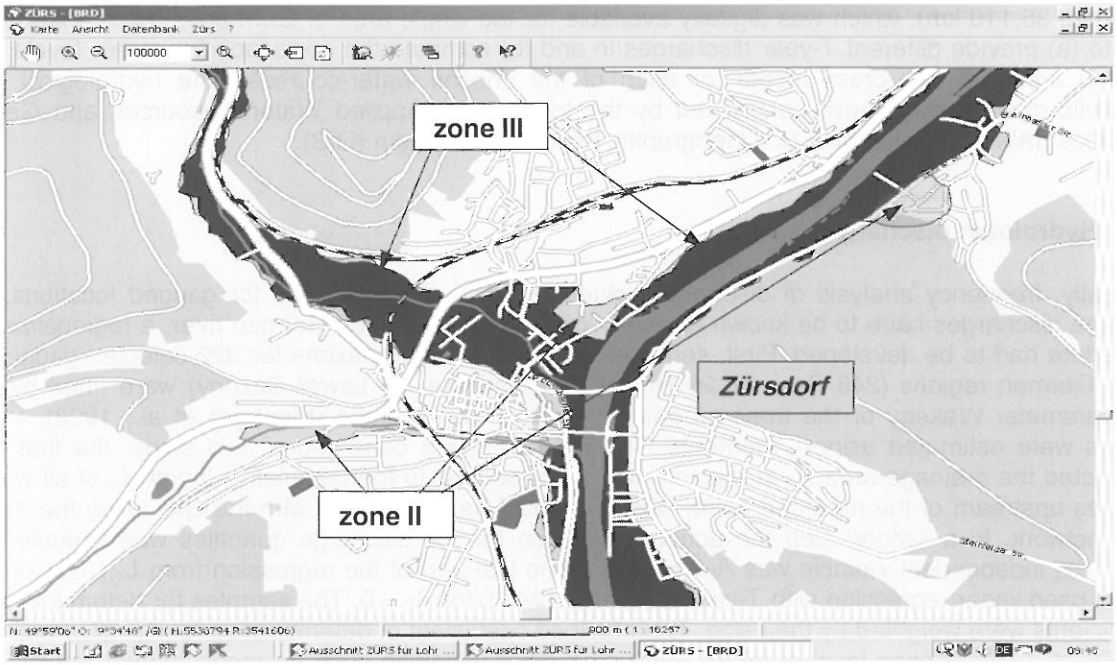

Figure 5-1: Example of a ZÜRS flood zone map (courtesy of German Insurance Association, GDV).

6 FLOOD PML ASSESSMENT FOR GERMANY

Like clients, insurance – and reinsurance – companies must protect themselves against high losses in order to assure their survival. Therefore, they are required to perform accumulation control, i.e. assess the probable maximum loss (PML) they may experience during an extreme event. Each company must decide on the reserves it needs and its reinsurance requirements. PML calculations are based on scenarios that assume a major event hitting a large area or an area with a high concentration of values. It is not obvious beforehand which scenario will determine the worst case for a given company as the expected losses depend on the company's portfolio, and particularly on the spatial distribution of its liabilities. For each company a different scenario may determine the PML.

PML models have been available for many years as a means of calculating maximum losses from earthquakes and windstorms. For the analysis of floods, such tools were not available until recently. Flood events are much more influenced by small-scale and local aspects, which include soil conditions and topography, the exact location of objects (elevation) and the effectiveness of flood control measures. Therefore, such models require considerably more detail and sophistication.

A model developed more or less parallel to the zonation model described above makes it possible for the first time to carry out accumulation analyses of flood events occurring in Germany. Eight different accumulation scenarios were chosen. The aim is to determine what liabilities of a given portfolio are affected and to estimate the probable losses for fictitious 10-year to 200-year flood scenarios.

The flood PML model considers only river floods. Flash floods after torrential rain are not included on account of the fact that they occur locally and therefore play a subordinate role in accumulation considerations. Floods caused by storm surges are not considered either since they are not insurable at present because of their gigantic loss potential.

In the PML analysis the potential of property damage is of interest. Therefore, the flooded settlement areas must be identified (spatial analysis). The expected losses are estimated based on the number of objects affected and on loss averages (portfolio analysis). The administrative units used are post code areas because portfolio data are aggregated in this form. The final step consists of summing up the loss values for all post codes in the regarded flood accumulation zone to obtain the probable maximum loss (accumulation analysis). The entire procedure consists therefore of five steps.

6.1 Hydrology: discharges

The hydrologic model component is practically identical to the one already described, with the difference that the discharges for three additional recurrence intervals (20, 100, 200 years) have to be determined. In the PML analysis it is no longer of interest which exposure a certain object has, but how many objects are flooded. The identification of the respective areas is based on the assumption that the *T*-year flood discharge occurs simultaneously along all water-courses of the considered river network. The assumption of simultaneity is justified although such a scenario is not possible in reality. The probability that this will happen in any one year is close to *1/T* only for small catchments. The larger the area and the corresponding river network, the smaller the probability that a *T*-year flood will occur everywhere at the same time. A 100-year flood peak in each of two rivers, for instance, will practically always generate a flood peak with a much lower frequency than once in 100 years downstream of their confluence. However, if the simultaneity condition is somewhat relaxed, it is theoretically possible that a 100-year peak will pass any location of a river basin during a single flood event, e.g. during a period of several days. Flood scenarios that comprise areas of several thousands of square kilometres cannot be associated with a probability of one in 100 years; their occurrence probabilities are much smaller.

6.2 Hydraulics: flooded areas

The second step, hydraulics, too is very similar to the one in the zonation model, except that flood control measures are not taken into account. While such measures may play a decisive role, in particular in scenarios with short return periods (10, 20, and possibly 50 years), dikes may also fail; and having the PML in view the possibility of failure becomes important. Using the direct output of the model also has the advantage that it may be updated more easily. The tedious manual work of incorporating the effects of flood control measures is thus avoided.

6.3 Spatial analysis: flooded settlement areas

The insured values can be assumed to be located within the boundaries of settlements. By integrating land-use information and superimposing it on the flooded areas by means of a Geographical Information System, the settlement areas affected by flooding can be identified. Insurance data are usually aggregated on the basis of administrative areas, typically post code areas. In Germany the five-digit post code areas are used, which are about 10,000 in number. This information is very rough when dealing with floods, but it is the only data base available and had therefore to be used. So far no distinction has been made between different types of settlement areas, although the information – in the form of GIS layers – is available. A refined breakdown into residential, commercial and industrial areas for the accumulation analysis of different classes of insurance is planned for the future. The result of the spatial analysis is a percentage of settlement area flooded within each post code zone and for each scenario.

6.4 Portfolio analysis: affected insurance contracts

The distribution of liabilities in the portfolio to be analysed is supplied by the insurer in the form of aggregated figures for each of the five-digit post code areas. The exact location of the insured objects is not known. Therefore one has to assume that the liabilities, i.e. the total sum insured within a post code zone, is distributed uniformly over the settlement area of this zone. For a single post code this assumption would definitely contain too much uncertainty. If however, as is the case in accumulation analysis, large regions are regarded with many post codes, the assumption of uniformly distributed liabilities is reasonable on average, particularly for mass business. Only in industrial business where relatively few objects with high concentrations of values at certain spots are regarded, this assumption may not be valid anymore. For a post code zone *i* the expected loss L_i for a given flood scenario is:

$$L_i = \frac{S_{f,i}}{S_i} \cdot r \cdot s \cdot (SI)_i \qquad (1)$$

where
L_i = total expected losses
$S_{f,i}$ = flooded settlement area
S_i = settlement area
r = loss frequency
s = average loss (in percent of sum insured)
$(SI)_i$ = total sum insured (liabilities)

All terms in the equation except the sum insured are subject to the respective scenario. The term "loss frequency" accounts for the fact that not each building located within the flooded area will suffer damage. Some objects are on a – maybe artificially – elevated position that is not shown in the digital elevation model, others may successfully apply individual flood control measures and thus avoid damage. In the term "average loss", which is given as a percentage of the total value of a building (or its contents), the results of extensive loss analyses and the experience on loss susceptibility in the different classes of insurance gathered over the years are incorporated.

6.5 Accumulation analysis: probable maximum loss

The last step in the analysis reveals the probable accumulation losses in different loss accumulation zones (LAZ's) for the portfolio under consideration. The accumulated losses are found by simply adding the losses expected in each post code area within a LAZ. It is extremely unlikely that a flood event will hit all or most of Germany at one and the same time. Extreme events are usually limited to specific regions, e.g. individual river basins. Consequently, loss accumulation zones had to be defined. It seemed reasonable to choose eight such zones (Figure 6-1). Five of them correspond to Germany's large river basins (Rhine, Danube, Odra, Elbe, Weser-Ems). Three further zones (South, Central, North) were defined as being zones that comprise parts of more than one basin. The central zone, for instance, embraces – besides the northern sub-catchments of the Danube in Bavaria – the catchment areas of the Main and Neckar, the areas on the left bank of the Rhine north of Karlsruhe, and the Middle and Lower Rhine Valley. This zone corresponds approximately to the area mainly affected in the 1993 Christmas flood.
The accumulation analysis is carried out separately for each of these loss accumulation zones. Fictitious events based on the modelled discharges serve as scenarios. For example, in the 100-year scenario 100-year discharges are assumed along all rivers in the loss accumulation zone being analysed. This produces a probable accumulation loss for every scenario. The resulting values are plotted on a PML graph that shows the losses for each scenario and forms the central result of the analysis (Figure 6-2). The critical region for the portfolio examined in Figure 6-2 is LAZ 4 (Elbe), and the probable maximum loss is about *€ 2.0m.*
There are, of course, limits of this kind of analysis. The various components (regionalization procedure, digital elevation model, river network, hydraulic model, allocation of liabilities, loss averages, etc.) are each subject to quite a high degree of uncertainty. The model's accuracy is therefore certainly not sufficient for local consideration of the flood risk. However, the spatial resolution and the accuracy of the information in the individual components of the flood model are geared specifically to the question of accumulation control and therefore treatment of large areas. Small-scale observations are not intended, let alone risk assessment for individual objects. Finally, as mentioned already, the applied discharge return periods cannot be compared directly with loss return periods and are therefore of restricted use in the process of premium calculation.

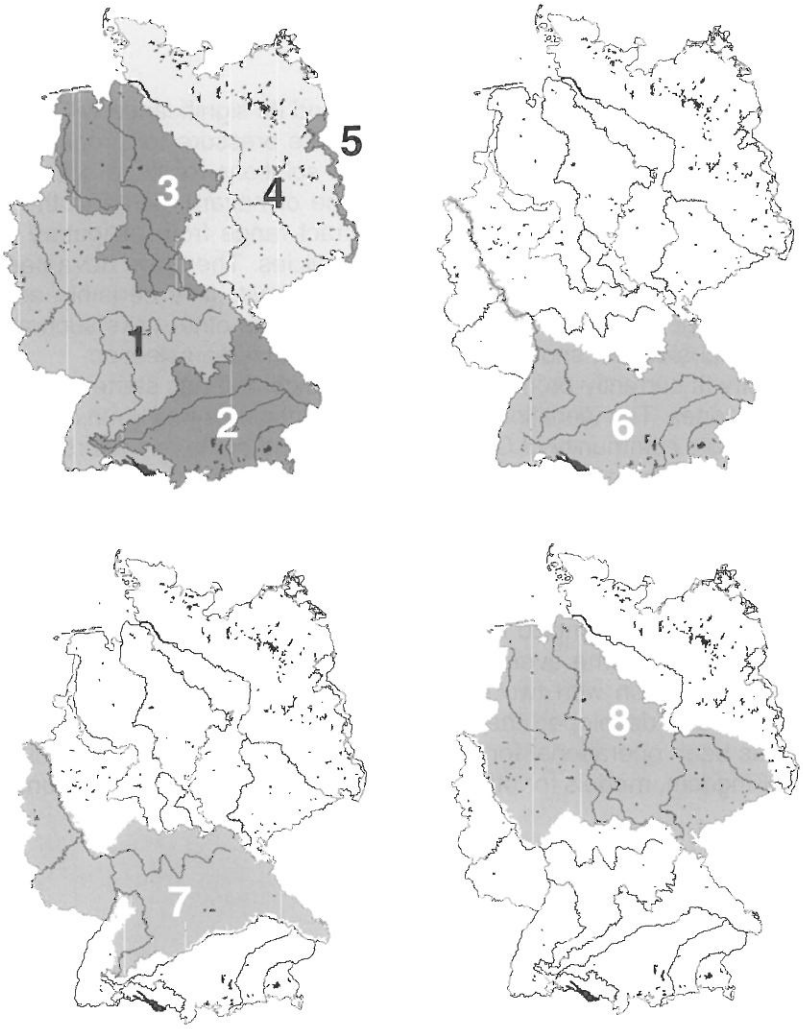

Figure 6-1: Loss accumulation zones (LAZ's) for Germany
1 Rhine, 2 Danube, 3 Weser-Ems, 4 Elbe, 5 Odra, 6 South, 7 Central, 8 North.

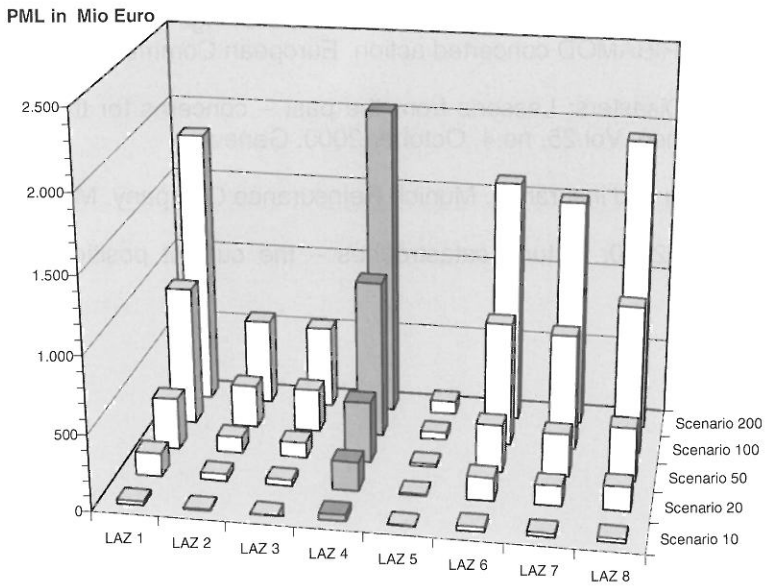

Figure 6-2: Probable maximum losses (PML) for eight loss accumulation zones (cf. Figure 6-1) and five flood scenarios corresponding to 10- to 200-year discharges.

7 CONCLUSION

Flooding has become an important topic for the insurance industry and its significance will continue to grow in the future. The increasing demand for insurance cover and the pressure for proper insurance concepts from all sides is forcing the insurance industry to develop solutions for flood cover. Various countries have already established insurance schemes for this type of hazard, some in the form of insurance pools, others on an individual basis. The types of contract range from obligatory to completely voluntary coverage, and from all-risk policies to flood-only policies. There are advantages and disadvantages in all these concepts and none can be declared the best. It is certainly advisable, however, to offer multi-hazard packages, thus combining the flood risk with other risks such as earthquake, landslide, windstorm, hail, subsidence, snow-load, etc. to avoid adverse selection.
In Germany, the insurance industry is currently promoting flood insurance and has started to tackle the problem by establishing flood risk zones. The identification of the different zones has been achieved in a concerted action not only by the whole community of German insurers (and some reinsurers) but also in close cooperation with public water resources authorities. Despite the fierce competition in the market the intention is clearly to come up with a unique zonation system valid for all companies that will even help the state in its efforts to enforce land-use planning that is compatible with the flood hazard.
Parallel to the primary insurers that need risk zoning for the purposes of acquisition and designing a premium structure, reinsurers – as part of their service to the primary insurance companies and in the interest of their own business – need risk zoning to calculate the expected losses that the insurance industry might face as the result of an extreme event threatening a company's existence. It was with this in mind that Munich Re in cooperation with two universities and the Institute for Applied Water Resources and Geoinformatics (IAWG) developed the world's first flood loss accumulation model for an entire country. The model has been operational for Germany since 1999. A similar model has just been developed for the United Kingdom, models for other countries will most likely follow soon.

REFERENCES

Kleeberg, H.-B. et al. (1998): Geoinfosystem "Überschwemmung Deutschland" (Geoinformation system "Flood Germany"). Report (in German) to Munich Reinsurance company. Unpublished

Kron, W. (1999a): The development of exposed areas. In: topics 2000: Natural catastrophes – the current position. Munich Reinsurance Company. Munich

Kron, W. (1999b): Insurance aspects of river floods. In: Proceedings of the European Expert Meeting on the Oder-Flood 1997 – RIBAMOD concerted action. European Communities. Luxembourg

Kron, W. (2000): Natural Disasters: Lessons from the past – concerns for the future. The GENEVA Papers on Risk and Insurance. Vol.25, no.4, October 2000. Geneva

Munich Re (1997): Flooding and insurance. Munich Reinsurance Company. Munich

Munich Re (1999): topics 2000: Natural catastrophes – the current position. Munich Reinsurance Company. Munich

A NATIONAL SYSTEM FOR FLOOD FREQUENCY ESTIMATION IN GREAT BRITAIN USING CONTINUOUS CATCHMENT SIMULATION: CONFIDENCE AND UNCERTAINTIES

Robert Lamb, Ann Calver and Alison L. Kay

Centre for Ecology & Hydrology, Wallingford, Oxfordshire, OX10 8BB, UK, rla@ceh.ac.uk, anc@ceh.ac.uk

SUMMARY

Continuous river flow modelling is being developed as a method for flood frequency estimation in Great Britain. The basic principle of the approach is to use conceptual rainfall-runoff modelling to generate synthetic flow data, from which information about flood frequencies can be extracted. One important aspect of the modelling methodology is the generalisation, or regionalisation, of rainfall-runoff model parameters to allow application at ungauged sites. Relationships have been sought between model parameters and catchment properties, based on parameter values established at a sample of gauged sites where 'as-ungauged' model performance can later be assessed.
This paper presents a method for estimating uncertainty in modelled flood data for the situation where the spatially generalised rainfall-runoff model parameters are used. Approximate confidence intervals can be constructed by Monte Carlo simulation. Results are presented to assess the confidence in flood frequencies estimated using continuous simulation, including comparisons with site-specific flow statistics.

Keywords: flood estimation, uncertainty, ungauged site, regionalisation

1 INTRODUCTION

This paper explores the calculation of uncertainty in modelled estimates of river flows, and, in particular, of flood frequencies. It presents a generalised approach to estimating river flood frequencies based on rainfall-runoff modelling. The modelling is on a continuous time basis and the estimation procedure is generalised to be applied at ungauged sites as well as those with calibration data.
The method is generic in principle. It may be viewed as the 'next generation' flood frequency estimation methodology following the Flood Studies Report (Natural Environment Research Council, 1975) and the Flood Estimation Handbook (Institute of Hydrology, 1999) which provide methods based on statistical analyses and event-based hydrograph approaches. Whilst continuous simulation can be applied at a detailed level for specific catchments, this paper focuses on spatially-generalised application (and associated uncertainties) whereby modelling is applied for any site, gauged or ungauged.

2 MODELS AND CALIBRATION

In principle, any appropriate rainfall-runoff model can be used to simulate flood responses in a particular catchment. For a national system, to be used for ungauged as well as gauged sites, certain considerations become important in choice of model. For the runoff models that are ultimately to be used for sites without flow data, generality of model structure is clearly important, but this must be balanced with parametric efficiency to mitigate problems of parameter uncertainty. This becomes especially significant when attempting to relate model parameters to catchment properties data because functional dependence between parameters can lead to great uncertainty in the derivation of the required empirical relationships. In the work reported here, two runoff models developed at the Institute of Hydrology were used, the Probability Distributed Model (PDM) of Moore (1985, 1993) and the Time-Area Topographic Extension (TATE) model of Calver (1993, 1996). These both have a variety of formulations and have been used in flood frequency modelling contexts with three to seven parameters. Both are conceptual stores-and-transfers hydrological models with an interpretation in physical process and utilise distribution functions to summarise spatial distributions of catchment runoff production.
Rainfall and river flow data from 40 gauged sites in Great Britain were used for model calibration. These calibration data are at an hourly time resolution. This was selected as a practical compromise for use over the set of catchments ranging in scale from 1 km^2 to 532 km^2 (mean 156 km^2) and with typical response times, indicated by the unit hydrograph time-to-peak (defined for British catchments according to the Flood Estimation Handbook (Institute of Hydrology, 1999) variable $T_p(0)$) of 3 hrs to 24 hours (mean 8 h). The hourly time series used for model calibration consist of, on average, 9 years of continuous data at each site. In total, the data set comprises more than 300 station years of continuous hourly data.

The choice of calibration method for model parameters at each sample catchment is related in part to the way subsequent relationships to catchment properties are sought (see below). Problems of calibration uncertainty in hydrological modelling are well-known; pragmatic solutions are, however, required in order to offer flood frequency estimates in a generalised framework. The approach of establishing a single set of model parameter values for a particular catchment can be valuable, provided care is taken in the calibration process. In general the experience in this work is that when automatic 'optimisation' techniques are used to determine parameter values considerable benefit is gained from also reviewing the results using hydrological judgement.

Objective functions which have been found to be helpful in quantitative comparisons include those related specifically to flood peak magnitudes (Lamb, 1999) as well as to overall goodness of fit of modelled and observed flow time series. Calibration was carried out at each gauged site using a combination of computationally intensive uniform random sampling of a wide parameter space with visual 'eyeball' fitting of flood peaks and hydrographs. Numerical criteria for calibration were two objective functions, O_{peak} and $O_{monthly}$. Function O_{peak} was the summed absolute differences between flood peaks extracted from simulated and observed flow data,

$$O_{peak} = \sum_{i=1}^{n} |Q_i - q_i| \quad (1)$$

where Q_i is the magnitude of the i^{th}-ranking extracted peak in the observed flow record, and q_i is the i^{th}-ranking peak in the simulated flows. Peaks were extracted as a partial duration series with an implied threshold such that a total of $3L$ peaks would be available for a L-year period of record. Function $O_{monthly}$ was the Nash and Sutcliffe (1970) efficiency for the modelled monthly-averaged flows.

The trade-offs between different parameter values suggested by the two objective functions were then resolved by carrying out further calibration based on visual inspection of simulated and observed data. Although introducing a subjective element, this also allows a greater degree of hydrological judgement to be introduced than adopting a simple automated rule for the final selection of the parameter values.

Figure 2-1 demonstrates the level of calibration achieved by parameter sparse models (in this case the PDM) on two catchments of contrasting flood response. Flood frequency curves have been derived from the modelled time series using standard partial duration series analyses (Naden, 1992) here using Poisson distributions for arrival times of peaks and generalised Pareto distributions for magnitudes.

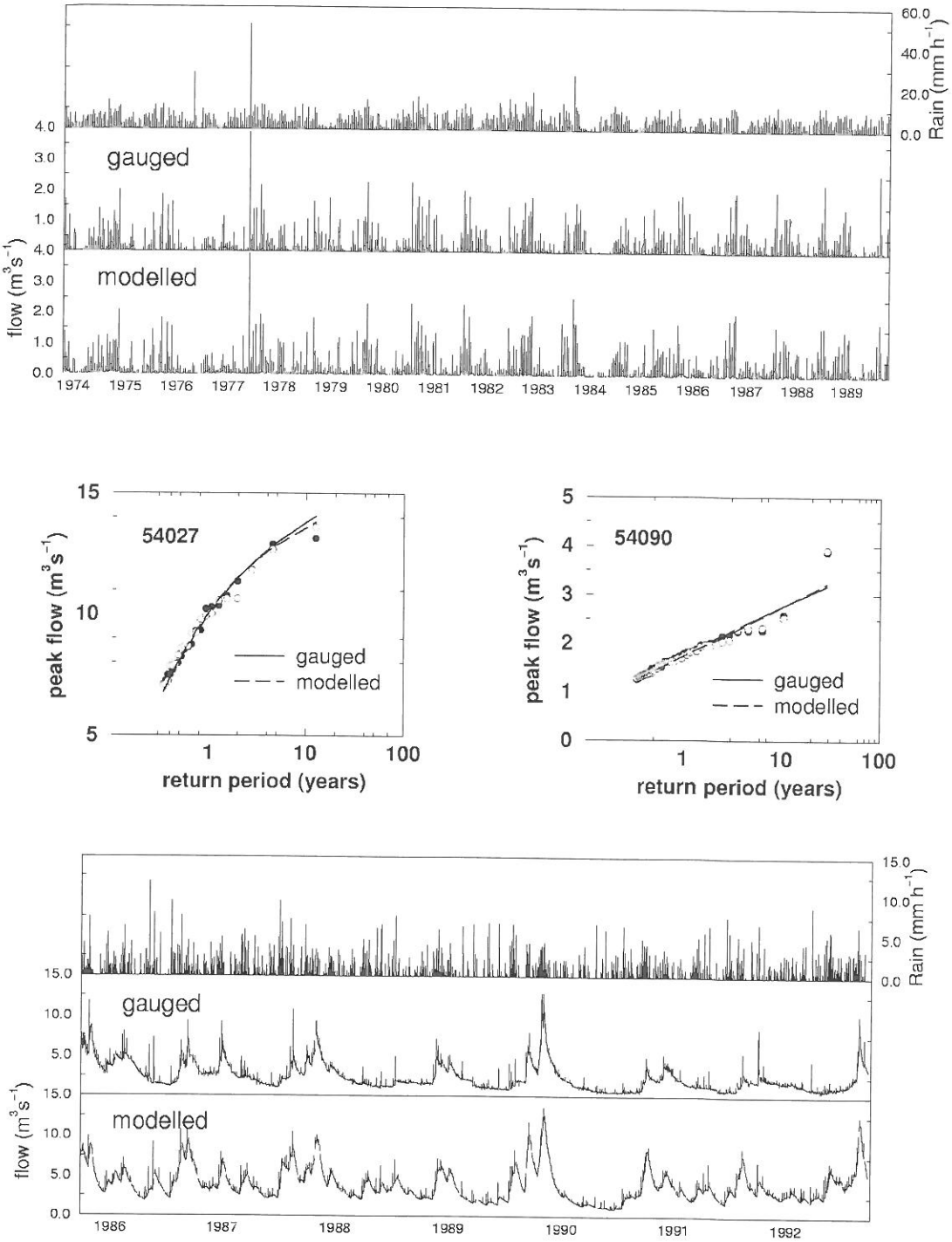

Figure 2-1: Calibration simulation results for two gauged sites of contrasting responses; (top, centre-right) 54090 the Tanllwyth, mid Wales and (bottom, centre-left) 54027, the Frome at Ebley Mill. Both simulations used the same simple, general conceptual model structure.

3 GENERALISATION TO UNGAUGED SITES

The catchment property data which allow generalisation of the method should ideally be easily obtainable, and offer physically plausible explanation of variance in calibrated model parameters. The major categories of catchment properties used were geological and soil material properties, catchment geometry and river network geometry indices, land-use and climate properties and standard hydrological indices (that can be derived without site flow data). Flood Estimation Handbook catchment descriptors are included. In practice, it may have to be accepted that some catchment properties

function in a surrogate rather than in a direct way and, in doing so, may combine the effects of some less succinctly expressed properties.
Pilot study results of applying univariate multiple regression to relate single 'best' estimates of model parameters to catchment properties were reported by Calver et al. (1999). This approach necessarily assumes that model parameters are independent, which is not entirely the case. In the univariate approach, calibrated values of model parameters at gauged sites are essentially treated as if they were 'independent observations' of the parameters.
A new 'sequential generalisation' approach aims to account for parameter covariance with few restrictive assumptions. In this approach the model parameter predictor equations were derived sequentially, accounting for effects that generalisation of earlier parameters have on later parameters. The approach is outlined in Figure 3-1, and more detailed descriptions can be found in Crewett et al. (1999, 2000) and Lamb et al. (2000a,b). In essence the approach seeks to address, to a practical degree, the difficulties of model equifinality, and to handle the assumptions of regression techniques in a way that is practical for conceptual hydrological modelling.

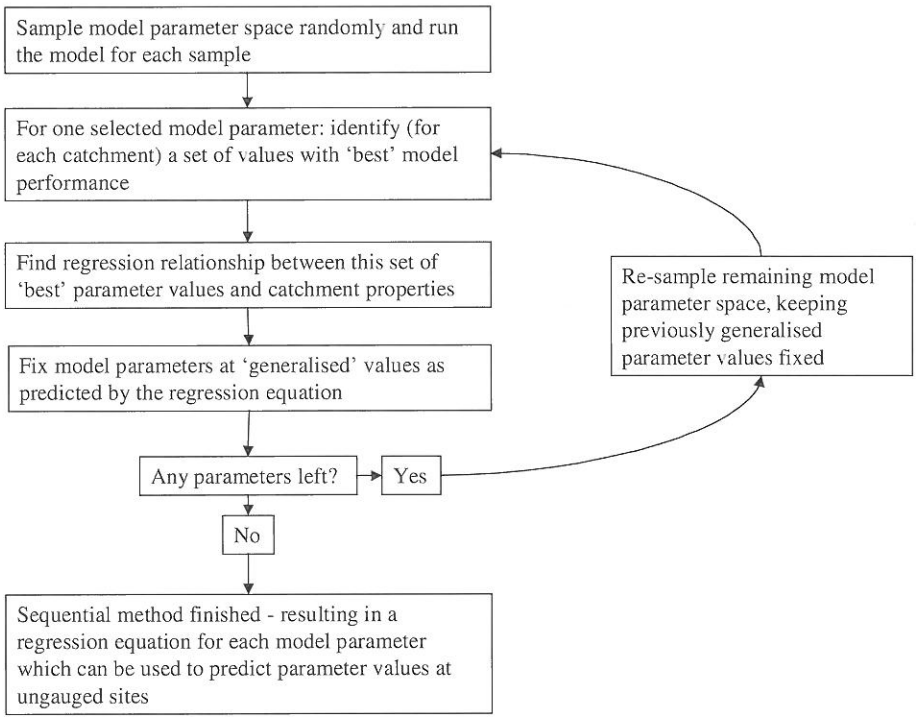

Figure 3-1: Outline flowchart for sequential calibration and generalisation.

Once model parameters can be predicted from spatial catchment properties data, the model(s) can be run for any site, given driving series of rainfall values. River flow time series can thus be derived, together with flood frequency and flow duration curves.
Figure 3-2 summarises the current level of performance of the method when applied to sites which have been treated as though ungauged, but with the real flow data retained for test purposes only. Part A of the figure shows how the measures of performance were derived and part B gives the numerical values for average return periods up to lengths appropriate to test in terms of the observation record length. Data are given for the first pilot system (as in Calver et al., 1999) and for subsequent improvements. These improvements (Lamb et al., 2000a,b) result from the reduction in the number of model parameters (in the case of the TATE) and in the adoption of the sequential method (in the case of the PDM). Subsequent refinements can incorporate the advantages of both sources of improved performance.

A

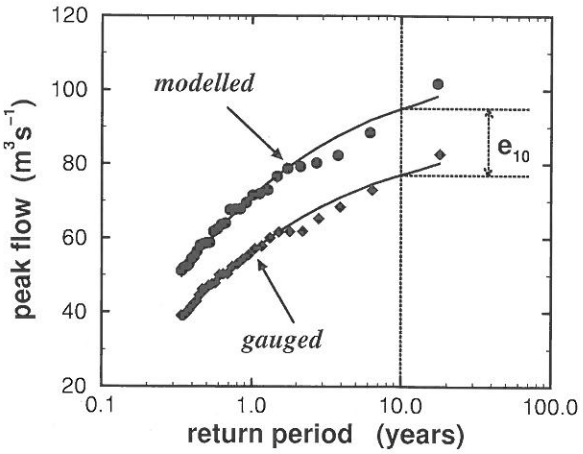

B

	Return period (years)	*1.0*	*2.0*	*2.33*	*5.0*	*10.0*	*20.0*
Model: TATE							
Pilot study*	Mean % error	31	31	32	33	35	38
	SD % error	29	31	32	33	35	36
New results (TATE3)	Mean % error	25	24	24	25	28	31
	SD % error	23	22	22	23	26	33
Model: PDM							
Pilot study*	Mean % error	42	40	40	40	42	45
	SD % error	35	33	32	34	37	44
New results (sequential)	Mean % error	22	23	24	24	26	27
	SD % error	18	18	19	20	21	23

**Calver et al. (1999)*

Figure 3-2: Part A is a schematic illustration of the 'residuals' used to assess flood quantile estimates. Individual errors e_T are subsequently scaled, so as to be expressed as a percentage of the gauged peak flow estimate for return period T (= 10 years in the example). Averages and standard deviations of these errors across all test catchments are shown in Part B.

4 UNCERTAINTY ESTIMATES FOR THE GENERALISED MODELLING

The summary of errors using 'as-ungauged' parameters provides a first indication of uncertainty in the spatial generalisation method, but only in gross terms for the group of calibration sites. More detailed estimates have been obtained by expressing model parameter estimates for the 'as-ungauged' site as distributions and using Monte Carlo simulation to produce corresponding distributions of simulated river flows and hence flood frequency curves. Approximate confidence intervals were then be computed from this simulated distributions. At this stage of research, the procedure has only been applied using the PDM catchment model.

For any catchment k, the as-ungauged estimate of a given PDM parameter is calculated from a regression equation as a function of $\mathbf{x}_k$, the vector of catchment properties at k. The as-ungauged parameter value is taken to be the mean μ_k of a distribution for which an estimate of the variance is $\sigma_d^2 = SS_r/d$, where SS_r is the sum of squares of the residuals and d is the degrees of freedom. The $100(1-\alpha)$% confidence limits of the estimate are then given (Draper and Smith, 1998) by

$$\mu_k \pm t(d,1-\alpha)\sigma_d \sqrt{\mathbf{x}_k (\mathbf{X}^T \mathbf{X})^{-1} x_k} = \mu_k \pm g_k(\alpha;d) \quad (2)$$

where $t(d, 1-\alpha)$ is the value from the t-distribution with d degrees of freedom with area $1-\alpha/2$ to its left and $\alpha/2$ to its right, $\mathbf{X}$ is the matrix with row i consisting of catchment properties for the i^{th} gauged catchment (and including a row for catchment k, if this is ungauged).

Equation (2) was used to produce cumulative distribution function $F(\theta_k)$ for each parameter at any site for which the required catchment properties are known by potting 1-α /2 against $\mu_k + g_k(\alpha, d)$ for α in [0,2].

For any target catchment, a distribution of hydrological model outputs (i.e. flow data) was then generated by running 1000 realisations of the PDM, randomly drawing values from the as-ungauged estimate distributions for each model parameter. The choice of the number of realisations was made after tests with values as large as 10,000 revealed very little difference in the outputs. For simplicity, we assumed in this experiment that the forcing (rainfall and PE) data are known with negligible uncertainty, at least when compared to the uncertainty about parameterisation of the hydrological model. The same, fixed, rainfall and PE data were therefore used to drive the hydrological model in each realisation of the PDM.

A partial duration series was extracted from each simulation, adopting an extraction rate of three peaks per year. This results in a total of (1000 x 3 x L) peaks being extracted in rank order of magnitude for each catchment, where L is the length of record for the catchment. The extraction rules stated in the UK Flood Studies Report (Natural Environment Research Council, 1975, Vol. 1) were followed. Approximate 90% confidence intervals were then constructed as follows for each catchment: For a given rank i (i = 1, ..., $3L$), the 1000 simulated POT data were arranged in a series in order of magnitude and the 50th and 950th values were recorded, counting in from each end of the series. Note that this procedure gives results that are based directly on simulated flood peaks, favoured here as the most straightforward approach. The curves shown as 'confidence intervals' are in fact piecewise linear interpolation between the point values. Possible alternatives would be to base the intervals on specified frequency distributions fitted to each simulated series.

Figure 4-1 shows a selection of results in terms of the approximate 90% confidence intervals constructed from the regression model estimates of PDM parameter distributions. The confidence intervals are accompanied by a curve indicating the mean-parameter estimate simulation, i.e. the best-estimate 'as-ungauged' simulation.

Also plotted are peaks extracted from the observed flow series along with a curve showing the generalised Pareto distribution (GPD), fitted to the observed peaks using probability weighted moments (Hosking, Wallis, 1987). The GPD is used because it has been found to be a suitable distribution for fitting peaks-over-threshold data for many UK catchments (Naden, 1992). The GPD curves are accompanied by 90% confidence intervals constructed using the likelihood ration method (Clarke, 1994).

In most cases the empirical flood data lie within the approximate 90% intervals constructed from the generalised-parameter PDM simulations. This result is interpreted as a partial validation of the spatially generalised modelling approach. It can only be partial, however, because the empirical flood frequency curves cross the simulated 90% intervals in other cases. Taking return periods of 2, 5 and 10 years for reference, the empirical curve plotted outside of the 90% intervals at one or more of these return periods for 14 of the study catchments. Overall there were four catchments in the study set of 40 where the observed flood peak data lie entirely outside of the 90% intervals.

The GPD confidence intervals consistently enclose the observed flood peak data. This is to be expected, given that the GPD was fitted directly to these data. However, the uncertainty about the GPD as a 'model' for the flood frequency data was not found to be markedly less than the uncertainty in the generalised hydrological model simulations. For many of the study catchments, the 90% GPD confidence intervals were found to be qualitatively comparable in width to the spatially-generalised hydrological model intervals. This can be interpreted tentatively to suggest that although the spatially generalised continuous simulation modelling is (not surprisingly) more likely to be 'wrong' for a particular catchment, it seems that where the method 'works', the uncertainty introduced by spatial generalisation of hydrological model parameters is not necessarily greater than the sampling uncertainty present when fitting a distribution directly to gauged flows.

In many cases, the GPD confidence intervals are much narrower for lower return periods, but then expand rapidly for longer return periods towards the tail of the distribution. Inspection of the confidence regions for the parameters of the GPD indicated that the GPD confidence intervals will almost always tend to expand steeply towards longer return periods, whereas this is not inevitable for the generalised CS intervals.

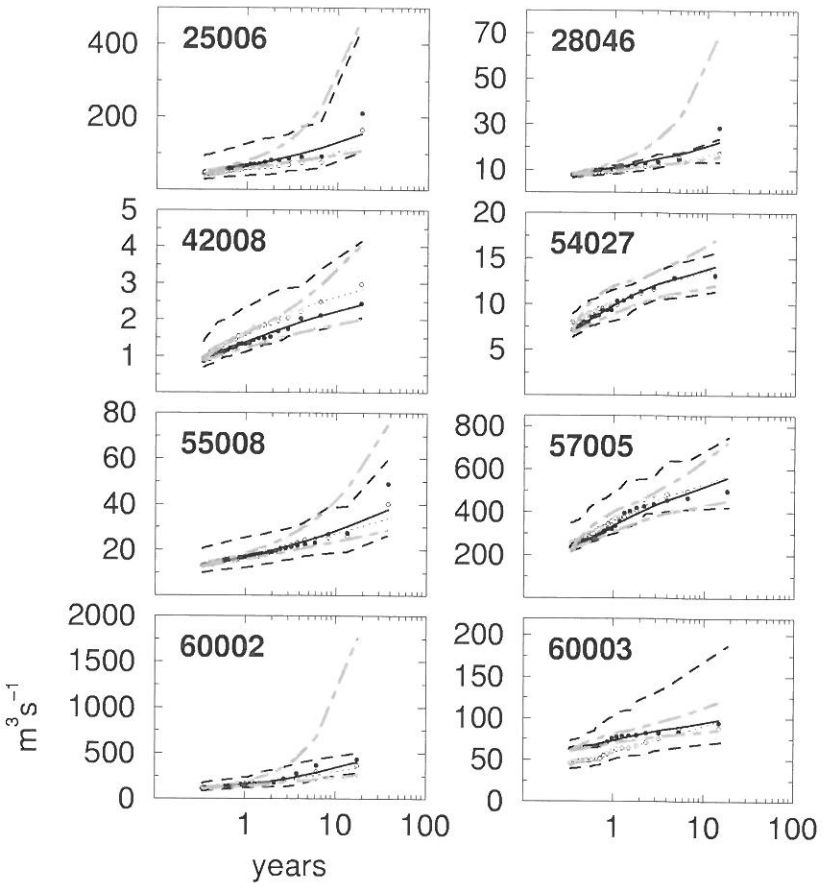

Figure 4-1: Flood frequency curves showing peak flow on vertical axes, plotted against average return period in years. Five digit numbers are UK National Water Archive catchment index numbers. Graphs show 90% simulated confidence intervals (- - - -) and mean simulations (····· ○), *treating catchments as ungauged. The GPD* (———) fitted to gauged peaks over threshold series (●) *is also shown, as are 90% confidence intervals for the GPD* (— · — ·), constructed using the likelihood ratio method.

5 CONCLUDING REMARKS

Confidence in the spatially generalised continuous simulation system to date is enhanced by the characterisation of the whole runoff response, including the flood response, across the conditions encountered in Britain. This includes catchments varying in area over three orders of magnitude and a mix of impermeable and permeable geologies. Further, when sites are treated as ungauged, and then the withheld observations are compared with spatially-generalised flood frequency results, average return periods up to those which can be tested are within pragmatic acceptance levels.
When confidence intervals are calculated for the 'as-ungauged' situation, comparatively few sites indicated a failure of the modelling or parameter generalisation. The degree of uncertainty in spatially generalised modelling varies between sites and is often no greater than for a site-specific distributional model fitted directly to the gauged flows.

ACKNOWLEDGEMENTS

This research has been funded by DEFRA Flood Management Division under R&D Projects FD0404 and FD1604. Some parts of these results have been published in the Proceedings of the Institution of Civil Engineers and in past conference proceedings of DEFRA, the British Hydrological Society and the Potsdam Conference on Advances in Flood Research.

REFERENCES

Calver, A. (1993): The time-area formulation revisited. Proceedings of the Institution of Civil Engineers: Water, Maritime and Energy, 101, 31-36. ICE. London.

Calver, A. (1996): Development and experience of the 'TATE' rainfall-runoff model. Proceedings of the Institution of Civil Engineers: Water, Maritime and Energy, 118, 168-176. ICE. London.

Calver, A., et al. (1999): River flood frequency estimation using continuous runoff modelling. Proceedings of the Institution of Civil Engineers: Water, Maritime and Energy, 136, 225-234. London.

Clarke, R. T. (1994): Statistical Modelling in Hydrology. Wiley. Chichester.

Crewett, J. et al. (1999): Spatial generalisation of model parameters for flood frequency estimation using continuous simulation: recent research advances. Institute of Hydrology report to Ministry of Agriculture, Fisheries and Food. Wallingford.

Crewett, J. et al. (2000): Spatial generalisation for flood frequency estimation by continuous simulation. Geophysical Research Abstracts, 2, EGS General Assembly, April 2000. Nice.

Draper, N. R., Smith, H. (1998): Applied Regression Analysis, 3rd Edition. Wiley. Chichester.

Hosking, J.R.M., Wallis, J.R. (1987): Parameter and quantile estimation for the Generalised Pareto distribution. Technometrics, 29, 339-349. American Statistical Association. Virginia.

Institute of Hydrology (1999): Flood Estimation Handbook (5 volumes). Institute of Hydrology. Wallingford.

Lamb, R. (1999): Calibration of a conceptual rainfall-runoff model for flood frequency estimation by continuous simulation. Water Resources Research, 35, 3103-3114. AGU. Washington.

Lamb, R. et al. (2000a): Progress in the spatial generalisation of 'continuous simulation' flood frequency modelling. In Toensmann, F. and Koch, M. (eds) River Flood Defence (volume 1), Kassel Reports of Hydraulic Engineering No. 9/2000, D-117-125. Herkules Verlag. Kassel.

Lamb, R. et al. (2000b): Relating hydrological model parameters and catchment properties to estimate flood frequencies from simulated river flows. Proceedings of the BHS 7th National Hydrology Symposium; September 2000, 3.57-3.64. Newcastle.

Naden, P.S. (1992): Analysis and use of peaks-over-threshold data in flood estimation. In: Floods and Flood Management, ed. A.J. Saul. Kluwer Academic, Dordrecht.

Nash, J.E. and Sutcliffe, J.V. (1970): River flow forecasting through conceptual models, 1, A discussion of principles. Journal of Hydrology, 10, 282-290. Elsevier. Amsterdam.

Natural Environment Research Council (1975): Flood Studies Report and Supplementary Reports. NERC, London.

Moore, R.J. (1985): The probability-distributed principle and runoff production at point and basin scales, Hydrological Sciences Journal, 30, 273-297. IAHS Press. Wallingford.

Moore, R.J. (1993): Real-time flood forecasting systems: perspectives and prospects. Proceedings of The British-Hungarian Workshop on Flood Defence, 6-10 September, 1993, VITUKI. Budapest.

METHODOLOGY OF TIME-SPACE FLOOD MODELLING IN CHANGING CONDITIONS

Vladimir Lobanov, Helen Lobanova

State Hydrological Institute, 23, Second Line, St. Petersburg, Russia, lobanov@EL6309.spb.edu

SUMMARY

Empirical-statistical methodology is suggested for time-space modelling of floods and their meteorological characteristics in changing conditions. The following main stages of such methodology include: modelling of floods and determination of their parameters for each year; modelling of flood parameters over the long-term period including extraction of homogeneous components connected with man's activity factors and different natural time scales (inter-annual, decadal, century, etc) and determination the kind of temporal models (stochastic or deterministic-stochastic) and their parameters; determination of homogeneous regions with the same tendencies of climate change in time series of floods; development of space models of flood for homogeneous regions and determination of their parameters. New methods have been developed for realisation of each stage of time-space modelling. Main of them: methods of intra-annual modelling, methods for extraction of homogeneous components of different time scales in long-term records, methods for determination of long-term climate changes and determination of homogeneous regions with the same tendencies of climate change and methods for dynamic spatial modelling. Application of developed methodology and methods is shown on some examples for Central England, North-West, North of European part and Far East regions of Russia.

Keywords: changing conditions, space-time modelling, homogeneous region, time scales

1 BACKGROUND

Today time model of floods is based on the distribution functions theory and is suitable for homogeneous and stationary conditions (Kritsky, Menkel, 1981; Rozhdestvensky, 1990). Such distribution function is described by three main parameters: mean (M), variation coefficient (Cv) and coefficient of skewness (Cs) which assume as constant values for long-term period. On the basis of these parameters any quantile of a given return period can be obtained as a design flood. The longest record of observations is the main assumption for effective assessment of parameters in stationary conditions, because the more a sample the smaller random errors of parameters (Kendall, Stuart, 1969). Therefore a restoration of the historical time series is a main condition for development of effective stochastic time model. Different approaches are used, but two of them are general: restoration on the basis of the same flood information in analogous sites with long-term records and using of precipitation-runoff models, when time series of meteorological factors have longer records. Spatial modelling of floods connects with interpolation or extrapolation of parameters of distribution function or design floods (quantiles) in any point of area, i.e. the same stable values. Main methods of spatial simulation are: lines of equal data, averaging, regional relationships with watershed descriptors, general precipitation-runoff models. Choice of homogeneous region is the main problem of the most approaches. As a rule, such region associates with the same level of main flood's factors of watershed (average annual rainfall, soil drainage type, relative percentage of lakes, reservoirs, forests, swamps, index of urban extent, baseflow index and other) or with a strong correlation with the main watershed descriptors such way, that an including of other basins over boundaries of this region makes worse this regional relationship. In a result, several methods can be used for a spatial modelling and a problem is how to choose the best result.

Modern changing conditions connected with joint "natural" dynamic and man's impact on climate, river channels, watersheds lead to necessity of analysis and modelling of dynamic properties of long-term time series of floods and parameters of spatial models. The first step is to separate influence of two main groups of modern factors: direct anthropogenic factors (land use, reservoir operation, etc) and factors of climate change and climate variability. Restoration of "natural" or "climatic" records of floods are fulfilled by different approaches too. Among them precipitation-runoff models with direct including of anthropogenic factors, water balance and regression equations, relationships with time series of analogous in natural conditions and other. As a result this first step allows obtain "climatic" records of floods and one or several time series of flood components connected with joint or separated impact of direct anthropogenic factors. Man's impact components are used as a corrective (scenario) to assess parameters of "climatic" flood models.

2 METHODOLOGY

Basic stone of suggested methodology for a time-space modelling is an empirical-statistical approach. This approach connects with explore data analysis and processing of observed data. Main problem is a development of the general model of space-time fluctuations of hydrometeorological characteristics, which takes into account seasonal variations, regular properties of long-term time series and fields. All space-time fluctuations of any hydrometeorological characteristic can be represented as a 3-dimensional array, where each direction (i,j,k) has the following interpretation:

- direction i represents an intra-annual cycle of variations (i =1,365 for daily values or i =1,12 for monthly values, number co-ordinates of floods, etc.);
- direction j represents a time series of interannual fluctuations (j =1,n, where n is a record period);
- direction k represents a spatial direction (k =1,m, where m is a number of stations over the area).

In the beginning of research a structure of the model for each direction is unknown and can be obtained only on the basis of analysis of empirical data. Therefore, the simplest way for a development of such general space-time model is step by step simulation. Creation of the common space-time model in this case connects with stepwise description over the each direction with generalization of fluctuations in some parameters of functions. Main stages of such approach will be as follows:

- step 1: modelling of intra-annual fluctuations for the each year (j) and for each observation site or station (k) with the result as parameters of the particular floods or intra-annual function;
- step 2: extraction and modelling of interannual fluctuations of different time scales for each site or station (k) with the result as homogeneous components of different time scales connected with processes of climate variability and long-term climate change and parameters of their time models;
- step 3: determination of homogeneous regions and modelling of spatial field for each homogeneous component of different time scale in the form of parameters of spatial model.

Development of spatial model is based on the spatial properties of the particular characteristic or parameter. The following kinds of spatial generalization can take place:

- averaging over the space if the general spatial gradient is less than random errors of data in the points;
- parameters of spatial distribution function, when spatial gradient is more than random errors and regular properties over the space are absent;
- parameters of space model when spatial gradient is more than random errors and space regular properties take place.

In the latter case, space model has a deterministic-stochastic nature as a rule and includes a regular spatial component connected with general regular properties and stochastic component connected with local properties (internal non-homogeneity of the field).

This way to describe the space-time fluctuations in full it means to obtain a kind of model for each of three directions, to obtained the coefficients and parameters for each model and to find interrelationships between these parameters.

3 TOOLS

3.1 Simulation inside annual time interval

Concerning flood events (snowmelt and rainfall floods) two main approaches for intra-annual generalization are suitable:

- determination of parameters (amplitude, volume, period, speed of increasing and reducing, etc) of each rainfall flood event or significant events;
- determination of parameters of seasonal function, when snowmelt flood characterizes the amplitude of intra-annual fluctuations and rainfall floods connects with synoptic processes.

In the first case the parameters of each flood or significant floods (peak over threshold – POT) are chosen (Institute of Hydrology, 1999) and the main problem how to assess an empirical probability of such non-regular floods when their time model is stochastic. In the second case the main problem to describe a seasonal function. In general case, the structure of seasonal (or intra-annual) function can be very complex, especially for such characteristics as precipitation and runoff. As a result a direct description of each year can be accompanied by significant difficulties. On the other hand, observations during each year are defined by general climate properties connected with the particular position of site on the Earth (as classical definition of "climate" – "klima"), as well as intra-annual fluctuations connected with synoptic processes. Therefore the simple way of intra-annual simulation is to connect of average seasonal conditions for a historical period with observed data within each

particular year. In this case only one assumption takes place about the same kind of seasonal function for each year and for a historical period and as a result - a linear relation between historical and particular season functions. The relationship between particular and historical conditions can be expressed by a following way:

(1) $$Y_{ij} = B1_j * Y_{im} + B0_j \pm E_{ij},$$

where:
- Y_{ij} is a hydrometeorological characteristic for the *i*-th period (daily, weekly, ten-day, monthly) of the *j*th year;
- Y_{im} is an average long-term (historical) function of intra-annual fluctuations of hydrometeorological data during a year;
- $B1_j$ is a coefficient describing a difference between amplitude of intra-annual function in the *j*-th year and amplitude of average long-term function ($B1_j$=1, if seasonal amplitude of *j*-th year equal the amplitude of historical seasonal function);
- $B0_j$ is a coefficient describing a difference of the minimum level of intra-annual function in the *j*-th year from a minimum average long-term intra-annual function ($B0_j$=0, if level of seasonal function of *j*-th year equal the level of historical seasonal function);
- E_{ij} are remainders from the relationship line between the particular and long-term conditions which characterise the processes of synoptic and macro-synoptic scales and can be presented by generalised characteristic as a standard deviation (S_{ej}) that is connected with an intensity of synoptic processes.

Equation (1) allows to represent the seasonal function as two coefficients (*B1* and *B0*) and one parameter (S_e), as well as to divide all intra-annual fluctuations into 2 parts: climatic part, connected with seasonal function (annual Earth rotation), and synoptic part, connected with atmospheric circulation.

3.2 Extraction and simulation of homogeneous components connected with climate variability and climate change

According to Climate Variability and Predictability Programme (CLIVAR, 1995), observed time series can be represented as a super-position of natural homogeneous components, connected with climate variability of different time scales (inter-annual, decadal, century) and long-term climate change component connected with anthropogenic impact:

(2) $$Z_{obs\text{-}y}=Z_{int}+Z_{dec}+Z_{cent}+Z_{ant},$$

where: $Z_{obs\text{-}y}$ is an observed characteristic of annual generalization (annual maximum flood, parameters of the particular flood and seasonal function, etc);
Z_{int} is natural homogeneous component of interannual time scale;
Z_{dec} is natural homogeneous component of decadal time scale;
Z_{cent} is natural homogeneous component of centennial time scale;
Z_{ant} is homogeneous component, connected with anthropogenic long-term climate change.

For time series of hydrological characteristics the additional components in (2) can be represented by influence of different factors of direct man's activities (regulation by reservoirs and dams, water intake and outtake, irrigation, etc). These components are extracted by different methods described, for example, in (Lobanova, 1997).
For extraction of homogeneous components connected with climate variability and climate change only the indirect statistical methods can be used. The existing methods, such as spectral and correlation analysis, moving average and smoothing need strong assumptions for processing time series, for example: harmonic function of cycles, constant period and amplitudes of cycles and other that could not be suitable for real time series of hydrometeorological characteristics. As a result, the two new methods have been developed: truncation method and method of smoothing of amplitudes of cycles. Two common assumptions have been given only:
- historical time series is a super-position of homogeneous components of different time scales;
- the extracted long-term climate change component is a sum of natural and anthropogenic ones.

The second assumption characterises that the joint component of long-term climate change ($Z_{cl.change}$) can be extracted only, if indirect methods are used. Really this component consists of two parts: natural (Z_{cent}) and anthropogenic (Z_{ant}) changes (Folland, 1996):

(3) $$Z_{cl.change} = Z_{cent} + Z_{ant}$$

In the first approximation the analysis and monitoring of climate change can be fulfilled on the basis of the complex process $Z_{cl.change}$. The separation of these two parts is possible by the physically based models or by a comparison of data in two different periods: during and before industrial period on the basis of the longest observed time series (more than 200-300 years) or using palaeodata.
First of the developed method is a truncation method which is based on a choice of homogeneous points in time series. In according to this method (Lobanov, 1995) any time series of meteorological characteristic can be present as a sum or a superposition of homogeneous components of different time scales, as (2). Common number of homogeneous is not known a priori, as well as their regular properties.
On the first step the homogeneous points belonging to the smallest time scale process are selected. These points are the all data except the minima of cycles, because the smallest scale process is absent in these minima. Therefore, these minima belong to the processes of the next time scale with period of cycles more than the smallest. These minima incorporate by continuous lines and the homogeneous process of the smallest time scale is picked out (truncated) from the rest part of composition. On the second step this procedure is returned and the smallest scale process will be the next with middle scale and so on. The main equation is:

(4) $$Z_j = [Z^*_{com.} - Z'_{com} f(Z_{min\,j})]$$

Z_j is a homogeneous j-th component,
$Z^*_{com.}$ is a sum of all residual components (including j-th),
Z'_{com} is a sum of all residual components (without j-th) as a function of minimums ($Z_{min\,j}$),
$Z_{cl.change.} = Z_m$ and m is a number of homogeneous components.

The second method of decomposition is based on the smoothing of amplitudes of cycles (Lobanov, 1998, Lobanov, Lobanova, 1999). This smoothing is based on the condition:

(5) $$Y_j = f(A_{ji}/2)$$

where A_{ji} is amplitude of i-th cycle.

Way of simulation of every extracted homogeneous component depends on the kind of the model of its time series. There are two kinds of time models the most suitable in hydrometeorology: stochastic and deterministic-stochastic. If any regular properties over the time are absent the model has a stochastic kind and time series can be represented as a frequency distribution function and described in whole by set of its parameters (average, variance, etc). If regular properties take place, the deterministic part of time model can be presented by different kinds of trend or autoregression equation. Analysis of regular properties over the time can be fulfilled for values per each year as well as for characteristics of cycles, such as: periods and amplitudes of cycles, their volumes, period and average speed for raising and falling branches of cycles, etc. Statistical methods and tests are used for an assessment of statistical significance of tendencies as well as for assessment of stationarity of generalised parameters of time series (average for several years, variance, etc.).

3.3 Simulation of spatial variations

Spatial modelling of floods includes two main parts: determination of homogeneous regions and determination of the parameters of spatial models in each homogeneous region. Separation of homogeneous region is based on the main common spatial factor. In changing conditions such factor can be significant (or non-significant) trends of modern climate change in time series and their direction (increasing or reducing), which may be obtained by methods 3.2.
Expanding of the common model on the space case includes three main kinds of generalizations:
- averaging over the space in the case when spatial gradient is less than the data errors;
- determination of the parameters of spatial distribution function when the spatial gradient is more than the data errors and regular properties over the space are absent;

- determination of the parameters of space model when the spatial gradient more than data errors and regular properties over the space take place.

Space model is obtained if range of spatial fluctuations is more than random errors. For a description of spatial fluctuation the linear model as kind (1) can be suggested. In this case the relationships are built between the field of hydrometeorological characteristic (annual, monthly, coefficients of the particular floods or intra-annual function, etc) in the particular year and mean historical field:

(6) $$Z_{kj} = A1_j * Z_{km} + A0_j \pm AE_{kj},$$

where:
- Z_{kj} is a field of hydrometeorological characteristic in *j*-th year for k-*th* station;
- Z_{km} is a historical field of a chosen hydrometeorological characteristic;
- $A1_j$ is a coefficient, which characterises a change of gradient of the field in the particular *j*-th year to the same gradient for a historical period;
- $A0_j$ is a coefficient, which characterises a change of level of the field in the particular *j*-th year to the same field level for the historical period;
- ASe_j (as a standard deviation of AE_{kj}) is a parameter of spatial variation of macro-synoptic processes and characterises internal non-homogeneity of the field in the particular year.

4 ANALYSIS OF FLOOD FACTORS. PRECIPITATION

4.1 Simulation in points

The analysis and simulation of monthly precipitation have been fulfilled for 6 the longest records at stations inside of Central England area and for 2 stations outside it: Rhayader and Chilgrove House. Three homogeneous components, connected with interannual, decadal climate variability and centural climate change, have been extracted for monthly, annual precipitation and coefficients of seasonal function for each station and their characteristics have been obtained.

The average period of cycles of interannual fluctuations (T_1) is equal 3 years for all months and year and 4 years for coefficients of seasonal model. Average periods of cycles of decadal climate variability are not stable for different months and coefficients and vary from 14-15 years to 25-27 years. The ratio K_1/K_2, which characterizes differences in variation of two processes is equal 2 in average. Contribution of the interannual process (Δ_1) varies from 76% to 88% for months and equal 21.5% only for annual values. It means that temporal generalization leads to smoothing amplitudes of cycles of small-scale processes. Climate change component is not such significant in a comparison with climate variability but has seasonal changes. Climate changes lead to an increasing of monthly precipitation for all months practically with the exception of cold season when precipitation are growing. Seasonal models have been obtained for each station too.

4.2 Spatial simulation

The first step for the development of spatial model is an assessment of homogeneous properties and a choice of homogeneous region. For this aim an analysis of contributions and tendencies of climate changes in monthly and annual precipitation has been fulfilled as well as for the coefficients of seasonal precipitation models. Seasonal functions of climate trends and their contributions are similar in the region of Central England and differ for stations outside this area. As a rule, the most part of trends in Central England region is located in a negative area. Stations in the region of Central England have similar season variations with maximum precipitation in summer – autumn period. Outside stations have seasonal function with maximum precipitation in autumn-winter period. Similarity of seasonal functions of precipitation and climate change trends give the possibility to obtain the relationships between them. These relationships are non-linear and statistically significant for the region and are absent for stations located outside the region.

Additional assessment of homogeneity of the chosen area has been fulfilled for coefficients and parameters of seasonal models. Climate trends for *B1, B0* coefficients and for parameter *Se* have been recalculated in % to mapping these values. Results of mapping are given in Figure 4-1. According these maps, all *B1*-coefficients have negative climate changes for the region stations and positive changes outside this area. Opposite, *B0*-coefficients have positive climate tendencies in the region and negative for other territory. Significance of climate changes for *Se*-parameters is enough low and

equal several percentages, but the general tendency of *Se* some reducing takes place in the region. This way, analysis of climate change in different characteristics of precipitation shows that the region of Central England can be assumed as a homogeneous region.

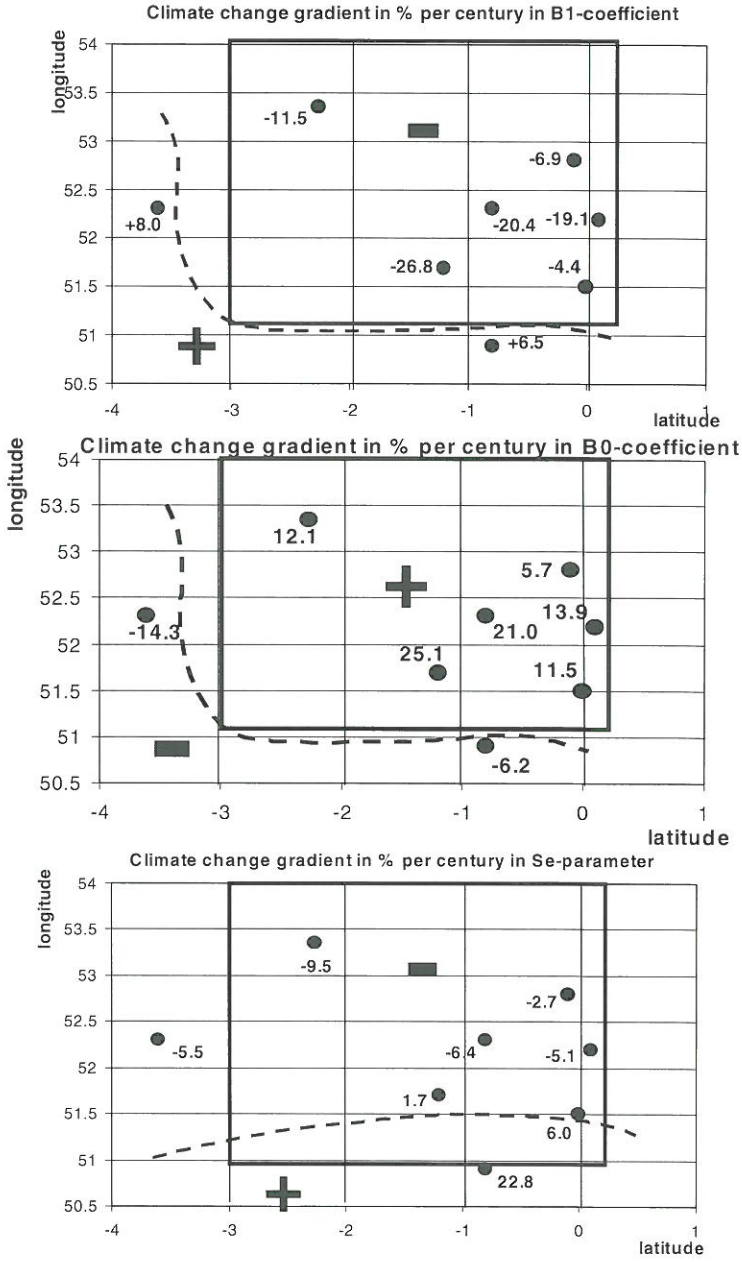

Figure 4-1: Spatial distribution of century gradient of climate change (in % per century) in coefficients of seasonal model of precipitation in the region of Central England and outside it.

Spatial models have been developed for monthly, annual precipitation and for parameters of seasonal models for time series in homogeneous region in according to the method described in item 3.3 this paper. As a result, *A1* and *A0* coefficients and parameters *ASe* of each spatial model have been calculated. Next step of the analysis has been connected with extraction of climate change components in time series of coefficients of spatial models and assessment of their contributions. Quantitative assessments of contributions of climate change in coefficients of general common time-space models are given in the Table 4-1.

Table 4-1: Contributions of climate change in time series of coefficients of time-space models (in % to general range of fluctuations).

Time par.	Station in homogeneous region						Space parameters		
	1	2	3	4	5	6	A1	A0	ASe
B1	-19.1	-26.8	-4.4	-11.5	-20.4	-6.9	-7.1	+7.7	-5.3
B0	+13.9	+25.1	+11.5	+12.1	+21.0	+5.7	-4.4	+14.0	-4.5
Se	-5.1	+1.7	+6.0	-9.5	-6.4	-2.7	-10.4	+5.9	-5.4
Year	+5.6	+7.4	-5.0	-19.2	-12.2	+2.1	-19.4	+11.4	+0.3

where:
1 – Cambridge, 2 – Oxford, 3 – Greenwich, 4 – Manchester, 5 – Althorp park, 6 – Podehole No.3

As follows from Table 4-1, fields of all coefficients (*B1, B0*) parameters (*Se*) of seasonal functions as well as a field of annual precipitation have a decreasing of gradients (*A1*-coefficient) or an increasing of homogeneity of the fields, increasing of the level of the fields (*A0*-coefficient and some small reducing of internal non-homogeneity of the fields (*ASe* -parameter). It means that the field becomes more high and plane.

5 MODELLING OF ANNUAL MAXIMUM RUNOFF. UK HOMOGENEOUS REGION

For assessment of climate changes the most long-term records of observations of annual maximums have been chosen inside of Central England homogeneous region. Unfortunately there were 14 such long-term time series only according the FEH data base. The same methods of extraction of long-term climate changes have been applied and contributions of climate trends are given in Table 5-1, where 10yr. is a method of consecutive averaging, *Ampl.* is a method of smoothing of amplitude of cycles and *Trunc.* is a truncation method for extraction of long-term climate change component. As it is seen from the Table 5-1, contributions of climate changes are different in some cases when different methods of extraction have been used. The most similar results take place for the most long-term time series. For these time series the climate change leads to a decreasing of maximum runoff with the exception the Trent River – site Trent Bridge, but this time series has the end of observation in 1969.

Table 5-1: Contributions of long-term climate change component in time series of annual maximum runoff.

No.	No reg.	River-Site	A sq.km	n, year	Contribution,% by method		
					10yr.	Ampl.	Trunc.
1	27021	Don - Doncaster	1256	110	-12.4	-8.4	-9.5
2	28070	Burbage Brook – Burbage	9.1	56	-2.5	11.2	-0.1
3	28804	Trent – Trent Bridge	7490	82	6.6	8.3	11.0
4	32002	Willow Brook - Fotheringhay	89.6	53	2.2	1.2	-0.2
5	32003	Harpers Brook – Old Middle Bridge	74.3	50	51.9	31.7	0.2
6	32004	Ise Brook – Harrowden Old Mill	194	50	-4.7	-17.9	-1.1
7	32006	Nene/Kislingbury - Dodford	223	53	4.4	5.3	3.5
8	32007	Nene Brampton – st.Andrews	232.8	53	20.1	11.9	1.5
9	32008	Nene/Kislingbury - Dodford	107.0	47	2.5	-15.6	2.4
10	38002	Ash - Mardock	78.7	53	-0.8	-5.3	0.3
11	39001	Thames - Kingston	9948	112	-6.7	-9.1	-12.3
12	39002	Thames – Days Weir	3444.7	57	-1.3	-6.8	-10.8
13	54001	Severn - Bewdley	4325	71	-4.5	-7.1	-6.5
14	54002	Avon - Evesham	2210	54	-0.4	-0.5	6.7

As a result, the assessment of climate changes in the time series of maximum runoff shows some decreasing of maximums for long-term time series with period of observation more than 70 years. The assessment of climate change for record with size less than 60-70 years is not reliable and on the other hand, any short-term jumping in records of maximum runoff can be caused by local factors of direct man's influence or climate variability. Spatial model of floods for Central England has been

developed and analysis of its coefficients showed that they have the same tendencies as for a spatial model of precipitation: decreasing of gradients (*A1*-coefficient), increasing of the level of the fields (*A0*-coefficient and some small reducing of internal non-homogeneity of the fields (*ASe* -parameter).

6 FLOOD AND TEMPERATURE FIELDS IN THE FAR EAST OF RUSSIA

The catastrophic floods in Primorski Territory of Russia are determined by monsoons from the Pacific Ocean. Therefore 30 time series of rainfall floods have been selected with the longest observations as well as the monthly air temperature in adjoining sector of the Pacific in the points of regular grids for period from 1891 to 1998 and for land area.
Temporal modelling of floods has been fulfilled separately for every time series. Truncation method has been used and the processes of three different scales have been obtained with an average period in 3 years for small-scale and in 12 years for middle-scale process. The exception was the Amur River (as intra-zones river) with periods in 4 years for small-scale and 25 years for middle-scale process. Any long-term trends in periods and amplitudes of cycles have not been obtained for process of small-scale, except the Bureja river with insignificant positive change. Cyclic variations take place in time series of cycle periods with step 2-3 units (cycles). For amplitudes of cycles such variations have periods in 2-3 units for the southern part and 3-4 units for the northern part of area.
Spatial modelling of temperature has been fulfilled for land and ocean area separately. It has been established that the *B0*-coefficients of dynamic spatial model have positive trend and the *B0*-coefficients have some decreasing from the 1920s and variance of errors increases from the 1960s. Therefore, the common level of land temperature field is increasing, as well as the intensity of macro-synoptic processes. At the same time there is some decreasing of spatial non-homogeneity of land temperature. For ocean sector when monsoons are born and moving the temporal models have been obtained for every points of regular grid at first. Three different-scale processes take place for every time series. The average cycle period has been equal 3 year for the northern and 4 year for southern part of ocean sector in the process of small scale. For middle scale average cycle period was 12 years for northern and 14-15 years for southern part. The same spatial non-homogeneity takes place for the part of large-scale process: decreasing trends in the northern and increasing trends in the south regions of ocean. In according to the space non-homogeneity, the spatial models have been obtained for the whole area as well as for two particular its parts: northern and southern. For the whole area it has been established the small increasing of homogeneity (decreasing of *B1*-coefficients) and macro-synoptic circulation (*Se*). For the northern part these results are more significant than for the southern one. As a conclusion, the spatial dynamic models allowed to obtain the increasing of the intensity of macro-synoptic circulation and the increasing of monsoon floods, which are connected with it.

7 ASSESSMENT OF STABILITY OF STOCHASTIC MODEL

As a rule, a stochastic model is used for assessment of design flood or flood of given return period. Really, they transfer today situation (distribution function) to future period. For the assessment of stability of such model the same 25 time series of annual maximum in UK has been chosen. Assessment of efficiency of approximation and extrapolation has been realised for a real situation, which takes place always for water projects. For this aim every record has been divided into two parts. First of them has been used for computations as analogues of observed record (calibration sub-sample). Computed values have been obtained for four return periods, which are equal empirical probabilities of the four first maximums in common time series of observation. In this case the period of future operation of water project has been equal a half of common period of observation or period of calibration sub-sample.
Computations of design annual maximum have been fulfilled by two software: WINFAP-FEH which realises methods of FEH (1999) and computer system DASHCA, which realises methods described in existing SNiP (1984) and new SNiP (2001), and applies in many projecting organisations of Russia. The differences between observed and computed values, which characterise the errors of 4 computed maximums, are given in Table 7-1 in %. These errors have different sign for different sites as well as sometimes for different quantiles of distribution for the same site. Mean modulus errors are less for all quantiles in the case when UK methods have been used. As a result, the average difference of errors is equal 4.5% only in the UK's methods favour. In general, these differences are connected with the feature, that in UK are used the more number of analytic distributions and enough flexible functions take place among them: Generalised Logistic, for example. These functions give a good fitting in complex cases, when other distributions (Kritsky-Menkel, for example) cannot do it.

Table 7-1: Errors (in %) between observed and computed annual maximums (4 first maximums) obtained by using of different software: WINFAP-FEH (UK) and DASHCA (Russia).

No	WINFAP-FEH (UK)					DASHCA (Russia)				
	4	3	2	1	Mean	4	3	2	1	Mean
1	24.4	23.2	-8.6	-4.0	15.1	23.3	21.7	-12.0	-7.4	16.1
2	58.2	13.5	10.0	-13.9	23.9	83.3	30.1	21.9	-6.1	35.4
3	-24.8	-21.0	-24.8	-13.8	21.1	-21.0	-18.4	-22.9	-13.8	19.0
4	-4.0	-3.3	4.2	13.7	6.3	-3.4	-3.8	1.8	7.4	4.1
5	-0.9	-1.7	6.6	21.0	7.6	-2.1	-3.7	2.6	9.8	4.6
6	-16.9	-12.6	-14.3	-29.0	18.2	-10.7	-8.8	-11.8	-29.4	15.2
7	-24.6	-34.3	-55.6	-45.0	39.9	-17.6	-30.9	-54.0	-45.3	37.0
8	-3.2	0.5	3.8	5.8	3.3	-2.4	0.6	3.3	1.5	2.0
9	23.3	26.6	35.0	-6.0	22.7	14.8	17.9	27.0	-6.7	16.6
10	-31.2	-30.7	-21.5	-10.9	23.6	-31.2	-31.7	-25.4	-19.1	26.8
11	7.1	8.7	9.2	17.0	10.5	2.8	3.0	1.4	6.0	3.3
12	8.2	13.6	19.2	-56.6	24.4	36.7	44.2	56.6	-37.8	43.8
13	-5.3	-9.9	-8.7	1.0	6.2	3.0	-2.7	-2.9	5.1	3.4
14	29.9	39.9	-5.6	6.1	20.4	35.0	43.7	-5.6	4.0	22.1
15	32.5	36.1	-5.5	-12.2	21.6	44.8	41.7	-3.3	-11.8	25.4
16	-4.6	-15.8	-25.3	-65.6	27.8	-4.4	-16.4	-26.4	-67.3	28.6
17	3.3	3.9	10.8	-9.8	7.0	0.0	0.8	8.5	-9.2	4.6
18	1.7	8.0	1.3	-17.1	7.0	2.9	18.7	9.7	-17.5	12.2
19	2.4	6.3	13.8	-2.9	6.4	10.1	11.8	16.9	-2.0	10.2
20	5.9	6.3	5.0	-40.9	14.5	-	-	-	-	-
21	-49.1	-60.9	-62.8	-62.0	58.7	-50.5	-62.0	-64.2	-63.7	60.1
22	-14.0	-26.7	-24.7	-20.3	21.4	-16.1	-28.8	-28.0	-24.6	24.4
23	-14.3	-8.0	-6.8	-3.5	8.2	-14.9	-11.6	-12.5	-13.1	13.0
24	-1.8	-2.1	2.0	8.5	3.6	-4.0	-5.2	-2.6	1.5	3.4
25	3.4	-8.2	-9.6	3.0	6.0	8.7	-4.1	-11.5	1.6	6.5
av	15.8	16.9	15.8	19.6	17.0	21.7	22.5	21.3	20.6	21.5

8 CONCLUSION

General empirical-statistical methodology and methods have been developed for time-space modelling of floods and their factors in changing conditions. In time series of floods and factors the components connected with climate variability and climate change have been extracted and their contributions have been obtained. Stability of stochastic models has been estimated and dynamics of parameters of spatial models in homogeneous regions has been analysed for Primorski Territory of Russia and Central part of UK.

REFERENCES

CLIVAR, A Study of Climate Variability and Predictability. Science Plan (1995): WCRP-89, WMO/TD No. 690 - 157 p.

Flood Estimation Handbook (1999): Institute of Hydrology, UK.

Folland, C. (1996): Current Climate Change: Can We Detect a Human Induced Influence? European Conference on Applied Climatology. Abstract Vol., Norrkoping, Sweden, May 1996, p. 3-4.

Kendall, M.G. and A. Stuart (1969): The Advanced Theory of Statistics, Vol.1-3, London.

Kritsky, S.N. and Menkel, M.F (1981): Hydrological bases of river runoff management. Science, Moscow, (in Russian).

Lobanov, V.A. (1995): Statistical Decision in Changing Natural Conditions. Proc. Int. Conf. on Statistical and Bayesian Methods in Hydrological Sciences, Paris, 20 pp.

Lobanov, V.A. (1998): Modelling of dynamic properties of hydrological processes. In: Hydrology in a Changing Environment (ed. by H.S.Wheater & C.Kirby), vol.1, 153-162. John Wiley/British Hydrological Society, Chichester, UK.

Lobanov, V.A., H.V. Lobanova (1999): Trends in Cold Climate Characteristics. In: Urban Drainage in specific climates. Cold climate. UNESCO Publ., 35 pp.

Lobanova, H.V. (1997): Assessment of Sustainable Floods and Water Resources Management by reservoirs in Russia. Proc. Int. Conf. LACAR97, Argentina, 10 pp.

Rozhdestvensky, A.V. (1990): Assessment of efficiency of hydrological computations. Gidrometeoizdat, St.Petersburg, (in Russian).

SNIP (Norm and Rules in Construction), Computation of main design hydrological characteristics. (2001): State Standard, Moscow, Ministry of Construction of Russia, in publish (in Russian).

SNIP-2.01.14-83 (Norm and Rules in Construction), State Standard. (1984): Moscow, Ministry of Construction of Russia, - 39 pp. (in Russian).

UNCERTAINTY ANALYSIS FOR FLOOD RISK ESTIMATION

Bruno Merz[1], Annegret Thieken[1], Günter Blöschl[2]

[1] GeoForschungsZentrum Potsdam (GFZ), Telegrafenberg, 14473 Potsdam, Germany, bmerz@gfz-potsdam.de, thieken@gfz-potsdam.de

[2] Institut für Hydraulik, Gewässerkunde und Wasserwirtschaft, Technische Universität Wien, Karlsplatz 13/223, 1040 Wien, Austria, g.bloeschl@email.tuwien.ac.at

SUMMARY

In order to be economically viable, flood disaster mitigation should be based on a comprehensive assessment of the flood risk. This requires the estimation of the flood hazard (i.e. runoff and associated probability) and the consequences of flooding (i.e. property damage, damage to persons, etc.). A number of studies have shown that the uncertainty associated with such estimates can be significant and that ignoring uncertainty through the use of mean or deterministic values can lead to decisions different from more informed decisions using uncertainty estimates.
Within the 'German Research Network Natural Disasters' project, the working group on 'Flood Risk Analysis' is investigating the complete flood disaster chain from the triggering event down to its various consequences. The working group is developing complex, spatially distributed models representing the relevant meteorological, hydrological, hydraulic, geo-technical, and socio-economic processes. In order to assess the flood risk and the uncertainty of the risk estimates these complex deterministic models are complemented by a simple stochastic model. The latter model consists of modules each representing one process of the flood disaster chain. Each module is a simple parameterisation of the corresponding more complex model. This ensures that the two approaches (simple stochastic and complex deterministic) are compatible at all steps of the flood disaster chain. The simple stochastic approach allows a large number of simulation runs in a Monte Carlo framework. These simulations are used to derive uncertainty bounds of the risk estimates. Additionally, the contributions of individual processes to the uncertainty of the risk estimation are identified.

Keywords: risk analysis, uncertainty analysis, flood damage estimation

1 INTRODUCTION

Flood defence systems are usually designed by specifying an exceedance probability and by demonstrating that the flood defence system prevents damage for events corresponding to this exceedance probability. This concept is limited by a number of assumptions and many researchers have called for more comprehensive design procedures (Plate, 1992, Bowles et al., 1996; Berga, 1998, Vrijling, 2001). The most complete approach is the risk-based design which strives to balance benefits and costs of the design in an explicit manner (Stewart, Melchers, 1997). For example, an optimal flood defence system, chosen from multiple options, can be found by minimising the life-cycle costs, i.e. the expected costs during the lifetime of the system. The costs also include failure costs which relate to the adverse effects of system failure (monetary damage, loss of life, injury, etc.). Failure is defined as a state where the system does not fulfil its purpose, i.e. it does not provide safety. For example, failure of a river levee occurs when the levee's hinterland is inundated, e.g. because of the river water level exceeding the levee crest or because of levee breach due to internal erosion.
In the context of risk-based design, flood risk encompasses the flood hazard (i.e. extreme events and associated probability) and the consequences of flooding. Ideally, a flood risk analysis should take into account all relevant flooding scenarios, their associated probabilities, their possible consequences and yield the full distribution function of the flood consequences.
Uncertainty is an inherent aspect of risk. Because risk analyses deal with extreme events which have rarely or never been observed at the time a decision has to be made, the uncertainty associated with risk estimates can be significant. Therefore, risk quantifications need to deal with uncertainty in some way (USACE, 1996; Carrington, Bolger, 1998). It has been shown that ignoring uncertainty through the use of mean or deterministic values can lead to decisions different from more informed decisions using uncertainty estimates (USACE, 1992; Petermann, Anderson, 1999).
So far, comprehensive flood risk and uncertainty analyses are an exception. Most analyses have been limited, e.g. by only considering a few failure scenarios or by not investigating the consequences of a

failure. Such limitations in the analyses have often been the result of a lack of data or lack of knowledge of the complex interactions in predicting extreme events and their consequences. With advances in data acquisition and widespread availability of high-speed computerised tools, comprehensive flood risk and uncertainty analyses are more feasible and are gaining increased attention. This is a development that certainly can be observed in the field of dam safety (Berga, 1998).
The purpose of this paper is to present the concepts and first results of a comprehensive flood risk and uncertainty analysis. The work is part of a larger project that aims at quantifying the spatial distribution of the flood risk along reaches of large rivers such as the Rhine. To this end, a methodology is being developed for analysing flood risks in river catchments.

2 CONCEPT OF THE RISK AND UNCERTAINTY ANALYSIS

Within the 'German Research Network Natural Disasters' (http://dfnk.gfz-potsdam.de), the working group on 'Flood Risk Analysis' has been investigating the complete flood disaster chain from the triggering event down to its various consequences: 'heavy rainstorms and/or snowmelt – runoff generation and runoff concentration in the catchment – flood routing – potential failure of flood protection structures – inundation – damage'. The current flood risk and possible changes in risk due to climate change, land use change and flood mitigation measures are to be derived for areas along the Rhine with particular attention to the City of Cologne. A further aim is to provide the end-users with an indication of the uncertainty of the risk estimates.

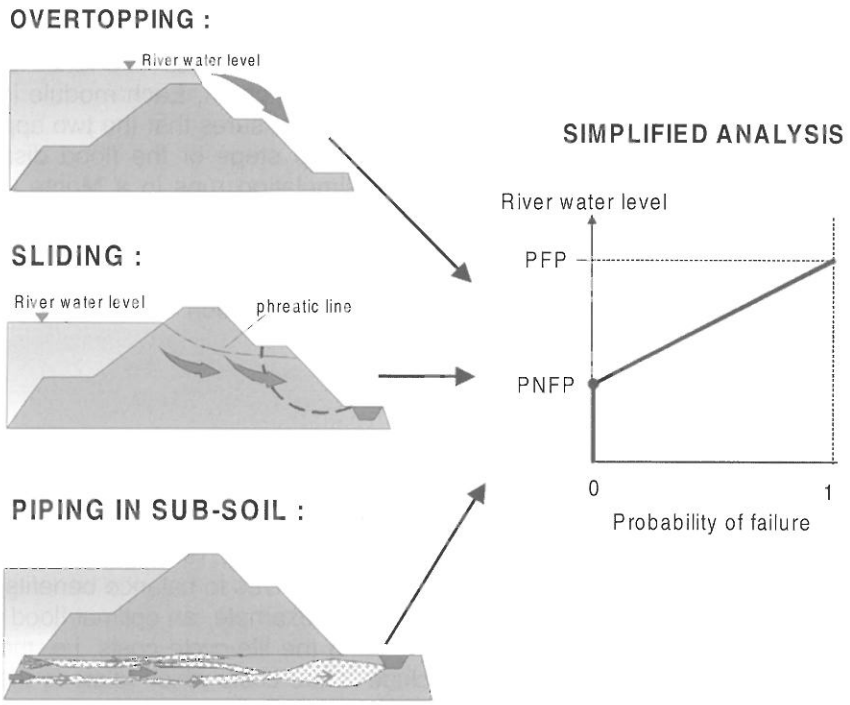

Figure 2-1: River levee performance: Deriving simple probabilistic parameterisations (right; PNFP: Probable Non-Failure Point; PFP: Probable Failure Point) for river breach from complex, physically-based, geo-technical studies (left).

The working group consists of eight sub-projects which study in detail the different processes of the flood disaster chain. For each element, complex, spatially distributed models are under development, representing the meteorological, hydrological, hydraulic, geo-technical, and socio-economic processes. The quantification of the flood risk and its uncertainty requires the combination of all processes of the flood disaster chain. Ideally, all models representing the different processes should be combined and many simulations should be run in order to derive the complete distribution function of flood damage. Such an approach is not feasible due to the enormous CPU and data requirements of the complex models. Therefore, in this project, these complex models are complemented by a simple stochastic model consisting of modules each representing one process of the flood disaster chain. Each module is a simple parameterisation of the corresponding more complex deterministic model. For instance, the complex deterministic representation of river levee performance consists of a physi-

cally-based, geo-technical model which describes the different failure mechanisms of river levees (breaching due to overtopping, sliding, piping in the sub-soil, etc.). The simple stochastic counterpart consists of a relationship for the probability of levee failure as a function of river water stage (Figure 2-1). The simple parameterisations are calibrated against the corresponding complex models. This ensures that the two approaches (simple stochastic and complex deterministic) are compatible at all steps of the process chain.
The simple stochastic approach allows a large number of simulation runs in a Monte Carlo framework. Such simulations are used to derive the flood risk of the target areas, e.g. the distribution function of the direct monetary flood damage of the City of Cologne. Furthermore, in a second order Monte Carlo simulation, uncertainty bounds of the risk estimates are derived.

3 CASE STUDY: FLOOD RISK OF COLOGNE

The feasibility of the simple stochastic approach is illustrated below for the case of the Rhine at Cologne. The model considers the following elements of the flood disaster chain: hydrological load, hydraulic transformation, damage in the flooded areas. In future, this reduced process chain will be extended by meteorological, hydrological, hydraulic and geo-technical processes to cover the complete flood disaster chain. For now, the parameters of the simple modules are derived from published data and studies that are based on complex deterministic models and data analyses. Once more comprehensive results from the complex models within DFNK are available, the parameters of the simple modules will be calibrated to the results of the complex models.

3.1 Model and Input Data

The risk and uncertainty analysis for the flood disaster chain of Cologne is based on the following data and assumptions.
The hydrological load, which is the first module, was derived from the flood frequency curve of the gauge Cologne/Rhine based on the annual maximum series from 1880 to 1990 (AMS18801999). In general, the uncertainty of frequency analyses of extreme events consists of model uncertainty and parameter uncertainty. To assess the model uncertainty, four distribution functions were fitted to AMS18801999: Gumbel, Pearson-III, Weibull and the Lognormal distribution. Figure 3-1 shows the four distributions and their agreement with the observed data for which the Weibull plotting positions were used. The parameter uncertainty was quantified by calculating the standard deviation of the mean estimated discharge for selected return periods T for each distribution function (Maniak, 1997):

(1) $$s_T = \beta_T \cdot \frac{s_{AMS}}{\sqrt{N}}$$

where: s_T: standard deviation of the mean estimated discharge with return period T,
β_T: coefficient for incorporating the skewness of the distribution function,
s_{AMS}: standard deviation of the sample,
N: sample size.

Based on Monte Carlo simulations (see below), the mean flood frequency curve and the uncertainty at selected return periods have been calculated (Figure 3-2). In the simulations equal weight was given to each of the four distributions functions.
The second module of the flood disaster chain transforms discharge values into river water levels, using the rating curve of the gauge Cologne/Rhine (hydraulic transformation). The transformation is based on measurements of discharge Q and water levels h to which, by means of least squares, the following equation was fitted, where a, b and c are coefficients (Figure 3-3):

(2) $$Q = a * (h - b)^c$$

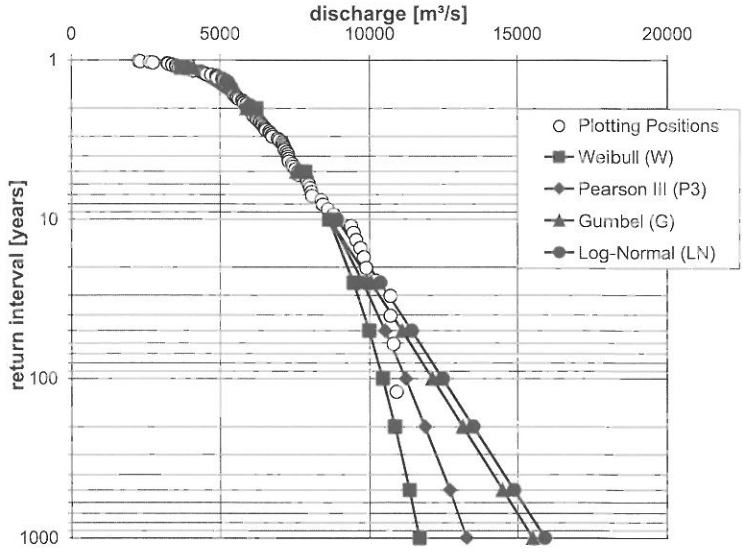

Figure 3-1: Fitting different distribution functions to the annual maximum flood series 1880-1999 of the gauge Cologne/Rhine.

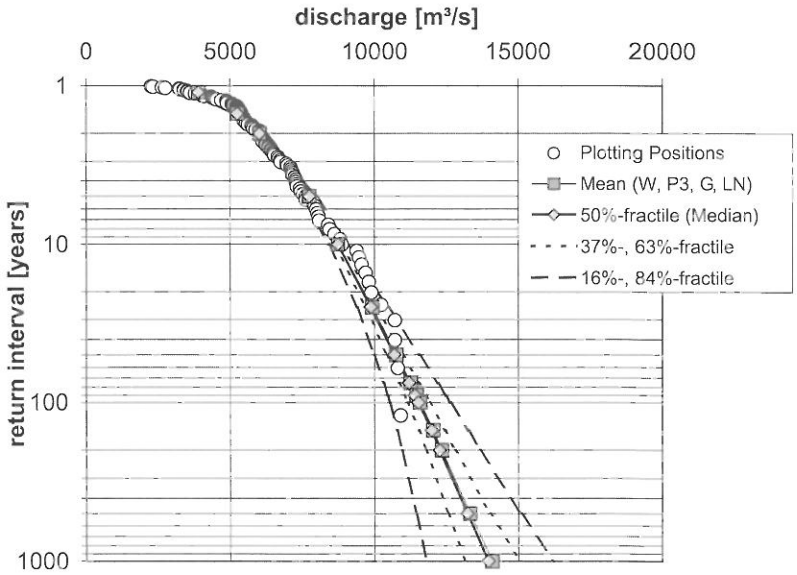

Figure 3-2: Mean flood frequency curve and its uncertainty from the Monte Carlo simulations.

It was assumed that the standard deviation of the discharge residuals (difference between measured and calculated discharge values) is a measure of the uncertainty of the hydraulic transformation. In order to consider the variation of uncertainty with increasing discharge, the discharge range was divided into classes (Figure 3-3). Figure 3-4 shows that the standard deviation of the residuals in the classes 0 - 3 increases with increasing discharge. Since class 4 is the extrapolation range where no measurements were available (Figure 3-3), the standard deviation for this class was estimated based on a linear extrapolation of the errors of the classes 0 – 3 (Figure 3-4).
The third module estimates the direct monetary damage in Cologne due to flood situations. These estimations are based on a damage function which relates the damage in the flooded areas to the river water level. The damage function of Cologne was derived from the unpublished studies of Rodriguez and Zeisler (1998) and ProAqua (2000). For selected river water levels, they simulated the extend of the inundation by a hydraulic model. Furthermore, they estimated the expected damage of all affected plots considering land use type (private housing, industry, etc.) and inundation depth. The sum of all damages within the inundation areas gave the total damage of Cologne at selected water levels (Figure 3-5).

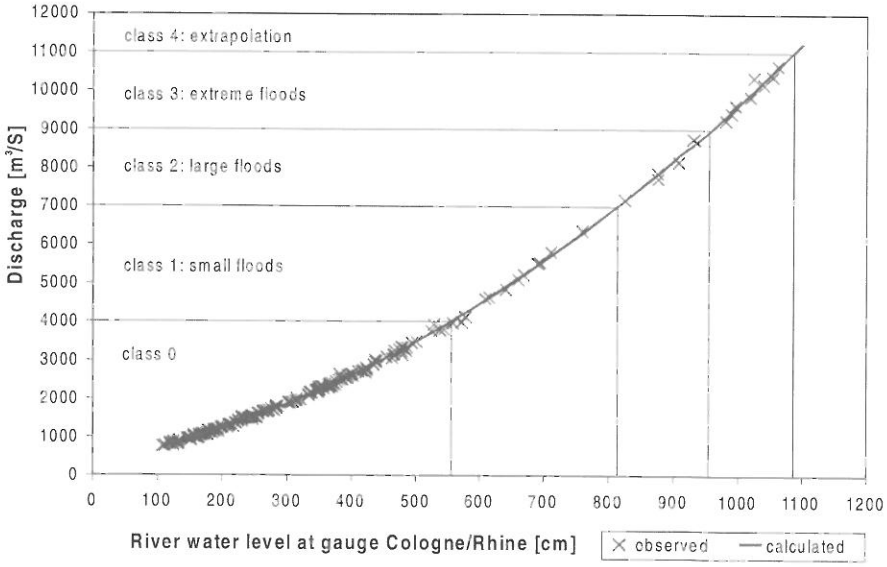

Figure 3-3: Discharge – water level measurements and rating curve of the gauge Cologne/Rhine.

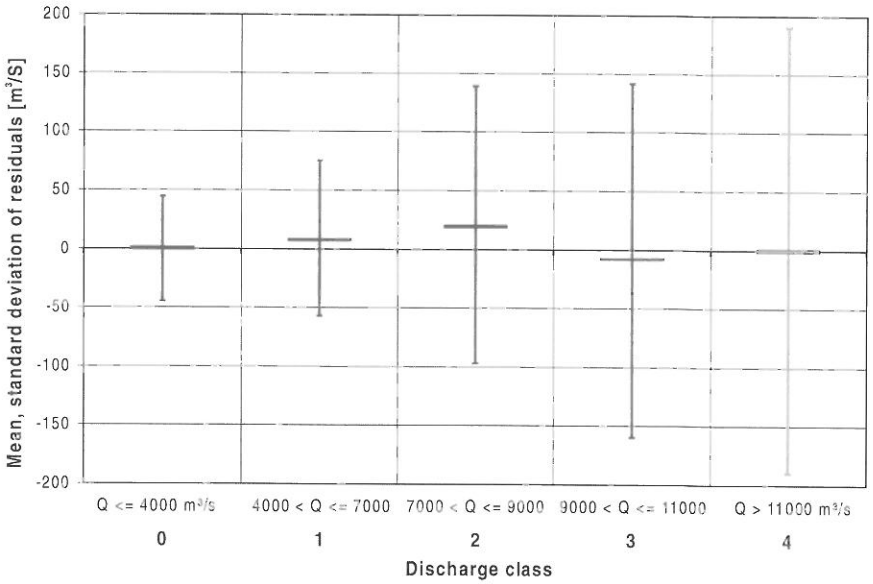

Figure 3-4: Mean values and +/- one standard deviation of the residuals for the different discharge classes at the gauge Cologne/Rhine.

This complex model was simplified by using the following equation from Kron and Thumerer (2001):

(3) $$D = \frac{SA_{in}}{SA} \cdot \frac{r}{100} \cdot \frac{d}{100} \cdot V$$

where: D: total direct property damage [DM],
SA: total settlement area [km²],
SA_{in}: inundated settlement area [km²],
r: damage frequency [%], which is the ratio of the actually damaged properties to the potentially damaged properties in the inundation area; r is assumed to take into account the damage-reducing effects of local flood defence and mitigation measures,
d: average property damage [% of the average property value],
V: sum of all property values [DM].

The parameters of this equation were derived from the results of Rodriguez and Zeisler (1998) and ProAqua (2000). The total settlement area in Cologne amounts to S = 230.27 km² (ProAqua, 2000). By means of land use information and the regional statistics of Nordrhine-Westphalia the sum of all property

values in Cologne was estimated to V = 177 billion DM (ProAqua, 2000). Since the analysis of Rodriguez and Zeisler (1998) and ProAqua (2000) did not consider local flood defence and precautions, the parameter r was set to 100 %. The parameters SA_{in} and d depend on the water level. For our simple model, the relationships of water level h versus inundated settlement area SA_{in} and water level h versus average property damage d were calibrated against the results of the above mentioned studies.
The uncertainty of these damage estimations is difficult to assess. Flood damage modelling is a field which has not received much attention and the theoretical foundations of damage models should be further improved (Wind et al., 1999). To estimate the uncertainty of the damage assessment it has been assumed here that the standard deviation of the inundated settlement area (SA_{in}) amounts to 10 % of the mean value and that the standard deviation of the average damage d amounts to 20 % of the mean value (Wind et al., 1999). For both parameters a normal distribution was assumed. The estimated sum of all property values in Cologne varies from 130 to 355 billion DM depending on the data source (estimates from Munich Re, Rodriguez, Zeisler, 1998, ProAqua, 2000). Since the actual shape of the uncertainty distribution will rarely be known, a triangular distribution was used according to USACE (1992). The most likely estimate amounts to 170-180 billion DM.

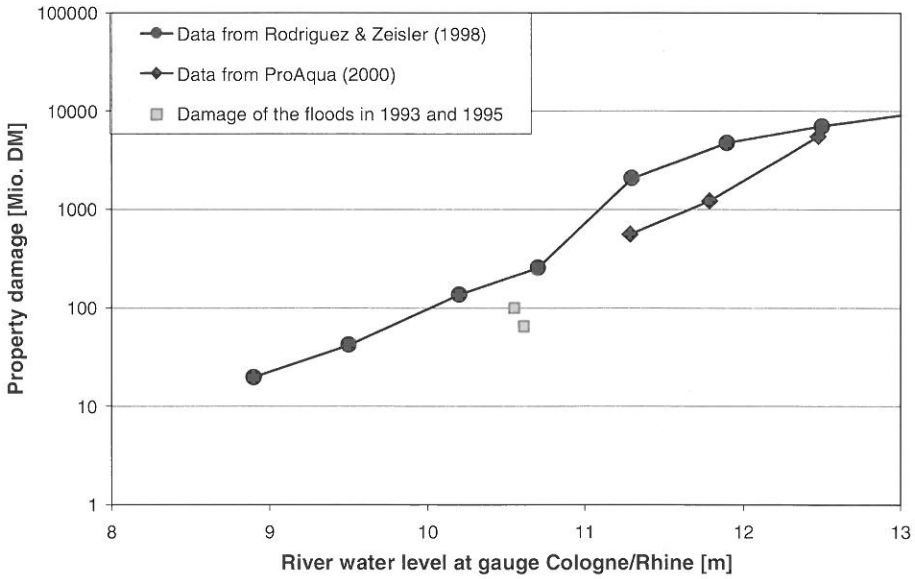

Figure 3-5: Estimation of direct property damage in Cologne as a function of the water level at the gauge Cologne/Rhine.

The three modules were combined in a first order Monte Carlo framework. A discharge was randomly chosen from a distribution function of discharge. This discharge was then transformed into a water level and afterwards into a property damage. By repeating this procedure 100000 times the distribution function of discharge is transformed into a distribution function of property damage. This distribution is plotted as a risk curve which gives the probability of events with damage exceeding a given level (complementary distribution function). In a further step, the uncertainty of the risk curve at selected return intervals has been assessed. To this end, a Monte Carlo simulation of second order has been performed which takes into account the uncertainty of the three processes.

3.2 First Results and Discussion

The results of the risk and uncertainty analysis for Cologne are summarised in Figure 3-6. The plots show the median flood risk curve (50%-fractile) and the 16%- and 84%-fractiles of the total uncertainty (i.e. +/- one standard deviation). Additionally, the contribution of the uncertainty of the different processes are shown. The risk curve has been calculated for return periods from 10 to 1000 years. For this range, the risk analysis yields direct monetary damages from 30 to 6000 million DM. The damage increases dramatically for events with return periods from 50 to approximately 100 years.
The simulations suggest that the uncertainty due to the flood frequency estimation is the dominant contribution to the total uncertainty (Figure 3-6a). Further research should focus on reducing this

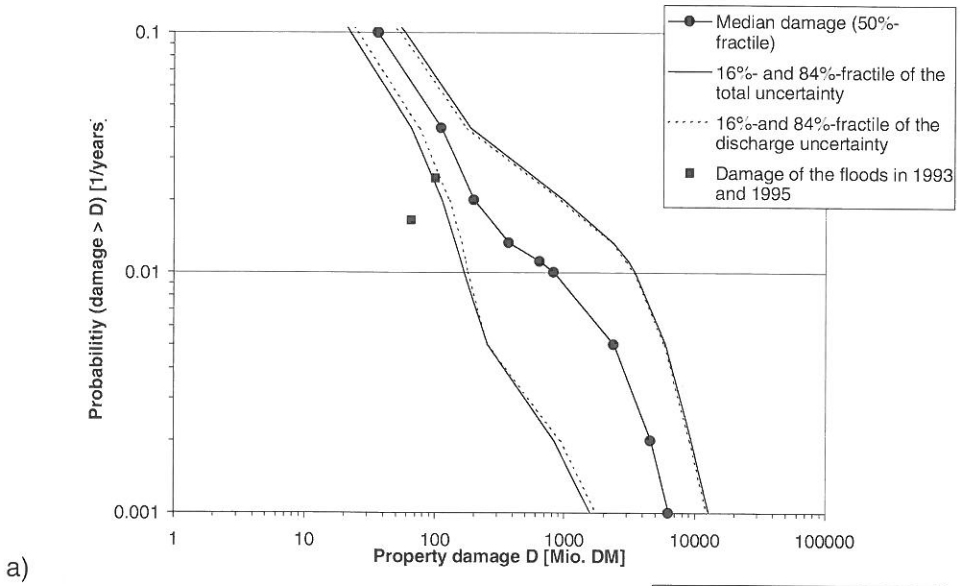

a)

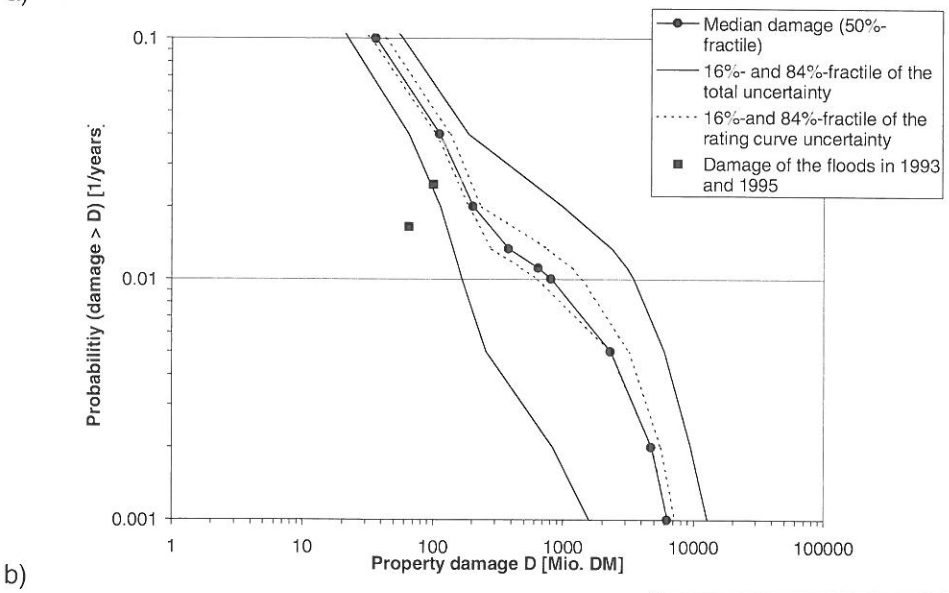

b)

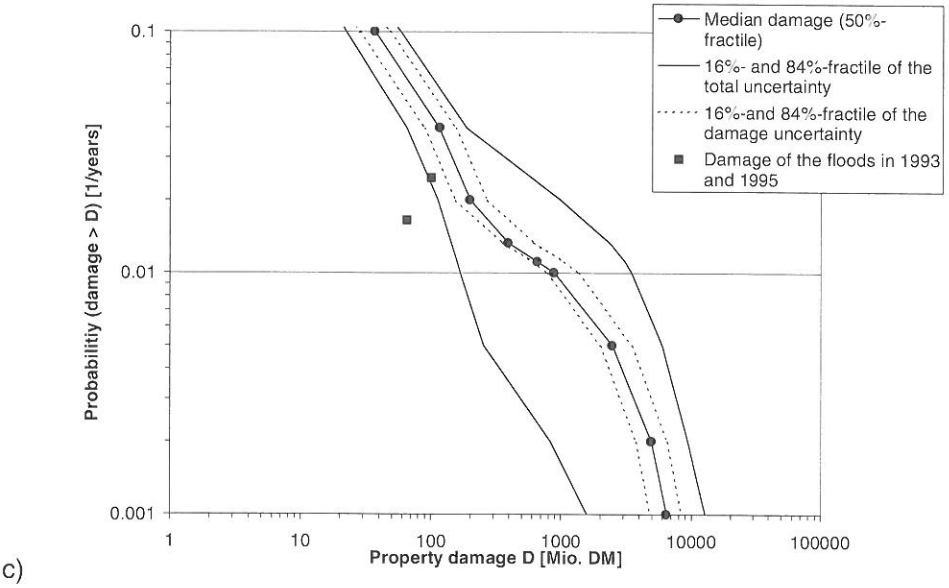

c)

Figure 3-6: Median flood risk curve for Cologne and estimates of the total uncertainty and the uncertainty due to the hydrological load (a); due to the hydraulic transformation (b); due to the damage function (c).

uncertainty. Possibilities are improved model selection for the flood frequency analysis and the use of rainfall-runoff modelling. Further issues that need clarification are the effect of the choice of sample (annual versus partial series) and the choice of the parameter estimation method on the uncertainty.
The uncertainty of the risk curve that is caused by the hydraulic transformation is almost negligible (Figure 3-6b). Its largest contribution occurs at return periods of approximately 100 years. This effect is caused by the characteristics of the flood defence system in Cologne. At water levels with return periods of approximately 100 years, the defence system starts to fail. Therefore, a small change in the water level may lead to a large change in the damage.
The uncertainty of the damage function contributes a large share to the total uncertainty for events with return periods up to 25 years (Figure 3-6c). For larger events the total uncertainty is dominated by the uncertainty of the flood frequency analysis. This result is surprising and needs further investigation. Flood damage data are rather scarce. The uncertainty of the damage function used for Cologne is a first rough assumption and will be improved by more detailed data analyses. Comparing with the estimates of flood damages in 1993 and 1995 the modelled property damages are too high. This may be due to the fact that local flood defense and mitigation strategies were not considered. Most damage models have in common that the direct monetary damage is obtained from the type and number of flooded objects and the inundation depth although it has been shown that the flood damage may depend on many factors. Some of these factors are flow velocity, duration of inundation, sediment concentration, availability and information content of flood warning, and the quality of external response in a flood situation (Penning-Rowsell, Fordham, 1994). Penning-Rowsell and Green (2000) found that the aggregated reduction of flood damage due to an early warning system and the effective response of residents will be 13 %, while Smith (1981) showed that actual damage in the residential sector was only 52.4 % of the potential damage. Wind et al. (1999) found differences of 35 % in municipal damages of the 1993 flood and the 1995 flood which were comparable in magnitude.
The effect of early warning and the degree of preparedness could be incorporated into the simple model by equation 3. Reducing parameter r from 100 % to 87 % leads to a shift of the complete risk curve. For example, the expected annual damage decreases from 44 million DM to 38 million DM.

4 CONCLUSIONS

A simple stochastic model was developed that allows to estimate the flood risk for large rivers. Furthermore, the model gives an indication of the uncertainty of the risk estimates. The quality of this uncertainty estimation depends on the quality of the assumptions about the uncertainty of the processes involved. The uncertainty of the flood damage model used here is a first assumption and needs further investigation. The feasibility of the model is illustrated for the case of the City of Cologne.
Even though the stochastic model is rather simple it is a comprehensive approach for the quantification of the flood risk. Further work will include additional processes and will focus on the calibration of the stochastic model against the more complex, spatially distributed models for the individual processes of the flood disaster chain.

ACKNOWLEDGEMENTS

Funding from the German Ministry for Education and Research (project number 01SFR9969/5) and data provision from the Institute of Hydrology, Koblenz, Munich Re; Munich and ProAqua, Aachen are gratefully acknowledged.

REFERENCES

Berga, L. (1998): New trends in hydrological safety. In: Berga, L. (ed.): Dam safety. Balkema. Rotterdam. pp. 1099-1106.

Bowles, D. et al. (1996): Risk assessment approach to dam safety criteria. Uncertainty in the Geologic Environment: From Theory to Practice. Geotechnical Special Publication No. 58, ASCE. p. 451-473.

Carrington, C.D., Bolger, P.M. (1998): Uncertainty and risk assessment. Human and Ecological Risk Assessment. Vol. 4(2): 253-257.

Kron, W., Thumerer, T. (2001): Überschwemmung in Deutschland. Versicherungswirtschaft. Vol. 56: 1370-1377.

Maniak, U. (1997): Hydrologie und Wasserwirtschaft. 4th Edition. Springer. Berlin. 650 pp.

Penning-Rowsell, E., Fordham, M. (1994): Floods across Europe: Flood hazard assessment, modelling and management. Middlesex University Press. London.

Penning-Rowsell, E.C., Green, C. (2000): New Insights into the appraisal of flood-alleviation benefits: (1) Flood damage loss information. Journal of the Chartered Institution of Water and Environmental Management. Vol. 14: 347-353.

Peterman, R.M., Anderson, J.L. (1999): Decision analysis: a method for taking uncertainties into account in risk-based decision making. Human and Ecological Risk Assessment. Vol. 5(2): 231-244.

Plate, E.J. (1992): Stochastic design in hydraulics: concepts for a broader application. Proc. Sixth IAHR Intern. Symposium on Stochastic Hydraulics, Taipei.

ProAqua (2000): Potentielle Hochwasserschäden am Rhein in Nordrhein-Westfalen. Studie im Auftrag des Ministeriums für Umwelt, Raumordnung und Landwirtschaft des Landes Nordrhein-Westfalen (unpublished).

Rodriguez, R., Zeisler, P. (1998): Ermittlung der Hochwasserschadenspotenziale in den überflutungsgefährdeten Gebieten der Stadt Köln. Gutachten im Auftrag der Stadt Köln, Hochwasserschutzzentrale (unpublished).

Smith, D.I. (1981): Actual and potential flood damage: a case study for urban Lismore, (New South Wales) NSW, Australia. Applied Geography. Vol. 1: 31-39.

Stewart, M.G., Melchers, R.E. (1997): Probabilistic risk assessment of engineering systems. Chapman and Hall, London.

USACE (U.S. Army Corps of Engineers), (1992): Guidelines for risk and uncertainty analysis in water resources planning. Institute for Water Resources, IWR Report 92-R-1. Fort Belvoir, VA. 62 pp.

USACE (U.S. Army Corps of Engineers), (1996): Risk-based analysis for flood damage reduction studies. Engineering Manual 1110-2-1619. Washington, DC.

Vrijling, J.K. (2001): Probabilistic design of water defense systems in The Netherlands. Reliability Engineering and System Safety. Vol. 74: 337-344.

Wind, H.G. et al. (1999): Analysis of flood damages from the 1993 and 1995 Meuse floods. Water Resources Research. Vol. 35(11): 3459-3465.

ON THE USE OF SIMULATION TECHNIQUES FOR THE ESTIMATION OF PEAK RIVER FLOWS

Armando Brath, Alberto Montanari, Greta Moretti

Faculty of Engineering, University of Bologna, Viale del Risorgimento 2, 40136 Bologna, Italy,
alberto.montanari@mail.ing.unibo.it

SUMMARY

In recent times, an increasing attention is being paid by hydrologists to simulation approaches for the estimation of the design flood flows. Such techniques may represent an attractive option when, due to the limited availability of historical information, an at-site or regional estimation of the design flood is not advisable. This study aims at testing the performances of a simulation procedure for estimating the flood frequency distribution. The proposed technique makes use of a multivariate stochastic point process for the generation of synthetic rainfall data, fractionally differenced ARIMA models for the generation of synthetic temperature data and a spatially distributed rainfall-runoff model for the simulation of synthetic flow runs referred to the river cross section of interest. An approximate approach for evaluating the uncertainty associated to the estimation of the peak flows is presented. The methodology has proven to be satisfactorily robust, in that the selected models resulted to be sufficiently reliable even when only short historical rainfall, temperature and river flows records are available for parameter calibration. In particular, the rainfall-runoff model can be parameterised even when river flows records are not available for the considered site, being the model parameters estimable by using upstream or downstream flow records. An application of the simulation technique to a small river basin (158 km^2 in area) located in Northern Italy is presented. As it was to be expected, the results show that the reliability of the approach strictly depends on the length of the historical records available. However, even when these latter are very short, useful indications about the shape of the flood frequency distribution can be derived.

Keywords: simulation, flood frequency, peak flow, distributed models, stochastic processes

1 INTRODUCTION

The damages due to flood and flash-flood events, in terms of both number of casualties and economic costs, are steadily increasing in the latest decades all over the world, ranking their impact at the top among weather-related natural hazards. For instance, in Italy a recent survey of flood events, carried out by the Italian National Group for the Prevention of Hydrogeological Disasters, shows the extreme vulnerability of Italian watersheds as far as floods are concerned. In fact there is an increasing need for effective measures for the reduction of such vulnerability, in the form of both flood warning system and engineering works for flood protection. In order to design an effective structural or management solution, in terms of both reduction of the flood risk and minimisation of the economic and environmental impact, one generally needs to obtain a reliable estimate of the maximum discharge and/or water volume that can be delivered during a flood, for an assigned probability of exceedance (or return period). This is usually called the "design flood" (NERC, 1975) and is estimated by making use of techniques for analysing the magnitude of extreme events.
The different approaches used by hydrologists for the estimation of the design flood can be classified into three main groups, namely, statistical, derived distribution and simulation techniques. The statistical methods attempt to estimate the frequency distribution of the extreme events by analysing observed records of peak river flows. When these latter are available for the river cross section of interest, an at-site estimation can be performed, by fitting the observed data using an appropriate extreme-value probability distribution. Kottegoda and Rosso (1997) present a variety of probability distributions that can be used to this end. The at-site estimation approach can rarely be used in practice, because of the limited number of flow gauging stations today available in most countries. Statistical design flood estimation for ungauged rivers can be performed by using regional techniques, such as the index flood method, the method of direct regression of quantiles and the method of regression for distribution parameters. The statistical methods are commonly applied in order to obtain an estimate of the peak discharge only but they can be employed for evaluating the flood volume too (Bacchi et al., 1993). The main limitation to the use of statistical approaches stems in their need for sufficiently extended peak flows observations recorded in the river cross section of interest or at least in its

neighbourhood. The minimum length of the historical record required for performing a reliable estimation increases with decreasing probability of exceedance of the estimated design flood.
The derived distribution approach is usually based on coupling a stochastic rainfall model with a rainfall-runoff model and, by means of such schematisation, aims at investigating the physical links which may relate some relevant behaviours of the flood frequency distribution with various selected geomorphoclimatic parameters of the watershed. In principle this approach can be applied even to ungauged catchements and, on one hand, is potentially able to provide useful indications of broad validity about the frequency of the extreme river flows. On the other hand, in order to allow the flood frequency distribution to be analytically or numerically derivable, one often needs to oversimplify the structure of the involved models, thus introducing significant approximations. Motivated by the pioneer work of Eagleson (1972), many authors provided in recent years scientific contributions about the derived distribution approaches (Cadavid et al., 1991; Raines and Valdes, 1993; Iacobellis and Fiorentino, 2000; Loukas, 2001).
The simulation approach is based on the use of rainfall-runoff models of varying complexity for generating river discharges from precipitation records. These latter can be derived from historical data, or obtained via rainfall generation models. The simulation approach aims to generate a synthetic series of peak river flows that can be used for inferring the flood frequency distribution of a given watershed. Since no limitation is imposed on the complexity of the involved models, which can be tailored to the specific case study, the simulation method might be successfully applicable for estimating the design flood, even to data limited catchments. In the past the simulations runs were mostly limited to the time span of single flood events, in order to limit the computational effort. This approach presents the disadvantages of requiring the specification of the initial soil moisture condition of the watershed and assuming that the return period of an extreme rainfall event is equal to the return period of the induced peak flows. This latter assumption was criticised by many authors (Dickinson, 1992). The increasing availability of computing powers makes now possible to move towards standard techniques for flood hydrograph estimation based upon the continuous simulation of flow. In fact, by running hydrological models continuously in time and analysing the flood peaks of the simulated flow series, it is no longer necessary to make the above assumption and, moreover, antecedent soil moisture is automatically accounted for by the hydrological model.
The reliability of the simulation approach for the estimation of the design flood in real world applications has yet to be fully proven. However, the results so far presented by the scientific literature are promising (Naden et al., 1996; Blazkova and Beven, 1997; Lamb, 1999; Cameron et al., 1999, 2000), though these first applications have shown the significant uncertainty which may affect the results. The requirement of reducing these uncertainties opens the door to numerous avenues of research. One of them is related to the question of consistency of rainfall-runoff model parameterisations for both continuous flow series and flood frequency simulation. Cameron et al. (1999) noted that this latter question has been so far poorly investigated and wondered: "if a model is provided with observed rainfall data, then will one or more parameter sets that provide acceptable hydrograph simulations also provide acceptable estimates of the frequency characteristics of the flood peaks?". To answer to this question is not an easy task and useful indications might be derived by developing some research case studies referred to gauged catchments.
The works by Cameron et al. (1999, 2000) can be considered a valuable guidance for applying the continuous simulation approach in order to derive the flood frequency distribution. The authors present an application to an extensively gauged catchment located in England, for which a 21-year record of rainfall and discharge observation is available. A 1000-year simulation run was obtained by applying a stochastic rainfall generator and the TOPMODEL rainfall-runoff model (Beven et al., 1984). Confidence bands for the estimated flood frequency distribution were derived by using the Generalised Likelihood Uncertainty Estimator (GLUE, Beven and Binley, 1992). The simulation approach provided an acceptable fit of the observed hydrographs and peak flow data. Nevertheless, the authors pointed out that further research is needed for improving the reliability of the estimation and concluded that there is a generic problem in current rainfall-runoff modelling and/or measurements techniques which could preclude the complete consistency of parameterisation in hourly hydrograph simulation and flood frequency estimation. This conclusion is particularly significant in view of the quite extensive historical data-base the authors had at disposal, which is very often unavailable in real world applications. Therefore, one may suspect that the uncertainties associated to the use of the simulation approach in poorly gauged catchments would be even more pronounced.
The study presented in this paper aims at providing a further contribution to the inspection of the performances of continuous simulation approaches for the estimation of the flood frequency distribution. Given that Cameron et al. (1999) pointed out the key effect exerted by the hydrological model on the estimation reliability, much of the present study has been devoted to testing an alternative rain-

fall-runoff approach, which has been specifically designed in order to meet the following requirements: (a) to allow a robust simulation of the peak flows even when only short records of historical data are available for model parameterisation, in order to be able to apply the model to data limited catchments; (b) to allow to constrain the range of the value of at least some of the model parameters by means of in-situ measurements or physical reasoning, in order to minimise the parameterisation uncertainty; (c) to provide very long simulation runs (up to one thousand years) at hourly time step in a reasonably limited time, even for medium-size basins; (d) to be able to be implemented even when a little information about the contributing area is available. The proposed rainfall-runoff model is spatially distributed and makes use of conceptual and physically-based schemes for the simulation of the hydrological processes at local scale. Rainfall input is provided by the multivariate generalised Neyman-Scott model (Cowpertwait, 1995) which was found in many occasions capable to fit the statistical properties and the spatial distribution of rainfall records referred to a wide range of climatic and orographic conditions.
The application of the proposed simulation procedure to a gauged watershed located in Northern Italy provided a good fit of the observed peak flows data. The reliability of the design flood estimation obviously depends on the length of the historical records available, but the application herein developed shows that satisfactory performances can be attained even when referring to scarcely gauged catchments.
The next section of the paper describes the study watershed. The third section aims at illustrating the simulation procedure, whose application is presented in the fourth section. The fifth section outlines the conclusions of the study.

2 THE STUDY WATERSHED

The simulation procedure herein proposed has been applied to the case study of the Samoggia River basin, located in Northern Italy, closed at the river cross section of Calcara (see Figure 2-1). The Samoggia River flows northwards across the Apennines Mountains and joins the Reno River upstream the city of Bologna. The basin area at Calcara is 158 km^2. The catchment is mostly mountainous, with a maximum and minimum altitude of 850 and 50 m a.s.l. respectively, while the main stream length is 60 km. The mountain areas are constituted primarily of soils and rocks of sedimentary origin, characterised by a low permeability which tend to decrease with increasing altitude. The upper part of the watershed is primarily covered by broad-leaved woods, which occupy about 10% of the basin area. The lower part of the basin is instead constituted by highly permeable alluvial fans, and is covered by farmlands and urbanised areas, these latter occupying less than 5% of the total basin extension. Because of their low permeability and their extension with respect to the total catchment surface, mountain areas contribute substantially to the formation of flood flows, which are

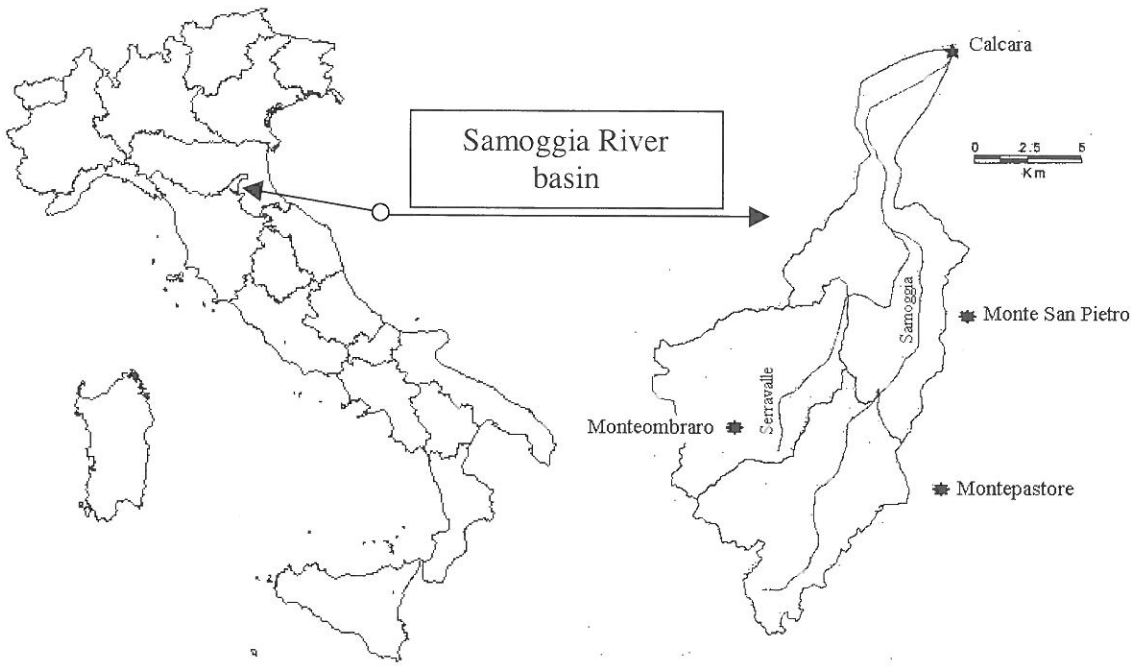

Figure 2-1: Location of the Samoggia River basin and the rainfall and river flow gauging stations.

primarily generated as infiltration excess runoff. The most critical precipitation and floods occur in Autumn and rarely in Spring and the annual maximum peak flow observed at Calcara in the period 1938-1997 is 452 m^3/s (1940). The annual rainfall depth averaged over the basin area and over the period 1959-1977 is 938 mm and the runoff coefficient, for the same period, is equal to 0.37. Basin topography is described by a Digital Elevation Model (DEM) whose resolution is 250 x 250 m, that is displayed in Figure 2-2. The hillslopes are significantly steep, since the slope of 44% of the basin area is comprised in the range 20%-10%.
The Samoggia River basin is monitored by raingauges and hydrometric stations managed by the Italian National Hydrographic Service. For the purposes of the present analysis, historical data of hourly river discharges at Calcara have been collected, for the period between January 1st, 1996 to December 31th 1996. 33 annual maximum peak flows observed at Calcara in the period 1938-1997 are also available (many observations are missing). Moreover, hourly rainfall depths over the basin are at disposal for the period between January 1st, 1994 to December 31th 1996. The rainfall data have been observed in three raingauges located on the basin or in the immediate neighbours (see Figure 2-1). They are located at Monte San Pietro (317 m a.s.l.), Montepastore (596 m a.s.l.) and Monteombraro (727 m a.s.l.). For this latter raingauge, 59 observation of annual maximum rainfall collected in the period 1938-1997 are also at disposal, for storm durations of 1, 3, 6, 12 and 24 hours. The maximum observed rainfall height for the 24-hour storm duration is 177 mm. Hourly temperature data recorded at Monteombraro in the period 1994-1996 are also available.
An extensive data-base of soil texture, soil type and soil use at local scale is at disposal too, retrieved from surveys carried out in the latter 10 years. Figure 2-3 reports a map of the relative permeability over the basin.

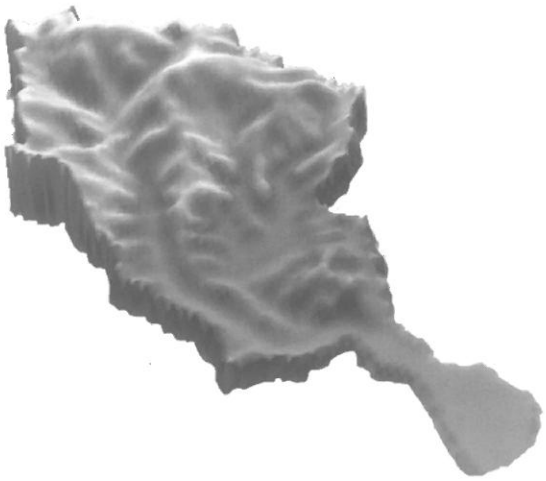

Figure 2-2: Digital elevation Model of the Samoggia River basin.

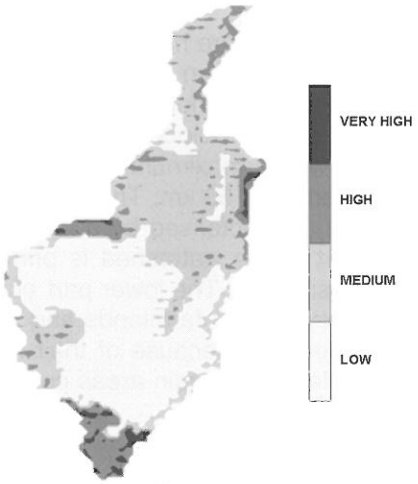

Figure 2-3: Map of the relative permeability of the Samoggia River basin.

3 OUTLINE OF THE SIMULATION PROCEDURE

The simulation procedure proposed herein is structured in the following steps: (a) generation of long runs of synthetic spatially distributed hourly rainfall data; this is achieved by using a stochastic rainfall model, whose parameters are estimated by fitting historical rainfall records. Given that the whole simulation procedure has to be reliable especially in the reproduction of the flood flows, the calibration of the rainfall model parameters has been performed by optimising the fit of some basic statistics of the hourly data and the fit of the annual maximum rainfall, for different storm durations, observed at the Monteombraro raingauge (the only raingauge where extreme rainfall observations are available). (b) generation of long runs of synthetic spatially distributed hourly temperature data; to this end, a stochastic fractionally-differenced ARIMA model has been fitted to the hourly temperature data observed at the Monteombraro raingauge and used to simulate a synthetic series referred to the same location. The cross-correlation between temperature and rainfall data was neglected because it turned out to be negligible in the historical series. Temperature data at local scale were obtained as a function of altitude by applying a standard temperature gradient of -0.006 degree centigrade per each elevation meter. (c) generation of long runs of synthetic hourly river flows data referred to the river cross section of Calcara. This is performed by fitting the proposed rainfall-runoff model using the available historical data and running the model itself by using the synthetic data produced in the previous steps as

meteoclimatic input. (d) Analysis of the extreme values of the synthetic river flows series in order to derive indications about the shape of the flood frequency distribution. In the following parts of this section the simulation procedure will be described with more detail.

3.1 Generation of synthetic rainfall data – The rainfall model

The simulation of spatially distributed rainfall data was obtained by applying a stochastic approach, namely the generalised multivariate Neyman-Scott rectangular pulses model (Cowpertwait, 1995), which represents the total rainfall intensity at time t as the sum of the intensities given by a random sequence of rain cells active at time t. The model is a generalisation of the well-known single-site Neyman-Scott rectangular pulses model (Rodriguez-Iturbe et al., 1987; Burlando, 1989).
In detail, the model represents the storm origins as occurrences of a Poisson process with rate λ, the arrival times being the same for any point in the catchment. The arrival of a storm origin at a catchment implies that the physical conditions necessary for rainfall have been met. However, rain only occurs at points in the catchment covered by rain cells. Each storm origin generates a random number of circular rain cells according to a Poisson process with rate ν. These cells are centred on the centroid of the raingauges and their radius is an independent exponential random variable with parameter γ. The waiting time, after a storm origin, for the starting time of a rain cell, is an independent exponential random variable with parameter β. Each rain cell has a random duration and a random intensity, where the intensity remains constant over the circular area covered by the cell and throughout the duration of the cell itself. Therefore, a pulse of rain is associated with each rain cell. The cell intensity and duration are both distributed exponentially with parameters μ and η. Each cell is characterised by a site-dependent probability to reach the ground level.
The total rainfall intensity at an arbitrary time t at a point m is the summation of the intensities of all cells active at time t that overlap point m. Such total rainfall intensity is scaled by a factor (which can be a function of the altitude). In order to account for seasonality, the model parameters can assume different values in each calendar month. Further details on the generalised multivariate Neyman-Scott model can be found in Cowpertwait (1995).
Since in the present case 3 raingauges are available, the total number of model parameters is equal to 12 for each calendar month. The monthly parameters of the rainfall model were estimated by applying the method of moments. This consists in minimising numerically the difference between the theoretical values of some basic statistics of the rainfall data, which are functions of the model parameters, and the corresponding values computed on the observed hourly rainfall data set. The statistics used for model estimation are the monthly mean, variance, proportion of dry hours, lag-one autocorrelations and lag-zero cross-correlation of the hourly data. In order to avoid inconsistency in the simulation of the extreme values, the parameter estimates were validated by verifying the capability of the model to reproduce the mean, variance and asymmetry of the annual maximum rainfall series observed in Monteombraro for the different storms durations.
Once that an optimal parameter set has been found, the capability of the model to fit the data has been checked by performing a statistical test based on simulation experiments. In detail, in order to check the fit of the mean, standard deviation, proportion of dry days and lag-one autocorrelation of the hourly data, 1000 samples of rainfall observations were simulated with a sample size equal to that of the historical series (3 years). On each sample the above statistics, averaged over the months and the raingauges, were computed and ranked. Then, the 2.5 and the 97.5 percentiles of the ranked values were assumed as 95% confidence limits for each of the statistics and compared with the ones computed on the historical records. The fit of the extreme values was tested by following an analogous procedure. Once that a long record of rainfall data was simulated, the annual maximum rainfall for storm duration of 1, 3, 6, 12 and 24 hours were extracted. 1000 different series of annual maxima were generated, with sample size equal to that of the correspondent historical data (59 data). The mean value, the standard deviation and the asymmetry of each of these samples were computed and ranked, thus obtaining their 95% confidence limits as described above. These too were compared with the analogous statistics computed on the observed data. Table 3-1 and 3-2 report the results of the above comparisons and show that the rainfall model provided a satisfactory fit of the observed rainfall. Only the proportion of dry hours is not well fitted by the model, which instead provides a good fit of the extreme values, that are of primary interest in the context of the present analysis. Figure 3-1 and 3-2 show a comparison between the frequency distribution of observed and simulated (1000-year sample) annual maxima, for storm duration of 1 and 24 hours.
Once the model parameters were calibrated, 1000 years of hourly spatially distributed rainfall data were generated to be used as input to the distributed rainfall-runoff model.

Table 3-1: Statistics of the historical samples of hourly rainfall. 95% confidence limits computed by simulation are reported between parentheses.

Mean (mm)	Standard deviation (mm)	Proportion of dry hours	Lag-1 autocorrelation
0.107 (0.081-0.119)	0.706 (0.591-0.893)	0.905 (0.917-0.935)	0.649 (0.443-0.691)

Table 3-2: Statistics of the historical samples of annual maximum rainfall for different storm durations. 95% confidence limits computed by simulation are reported between parentheses.

Storm duration	Mean (mm)	Standard deviation (mm)	Asimmetry
1	25.0 (21.2 – 26.6)	11.1 (8.4 – 14.0)	12.1 (6.8 – 16.5)
3	40.2 (34.7 – 42.1)	14.7 (10.9 – 19.2)	16.8 (8.5 – 23.7)
6	50.9 (44.3 – 52.8)	16.7 (12.6 – 20.3)	17.5 (10.3 – 22.0)
12	68.6 (59.1 – 72.5)	25.7 (19.1 – 32.4)	28.8 (16.0 – 39.4)
24	86.3 (73.2 – 92.2)	37.4 (26.4 – 52.5)	45.6 (24.4 – 74.3)

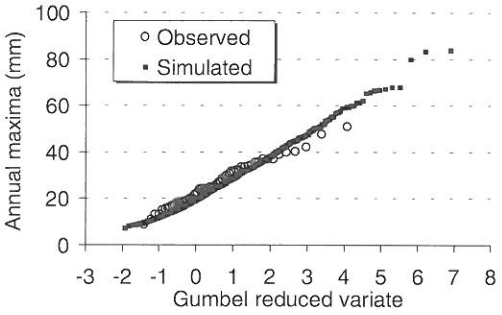

Figure 3-1: Monteombraro raingauge. Compa-rison between the frequency distribution of observed and simulated annual maximum rainfall for storm duration of 1 hours.

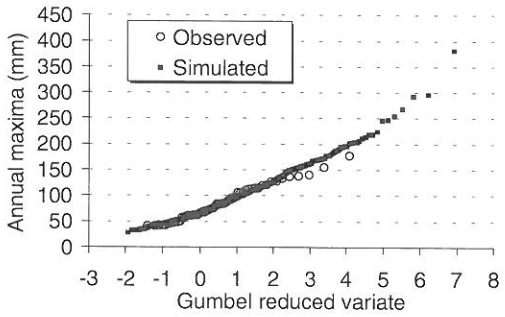

Figure 3-2: Monteombraro raingauge. Comparison between the frequency distribution of observed and simulated annual maximum rainfall for storm duration of 24 hours.

3.2 Generation of synthetic temperature data – The temperature model

The generation of synthetic hourly temperature records, referred to Monteombraro, was carried out by applying a linear stochastic approach, namely a fractionally differenced ARIMA model (FARIMA). In many occasions this class of models turned out to be able to fit well the autocorrelation structure of temperature series which, for increasing lag, is very often affected by a slow decay that may suggest the presence of long-term persistence. FARIMA models, that are characterised by a high flexibility in their autocorrelation structure, are capable of fitting long-term persistence by means of the fractional differencing operator. Model fitting was carried out on a monthly basis, in order to account for the non-stationarity of the autorrelation structure of the data. Parameter estimation was performed by applying an approximate maximum likelihood approach. The daily periodicity in the temperature records was preliminarily removed by applying the harmonic regression method. We do not provide a detailed description of the generation of the synthetic 1000-year hourly temperature record, which is based on the application of well-known techniques. Major details on FARIMA models and the simulation procedure herein applied can be found in Montanari et al. (1997, 2000).

3.3 Generation of synthetic river flows data – The rainfall-runoff model

The distributed continuous-simulation rainfall-runoff model used herein has been conceived in order to be applicable to a wide spectrum of real-world case studies, even when only a limited historical database of hydrometeorological and geomorphological records is available. Therefore, particular care has been taken in order to develop a robust approach, which is primarily in charge of providing a suffi-

ciently reliable reproduction of the peak flows. In order to limit the information needed for model parametrisation, many of the hydrological processes involved in the rainfall-runoff transformation have been schematised using conceptual approaches. These need to be parametrised on the basis of some historical hydrometerological records and therefore the need for observed data is not eliminated. However recent researches (Brath et al., 2001) proved the efficiency and the robustness of the proposed model when applied to data limited catchments, especially in comparison with lumped approaches. Such efficiency is believed to be due to the capability of the model to take advantage from the spatially distributed description of basin topography, soil type and use.

The catchment hydrologic response is determined by the composition of the two processes of hillslope runoff and channel propagation along the river network. The model discretises the basin in square cells coinciding with the pixels of the DEM. The river network is automatically extracted from the DEM itself by applying the D-8 method (Band, 1986; Tarboton, 1997), which allows to estimate the flow paths and the contributing area to each cell. In detail, the network determination is carried out by first assigning to each DEM cell a maximum slope pointer and then processing each cell in order to organise the river network. Digital pits are filled in a preprocessing step, before extracting the channel network from the catchment DEM. Each cell receives water from its upslope neighbours and discharges to its downslope neighbour. For cells of flow convergence, the upstream inflow hydrograph is taken as the sum of the outflows hydrographs of the neighbouring upslope cells. Distinction between hillslope rill and network channel is based on the concept of constant critical support area (Montgomery and Foufoula-Georgiou, 1993). Accordingly, rill flow is assumed to occur in each cell where the upstream drainage area does not exceed 0.5 km^2, while channel flow occurs otherwise.

The interaction between soil, vegetation and atmosphere is modelled by applying a conceptual approach. The model firstly computes the local rainfall $P_l[t,(i,j)]$, for each DEM cell, by interpolating the observations referred to each raingauge through an inverse distance approach. Then, for each cell of coordinates (i,j) a first rate of the rainfall depth is accumulated in a local reservoir (interception reservoir) which simulates the interception operated by the vegetation. The capacity of such interception reservoir is equal to $Cint \cdot S(i,j)$, where Cint is a calibration parameter (constant in space and time) and S(i,j) is the local soil storativity. This latter is computed depending on soil type and land use accordingly to the Curve Number method (CN method, Soil Conservation Service, 1972). Once that the interception reservoir is full of water, the exceeding rainfall reaches the ground surface. Then, the surface and sub-surface flows are computed according to a modified CN approach, that is able to simulate the redistribution of the soil water content during the inter-storm periods. In detail, it is assumed that in correspondence of each DEM cell a linear reservoir (infiltration reservoir) is located at the soil level, which collects the infiltrated water. The local surface runoff and infiltration are computed accordingly to the relationship

$$\frac{P_n[t,(i,j)]}{P[t,(i,j)]} = \frac{F[t,(i,j)]}{H \cdot S(i,j)} \quad , \tag{1}$$

where $P[t,(i,j)]$ is the intensity of rainfall which reaches the ground at time t, $P_n[t,(i,j)]$ is the intensity of surface runoff, $F[t,(i,j)]$ is the water content at time t of the infiltration reservoir located in correspondence of the cell (i,j) and $H \cdot S(i,j)$ is the capacity of the infiltration reservoir itself, computed by multiplying a calibration parameter H for the soil storativity previously introduced.

The outflow $W[t,(i,j)]$ from the infiltration reservoir to the subsurface river network, which is assumed to coincide with the surface one, is computed accordingly to the linear relationship

$$W[t,(i,j)] = F[t,(i,j)]/H_s \quad , \tag{2}$$

where H_s is a calibration parameter. H and H_s are assumed to be constant with respect to both space and time.

The parameters H and Cint exert a significant influence on the simulation of the peak river flows. In the context of the present study they were evaluated by means of a trial and error procedure, by optimising the fit of the flood flows and the runoff coefficient of the basin. Calibration experiments performed on different Italian watersheds have shown that the value of the parameter H is often comprised in the range (0.05-0.6), while the parameter Cint is often close to 0.2, which is the value suggested by the CN method. The parameter H_s was calibrated by optimising the shape of the falling limb of the hydrograph and is scarcely effective on the peak flows. A first attempt value for H_s is the expected drying time of the soil column.

The hourly intensity of potential evapontranspiration $E_p[t,(i,j)]$ is computed at local scale by applying the radiation method (Doorembos et al., 1984). When some water is stored in the interception reservoir, the effective evapotranspiration $E[t,(i,j)]$ is assumed to be equal to $E_p[t,(i,j)]$ and is subtracted from the water content of the interception reservoir itself. When this latter is empty, or is emptied while subtracting the evapotranspiration rate, the remaining part of $E_p[t,(i,j)]$ is subtracted from the water content of the infiltration reservoir. In this case, it is assumed that $E[t,(i,j)]$ is varying linearly from 0 when $F[t,(i,j)] = 0$, to $E_p[t,(i,j)]$ when $F[t,(i,j)] = H \cdot S(i,j)$. Evapotranspiration is the only source of water losses in the model.
By combining the equations (1) and (2) and taking the effective evapotranspiration into account, the mass-balance equation for the infiltration reservoir can be written as

$$\frac{dF[t,(i,j)]}{dt} = -\frac{F[t,(i,j)]}{H_s} - E[t,(i,j)] + P[t,(i,j)]\left\{1 - \frac{F[t,(i,j)]}{H \cdot S(i,j)}\right\}, \quad (3)$$

and is numerically solved by applying the second-order Runge-Kutta method.
Surface and sub-surface flows are propagated towards the basin outlet by applying the variable parameters Muskingum-Cunge model. Extensive details can be found in Cunge (1969) and Orlandini et al. (1999) for surface and sub-surface propagation respectively. For the surface flows, the kinematic celerity is computed by considering rectangular river cross section with fixed width/height ratio. This latter parameter and the channel roughness can assume different values along the river network and on the hillslopes. In particular, the channel roughness in the river network is allowed to vary from a minimum to a maximum value depending on the contributing area according to a linear relationships. For the sub-surface flows, the kinematic celerity is instead computed as a function of the saturated hydraulic conductivity of the soil.
It is interesting to note that the model describes in a simplified manner the dynamics of sub-surface flows. In particular, it does not distinguish between near-surface and deep water flow, and assumes that the parameters H and Hs are constant with respect to both space and time. This simplified description has been used in order to reduce the number of model parameters and, consequently, the amount of historical data required for their calibration. On the other hand, one may expect a significant approximation in the simulation of the lower river discharges, especially when referring to highly permeable basins. Moreover, the formation of the surface runoff is modelled according to a scheme that is very similar to the one adopted by the CN model, which is considered by many authors as an infiltration excess approach (Beven, 2000). Therefore one may expect that the proposed model is better suited for basins characterised by low permeability and prevalently impervious hillslopes, where the surface runoff is more likely to be given by excess of infiltration instead of excess of saturation.

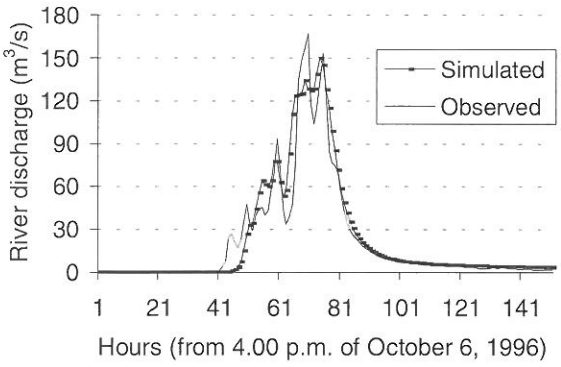

Figure 3-3: Flood event of October 8, 1996. Comparison between observed and simulated hydrographs.

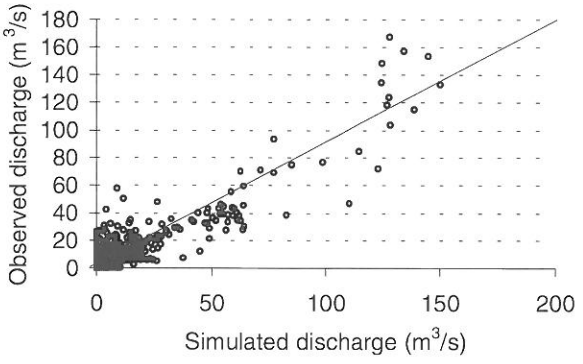

Figure 3.4: Year 1996. Dispersion diagram of observed versus simulated hourly discharges.

Table 3-3 reports a list of the model parameters and indicates which ones were estimated by in-situ measurements or physical reasoning and which ones were instead derived by manual calibration. This latter was performed by comparing observed and simulated hourly river flows of the flood event occurred on October 8, 1996. Figure 3-3 shows a comparison of the observed and simulated flood hydrographs. The model was validated by simulating the hourly flows of the whole year 1996. In Figure 3-4 a diagram of observed versus simulated 1996 hourly flows greater than 20 m^3/s is reported.

Table 3-3: Rainfall-runoff model parameters and their values. These latter were partly optimised by calibration (calibrated) and partly estimated by in-situ measurements or physical reasoning (estimated).

Parameter	Symbol and dimension	Method of estimation	Estimated values
Strickler roughness for the hillslopes	k_{sv} [$m^{1/3}s^{-1}$]	Calibrated	4.6
Channel width/height ratio for the hillslopes	$w_{v\,[-]}$	Calibrated	500
Maximum and minimum Strickler roughness for the channel network	K^0_{sr} , K^1_{sr} [$m^{1/3}s^{-1}$]	Estimated	25-45
Channel width/height ratio for the channel network	$W_{r\,[-]}$	Estimated	10
Constant critical source area	A_0 [km^2]	Estimated	0.5
Saturated hydraulic conductivity	K_i [cm s^{-1}]	Calibrated	1.0
Bottom discharge parameter for the infiltration reservoir capacity	H_s [s]	Calibrated	79095
Multiplying parameter for the infiltration reservoir capacity	H [-]	Calibrated	0.08
Multiplying parameter for the interception reservoir capacity	Cint [-]	Calibrated	0.65

Table 3-4: Absolute mean relative error in the simulation of the 1996 hourly flows for different threshold levels.

> 0 m^3/s	> 5 m^3/s	> 10 m^3/s	> 30 m^3/s	> 50 m^3/s	> 100 m^3/s
56%	47%	44%	40%	23%	14%

All the parameters that were optimised by calibration assumed physically realistic values. The Nash-Sutcliffe coefficient of efficiency for the simulation of the 1996 hourly flows is 0.82. Table 3-4 reports the absolute mean relative error in the simulation of the 1996 flows for different threshold levels. It can be seen that the model performances are improving with increasing flows.

3.4 analysis of the river flow simulation uncertainty

Quantifying the uncertainty associated to the flood frequency simulation allows one to assess the reliability of the obtained flood estimates. The evaluation of the uncertainty in rainfall-runoff modelling is a topical issue in hydrology. Cameron et al. (1999) used the GLUE method (Beven and Binley, 1992) for estimating the uncertainty associated to their simulations. A similar approach was recently proposed by Kuczera and Parent (1998). These techniques are based on performing repeated simulations of rainfall and runoff records for different parameter values and can hardly be applied in the context of the present analysis. In fact, when the complexity and the number of parameters of the simulation model increase, these methods become highly computer intensive. Therefore an approximate approach is herein introduced for the estimation of the hydrologic uncertainty, that is based on the analysis of the rainfall-runoff model errors in the simulation of the historical sample.
The proposed method relies on some basic assumptions, namely: (a) the uncertainty in rainfall and temperature modelling (precipitation and temperature uncertainty) is not significant with respect to the uncertainty in rainfall-runoff modelling (hydrologic uncertainty) and therefore can be neglected. (b) the rainfall-runoff model errors e(t) are outcomes of a random variable E. The probability distributions of E, is Gaussian and its parameters are dependent on the value of the simulated river flow. (c) The width of the confidence interval of the simulated Q(t) is linearly varying with Q(t) itself.
The authors are fully aware of the approximations introduced by neglecting the precipitation uncertainty. In the present study the rainfall model provided a good fit of the historical records and thus the approximation was believed acceptable. Research studies are currently on going for estimating the uncertainty associated to the Neyman-Scott model simulations.
The hydrologic uncertainty is evaluated by estimating the range of the simulation error with 1-α probability of coverage, where α is the level of significance of the confidence bands. The range is expected to be non-stationary, since it depends on the value of the river discharge. Hence the estimation of the range width was carried out by referring to I different non overlapping classes of increasing water flows. Under the assumption of Gaussian distribution of the error, the upper and lower limits of the above range for the i-th class can be expressed as

(3) $$w_+^{\alpha}(i) = \mu_E(i) + k\,\sigma_E(i)\ ,\ w_-^{\alpha}(i) = \mu_E(i) - k\,\sigma_E(i)\ ,\quad i = 1,.....I,$$

where $\mu_E(i)$ and $\sigma_E(i)$ are the mean and standard deviation of the e(t) comprised in the i-th class and k is the $1-\alpha/2$ quantile of the Student's t distribution with N(i)-1 degree of freedom. Here N(i) is the number of model errors in the i-th class. In order to relate with an analytical relation the above range limits to the value of the simulate river discharge, a linear relationship was found to provide a reasonable approximation in the context of the present case-study. In detail, the procedure is structured in the following steps. 1) Collect a sample as large as possible of pairs Q(t),e(t) of simulated river flows and correspondent model errors. Rank the pairs accordingly to increasing Q(t) and divide them in an arbitrary number of non-overlapping classes. Accordingly to our experience, 10 classes are sufficient, with the last of them collecting all the pairs whose Q(t) is greater than the 20-year return period peak flow. When dealing with short samples, as in the case of the present study, it may be necessary to join some of the classes in order to assure that at least 30 pairs are comprised in each of them. Let us indicate with n the number of the identified classes. 2) Compute the mean $\mu_E(i)$ and standard deviation $\sigma_E(i)$ of the e(t) comprised in each i-th class. 3) Compute the quantities $w^{\alpha}_+(i)$ and $w^{\alpha}_-(i)$. Compute also the mean $\mu_Q(i)$ of the Q(t) in each class. 4) Fit two linear relationships, the first on the n pairs $w_+^{\alpha}(i)$, $\mu_Q(i)$ and the second on the n pairs $w_-^{\alpha}(i)$, $\mu_Q(i)$, thus obtaining the relationships $w^{\alpha}_+(Q)$ and $w^{\alpha}_-(Q)$ which relate the simulated flow Q(t) to the widths of the its confidence bands. In order to account for the uncertainty in the estimation of the linear regression coefficients, their 95% confidence limits were used in order to express the confidence band width. 4) Compute the $1-\alpha$ confidence interval for the simulated river flow with the relationships $Q^{\alpha}_+(t) = Q(t) + w^{\alpha}_+(Q)$ and $Q^{\alpha}_-(t) = Q(t) - w^{\alpha}_-(Q)$.
In the present analysis, since a short sample of historical flows is only available, it was necessary to limit the number of classes to the value n = 3. After performing the estimation procedure described above, the following equations were obtained for the width of the 90% confidence bands,

(4) $$w_+^{\alpha}(Q) = 9.36 + 0.61Q\ ,\ w_-^{\alpha}(Q) = -9.43 - 0.75Q \qquad [m^3/s].$$

The coefficient of determination of the two linear regressions (4) are 0.86 and 0.93 respectively. It is advisable not to extrapolate (4) beyond the value of the maximum observed river discharge contained in the data-base used for obtaining the confidence bands, in order to avoid unreliable estimations.

4 SIMULATION RESULTS

The 1000-year long rainfall and temperature records which were simulated using the stochastic models described in the Section 3.1 and 3.2 were used as meteoclimatic input to the rainfall-runoff model. The annual maximum hourly peak flows were extracted from the synthetic river discharge record, thus obtaining a 1000-size sample of flood flows to be compared with the available historical data-set. In order to verify the reliability of the simulation procedure on an objective basis, a statistical test based on resampling the simulated annual maxima was performed. In detail, 1000 different samples with size equal to that of the historical series (33 data) were extracted from the simulated 1000-year record of annual maximum peak flow. The mean, standard deviation and asymmetry of these simulated samples were computed and ranked. Then, the 2.5 and the 97.5 percentiles were assumed as 95% confidence limits for the respective statistics and compared with the analogous values computed on the historical record. The results of such comparison are reported in Table 4-1 and show that the hypothesis of good fit cannot be rejected. Figure 4-1 shows a comparison between the frequency distribution of observed and simulated annual maximum peak flow.
From Figure 4-1 one can note an underestimation of the lower peak flows, which is probably due to the approximation introduced in the modelling of the dynamics of the sub-surface flows. The mean values of observed and simulated annual maximum peak flows are 148 and 166 m^3/s respectively.

Table 4-1: Mean, standard deviation and asymmetry of the historical sample of annual maximum peak flow. 95% confidence limits computed via simulation (see text) are reported between parentheses.

Mean (m^3/s)	Standard deviation (m^3/s)	Asimmetry
166.5 (106.0 – 191.6)	113.8 (82.1 – 175.2)	120.1 (63.6 – 210.1)

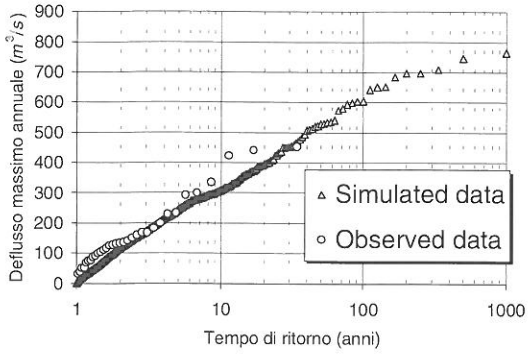

Figure 4-1: Comparison between observed and simulated flood frequency curves.

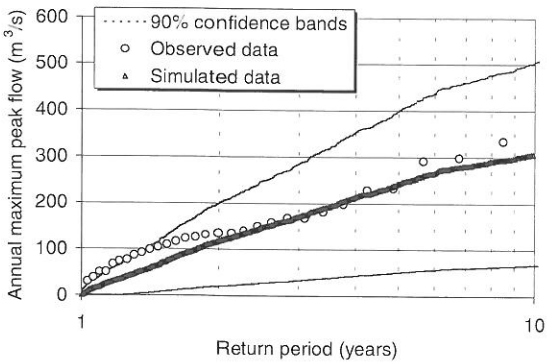

Figure 4-2: 90% confidence bands of the simulated river flows computed as described in Section 4.

Figure 4-2 shows the 90% confidence interval for the simulated river flows of the Samoggia River. It is quite wide, because of the limited extension of the observed record. This is to be expected, since the confidence bands quantify the uncertainty associated to the estimation and therefore their width have to increase with decreasing data availability. In particular, a large estimation uncertainty for the mean $\mu_E(i)$ and variance $\sigma_E(i)$ results when a few model errors e(t) are only available. From Figure 4-2 it can be noted that almost all the observed annual maximum peak flows are comprised between the confidence bands, with a few exceptions for some lower river flows.

5 CONCLUSIONS

This paper presents a simulation procedure for the estimation of the flood frequency distribution. The proposed technique makes use of a multivariate stochastic point process for the generation of synthetic rainfall data, a fractionally differenced ARIMA models for the generation of synthetic temperature data and a spatially distributed rainfall-runoff model for the simulation of synthetic river flows runs referred to the river cross section of interest. The simulation procedure was developed paying particular attention for assuring a satisfactory robust reproduction of the flood flows, even for data limited catchments. An approach for evaluating the uncertainty associated to the estimation is presented, along with an application to a case study of a river basin located in Northern Italy. The methodology has proven to be satisfactorily robust, in that the selected models could be shown to be sufficiently reliable even when only short historical rainfall, temperature and river flows records are available for model calibration. In particular, the observed flood frequency distribution resulted to be satisfactorily simulated, especially in view of the limited length of the historical data-base in this case available for calibrating the model parameters.

ACKNOWLEDGEMENTS

The work presented here has been partially supported by the Ministry of University and Research in Science and Technology (MIUR) of Italy through its national grant to the program on "Hydrological safety of impounded rivers", and by the National Research Council of Italy, National Group for the Prevention of the Hydrogeological Disasters, contract n° 0000489PF42. Comments from an anonymous Reviewer were greatly appreciated.

REFERENCES

Bacchi, B. et al. (1993): Analysis of the relationships between flood peaks and flood volumes based on crossing properties of river flow processes. Water Resour. Res., 28, 2773-2782. AGU. Washington D.C.

Band, L.E. (1986): Topographic partition of watersheds with digital elevation models. Water Resour. Res., 22, 15-24. AGU. Washington D.C.

Beven, K.J. (2000): Rainfall-Runoff modeling. John Wiley. London.

Beven, K.J., Binley, A. (1992): The future of distributed models: model calibration and uncertainty prediction. Hydrol. Proc., 6, 279–298. John Wiley. London.

Beven, K.J. et al. (1984): Testing a physically-based flood forecasting model (TOPMODEL) for 3 UK catchments. J. Hydrol., 69, 119–143. Elsevier. Amsterdam.

Blazkova, S., Beven, K.J. (1997): Flood frequency prediction for data limited catchments in the Czech Republic using a stochastic rainfall model and TOPMODEL. J. Hydrol., 195, 256–278. Elsevier. Amsterdam.

Brath, A. et al. (2001): Comparing the calibration requirements and the simulation performances of lumped and distributed hydrological models: an Italian case study. Abstract presented at the AGU Spring Meeting, Boston, May 2001, Eos. Trans. AGU, 82, Spring Meet. Suppl., Abstract H31D-04.

Burlando, P. (1989): Stochastic models for the predictions and simulations of rainfall in time (in Italian). Ph.D Thesis. Politecnico di Milano. Milan.

Cadavid, L. et al. (1991): Flood-frequency derivation from kinematic wave. J. Hydrol. Engng., 117,489-510. ASCE. Reston.

Cameron, D. et al. (1999): Flood frequency estimation by continuous simulation for a gauged upland catchment (with uncertainty). J. Hydrol., 219, 169-187. Elsevier. Amsterdam.

Cameron, D. et al. (2000): Flood frequency estimation by continuous simulation (with likelihood based uncertainty estimation). Hydrol. Earth Syst. Sci., 4, 23-34. EGS. Katlenburg-Lindau.

Cowpertwait, P.S.P. (1995): A generalized spatial-temporal model of rainfall based on a clustered point process. Proc. of the R. Soc. of London, Series A, 450, 163-175. London.

Cunge, J.A. (1969): On the subject of a flood propagation computation method (Muskingum Method). J. Hydraulic Res., 7, 205-230. IAHR. Madrid.

Dickinson, W.T. et al. (1992): Extremes for rainfall and streamflow, how strong are the links? Can. Water Resour. J., 17, 224-236. AGU. Washington D.C.

Doorembos, J., et al. (1984): Guidelines for predicting crop water requirements. FAO Irrig. Drainage Pap. Rome.

Eagleson, P.S. (1972): Dynamics of flood frequency. Water Resour. Res., 8, 878–898. AGU. Washington D.C.

Iacobellis, V., Fiorentino, M. (2000): Derived distribution of floods based on the concept of partial area coverage with a climatic appeal. Water Resour. Res., 36,469-482. AGU. Washington D.C.

Kottegoda, N.T., Rosso, R. (1997): Statistics, Probability And Reliability Methods for Civil and Environmental Engineers. McGraw-Hill. New York.

Kuczera, G., Parent, E. (1998): Monte Carlo assessment of parameter uncertainty in conceptual catchment models: the Metropolis algorithm. J. Hydrol., 211, 69, 85. Elsevier. Amsterdam.

Lamb, R.L. (1999): Calibration of a conceptual rainfall-runoff model for flood frequency estimation by continuous simulation. Water Resour. Res., 35, 3103-3114. AGU. Washington D.C.

Loukas, A. (2001): Flood frequency estimation by a derived distribution procedure. J. Hydrol., 255, 69-89. Elsevier. Amsterdam.

Montanari, A. et al. (1997): Fractionally differenced ARIMA models applied to hydrologic time series: identification, estimation and simulation. Water Resour. Res., 33, 1035-1044. AGU. Washington D.C.

Montanari, A. et al. (2000): A seasonal fractionally differenced ARIMA model applied to the Nile River monthly flows at Aswan. Water Resour. Res., 36, 1249-1260. AGU. Washington D.C.

Montgomery, D.L., Foufoula-Georgiou, E. (1993): Channel network source representation using digital elevation models. Water Resour. Res., 29, 3925-3934. AGU. Washington D.C.

Naden, P.S. et al. (1996): Impact of climate and land use change on the flood response of large catchments. Proceedings of the 31st MAFF Conference of River and Coastal Engineers, Keele, UK, July 1996, 2.1.1–2.1.16.

NERC (1975): Natural Environment Research Council Flood Studies Report. Whitefriars Press. London.

Orlandini S. et al. (1999): On the storm flow response of upland Alpine catchments. Hydrol. Proc., 13, 549-562. John Wiley. London.

Raines, T.H., Valdes, J.B. (1993): Estimation of flood frequencies for ungauged catchments. J. Hydrol. Engng, 119, 1138-1154. ASCE. Reston.

Rodriguez-Iturbe, I. et al. (1987): Some models for rainfall based on stochastic point processes. Proc. of the R. Soc. London, Series A, 410, 269-288. London.

Soil Conservation Service (1972): National Engineering Handbook, section 4, Hydrology. U.S. Dept. of Agriculture. Washington D.C.

Tarboton, D. G. (1997): A New Method for the Determination of Flow Directions and Contributing Areas in Grid Digital Elevation Models. Water Resour. Res., 33, 309-319. AGU. Washington D.C.

REGIONALISATION MODEL FOR FLOOD EVENTS IN BADEN-WUERTTEMBERG BASED ON A MULTIPLE LINEAR REGRESSION MODEL

Peter Neff, Jürgen Ihringer

Institute of water resources planning, hydraulic and rural engineering (IWK), department of hydrology, Kaiserstrasse 12, 76128 Karlsruhe, Germany, iwk@uni-karlsruhe.de

SUMMARY

In water resources development indexes of flood peaks are necessary for construction planning or for estimating a risk potential. Generally these indexes are available only for sites where gauges are and not for the development site. Furthermore caution is required for the reliability of the gauge indexes as the time series of the discharge often are quite short or not reliable. While creating the regionalisation model a spatial adjustment of all gauge indexes was conducted before applying them to the multiple regression model. The model now enables the estimation of the flood peaks at nearly any site. The regionalisation model is available on CD with a special ArcView surface.

Keywords: regionalisation model, flood peak estimation, multiple regression model

1 INTRODUCTION

The regionalisation model for flood events of Baden-Wuerttemberg is a multiple regression model for the area-wide estimation of the flood peak discharges created for the use in water resources development. The model is the continuation of an older procedure for estimating flood events in Baden-Württemberg (LfU, 1983; LfU, 1988). It is based on factors, which nearly all can be derived from topografic maps (Lutz, 1984). It was developped in collaboration with the Landesanstalt fuer Umweltschutz Baden-Wuerttemberg which provided all the data about the gauges. The aim was to develop a robust model for easy use which also contains the possibility of actualisation and continuation.
Time and again in water engineering business values of flood peaks are required for planning buildings like bridges, weirs, power plants or flood control reservoirs, but normally there is no reliable data available. Only for gauges are there more or less certain values existing. And even the certainty of these data depends on a lot of factors such as length of the time series and the quality of the discharge rating curve. During the processing of the regionalisation model for flood events in Baden-Wuerttemberg a spatial comparison of the gauges was conducted. Gauges that did not fit into the spatial structure and showed other behaviour than surrounding gauges were examined more closely. The discharge rating curves were controlled and some of them were hdraulically revised. With the help of the regionalisation model it then became possible to estimate flood peak discharges at nearly any site in Baden-Wuerttemberg for the return periods from 2 years up to 200 years.

2 DESCRIPTION OF THE AREA OF INVESTIGATION

Baden-Wuerttemberg is situated in the south-west of Germany and covers about 35000 km². In regard to the relief, the geology and the land use this region is quite inhomogeneous. Granitic mountainous regions as well as agricultural regions with loess coverage can be found. Also great gravel accumulations as in the Rhine Valley can be found. The elevation ranges between 90 m at the river Rhine and nearly 1500 on the top of the Feldberg in the black forest mountains. Baden-Wuerttemberg is divided by the watershed between the Rhine and the Danube. The tributaries of these two rivers have very different slopes. The mean annual precipitation ranges from about 550 mm to about 2000 mm.

3 THE MODEL

The regionalisation model is based on a multiple linear regression approach. Using the model the flood peak discharges at nearly any site without measurements can be described with catchment parameters. To develop the model first the flood peak discharges for the different return periods (2 years up to 200 years) had to be derived from the time series of the gauges with the help of the extrem value statistics. All in all 335 gauges with usable time series were available. In a second step

the 8 different parameters of the catchments were acquired. At last the following regression model (equation 1, 2, 3) could be derived which allows the estimation of the flood peak discharges of the different return periods as a function of the 8 catchment parameters.

(equation 3-1):

(1)
$$\ln(Y_T) = C_0 + C_1 \cdot \ln(A_{Eo}) + C_2 \cdot \ln(S+1) + C_3 \cdot \ln(W+1) + C_4 \cdot \ln(I_g) + C_5 \cdot \ln(L) + C_6 \cdot \ln(L_C) + C_7 \cdot \ln(hN_G) + C_8 \cdot \ln(LF)$$

(2) for T = 1 [a]: $MHq = Y_t$

(3) for T = 2, 5, 10, 20, 50, 100 [a]: $Hq_T = MHq * Y_T$

with:
MHq : Mean annual maximum discharge per unit area [$m^3/(s*km^2)$]
Hq_T : Maximum discharge per unit area of return period T [$m^3/(s*km^2)$]
C_0 - C_8 : regression coefficients

Factors:
As input for the regionalisation model only gauges are used which show a time series of discharge with at least 10 years. The data of these gauges are used only if they show no trend and the gauges are not influenced by anthropogeneous factors like flood control reservoirs. The uncontaminated parts of a few time series were separated from the rest reflecting anthropogeneous influence and used. Figure 3-1 shows a gauge influenced by a flood control reservoir. All in all 335 gauges comprising more than 15000 years of observation were used for developing the regionalisation model. The mean length of observation is about 45 years. To the qualified gauges a suitable distribution function was fitted in order to derive the flood peak discharges for the different return periods (2 years up to 200 years). Table 3-1 shows the different used distribution functions. The flood peak discharges which were raised in this way are the dependent variables in the regionalisation equation.

Table 3-1: analytical distribution functions for the statistical analysis of the flood peak for several return periods.

	distribution function	**number of paramters**
1	Log-Normal distribution	2
2	Log-Normal distribution	3
3	Gumbel distribution	2
4	Log-Gumbel distribution	2
5	Gamma distribution	2
6	Log-Gamma distribution	2
7	Pearson-III distribution	3
8	Log-Pearson-III distribution	3
9	Weibull distribution	2
10	Log-Weibull distribution	2
11	Weibull distribution	3
12	Log-Weibull distribution	3
13	empirical distribution	-

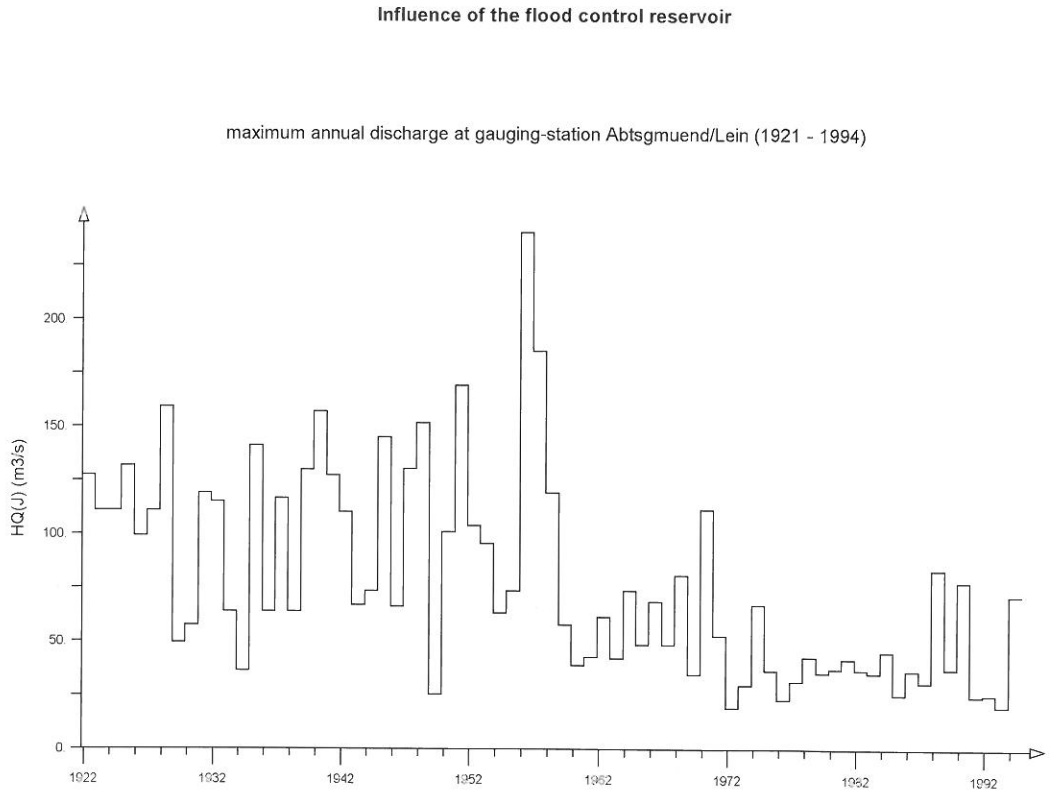

Figure 3-1: Influence of a flood control reservoir on the time series since 1960.

3.1 Catchment parameters (Independent Variables)

The independent variables for the regression calculation are catchment parameters which have been tried and tested in many rainfall runoff models and are easily derived from topographic maps. For the development of the model some of the catchment parametes were calculated automatically with the help of GIS (ArcInfo) on the basis of of the digital elevation model of Baden-Wuerttemberg with a grid size of 50 x 50m. The following parameters are used in the regression model:

1. AE: Area of the catchment in km^2: This parameter is derived from the digital elevation model

2. S: Coverage [%]: urban area in relation to the area of the whole catchment. This parameter was derived from a satellite scene.

3. W: Coverage [%]: forestal area in relation to the area of the whole catchment. This parameter is derived from a satellite scene.

4. IG: weighted slope [%]: as simple measurement for the slope properties in the catchment along the longitudinal section of the river. This parameter was derived from the digital elevation model.

5. L: Length of flow path from watershed to gauge [km]: This parameter was derived from the digital elevation model

6. LC: Length of flow path from the center of the catchment to gauge [km]: This parameter was derived from the digital elevation model.

7. N: Mean annual precipitation [mm]: This parameter could be provided area-wide by the DWD (Deutscher Wetterdienst)

8. LF: empirical landscape factor [-]: Whereas the parameters 1 to 7 are directly available in digital form or can be derived from the digital elevation model of Baden-Wuerttemberg using special routines, the landscape factor is a dimensionless parameter which was at first acquired empi-

rically for the whole area. In closer examination parameters 1 to 7 proved insufficient for obtaining satisfying results. In fact it was necessary to introduce another factor to consider the regional differences in the flood genesis. It was obvious that the geology has a great influence. Since the factor geology cannot be described numerically it was necessary to derive the landscape factor empirically. So in an iterative process the values of the landscape factor were assigned to the different geological units for the whole extent of Baden-Württemberg so that the spatial pattern of the landscape factor is more or less the same as the distribution of the geological units. The comparison of the of the geology and of the landscape factor maps show a very good conformance. The frequencies of the landscape factors are shown in Figure 3-2.

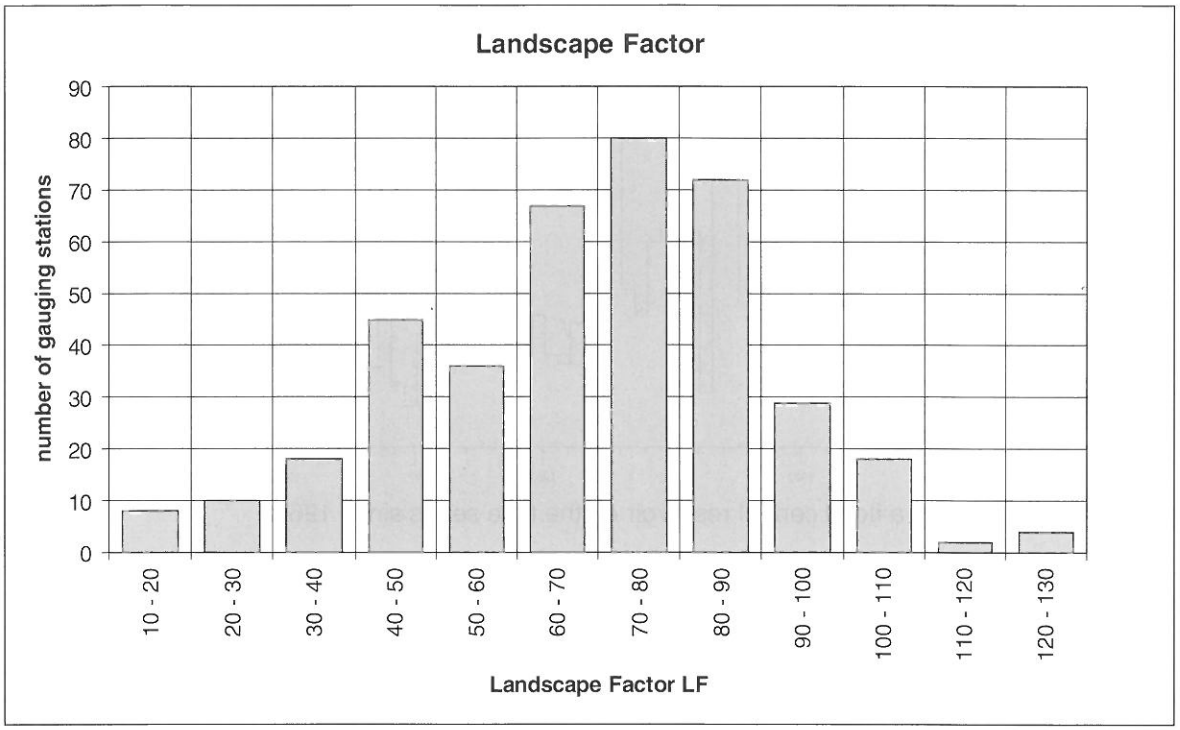

Figure 3-2: Frequency of landscape factor (in classes).

Table 3-2: regression coefficients for the regionalisation model.

return period	coefficients for the several facors for the regression model								
	C_0	C_1 (A_{Eo})	C_2 (S+1)	C_3 (W+1)	C_4 (I_g)	C_5 (L)	C_6 (L_C)	C_7 (hN_G)	C_8 (LF)
MHq	-17.0745	-0.3090	0.1105	-0.2044	-0.0710	0.2667	-0.1059	1.4799	1.5800
Hq_2	-1.3858	-0.0311	0.0055	-0.0713	-0.0517	0.0669	-0.0276	0.2361	-0.0307
Hq_5	1.1075	-0.0063	-0.0199	0.0037	0.0206	-0.0045	0.0200	-0.1243	0.0215
Hq_{10}	2.4326	0.0134	-0.0308	0.0410	0.0629	-0.0491	0.0405	-0.3138	0.0455
Hq_{20}	3.5938	0.0308	-0.0416	0.0661	0.1053	-0.0763	0.0490	-0.4773	0.0628
Hq_{50}	4.8795	0.0501	-0.0503	0.1017	0.1526	-0.1017	0.0530	-0.6618	0.0797
Hq_{100}	5.7391	0.0674	-0.0556	0.1221	0.1860	-0.1269	0.0564	-0.7824	0.0897
Hq_{200}	6.5645	0.0767	-0.0585	0.1456	0.2232	-0.1302	0.0551	-0.9011	0.0936

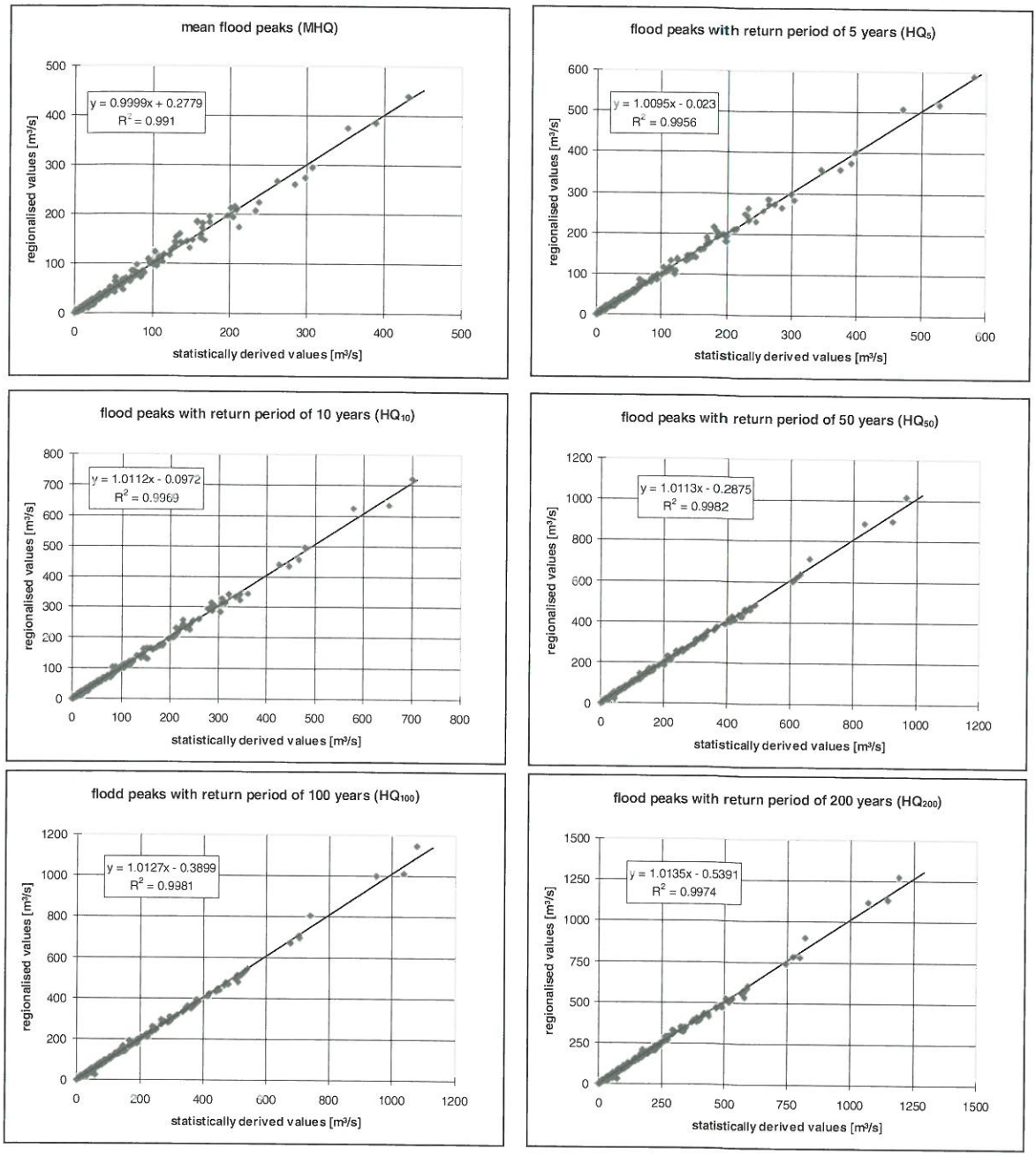

regionalised flood peaks in comparison to statistically derived values for the different return periods

Figure 3-3: comparison of regionalised values and values derived from the statistical analysis.

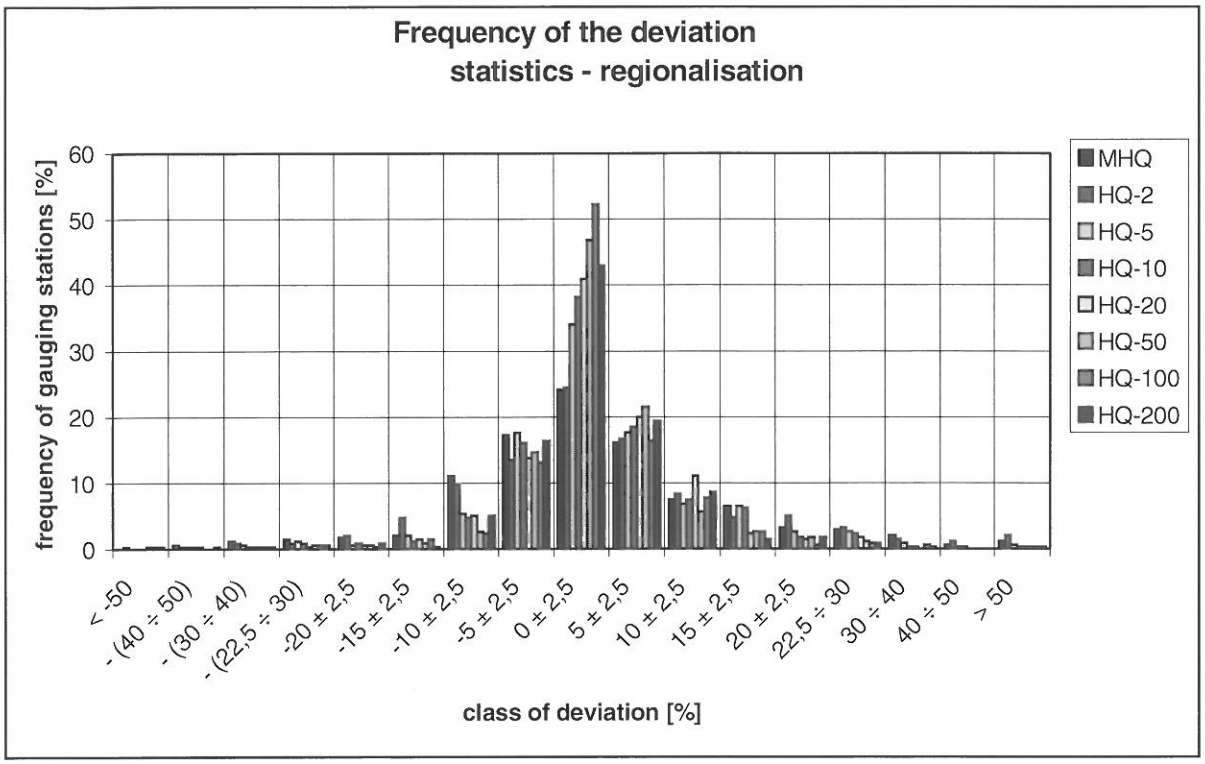

Figure 3-4: Frequenzy of deviation of the regionalised flood peaks from the flood peaks derived from the statistical analysis.

4 RESULTS

The comparison of the regionalised flood values and the values which are derived from the extrem value statistics shows a very good match (Figure 3-3). As shown in Figure 3-4 about 90 percent of the deviating gauges are situated in the zone < 10 percent. Also a very high correlation between the regionalised values and the values derived from the extreme value statistics is obvious. In Table 3-2 the regression coefficients for all return periods and all factors are shown. If these coefficients are illustrated as in Figure 4-3 a plausible progression of the coefficients with the increasing return period becomes clear.
Since the included gauges cover nearly the whole spectrum of all existing geological units in the area it seems to be maintainable to transfer the model to the whole extent of Baden-Wuerttemberg. It was applied to about 3500 predetermined sites in Baden-Wuerttemberg. But at first the determined values could only be verified for the gauges, as there are no other available statistics for these 3500 sites. One illustration of the results is a map of the maximum discharges per unit area for the different return periods. Figure 4-2 shows this discharges for the return period of 100 years.

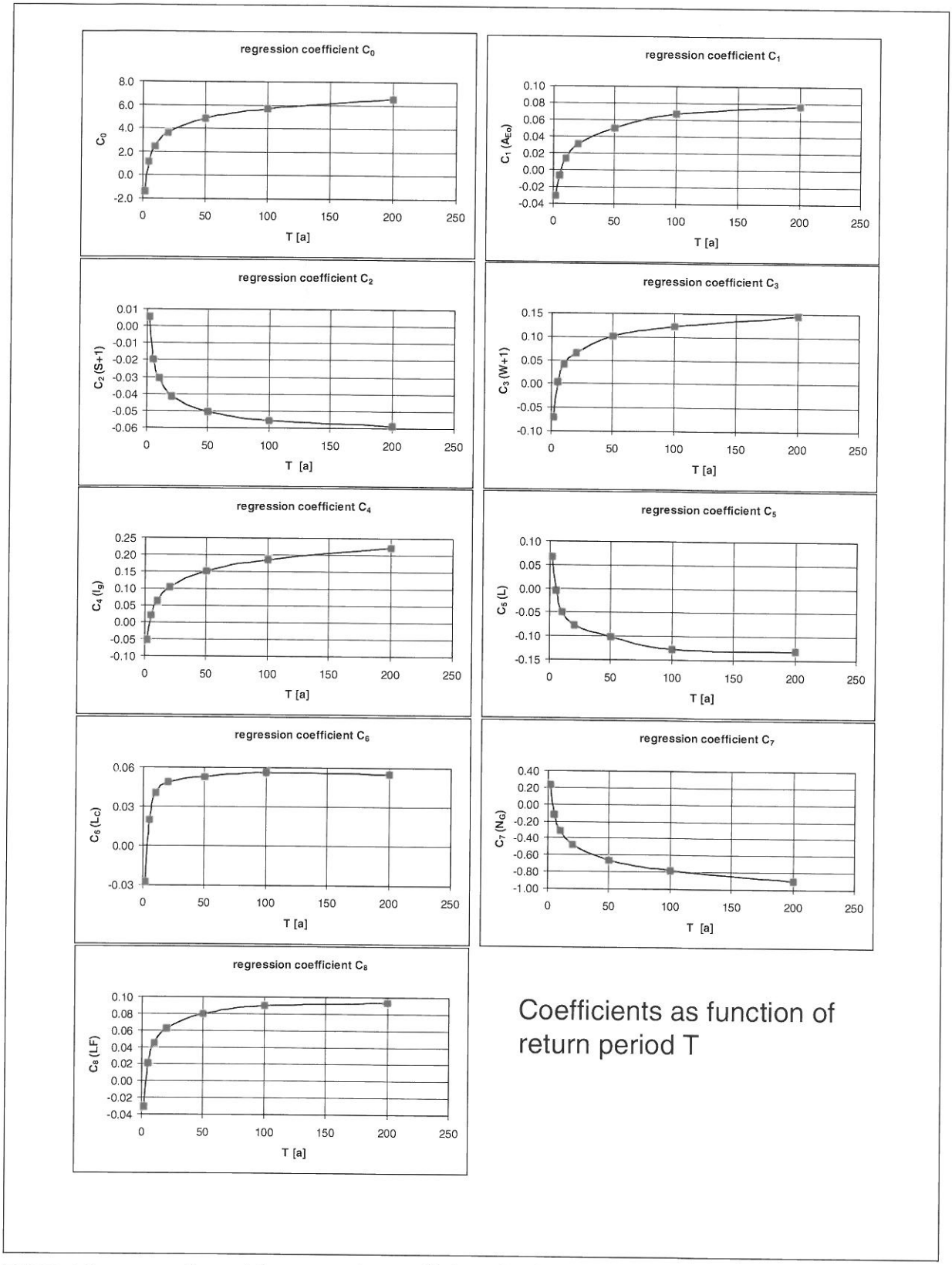

Figure 4-1: comparison of the regression coefficients for the different return periods.

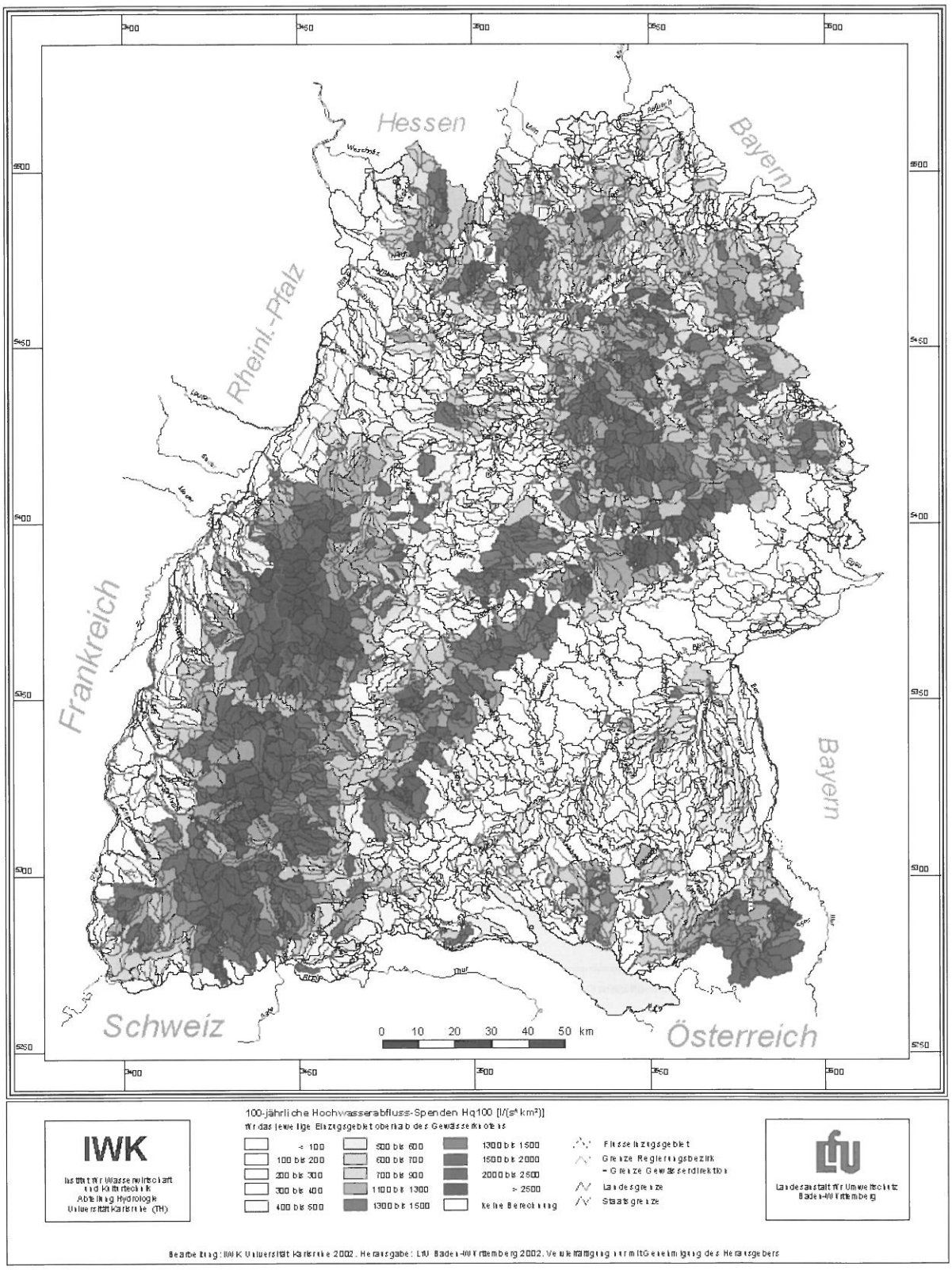

Figure 4-2: regionalised discharges per unit area for the return period of 100 years.

4.1 PLAUSIBILITY CHECK WITH LONGITUDINAL FLOOD SECTÍONS

A plausibility check of the regionalised peak flood discharges could be realised with generated longitudinal sections along 160 selected streams. With the help of these sections which also contain the gauges a very fast and simple visual plausibility-check was possible. At a glance it is possible to recognize decreasing peak flood discharges along a stream (Figure 4-3) For nearly all of the 160 longitudinal sections plausible calculated values arose.

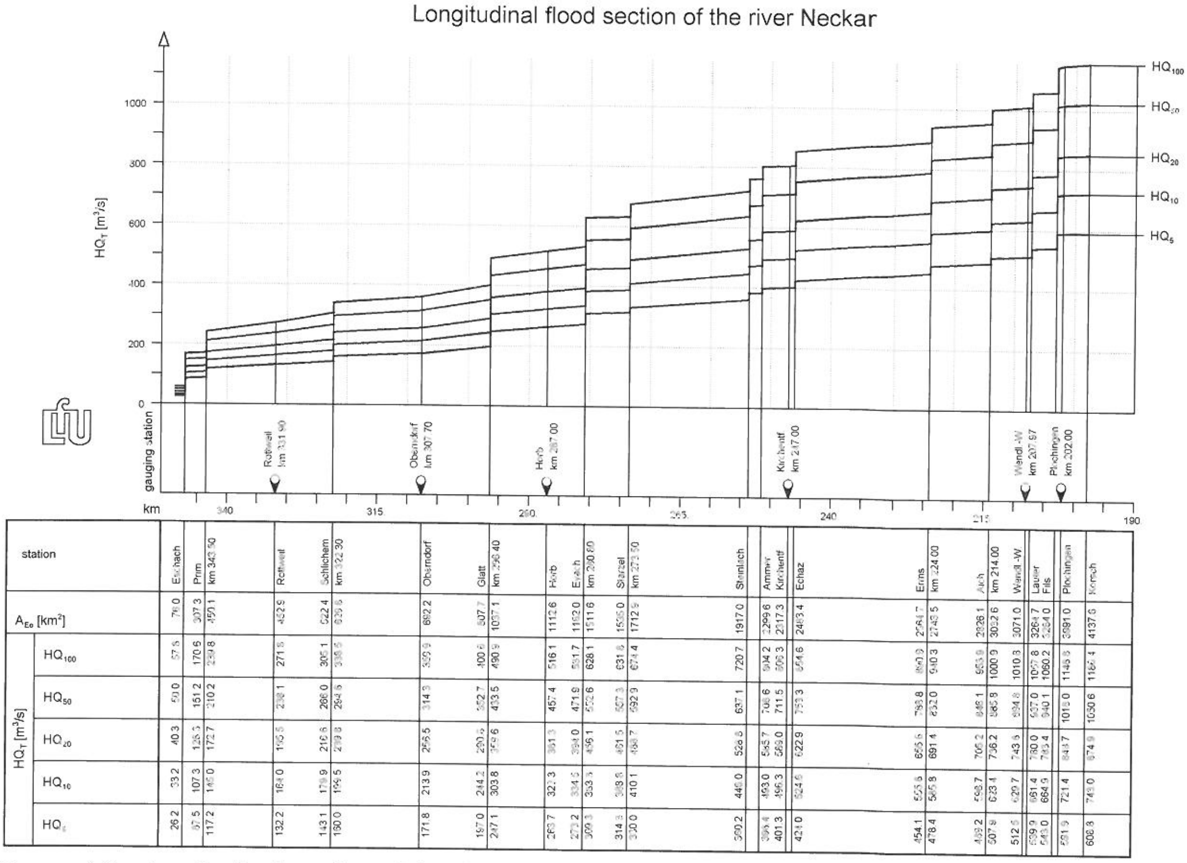

Figure 4-3: longitudinal section of the river "Neckar".

4.2 Limits for the application of the regionalisation model:

The regionalisation model for flood events in Baden-Wuerttemberg is in principle applicable area-wide. But in following situations the model can contain a fuzziness and should be used with caution:

- anthropogenic interventions may influence the flood generating processes. Above all flood control reservoirs can change the behaviour of the hydrograph.
- in carstic regions: in carstic regions the phreatic divide is often unknown and cannot be used for the regionalisation model.
- when small brooks enter a gravel accumulation infiltration may occur which can reduce a peak flood. This effect takes place primarily in the Rhine valley

5 CONCLUSIONS

The regionalisation model for flood events in Baden-Wuerttemberg is a simple, practical, multiple linear regression model to estimate the flood peak values of different return periods for nearly any site along streams. Of course there are dependencies of different parameters and also a certain multicollinearity which cannot be excluded when using such catchment parameters but one the other hand it was the main aim to develop a quite simple model and the results are quite plausible and the model is suited for the practical daily use. So it is already used in the water resources development of Baden-Wuerttemberg.

The flood peak values for different return periods (2 years up to 200 years) for about 4000 predetermined sites along streams have been calculated and are stored in a database. With a special ArcView coding the user can work interactively to find the required data. The whole application is available on CD (system requirements: pre-installation of MS-Access including ODBC and ArcView (ESRI)). Figure 5-1 shows a view of the application.
It is presently being investigated whether an analog model can be derived for mean water and low water.

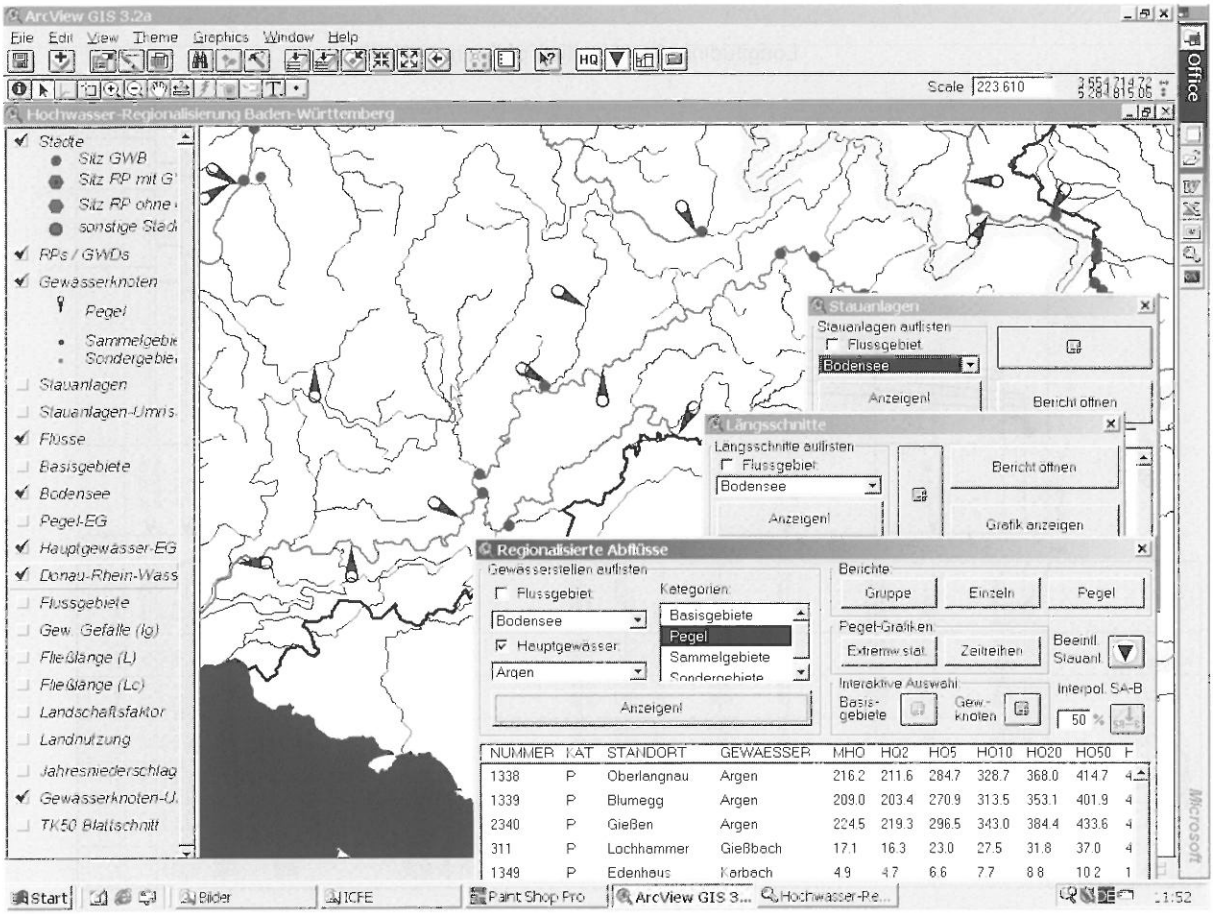

Figure 5-1: Surface of the CD application of the regionalisation model for flood events.

REFERENCES

LfU (1983): Hochwasserabflüsse in Baden-Württemberg – Donau und Neckargebiet. Handbuch Hydrologie Baden-Württemberg; LfU Baden-Württemberg

LfU (1988): Hochwasserabflüsse in Baden-Württemberg – Bodensee- und Rheingebiet, Maingebiet. Handbuch Hydrologie Baden-Württemberg; LfU Baden-Württemberg

Lutz, W. (1984): Berechnung von Hochwasserabflüssen unter Anwendung von Gebietskenngrößen. Mitteilungen des Instituts für Hydrologie und Wasserwirtschaft, Universität Karlsruhe, Heft 24

REGIONAL ESTIMATION OF MODEL PARAMETERS – A CASE STUDY IN WESTERN EUROPE

Markus Niggli, Benoit Hingray, André Musy

HYDRAM, Ecole Polytechnique Fédérale de Lausanne, 1015 Lausanne,
Markus.Niggli@epfl.ch, Benoit.Hingray@epfl.ch, Andre.Musy@epfl.ch

SUMMARY

A methodology for estimating regional parameters for a conceptual rainfall-runoff model is presented in this paper. This study is a part of the WRINCLE project where the objective was to provide detailed future climate and hydrological information for Europe in an accessible format. The development of a methodology for estimating river water resources characteristics (hydrological regime, flow duration curves) directly from meteorological inputs and catchment was required. This was achieved within a theoretical framework relating first and second order moments of daily discharge to rainfall parameters and potential evapotranspiration as a function of basin parameters used in a conceptual lumped rainfall-runoff model. The rainfall-runoff model has 5 parameters, which are estimated using a set of about 40 calibration catchments of about 500 km^2 each, distributed throughout Western Europe. The model was fitted with a search procedure that minimises the sum of squares of difference between observed and predicted daily discharge. Multivariate analysis techniques were applied to explain the variability of the parameters, using catchment data (soil, land cover, river network, topography, etc.), easily available for all of Europe. The model performance was tested for 5 catchments that were not included in the calibration and the regionalisation study. This analytical approach, which requires some assumptions but does not require simulations for discharge predictions, may be more appropriate for producing detailed maps at the European scale. As an example, this paper shows how it is possible to produce a flow duration curve gridded map for all of Western Europe (0.25° latitude/longitude spatial resolution). A simple statistical distribution, which parameters can be derived from the analytical outputs of the rainfall-runoff model, was used for that purpose. Finally some remaining issues facing flood estimation for large areas under a future climate are exposed in the conclusion.

Keywords: climate change, regionalisation, analytical rainfall-runoff model, water resources

1 INTRODUCTION

This paper presents our major results in the project WRINCLE (Water Resources: the INfluence of CLimate change in Europe) where the objective was to assess the influence of climate change in Europe and to produce maps for different climate projections (WRINCLE, 2001). Our contribution to this project was to develop a methodology to estimate river discharge characteristics directly from rainfall parameters and basin properties. The aim is to generate discharge statistics useful for characterising water resources, i.e. mean flows and flow duration curves rather than extreme value distributions, since meaningful flood frequency information cannot be generated on a pan-European scale for future climate. This aim is achieved with an analytical approach relating river discharge statistics to the parameters of a conceptual hydrological model and those of simple rainfall model. The time resolution is one day, in order to produce flow duration curves. The area of study is Western Europe (European Community plus Norway and Switzerland) because of data availability. This approach requires several assumptions but doesn't require simulations for discharge predictions, these latter being highly time consuming. It is therefore more appropriate for producing maps at the European scale. It requires the development of a simple calibration and regionalisation procedure to estimate model parameters, which can be reasonably applied for the area of study.

2 THE PROPOSED HYDROLOGICAL MODEL

2.1 Theoretical principles

The model used for rainfall-runoff transformation is based on a deterministic, lumped, conceptual and "storage oriented" representation of the catchment. It has two inputs: the total rainfall *(PTOT)* and the Potential Evapotranspiration *(PET)*. As shown in Figure 2-1, the total hydrograph is divided into a fast

(Qquick) and slow component *(Qbase)*. The infiltration process is described by a reservoir with a maximum storage capacity. The storage level *S* at time *t* governs the amount of actual evapotranspiration *(ET)*, net rainfall *(PN)* and base flow *(Qbase)*. The net rainfall is routed through a single linear reservoir to produce the fast contribution. The model has three basic parameters (soil maximum water storage *A*, base flow recession coefficient *k* and constant *k2* in the linear transfer function). The two parameters *CF1* and *CF2* represent critical filling rates of the "base flow" reservoir.

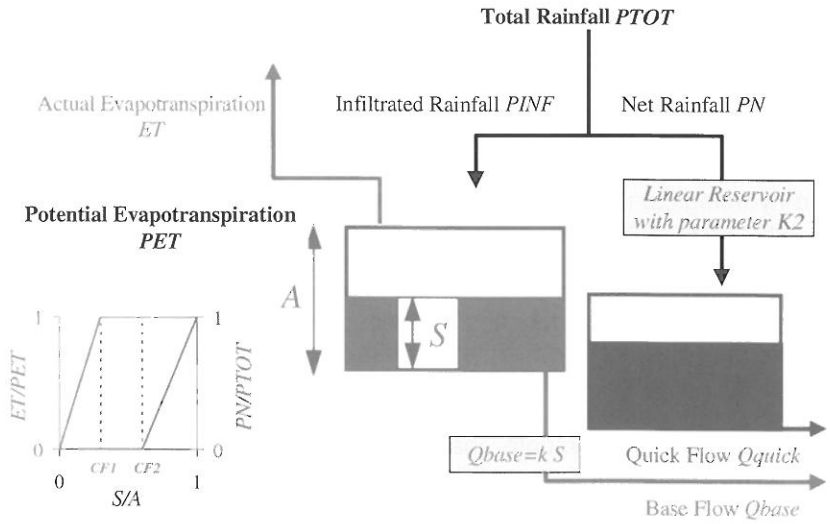

Figure 2-1: Hydrological model description.

For catchments affected by snowmelt, the rainfall input *PTOT* can be transformed into snowmelt and liquid precipitation. The simple degree-day method *(WMO, 1986)*, which requires only temperature time series as additional inputs can be used.

2.2 Development of an analytical solution

The analytical expressions for the mean and variance can be determined for the four following cases depending on the filling rate *S/A* of the reservoir producing the base flow (Table 2-1).

Table 2-1: The 4 cases for the filling rate of the "base flow reservoir".

j	Situation
1	*S/A<CF1* and *S/A<CF2*
2	*S/A<CF1* and *S/A>CF2*
3	*S/A>CF1* and *S/A<CF2*
4	*S/A>CF1* and *S/A>CF2*

The linear differential equation governing the temporal variation of *S* at time *t* can be written as following:

$$\frac{dS(t)}{dt} = \beta_j(t) + \alpha_j(t)S(t) \tag{1}$$

where $\beta_j(t)$ and $\alpha_j(t)$ are coefficients depending on meteorological inputs and the model parameters. Both coefficients are different for each case *j* described in table 2-1. For instance if *j*=1, we have:

$$\alpha_1(t) = -\left(\frac{PET(t)}{A \cdot CF1} + k\right) \tag{2}$$

$$\beta_1(t) = -PTOT(t) \tag{3}$$

The structure of equation for S can then by defined as following:

$$S(t) = \frac{\exp(\alpha_j \Delta t)(\alpha_j S(t-dt) + \beta_j) - \beta_j}{\alpha_j} \quad (4)$$

In order to derive an analytical solution for the first and second order moments, the following assumptions are needed:

- *Simple distributions for the rainfall and the potential evapotranspiration processes within a month must be assumed.* In our case the rainfall process is described with a discrete distribution when there is no rain, or a continuous one, with an exponential law, otherwise. The daily potential evapotranspiration for month *m* is kept constant *(PET(t,m)=PET(m)).*
- *The meteorological input (averaged rainfall and potential evapotranspiration) must be spatially uniform over the entire catchment.* This assumption is due to lumped character of the model, which doesn't capture the non-linearity of the hydrologic response in case of spatially heterogeneous meteorological conditions. Therefore, to limit the uncertainty introduced by lumped handling of rainfall and potential evapotranspiration, catchment size is restricted to 1000 km^2.
- *The catchment is not affected by snowmelt.* This assumption restricts the use of the analytical model to catchments without a significant snowmelt component. Indeed no analytical solution of the model could be found when taking into account snowmelt. It is of course possible to run simulations with transformed meteorological input (snowmelt and liquid precipitation instead of measured precipitation). This can only be done with the numerical version of the model.

The expected value and the variance of the stock process, net rainfall and total flow can be then derived for each case *j* by analytical integration over the possible values of *Ptot* (that is between 0 and infinity). The full mathematical description of the analytical model is given in Niggli et al. (2001). Actually, the model is a combination of 4 different models. If we consider that the distribution of the discharge produced by the model is a compound distribution of the 4 situations, then the expectancy $E_m(Q)$ and the variance $Var_m(Q)$ for month *m* can be written as (Benjamin and Cornell, 1970):

$$E_m(Q) = \sum_{j=1}^{4} p_{jm} \cdot E_{jm}(Q) \quad (5)$$

$$Var_m(Q) = \sum_{j=1}^{4} p_{jm} \cdot Var_{jm}(Q) + p_{jm} \cdot (E_{jm}(Q) - E_m(Q))^2 \quad (6)$$

where $E_{jm}(Q)$ and $Var_{jm}(Q)$ are respectively the mean and the variance associated to the four situations described in table 2-1; p_{jm} is the probability of *S/A* being in the case *j*. The different values of p_{jm} are not known *a priori* and have to be related to meteorological and physiographic variables by multivariate analysis.

3 REGIONALISATION STUDY

In order to derive runoff maps for western Europe, a regionalisation study is necessary. This was done in the following way:

- data collection for selected gauged catchments across Western Europe,
- model calibration for a subset of the selected catchments and,
- multivariate analysis in order to derive models parameter from catchments characteristics.

The catchments not used in the calibration and the multivariate analysis are used for validation.

3.1 Data collection

The discharge data were obtained mostly from the FRIEND database (Gustard, 1993), where the catchments are not strongly affected by the anthropogenic activities (dam, lake regulation, urbanization) and have an area comprised generally between 200 and 500 km^2. We selected 40 catchments where a concomitant meteorological station (rainfall, temperature), providing daily time series, is located nearby the catchment (cf. Figure 3-1). These time series were collected during the WRINCLE project from various European meteorological institutes. Another important source of time series is the MAP daily rainfall database (Frei and Schär, 1998). These are Alpine precipitation fields constructed by spatial analysis of rainfall gauge observations onto a 25 km regular grid. Spatially averaged rainfall for each catchment was then derived using the Thiessen polygons method or an elevation-rainfall gradient. Catchment daily time series of potential evapotranspiration (*PET*), assuming a constant value within a month, were obtained from the baseline *PET* derived by the Climate Research Unit (CRU), University of East Anglia (WRINCLE, 2001). The Penman-Monteith formulation recommended by the Food and Agriculture Organisation (FAO) for a reference vegetation cover (crop) was used.
The catchment characteristics were obtained from vectorial or raster data sets easily available for all of Europe. Catchments boundaries were determined by the river network from the Digital Chart of the World (DCW) and by contour maps derived by the 1-km GLOBE Digital Elevation Model. Both data sets can be downloaded from the World Wide Web, at the following addresses:

- http://www.maproom.psu.edu/dcw/ and
- http://www.ngdc.noaa.gov/seg/topo/globe.shtml.

This method gives a typical error in drainage area of 10%, when compared to the values of drainage area given in the FRIEND database. The GLOBE data were also used to calculate mean elevation and slope for the selected catchments. Land cover data were obtained from the Eurasia Land Cover database (EDC). Again, these data can be downloaded from the World Wide Web (http://edcdaac.usgs.gov/glcc/glcc.html). The data are grouped in several classification schemes. One of them is the 17-way IGBP scheme (Belward,1996). A further classification into 3 fundamental types was made:

- Natural Vegetation: IGBP Class 1 to 11 and 50% of class 14
- Croplands: IGBP Class 12 and 50% of class 14
- No vegetation: IGBP Class 12, 15 and 16

Figure 3-1: Geographical distribution of the catchments used in the model calibration and regionalisation study.

The soil data were derived from the digital version of the FAO World Soil Map (FAO, 1995), giving a polygonal coverage. The vectorial data were laid over a raster grid with 0.1° latitude/longitude resolution. In each grid cell, the dominant soil texture class was determined. Saturated hydraulic conductivity, water content at saturation and profile available water content can then be derived using a pedotransfer function (Saxton et al., 1986).
Finally annual and monthly rainfall and potential evapotranspiration (FAO recommended Penman-Monteith formulation) for a spatial resolution of 0.5° lat/long were derived from the monthly baseline fields of climatic variables used in WRINCLE (WRINCLE, 2001).
Table 3-1 resumes the catchments characteristics derived from the available European datasets:

Table 3-1: Raster data used in the regionalisation study. The column "resolution" corresponds to the resolution of the data displayed in a raster form (i.e. length of an elementary grid cell).

Variable	Symbol	Resolution	Unity
Area	AREA	1 km	km^2
Altitude	ALT	1 km	M
Slope	SLOPE	1 km	°
Temperature	TEMP	~ 50 km	°C
Annual Rainfall	ANRAIN	~ 50 km	mm
Rainfall for month *m*	RAINm	~ 50 km	mm
Annual *PET*	ANPET	~ 50 km	mm
PET for month *m*	PETm	~ 50 km	mm
Natural vegetation	NAT	1 km	%
Croplands	CROPS	1 km	%
Bare or urbanized soils	BARE	1 km	%
Soil Moisture at saturation	THETA	~ 10 km	%
Saturated hydraulic conductivity	KS	~ 10 km	cm/h
Profile Available water content	PAWC	~ 50 km	mm

3.2 Model calibration

For a fixed set of values of *CF1* and *CF2*, the following methodology of calibration was applied in the study:

- Determining the best relationship between the two parameters governing the base flow (*A* and *k*). Preliminary studies showed that these two parameters are highly correlated. Figure 3-2 (left) shows the non-uniqueness of the optimal parameter set *A* and *k*. Actually, there are many sets of values for *A* and *k*, which can be considered as optimal. A power function provides a fair approximation of the relation between the different optimal parameter sets (*A, k*). The parameters of the power function are determined so that the base flow component of the model reproduces the best a reference base flow. A least square minimization function is therefore used. The reference base flow (or "observed" base flow) is obtained from the observed discharge series and an algorithm for hydrograph separation ("Base Flow Index" method presented in Gustard (1989)).
- Determining the best parameters *A* and *k2* (quick flow parameter) for the total flows with the least square minimisation function. In that case, the simulated discharge (base flow plus quick flow) is compared to the observed discharge. For each value of *A* in the calibration runs, the parameter *k* was computed using the relationship found at the first step of the calibration. In Figure 3-2 (right), an example of response surface of the least square error is given. Contrary to the first step, a unique set of optimal parameters *A* and *k2* can be found.

This method of calibration is simple and robust, and takes into account the dependence between the parameters *A* and *k*. The rainfall input is transformed into snowmelt and liquid precipitation for Scandinavian and Alpine catchments, using the degree-day method. It was found that for catchments with an average annual temperature lower than 5°C, the snowmelt compound needs to be taken into consideration. The degree-day method parameters, critical melt temperature and melt rate factor, are set to 0°C and 3.5 mm/°C/day respectively (*WMO, 1986*). Additionally, temperature recorded at the closest station was corrected by a constant multiplication factor, assuming that the temperature-elevation

gradient is 0.65°C/100m. *CF1* and *CF2* were fixed to 0.6 and 0.4 respectively. This is one of the numerous sets which allow for an acceptable, unbiased reproduction of the daily discharge.

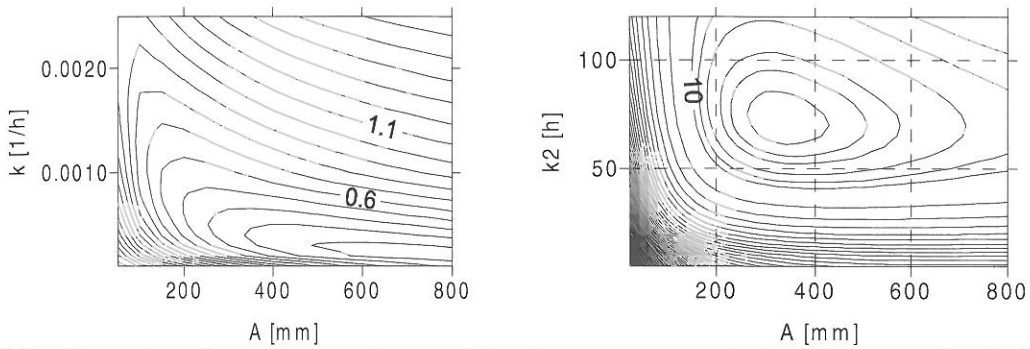

Figure 3-2: Examples of response surfaces, giving the square error between observed and simulated daily discharge for different couples of *A-k* values (left) and *A-k2* values (right).

The performance of the model with calibrated parameters was assessed with the *NS* goodness-of-fit criterion (Nash and Suttcliffe, 1970) and the bias (*PBIAS*), at a daily time step. *PBIAS*, the relative mean value of the residual between the observed and simulated flow, measures the tendency of under- or over- estimation of the model; the optimal value is 0. *NS* measures the fraction of the variance of the observed flows explained by the model; the optimal value is 1. The obtained *NS* values are between 0.20 and 0.80 (with an average of approximately 0.5) and the *PBIAS* between –0.5 and +0.5 (average 0). In other words, the simulated discharge is unbiased and explains 50% of the observed discharge. The model performance is more or less similar for all regions of Western Europe. Very dry catchments from Southern Mediterranean areas, as well as alpine catchments with an important snowmelt component or catchment representative of a temperate climate, are for instance equally well simulated.

3.3 Multivariate analysis

Multivariate analysis techniques (correlation analysis and stepwise regression) were applied to explain the variability of the parameters *A, k* and *k2* using the derived catchment data (cf. table 3-1). The 40 calibration catchments were used to fit the model parameters. Preliminary analysis involved investigation into correlation within and between the catchment characteristics and the model parameters coupled with graphical evaluation of scatterplots to identify possible interdependencies. Subsets of independent catchment characteristics were then created (value of coefficient of determination R^2 lower than 0.5) and a stepwise regression analysis was performed with these different subsets. The presence of variables retained in the final regression equation must also be explained physically (hydrological significance). It is worth noting that because of its strong correlation with *A*, *k* was not obtained directly. First a regional relation between the optimal values of the logarithms of *A* and *k* was derived by linear regression. The residuals of this relation were then regionalised and used to derive *k*. In order to ensure that the different variables are more or less normally distributed and to avoid inconsistencies (for instance negative values for the explained variables), we have chosen to work with log-transformed variables. The following equations were obtained:

(7) $$A = 28 \cdot (CROPS + 1)^{0.40} \cdot PAWC^{2.1} \cdot ANPET^{-1.2}$$

(8) $$k = 0.0373 \cdot A^{-0.92} \cdot PAWC^{1.34} \cdot ANPET^{-1.27} \cdot ALT^{0.37}$$

(9) $$k2 = 18'600 \cdot (TEMP + 10)^{-1.8} \cdot SLOPE^{-0.08}$$

Except *SLOPE* in Equation (9), all explaining variables are significant at the 10% level. The determination coefficients R^2 are between 0.35 and 0.65, which is similar to result obtained in other studies (Abdullah and Lettenmaier, 1997 or Sefton and Howarth, 1998). Unsurprisingly, *CROPS* (the proportion of croplands, in general associated to deep soil and moderate slopes) and *PAWC* are positively correlated to *A* in Equation (7). The presence of *PET* and TEMP in the relationships may be due to model simplifications and/or errors in the hydrologic process description. This seems to affect espe-

cially drier Mediterranean catchments, where *A* and *k2* are generally lower, indicating a quicker runoff response. An explanation for these low values may be that the Mediterranean catchments are prone to flash floods, which cannot be accurately captured by daily data. On the other hand, *k2* is generally higher for Scandinavian and Alpine catchments, i.e. catchments were the snowmelt needs to be modelled. Again, simplifications or unaccounted-for errors may explain these higher values. As mentioned above, *SLOPE* in Equation (9) is not statistically significant at a 10% level, but was retained because of its significance for quick flow responses. It is worth noting that if the regression is performed only for catchment without a snowmelt component, *SLOPE* becomes significant at a 10% level. The higher value of *k2* for Alpine catchments affected by snowmelt may hide the role of *SLOPE*. Finally, as mentioned above, *A* is strongly correlated to *k*, explaining its presence in Equation (8). *PAWC*, *PET* and *ALT* explain the variance of the residuals of the *log(k)–log(A)* relationship. For instance, if the residuals are negative, the recession parameter is lower than expected by the *log(k)–log(A)* relationship. In Equation (8), low values of *PAWC*, high values of *PET* and low values of *ALT* (strongly correlated to *SLOPE*) are logically associated to negative values of the residuals.
Note that presence of climatic variables in the regression equations leads to different model parameter values for present and future climate. Generally, the calculated values for *A*, *k* and *k2* are lower for the future climate projection. The scatterplot representing parameters *A* and *k* for calibration and 5 control catchment is given in Figure 3-3 for two cases: a) locally fitted parameter; b) parameter calculated with regression Equations 4.4 and 4.5. The regression equations produce realistic model parameter values for *A* and *k*. The same conclusion can be drawn for parameter *k2*.

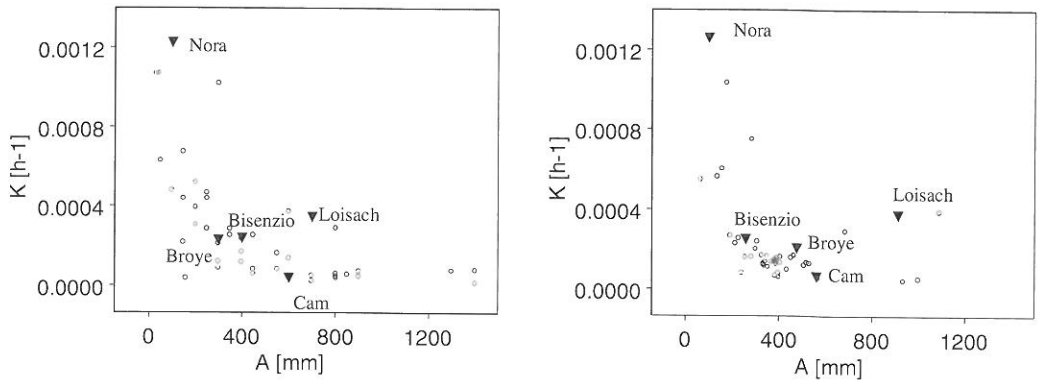

Figure 3-3: Parameters *A* and *k*: comparison between locally fitted (left) and regionalised value (right). The black triangles correspond to the catchments used for control.

The above equations were obtained for catchments distributed throughout Western Europe and it is proposed that they are applicable for all similar catchments (smaller than 1000 km^2 and with similar physiographic characteristics).
Figure 3-4 compares observed and simulated daily discharge time series for a catchment, which was not used in the model calibration and the regionalisation study. The parameters *A*, *k* and *k2* were calculated with Equations (7), (8) and (9). The agreement is satisfactory, except for peak flows, which are underestimated. This tendency of underestimation, which is also observed for the other catch-

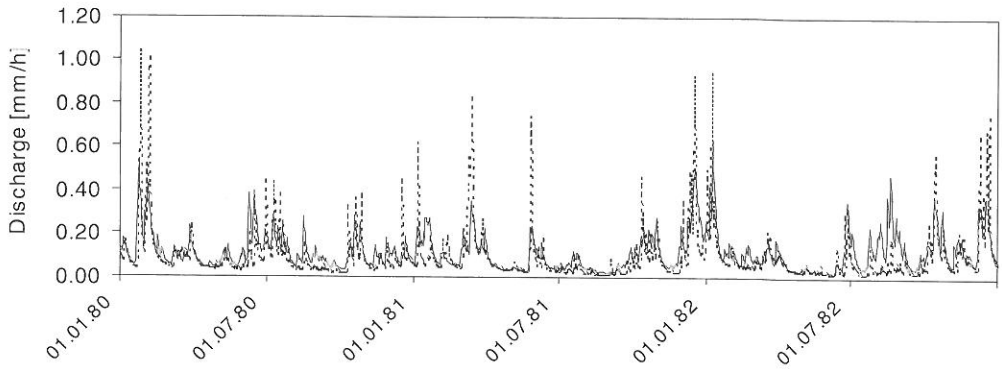

Figure 3-4: observed (dashed line) and simulated daily discharge for the Broye catchment (Switzerland).

ments, is essentially due to the simplification of the hydrological processes made by the model. However, despite these limitations, the model reproduces fairly well the monthly mean and variance of the daily flows, which is our major objective in this study.
The weighting coefficients p_{jm} in Equations (5) and (6) were also determined by statistical regressions (cf. Niggli et al., 2001 for more details). They need to be assessed if the analytical form of the hydrological model is used.

4 APPLICATION: GRIDDED FLOW DURATION CURVE FOR WESTERN EUROPE

In its analytical form, the model is suited for discharge estimation for many sites over a large geographical area. Basically, all the discharge characteristics, which require only the estimation of the monthly mean and variance of daily discharge, can be produced for ungauged catchments or grid cells with an area up to 1000 km^2. For instance, the hydrological regime can be easily constructed by plotting the mean value of discharge against the month of occurrence. In this paper we show how it is also possible to assess the effect of climate change on flow duration curves in Western Europe for each grid cells of 0.25° latitude/longitude. This spatial resolution was chosen because it corresponds to a size of approximately 600 km^2, which is within the domain of validity regarding the catchment area.
A flow duration curves represents the relationship between magnitude and frequency of daily (or monthly) streamflow Q for a particular river basin, providing an estimate of the time a given streamflow was equalled or exceeded over a period. In order to reproduce a flow duration curve, using the information given by the analytical model, a cumulative distribution function (*cdf*), which fulfil the following conditions must be chosen.

1. Its parameters can be expressed in terms of the first and second order moments of daily discharge (at an annual level) and;
2. The quantiles of the *cdf* are positive real numbers.

The 2-parameters log-normal distribution was selected. Niggli et al. (2001), have shown that this distribution is able to reproduce reasonably well the flow duration curves in Western Europe. The probability distribution function (*pdf*) of the log-normal distribution can be written as follows:

$$f(Q) = \frac{1}{Q \cdot b \cdot \sqrt{2\pi}} \exp\left(- \frac{(\log(Q) - a)^2}{2 \cdot b^2} \right) \tag{10}$$

The parameters a and b of the law can be defined using the method of moments (Haan, 1977):

$$a = \frac{1}{2} \cdot \log\left(\frac{E(Q)^2}{CV(Q)^2 + 1} \right) \tag{11}$$

$$b = \sqrt{\log(CV(Q)^2 + 1)} \tag{12}$$

where $E(Q)$ and $CV(Q)$ are respectively the annual mean and coefficient of variation of the daily streamflow.
To obtain $CV(Q)$ we have to estimate the annual variance $Var(Q)$ on the basis of the monthly variances $Var_m(Q)$ obtained from Equation (6). Again, if the distribution of the daily discharge can be considered as a compound distribution of monthly distributions, then the same formula as Equation (6) can be used:

$$Var(Q) = \sum_{m=1}^{12} n_m \cdot Var_m(Q) + n_m \cdot (E_m(Q) - E(Q))^2 \tag{13}$$

where $Var_i(Q)$ and $E_i(Q)$ are respectively the variance and the mean of the observed daily discharge for month i. n_m is the number of days within the month m. The *cdf* is derived from the *pdf*, using a numerical approximation (for instance the one proposed by Tukey (1960)).

The flow duration curve and various percentile flow can then by reproduced with this *cdf* for all grid cells in Europe on the basis of the model development presented in this paper. Figure 4-1 (left) shows for example, the areas where the simulated 95-percentile flow should be reduced under a future climate by more than 50%. The drier areas around the Mediterranean Sea show the greatest sensitivity to climate change, while northern areas seem less affected. These results are the combination of lower mean runoff (decrease of a parameter) and higher flow variability (increase of *b* parameter i.e. steeper flow duration curves). An example of typical flow duration curves for Mediterranean areas is given in Figure 4-1 (right).
The data representative for the current climate are based on the monthly fields of climatic variables developed by New et al. (1999, 2000) as well as observed daily time series of 131 European rainfall stations for the reference period 1960-1990. The data for the future climate were obtained from GCM outputs for a typical greenhouse gases scenario and recent downscaling techniques. More details for the climatic inputs can be found in WRINCLE (2001).

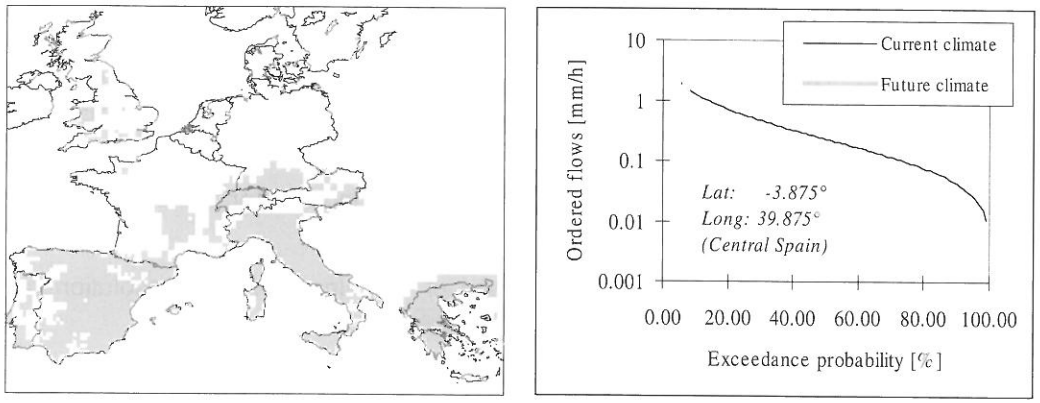

Figure 4-1: Left: Grid cells were the 95-percentile flow (equalled or exceeded 95% of the time) is the most affected by climate change. Cells are displayed in grey when the simulated 95-percentile flow is reduced by more than 50%. Right: An example of flow duration curves obtained for a grid cells located in Central Spain.

5 CONCLUSIONS

This paper has summarised a methodology able to assess the potential effects of climate change on water resources characteristics in Western Europe. The case of flow duration curves is presented and reveals that the most sensitive areas in terms of low flow decreases (for instance daily flow quantile exceeded 95% of the time) are the Mediterranean areas. Changes in monthly values of mean discharge and discharge variance as well as the model parameters are provided in a digital atlas for all 0.25° latitude/longitude grid cells of Western Europe (cf. http://www.ncl.ac.uk/wrincle). These results were obtained with a simple conceptual rainfall-runoff model, which enables the analytical derivation of the daily mean and variance at a monthly or annual level. The model parameters are regionalised, using gauged catchments distributed throughout the area of study and a log-normal distribution can reproduce reliably the flow duration curves.
Caution should be exercised in applying the methodology for conditions outside the range over which it was fitted. Moreover, the analytical model cannot be applied for catchment or grid cells where the snowmelt contribution is significant. Note that for these cases, the rainfall-runoff model, in its numerical form, could be especially useful. Snow-accumulation and snowmelt processes can be taken into account in that case. The derivation of discharge statistics with numerical simulations involves the use of long term observed or hypothetical daily time series for rainfall, temperature and potential evapotranspiration. The numerical form of the rainfall-runoff model can also be used, for some particular areas, in order to refine the results obtained by the analytical form.
No assessment of the possible change in flood occurrence or magnitude was made in the WRINCLE project. These hydrological variables cannot be assessed with enough confidence with the currently available climate scenarios. A major problem is indeed the inability of the GCMs and the downscaling method to give reliable information for rainfall at hourly time steps and a finer spatial resolution than presented in this paper. The rainfall-runoff model also has limitations, arising primarily because of the necessity of working with an analytical approach at the European scale. A big amount of model simplifications are therefore needed for the derivation of the mean and the variance of the flows (for instance

the model should be linear and lumped). Moreover, higher order moments estimations are certainly necessary if the aspect of flood estimation is addressed. Even if the estimation of the climatic inputs for changed climate could be improved in the future, there are still major obstacles for deriving flood information over a such large area as western Europe. For smaller areas, it is recommended to use numerical models where the complexity of the hydrological systems can be better taken into account.
As mentioned above, developments for a better simulation of the flows are certainly required. The proposed model provides nevertheless the potential for improving understanding of runoff and flow patterns over large areas. The model is also very useful in qualitative water resources assessment and long-term forecasting.

REFERENCES

Abdulla, F. A., Lettenmaier, D. P. (1997): Application of regional parameter estimation schemes to simulate the water balance of a large continental river. Journal of Hydrology, 197, 258-285.

Belward, A. S. (1996): The IGBP-DIS Global 1 Km Land Cover Data Set "Discover" Proposal and Implementation Plans. Report of the Land Cover Working Group of IGBP-DIS, IGBP-DIS Working Paper 13. IGBP Data And Information System Office, Toulouse, France.

Benjamin, J. R., Cornell, C. A. (1970): Probability, statistics and decision for civil engineers. Mac-Graw Hill, United States of America.

Frei, C., Schär, C. (1998): A precipitation climatology of the Alps from high-resolution rain-gauge observations. International Journal of Climatology, 18, 873-900.

Gustard, A. (1993): Flow Regime from International Experimental and Network Data Sets (FRIEND). Institute of hydrology. Wallingford.

Haan, C. T. (1977): Statistical methods in hydrology. Iowa State University Press.

Nash, J.E., Sutcliffe, J.V. (1970): River flow forecasting through conceptual models. Part I, a discussion of principles. Journal of Hydrology, 10, 282-290.

New, M. et al. (1999): Representing twentieth-century space-time climate variability. Part 1: Development of a 1961-90 mean monthly terrestrial climatology. Journal of Climate 12, 829-856.

New, M. et al. (2000): Representing twentieth-century space-time climate variability. Part 2: Development of 1961-90 monthly grids of terrestrial surface climate. J. of Climate 13, 2217-2238.

Niggli, M. et al. (1999): Projet GESREAU: Régionalisation courbes de débits classés du canton de Vaud. Rapport IATE/HYDRAM. EPFL, Lausanne.

Niggli, M. et al. (2001): WRINCLE: A methodology for producing runoff maps and assessing the influence of climate change in Europe. HYDRAM. EPFL, Lausanne.

Sefton, C. E. M., Howarth, S. M. (1998): Relationships between dynamic response characteristics and physical descriptors of catchments in England and Wales, Journal of Hydrology, 211, 1-16.

Tukey, J. W. (1960): The practical relationship between the common transformation of percentages of fractions and of amounts. Technical Report N°36, Statistical Research Group. Princeton, New Jersey.

WMO (1986): Intercomparison of models of snowmelt runoff. Operational Hydrology Report No 23 (WMO No 646). World Meteorological Organisation, Geneva.

WRINCLE (2001): Water resources: influence of climate change in Europe: Final report, EU Environment and Climate Research Program ENV4-CT97-0452. Ed. C. G. Kilsby, Water Resource Systems Research Laboratory. University of Newcastle, United Kingdom.

REGIONAL FLOOD ESTIMATION EXPERIENCES IN NEW ZEALAND

Charles P. Pearson

National Institute of Water and Atmospheric Research (NIWA), PO Box 8602, Christchurch, New Zealand, c.pearson@niwa.co.nz

SUMMARY

Development of improved understanding of flood frequency behaviour in New Zealand using regional methods is described. By 1990, geographic flood regions, flood estimation contour maps and the Extreme Value Type I (EV1) distribution had been prescribed as part of regional flood estimation schemes. Some advances on regional flood estimation for New Zealand since 1990, based upon the method of L-moments, were: use of catchment characteristics rather than regions to group small catchments; identification of EV2 tendencies in flood peak and storm rainfall annual maxima; use of peaks over a threshold sampling for regional analyses; use of the Two-Component Extreme Value (TCEV) distribution for regional studies.

Keywords: New Zealand, regional flood frequency, L-moments, extreme value distributions

1 INTRODUCTION

For a river location, the probability distribution $F(x)$ of flood peaks is a basic characteristic of that location. Flood frequency analysis aims to identify and estimate $F(x)$ at river locations with flow records (at-site flood frequency), extrapolate with this distribution to low probability events, and transfer information spatially to river locations without flow records (regional flood frequency). For effective regional flood frequency it is important to understand the physical processes which influence the upper tail of $F(x)$. Factors include climate (storm characteristics), catchment physiography (topography, slope, soil properties, geology, vegetation, land-use), catchment scale (drainage area, hillslope versus channel processes, Blöschl 1996) and river hydraulics (channel networks, lakes, river gorges, Wolff and Burges 1994).
Two regional flood frequency studies of New Zealand were carried out in the 1980s (Beable and McKerchar 1982, McKerchar and Pearson 1989). These are described briefly in Section 2. Advances on these methods since 1990 are described in Section 3, with a view to implementing a further national study.

2 NATIONAL FLOOD STUDIES OF THE 1980s

New Zealand has a temperate and maritime climate. Its rugged relief especially in the South Island (i.e. the Southern Alps regions, Weingartner and Pearson 2001), leads to orographically enhanced storm rainfalls and extreme floods. Underpinning national flood studies described below have been national and regional hydrometric networks and databases. Pearson (1998) documents hydrometric recording in New Zealand. Both regional and national databases benefit from quality assured data collection programmes (see e.g. Mosley and McKerchar 1989, Hudson et al. 1999). For each of the national flood studies, additional careful quality checks were carried out (checking stage-discharge rating curves and gaps in records) to obtain annual maximum flood series for analysis.

2.1 Beable and McKerchar (1982)

Beable and McKerchar (1982) followed the regional index flood approach of the British flood studies report (NERC 1975). More than ten regions were identified for estimation of mean annual flood ("index flood") and dimensionless flood frequency quantiles (growth curves). Mean annual flood was estimated using multiplicative regression equations with catchment characteristics as independent variables, such as basin area (A), rainfall, slope etc. Distributions used for the flood frequency growth curves were either the EV1 or EV2 distributions. Beable and McKerchar's work substantially improved upon earlier methods, which were based mainly upon storm rainfall statistics. Mosley (1981) used a clustering approach of specific mean annual flood and coefficient of variation of annual maxima to confirm the flood regions identified by Beable and McKerchar.

2.2 McKerchar and Pearson (1989)

Almost a decade later, McKerchar and Pearson (1989, 1990) updated this work using an index flood method based upon contour maps. Mean annual flood (divided by $A^{0.8}$, 343 catchments) and dimensionless 100-year return period flood (Q_{100}, 275 catchments) were mapped for New Zealand, and used as the basis of a flood estimation procedure. The EV1 distribution was shown to be satisfactory against the Generalised Extreme Value (GEV) distribution alternative (EV2, EV3) for most annual maximum flood peak series, although series from small catchments (A < 100 km^2) and from catchments of eastern regions did not match this distribution so well. For larger catchments (A > 100 km^2), mean annual flood and Q_{100} had prediction standard errors of 17% and 30%, respectively. Figure 2-1 shows the contour maps for the South Island.

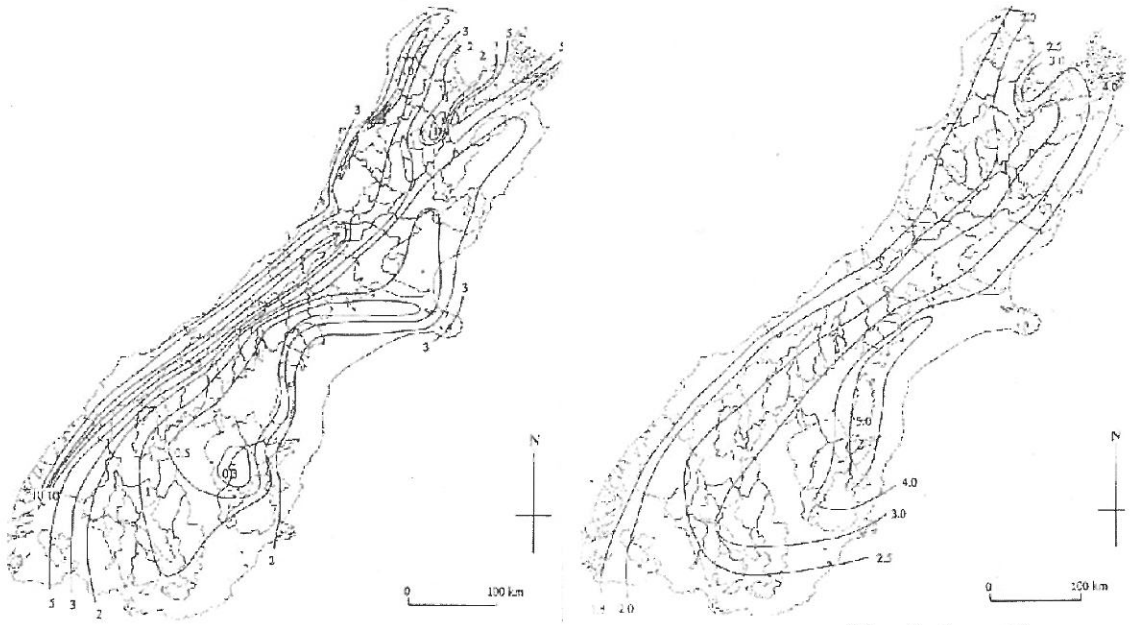

Figure 2-1: South Island contours of (left) specific mean annual flood (Q / $A^{0.8}$, m^3 s^{-1} km$^{-1.6}$) and (right) dimensionless 100-year flood (Q_{100} / Q) (McKerchar and Pearson 1989, 1990).

3 EXPERIENCES AND PROGRESS SINCE 1990

3.1 L-moments

Regional L-moments methods developed by Hosking and Wallis (1993, Hosking 1990) allowed testing of groups of catchments for homogeneity with respect to flood frequency and identification of the most appropriate distributions for these groups. L-moment ratio plots of L-kurtosis versus L-skewness assist greatly in specifying upper tail behaviour of flood series distributions, $F(x)$ (Vogel and Fenessey 1993). Follow-up studies (Pearson 1991a, 1991b) to the national studies used L-moment statistics to show that for some catchments, the EV2 distribution was more appropriate than the EV1 distribution for the McKerchar and Pearson flood data set (Figure 3-1). Numerous regional studies since have used these tests to identify EV2-tendencies in many New Zealand flood series (including those of the North Island), particularly for eastern regions where flooding is less frequent on an annual basis. In eastern regions (e.g. coastal Canterbury of the central South Island), annual maximum series had predominantly low flood peaks, punctuated by a few relatively large values. In general, the EV1 distribution was found to be satisfactory for the flood frequency of western New Zealand, but elsewhere the EV2 was more appropriate – Figure 3-2 shows the L-moment ratios of the Canterbury (eastern) region of the South Island compared with those of the West Coast region to the west. Later L-moment studies have shown that even western regions have some EV2 tendencies. This may be caused by non-stationarity of flood series over different time periods (e.g., decades, see McKerchar, this volume).

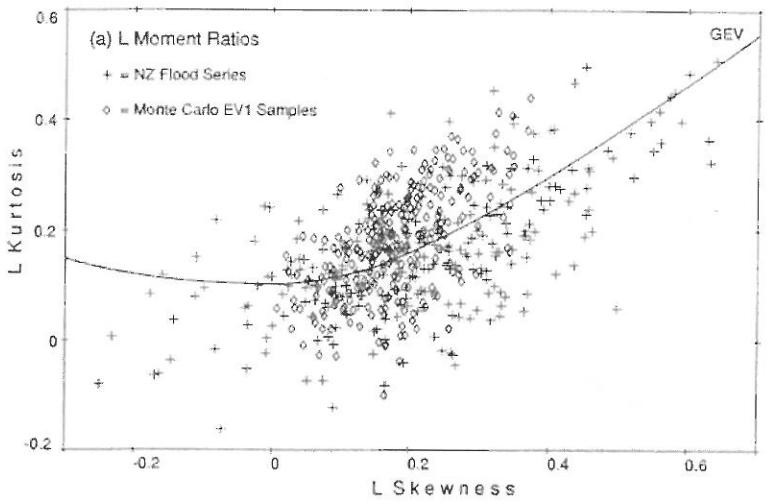

Figure 3-1: L-moment ratios of 275 New Zealand flood series, showing the three-parameter GEV (curve) distribution (Pearson 1991a). The two-parameter EV1 distribution is represented by point (0.17, 0.15) on the GEV curve. New Zealand flood series have greater variability than expected for the EV1 distribution (Monte Carlo values).

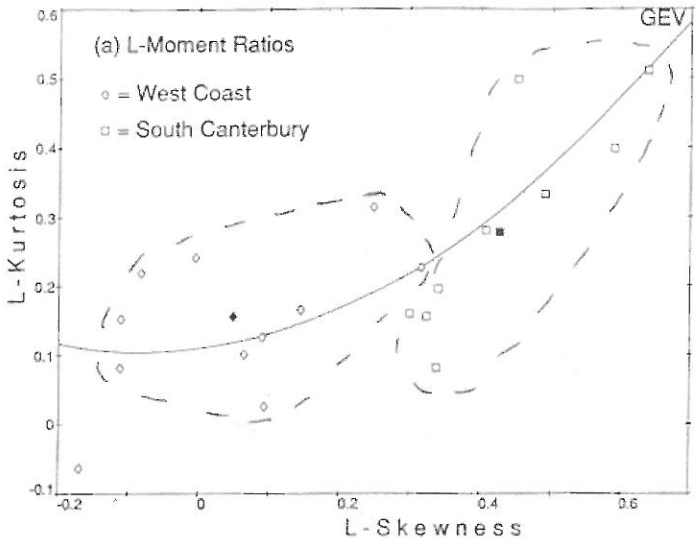

Figure 3-2: L-moment ratios of the Canterbury (eastern, South Canterbury) region of the South Island compared with those of the West Coast region to the west.

3.2 Small Catchments

For over 100 small catchments (A < 100 km^2) of the McKerchar and Pearson data set, a study using sub-groupings based on catchment characteristics was carried out (Pearson 1991b). Characteristics used included catchment geology and soil parameters. Optimal groupings were found using storm rainfall and catchment slope parameters with L-moment ratios in a grouping scheme developed by Wiltshire (1985). The groups were not contiguous regions. Figure 3-3 shows the regional flood frequency growth curves for six identified groups. The EV2-tendencies were greatest for catchments with low storm rainfalls and high catchment slopes. For all but the high rainfall groups, the McKerchar and Pearson EV1 Q_{100} / Q estimates are shown to be underestimates.

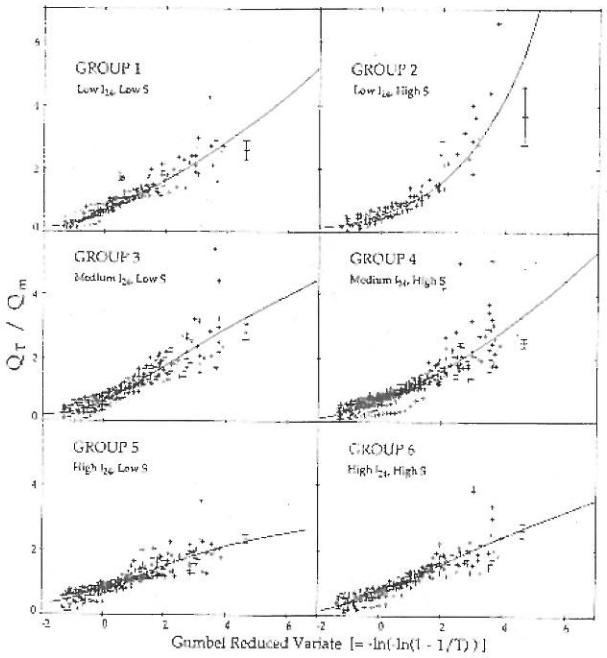

Figure 3-3: Flood frequency growth curves for six groups of small catchments, based upon rainfall (I_{24}) and slope (S) characteristics (Pearson 1991b). Confidence error bars (95% level) are shown for McKerchar and Pearson (1989, 1990) EV1 Q_{100} / Q estimates for each group of catchments.

3.3 Peaks Over A Threshold Sampling

The value of using peaks over a threshold series compared with annual maximum flood series was investigated in a regional context (Madsen et al. 1997), for the east and west South Island regions. Peaks over a threshold selection of flood data allowed a two-fold or greater increase in series sample size (n). Rather than identifying east and west regions, an optimal partitioning was achieved using the Pearson (1991b) scheme with annual rainfall – west catchments had rainfall over 1300 mm, whereas east catchments were below this threshold. In general, the Exponential distribution was found to be satisfactory for the flood frequency of the peaks over a threshold series of the western catchments, and the Generalised Pareto distribution was more appropriate for the east. These results were equivalent to the EV1 and EV2 findings for annual maxima of the west and east respectively (Section 3.1 above). More importantly, Figure 3-4 shows that the use of larger flood sample sizes for peaks over a threshold series (versus annual maxima series) leads to greater precision in the L-moment ratios plane, and hence greater ability to identify homogeneous groupings and corresponding distributions.

3.4 Distribution of Storm Rainfalls

The EV2 tendencies in many New Zealand annual maxima flood series are associated with both climatic and land factors. However, Tomlinson (1980) concluded that the EV1 distribution was satisfactory to estimate frequencies of annual maximum storm rainfalls in New Zealand. An L-moments study (Pearson and Henderson 1998) checked the applicability of the EV1 distribution for annual maximum storm rainfalls for durations 1, 6 and 24 hours. The EV2 distribution was found to be more applicable for most of New Zealand, in that the shape parameter k of the GEV distribution was predominantly negative. Figure 3-5 shows the growth curve for 24-hour storm rainfalls for the southern region of the South Island, indicating the extent of underestimation by the EV1 distribution at higher return periods.

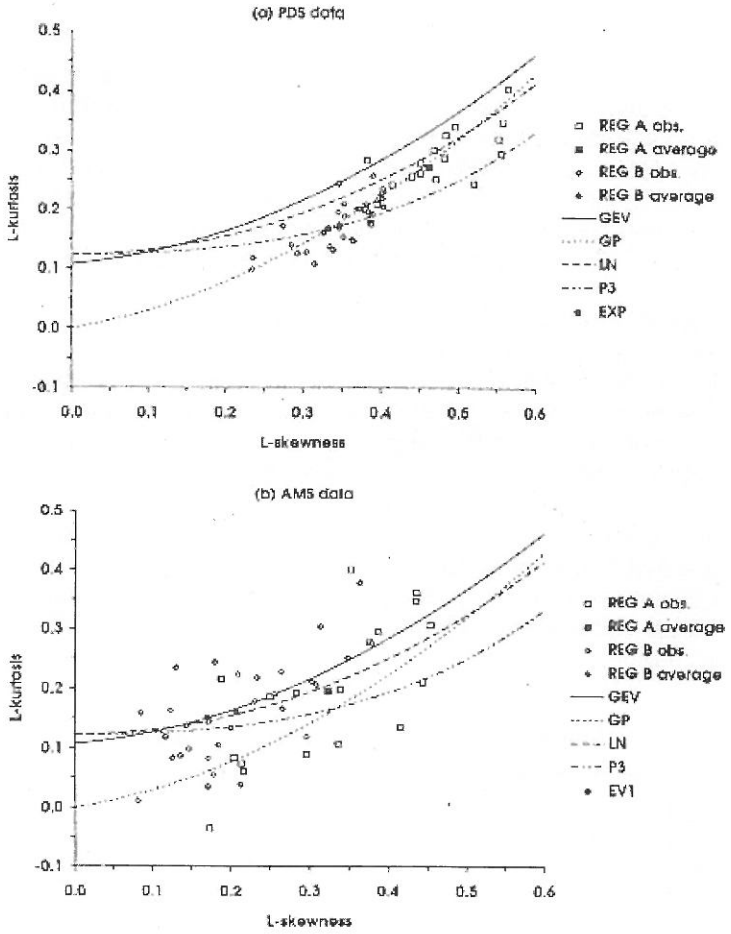

Figure 3-4: Plots of L-kurtosis v L-skewness for east (Region A) and west (B) regions of the South Island, for peaks over a threshold sampling (upper plot; largest 2*n* floods selected at each site) and for annual maximum series (lower plot; *n* flood peaks).

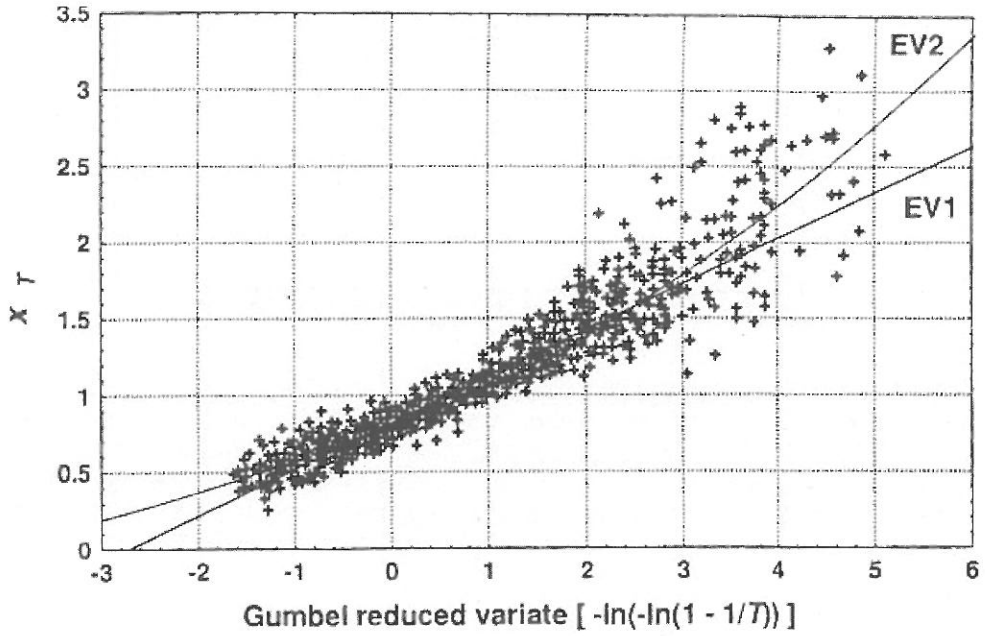

Figure 3-5: Regional storm rainfall frequency growth curves for 83 series of eastern Southland (south-eastern South Island) annual maximum 24-hour duration storm rainfalls, with fitted EV2 (curve) and EV1 (line) distributions.

3.5 Two-Component Extreme Value Distribution

The EV2 tendencies of flood series from Canterbury rivers (central, east South Island) were investigated further by Connell and Pearson (2001). Rather than the extreme curvature of some EV2 distributions, the more conservative approach of the Two-Component Extreme Value (TCEV) distribution (Rossi et al. 1984, Beran et al. 1986) was used, which is equivalent to two EV1 distributions. The TCEV distribution comprises a frequent basic series and an infrequent outlying series.
Analysis of annual maximum flood series from Canterbury showed that the TCEV distribution fits many of these series, and that the TCEV is a better distribution to use for regional flood studies than the EV2 distribution.
Distinct regions were identified for Canterbury using L-moment ratios (Figure 3-6). The South Canterbury East Coast Rivers have a marked two-component tendency while the North Canterbury East Coast Rivers have a lesser but significant two-component tendency. The difference in severity of the TCEV tendencies between the north and south East Coast rivers was due to orographic effects and alignment of the upper catchment boundary (Figure 3-7). South East rivers receive severest storm rainfall from warmer north-easterly storms, whereas North East rivers receive most rainfall from cooler south-easterly storms.
For Main Divide Rivers (Figure 3-6, 3-7), the third Canterbury region, the predominant storm direction is from the west. This was strong enough to be the only EV1 process evident in the flood series and hence this distribution continues to be the preferred option for these (and West Coast) rivers. As EV2 tendencies exist in flood series from some West Coast rivers, some weak TCEV signals were detected in some series from this region.

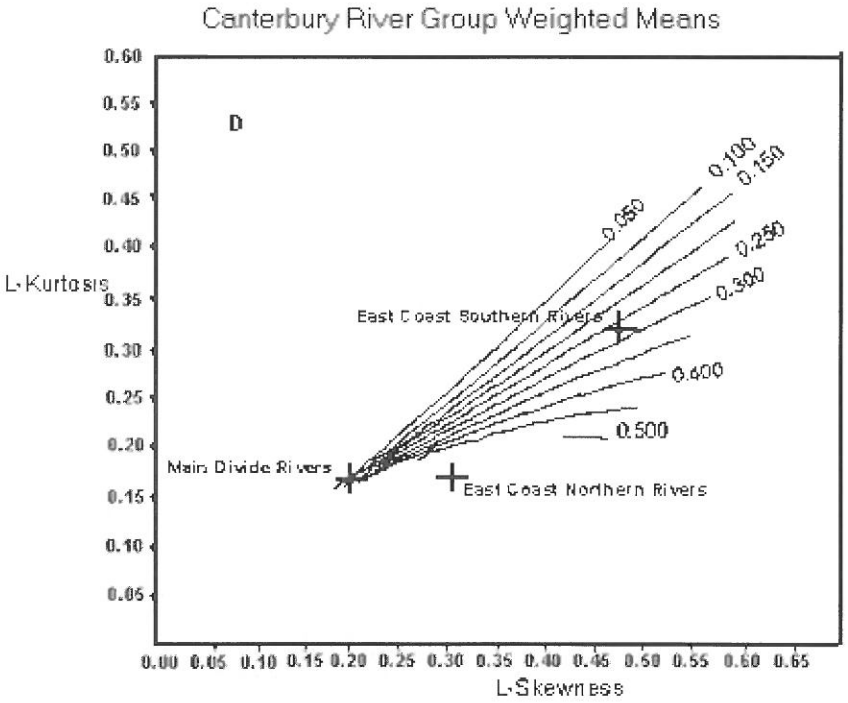

Figure 3-6: Weighted average L-moment ratios for three Canterbury regions: Northern East Coast Rivers, Southern East Coast Rivers, Main Divide Rivers. Curves on the plots represent the TCEV distribution for various probabilities of an annual maximum flood value coming from the outlier series. The EV1 distribution has coordinates at the apex (0.17, 0.15) of the TCEV curves, i.e., the case of only one component of the TCEV distribution. A similar TCEV distribution plot was presented in Gabriele and Arnell (1991).

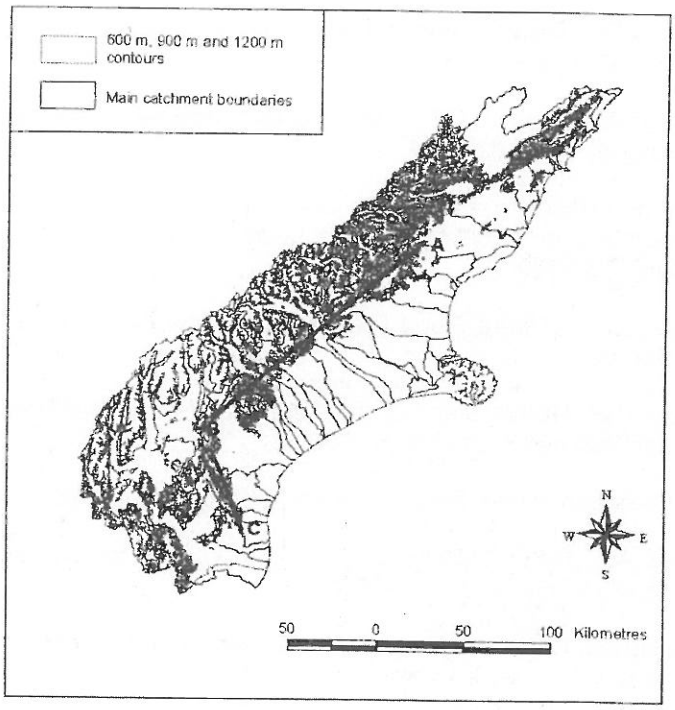

Figure 3-7: Divide axes (lines AB and BC, B obscured) for Canterbury East Coast rivers. Main Divide rivers are west of these axes.

4 CONCLUSIONS

The experiences reported in Section 3, and additional data and better methods available since the national flood studies of the 1980s (Section 2), provide a basis for revisiting a national flood procedure for New Zealand flood frequency estimation. Other methods under investigation include: using improved physically-based rainfall-runoff models now available with continuous rainfall simulations and data; more studies on the importance of scaling and multi-scaling of flood peaks; use of hierarchical Bayes methods for super-parameters of $F(x)$ (e.g. Gabriele and Arnell 1991, Ribeiro-Correa and Rousselle 1993); development of a peaks over a threshold equivalent to the TCEV distribution; and GIS methods to delineate parameters of $F(x)$ with river channel networks (as per the Swiss Hydrological Atlas, e.g. Weingartner 1999). Issues remaining include clarifying the role of climate-related non-stationarity in both storm rainfall and flood processes and data series, and effects of changing land-use.

REFERENCES

Beable, M.E., McKerchar, A.I. (1982): Regional Flood Estimation in New Zealand. Water and Soil Technical Publication No. 20, Ministry of Works and Development, Wellington, 132p.

Beran, M., Hosking, J.R.M., Arnell, N. (1986): Comment on "Two-component extreme value distribution for flood frequency analysis". Water Resources Research 22, 263-266.

Blöschl, G. (1996): Scale and Scaling in Hydrology. Wiener Mitteilungen Band 132, Institut für Hydraulik, Gewässerkunde und Wasserwirtschaft Technische Universität Wien, 346p.

Connell, R.J., Pearson, C.P. (2001): Two-component extreme value distribution applied to Canterbury annual maximum flood peaks. Journal of Hydrology (NZ) 40(2),105-127.

Gabriele, S., Arnell, N.(1991): A hierarchical approach to regional flood frequency analysis. Water Resources Research 27(6), 1281-1289.

Hosking, J.R.M., (1990): L-moments: analysis and estimation of distributions using linear combinations of order statistics. Journal of Royal Statistical Society B, 52, 105-124.

Hosking, J.R.M., Wallis, J.R. (1993): Some statistics useful in regional frequency analysis. Water Resources Research 29(2), 271-281.

Hudson, H.R., McMillan, D.A., Pearson, C.P. (1999): Quality assurance in hydrological measurement. Hydrological Sciences Journal 44(5), 825-834.

Madsen, H., Pearson, C.P., Rosbjerg, D. (1997): Comparison of annual maximum flood series and partial duration series methods for modeling extreme hydrologic events. 2. Regional modeling. Water Resources Research 33(4), 759-769.

McKerchar, A.I., Pearson, C.P. (1989): Flood Frequency in New Zealand. Publication No. 20, DSIR Hydrology Centre, Christchurch.

McKerchar, A.I., Pearson, C.P. (1990): Maps of flood statistics for regional flood frequency analysis in New Zealand. Hydrological Sciences Journal 35(6), 609-621.

Mosley, M.P. (1981): Delimitation of New Zealand hydrologic regions. Journal of Hydrology 49, 173-192.

Mosley, M.P., McKerchar, A.I. (1989): Quality assurance programme for hydrometric data in New Zealand. Hydrological Sciences Journal 34(2), 185-202.

Natural Environment Research Council (1975): Flood Studies Report, Volume 1. Natural Environment Research Council, London.

Pearson, C.P. (1991a): New Zealand regional flood frequency analysis using L-moments. Journal of Hydrology (NZ) 30(2), 53-64.

Pearson, C.P. (1991b): Regional flood frequency for small New Zealand basins, 2, Flood frequency groups. Journal of Hydrology (NZ) 30(2), 77-92.

Pearson, C.P. (1998): Changes to New Zealand's national hydrometric network in the 1990s. Journal of Hydrology (NZ) 37(1), 1-17.

Pearson, C.P., Henderson, R.D. (1998): Frequency distribution of annual maximum storm rainfalls in New Zealand. Journal of Hydrology (NZ) 37(1), 19-33.

Ribeiro-Correa, J., Rousselle, J. (1993): A hierarchical and empirical Bayes approach for the regional Pearson type III distribution. Water Resources Research 29(2), 435-444.

Rossi, F., Fiorentino, M., Versace, P. (1984): Two-component extreme value distribution for flood frequency analysis. Water Resources Research 20(7), 847-856.

Tomlinson, A.I. (1980): The frequency of high intensity rainfalls in New Zealand, Part I. Water and Soil Technical Publication No. 19, Ministry of Works and Development, Wellington, 36p.

Vogel, R.M., Fennessey, N.M. (1993): L-moment diagrams should replace product moment diagrams. Water Resources Research 29(6), 1745-1752.

Weingartner, R. (1999): Regionalhydrologische Analyse – Grundlagen und Anwendungen. Beitrage zur Hydrologie der Schweiz, 37, Bern.

Weingartner, R., Pearson, C.P. (2001): A Comparison of the hydrology of the Swiss Alps and the Southern Alps of New Zealand. Mountain Research and Development 21(4), 370-381.

Wiltshire, S.E., (1985): Grouping basins for regional flood frequency analysis. Hydrological Sciences Journal 30(1), 151-159.

Wolff, C.G, Burges, S.J. (1994): An analysis of the influence of river channel properties on flood frequency. Journal of Hydrology 153, 317-337.

ROBUSTNESS OF TWO FLOOD ESTIMATION METHODS WITH DATA AVAILABILITY

Charles Perrin and Claude Michel

Cemagref, Parc de Tourvoie, BP 44, 92163 Antony Cedex, France, charles.perrin@cemagref.fr

SUMMARY

This study evaluates the usefulness of using a rainfall-runoff model to produce streamflow series for flood estimation. It compares the classical method of flood estimation based on the adjustment of statistical laws with an approach based on rainfall-runoff model in conditions of reduced availability of streamflow data. Results on a sample of 40 French catchments indicate that the advantage of having larger samples of maximum annual floods thanks to the use of a rainfall-runoff model is balanced by problems of model efficiency, hence limiting the worth of using a rainfall-runoff model for flood estimation only to catchments where the model performs satisfactorily. The use of an objective function that puts more weight on flood peaks improves the quality of flood estimates.

Keywords: Flood estimation, rainfall-runoff model

1 INTRODUCTION

The classical approach to estimate design floods of medium return periods (say between 10 and 50 years) is based on adjusting statistical laws (typically log-normal, Gumbel or log-Pearson III laws) on a set of maximum annual flood values provided by streamflow records. For such return periods, the ideal situation is to have records longer than the return period of interest. In this case, the design flood is just calculated and there is no problems of extrapolation.
However such long streamflow records are seldom available on the location of interest and the fitting of statistical laws must be carried out on a limited number of maximum annual flood observations. This limitation as to observation data tends to reduce the reliability of the adjusted law and one is faced with problems of extrapolation. Therefore, when streamflow data are scarce, one can be concerned with the accuracy of the values of floods estimated by statistical methods.
An alternative approach for flood estimation is to use a rainfall-runoff model. The model can be calibrated against streamflow records even when only two or three years of data are available. Then it can be run with longer rainfall time-series (generally of larger availability) to determine the required flood estimate. The limit of such a method may arise from the difficulty of the rainfall-runoff model to simulate flood peaks with good accuracy. Several authors already proposed the application of rainfall-runoff models in the context of flood estimation (see e.g. Fontaine, 1995; Cameron et al., 1999; Lamb, 1999).
The purpose of this paper is to assess the robustness of both flood estimation approaches with the availability of streamflow data, which means in fact, to evaluate the worth of extending streamflow records using a rainfall-runoff model when only short time-series are available.

2 ASSESSMENT METHODOLOGY

2.1 Test catchments

The classical statistical method and the approach based on rainfall-runoff modelling were compared on a set of 40 catchments in France. Their location is shown in Figure 2-1. They have different climatic characteristics, with oceanic influences in the western part of France or Mediterranean in the southern part of the country. Some of the basins are situated in the centre or eastern part of France and their regime may be influenced by snowmelt of temporary snow covers. Catchment area is rather small, ranging from 8.9 to 356 km^2.
At least 21 years of daily data were available for each catchment. Between one and nine raingauges were used to calculate catchment mean areal rainfall. The only criterion for catchment selection was the length of available record at the time of the study, to avoid any bias due to modelling considerations. A quite large sample of catchments was used to get results statistically significant.

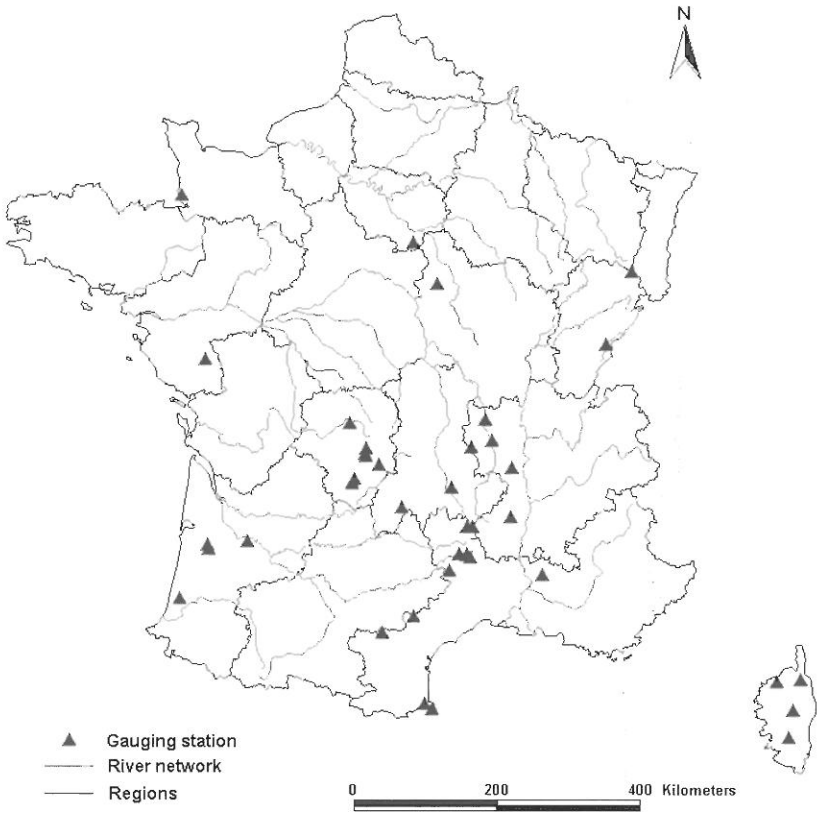

Figure 2-1: Location map of the 40 French catchments.

2.2 Description of tests

Although extreme floods estimations are often of interest for design purposes, there is little chance to have such rare events be recorded in short time series typically of a few decades. Therefore, it is almost impossible to know the true value of the peak flood on a given catchment for long return periods (say 1000 years), that can be only estimated by calculus and extrapolation.
Since the aim of this work is to compare the efficiency of two flood estimation methods, their efficiency can only be assessed by referring to a known value (or good estimate). Given the length of our data sets, we have chosen to concentrate on the 50-year daily flood, which will require only small extrapolation to be determined.
For each catchment (indexed by i), the whole set of data has been used to fit the best 2-parameter probability distribution function (pdf) to the sample of annual maximum daily flows. Then the 50-year daily flood (Q_i) has been derived from this pdf and this estimation has been hold as the best estimate at hand.
The assessment of flood estimation methods was carried out by considering a reduced availability of streamflow data, with 7- and 4-year long data sets. For each catchment, the whole period of record has been divided into 7-year (then 4-year) periods (indexed with the letter j). For each sub-period, both flood estimation methods have been applied. First, the best pdf estimated from the sample of the maximum annual flows and the 50-year flood has been estimated (noted QF_{ij} for the *jth* period and the *ith* catchment). Second, a conceptual rainfall-runoff model has been calibrated using observed daily rainfall and daily flow data of the same sub-period. Using the whole set of rainfall data, the calibrated model is then run in simulation mode to give a longer series of modelled daily flow data. This new series can produce a larger sample of annual maximum flows and, having determined the best pdf, this simulated series of data can yield an estimate of the 50-year daily flood (noted QM_{ij}).
The test consists in comparing QF_{ij} and QM_{ij} as alternative estimations of Q_i.
Of course one could also have coupled the rainfall-runoff model with a stochastic rainfall generator to generate longer time-series of streamflow (see for example Cameron et al., 1999). However, we preferred to concentrate here on rainfall-runoff modelling issues and use only observed rainfall data.

2.3 Assessment criterion

Given the large set of catchments, a statistical measure was used to compare the performances of both approaches. The chosen criterion is the standard error of each method calculated on the whole set of catchments by comparison to the reference floods. To avoid bias in this calculation due to the difference of flood magnitudes between catchments, a prior logarithmic transformation of flood estimates was done. The assessment criterion is then given by:

(1) $$s_F = \sqrt{\frac{1}{N-1}\sum_{i,j}\left[\ln\left(\frac{QF_{ij}}{Q_i}\right)\right]^2}$$

for the classical pdf approach, and:

(2) $$s_M = \sqrt{\frac{1}{N-1}\sum_{i,j}\left[\ln\left(\frac{QM_{ij}}{Q_i}\right)\right]^2}$$

for the method using the rainfall-runoff model.

3 MODELLING TOOLS

3.1 Classical approach

Given that the form of the pdf for a given sub-period is not known a priori, a set of possible pdfs was considered. The two basic pdfs forms chosen here are the Gaussian pdf and the Gumbel pdf. In each case, four different variants were tested corresponding to four transformations of the data of annual maximum flood: raising the peak flows successively to powers 1, 0.5, 0.333 and using the log-transformation. Consequently eight candidate pdfs are available. For each sub-period, all pdfs were tested and the one yielding the best curve fitting was selected to estimate the flood quantile under study.

3.2 Approach using a rainfall-runoff model

Most existing rainfall-runoff models can be applied in the context of flood estimation. Fontaine (1995) used the event-based HEC-1 model, Cameron et al. (1999) and Lamb (1999) applied continuous modelling with TOPMODEL and PDM model respectively. Here a continuous model was also preferred, avoiding the tricky problem of determination of initial conditions prior to flood events. The rainfall-runoff model used in this study is the four-parameter GR4J model. A schematic diagram of the model is given in Figure 3-1. The model was derived by Perrin (2000) from a previous version detailed by Edijatno et al. (1999). One of the characteristics of this model is its parsimony in terms of parameters, which limits problems of over-parameterisation and difficulties in determining parameters values during calibration. The four model parameters are the water exchange coefficient, the capacity of the non-linear routing store, the time-base of the unit hydrographs and the capacity of the soil moisture accounting store. They were calibrated with a local search optimisation method. The Nash and Sutcliffe (1970) criterion chosen as objective function puts naturally more weight on flood peaks and is therefore well suited for this type of application. The first year of each calibration sub-period was used for model warm-up.
Although we have applied here a single model to all test catchments, the ideal situation in operational conditions would have been of course to test several models for each catchment and select the best performing one.

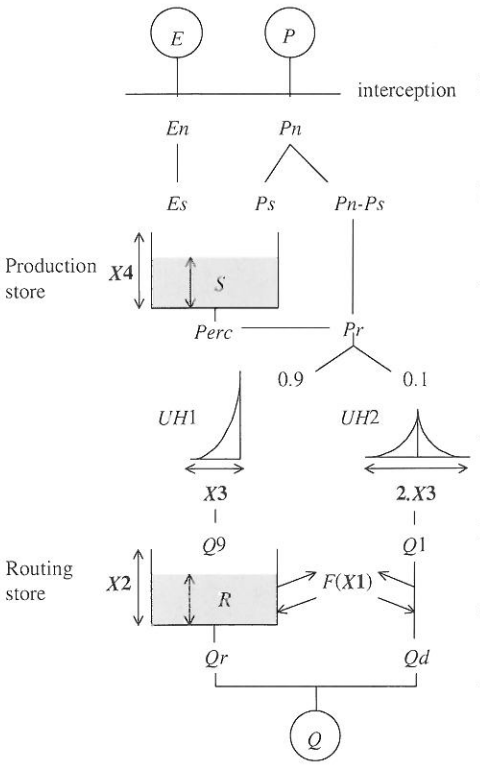

Interception (E : potential evapotranspiration; P : precipitation)

$if\ P \geq E, Pn = P - E, En = 0$

$else \quad Pn = 0, \quad En = E - P$

Production

$$Ps = \frac{Pn.\left(1-\left(\frac{S}{X4}\right)^2\right)}{1+\frac{Pn}{X4}\left(1+\frac{S}{X4}\right)} \qquad Es = \frac{En.\frac{S}{X4}\left(2-\frac{S}{X4}\right)}{1+\frac{En}{X4}\left(2-\frac{S}{X4}\right)} \qquad S = S + Ps - Es$$

Percolation

$$Perc = S - \left(S^{-4} + \left(\frac{9}{4}.X4\right)^{-4}\right)^{-\frac{1}{4}} \qquad S = S - Perc \qquad Pr = Pn - Ps + Perc$$

Unit Hydrograph ordinates

$$UH1(j) = SH1(j) - SH1(j-1)$$

with $\quad 0 \leq j \leq X3, SH1(j) = \left(\frac{j}{X3}\right)^{\frac{5}{2}}$

$\quad j > X3, \ SH1(j) = 1$

$$UH2(j) = SH2(j) - SH2(j-1)$$

with $\quad 0 \leq j \leq X3, SH2(j) = \frac{1}{2}\left(\frac{j}{X3}\right)^{\frac{5}{2}}$

$\quad X3 < j \leq 2.X3, SH2(j) = 1 - \frac{1}{2}\left(2 - \frac{j}{X3}\right)^{\frac{5}{2}}$

$\quad j > 2.X3, \ SH2(j) = 1$

Water exchanges

$$F = X1\left(\frac{R}{X2}\right)^{\frac{7}{2}}$$

Direct flow component

$$Qd = \max(0, Q1 + F)$$

Non linear routing store

$$R = \max(\varepsilon, R + Q9 + F) \qquad Qr = R - \left(R^{-4} + X2^{-4}\right)^{-\frac{1}{4}} \qquad R = R - Qr$$

Total streamflow

$$Q = Qr + Qd$$

Figure 3-1: Structure of the GR4J rainfall-runoff model.

4 RESULTS AND DISCUSSION

4.1 Calibration of the rainfall-runoff model

The extension of streamflow time-series using a rainfall-runoff model requires that the model performs satisfactorily on the study catchment. In our tests, the model was successively calibrated on each sub-period. On the whole catchment sample, 127 and 177 calibrations were performed on the 7- and 4-year sub-periods respectively.

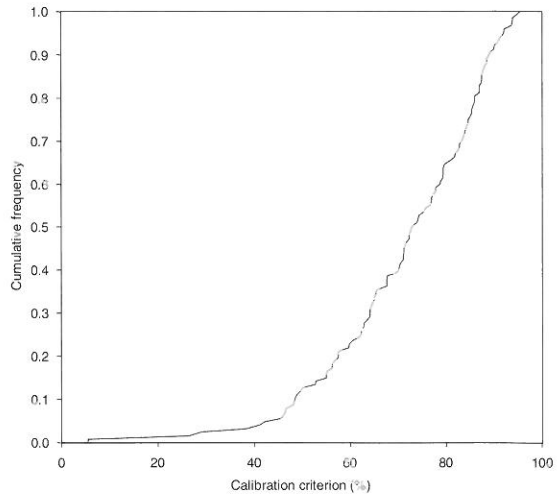

Figure 4-1: Distribution of criteria obtained in calibration on the sample of catchments with 7-year sub-periods.

Figure 4-1 illustrates the distribution of calibration criteria obtained with the 7-year sub-periods. It indicates that 65 % of efficiency criteria are lower than 80 %. So the model has some difficulties to perform satisfactorily on a good part of the test catchments. Given that the calibration objective function puts more weight on flood peaks, it means that the model does not manage to match peaks with good accuracy on those catchments.
Similar results were obtained with the shorter sub-periods, with 60 % of calibration runs under 80 % of efficiency.
The problem of model efficiency in simulating flood peaks has several well-known origins, among which are the inadequacy of model structure, the uncertainties associated with streamflow gauging or rainfall measurement or the problems of parameter determination. These aspects in the context of flood estimation are discussed for example by Fontaine (1995). On some catchments, the influence of snow-melt which is not accounted for in the selected model may also be a source of problem in simulations.

4.2 Results of flood estimation

The 50-year flood was estimated using both approaches. Results are given in Table 4-1 One distinguishes results obtained on the whole sample of catchments, and results obtained on sub-periods where the rainfall-runoff performs satisfactorily (criterion above 80 %) or not. In general, results show that the classical approach is more satisfactory than the method using a rainfall-runoff model. This advantage is even larger when one considers sub-periods where the model does not perform satisfactorily. However, when one considers the sub-periods where the model is good, the trend is reversed, showing the usefulness of using the rainfall-runoff model for increasing the sample of maximum annual flood.
The same behaviour can be observed either for 7-year or 4-year sub-periods, which means that the robustness of the methods does not change much when data availability decreases.

Table 4-1: Results of flood estimation of the classical approach (S_F) and the approach with the rainfall-runoff model (S_M).

		S_F	S_M
7-year sub-period	Whole sample of sub-periods	0,51	0,62
	Sub-periods with low model efficiency	0,58	0,75
	Sub-periods with high model efficiency	0,34	0,26
4-year sub-period	Whole sample of sub-periods	0,54	0,65
	Sub-periods with low model efficiency	0,59	0,78
	Sub-periods with high model efficiency	0,48	0,38

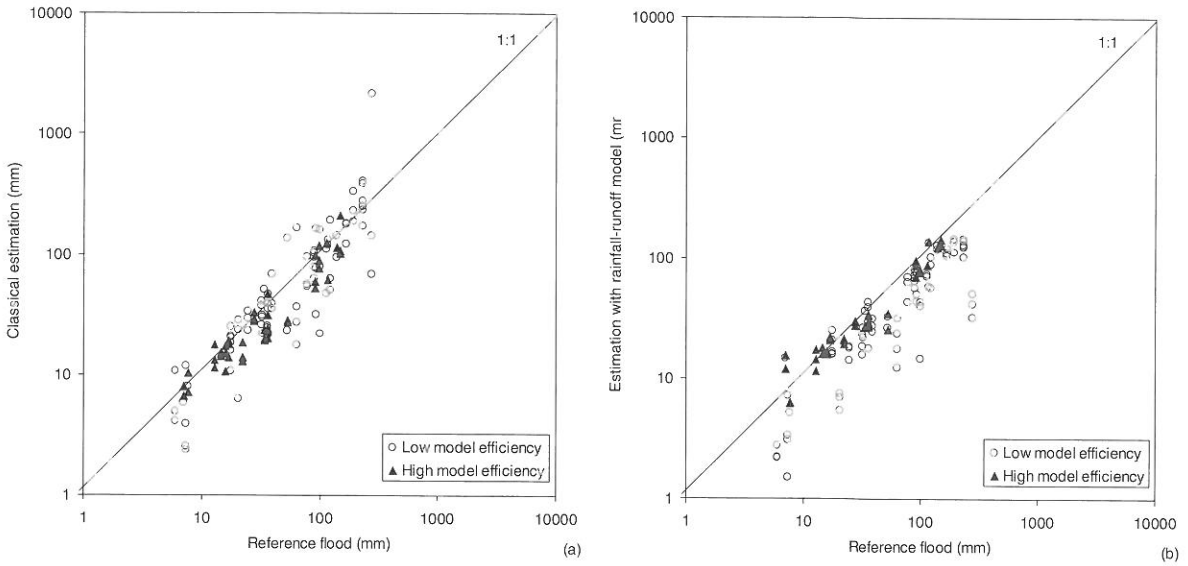

Figure 4-2: Plots of classical estimation (a) and estimation with the rainfall-runoff model (b) against reference flood in the case of 7-year sub-periods.

Figure 4-2 shows the correspondence between the reference floods and the estimations provided by both methods in the case of the 7-year sub-periods. It indicates that the lower efficiency of the rainfall-runoff based method may come from the fact that the model seems to underestimate flood peaks on many test catchments, therefore also underestimating the 50-year flood. In contrast, flood estimations seem evenly dispersed between under- and overestimation for the classical method. The results are very similar in the case of the 4-year sub-periods.

4.3 Tentative improvement of modelling efficiency

The overall lower efficiency of the method based on the rainfall-runoff model originates in the difficulty of the rainfall-runoff model to match flood peaks. To try to better capture catchment behaviour between flood periods, an attempt was made to change the objective function used for model calibration. The study by Lamb (1999) discusses this issue of objective function selection during the calibration procedure. Here we kept a single form of objective function but changed the target variable. Instead of taking streamflow as target variable in the objective function, a transformed value of streamflow was chosen. The prior transformation on streamflow was a power transformation with exponent 2 and 3. This puts even more weight on large model errors during flood peaks.
Results on the total catchment sample (see Table 4-2) indicate that better performances can be achieved in the estimation of the 50-year flood, and both methods become almost equivalent. However the exponent 3 does not bring much improvement in comparison with exponent 2.

Table 4-2: Results of flood estimation of the classical approach (S_F) and the approach with the rainfall-runoff model (S_M).

	Objective function	S_F	S_M
7-year sub-period	Nash(Q)	0.51	0.62
	Nash(Q^2)	0.51	0.50
	Nash(Q^3)	0.51	0.47
4-year sub-period	Nash(Q)	0.54	0.65
	Nash(Q^2)	0.54	0.56
	Nash(Q^3)	0.54	0.53

Table 4-3 shows values of ratios between the values of floods estimated by the different methods and the reference floods for the 7-year sub-periods. The use of the prior transformation on streamflow during model calibration effectively narrows the range of under- or overestimation of the 50-year floods. However, the underestimation for most sub-periods still remains: the median ratio is still much lower than unity even when using the transformation of streamflow.

Table 4-3: Characteristic values of the distributions of ratios between 50-year flood estimates and reference flood in the case of 7-year sub-periods.

	Percentile 0.1	Median Value	Percentile 0.9
Classical method	0.50	0.94	1.41
R-R method with OF(Q)	0.37	0.76	1.17
R-R method with OF(Q^2)	0.48	0.79	1.08
R-R method with OF(Q^3)	0.51	0.83	1.12

5 CONCLUSION

The study showed the influence of low efficiency of the rainfall-runoff model on the quality of flood estimations. On the whole sample of test catchments, the improvement brought by the rainfall-runoff model did not appear clearly, except for cases where the model performs satisfactorily.
The use of an objective function that puts a lot of weight on errors on flood peaks brings improvement in the results. It makes the approach based on the rainfall-runoff model of almost equivalent efficiency as the approach based solely on statistical fits, in cases of low availability of streamflow data. Of course, in cases where only one or two years of streamflow data are available, statistical adjustment are not possible and the use of a rainfall-runoff model becomes more worthwhile.

An alternative solution to compensate for the difficulty of the rainfall-runoff model to capture flood peaks in this context could be to adopt a two-step approach, by using a correction on streamflows simulated by the model, which avoids to have a bias on modelled floods. This is similar to the approach adopted by Yang and Michel (2000) in their methodology for flood forecasting.
This study may also indicate that models still have to experience a substantial increase in accuracy to be successfully used in flood estimation on whatever gauged catchment.

ACKNOWLEDGEMENTS

Rainfall and streamflow daily data were provided by the PLUVIO data base of Météo-France and the the HYDRO data base of the French Ministry of Environment respectively. This research received financial support from the Programme National de Recherches en Hydrologie (PNRH) of the Institut National des Sciences de l'Univers.

REFERENCES

Cameron, D.S. et al. (1999): Flood frequency estimation by continuous simulation for a gauged upland catchment (with uncertainty). Journal of Hydrology, Amsterdam, The Netherlands, 219, 169-187.

Edijatno et al. (1999): GR3J: a daily watershed model with three free parameters. Hydrological Sciences Journal, Wallingford, UK, 44(2), 263-277.

Fontaine, T.A. (1995): Rainfall-runoff model accuracy for an extreme flood. Journal of Hydraulic Engineering, New-York, USA, 121(4), 365-374.

Lamb, R. (1999): Calibration of a conceptual rainfall-runoff model for flood frequency estimation by continuous simulation. Water Resources Research, Washington, USA, 35(10), 3103-3114.

Nash, J.E., Sutcliffe, J.V. (1970): River flow forecasting through conceptual models. Part I - A discussion of principles. Journal of Hydrology, Amsterdam, The Netherlands, 27(3), 282-290.

Perrin, C. (2000): Vers une amélioration d'un modèle global pluie-débit au travers d'une approche comparative. PhD thesis, INPG (Grenoble) / Cemagref (Antony), France, 530 p.

Yang, X., Michel, C. (2000): Flood forecasting with a watershed model: a new method of parameter updating. Hydrological Sciences Journal, Wallingford, UK, 45(4), 537-546.

MODEL OF SNOW COVER FORMATION AND METHODICS FOR THE LONG-TERM PREDICTION OF INFLOW INTO WATER RESERVOIRS DURING THE FLOOD SEASON

Felix Pertziger[1], Michael Baumgartner[2], Timur Kobilov[1], Alexey Schultz[3], Ludmila Vasilina[1]

[1] Hydrometeorological Survey, Republic of Uzbekistan, felix@rch.uz

[2] MFB GeoConsulting, Switzerland, contact@mfb-geo.ch

[3] Swiss Aral Sea Mission, Uzbekistan, alexey@rch.uz

SUMMARY

The long-term predictions of runoff are of great interest for Central Asian water management, agricultural and hydropower production authorities.
A research has been made to use remote sensing data together with the model of snow cover formation to predict at the end of March the total water inflow into a reservoir during the flood season (April - September).
A two parameters model of snow cover formation was developed and tested to fit both temporal (year-to-year) and spatial (3D) pattern of snow cover extent over the basin. Snow covered areas were revealed from AVHRR images acquired at the end of March during 1989 - 2001. These thirteen maps of snow cover extent have been used for the parameter calibration. A consequent series of seasonal snow line positions has been compared with modeling results to validate the simulation performance.
The water inflow into the reservoir during the flood period has been plotted against computed snow amount at the end of March over 11000-km^2 watershed. A linear regression equation explains 86% of runoff variations, there is no flood season with error of prediction bigger than admissible threshold. The developed forecasting technique proves to be of high performance. It is applicable for long-term runoff predictions at any snow-fed mountainous river with similar seasonal pattern of precipitation and availability of climate stations.

Keywords: runoff, prediction, snow cover, model

1 INTRODUCTION

The long-term prediction of runoff is of great interest for Central Asian water management, agricultural and hydropower production authorities.
A research has been made to use remote sensing data together with the model of snow cover formation to predict at the end of March the total water inflow into a reservoir during the flood season (April - September). The reservoir is designed both for power production and irrigation in a country capital oasis (Tashkent, Uzbekistan).

2 INPUT DATA

The following hydrological and climatic information has been collected from archives and compiled into Excel® workbook:

- 10-days precipitation totals measured at 11 stations during the cold seasons (October - March) of 1989 - 2001;
- 10-days average air temperature measured at 6 meteorological stations during the same years;
- Inflow to the reservoir during the "vegetation" period (April-September) in 1989 - 2000.

NOAA AVHRR data of the study area at the end of March of 1989-2001 (13 scenes in total) have been used for identifying the snow cover extent over the basin. For the period 1989 - 1997 data were downloaded from **www.saa.noaa.gov**. For the last four years such information was acquired in the framework of the World Bank Project 2.1 "Improvement of Hydrometeorological Surveys in Central Asia" (Flow Forecasting) financed by Swiss State Secretariat of Economic Affairs and Swiss Development Cooperation (Kobilov et al., 2000).
The last type of input data was the digital elevation model (DEM) of the watershed. The DEM developed within the above mentioned project has been resampled to reduce the processing time. Figure 2-1 shows the basin for Charvak Reservoir and the location of the climatic stations used in this work.

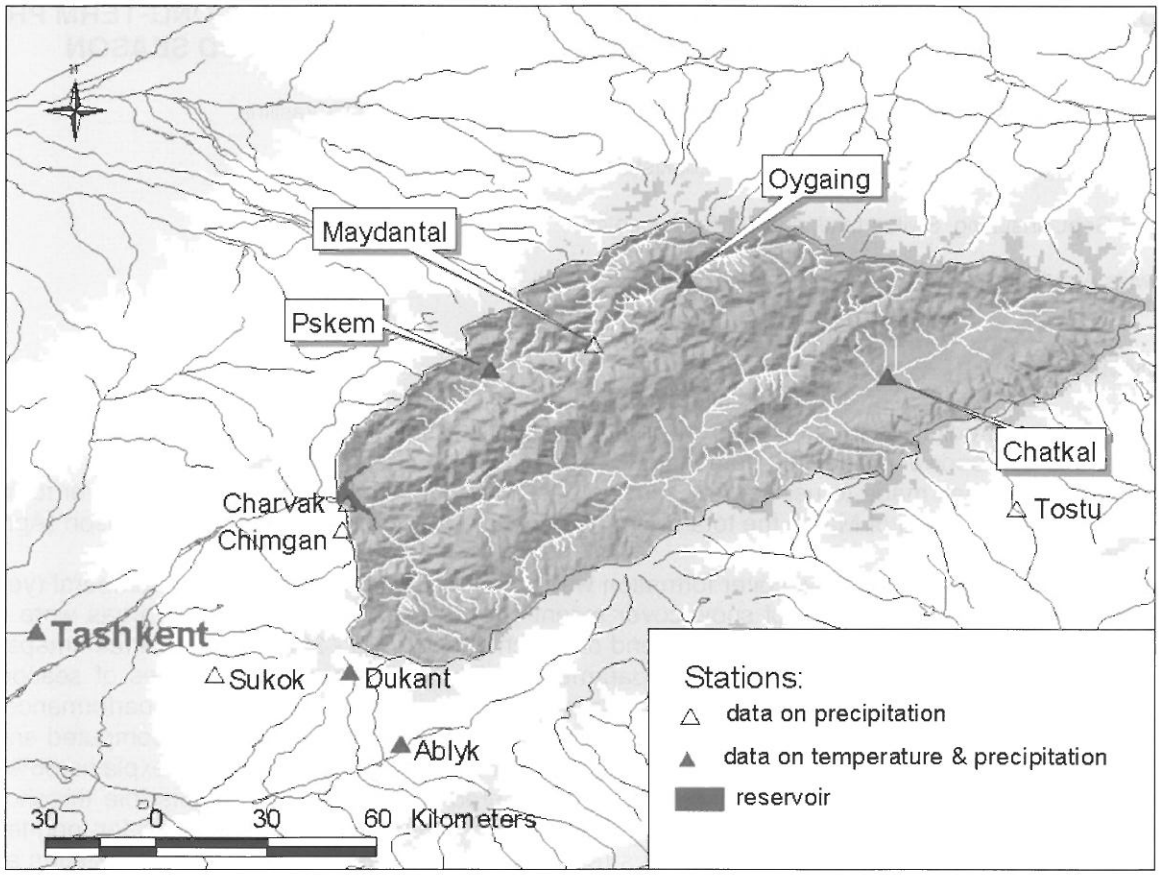

Figure 2-1: Location of the climatic stations.

3 DATA PREPROCESSING

As a first step, climate data have been mapped with the help of Anusplin software package (Hutchinson, 1999), devoted for spline fitting surfaces (particularly climatic) from noisy data as functions of one or more independent variables. Longitude, latitude and elevation of the stations were used as variables. An advantage of Anusplin is that input data can be submitted both in a point and grid format. The Spatial extent and the resolution of the output grid depend upon the resolution of the DEM (elevation has been used as a third variable). In a whole, 18 (due to a number of 10-days periods in October-March) maps of precipitation totals and 18 maps of air temperature have been constructed for each of the 13 years.

4 CALIBRATION: SNOW COVER FORMATION MODEL

It is assumed that 10-days snow accumulation (S) at any point (grid cell) in the basin is equal to the solid part of precipitation (snow):

$$S_d = \begin{cases} X_d, \vartheta_d < \vartheta_0 \\ 0.5X_d, \vartheta_d = \vartheta_0, \\ 0, \vartheta_d > \vartheta_0 \end{cases} \quad (1)$$

where X is precipitation [mm], ϑ is air temperature [°C], ϑ_0 is snow-rain temperature threshold (parameter #1), d is 10 days period number (d = 1,2 .. 18). An example for the computation of S for a single cell during one season is shown in Figure 4-1a.

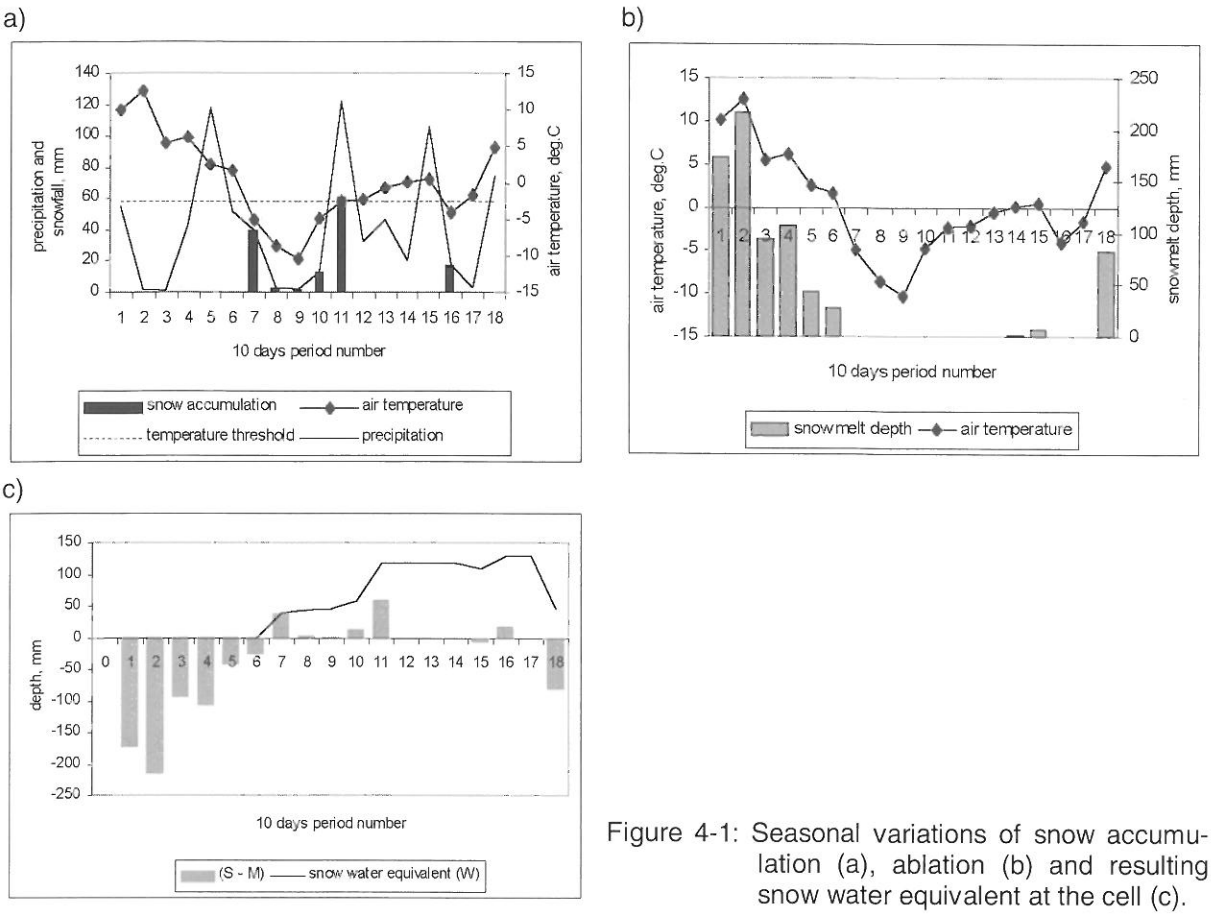

Figure 4-1: Seasonal variations of snow accumulation (a), ablation (b) and resulting snow water equivalent at the cell (c).

Similar to the degree-day method it was assumed that the 10-days snowmelt depth (*M, mm*) occurs only under positive air temperatures and M is proportional to the latter:

(2) $$M_d = \max(\alpha\vartheta, 0),$$

where α is the snowmelt factor (parameter #2). An example of M computation for a single cell during one cold season is shown in Figure 4-1b.

The 10-days change in snow water equivalent (ΔW) was calculated as a difference of snow accumulation and ablation:

(3) $$\Delta W_d = S_d - M_d$$

,

And finally, the water equivalent at time d has been computed by aggregation of changes:

(4) $$W_d = \max(W_{d-1} + \Delta W_d, 0).$$

It has been reasonably assumed that there is no snow all over the basin at the end of September which is traditionally considered as the start of the hydrological year, i.e. $W_0 = 0$. An example of the seasonal pattern of W at a single point is shown in Figure 4-1c.

The following function has been used as target during the search of numeric values of the parameters ϑ_0 and α:

(5) $$T = \frac{\sum_{k=1}^{m}\sum_{j=1}^{n}\left|sign\left(C_{k,j}\right) - sign\left(W_{k,j}\right)\right|}{m},$$

where k is year number; m is total number of years (13 in our case); j is cell number; n is a total number of cells in the snow map grid minus the number of cells with "No Data" attributed,

(6) $$sign(x) = \begin{cases} 1, x > 0 \\ 0, x = 0 \\ -1, x < 0 \end{cases}$$

(7) $$C = \begin{cases} 1, \text{snow covered cell} \\ 0, \text{snow free cell} \end{cases}$$

In simpler terms, a combination of parameters ϑ_0 and α was searched, which will result in a best fitting of snow cover patterns by trying to reduce a number of mismatched cells. Such cells are shown in Figure 4-2c in dark.

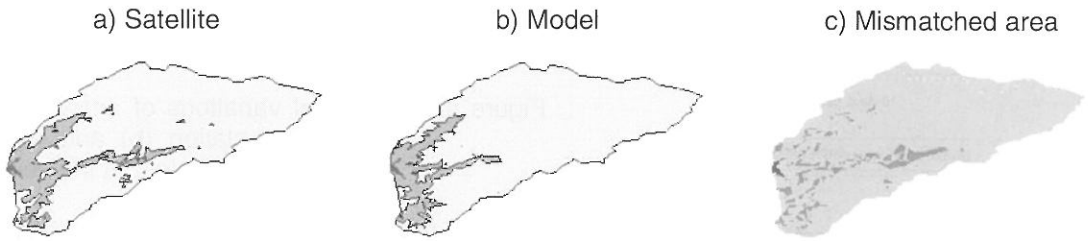

Figure 4-2: Intercomparison of measured and simulated snow cover extent, March 2000.

The code described in Bunday (1988) has been used as a search procedure. It turned out that metric T reaches the minimum under ϑ_0 = -2.5^{0}C and α = 18.5 mm/(^{0}C·10 day). Examples of measured and simulated snow patterns for two extreme years are shown in Table 4-1.

Table 4-1: Comparison of measured and computed snow pattern on March 1993 and 2000.

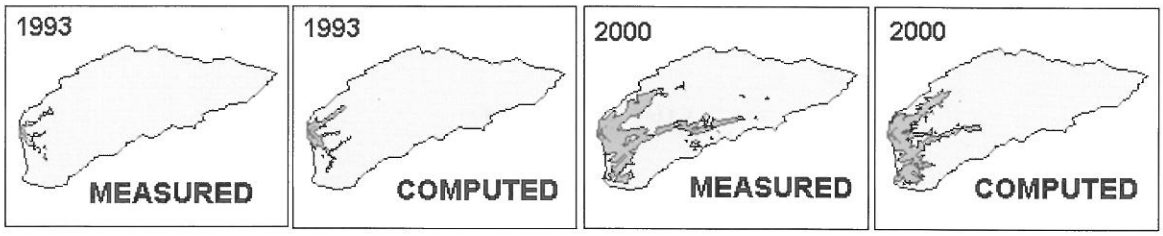

The correlation coefficient between measured and computed snow-covered areas for 13 years equals to 0.80. This proves the good performance of the proposed snow cover formation model in fitting year-to-year variations of the snow cover extent. Nevertheless it was decided to check the capability of the model in respect to spatial variations of the amount of snow within the basin.

5 VALIDATION: SNOW COVER FORMATION MODEL

A consequent series of seasonal snow line positions can be used for revealing a pattern of snow cover ablation. Under the same temperature regime, the snow will melt earlier from a site with smaller snow reserves than from a site with larger reserves (later melting). Elevation is the most significant factor defining an air temperature pattern over a medium sized basin, like Charvak water reservoir. If the model

estimates a direct proportion between date of snow ablation and snow water equivalent within an elevation zone, it is a good evidence of the model performance.
The set of 14 satellite images acquired during the melt season of 1999 has been used to compile a map of the dates of snow cover ablation (or disappearance). It has been assumed that at any vertex describing the shape of the snow covered area, the date of image acquisition is the date of snow cover disappearing/melting away. The map is shown in Figure 5-1a. The snow cover model output is a map of snow water equivalent (SWE) at the end of March. The 1999 map of SWE is shown in Figure 5-1b. As a next step, a watershed has been subdivided into 7 elevation zones and for each of them an average value for the date of snow ablation and water equivalent was estimated. Corresponding trends are shown in Figures 5-1c and 5-1d, respectively. The subtraction of trends gave anomaly patterns for the discussed features of the snow cover regime. They are presented in Figures 5-1e and 5-1f, respectively.

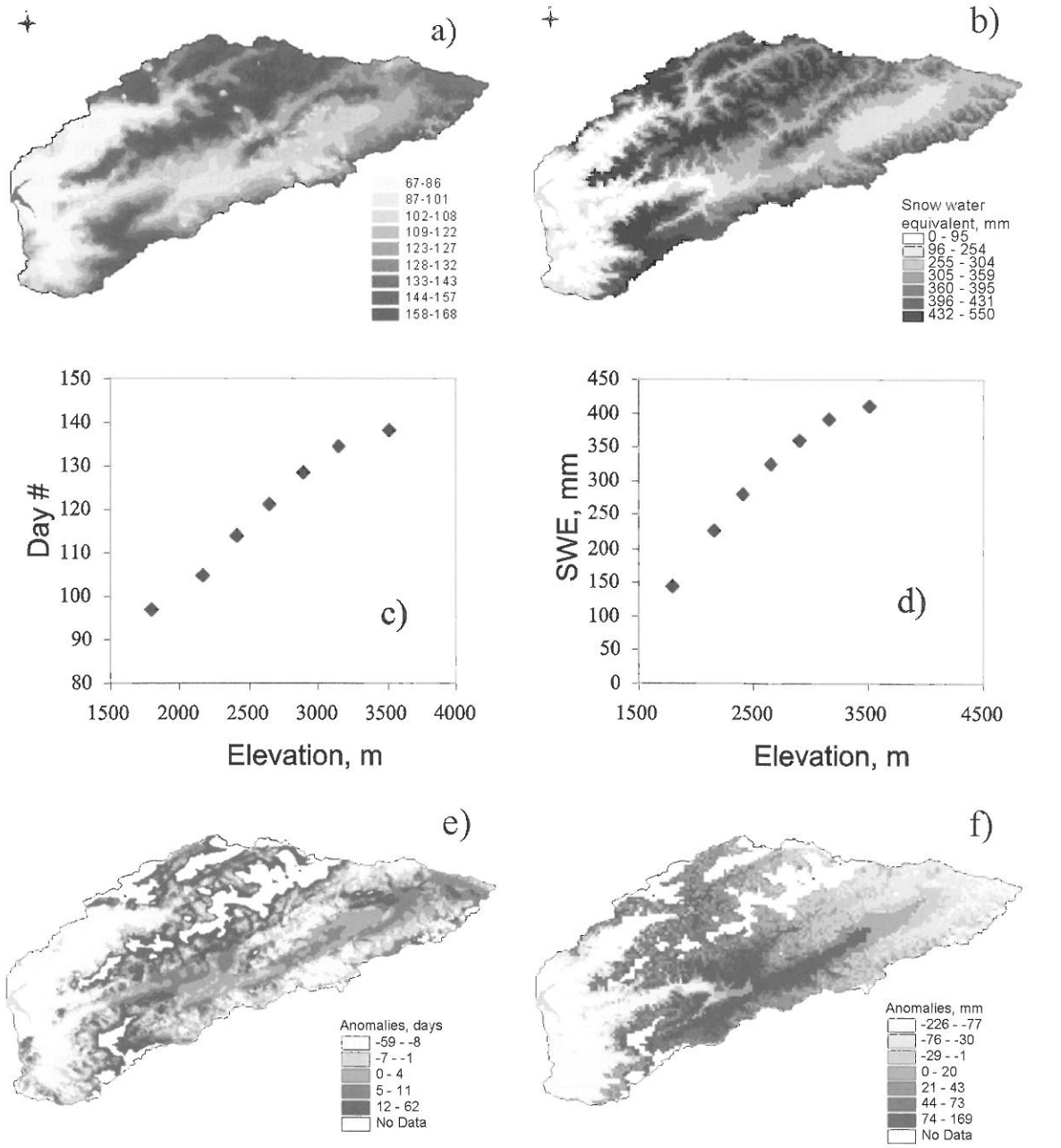

Figure 5-1: The 1999 maps of the day of snow cover ablation (a) and snow water equivalent (b), their trends versus elevation (c, d) and anomaly pattern (e, f).

There are a lot of similar features in the last two maps; for example a big area in the South of the reservoir has negative anomalies for both, the date and the water equivalent.
As a final step, the anomalies of the date of ablation were summarized with those of the snow water equivalent. The results have been compiled in Figure 5-2 making the relationship between the discussed features more evident.

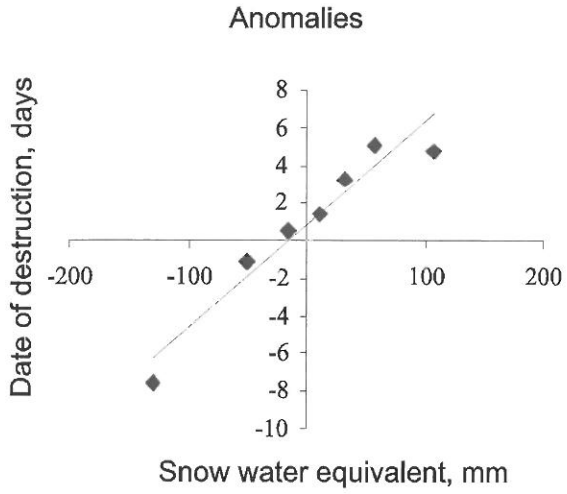

Figure 5-2: Relationship between anomalies of snow water equivalent at the end of March, 1999 and the date of snowpack ablation during the 1999 melting season.

As one can see, a highly reliable model of snow cover formation within the mountainous river basin has been developed. The model fits both, the spatial (3D) and temporal changes of snow cover extent and water equivalent.
The approach used for the model parameter calibration is similar to the one known in the USSR school of hydrology as the "method of heat evince" (Denisov, 1967). The difference is that here a 3D-fit of snow cover pattern was implemented instead of using a single variable, which was the elevation of snow line.

6 LONG-TERM FORECAST OF WATER INFLOW

The computed snow amount at the end of March within a basin has been compared with the water inflow into the reservoir during the flood period (April - September). The corresponding plot, the regression equation and the coefficient of determination are shown in Figure 6-1.

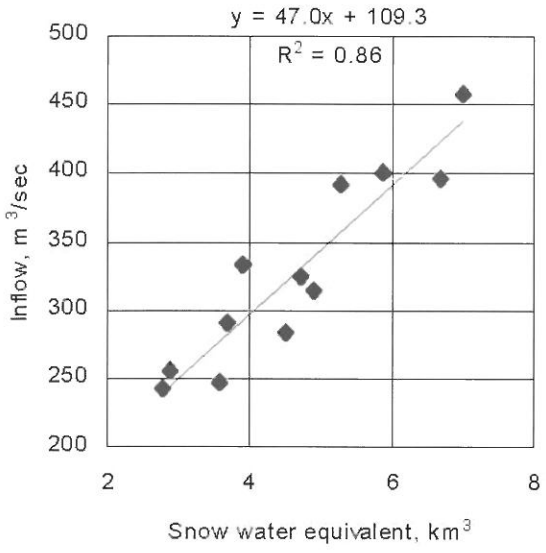

Figure 6-1: Relationship between water accumulated in the snow pack at the end of March and the inflow to the reservoir during April-September, 1989-2000.

The equation explains 86% of the variations of the inflow to the reservoir. If traditional predictors would be used, the scores will be significantly lower. For example the best correlation of the runoff serie and precipitation totals during October-March results in $R^2 = 0.72$.
The threshold value of error (S_{lim}) for long-term hydrological forecasts of the discharge (Q) is calculated by:

(8) $$S_{lim} = 0.674\sigma_Q,$$

where σ_Q is standard deviation of discharge. The forecast is considered as accurate if $|Q_{mes} - Q_{pred}| \leq S_{\lim}$. In our case S_{lim} = 47 m^3/s. Table 6-1 compares the measured and predicted discharges. As one can see, there is no year with an error bigger than the admissible threshold.

Table 6-1: Measured and predicted inflow into Charvak Water Reservoir during March-September.

Year	Snow Water Equivalent, km^3	Q_{mes}, m^3/s	Q_{pred}, m^3/s	$\|Q_{mes} - Q_{pred}\|$, m^3/s	$\|Q_{mes} - Q_{pred}\| \leq S_{\lim}$
1989	3.58	246	277	31	TRUE
1990	5.89	401	386	15	TRUE
1991	2.89	256	245	11	TRUE
1992	4.91	315	340	25	TRUE
1993	5.28	391	357	34	TRUE
1994	6.68	396	423	27	TRUE
1995	4.49	284	320	36	TRUE
1996	4.73	324	332	8	TRUE
1997	3.71	291	283	8	TRUE
1998	7.02	458	439	19	TRUE
1999	3.91	333	293	40	TRUE
2000	2.78	242	240	2	TRUE
2001	4.37	-	**315**	-	

It means that a highly efficient method of long-term (6 months lead-time) prediction of runoff has been developed. Due to the equation shown in Figure 6-1, an expected inflow into the reservoir in 2001 will be 315 ± 47 m^3/s.
Let's note that the study has not been targeted on a better correlation between modeled snow amount and runoff, it was directed to a fitting of snow cover extent.

7 SOFTWARE

The software is Microsoft Excel ® 97 workbook containing climatic data in separate sheets. It is built in VBA code capable to compile a set of required input maps, make a search for parameters of the snow cover model, and derive an updated forecasting value of runoff. The built-in procedure controls the identity of spatial extent of snow maps, sets of stations and data completeness.
To produce the forecast for any additional year, one has to perform next steps: a) compile two sheets with 10-days data on air temperature and precipitation recorded at specified stations during the cold season; b) update the database by missing values of runoff (for example, at the end of March 2002, the inflow during April - September, 2001 has to be entered in a proper place in a book) and c) prepare the binary version of the snow cover map for the end of March.
The software can easily be customized for any other basin-object. There are no difficulties in transferring it to other personal computers.

8 RESULTS AND CONCLUSION REMARKS

- A reliable model of snow cover formation within mountainous river basin has been developed. The model fits both spatial (3D) and temporal changes of snow cover extent and water equivalent;
- The combination of a traditional approach with remote sensing information results in a highly efficient technique for long-term (6 months lead-time) prediction of inflow into Charvak Water Reservoir. An expected inflow into reservoir in April-September, 2001 will be within the limits of 315 ± 47 m^3/s. (In fact it was 312 m^3/s, which is an additional proof of the high performance of the developed prediction technique);
- This robust technique can easily be implemented for any snow-fed mountainous river with similar seasonal patterns of precipitation and availability of climatic stations.

REFERENCES

Kobilov, T. et al. (2001): Operational technology for snow-cover mapping in the Central Asian mountains using NOAA-AVHRR data. Remote Sensing and Hydrology 2000 (Proceedings of a symposium held at Santa Fe, New Mexico, USA, April 2000). IAHS Publ. no. 267, 2001, p. 76 - 80.

Hutchinson, M. (1999): ANUSPLIN Version 4.1. User Guide /The Australian National University. Centre for Resource and Environmental Studies, Canberra, CRES, ISBN 086740 512 0.

Bunday, B. (1988): Basic optimization methods. Nauka, Moscow (in Russian), 128 pp.

Denisov, Yu. (1967): The model of snow cover formation within the mountainous basins. Hydrology & Meteorology, (in Russian), p. 75 - 81. [Денисов Ю.М. Модель формирования снежного покрова в горных бассейнах. //Метеорология и гидрология. - 1967 - №5., с. 75 - 81.]

THE APPLICATION OF FLOOD MODELLING AND MAPPING FOR MANAGING FLOOD RISK IN THE UK

Harvey J. E. Rodda[1] and Agnete Berger[2]

[1] Peter Brett Associates,16 Westcote Road, Reading, UK, hrodda@pba.co.uk

[2] Risk Management Solutions Ltd, 10 Eastcheap, London, UK, agnete.berger@rms.com

SUMMARY

This paper discusses different modelling and mapping approaches that have been implemented in the UK to assess flood risk, highlighting the issues of scale and accuracy as required for different purposes. Two approaches to identify flood risk may be distinguished. Firstly a design approach, where specific flood return periods are modelled using a range of techniques to define flood envelopes for planning and engineering purposes. This approach covers both the countrywide scale to the detailed hydrodynamic modelling of specific river reaches. Secondly a stochastic event-based approach that simulates the full range of flood return periods up to and beyond 1000 year return period on each river, and assesses the likelihood of separate rivers in the UK flooding during the same flood event for the purposes of insurance and re-insurance risk pricing.

Keywords: flood mapping, flood modelling, risk, insurance

1 INTRODUCTION

The application of mapping and modelling techniques to identify areas at risk from river flooding is a well-established practice. This information is of great importance to planners, developers and engineers to understand the risks of inundation associated with existing and new buildings, and more recently to the insurance industry for setting premiums and identifying potential losses from a flood event. This paper identifies and discusses two different approaches that have been used to assess flood risk by mapping and modelling. Firstly the design approach, where specific return periods are modelled using a range of techniques to produce flood risk maps ranging in resolution from a countrywide scale to individual river reaches over a few kilometres. The flood extent is always mapped to a design flood level, commonly the 1 in 100 year flood. These types of maps are very good for planning purposes, but one major disadvantage is that they do not consider the relationships between the degree of flooding for individual river basins. This is of particular importance for the insurance industry where, besides pricing each individual risk, the primary insurer needs to quantify the level at which reinsurance cover is required to cover flood event losses and the re-insurer needs to control portfolio risk aggregation. This issue has been addressed by a second stochastic event-based approach used to develop the RMS UK River Flood model. The model uses a stochastic set of flood events to assign the risk of a certain depth of flooding for any 7-figure postcode in the UK for a given event, using a combination of physically-based meteorological, hydrological and hydrodynamic modelling and probabilistic sampling techniques.

2 DESIGN APPROACH

2.1 Indicative Flood Plain Maps

In the United Kingdom, a major undertaking of the Environment Agency in the past couple of years has been the publishing of indicative flood plain maps (IFPM). The IFPM programme is a ministerial requirement stemming from the large Easter 1998 floods. The directive states that all rivers in the United Kingdom will have flood extent maps developed to encompass the 100 year flood in the fluvial reaches and 200 year flood in tidal reaches. This directive is in effect the substance of Section 105 of the Water Resources Act 1991 which places a requirement on the Environment Agency to supply local authorities with flood risk maps. This is to be completed using a range of assessment, modelling and mapping techniques depending on the location and site constraints.
The IFPM were produced as an interim measure to provide an indication of the flood risk areas in the wake of the Easter 1998 floods. The flood map envelopes were produced using a combination of tech-

niques including: the worst known flood extent based on historical information, photos and resident discussions; existing maps of land liable to flood (produced in 1981 under Section 24), the Institute of Hydrology flood risk map for England and Wales (Morris, Flavin, 1995), and the 5m AOD contour digitised from 1:10,000 scale maps.
As these maps were produced as an interim measure there a number of inaccuracies in the flood envelopes and a more detailed mapping programme is being undertaken for the Environment Agency which includes the application of detailed hydrological and hydraulic models. The problems with the IFPM include flood envelopes crossing sloping ground and including high ground not at risk, flood levels differing across the flood plain and not following the lie of the floodplain. A review of IFPM for specific reaches using high-resolution topographic data highlighted the inaccuracy of the IFPM, as illustrated in Figure 2-1. In addition, the Institute of Hydrology flood risk map, which has been incorporated into sections of the IFPM is based on a 50m DTM. At high resolution this gives a stepped outline which in reality does not occur.

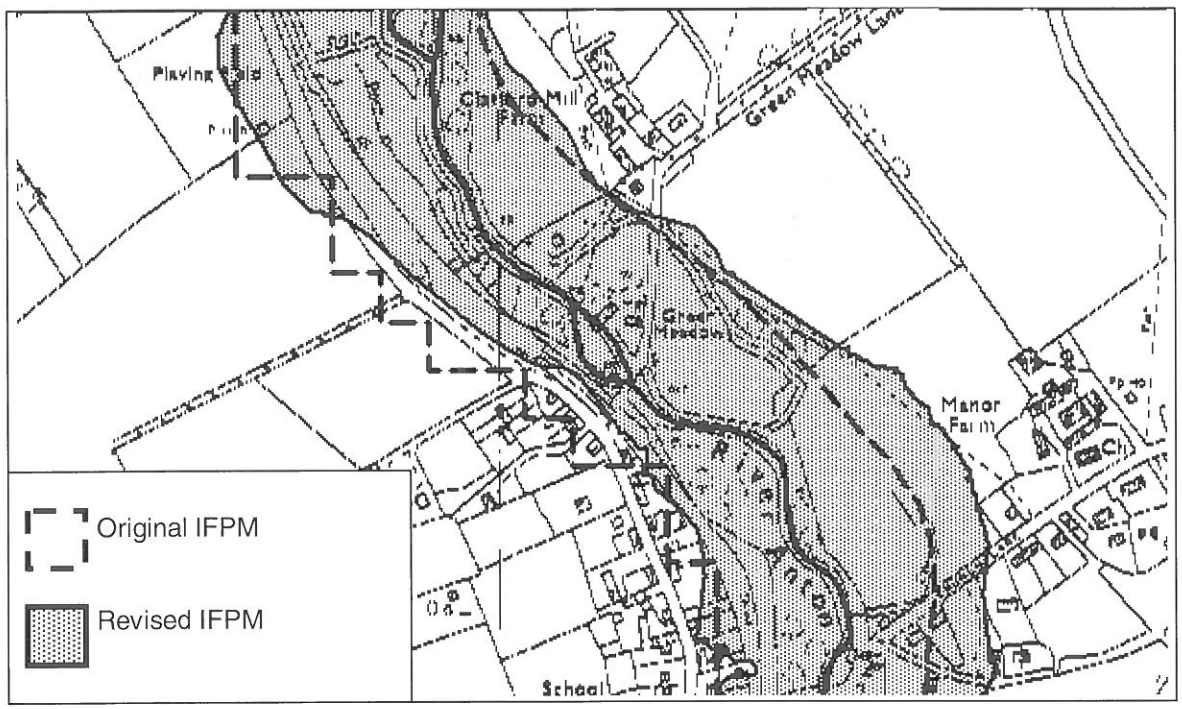

Figure 2-1: A comparison of original and revised Indicative Floodplain Maps (IFPM) for the River Anton in Southern England. The angular outline of the original map is from the use of a 50m DTM to define the flood envelope.

2.2 Section 105 Mapping

The programme of more detailed flood plain mapping is termed Section 105 Mapping and it is currently being undertaken for all designated main river reaches in England and Wales. The main output is the 100 year flood envelope, but also 5, 10, 20, 50 and 1000 year envelopes are being produced. The mapping is being undertaken by a number of consultancy companies selected by the Environment Agency, and the procedure undertaken follows rigid Agency specification guidelines for hydrological and hydrodynamic modelling and mapping of the flood extent.

2.2.1 Hydrological Modelling

The design flows required to produce the flood envelopes are derived using procedures from the Flood Estimation Handbook (Institute of Hydrology, 2000). Peak design flows (e.g. 100 year) can be obtained for ungauged and gauged catchment using a statistical technique based on the pooling of annual maximum flows from catchments with similar specified catchment descriptors for area, wetness and soil properties, and attenuation from lakes and reservoirs. Unit hydrographs are also derived using catchment descriptors, and these are then used to simulate historical flood events and the outputs

are calibrated using observed flows at gauged catchments. In the case of ungauged catchments, hydrographs are calibrated to a gauged site further downstream. The finalised hydrographs are then used as the boundary condition inputs to the hydrodynamic model.

2.2.2 Hydrodynamic Modelling

A detailed hydrodynamic model is employed to calculate the water levels at a number of points or nodes along the river reach. Commercial modelling software such as ISIS or Mike 11 is required for this stage of the mapping, and levels can be calculated to the nearest mm. These models require detailed survey information including extended channel cross sections (commonly at 100m intervals), and all structures along the length of the reach, such as bridges, culverts, defences and flood storage areas. Due to the detailed nature of these models, simulations are concentrated in small areas or "hot spots". These are in urban areas where property is at risk and flooding has been recorded, in areas where new development is proposed, and in places where problem flood defences have been identified through defence surveys. Flood levels in areas outside of the hotspots, mostly rural, uninhabited land, are derived using kinematic routing methods included in the hydrodynamic software.

2.2.3 Flood Envelope Mapping

The water levels predicted by the hydrodynamic model are then used to generate a flood surface. Using GIS, a triangular irregular network (TIN) is built from the predicted level at each extended cross section. This gives a flood surface in m AOD, which can be converted into a flooded extent through subtracting the actual ground surface elevation given by an accurate DTM, preferably from a ground survey with 1 m horizontal and 1 cm vertical resolution. Where ground survey data is not available high resolution DTMS from photogrammetry and LiDAR can be used
This procedure can be repeated for different return period floods, and once calibrated hydrological and hydrodynamic models are in place further simulations and mapping can be undertaken more quickly.

3 STOCHASTIC EVENT-BASED APPROACH

In the UK river basins are relatively small so large floods characteristically affect many separate rivers during the same event (e.g. Easter 1998, Autumn 2000). The RMS UK River Flood model was developed in order to capture both the correlation of flooding on separate rivers during a flood event and the full range of flood return periods on each river up to and beyond the 1000 year discharge. A stochastic event set of over 2000 flood-inducing rainfall events is coupled dynamically with a runoff model, and a hydrological model is used to determine maximum flood extent and depth, taking account of flood defences. Flood risk is modelled in terms of the insured damage or loss to a range of building types over the full range of flood event return periods for the whole country at 7-figure postcode resolution (average of 15 properties per 7-figure postcode).

3.1 Rainfall Stochastic Event Set

The stochastic event set is based on a comprehensive historical catalogue of 528 flood events covering 1870-2000 that represents the range of flood-inducing rainfall event types that affect the UK, their rates of occurrence and severity. Widespread flooding during the winter months is caused by single or consecutive frontal events associated with the westerly track of Atlantic extra-tropical cyclones. Flash floods during the summer months result from mesoscale convective systems (MCCs), clusters of intense thunderstorm cells within a mesoscale region of stratiform rain that affect the southern part of the UK, and localised thunderstorms that can occur anywhere. The flood-inducing rainfall events are modelled as clusters of at least one event in order to represent floods resulting from a sequence of rainfall events. Frontal and MCC events are defined using a combination of ten parameters (e.g. axis lengths, bearing, rainfall, number and spacing of events) by importance sampling to ensure proper representation of rare, extreme flood events. The flood-inducing rainfall events are modelled as they evolve on an hourly basis using a rainfall profile to simulate the growth and decay of rainfall over a point and orographic enhancement grids to represent the proven increase in rainfall with altitude. Thunderstorms are modelled as a series of stationary ellipses with a single value of rainfall intensity using Monte Carlo simulation based on the annual average frequency distribution of thunderstorms for

1961-1990. Modelled rainfall over a series of return periods and time periods has been calibrated with corresponding Flood Studies Report (FSR) and Flood Estimation Handbook (FEH) data (NERC, 1975; Institute of Hydrology, 2000).

3.2 Hydrological Model

The modelled river network balances the requirement to include catchments throughout the UK that are characterised by a high potential for insured loss by the full range of flood event types and hydrological modelling efficiency (Figure 3-1). The modelled maximum hourly rainfall is converted into runoff in each of the 626 catchments modelled using a modified US Soil Conservation Service equation (Webster, Ashfaq, 2002) that includes a stochastic antecedent index based on daily flow records to model the effect of catchment antecedent wetness on the soil term. Runoff is converted into discharge by using a modified triangular unit hydrograph technique (NERC 1975; Institute of Hydrology, 2000). Individual catchment characteristics derived from a 1km and 50m DTM are used to calculate the time to peak for each catchment, and each hourly hydrograph is combined to give the event storm hydrograph. Total discharge for each catchment includes the antecedent flow, the product of the catchment stochastic antecedent index and the bankfull discharge. The discharge is routed downstream at hourly time steps using established hydraulic techniques partly based on the RIBAMAN model (HR Wallingford, 1994) and a unique catchment numbering system used in developing the United States Geological Survey HYDRO1K data set (Verdin, 1997). Output from the hydrological model has been compared against data from the FEH and recent flood events, and the correlation of high flows in multiple rivers has been calibrated against maximum annual flow records for 274 gauges. Thunderstorm events frequently cause flooding without the direct involvement of a river, especially in urban areas, and are therefore modelled separately from the rainfall-runoff and hydrological model.

Figure 3-1: River network modelled by the RMS UK River Flood model with detail showing the individual catchments modelled within the Thames basin.

3.3 Hydrodynamic Model

Depth above bankfull is derived from the maximum discharge using rating curves. The rating curves are based on modelling channel and floodplain flow for a series of depths above bankfull in each catchment using GIS analysis of a 50m DTM, and have been calibrated against standard depth-discharge relationships supplied by the Environment Agency. The over-bankfull depth is propagated over the floodplain of each catchment using a 50m horizontal- and 1m vertical-resolution DTM by identifying the area of the floodplain flooded by each river cell within each catchment. The total extent and depth of the flood event is computed to include the effect of backing up as controlled by the relationship between the flow return period of individual catchments and catchment hierarchy. Flood extents have been calibrated with RMS and other published surveys of past floods. Due to the unavailability of detailed information on the

location, standard of protection and maintenance of defences in the UK, a probabilistic model is used to simulate protection against floods of different return periods. The probabilistic model provides an envelope of uncertainty around Department of the Environment, Forests and Rural Affairs guidelines, and based on detailed research on the performance of defences during recent flood events, the modelled uncertainty differentiates between rural areas and four categories of urban areas. The actual flood depth is derived for each 7-figure postcode unit within the floodplain.

3.4 Flood Risk

Flood risk is quantified by using damage curves for a range of building types to model the percentage insured loss related to depth of flooding for frontal and MCC flood events, and to rainfall intensity for thunderstorm events. The flood risk, in terms of insured loss, can thus be quantified for flood events of specific return periods and as the average annual loss at the resolution of the country or 7-figure postcode unit (Figure 3-2).

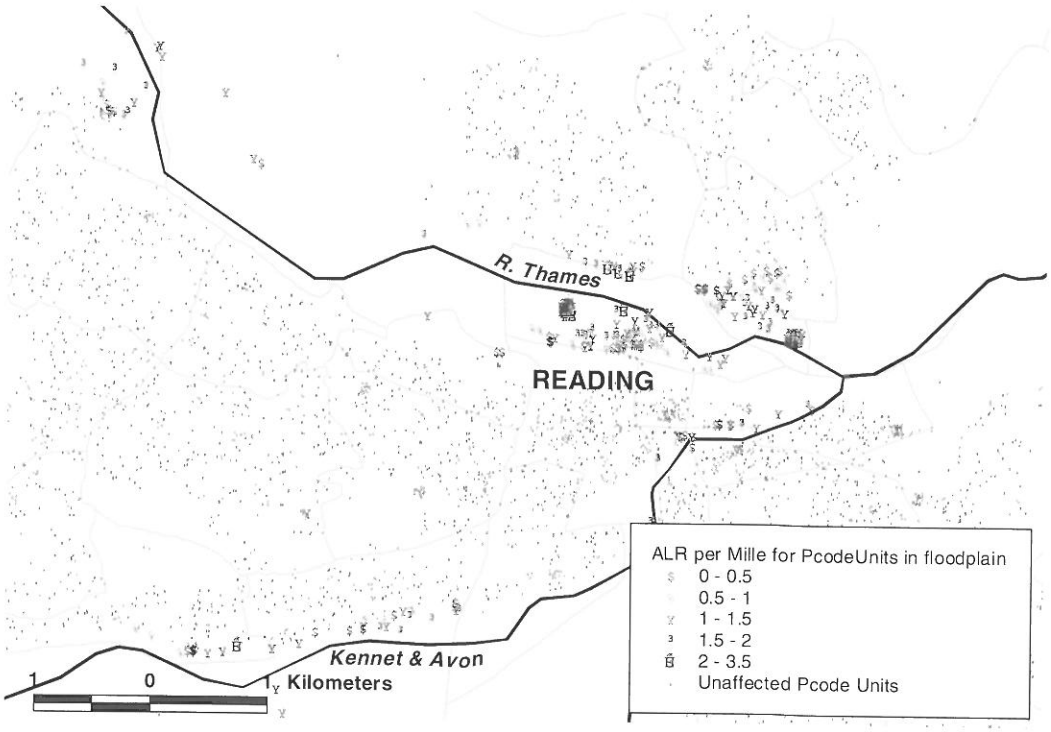

Figure 3-2: Flood risk is quantified as the average annual insured flood loss relative to the insured value at risk (per £1000) for 7-figure postcode units as illustrated for the town of Reading. The boundaries of 5-figure postcode sectors are shown in the background.

4 CONCLUSIONS

The different modelling and mapping approaches that have been implemented in the UK to assess flood risk cover a range of study scales to meet the requirements of different users. The demand for detailed reach-specific modelling undertaken under Section 105 mapping is likely to increase following a recent Government planning document (Department of Transport, Local Government and the Regions, 2001) which requires a flood risk assessment for any planning application located within a flood plain as indicated by the IFPM. Similarly, with total insured UK flood losses exceeding £1billion since 1998, insurers and re-insurers require appropriately scaled models to quantify their exposure to flood risk.

ACKNOWLEDGEMENTS

The authors would like to acknowledge the Environment Agency for initiating and funding the Section 105 Mapping programme, as described in this paper. The team that developed the RMS UK River Flood model includes Michael Drayton, Paul Burgess, Edida Rajesh, Ramesh Karunakaran, Vineet Jain and Elizabeth Couchman. Harvey Rodda worked on the RMS UK River Flood model whilst employed by Risk Management Solutions.

REFERENCES

Department of Transport, Local Government and the Regions (2001): Planning Policy Guidance Note 25 development and Flood Risk. The Stationary Office. Norwich, UK.

Institute of Hydrology (2000): Flood Estimation Handbook. Wallingford, UK.

Morris, D. G., Flavin, R. W. (1995): Flood Risk Map for England and Wales. Institute of Hydrology Report No. 30. Wallingford, UK.

HR Wallingford (1994): RIBAMAN Use Manual Version 1.22A. HR Wallingford Ltd. Wallingford, UK.

Webster, P., Ashfaq, A. (2002): Comparison of UK Flood Event Characteristics With Design Guidelines. Institute of Civil Engineers Water and Maritime Engineering Journal, accepted for publication.

NERC (1975): The Flood Studies Report. Wallingford, UK.

Verdin, K. L. (1997): A System for Topologically Coding Global Drainage Basins and Stream Network. USGS EROS Data Centre Distributed Archive Center
(URL: http://edcdaac.usgs.gov/gtopo30/hydro/P311.html- Accessed July 2000)

CORRELATION BETWEEN BASIN CHARACTERISTICS AND EXTREME FLOOD VALUES

Robert Schatzl

Amt der Steiermärkischen Landesregierung, Fachabteilung 3a - Referat 1 Hydrographie, Stempfergasse 7, A-8010 Graz, robert.schatzl@stmk.gv.at

SUMMARY

In this paper an analysis of the correlations between general basin characteristics and extreme flood values is made. For this purpose, 153 gauges over the whole Styria were selected with recording periods greater than 5 years. The flood values with return periods of 1, 5, 10, 30, 50 and 100 years were calculated according to DVWK-Regel 101, whereas the basin characteristics were determined using a software based on ArcView GIS 3.2 and Spatial Analyst 1.1. The most important results and some aspects for further investigations are shown in this report.

Keywords: extreme flood values, catchment characteristics, correlations, ArcView GIS

1 INTRODUCTION

One of the most important tasks of the Hydrographical Service of the Styrian Government is to calculate extreme values of discharge in gauged and especially ungauged basins for planning purposes in and around the concerned river. Due to the fact that there are dependencies between some basin characteristics and the discharge as it is shown in many works (i.e. Uhlenbrook et al., 2000), this investigation is made to find correlations between extreme values recorded at gauges and general characteristics in the concerned basins such as land use, precipitation amount, height of the terrain and others. The analysis is made for gauges with recording periods greater than 5 years, whereas for the correlations with extreme flood values (return period 30, 50 and 100 years) only gauges with recording periods greater 10, 16 and 33 years were used according to the guidelines of DVWK-Regel 101 (1997).

2 DATA BASIS

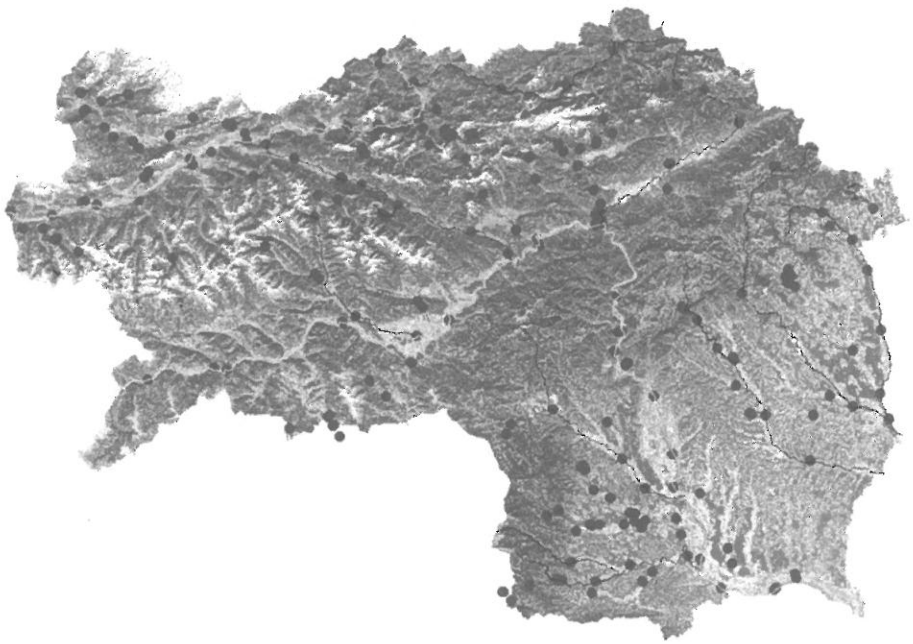

Figure 2-1: Map of Styria with the location of the gauges and the greater rivers.

153 gauges over the whole Styria were used for the analysis. A map with the location of these gauges is shown in Figure 2-1. It must be mentioned that only 96 of these 153 gauges are still in operation. In Figure 2-2 an overview is given about the recording periods of all the gauges.

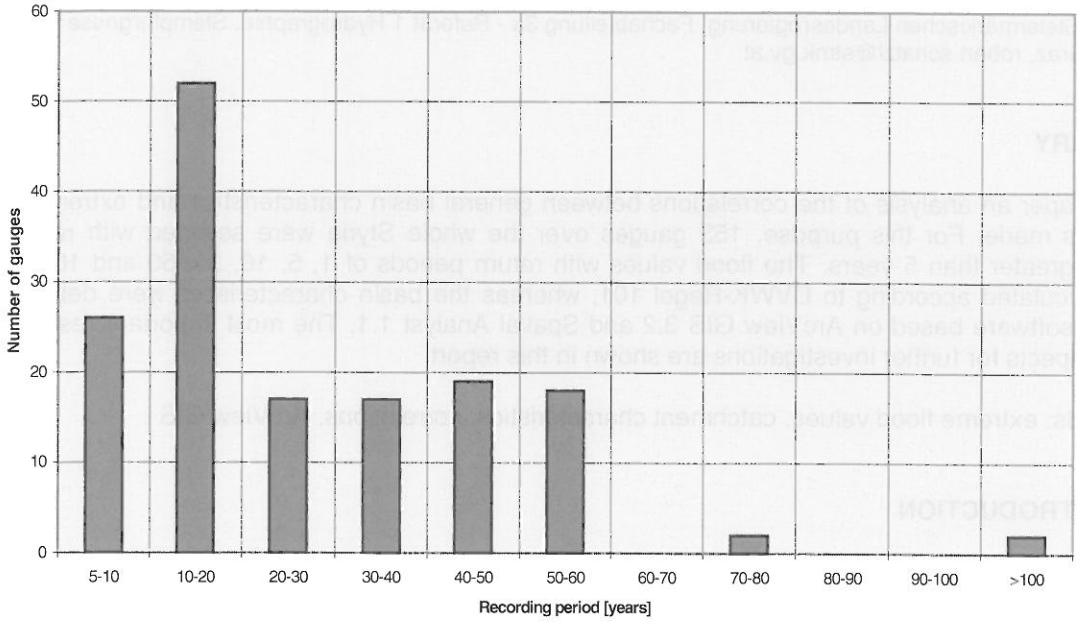

Figure 2-2: Number of gauges dependent on the recording period.

In Figure 2-2 it can be seen that the greater part of the gauges has recording periods < 20 years. But there is also a significant number of gauges with recording periods between 20 and 60 years, which can be used for the calculation of flood values with return periods > 50 years. In Figure 2-3 the distribution of the catchment areas of the 153 gauges is shown.

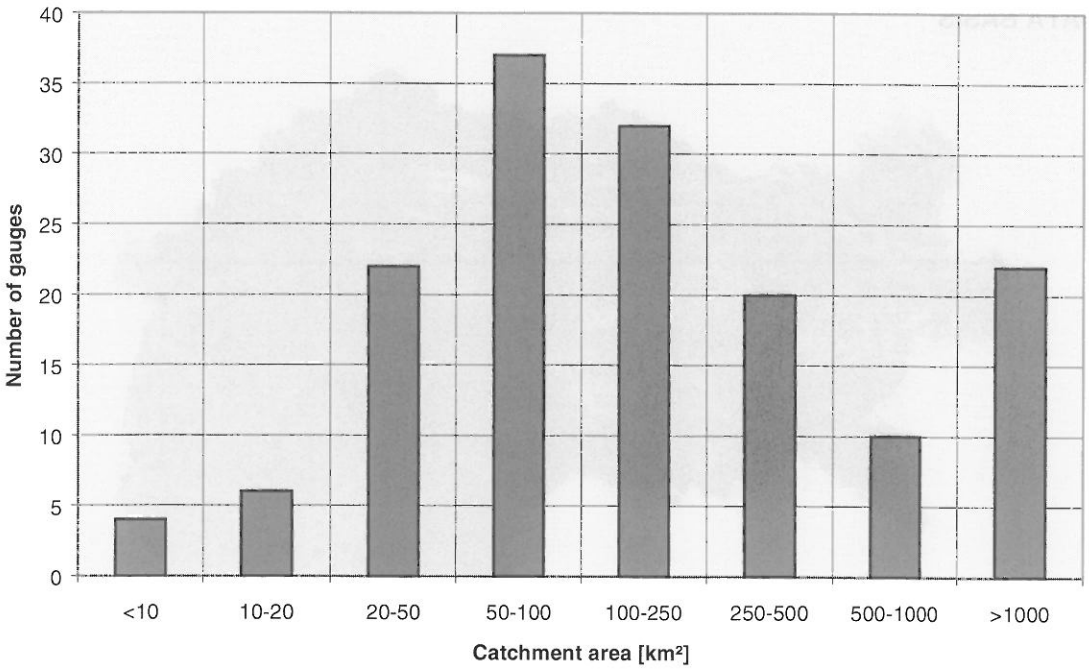

Figure 2-3: Distribution of the catchment areas of the gauges.

Therefore, the greater part of the gauges has catchment areas between 50 and 250 km², but there are also about 20 gauges with catchment areas > 1000 km² especially at the rivers Enns and Mur (Figure 2-1), which are the two main rivers of Styria.

3 CALCULATION OF FLOOD VALUES

The calculation of flood values at the selected gauges was made as mentioned above according to DVWK-Regel 101 (1997) with use of a software package named HQ-EX 2.0 (WASY, 1997). In figure 3-1 an example of such a calculation is shown by means of the gauge Sagbauer/Gradenbach.

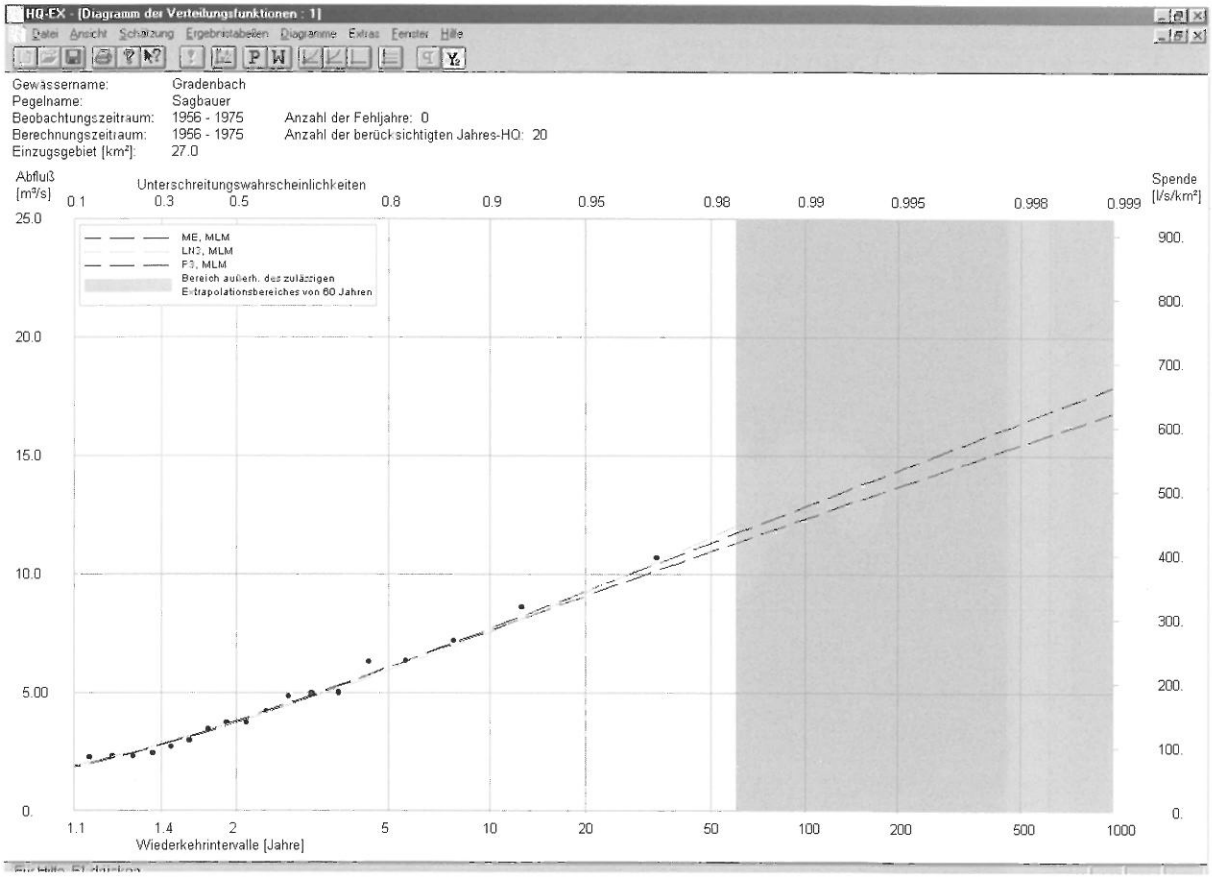

Figure 3-1: Calculation of flood values with HQ-EX 2.0.

In Figure 3-1 the results of the calculation of the flood values for the gauge Sagbauer/Gradenbach can be seen with a recording period of 20 years. According to DVWK-Regel 101 the annual series is used, whereas the inadmissible extrapolation area is marked in grey due to the rule that an extrapolation is only useful within a period of 3*n years with n equals the number of the recording years. Therefore the flood values of all 153 gauges were calculated with this software and stored in an excel-sheet.

4 CALCULATION OF BASIN CHARACTERISTICS

The calculation of the basin characteristics was made with the use of a software tool based on ArcView GIS 3.2 and Spatial Analyst 1.1 (Volk, 2000; Volk & Schatzl, 2001). Based on the Digital Elevation Model (DEM) of Styria with a resolution of 25 x 25 m it is possible to determine the following basin characteristics for any point in a catchment:

- Catchment area
- Mean, maximum and minimum value and distribution of
  - height
  - slope
  - exposition

- Mean, maximum and minimum value of
  - annual precipitation
- Total length of the river network
- Density of the river network
- Land use

In Figure 4-1 a calculation of basin characteristics with this software tool is shown by means of the gauge Sagbauer/Gradenbach. The calculated catchment area can be seen in an ArcView GIS 3.2 view, the values of the basin characteristics are stored as ASCII-file automatically by the software and then transformed into the Excel-sheet mentioned above.

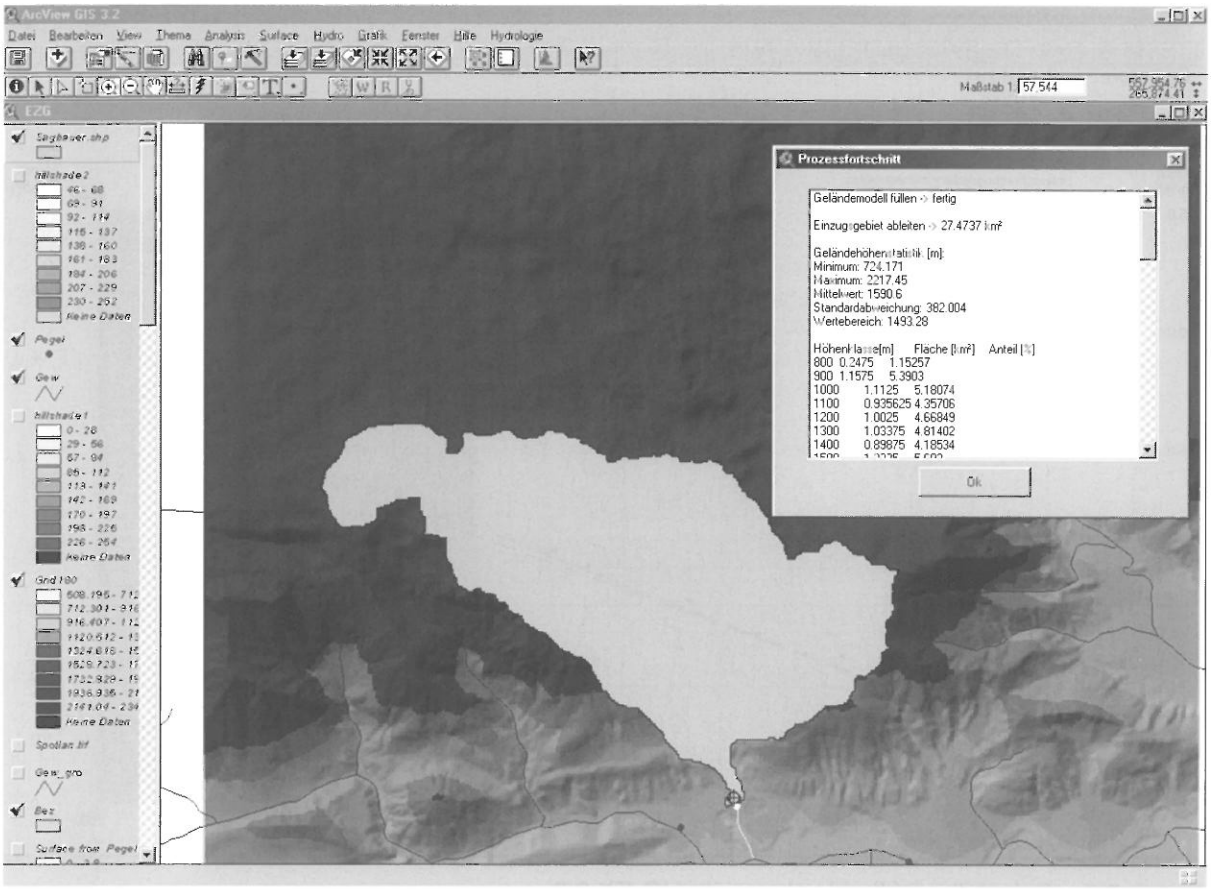

Figure 4-1: Calculation of a catchment (Sagbauer/Gradenbach) with the software tool and basin characteristics as ASCII-file.

5 CORRELATIONS BETWEEN BASIN CHARACTERISTICS AND DISCHARGE VALUES

In the last years many investigations have been made to find correlations between discharge values and special basin characteristics. The aim of many of this studies was to analyse the processes of runoff generation and runoff concentration (Uhlenbrook & Leibundgut, 1997; Naef et. Al, 1998, Peschke et al., 1998). There are also many investigations where the importance of the saisonality of floods is addressed (Black & Werritty, 1997; Burn, 1997; Magilligan & Graber, 1996; Merz et al., 1999; Piock-Ellena et al., 2000). A good summary of studies in this direction gives Uhlenbrook et al. (2000). Therefore this study can be seen as validation of former results with the aim to create a basis for a software tool, where flood values can be estimated based on selected basin characteristics. In the following, the correlations between basin characteristics and the calculated discharge, especially flood values were analysed and the most important results are shown. A summary of the results is shown in Table 5-1.

5.1 Catchment area

First, the correlations between flood values and the catchment area are handled. It can be recognised that there is a strong correlation between the mean annual discharge (MQ) and the catchment area (r^2 ~ 0.93). The same is valid for the HQ_1 value (flood value with return period of 1 year). This correlation decreases when HQ_{30} or HQ_{100} are considered but the correlation coefficient r^2 is still about 0.66.

5.2 Elevation

There is a relatively poor correlation (r^2 = 0.32) between the mean annual specific discharge [l/sha] and the mean value of the elevation of each catchment, but when Hq_1, Hq_{30} and Hq_{100} [all in l/sha] are considered, it can be recognised that there is almost no correlation between these values and the elevation (r~0).

5.3 Slope

Almost the same as for the height can be seen if the mean value of the slope of the catchment is correlated with the specific discharge values. The correlation coefficient for the mean annual specific discharge is about r^2 ~ 0.3, but there is also almost no correlation between Hq_1, Hq_{30} and Hq_{100} and the slope.

5.4 Exposition

There is no correlation between the specific discharge values and the exposition. Even the mean annual specific discharge shows no dependency.

5.5 Mean annual precipitation

There are relatively strong correlations between the mean annual specific discharge and the mean annual precipitation (r^2 = 0.51), there are also even if poor correlations (r^2 = 0.18) between Hq_1 and the mean annual precipitation, no correlations show Hq_{30} and Hq_{100}. These results are corresponding to studies of Blöschl (1999) and Uhlenbrook (2000).

5.6 Length of river network

A strong dependency between the discharge values (MQ, HQ_1, HQ_{30} and HQ_{100}) and the total length of the river network in the catchment can be seen. The correlation coefficient r^2 lies between 0.6 and 0.7.

5.7 Density of river network

A poor correlation between the mean annual specific discharge and the density of the river network in the catchments can be recognised, no correlations can be seen for Hq_1, Hq_{30} and Hq_{100}.

5.8 Land use

As the analysis has shown, there are no correlations between land use and the discharge values in the considered catchments. As example, Table 5-1 shows the correlations by means of the proportion of wooded areas on the whole area in %.

5.9 Correlation between mean annual discharge and flood values

It have shown that there are strong correlations between the flood values and the mean annual discharge especially for HQ_1 and HQ_{10} (r^2 ~ 0.95), but also for HQ_{30} and HQ_{100}, the correlation coefficient r^2 is about 0.57. That means if the mean annual discharge can be determined with a certain accuracy from the basin characteristics, it would be possible to estimate at least HQ_1 and HQ_{10} relative exactly. For HQ_{30} and HQ_{100}, the accuracy of the estimation gets lower, but it is still possible to define a certain range for these values.

Table 5-1: Correlations (R^2) between selected basin characteristics and flood values.

Flood value / Basin Characteristic	MQ [m³/s] or *Mq [m³/skm²]*	HQ1 [m³/s] or *Hq1 [m³/skm²]*	HQ30 [m³/s] or *Hq30 [m³/skm²]*	HQ1000 [m³/s] or *Hq100 [m³/skm²]*
Catchment area	0.94	0.94	0.67	0.67
Elevation	*0.32*	*0.01*	*0*	*0*
Slope	*0.35*	*0*	*0*	*0*
Exposition	*0.02*	*0.03*	*0.03*	*0.02*
Mean annual precipitation	*0.51*	*0.19*	*0.09*	*0.05*
Length of river network	0.63	0.67	0.69	0.68
Density of river network	*0.23*	*0*	*0*	*0*
Land use	*0*	*0*	*0*	*0*

6 CONCLUSIONS

The analysis of correlations between discharge values (mean annual discharge and flood values) and general basin characteristics at 153 gauges over the whole Styria has shown the following results: there are strong correlations between flood values and the catchment areas (r^2 ~ 0.7), also between the flood values and the length of the river network in the considered catchments (r^2 ~ 0.7). Poor or no dependencies can be seen between the flood values and the mean value of the height of the catchments, slope, exposition, mean annual precipitation, density of river network and the land use, although it must be stated that the correlation between these characteristics and the mean annual discharge is stronger to a certain degree, especially concerning the mean annual precipitation [r^2 ~ 0.5). Very strong correlations can be seen between the mean annual discharge and the flood values of the lower return periods (HQ_1 and HQ_{10}), but also for the extreme flood values HQ_{30} and HQ_{100}, the correlations are still high (r^2 ~ 0.57). Based on these results, the development of a regression model based on ArcView GIS for the estimation of the mean annual discharge and further for the extreme flood values in ungauged catchments based on selected basin characteristics will be the next step.

REFERENCES

Black, A.R., Werritty, A. (1997): Seasonality of flooding: a case study of North Britain. In: Journal of Hydrology 195, 1-25.

Blöschl, G., Piock-Ellena, U., Merz, R., Gutknecht, D. (1999): Prozessorientierte Regionalisierung von Hochwässern. In: Schriftenreihe des Fachgebietes Wasserbau und Wasserwirtschaft der Universität Kaiserslautern.

Burn, D.H. (1997): Catchment similarity for regional flood frequency analysis using seasonality measures. Journal of Hydrology 202, 212-230.

DVWK-Regel 101 (1997): Statistische Analyse von Hochwasserabflüssen. Unveröffentlichter Entwurf. DVWK-Geschäftsstelle, Gluckstrasse 2, 53115 Bonn

Magilligan, F.J., Graber, B.E. (1996): Hydroclimatological and geomorphic controls on the timing and spatial variability of floods in New England, USA. In Journal of Hydrology 178, 159-180.

Merz, R., Piock-Ellena, U., Blöschl, G., Gutknecht, D. (1999): Seasonality of flood processes in Austria. In: IAHS Publ. No. 255, 273-278.

Naef, F., Scherrer, S., Faeh, A. (1998): Die Auswirkung des Rückhaltevermögens natürlicher Einzugsgebiete bei extremen Niederschlagsereignissen auf die Größe extremer Hochwässer. vdf, Hochschulverlag an der ETH Zürich.

Peschke, G., Etzenberg, C., Müller, G. (1998): Experimental analysis of different runoff generation mechanisms. In: Bueck, J. et. Al. (1998): Proceedings of the ERB - Conference on Catchment Hydrology and Biochemical Processes in Changing Environment, Liblice.

Piock-Ellena, U., Pfaundler, M., Blöschl, G., Burlando, P., Merz, R. (2000): Saisonalitätsanalyse als Basis für die Regionalisiserung von Hochwässern. In: Wasser, Energie, Luft. 92. Jahrgang, 2000, Heft ½, 13-21, Baden, Schweiz.

Schatzl, R., Volk, G. (2000): Automatisierte Einzugsgebietsausweisung auf der Basis ArcView GIS 3.2 und Spatial Analyst 1.1. Unveröffentlichter Bericht, Hydrographischer Dienst Steiermark. Graz.

Uhlenbrook, S., Leibundgut, Ch. (1997): Abflussbildung bei Hochwasser. Wasser und Boden, 9, 13-22.

Uhlenbrook, S., Steinbrich, A., Tetzlaff, D., Leibundgut, C. (2000): Zusammenhang zwischen extremen Hochwassern und ihren Einflussgrößen. Klimaveränderung und Konsequenzen für die Wasserwirtschaft – Fachvorträge beim KLIWA-Symposium, 29.-30. November 2000. Karlsruhe.

Volk, G. (2000): Application of Spatially Distributed Hydrological Models for Risk Assessment in Headwater Regions. In Haigh, M. and Krecek, J. (eds.): Environmental Reconstruction in Headwater Areas, NATO Sciences Series 2. Environmental Security – Vol. 68, Kluwer Academic Publishers. Dordrecht.

WASY (1997): HQ-EX, Version 2.0, Benutzerhandbuch. Gesellschaft für wasserwirtschaftliche Planung und Systemforschung mbH. Berlin.

INFERNO – INTEGRATION OF REMOTE SENSING DATA IN OPERATIONAL WATER BALANCE AND FLOOD PREDICTION MODELLING

Werner Schulz[1], Ute Merkel[1], Heike Bach[2], Florian Appel[2], Ralf Ludwig[3], Alexander Löw[3], Wolfram Mauser[3]

[1] Landesanstalt für Umweltschutz Baden-Württemberg, Hochwasser-Vorhersage-Zentrale, Benzstrasse 5, D-76185 Karlsruhe, Germany, werner.schulz@lfuka.lfu.bwl.de

[2] VISTA Geowissenschaftliche Fernerkundung GmbH, Luisenstr. 45, D-80333 München, Germany, bach@vista-geo.de

[3] Institute of Geography, Chair of Geographical Remote Sensing, University of Munich, Luisenstr. 37, D-80333 München, Germany, a.loew@iggf.geo.uni-munechen.de

SUMMARY

Methods to accurately assess and forecast flood discharge are a fundamental requirement in practical hydrology. However, existing rainfall-runoff models, seldom consider the spatial characterisation of the land surface, which is essential for an accurate description of processes relevant for runoff formation. Stable information or information with low temporal frequency can be gathered by mapping or using remote sensing data. However, land surface parameters of high temporal variability, like snow properties and soil moisture, can as yet not be spatially measured with the temporal frequency required.
The improvement of operational flood forecast systems requires the improvement of spatial input parameters. Remote sensing methods have a high potential to achieve this goal and to make model parameterisation regionally transferable. To prove and demonstrate this, the INFERNO (Integration of remote sensing data in operational water balance and flood prediction modelling) project has been set up, funded by the German Aerospace Center DLR (Kz: 50EE0053).
The potential of using multisensoral ENVISAT data for operational flood forecast will be analysed using test cases and demonstration runs in the operational flood forecast centre of Baden-Württemberg (HVZ) in Karlsruhe (Southwest Germany). ENVISAT will be put in orbit in January 2002 and will provide a valuable set of applicative, optical and microwave remote sensing observations. Methodologies are under development to synergistically use different ENVISAT-sensors (microwave and optical) for a better spatial mapping and quantitative determination of soil moisture and snow properties with a sufficient temporal frequency for runoff modelling. In the HVZ these new data sources and respective model components of snow and soil water dynamics will be integrated in the continuously operated water balance model LARSIM (Large Area Runoff Simulation Model).
Until ENVISAT data are available, software tools are developed and products are generated using existing sensors with similar specifications. First results of the concept realisation are demonstrated for the 1998/99 winter season in the mesoscale catchment of the Neckar river in Baden-Wuerttemberg.

Keywords: Operational Flood Forecasting, Modeling, HVZ, LARSIM, Remote Sensing, ENVISAT

1 INFERNO - PROJECT CONCEPT AND BACKGROUND

In 1991, the German federal state of Baden-Württemberg founded the Flood Forecasting Centre (HVZ), as part of its Environmental Protection Agency (Landesanstalt für Umweltschutz Baden-Württemberg LfU). Ever since, the HVZ is responsible for flood monitoring along most rivers in Baden-Württemberg, among them its largest Upper Rhine and Neckar. In the case of flood, forecasts are calculated and provided hourly. The results are presented to the public via different media like phone, fax, internet etc. (Schulz, 2000; Homagk, 1998). The HVZ aims to publish data about ongoing and upcoming floods rapidly and reliable. These data include recorded water levels of about 140 gauges, precipitation measurements of about 170 stations, precipitation forecasts (calculated and provided by the German Weather Service (DWD)) and the calculated water level forecasts for 35 gauges in Baden-Württemberg. Forecast times range from 8 to 48 hours (Homagk, 1998).
At the end of the year 2000, the HVZ started the project InFerno. It has been established to test the potential and applicability of remote sensing data for improving operational flood forecasting and water balance modelling by retrieving information for model parameterization and data assimilation. The focus has been given to the quantitative retrieval of soil moisture, spatial snow distribution and snow properties to improve the simulation of the snowcover and snowmelt (step 1) and the discharge forecast by using

soil moisture data (step 2). The project consortio consists of three partners. The flood forecasting centre HVZ will define the required remote sensing products from an operational hydrologist perspective. The scientific research, which is needed to develop algorithms to generate these products, is conducted by the Institute for Geography of the University of Munich. The value adding company VISTA serves as the integrating link between research and hydrologists through the transcription and extension of the research results into operational processes and tools. It will be a common issue to understand, how these products can be assimilated in the available hydrological models and what model modifications have to be performed to suitably consider this new spatial information source.

2 THE LARGE AREA RUNOFF SIMULATION MODEL LARSIM

Among other models, the HVZ applies the water balance model LARSIM (**L**arge **A**rea **R**unoff **Si**mulation **M**odel) to calculate flood forecastings for several gauges in Baden-Württemberg. LARSIM enables continuous spatially distributed process simulations of the water balance terms for mesoscale catchments (Bremicker, 2000). Based on the river basin model FGMOD (Ludwig, 1982), LARSIM requires detailed spatial information about the simulated catchment area like land use (classified from satellite imagery), topography (DEM), vectorized river network and field capacities of soils. The water balance model incorporates not only the runoff generation in the area and the translation and Retention in river channels, but also the processes of interception, evapotranspiration, water storage in soils and aquifers, snow accumulation and snowmelt (Bremicker and Gerlinger, 2001). Required dynamic input data for LARSIM are time series of precipitation, wind velocity, air temperature, air pressure, air humidity and global radiation. The operational working model uses one-hour values, collected daily or, while a storm event, hourly.
Snowmelt can significantly contribute to river floods. Many severe flood events in Baden-Württemberg comprise snowmelt and heavy rain. An example for the difficult operational work in this case is the flood of February 1999. Due to a snowmelt forecast of insufficient quality from February 19th, the HVZ published overestimated waterlevel-forecasts for the river Neckar during the starting hours of the flood event. Only with a revised snowmelt forecast, received at 10 a.m. on February 20th, the newly calculated water level forecast showed satisfying quality. InFerno intends to provide methods to prolong the time period of reliable forecasts.

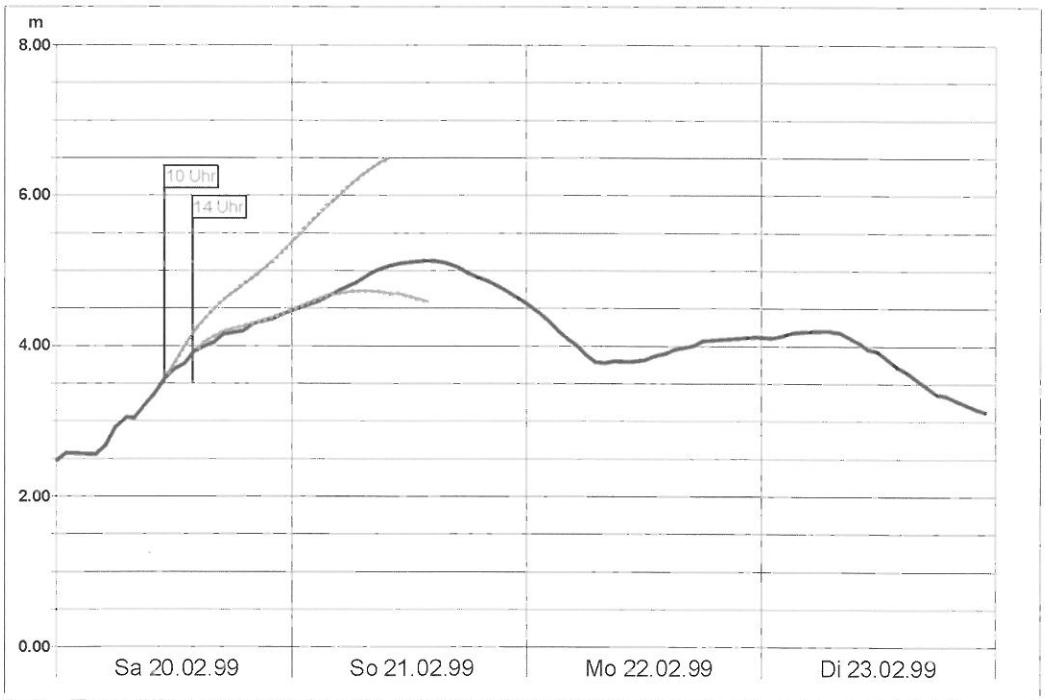

Figure 2-1: Two different operationally calculated water level forecasts at gauge Heidelberg along the river Neckar. Differences depend on the quality of the snowmelt forecast.

2.1 The LARSIM Snow Module

In its process description, LARSIM considers both the accumulation and melting of a snowpack. Snow accumulation is determined by precipitation and a critical temperature T_{crit} of the near surface air temperature. Actual air temperature is spatially interpolated from on line collected point measurements. For $T_{actual} < T_{crit}$ precipitation is modelled as snowfall. T_{crit} can be individually alleged for each raster cell.
The computation of the potential snowmelt rate is based on an energy balance approach and is performed by an extended version of the Knauf method (Knauf, 1980). Potential snowmelt is hereby considered a function of wind velocity, air temperature, intensity of precipitation and global radiation.
An increase of snowmelt does not necessarily lead to immediate runoff. Several stages of snow metamorphosis are possible, in which liquid water can be stored in the snowpack. The retention of liquid water in the snowlayer will consequently lead to a structural change and hence a compaction of the snowlayer. In LARSIM, this process is represented by the snow density, which rises with increasing snow compaction. Once a critical snow density is reached, further energy input will initialise the actual melting process and runoff will occur. Snow compaction and actual snowmelt are calculated using the approach of Bertle (1966).

2.2 Application in the Neckar Watershed and Model Performance

LARSIM has been applied to the Neckar basin (catchment area approx. 14 000 km²). Figure 2-2 shows results of the LARSIM modelled snow depth (left) and snow water equivalent (right) for February 18th 1999.

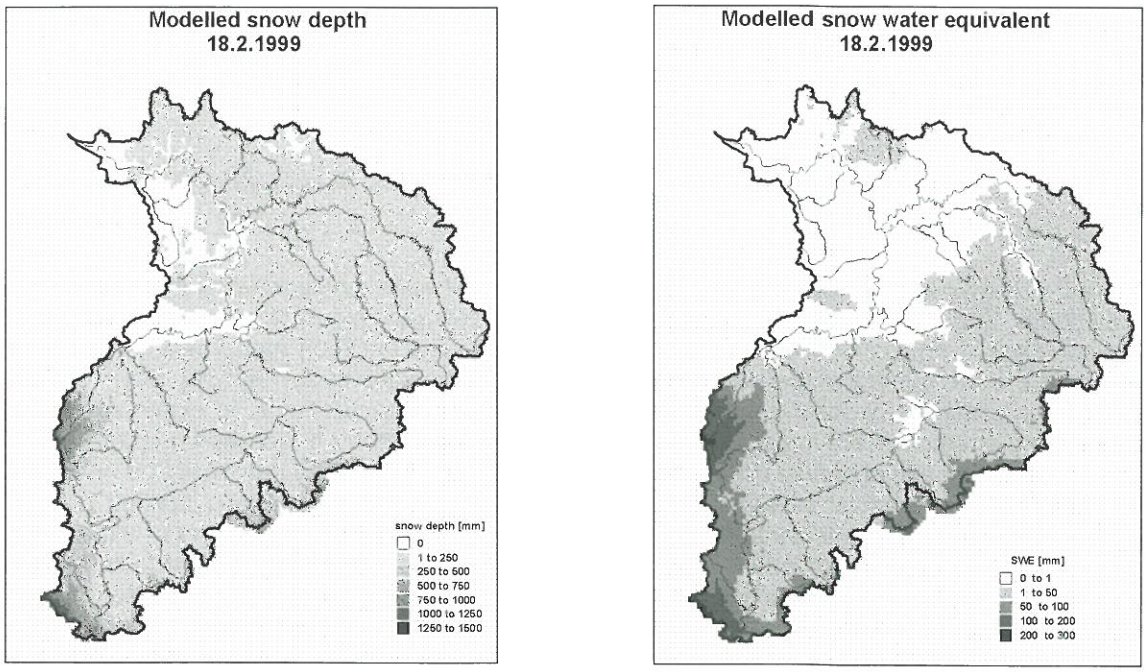

Figure 2-2: Modelled snow depth (left) and snow water equivalent SWE (right) of the Neckar basin on February 18th, 1999.

While nearly the whole catchment is snow covered on Feb. 18th, distinct maxima of snow water equivalent can be located in the mountainous areas of the "Schwarzwald" and the "Schwäbische Alb".
The LARSIM model results are evaluated with measurements of snow depth and SWE, performed by the German Weather Service (DWD). The DWD operates 50 snow gauges in the Neckar catchment, where snow depth and SWE were taken three times a week. This data is immediately transmitted and can hence be used for operational modelling. Additional, the DWD maintains another 120 stations in the Neckar basin. Their measurements are available at an offline level and are therefore only applicable for the modelling of historic events. Figure 2-3 outlines a comparison of measured DWD data with the results of the LARSIM model for the winter season of 1998/99 at two locations in the watershed (Freudenstadt and Schwäbisch Hall/Teuresdorf).

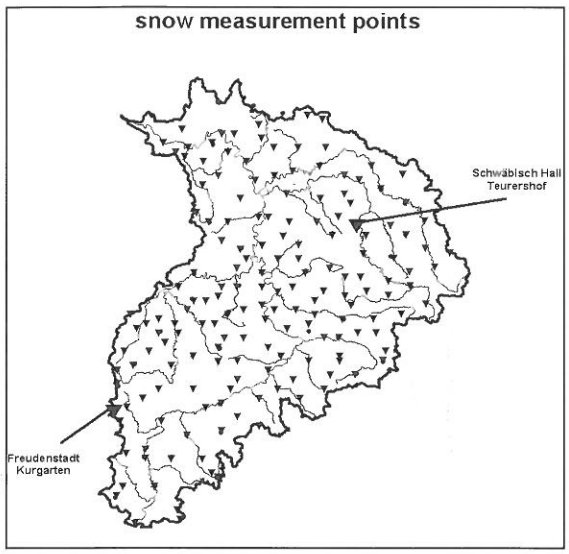

Figure 2-3: Location of DWD snow gauges (left); comparison of modelled and calculated snow depth in 'Freudenstadt-Kurgarten' 800m +NN (below left) and 'Schwäbisch Hall-Teurershof' 365m+NN (below right), winter season 1998/99.

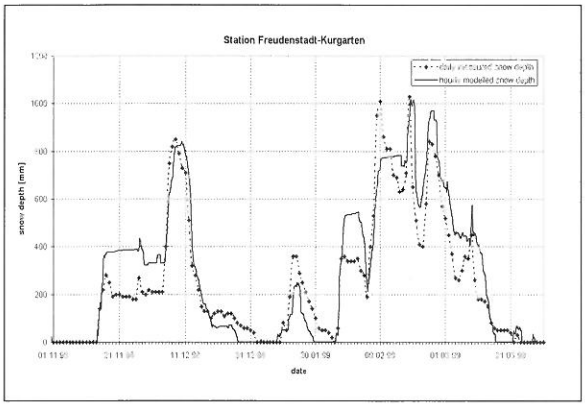

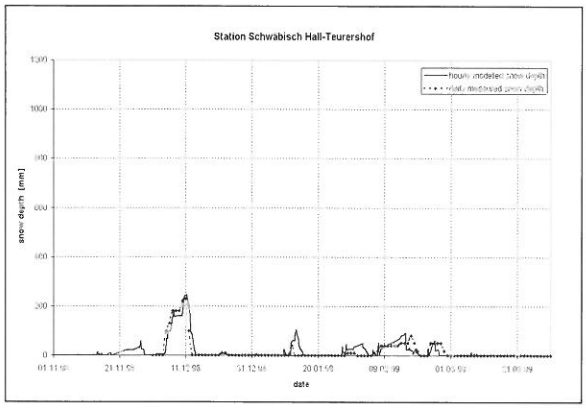

Figure 2-3 shows only partly satisfying correspondence between measured and calculated values of snow depth. The viewgraphs not only illustrate considerable deviations in snow depth but also highlight conditions of major concern due to opposing devolutions between model results and measurements, where the current model assumptions and parameterisations do not hold. On this basis, the spatial representation of snow cover interpolated from point measurements is extremely critical and requires improvement. This major drawback can be counteracted by a focussed utilisation of remote sensing data. The actual spatial distribution of snowcover in a watershed can easily be determined by the interpretation of optical satellite imagery (Figure 2-4 and 2-5; the method applied is described below in chapter 3). While this information can be used to highlight obvious errors in the snow model performance, it is a central research issue to determine the responsible factors for actual deviations of modelled and measured snow properties in time and in space and to guide the way to an optimized parameterisation of the applied snow model. In this respect it is necessary to combine satellite imagery with actual point measurements to identify current obstacles in model parameterization and to provide robust algorithms for an operational real-time tracking of model parameters in case of contradiction. While Figure 2-4 shows an example of reasonable agreement between classified snowcover from satellite imagery (left), LARSIM modelled snow depth (center) and DWD point measurements (right; black stars indicating measured snow) for February 26th 1999, Figure 2-5 points out recognisable differences in snow cover between satellite imagery and LARSIM results. LARSIM considerably overrates snowmelt for February 26th to 27th 1999. However, it also becomes obvious that the weather-dependancy of optical satellite imagery (partial obstruction of sight due to cloud cover in the south-east of the watershed) requires additional information sources that can furthermore provide information about the energetic stage of the snowpack, which can be allusively derived from the determination of the snowpacks liquid water content by means of microwave imagery. The respective procedure is described in chapter 3.2.1.

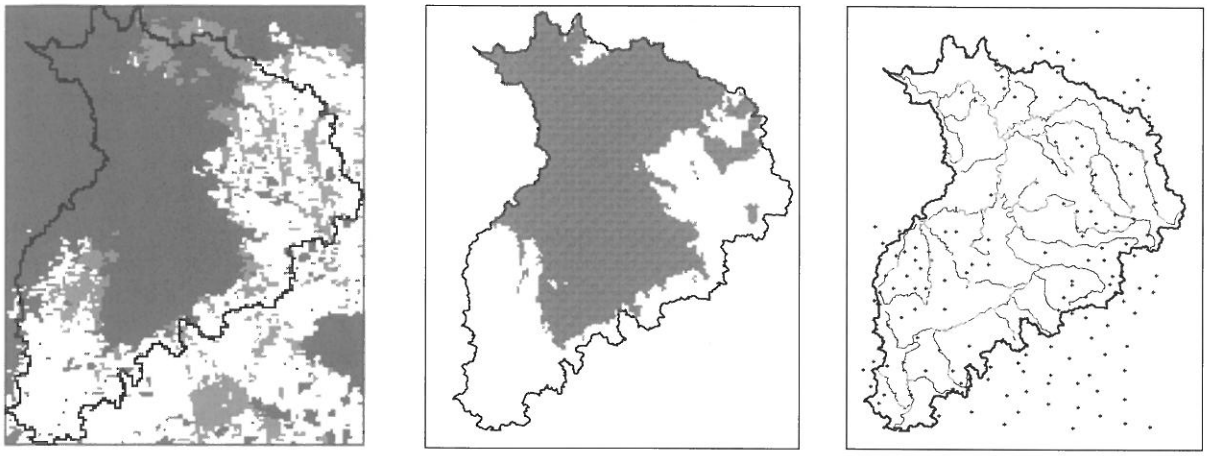

Figure 2-4: Comparison of snow covered area detected by optical sensor (left), snow cover modelled by LARSIM (middle) and DWD point measurements (right) of the Neckar basin on February 26th, 1999.

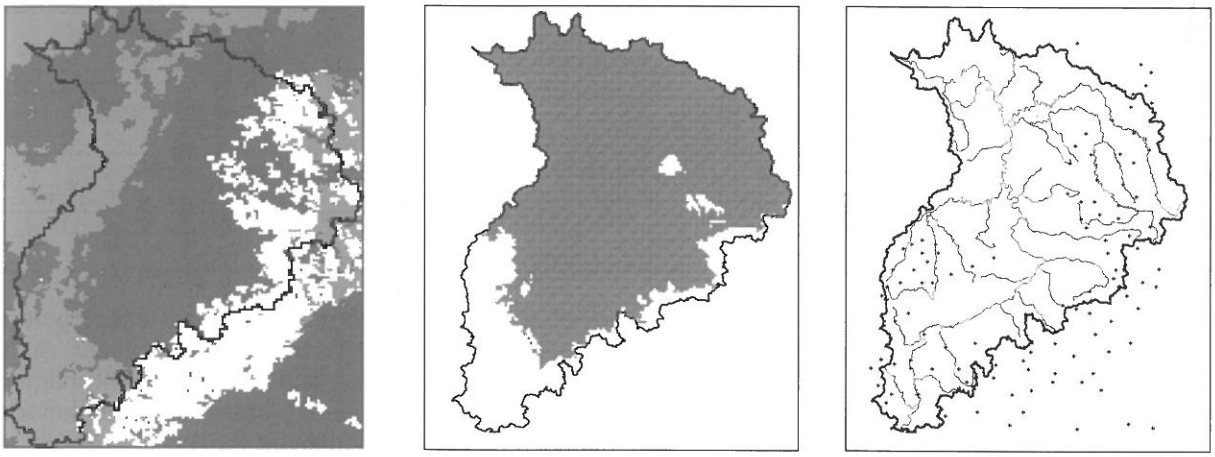

Figure 2-5: Comparison of snow covered area detected by optical sensor (left), snow cover modelled by LARSIM (middle) and DWD point measurements (right) of the Neckar basin on February 27th, 1999.

3 THE ROLE OF REMOTE SENSING IN FLOOD FORECASTING

The potential of remote sensing data has gained increasing consideration in numerous hydrological applications. The possibility to image spatial characteristics and to retrieve manifold quantitative information over large areas has been recognized as a useful tool in complex water-related issues, such as water balance modeling or yield estimation. However, due to the coarse temporal resolution of available imagery, the utilization of remote sensing is yet uncommon in the field of flood forecasting and flood management, where information on soil moisture and snow properties, as fundamentally steering parameters for floods, needs to be provided at a high temporal frequency. Nevertheless, an accurate description of the land surface is essential to model the processes involved in runoff formation. In this respect, remote sensing facilitates an improvement of spatial input parameters and accounts for regional transferability of the models in use. Sensors of the new generation will be able to provide the required information at sufficient temporal intervals and will hence counteract current limitations of applying remote sensing for the objectives of flood research in general and operational flood forecasting systems in particular.

The project InFerno has been originated to evaluate the capabilities of remote sensing with respect to operational flood forecasting and management. Based on existing and on-going research initiatives for the derivation of soil moisture and snow properties, new methodologies are being developed and are brought to an operational level, by means of algorithm retrieval and software development for automatically processing remote sensing data and to assimilate remote sensing information in the relevant hydrologic model. The synergetic use of different remote sensing sensors (microwave and optical) will be inevitable to obtain meaningful results in this respect. It will furthermore be of central importance to

solve the difficult scaling issue, i.e. transporting hydrological process description in terms of model parameterization across the various spatial and temporal scales at which these processes occur as against the availability of remote sensing data.

3.1 Sensors

In order to successfully apply remote sensing information in the field of flood forecasting, a sensor is needed which provides good spatial and spectral coverage in combination with a high temporal frequency. Significant and reliable products in the sense of InFerno will be made possible with the launch of ESA´s ENVISAT (scheduled for January 2002), which will provide a valuable set of applicative, optical and microwave earth observations. Methodologies are under development to synergetically use the different (microwave and optical) ENVISAT-sensors ASAR, MERIS and AATSR for a better spatial mapping and quantitative determination of soil moisture and snow properties, such as snow wetness and snow water equivalent.

Table 3-1: ENVISAT sensors used in the InFerno project.

Sensor	ASAR	MERIS	AATSR
Name	Advanced Synthetic Aperture Radar	Medium Resolution Imaging Spectrometer	Advanced Along-Track Scanning Radiometer
Spectral features	C-Band SAR System HH / VV Polarization available	Imaging Spectrometer 15 channels in the 390 ... 1040 nm range	High resolution radiometer 7 channels in VIS/NIR/TIR
Spatial features	Resolution: 100m Scene: 400 x 400 km	Resolution: 300m Scene: 575 x 575 km	Resolution: 500 Scene: 1150 x 1150 km
Principle Appliance	- Soil moisture - Wet Snow	- Land Use - Snow covered area	- Snow covered area

In a first project phase, i.e. until ENVISAT data is available, algorithm retrieval, software development and product generation is performed using existing sensors with ENVISAT-similar specifications, such as ERS, RADARSAT and NOAA-AVHRR. The developed methodologies and tools are then adapted to ENVISAT data in a second project phase, where ASAR data will be used to determine near surface soil moisture and wet snow cover, while MERIS and AATSR will be employed for the delineation of snow covered areas and the mapping of land use.

3.2 Remote Sensing Objectives in InFerno

Thoroughly processed remote sensing data is expected to serve as a valuable source of information to deliver spatially distributed parameters of snow properties and soil moisture. These highly dynamic land surface characteristics are crucial for the prediction and modeling of floods, since they largely determine the rapidly changing retention and runoff producing capacities of a watershed. It is therefore necesssary to provide reliable information of the spatially distributed energetic stage of a snowpack and/or the initial soil moisture condition prior to a possible flood event.

3.2.1 Remote Sensing of Snow Properties

Detecting Snow Covered Areas (SCA)
The spectral characteristics of snow can be used to derive snow cover maps from optical remote sensing data. Problems occur in the discrimination between snow and clouds. Derrien (1993) and Dozier (1989) have individually developed similar indices for the derivation of Snow Covered Area (SCA) from optical remote sensing data (in InFerno, the Derrien method is used for NOAA-9 to NOAA-14, the Dozier method for NOAA-16). These methods can be used to delineate snow cover from other surfaces and to distinguish snow from clouds by their respective spectral signatures. It is based on the fact that in contrast to clouds, snow covered surfaces show a low reflectivity in the shortwave-infrared section of the electromagnetic spectrum, while both surfaces have high reflectances in the visible. The assignment of each pixel is conducted by applying empirically determined thresholds to an index image, resulting in a classification distinguishing snow, clouds and areas free of snow.

In 2001, an operational processing chain has been developed and was implemented to automatically process snow cover maps from NOAA-AVHRR data for Southern Germany. It fully preprocesses the satellite imagery (e.g. calibration, navigation, geocoding) and performs the calculation of the Derrien or Dozier index. Figure 3-2 shows an example of a SCA map of the Neckar watershed using the Derrien index approach.

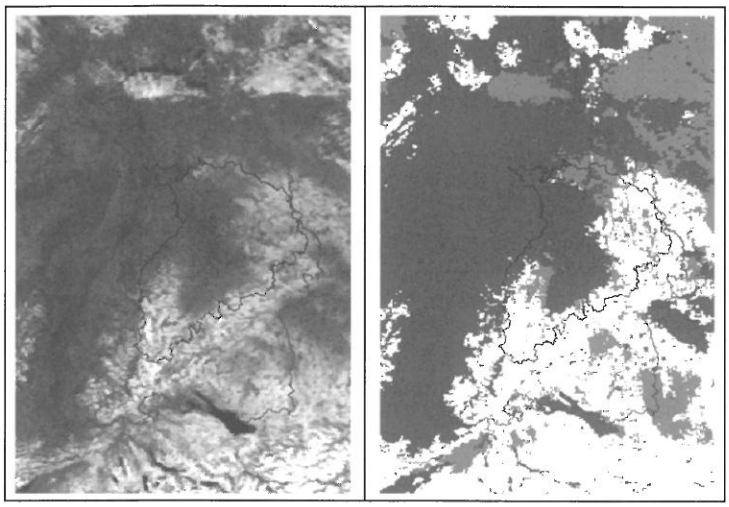

Figure 3-6: (left) NOAA-AVHRR image from February 26nd 1999 (*NOAA channels 1,2).*

Figure 3-7: (right) Snow Covered Area using the index method of Derrien.

Wet Snow Distribution

The use of optical remote sensing data is limited to cloud free areas, which restricts its usability in operational terms. To bridge this gap, InFerno follows a synergetic multisensoral approach, taking advantage of the fact that wet snow can be detected from weather-independent Synthetic Aperture Radar (SAR) data. The backscatter coefficient of a snow-covered area comprises information of the air/snow interface (1), the snow/ground interface (2), the ground (3) and volume scattering in the snowpack (4) (Fung, 1994). The latter can be determined when all other influences are individually eliminated.

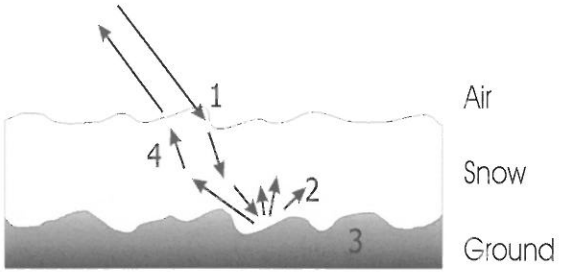

Figure 3-8: Backscattering terms of a snow-covered area in the microwave spectrum.

Dry snow is transparent for C-band SAR data (5.3 GHz, as used onboard ERS, RADARSAT and ASAR), with the backscattered signal being significantly dominated by the underlying soil properties. Mätzler (1987) showed that the liquid water content of the upper snow layer (0 – 5 cm) has an evident influence on the microwave penetration depth. While dry snow has a penetrability of about 60 m (!), a liquid water content of 3 Vol. % reduces the penetration depth to 0.3 m. The strong absorption of the signal in the upper layer obviates the signal from the underlying soil, with a signal reduction of 3-6 dB. Nagler and Rott (Nagler et al., 2000, Rott, 2000) have made use of this large backscatter deviation for a methodology to map areas with a wet snow cover and hence display regions of increased flood risk. The method has been successfully adapted to classify wet snow areas in the Neckar watershed by applying a threshold of 2-3 dB (Figure 3-4). It has shown validity for ERS imagery, which is characterized by a low incidence angle of 23°. Baghdadi et al. (2000) applied the algorithm to RADARSAT standard image data and determined that the higher incidence angle of about 47° lead to diminished differences of about 1 dB between reference and snow image. ENVISAT ASAR will provide images with high temporal frequency of about 3 days with different incidence angles and dual polarization and will therefore provide deeper insight to this important and yet unsolved issue.

While most studies on wet snow area estimation were conducted in alpine areas, the project area of InFerno lies in the low mountainous area of the Neckar watershed, where the small scale heterogeneity of land use shows explicit backscatter variability due to the respective differences in surface roughness. In order to quantitatively improve classification results, these differences are compensated applying land use dependent thresholds.

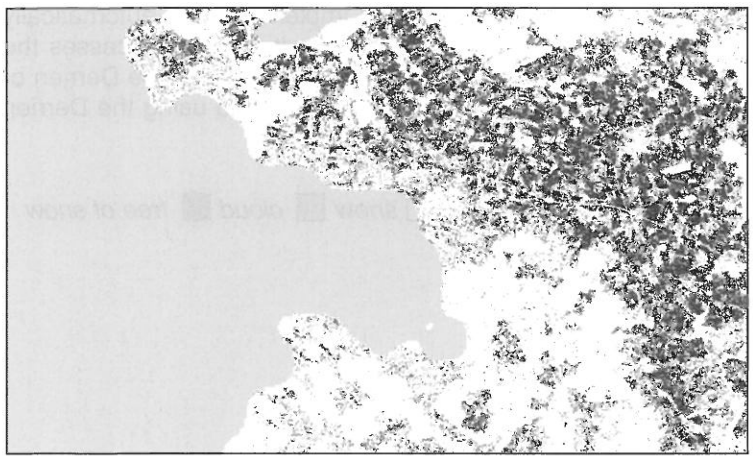

Figure 3-9: Wet Snow Mapping depending on snow cover map, landuse and SAR ratio.

3.2.2 Remote Sensing of Soil Moisture

It is a future task to improve forecasts especially for middle-sized and small catchment areas and to install an early flood-warning system for floods in smaller catchments (Homagk, 1998). Therefore, the soil moisture condition prior to heavy rainfall is one of the determining factors for flood generation. Information on soil moisture is most critical and hence needed in the starting phase of a flood, when conventional methods, that are based on the observation of water level rises, can not yet be applied. For the near surface soil layer, radar data (e.g. ERS SAR) can be used to extract soil moisture in a spatially distributed way. Thus, this information can be used to initialise the flood model according to the actual soil moisture conditions.

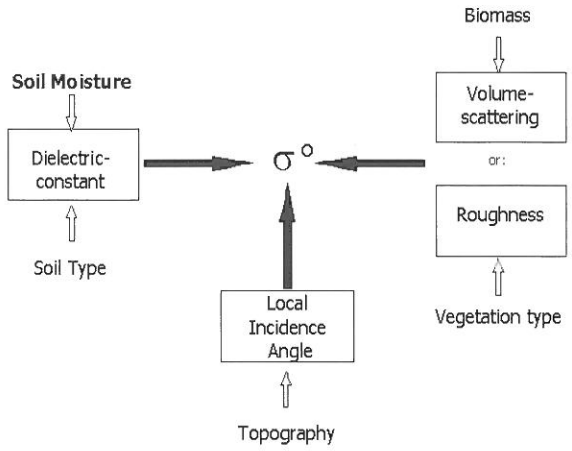

Figure 3-10: Soil moisture retrieval from ERS data using the described approach.

Within InFerno, the soil moisture is derived from SAR data using a method developed by Rombach & Mauser (1997) and Riegler & Mauser (1998). It is based on an empirical compensation of the different terms affecting the radar backscattering (Figure 3-5). First topographical influences are corrected considering the local incidence angle of each pixel illuminated by the microwave beam. Land use dependent roughness effects and biomass dependent volume scattering are compensated and the dielectric constant of the underlying soil is estimated. Depending on soil physical properties, corrections are made to invert volumetric soil moisture from the determined dielectric constant. This method has been successfully applied in various micro- and mesoscale catchments (Mauser et al., 2000; Oppelt et al., 1998).
The estimated soil-moisture at the upper layer will be linked with the water balance model LARSIM. The possibilities of a connection between Radar data derived soil moisture and a hydrological model could be shown for the Ammer catchment (~ 700 km^2) at the Northern Bord of the alps, where the simualation of the 'Whitsun flood' 1999, using topical soil moisture information derived from the ERS data, shows a close correspondence between the measured and modeled peak discharge and discharge volume (Bach, 2000).

Characteristic for the InFerno approach is the combination of station measurements, remote sensing data, GIS data layers on land surface parameters like elevation, land use, soil type through data assimilation in a flood model.

4 CONCLUSION

The project InFerno has been originated to evaluate the capabilities of remote sensing with respect to operational flood forecasting and management. In this sense, the project setup is breaking new ground in several ways, i.e. by operationally assimilating remotely sensed data and retrieved information into existing information systems and hydrologic models. The major challenge of the project lies in the implementation of algorithms developed for a multisensoral synergy and the creation of robust, operationally applicable remote sensing products. The involved partners are confident to achieve this ambitious goal, by placing the research matters of the project on the enhancement of existing procedures and on a broad expertise in the fields of remote sensing, software development, hydrologic modeling and operational flood forecasting.

ACKNOWLEDGEMENT

Funding of the project InFerno (project no. 50EE0053) by the German Aerospace Center (DLR) is gratefully acknowledged. Teh European Space Agency (ESA) supported this work through its PI program.

REFERENCES

Bach, H. et al. (2000): Application of SAR-data for flood modelling in Southern Germany. Proceedings of ERS-ENVISAT-Symposium Gothenburg 2000, Looking down to Earth in the New Millennium. ESA SP-461, p.123.

Baghdadi, N. et al. (2000): Potential and Limitations of RADARSAT SAR Data for Wet Snow Monitoring. IEEE Transactions on Geoscience and Remote Sensing. (38) 1. 316-320.; New York

Bertle, F. (1966): Effects of snow compaction on runoff from rain on snow. Engineering monographs No 35, Washington D.C.

Bremicker, M., Gerlinger, K. (2001): Operational application of the water balance model LARSIM in the Neckar basin. In: Runoff Generation and Implications for River Basin Modelling - Proceedings of the International Workshop 9.-13. October 2000, p. 306 - 312. Freiburger Schriften zur Hydrologie, Institut für Hydrologie, University of Freiburg, Band 13.

Bremicker, M. (2000): Das Wasserhaushaltsmodell LARSIM - Modellgrundlagen und Anwendungsbeispiele. Freiburger Schriften zur Hydrologie, Institut für Hydrologie, University of Freiburg, Band 11.

Derrien, M. et al. (1993): Automatic cloud detection applied to NOAA-11 AVHRR imagery. Remote Sensing of Environment (46). 246-267; New York, Amsterdam

Dozier, J. (1989): Spectral signature of alpine snow cover from Landsat Thematic Mapper. Remote Sensing of Environment. Vol. 28; New York, Amsterdam.

Fung, A. (1994): Microwave Scattering and Emission Models and Their Applications. Artech House Inc. Norwood.

Homagk, P. (1998): paper, held at workshop of the German Weather Service and the Czech Weather Service in Prague, May 1998.

Knauf, D. (1980): Die Berechnung des Abflusses aus einer Schneedecke. In DVWK-Schriften, Heft 46: Analyse und Berechnung oberirdischer Abflüsse S.95-135; Bonn.

Ludwig, K. (1982): The program system FGMOD for calculation of runoff processes in river basins. Zeitschrift für Kulturtechnik und Flurbereinigung 23, 25-37; Berlin, Hamburg.

Mätzler, C. (1987): Application of the interaction of microwaves with natural snow cover. Remote Sensing Reviews. (2), Amsterdam. 259-387.

Mauser, W. (1984): Calculations of Flood-Hydrographs Using Satellite-Derived Land-Use Information. Adv. Space Res., (4) 11. 211-216.

Mauser, W., Stolz, R., Schneider, K., Bach, H (2000): Comparison of ERS-SAR data soil moisture distributions with SVAT model results. Proceedings of ERS-ENVISAT-Symposium Gothenburg 2000, Looking down to Earth in the New Millennium, ESA SP-461, Noordwijk.

Nagler, T. et al. (1998): SAR based Snow Cover Retrievals for Runoff Modelling. 2nd Workshop on Retrieval of Bio- and Geophysical Parameters from SAR Data for Land Applications, ESA SP-441, Noordwijk pp.511-518

Oppelt, N. et al. (1998): Mesoscale soil moisture patterns derived from ERS data. Proceedings of the EUROPTO-SPIE conference Barcelona. SPIE Vol. 3499. pp. 41-51.

Riegler G., Mauser W. (1998): Geometric and radiometric terrain correction of ERS SAR data for applications in hydrologic modelling. Proc. IGARSS'98, Seattle, pp. 2603-2605.

Rombach, M., Mauser, W. (1997): Multi-annual analysis of ERS surface soil moisture measurements of different land uses. In: Proc. of the Third ERS Symposium: Space at the Service of Our Environment, Florence 1997, ESA-SP- 414, Volume I, May 1997, pp. 27-34.

Rott H. et al. (2000): Hydalp - Hydrology of Alpine and High Latitude Basins: Final Report.

Schulz, W. (2000): Hochwasservorhersagesystme in Baden-Württemberg für die obere Donau. XX Konferenz der Donauländer, Bratislavia, Slovakia, 4-8. September 2000 (CD-ROM)

REGIONALIZED FLOOD ESTIMATION AT UNGAUGED SITES SUPPORTED BY GIS

A.H. Schumann[1], B. Pfützner[2]

[1] Ruhr- University Bochum, Institute for Hydrology, Water Management and Environmental Techniques, Germany, 44780 Bochum, andreas.schumann@ruhr-uni-bochum.de

[2] Bureau for Applied Hydrology, Wollankstr. 117, Germany, 13187 Berlin, Bernd.Pfuetzner@bah-berlin.de

SUMMARY

Regional flood frequency analyses are an attempt to explain the spatial variability of flood statistics by deterministic relationships to watershed characteristics. Many problems are connected with this approach. Some of them are presented here: the year and site effects, specific problems of multiple regression analysis and the scale problem. Special emphasis should be given to the problems of homogenous flood regions. At some practical examples ways to overcome some of these problems are discussed. Especially it is shown how regional flood analysis can benefit from Geographic Information Systems (GIS). GIS are very helpful in regionalized flood estimation as the can be used to provide watershed characteristics in an efficient way. The option to visualize the results of the regionalization e.g. by regional flood maps, is very helpful to explore the specific spatial distribution of flood risk within the region of interest. Also other visualization e.g. by comparison of the results of flood statistics at ungauged and gauged sites can be provided by utilization of the GIS. By a case study for a mountainous region in Germany it is shown that many theoretical based solutions for the problem of regionalization are limited by the spatial heterogeneity of hydrological processes and scale effects.

Keywords: Regional flood frequency analysis, watershed characteristics, multicollinearity, spatial heterogeneity

1 INTRODUCTION

In general flood probabilities can be estimated from runoff series by frequency analysis. Unfortunately runoff data are seldom available at the site of interest where flood probabilities are needed. By regionalization of flood statistics these problems should be solved. This approach of regional flood frequency analyses is based on the assumption that statistical information derived at gauges can be linked with climatic data and physical characteristics of their watersheds to estimate regional valid relationships which could be used to assess flood statistical characteristics at ungauged locations. Regionalization is an attempt to explain hydrological statistics by characteristics and parameters which are relevant in a deterministic sense for floods. The development of each single flood event depends strongly from coincidences of many different event specific factors (e.g. precipitation, state of the catchment). Any selection and ranking of watershed characteristics with the aim to describe their influence on the statistical characteristics of flood series will be an imperfect attempt. In this paper some general problems of regional flood frequency analyses are described together with options to overcome them. These problems are:

- the year and site effects (the multisite runoff data used for frequency analyses are derived from series with different length and different quality of discharge data.)
- the problems of multiple regression analysis (esp. multicollinearity)
- the scale problem
- the definition of homogenous flood regions.

Unfortunately the demand for further research with regard to these problems is contradictory to the present need to provide applicable solutions for flood frequency estimations at ungauged sites. The problems mentioned above should not be neglected completely as it is done in many studies. Examples from the practice of development and application of regional flood frequency analyses done by the authors will underline this.

2 THE PROBLEMS OF REGIONAL FLOOD FREQUENCY ANALYSES

2.1 The general problems of flood frequency analyses at a single gauge

Basis for any regionalization is a flood frequency analysis at each gauging station within the region. The raw data should fulfil some basic criteria as homogeneity and consistency. Other problems consist in the selection of an appropriated distribution function and the way how outliners should be considered. These decisions are very important for the following regionalization as the range of flood statistics at the different gauging stations within a region is determined by them. These problems can not be handled without cooperation with the local hydrologists. The preferred practice of flood frequency analyses in the region has to be considered (e.g. the utilization of a certain distribution function or the handling of outliers). If e.g. the Gumbel- Distribution is used within a region, the utilization of the Pearson-3- Distribution will generate significant higher values for flood events with low exceedance probabilities. Here the results of regionalization could differ significantly from the flood statistics which are used within this region. The common practice of frequency analysis should be considered in regional flood frequency analysis to produce consistent results after regionalization.
Unfortunately often the cooperation between the producers of hydrological data and the users of these data is not ensured. The assumption that flood peaks at a gauge could be estimated with a accuracy of some percent is unreasoned. The range of uncertainty is widening with flood events which are rather seldom. Unfortunately these events affect the shape of the distribution function often significantly. From our analyses plus/minus 30 percent seems to be an appropriated range of uncertainty for flood peaks with an empirical frequency of 0.05 and lower. But also the consistency of data within runoff series is very problematic. Often continuous registrations of runoff values are not available during the whole period of observation. The utilization of discrete daily observations is worse than a lack of flood data as it influences the statistical results significantly. In such cases the flood peaks will be missed temporarily. This could cause large differences in the statistical moments of higher orders between neighbouring stations. Often such specific problem becomes not evident without an attempt to regionalise the flood statistics at different gauges. It is a rather simple statement that the results of the regionalization can not be more accurate than the raw data. However more important is the fact that the regionalization itself varies accordingly to the uncertainty of discharge data. The consideration of uncertainties of flood series which may affect the results of regionalization in a unexpected way is very important. Any minimization of the residuals during the regionalization without consideration of the limitations of the data is problematic for any application of the resulting methodology on ungauged watersheds.

2.2 Some specific problems of regionalization

2.2.1 Multicollinearity and the specific spatial characteristic of hydrometrical networks

The term "Multicollinearity" describes the problem in multiple regression analysis that two or more independent variables are highly correlated. This makes it difficult if not impossible to determine their separate effects on the dependent variable. Such multiple regressions are the main tool of regionalization. Unfortunately multicollinearity is a problem for regionalized flood estimation which results from the specific structure of gauging networks and morphological and soil characteristics within river basins. In mountainous regions e.g. the elevation determines many watershed characteristics. If the elevation of the watershed is high the soil permeability is often small, the slope is high, forest is the dominating land-use and the area of the watersheds is small. To demonstrate these relationships with an example the coefficients of correlation between the mean elevation and some other catchment characteristics for a mountainous region in Germany are shown in Table 2-1. Obviously are all of these characteristics strongly correlated with elevation. There are two ways to handle multicollinearity: to exclude correlated catchment characteristics from the analysis or to use multivariate statistics e.g. by principal components to combine correlated characteristics. The first approach leads to a definition of a main catchment characteristic which is most important to describe the spatial heterogeneity within the region of interest (in the example of Table 2-1 the elevation).

Table 2-1: Coefficients of correlation between the mean elevation and some other catchment characteristics for 11 catchments in the Harz mountainous region.

	P6h100[1)]	Average Day of the yearly flood within the year	Relative are with low soil permeability	Relative Area with thin soil cover	Percentage Forests	Mean Slope
Elevation of the watershed	0.795	-0.851	0.707	0.798	0.847	0.592

[1)] P6h100 precipitation with 6 hours duration and an interval of occurrence of 100 years

Another problem which becomes less evident than multicollinearity arises from the correlation between annual floods at different stations (Hosking and Wallis, 1988). Especially if in a particular year a heavy rainfall over a large area results in large floods at many flow-recording stations the flood series are cross-correlated. Connected with this problem, the statistical parameters derived from periods of different lengths will be influenced by the stochastic character of large floods which modify the variance values of short time series significantly. Short records can include sequences of years that are wetter or drier than the average. An separation of these year and site effects by generalized linear models was proposed by Clarke (2001).

2.2.2 How to specify regions?

The definition of homogeneous regions is fundamental for each regional analysis. These regions specify the set of catchments between which we can transfer or scale information. Gupta et al. (1994) defined a set of catchments as homogeneous if we can relate their hydrological properties (such as flood and rainfall frequencies, stream lengths and slopes) using a scale function that only involves catchment size, and not location within the region. This definition is very helpful as it is shown by the example in Figure 2-1. In this example a relationship between the mean specific annual floods and the watershed area is used to subdivide 66 gauges within a political defined region into two flood regions which are strongly related to the elevation of the watersheds.

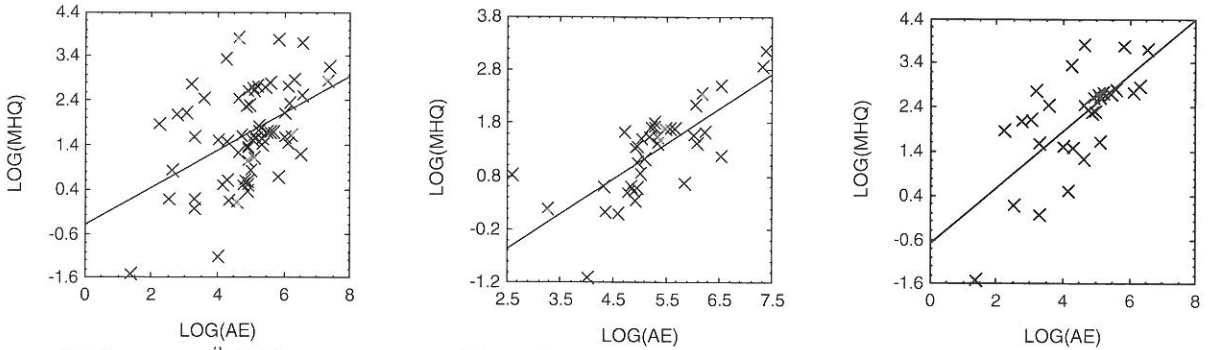

Figure 2-1: Example for a definition of two regions by scaling of the mean annual flood with the catchment area.

In contradiction to this definition by scaling, regions are often specified by their catchment properties. To define regions by objective techniques according to catchment properties multivariate statistics such as cluster analysis is applied (Burn, 1989), (Acreman and Sinclair, 1986). More recently, several researchers have addressed the definition of focused pooling techniques, which specifically design the homogeneous group of basins for a site of interest. The focussed pooling group is identified using catchment similarity measures rather than geographical location. By introduction of focused pooling techniques fixed and contiguous regions were replaced by flexible and overlapping groups that are not necessarily geographically contiguous. The practical problems of this approach consist in the classification of ungauged sites. The relative performance of four hydrological similarity measures used to form homogeneous pooling groups for regional frequency analysis was presented by Castellarin et al. (2001). One pair of similarity measures is based on seasonality indexes that reflect the timing of extreme events. A further pair of measures considers a characterization, at the basin scale, of the frequency distribution of rainfall extremes and the extent of the impervious portion of the catchment. The results demonstrate that similarity measures based on seasonality indexes are effective for esti-

mating extreme flow quantiles for the study area. (We received a similar result in our studies, described below). Unfortunately for ungauged catchment this specification of seasonality is not available. For ungauged catchments, a similarity measure incorporating both rainfall statistics and permeability information was proposed by these authors as most effective.
Often the definition of regions is limited by the scale problems. The scale problem describes the different behaviour of small and large watersheds. It is closely connected with the spatial heterogeneity of the catchment characteristics. Often large watersheds cover different flood regions or the flood conditions at a gauge are determined by a part of its watershed only. As the number of gauges is often small it can not be avoided to use different gauges situated in the longitudinal section of the same river. Here a general deficit of regional analyses in mountainous regions becomes evident: If the flood characteristic of a runoff series at a gauge is related to the entire catchment we neglect the heterogeneity in it. In general the runoff is viewed as the integrated result of all hydrological processes within a drainage area. This assumption is more or less violated if the flood generation is spatially limited to some parts of the catchment only. The spatial heterogeneity of flood generation can be caused by event-specific factors (e.g. rainfall distribution), but also by heterogeneities which result from different physical characteristics of sub-catchments within the basin, e.g. from the specific flood processes in headwaters. In such cases the flood characteristic of a river, which drains a larger, heterogeneous area will be different at different locations along its course. Especially the flood characteristics of smaller catchments will be more affected by their headwaters. Further downstream these peaks will be reduced by diffusion. In some cases we have to consider tubes of higher flood risks along rivers with flood producing headwaters. These tubes can be embedded in regions with lower risk and end by the impact of the diffusion on the flood peaks and the average effect of larger basins which compensates such heterogeneities. In Figure 2-2 three different flood regions are mapped. In region 3 gauges at rivers which originates in region 2 show different flood characteristics than gauges at the outlet of smaller catchments which are located in region 3 completely.

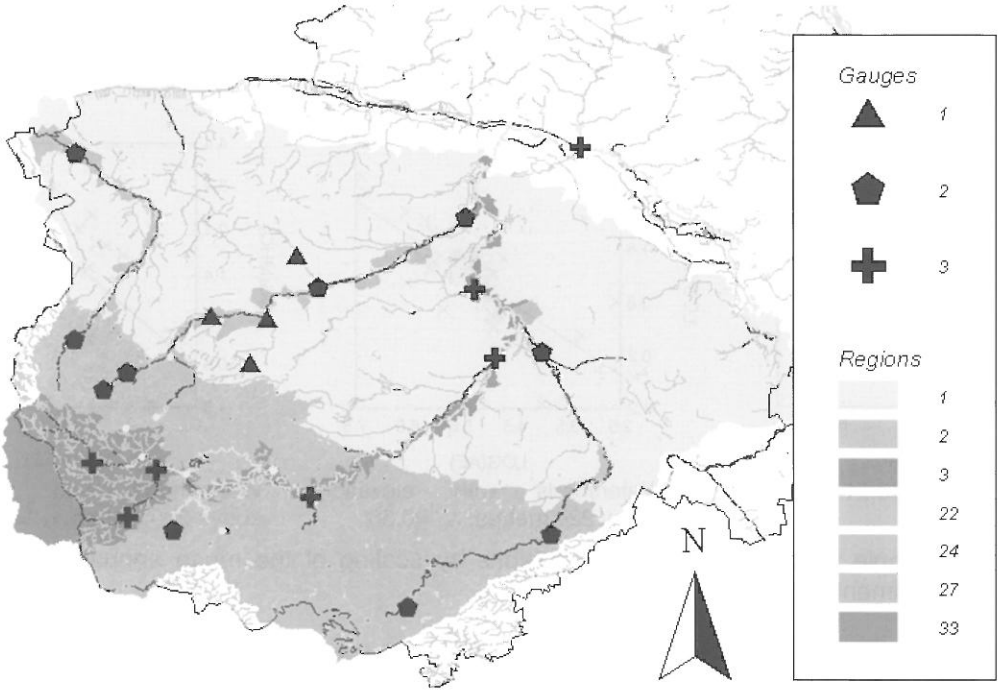

Figure 2-2: Map of the three flood regions in the eastern part of the Harz mountains.

3 APPLICATION OF GEOGRAPHIC INFORMATION SYSTEMS IN REGIONAL FLOOD FREQUENCY ANALYSES – A CASE STUDY

Regional flood frequency analysis can benefit manifold from the option to use spatially distributed information, offered by Geographic Information Systems. By application of a GIS regionalization of flood statistical information can be based on a wider spectrum of catchment characteristics estimated with lower efforts. A GIS offers unique opportunities to visualize the results of regionalization in an interactive way. This could be used e.g. to specify flood homogenous regions. Finally the developed

methodology for regionalized flood estimation can be applied on ungauged watersheds within the framework of the GIS in a very user-friendly way.
In the following the results of a regional flood frequency analysis for a political region in Germany are presented. Within this region different natural units can be distinguished from the east part of the Harz Mountains with an elevation around 900 metres a.s.l. downwards to the valley of the River Elbe and the lowlands of East Germany.

Data base
In total only 66 gauges were available for flood analysis in this region. The average size of the catchments is 260 km^2, only 17 percent (11 watersheds) are smaller than 25 km^2, 26 catchments have an area between 100 and 200 km^2 and 7 catchments have an area above 500 km^2. Unfortunately were 20 percent of the time series shorter than 20 years. Observation periods of more than 30 years were available only at 43 percent of all gauges. The GIS data base consists in Land Use data, maps of soil characteristics, slope and elevation, a digitised river network, digitised catchment boundaries and a spatial order scheme of drainage areas which was based on a subdivision of all catchments into small drainage areas defined by nodes of the river network. In general the average size of these area elements was around 1 km^2. Based on storm statistics of the German Weather Service (Kostra, 1997) also maps of extreme rainfall with durations between 15 minutes and 72 hours and recurrence intervals between 1 and 100 years were available.
First of all the yearly flood series at a gauges were statistical analyzed. To derive comparable distributions functions at different gauges the series of annual flood peaks were normalised by division with the mean yearly flood values. For all gauges different types of distributions were applied using product moments and L- moments and validated by regression analyses between the computed quantiles of the distribution and the empirical probabilities of the measured annual flood peaks. To support the selection of regional valid distribution functions the L- Moment- Diagram was used. In this diagram (Vogel et al., 1993) (Figure 3-1) the theoretical relationships between the third and fourth Probability Weighted Moments are compared with quotients of the empirical moments, generated for each gauge. It can be seen from Figure 3-1 that no clear preference for a specific distribution becomes evident. However the yearly flood series for catchments in the mountainous upper part of this region seems to be more related to the Generalized Extreme Value Distribution than gauges in the lowlands which tend more to the Pearson-3-Distribution.

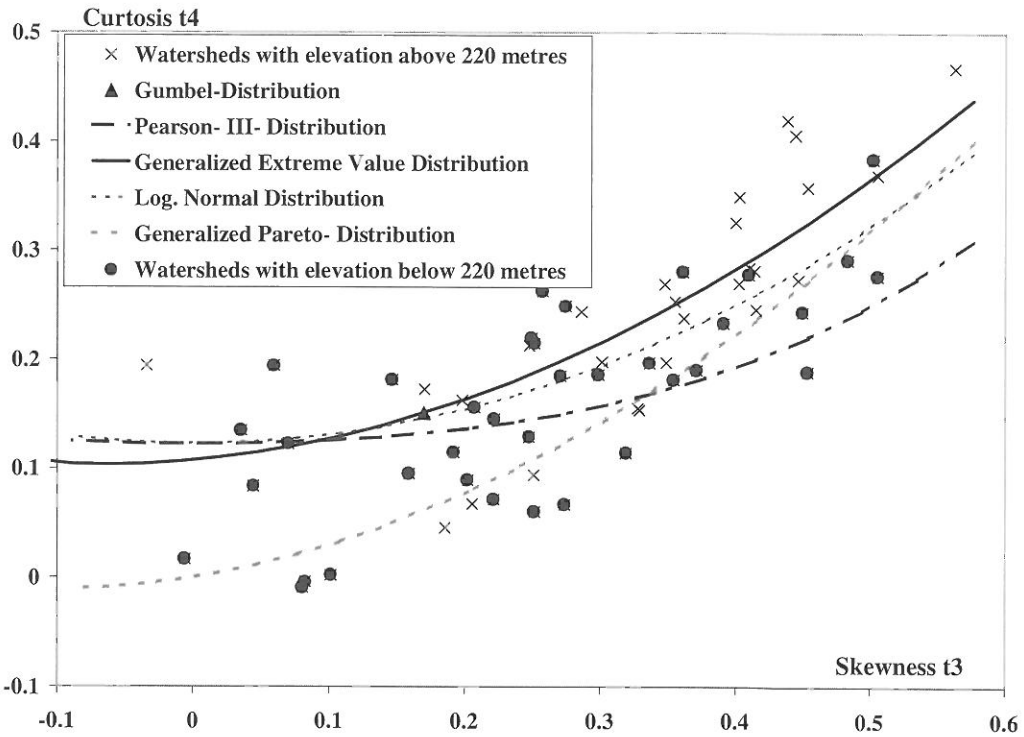

Figure 3-1: Diagram of L- Moments t3 and t4 for different distribution functions and empirical quotients at the different gauges (points).

In the next step of this analysis, the region was differentiated into the mountainous part and the lowlands. To avoid the problems of multicollinearity of catchment characteristics and considering the small number of gauges in relation to the heterogeneous flood situation in the mountainous part the most significant catchment characteristic was selected here and related to the quantiles of the flood distributions at the gauges. By an analysis of the correlation matrix between all catchment characteristics available it became obvious that the mean elevation explained most of the variability of all other characteristics (Table 2-1). The mean elevation Hmean was strongly correlated with the mean annual specific flood Mhqs:

(1) $$Mhqs = -201.348 + 0.983023*Hmean$$

This correlation explains 79 percent of the variance of the specific mean annual flood values but it was not applicable for regionalization as the variance itself is high. This problem could be solved by an further differentiation into three flood regions. The mountainous region was subdivided by three different relationships between elevation and the specific mean annual flood values. In the further analysis the scaling with the area was replaced by a scaling with elevation as the catchment area size was strongly related to the mean elevation of the watershed. In the next step the shape of the distribution function was described by regressions between the quantiles and catchment characteristics. The yearly floods were related to the mean annual flood and the quantiles of the Generalized Extreme Value distribution were estimated for recurrence intervals of 2, 5, 10, 20, 25, 50, 100 and 200 years. Again all catchment characteristics were tested in their relevance to describe the variance of the different quantile values. The strongest relationship was found with the characteristic "drainage density". It is interesting that the influence of this characteristic depends strongly from the specific recurrence interval as it is shown in Figure 3-2.

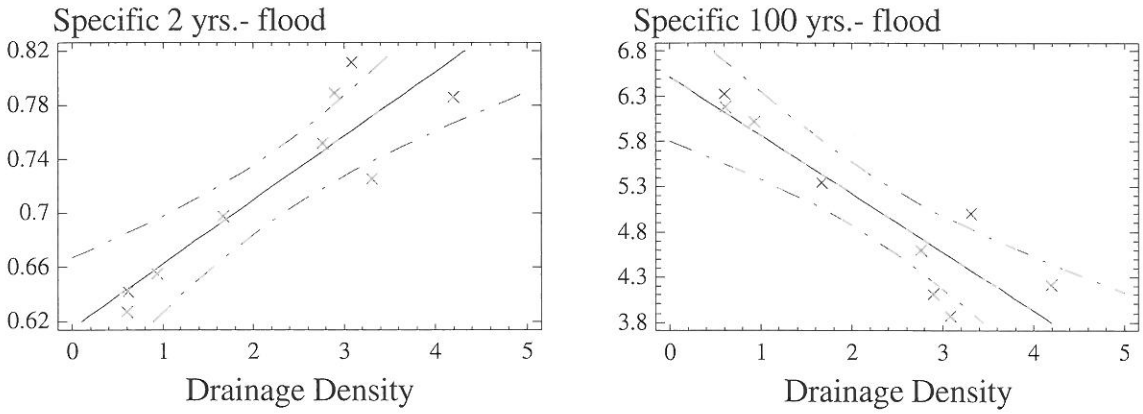

Figure 3-2: Regressions between drainage density and 2 yrs. or respectively 100 yrs. specific floods.

For a low exceedance probability the related quantiles decline with increasing drainage density but for high exceedance probability the related quantiles increase with drainage density. This phenomenon can be explained by the influence of the soil storage capacity on flood probabilities. If the drainage density is high the soil storage capacity is in general low. Rainfall events produce very often floods in such catchments, the rise of the distribution is relatively small as the shape of it depends mainly from the statistics of rainfall. If the drainage density is low and the soil storage capacity high, an extreme flood is caused by joint probabilities of precipitation and extreme wet soil conditions. A flood event which is very seldom results here from high precipitation values and simultaneously a high soil moisture at the beginning of the rainfall event. The slope of the distribution is higher in such catchments, as the extremes differ here more from the average conditions.
For the lowlands the regionalization was done in a different way. Here the elevation is less important than in the mountainous region. Considering the joint impact of soil permeability and precipitation, the flood quantiles were related to extreme precipitation values with the same probability. This approach is based on a simplified conceptual representation of the process of transformation of intense rainfall into runoff by the Rational Method. It assumes that the average value of the annual maximum peak discharge is related to the average value of the annual maximum rainfall depths within a duration equal to the time of concentration of the watershed (Brath et al., 2001). For the region analysed here different durations and exceedance probabilities for extreme rain events were available from the maps of storm statistics, provided by the German Weather Service. By application of the GIS values of the time of concentration for each watershed were estimated. The specific flood quantiles were related to the

sums of rainfall with the same exceedance probability and a duration chosen accordingly to the time of concentration. These quotients (in the following called "peak runoff coefficients") were estimated for recurrence intervals of T=2, 5, 10, 20, 25, 50, 100 years and related to catchment characteristics. This was done by multiple regressions. To ensure a normal distribution of the variables the independent and dependent variables were transformed by Box-Cox- Transformations. Again different soil characteristics, land use and geomorphologic characteristics were used: drainage density, soil depth, are with small permeabilities, urban areas, forest, impervious areas, slope, main flow direction, a parameter to characterise the shape of the watershed in comparison with a circle, elevation of the watershed etc.. In total 37 gauges were located within the lowland region. These watersheds were differentiated into three groups which showed different behaviour with regard to the relationships between the peak runoff coefficients and the catchment characteristics. Unfortunately 9 gauges showed unusual residuals in the multiple regressions. A detailed data analysis of these data showed serious errors within these time series. These gauges were removed from the sample. Within all regressions the catchment area had the highest influence on the peak runoff coefficients. In two of the three groups also the urban area had an significant impact. In one group the elevation was more important. The resulting mean errors of the estimated peak runoff coefficients were around 10 percent. By a visualization of the results within the GIS it became evident that the flood regions were not geographically contiguous (Figure 3-3). A discriminant analysis of the gauged watersheds with the aim to specify discriminant functions which could be used to classify ungauged watershed was not successful. From the relative small numbers of gauges within each flood region resulted non-significant classifications. However the following criteria were most important for the specification of memberships to a flood region: the soil permeability, soil depth and the seasonal distribution of the yearly floods. In Figure 3-3 the seasonality of the yearly floods is shown by charts for the different gauges. Obviously is the spatial heterogeneity of the occurrence of summer floods considerably. Neighbouring watersheds show different seasonal distribution of floods, which cause significant differences in the statistical parameters and between the fitted distribution functions.

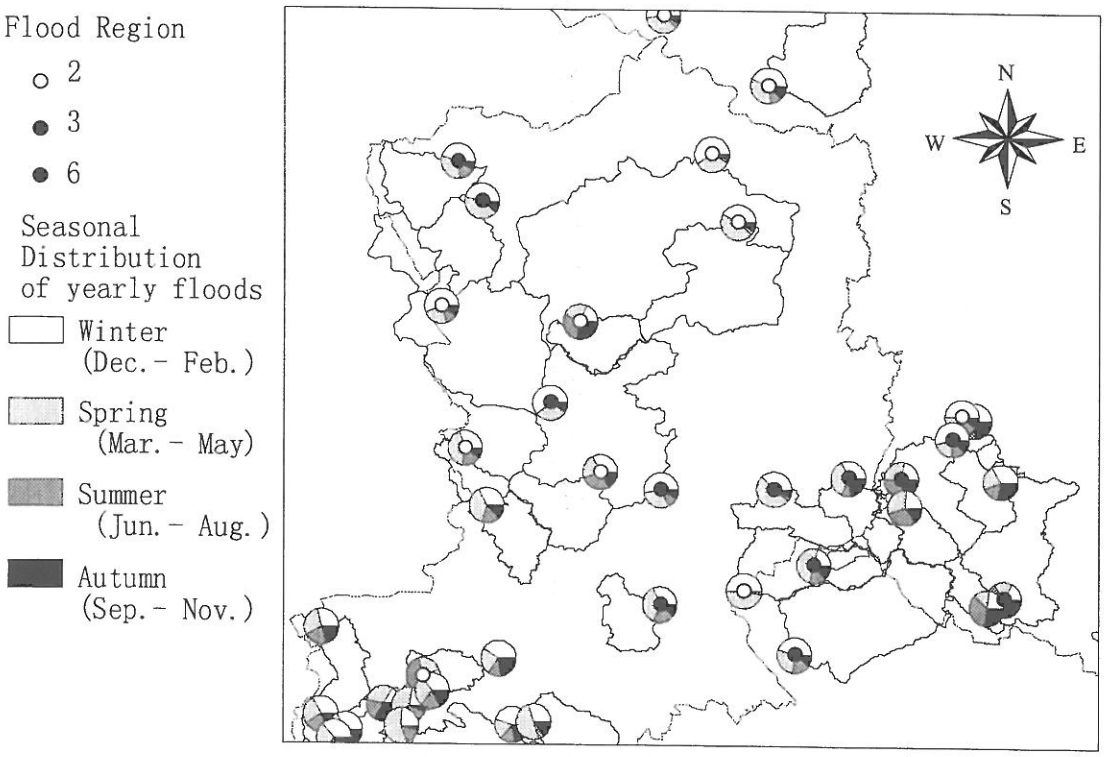

Figure 3-3: Seasonal characteristics of yearly floods and flood regions.

This spatial heterogeneity can not be explained by watershed characteristics. It seems to be more related to the regional features of flood producing weather conditions. A mapping of these local conditions would not solve the problem as the gauging network is not covering the whole region. Only if we neglect this spatial heterogeneity by renunciation of a definition of flood regions we could define a regional valid methodology applicable on all gauges in the region. This simplification reduced the accuracy of the methodology to estimate quantiles from 10 percent to 30 percent. Nevertheless under consideration of the uncertainties to measure flood peaks at gauges this accuracy seems to be still tolerable.

A GIS- based software solution was developed to apply the developed methodology with the aim to estimate at any point of the river network the flood statistics automatically under consideration of its location with regard to the flood regions (three region in the mountainous part, one region in the lowland) and the specific characteristics of the drainage area. To avoid a time consuming repeated analysis of the GIS data base to estimate the drainage area and other watershed characteristics the data base was pre-processed. For all small drainage area elements the characteristics were estimated and stored in a data bank. For each location of the river network the drainage area upstream can be estimated by an aggregation of these small drainage areas. This approach can be used to produce a flood map for the study area. The procedure to estimate the flood statistics at any location of the river network consists of the following steps of the developed software tool:

- select the site of interest from maps of the region which are provided in different scales,
- the physical characteristics (e.g. area, land use, soil characteristics etc.) are estimated for the watershed selected automatically
- the flood statistical information are derived from these characteristics.
- the results are compared with statistical data at neighbouring gauges and with previous statements about floods for this location or other sites close to it.

In the last step the user can select one or combine the three different flood statistical information (regionalization, information at gauges, previous statements about flood statistics) to make his statement which is used within a report generator.

4 CONCLUSIONS

All flood frequency analyses are strongly limited by scale effects. Methods to estimate flood statistics for ungauged drainage areas will be mostly applied on very small catchments (e.g. between 1 or 10 km^2). Unfortunately these methods were often derived from runoff data which were measured at gauges with drainage areas between 100 or 1000 km^2. The impact of this scale effect will be aggravated by the heterogeneity of flood generation within such catchments. Especially in mountainous river basins the flood statistics could be determined by the headwaters only. During the regionalization the location, extension and heterogeneity of the drainage area is more important than the location of the gauge. This complicates the definition of flood regions significantly.

The attempt to explain statistical characteristics by parameters which have an impact on floods in a deterministic way is limited by the complexity of flood generation. Often watershed characteristics (e.g. soil, land cover, seasonality, elevation, slope, geology, precipitation, drainage area) are specified by general patterns of natural conditions. Thus multiple regressions which are used to estimate flood statistical parameters from these characteristics are mostly influenced by multicollinearity. In our study for a mountainous region in Germany it was shown that the complexity of flood generation can be described by one or two characteristics only (by elevation and drainage density) which characterices this spatial pattern.

The problem of overlaying impacts of precipitation and physical watershed characteristics can be solved partially by a separation of the impact of precipitation. Here the specific flood quantiles were related to the sums of rainfall with the same exceedance probability and a duration chosen accordingly to the time of concentration.

If the heterogeneity of flood generation within a region is high we can not explain it sufficiently. We should honest specify the uncertainties of flood estimations for ungauged watersheds instead to hide these problems by maps or statistical tricks.

In general regional flood frequency analysis is complicated by a insufficient data base, scale effects and the complexity of flood generation. There is no general and simple way how a regionalization could be done as it depends from many different factors (availability of data and information, specific characteristics of the region of interest and heterogeneity of flood statistical characteristics).

REFERENCES

Acreman, M.C., Sinclair, C.D. (1986): Classification of drainage basins according to their physical characteristics, and application for flood frequency analysis in Scotland. Journal of Hydrology, 84 (3), p. 365-380

Brath, A. et al. (2001): Estimatine the index flood using in direct methods, Hydrological Science Journal, 46 (3) June 2001, p. 399 –418

Burn, D.H. (1989): Cluster analysis as applied to regional flood frequency. J. Water Resources Planning and Management 115 (5), p. 567 - 582.

Castellarin, D.H. et al.(2001): Assessing the effectiveness of hydrological similarity measures for flood frequency analysis, Journal of Hydrology 241 (2001) p. 270-285

Gupta, V. K., D. R. Dawdy: 1994 Regional analysis of flood peaks, in "Advances in Distributed Hydrology", edited by R. Rosso et al., p.149–168, Water Resour. Publ., Highlands Ranch, Colorado, USA

Hosking, J.R.M., Wallis, J.R. (1993): Some Statistics Useful in Regional Frequency Analysis, Water Ressources Research, Vol. 29,NO. 2, p. 271- 281, Feb. 1993

KOSTRA (1997): Starkniederschlagshöhen für Deutschland, Offenbach a. Main 1997, Selbstverlag des Deutschen Wetterdienstes

Vogel, R.M. et al. (1993): Floodflow frequency model selection in Australia, Journal of Hydrology, 146, p. 421- 449

FLOOD RISK MODELLING OF BABAI RIVER IN NEPAL

Rajesh Raj Shrestha, Stephan Theobald and Franz Nestmann

Institute for Water Resources Management, Hydraulic and Rural Engineering, University of Karlsruhe,
D-76128 Karlsruhe, Germany
shrestha@iwk.uni-karlsruhe.de, theobald@iwk.uni-karlsruhe.de, nestmann@iwk.uni-karlsruhe.de

SUMMARY

Flood risk involves a complex interaction of hydrology and hydraulics of river flow with potential of damage to the surrounding floodplains. The understanding of this interaction can be facilitated through an integrated system of hydraulic numerical models and Geographic Information Systems (GIS). This paper describes such an application with a case study from Babai River in Nepal for flooding in natural conditions.
The basic components of the model include; preparation of digital terrain model, calculation of water surface profiles, delineation of flood areas and assessment of risk. The methodology is illustrated with the application of HEC-RAS numerical model, and ARC/INFO and ArcView GIS. HEC-GeoRAS extension for ArcView GIS is used as an interface between the two systems for pre and post-processing. The application is extended to risk assessment through the use of spatial analysis functionality of GIS. The approach adopted for this study is based on the division of risk into vulnerability, associated with land use pattern, and hazard associated with hydrological and hydraulic parameters. Based on the analyses of these risk components, various relationships such as discharge-flood area and flood depth-land use are developed. A series of maps are also prepared depicting these relationships for the visualisation of results. This gives a new perspective to the modelled data and provides an effective and efficient decision making tool.

Keywords: river modelling, geographic information system, vulnerability, hazard, risk.

1 INTRODUCTION

Understanding the relationship between flood water and its surrounding is crucial in limiting the effects of flood induced disasters. Since floodplain management contains a number of semi-structured and non-structured problems, modelling capability is important to grasp and manage flood damage reduction systems (Simonovic, 1998). Hydraulic and hydrologic numerical models provide such capabilities, and are now well established, standard tools for modelling flows in rivers. The integration of these tools with the Geographic Information Systems (GIS) adds a spatial dimension to modelling systems and offers tools for more objective analyses and fast and transparent decision making. These tools also provide powerful and versatile means for further analyses such as flood risk modelling and assessment of various alternatives for flood protection.
There are a number of commercial and non-commercial software applications developed for this purpose. As for an example, the Institute for Water Resources Management, Hydraulic and Rural Engineering (IWK), University of Karlsruhe has developed a GIS - supported flood model for *Necker River*. This has been undertaken at the request of the Water Management Administration of *Baden Württemberg* in the context of project "*Integrierende Konzeption Neckar Einzugsgebiet* (IKONE)" (Oberle et al., 2000). The simulation of river flow is carried out by the one-dimensional model CARIMA from the *Laboratoire d'Hydraulique de France (*Grenoble*)* and the spatial data processing is done using ARC/INFO and ArcView GIS. Under the same project, the IWK has developed and transferred customised tools adapted to the requirements of state administration authorities. This consists of an interface for steady flow numerical computation as well as generation of inundation zones. This enables users with little GIS experience to perform complex task sequences in an automated manner using structured graphical user interface.
A popular application in this area is the interface between HEC-RAS and GIS. HEC-RAS developed by the US Army Corps of Engineers, Hydraulic Engineering Centre is one of the most widely used tools for the calculation of one-dimensional steady flow water surface profiles in rivers. To facilitate the exchange of data between the HEC-RAS and the GIS for pre and post processing, HEC-GeoRAS extension for ArcView GIS has been developed through a cooperative research between the Environmental Systems Research Institute and the Hydraulic Engineering Center.
The main objective of the research described in this paper is to extend this application to a systematic and objective assessment of flood risk (Shrestha, 2000). A case study from Babai River in Nepal

demonstrates the application for flooding in natural conditions. This paper describes the methodology using HEC-RAS, ARC/INFO and ArcView GIS, and HEC-GeoRAS extension for ArcView GIS.

2 FLOOD RISK ASSESSMENT

Flood risk involves a complex interaction of hydrology and hydraulics of the river flow with the potential of damage to the surrounding floodplains. The element of risk has both spatial and temporal domains and is also a function of level of human intervention to the surrounding floodplains. Plate (2000) described that the flood risk assessment requires a clear understanding of the causes of a potential disaster, which includes both the natural hazard of a flood, and the vulnerability of the elements at risk, which are people and their properties. Flood risk assessment therefore consists of understanding and quantifying this complex phenomenon.

Several researches have defined methodologies for flood risk assessment. Gilard (1996) presented an approach that divides the flood risk into the factors of vulnerability and hazard. He described vulnerability as the sensitivity of land use to the flood phenomenon, which depends only on land use type and social perception of the risk. The second factor, hazard, depends only on the flow regime of river and is independent of land use of floodplains. Consequently, same flow will flood the same area with the same physical parameters, whatever should be the real land use.

Boyle et al. (1998) discussed the assessment of expected damage due to flood in terms of four primary steps. These include: (1) hydrological frequency analysis; (2) hazard assessment; (3) hazard exposure analysis; and (4) damage assessment. In this methodology, the hydrological frequency analysis is based upon historical records and provides an estimate of exceedance probability or recurrence interval of a flood event of a particular magnitude. The hazard assessment divides risks posed by a flood event into tangible and intangible damages. After identifying the potential hazards, next step in the assessment process includes the estimation of extent and severity of damages in terms of the hazard exposure analysis, usually defined by the parameters like flood water depth and velocity. The damage assessment involves estimating the impact of likely exposure in terms of cost of replacing and restoring affected areas.

The flood vulnerability and hazard assessment can be undertaken as outlined in the three approaches by Rejeski (1993). In the first approach, a simple *binary (nominal) model* describes vulnerability as either present or absent in a particular area. The second approach, *weighted (ordinal) model,* describes spatial and temporal distribution of the flood hazard by ranking locations within the hazard area according to its severity. The third approach is the *quantitative (interval ratio) model,* which assigns numbers to locations that quantify the unit hazard factor.

3 METHODOLOGY

The methodology adapted in this study follows the approach developed by Gilard (1996). A conceptual flood risk model is defined by differentiating the hazard and the vulnerability components in terms of probability and spatial distribution. In this conceptual model, probability in hazard terms is defined as the return period of flood occurrence, which is related to the flood hydrology, while in vulnerability terms it is either presence or absence of the flood of a particular return period in a certain area. Similarly, the spatial distribution in hazard refers to flow in river channel and flood plains, which is related to river hydraulics, while in vulnerability terms this refers to land use type of the area under the influence of flood. After defining this conceptual model, the vulnerability assessment is conducted using of the *binary model*, based on presence or absence of flood of a particular intensity in a particular land use type. The *weighted model* is used for the hazard assessment according to the flood water depth. The results of these two analyses are combined together for the flood risk assessment. This risk assessment process is automated through a customised graphical user interface in the ArcView GIS. For this purpose, a user extension is developed using the Avenue programming language. The structure of the floodplain mapping and flood risk assessment model is shown in Figure 3-1.

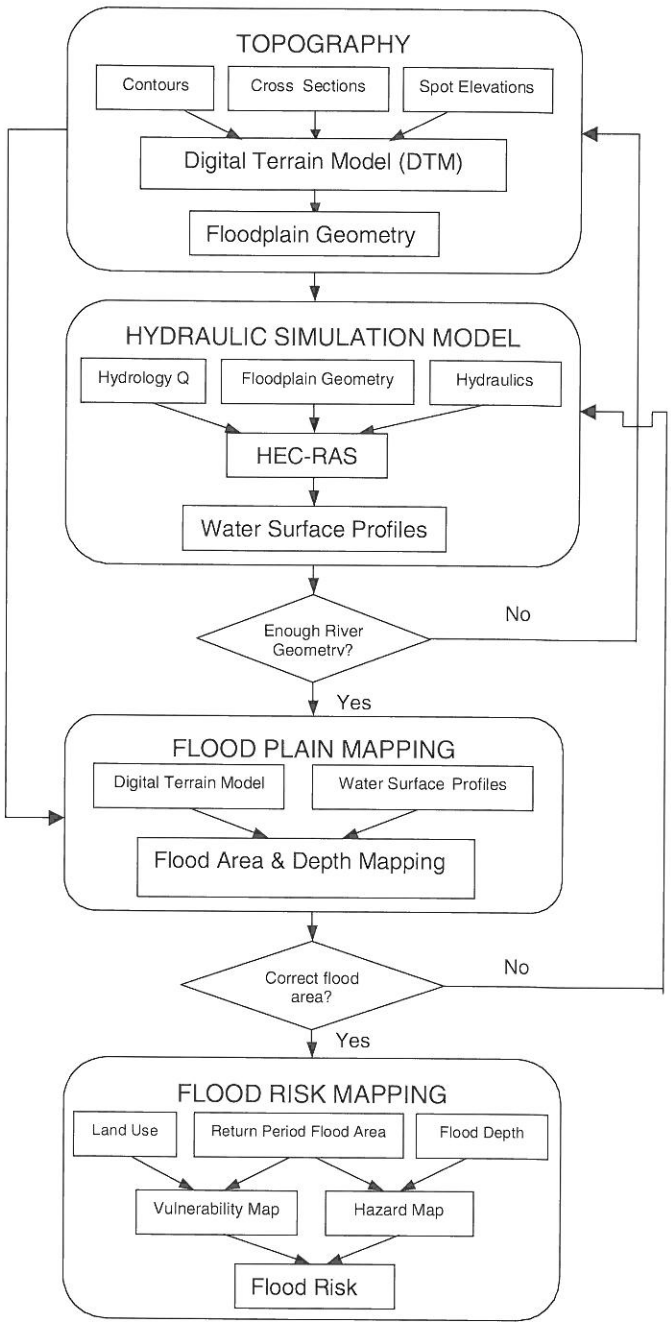

Figure 3-1: The Structure of the Floodplain Mapping and Flood Risk Assessment Model.

4 CASE STUDY

Nepal is predominantly a mountainous country with mountains constituting about 83 percent of land. The remaining 17 percent of land bordering India is flat Terai Plain, also known as the Indo-Gangetic Plain. It is this Terai plain, which is most vulnerable to the phenomenon of flooding every year. As rivers emerge into the plains from steep and narrow mountain gorges, they spread out and their gradient decrease abruptly with three major consequences: deposition of bed load, changes in rivers course and frequent floods (Jollinger, 1979). The problem of floods is aggravated by heavy precipitation in the monsoon season, which brings about 80 percent of total mean annual rainfall of about 1500 mm in the period between June and September. Much of this monsoon precipitation occur as a series of intense, localised storms, with bulk of precipitation occurring during 30 to 40 storm events, each of which result in between 25 to 100 mm precipitation (Alford, 1993).

Babai River in the mid-western region of Nepal, which is about 500 km South-West of Kathmandu, is one of the most flood prone rivers in the country (Figure 4-1). The river originates in the mountainous region, also known as the Mahabharat Range and has a catchment area of 3000 km^2. It emerges into the Terai plain through an irrigation barrage located at the foothills of mountains. The river flows through the length of about 43 km in the Nepalese Terai before flowing into India. The administrative headquarters of Bardiya district - Gulariya Municipality is located at the right bank of Babai River in Nepal-India border. The Municipality suffers extensive damage due to floods in Babai River in a regular basis. This study focuses on the most flood prone area of the river, extending from the up-stream barrage to the Indian border.

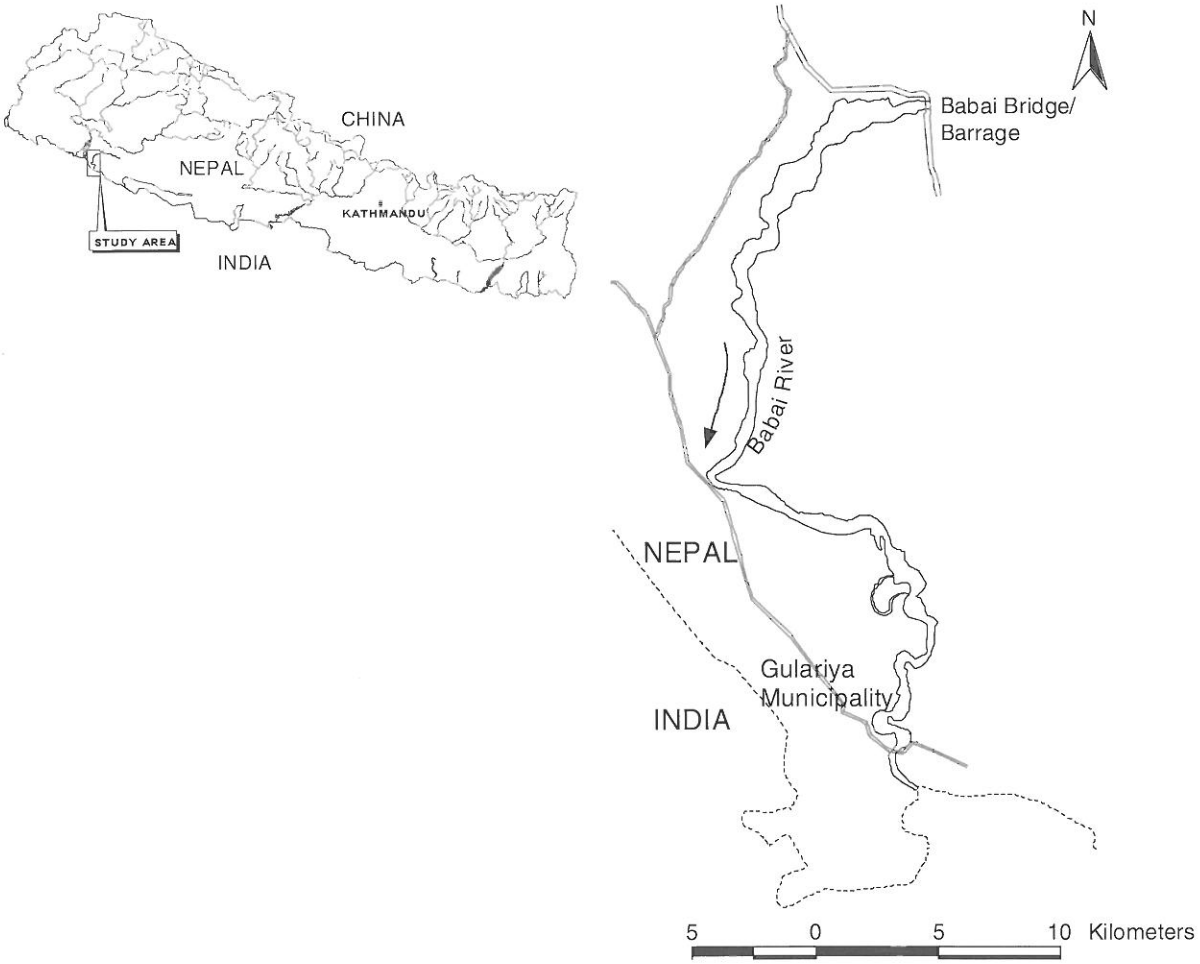

Figure 4-1: The Location Map of the Study Area.

A feasibility level flood mitigation plan study has already been carried out under "*The Study on Flood Mitigation Plan for Selected Rivers in the Terai Plain in the Kingdom of Nepal*" (FMP) by Japan International Cooperation Agency (JICA) in collaboration with His Majesty's Government of Nepal (HMG/N), Department of Irrigation (DOI) (JICA/DOI, 1999a, 1999b & 1999c). The FMP study prepared flood risk maps for the area based on the field investigation. The present study focuses on more knowledge based modelling system for a systematic assessment of flood risk.

4.1 Model Development

Various levels of digital and analog data in Babai River floodplains are prepared for the study. Contours at interval 2.5 m, spot heights, river systems, roads and settlement are digitised as ARC/INFO coverages from 1:10000 topographical map (1998) prepared for the FMP study (JICA/DOI, 1999c). Cross sections at intervals of about 1 km from the river survey of 1998 are used. The elevation data from contours, spot elevation and river cross sections are incorporated to prepare the digital terrain model of 10 m grid cell size.

In addition, digital database of river systems and land use classification are acquired from the International Centre for Integrated Mountain Development (ICIMOD). The land use information is based on 1:50000 map and includes the classes namely; settlement, wetland, mixedland and dryland cultivated, grazing land, plantation and hardwood forest and river.
The one-dimensional HEC-RAS model is used for the steady flow water surface profiles computation. The model is calibrated with 1995 flood marks. The water surface profiles are computed for floods of 2, 5, 10, 20, and 50 year return periods. The probability of floods of different various return periods were taken from the FMP study are given in Table 4-1.

Table 4-1: Probable Discharges of Babai River (m^3/s).

Return Period (yr)	Q_2	Q_5	Q_{10}	Q_{20}	Q_{50}
Flood Discharge (m^3/s)	2360	4070	5210	6300	7700

After the computation of water surface profiles in HEC-RAS, the water levels are imported to ArcView GIS using the functionalities of HEC-GeoRAS extension. The extension also facilitates the automated generation of flood grids and bounding flood polygons. The detailed procedure for pre and post processing using HEC-GeoRAS extension is given in Hydraulic Engineering Center (2000).

4.2 Flood Vulnerability Analysis

The flood vulnerability is a function of land use characteristics of areas under the exposure of flood. That is, a flood of same exceedance probability will have different levels of vulnerability according to land use characteristics and consequently potential for damage. Obviously vulnerability level will be higher in the settlement area as compared to the forested area. The vulnerability analysis therefore consists of identifying land use areas under the potential influence of flood of a particular return period. For this purpose, vulnerability maps are prepared by clipping the floodplain land use themes with the flood area polygons for each of the flood events being modelled. This depicts the presence or the absence of flood of a particular return period as a binary model (Figure 4-2A). The land use areas under the influence each flood events are reclassified for the calculation of total vulnerable areas (Figure 4-2B).

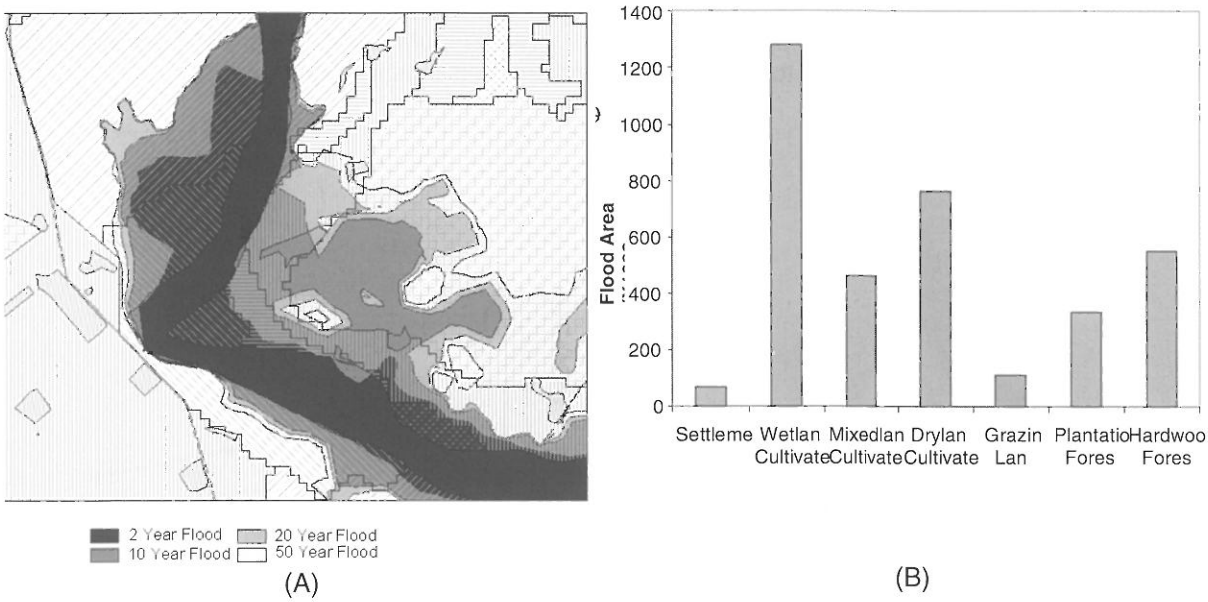

Figure 4-2: (A) Flood Vulnerability by Return Period
(B) Flood Vulnerability Classification for 20 Year Flood.

4.3 Flood Hazard Analysis

The hazard aspect of flood risk is related to the hydraulic and the hydrological parameters. This implies that the same flood will affect a particular area with the same hydraulic properties regardless of the land use types. Hazard level may be defined by parameters such as water depth and exceedance probability of flood events. In order to examine the relationship between flood discharges with flood depths and total flood areas, curves are plotted between these parameters (Figure 4-3A and 4-3B).

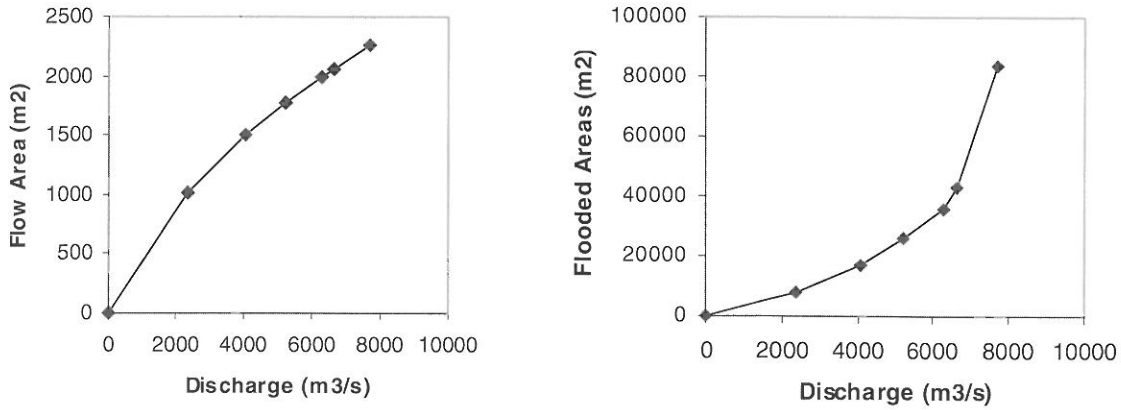

(A) (B)

Figure 4-3: Flood Hazard Relationships: (A) Flow Area versus Discharge; (B) Total Flood Area versus Discharge.

Figure 4-3A is a typical plot of flow area and discharge in a cross section. This exhibits a gradual reduction of the slope of relationship curve with the increase in discharge. However, the relationship between discharge and total flood area as shown in Fig. 4-3B depicts totally opposite trend. This relationship curve has a steeper slope with the increase in discharge, indicating a higher rate of increase in flood area.

For the quantification of flood hazard and potential of damage, water depth is a determining parameter. For this purpose, the weighted model is used ranking hazard level in terms of the water depth. The hazard levels are determined by reclassifying flood grids as flood depths polygons bounding water depths at intervals of 0.5, 1.0, 1.5, 2.0, 2.5, 3.0, 4.0 and >6.0 m (Figure 4-4A). The areas bounded by the flood depth polygons are calculated to derive depth-flood area relationship (Figure 4-4B).

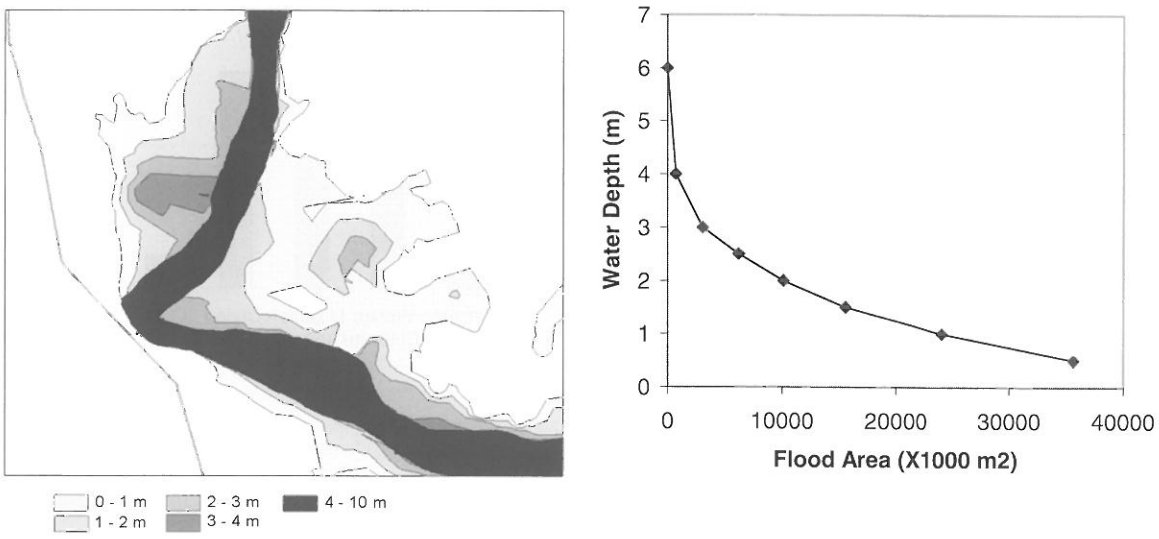

(A) (B)

Figure 4-4: Hazard for 20 Year Flood: (A) Average Depth of Flooding; (B) Water Depth - Flood Area Relationship.

4.4 Flood Risk Analysis

The flood risk analysis includes combination of the results of both, the vulnerability analysis and the hazard analysis. The relationship between land use vulnerability and flood depth hazard classes defines the risk level in a particular area. Flood risk maps prepared by overlaying flood depth grids with land use polygons depict this relationship (Figure 4-5A). The land use and hazard classes are translated into colour classes for the visualisation of the level of hazards in the vulnerable areas. Further analyses are performed by intersecting flood depth polygons with land use vulnerability polygons. The resulting attribute tables are reclassified to develop the land use - flood depth relationship (Figure 4-5B). This shows the potential flood areas not only in terms of land use vulnerability classes but also water depth hazard classes.

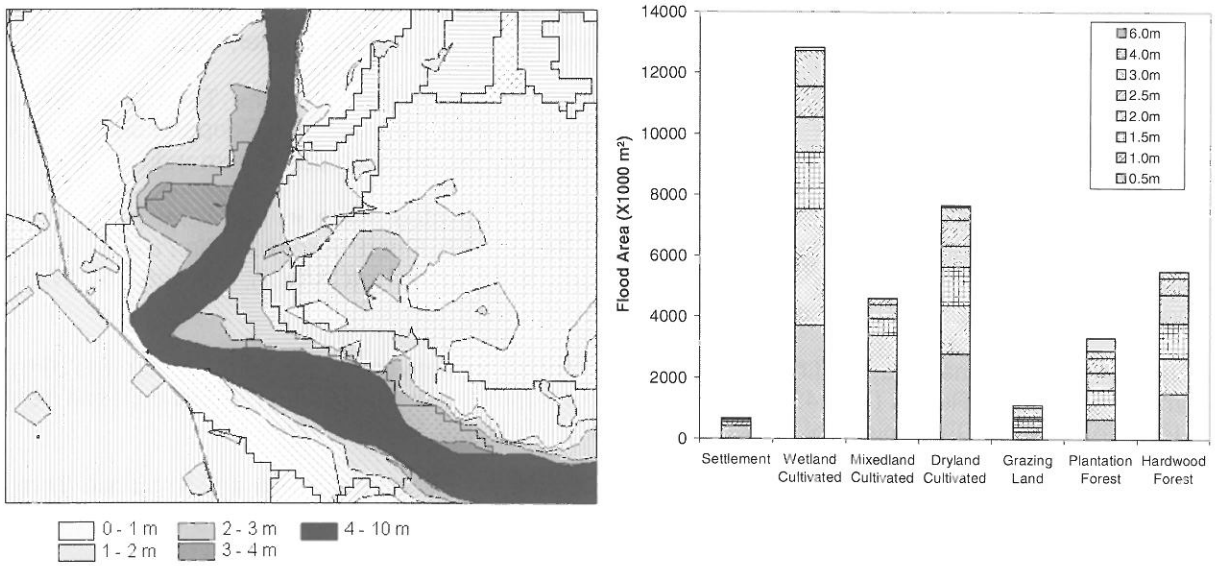

(A) (B)

Figure 4-5: Flood Risk for 20 Year Return Period: (A) Flood Risk Map; (B) Land Use - Flood Depth Relationship.

5 DISCUSSION AND CONCLUSIONS

The computation of water surface profiles using hydraulic numerical models and displaying the results in the GIS is gaining in increasing application, especially in Europe and North America. However, such applications are limited in countries like Nepal, where the availability of river geometric, topographic and hydrological data are also very limited. The situation of river flooding in Nepal is also completely different, there are much higher variations in the river flows and rivers are completely unregulated. This study presents an approach of conducting a similar study for flows in natural conditions. The available tools and methodologies are adopted and modified according to the requirements of this study. In the context of this study, this approach facilitates a transition from a flood hazard model based on the field investigation to a knowledge-based model that can be related to flood intensity and land use classes.

From the technological viewpoint, these tools provide efficient and effective means for an automated floodplain mapping and analysis. These methods and techniques offer a knowledge based flood model incorporating an objective quantification of the risk. The assessment of risk has given a new perspective to the modelled data. A series of maps are also prepared depicting these relationships for the visualisation of the results. These graphical representations of the flood risk in terms of relationship curves and maps help in better understanding of the perception of risk. This will also help planners and decision makers with an objective decision making tool for the implementation of appropriate flood protection measures.

REFERENCES

Alford, D. (1992): Hydrological aspects of the Himalayan Region, ICIMOD Occasional Paper No. 18, International Centre for Integrated Mountain Development (ICIMOD), Kathmandu

Boyle, S. J. et al. (1998): Developing geographical information systems for land use impact assessment in flooding conditions, Journal of Water Resources Planning and Management, ASCE 124 (2), pp. 89-98, Reston, Virginia

Gilard, O. (1996): Flood risk management: risk cartography for objective negotiations, 3rd IHP/IAHS George Kovacs colloquium, UNESCO, Paris

Hydraulic Engineering Center (2000): HEC-GeoRAS An extension for support of HEC-RAS using ArcView, User's Manual, US Army Corps of Engineers, Hydrological Engineering Center, Davis, California

JICA/DOI (1999a): The study on flood mitigation plan for selected rivers in the Terai plain in the Kingdom of Nepal, Final Report (Vol. 2: Main Report). Japan International Cooperation Agency/ Department of Irrigation (JICA/DOI), Ministry of Water Resources, HMG/Nepal, Kathmandu

JICA/DOI (1999b): The study on flood mitigation plan for selected rivers in the Terai plain in the Kingdom of Nepal, Final Report (Vol. 3: Supporting Report, A7: Flood Mitigation Plan/Babai River). Japan International Cooperation Agency/Department of Irrigation (JICA/DOI), Ministry of Water Resources, HMG/Nepal, Kathmandu

JICA/DOI (1999c): The study on flood mitigation plan for selected rivers in the Terai plain in the Kingdom of Nepal, Final Report (Vol. 4: Data Book). Japan International Cooperation Agency/ Department of Irrigation (JICA/DOI), Ministry of Water Resources, HMG/Nepal, Kathmandu

Jollinger, F. (1979): Analysis of river problems and strategy for flood control in the Nepalese Terai, Department of Soil and Water Conservation, Ministry of Forest, HMG/Nepal, Kathmandu

Oberle, P. et al. (2000): GIS-supported flood modelling, by the example of River Necker, International Symposium on Flood Defence, University of Kassel, Kassel

Plate, E. J. (2000): Flood risk and flood management, European Conference on Advances in Flood Research, Potsdam Institute for Climate Impact Research (PIK), pp 330-343, Potsdam

Rejeski, D. (1993): GIS and risk: a three culture problem, Environmental Modelling with GIS, M. F. Goodchild, B. O. Parks and L. T. Steyaert, eds., Oxford University Press, New York

Shrestha, R. R. (2000): Application of geographic information system and numerical modelling tools for floodplain analysis and flood risk assessment of Babai River in Nepal, M. Sc. thesis, Resources Engineering, University of Karlsruhe, Karlsruhe

Simonovic, S. P. (1998): Decision support system for flood management in the Red River basin, International Joint Commission Red River Task Force, Slobodan P. Simonovic Consulting Engineers Ltd., Winnipeg

REGIONAL FLOOD FREQUENCY ANALYSIS: IDENTIFICATION OF PHYSICAL REGIONAL TYPES

Lubomír Solín

Institute of Geography, Slovak Academy of Science, Štefánikova 49, 814 73 Bratislava, Slovakia, solin@savba.sk

SUMMARY

The paper concentrates upon application of the regional flood frequency analysis in Slovakia with an emphasis on the problem of identification of physiographic regional types of basin. The aim of the paper is to obtain knowledge of basin characteristics controlling the spatial variability of the at-site statistics of flood frequency behaviour and applies them in numerical and logical procedures for identifying regional units in the space of basin characteristics. The regional units are subsequently tested in terms of homogeneity of flood frequency behaviour within region and heterogeneity between regions. The conclusion identifies the best methods for identifying the regional units in the space of basin characteristics for forming regional flood frequency curves.

Keywords: regional flood frequency, basin characteristics, *L*-moment, cluster analysis, logical division

1 INTRODUCTION

Regional flood frequency analysis is an efficient tool for estimating of the *T*-year quantiles for basins with a relatively short gauging or for basins, which completely lack gauging. It is based on the concept of similar character of flood frequency behaviour in the framework of the defined regional unit and the estimate of the *T*-year quantiles is carried out using the regional frequency curve instead of the at site-distribution curve. The index flood model

$$Q_i(F) = \mu_i\, q(F) \tag{1}$$

introduced into hydrological literature by Dalrymple (1960) is a very frequently used model, which formally expresses the concept of the regional frequency analysis. Cunnane (1988), Hosking, Wallis (1977), present a review of additional ways of constructing the regional flood frequency curve. The symbol $Q_i(F)$ in equation *(1)* is the estimated *T*-year quantile for the *i-th* basin in the regional units. Further μ_i is index flood, which can be any location parameter of distribution. The mean of the at-site annual maximum streamflow data is very often used. The remaining symbol $q(F)$ is the regional growth curve, a dimensionless quantile function, which is the same for every site in the regional unit. However, the presumption of an identical regional growth curve at different sites will never be exactly valid in practice. Accurate delimitation of regional units is the only way to attain a certain approximation. Identification of regional units and specification of the regional growth curve are the key elements in regional flood frequency analysis. The more accurately we identify regional units with regard to flood frequency behaviour, the more consistent the regional growth curve with data and the more precise the *T*-year quantile estimate.

The efficiency of the *T*-year quantile estimate by means of regional frequency curve increases, if the regional units are identified in the space of basin characteristics (Hosking, Wallis, 1997). Even in case the regional units were identified directly in the space of hydrological characteristics (e.g. Mosley, 1981) it is indispensable to make additional physical justification of spatial location of relatively hydrological homogeneous classes if we want to increase the efficiency of the use of the regional frequency curve. Division of the interest area into regional units for regional flood frequency analysis though, differs in certain aspects from the traditional regional taxonomy:

a) regional variability of flood frequency behaviour is studied in the framework of a sample of basins which is a portion of a much larger population that is the true object of interest. This means that the selected set of basins should represent the population. An exhaustive characterisation of regionalization of interested area is then achieved with classification of all basins of population into the regional units identified in a sample. Basins are classified into regional units by different methods using relevant basin characteristics
b) although the basins are clustered into regional units on the basis of similarity in terms of basin characteristics, a high degree of dissimilarity among the regional units and similarity within the

regional units in terms of flood frequency behaviour, is also required. This is the reason why the created classification schemes in the space of basin characteristics must be subsequently tested from the point of view of hydrological consequences. Thus, the regional taxonomy for flood frequency analysis is more focused on identifying the regional structure of flood frequency behaviour in linkage to basin characteristics than on discovering the classes of the basin characteristics or at-site statistics only.

The paper is aimed at obtaining the knowledge on basin characteristics controlling spatial variability of at-site statistics of flood frequency behaviour and to implement them into the numerical and logical procedures used for identifying regional units in the space of basin characteristics. The conclusion, which of the methods of identifying the regional units is the best for forming the regional flood frequency curve is then made on the basis of testing regional units in terms of their hydrological consequences: dissimilarity of the regional at-site statistics between them and similarity of at-site statistics between sites within them.

2 A BRIEF SURVEY OF LITERATURE

Grouping of basins into regional units by numerical methods of hierarchic and non-hierarchic cluster analysis is the preferred approach to the subject (Wiltshire, 1986b; Acreman, Sinclair, 1986; Burn, Goel, 2000). The well-defined rules of their utilisation give an impression of an objective method. However, cluster analysis requires adoption of a whole set of subjective decisions concerning the choice of basic units, their attributes, measure of similarity, clustering algorithm, number of defined classes (Andeberg, 1972; Gordon, 1981). These decisions influence the final results of clustering. It is rather a rule than an exception that the choice of basin characteristics influencing the spatial variability of hydrological characteristics is based more on logical consideration than on the results of mathematical and graphical analysis. Those characteristics of basins, which are easily found from the topographic and thematic maps, are usually taken into account.

The alternative way of clustering relies on the logical division. The basic principles of regionalization by the method of logical division were analysed by Grigg (1969) and Armand (1972). In connection with regional flood frequency analysis it was applied, for instance by Wiltshire (1986a). Apart from preservation of certain logical rules (division should be exhaustive, classes should exclude each other, division should proceed at every stage upon one principle), the key principle of a logical division is the assessment of differentiating characteristics, which are important for the purpose of the division. Thus, division explicitly presupposes that there is some understanding of the causes of differences between the objects studied.

Another approach, also called „regionalization without regions" (Acreman, Wiltshire, 1987) or „region of influence" (ROI) by Burn (1990) relies on the idea that each basin can have its own region consisting of basins, which are similar from the point of view of their physical or hydrological characteristics. Regional units defined on the basis of this principle though, in contrast to the regional units defined by numerical or logical approach are not disjunctive and a problem with their cartographic presentation emerges.

The regional units defined in the space of basin characteristics are subsequently tested in terms of homogeneity of flood frequency behaviour within a region and heterogeneity between regions. As the hydrological data for a given site may be best fitted by any of several theoretical distributions according Mosley (1981), it is better if testing of homogeneity of flood frequency behaviour within and heterogeneity between physiographic regional units is carried out on the basis of summary statistics of the at-site data than on the basis of parameters of some of distribution functions. Wiltshire (1986c) divides the test of regional homogeneity into two basic groups 1) distribution-free test, and 2) distribution-based test. The first group of tests is based on the assumption that the dimensionless flood frequency values have a similar slope on probability a plot, which is related to the at-site dispersion measure of dimensionless flood frequency values. Homogeneity is then tested by statistics, which expressed dispersion of the at-site data around the regional value (Wiltshire, 1986a). Chowbury et al. (1991) proposed to test the regional homogeneity with regards to combination of the *L*-moment ratios. When testing the regional homogeneity on the basis of a distribution-based test, a priori the type of parent at site distribution is selected and whether the parameters of distribution at particular sites are consistent with the proposed regional distribution is tested (Greis, Wood, 1981; Lettenmaier, Potter, 1985; Wiltshire, 1986b; Lettenmaier et al., 1987; Chowbury et al., 1991; Rosbjerg, Madsen, 1995; Hosking, Wallis, 1997). Testing of heterogeneity of regional units in terms of flood frequency behaviour is normally carried out by *F* test (Wiltshire, 1986a; Acreman, Sinclair, 1986).

3 METHODOLOGY

3.1 Sample of basins, basin characteristics and at-site statistics

Regional units of flood frequency behaviour are identified firstly in the sample of basins representing some population, which is generally understood as a set of basic units continuous in space, not overlapping, covering the territory of interest in an exhaustive way and in an ideal case having same size. In our case, the population is defined as a set of spatially continuous not overlapping small basins (area under 200 km^2) corresponding to the „blue line", which are drawn from hydrological maps at scale 1:50 000. An exhaustive partition of Slovakia includes more than 5,000 such small basins. A sample of this population should be made by the method of random selection in order to guarantee its representativeness. Unfortunately, in many cases, including this, the choice of sample using the random selection method is not possible because a limited number of small basins are gauged. Representativeness of a sample in such cases is secured by intentional choice relying on logical judgement. The selected set of gauged small basins represents the main physiographic features of Slovakia: the basic macroforms of relief, (mountain range, basin, lowland) and diversity of substrate classes (crystalline, limestone, dolomite, flysch, volcanic rocks, and loess). This intentional choice resulted in a sample of 158 small basins.

From the database of basin characteristics (Solín et al., 2000) the following were taken into account: 1) mean annual precipitation in the period 1976-1995, 2) maximum altitude, 3) mean altitude, 4) relative altitude, 5) mean inclination of slopes, 6) aspect: percentage of slopes in the basins oriented to the north, 7) classes of permeability of rock complexes 8) classes of permeability of weathering mantle, 9) percentage of urbanized and technicized areas, 10) percentage of arable land 11) percentage of forest, 12) percentage of meadows and pastures, and 13) percentage of alpine meadows and rock relief. The characteristics were obtained by overlaying layers of the digital model of relief (Šúri et al., 1997), land cover (Feranec et al., 1996), hydrogeology (Porubský, 1980), isohyetes (Faško, 1998) by the layer of the small basins (Solín, Grešková, 1999) in the environment of GIS.

For each selected basin hydrological data on the mean daily maximum annual runoff of a 20-year period 1976-1995 were available. The primary hydrological data were transformed into the normalized form by dividing the values of the mean daily maximum annual discharges by their arithmetical average.

The at-site statistics, which describe the shape of flood frequency distribution (location, variation, skewness and curtosis) were estimated by the *L*-moments method (Hosking, Wallis, 1997). The sample *L*-moments are defined as follows:

(2) $$l_1 = b_0$$

(3) $$l_2 = 2b_1 - b_0$$

(4) $$l_3 = 6b_2 - 6b_1 + b_0$$

(5) $$l_4 = 20b_3 - 30b_2 + 12b_1 - b_0$$

where b_0 to b_3 are sample estimates of probability weighted moment β_r according to

(6) $$b_r = n^{-1} \sum_{j=r+1}^{n} \frac{(j-1)(j-2)\ldots(j-r)}{(n-1)(n-2)\ldots(n-r)} x_{j:n}$$

where $x_{j:n}$ is the ordered sample of the dimensionless mean daily maximum annual runoff, where $x_{1:n} < x_{2:n} < x_{n:n}$. *L*-moments ratios:

(7) $$t = l_2 / l_1$$

(8) $$t_3 = l_3 / l_2$$

(9) $$t_4 = l_4 / l_2$$

then express the sample coefficients of *L*-variation (*L*-Cv), *L*-skewness and *L*-curtosis respectively. The values t, t_3 and t_4 were determined for each basins of the selected set.

3.2 The relationship between the basin characteristics and at-site statistics

It is considered that among the at-site statistics, the coefficient of *L*-variation (*L*-Cv) has a larger effect on estimates of extreme quantiles than *L*-skewness or *L*-curtosis (Hosing, Wallis, 1997), because it influences the slope of the dimensionless growth curve. This is the reason why emphasis is laid upon identifying regional variability of *L*-Cv. Firstly basin characteristics controlling the spatial variability of *L*-Cv are determined and secondly their differentiation values, which delimit the distinctly different groups of basins in terms of *L*-Cv are identified. The assessment of the influences of the considered basin characteristics on the spatial variability of *L*-Cv can be done by numerical methods. For example, the method of partial coefficient of correlation, the method of reduction of variance or factor analysis can be used. However, the numerical methods do not allow for identifying of differentiation values of basin characteristics. Regarding the aim of the analysis the graphical method (point plot) for analysing the relation of *L*-Cv versus basin characteristic is preferable. Values of *L*-Cv are on the co-ordinate *y* and the basin characteristic values are on the co-ordinate *x*. Dispersion of points suggest then the degree of dependence and differentiation values can be read at plot.

3.3 Identification of regional units in the space of basin characteristics

Regional types of flood frequency behaviour are identified only in the space of basin characteristics controlling spatial variability of *L*-Cv by two approaches: i) the method of hierarchic and non hierarchic cluster analysis and ii) the method of logical division. In the sense of terminology used by regional taxonomy (Fischer, 1987, Bezák, 1996) the regional type, in contrast to other regional unit - region, represents a set of the basic spatial units, which are not contiguous in geographical space.
In the case of application of hierarchic methods the basins are clustered into classes by the method of average linkage and the centroid method. In both cases the Euclidean distance expresses the measure of similarity. In the first case, two such clusters having minimum average distances are joined into one cluster. In the second case those two clusters with similar centroid are merged. From non-hierarchic methods the method of *K*-means is used. The algorithm attempts to minimize the total sum within cluster variance. The minimum value of the overall sum of the within cluster dispersion is reached by iterative relocation of the units between an a priori chosen number of clusters. For more information on the clustering algorithms of the quoted numerical methods, see for instance Andeberg (1972) or Gordon (1981). The statistical software GENSTAT was used for their application.
By method of logical division basins were discriminated into classes, which where created on the basis of differentiation values of basin characteristics controlling the spatial variability of *L*-Cv. Besides logical division on the basis of single basin characteristics their mutual combination was also applied.

3.4 Testing of heterogeneity between and the homogeneity within the identified regional types from the point of view of *L*-Cv

The regional types identified by different ways in the space of basin characteristics are tested in terms of three categories of hydrological consequences:
1) hydrological efficiency of the classification scheme as a whole. The zero hypothesis on equality of population regional values τ^{Rk} that is $H_0 = \tau^{R1} = \tau^{R2} =, \ldots, \tau^{Rk}$ is tested. The testing criterion is the empirical value *F* that is expressed by the equation

$$F = \frac{\sum_k \left(t^{Rk} - t^T\right)^2 / k - 1}{\sum_k \sum_j \left(t_{jk} - t^{Rk}\right)^2 / n_T - k} \tag{10}$$

where
t^T is the total arithmetic mean of t_j values of the chosen set
t^{Rk} is the arithmetic mean of t_j values of the *k-th* regional unit
t_{jk} is the value *t* in *j-th* basin of the *k-th* regional unit
k, n_T are the number of regional units and the total number of basins respectively

If the empirical F value is higher than the value F distribution at the significance level $\alpha_{0,05}$, then the hypothesis on equality of regional values τ^{Rk} is rejected. The higher the empirical F value, the more accurately is the regional variability L-Cv expressed through regional types identified in the space of basin characteristics.
2) heterogeneity of regional types in terms of regional values τ^{Rk}. The zero hypotheses that there is no difference between regional values τ^{Rk} that is H_0: $\tau^{R1} - \tau^{R2} = 0,\ldots,H_0$: $\tau^{Ri} - \tau^{Rk} = 0$ are tested. The hypotheses are tested by the method of pairwise comparison (Neter et al., 1985). Let the difference δ between the population regional values τ^{Ri}, τ^{Rm} be

(11) $$\delta = \tau^{Ri} - \tau^{Rm}$$

The point estimator of δ is

(12) $$\hat{D} = t^{Ri} - t^{Rm}$$

Assuming that t^{Ri} and t^{Rm} are independent, the estimated variance of δ is

(13) $$s^2\left(\hat{D}\right) = MSE\left(1/n_i + 1/n_m\right)$$

where MSE is the mean square error. Then the confident interval for δ is

(14) $$\hat{D} \pm t(1-\alpha/2;\, n_t - k)\, s\left(\hat{D}\right)$$

Zero hypotheses on no difference between regional values τ^{Rk} are rejected if at the significance level $\alpha_{0,05}$ zero is not part of the confident interval.
3) homogeneity of the at-site values within the regional type. The zero hypotheses that there is no difference between at-site L-Cv values in the regional type is tested. The testing criterion is the S statistic used by Wiltshire (1986a). The statistic S has χ^2 distribution and compares differences between the at-site L-Cv values and the regional L-Cv value with differences, which are the result of sampling variation of L-Cv and which would occur in the case that the regional type was homogeneous. The form of S statistic is

(15) $$S = \sum_j \frac{\left(t_j - t^{Rk}\right)^2}{u_j}$$

where u_j is sampling variation of L-Cv, which is given by

(16) $$u_j = V/n_j$$

where V term is the average of the jack-knife variance (Parr, 1983), which was computed for each site within the regional type. The zero hypothesis is rejected, if S statistic value is higher than the value χ^2 distribution at the significance level $\alpha_{0,05}$.
Beside the homogeneity assessment of the regional type basins (outliers) of which L-moment ratios are not concordant with the variance within regional type were also identified according discordance measure, which was introduced by Hosking, Wallis (1997). The level of discordance is defined as

(17) $$D_i = \frac{1}{3} N \left(\mathbf{u}_i - \bar{\mathbf{u}}\right)^2 \mathbf{A}^{-1} \left(\mathbf{u}_i - \bar{\mathbf{u}}\right)$$

where

(18) $$\mathbf{u}_i = \left[t^i\ t_3^i\ t_4^i\right]$$

$\bar{\mathbf{u}}$ = group average of $\mathbf{u}_i$ and

$$\mathbf{A} = \sum_{i=1}^{N} \left(\mathbf{u}_i - \bar{\mathbf{u}}\right)\left(\mathbf{u}_i - \bar{\mathbf{u}}\right)^T$$

The critical value of statistics D_i changes with the number of basins in the regional unit. The critical value equals 3 for 15 and more basins. Basins with such or higher value are considered as outliers and require additional examination of why this value is so high.

4 RESULTS ACHIEVED

Analysis of point plots suggested that from thirteen considered basin characteristics only mean annual precipitation and mean altitude of the basin have an important influence on the spatial variability of *L*-Cv (Figure 4-1, Figure 4-2). The awaited influence of forestation or permeability of basin on the spatial variability of the *L*-Cv values did not appear at this hierarchic level. The selected range of basin areas (small basins) eliminated the effect of basin size. Values of *L*-Cv decrease with increasing values of the annual precipitation or mean altitude of the basin. These two characteristics
also control the water yield of the basin represented by its mean annual runoff (Solín, Cebecauer, 2000). Therefore the *L*-Cv values decrease with increasing mean annual runoff too (Figure 4-3). This agrees with the knowledge pointed out by Wiltshire (1986a) that the driest basins will tend to experience a range of soil moisture conditions, which in turn result in a range of percentage runoff and hence a range of flood magnitudes. Basins in a high rainfall region will tend to generally uniformly large floods with correspondingly little variation in the annual maximum series.

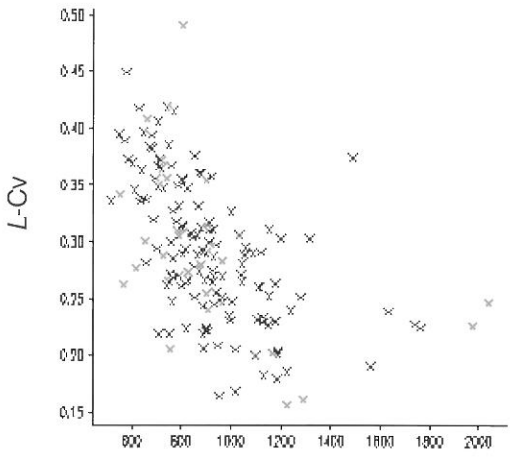

mean annual precipitation (mm)

Figure 4-1: Relationship *L*-Cv vs precipitation

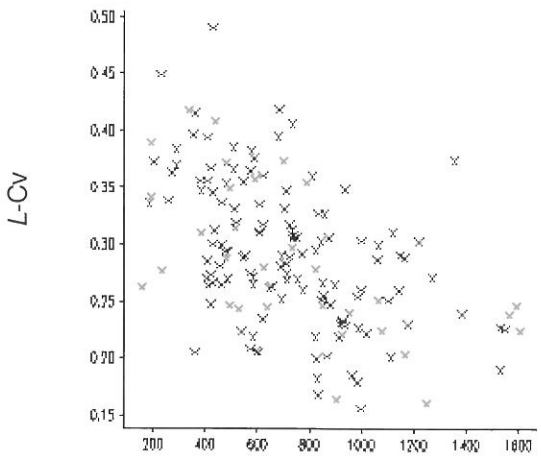

mean altitude (m a.s.l.)

Figure 4-2: Relationship *L*-Cv vs altitude.

On the basis of analysis of point plots: *L*-Cv versus mean annual precipitation, *L*-Cv versus mean altitude and *L*-Cv versus mean annual runoff of basin the following differentiation values were identified: 700, 950, and 1 500 mm; 300, 800, 1 500 m a.s.l.; 150, 300, 500, and 1 000 mm respectively, which delimit the different groups of basins in terms of the *L*-Cv values. The number of differentiation values then suggests that, in the space of mean annual precipitation and mean altitude or in the space of annual average runoff four or five regional units should be delimited.
Identification of four regional units by average linkage method and group average in the space of the mean annual precipitation and mean altitude was achieved by a cutting dendogram at the level of similarity of 94 or 95.5% respectively. In case of using the *K*-means methods, four classes of basins were determined a priori. The differentiation values of mean annual precipitation suggest formation of the following classes by logical division: *I*) less than 700 mm, *II*) 701-950 mm, *III*) 951-1 500 mm, and *IV*) more than 1 500 mm. On the basis of differentiation values of mean altitude the following classes were formed: *I*) less than 300 m a.s.l., *II*) 301-800 m a.s.l., *III*) 801-1 500 m a.s.l. and *IV*) more than 1 500 m a.s.l. A further four regional types were identified on the basis of combination of the mean annual precipitation and the mean altitude (Figure 4-4): *I*) annual precipitation (P) less than 950 mm and mean altitude (A) less than 325 m a.s.l., *II*) P - less than 950 mm and A - 351-700 m a.s.l., *III*) P- less than 950 mm and A- more than 700 m a.s.l., *IV*) P- more than 950 mm and A - more than 700 m a.s.l. Finally the basins were also clustered into five regional units on the basis of the differentiation values of the mean annual runoff: *I*) less than 150 mm, *II*) 151-300 mm, *III*) 301-500 mm, *IV*) 501-1 000 mm, *V*) over 1 000 mm.

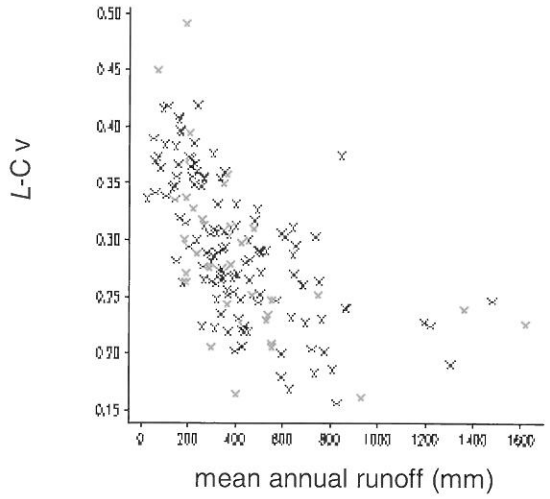

Figure 4-3: Relationship *L*-Cv vs runoff

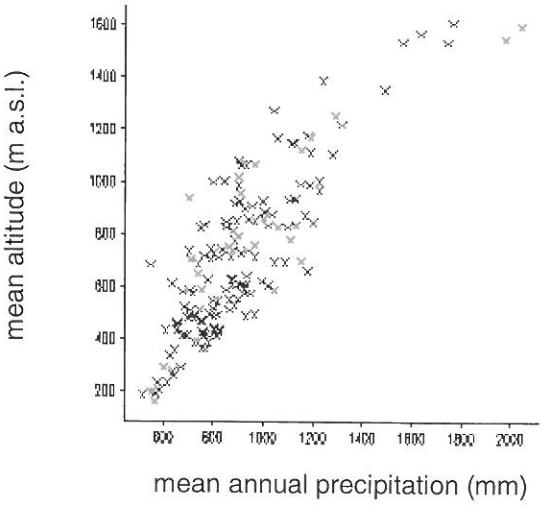

Figure 4-4: Relationship altitude vs precipitation.

Table 4-1 presents the basic hydrological consequence of the regional types delimited in the space of mean altitude, mean annual precipitation and mean annual runoff by different methods. The regional values t^{Rk} decrease from regional type *I* to regional types *IV* or *V*. Regional type *I* includes basins with low values of mean altitude, mean annual precipitation and mean runoff and in the regional type *IV* basins with the highest values of the above-mentioned characteristics prevail.

Table 4-1: Regional values of *L*-Cv and the number of basins in the regional types delimited by different methods.

method of regional typification	regional types t^R / number of basins				
	I	*II*	*III*	*IV*	*V*
HC-average linkage	*0,3304*/68	*0,2624*/69	*0,2503*/12	*0,2464*/7	
HC-group average	*0.3609*/13	*0,3118*/74	*0,2561*/50	*0,2489*/19	
NHC-K means	*0,3354*/51	*0,2937*/54	*0,2412*/44	*0,2464*/7	
LD-altitude	*0,3525*/11	*0,3108*/87	*0,2505*/52	*0,2252*/6	
LD-precipitation	*0,3539*/24	*0,3003*/82	*0,2450*/35	*0,2252*/6	
LD- P + A	*0,3579*/12	*0,3167*/60	*0,2903*/34	*0,2426*/50	
LD- average runoff	*0,3657*/17	*0,3317*/40	*0,2756*/56	*0,2415*/37	*0,252*/6

HC – hierarchical cluster analysis, NHC – nonhierachichal cluster analysis, LD – logical division

The results of testing the overall hydrological efficiency as well as significance of pairwise differences of regional values of *L*-Cv between the regional types identified by different methods are given in Table 4-2.

Table 4-2: Results of the tests of hydrological consequences.

method of regional typification	*F*-test	non significant confidence interval for δ
HC-average linkage	22,65	2-3, 2-4, 3-4
HC-group average	21,68	3-4
NHC-K means	27,68	3-4
LD-altitude	21,18	3-4
LD-annual precipitation	28,33	3-4
LD-P+A	25,19	-
LD-average runoff (5)	30,21	4-5
LD- average runoff	40,07	-

The critical value of *F* distribution at the significance level $\alpha_{0.05}$ for 3 and 152 degrees of freedom is 2.43. The zero hypothesis on equality of regional values τ^{Rk} is rejected by all methods. With regard to the small differences among *F* values (with the exception of clustering the basins into regional types by logical division on the basis of mean annual runoff), any of the quoted methods could be used for

clustering basins into regional types. However, the pairwise comparison of the differences between regional values t^{Rk} shows a distinct difference among methods in terms of justification of the identified number of regional types from the hydrological point of view. Only two regional types can be delimited by the method of average linkage. The differences between the regional types *II*, *III* and *IV* in terms of the regional values t^{Rk} are not statistically significant and hence they are not heterogeneous. The regional types delimited by the group average, *K*-means, logical division (LD-altitude, LD-precipitation) more accurately identify regional variability of *L*-Cv. In this case delimitation of three regional types is justified. There is no statistically significant difference from the viewpoint of regional values t^{Rk} only between the regional types *III* and *IV*. All four regional types show statistically significant differences between the regional *L*-Cv values, when they are identified by the LD-P+A method. Further precision of the *L*-Cv regional variability can be attained, when regional units are delimited on the basis of mean annual runoff. Delimitation of four regional units on the basis of differentiation values 150, 300, and 500 m results in *F* ratio value 40.07 and all pair differences between the regional values t^R are statistically significant. In case of identification of five regional types as was originally suggested by four differentiation values, there is no statistically significant difference between fourth and fifth regional type in terms of t^R.

Homogeneity of regional types from the viewpoint of the at-site *L*-Cv values was numerically tested only in case of regional units delimited on the basis of average annual runoff by the method of logical division (LD-average runoff), because it is the best way of identifying the regional variability of *L*-Cv compared with all the considered ways. The discordance measure was also calculated for each basin of regional type in this case. The result of comparing the calculated values of statistic *S* with the critical values χ^2 distribution at the significance level $\alpha_{0.05}$ suggests that the delimited regional types are homogeneous from the point of view of the at-site *L*-Cv values (Table 4-3). No outliers occur in the regional type *I* (basins with D_i more than 3). In the regional type *II* there are three basins having D_i value larger than 3 (Hanušovce nad Topľou - Medziansky creek: D_i =3.804, Sološnica-Sološnický creek: D_i = 4.899, Oslany-Oslanský creek: D_i = 3.625). The regional type III contains one basin (Valča-Hlinický creek: D_i = 3,461) and the regional type IV also contains one basis (Ľubochňa - *Ľubochniansky creek:* D_i = 3.461) with the value D_i larger than 3.

Table 4-3: Results of testing the homogeneity of regional types identified by the LD-average runoff method.

	Regional types			
	I	*II*	*III*	*IV*
S statistic	0.384	1.642	2.215	2.579

5 CONCLUSION

Identification of the regional units of flood frequency behaviour expressed by the coefficient of *L*-variation (*L*-Cv) in the space of basin characteristics is the first step of the regional flood frequency analysis. The regional units were identified in the space of mean annual precipitation and mean altitude, which control spatial variability of *L*-Cv values by hierarchic and nonhierachic cluster analysis and by logical division. Mean annual runoff as another characteristic controlling spatial variability of *L*-Cv was taken into account. In the space of mean annual precipitation and mean altitude or in the space of annual average runoff the number of differentiation values suggests that four or five regional units should be delimited. The study emphasises the testing of heterogeneity between the regional types from the point of view of their regional *L*-Cv values by the method of pairwise comparison. It is not justified to delimit the regional types, which are homogeneous but are not distinct inter se as two different regional types. The pairwise comparison of the differences between regional *L*-Cv values shows that the best way of grouping small basins into regional types is reached by the logical division based on combination of differentiation values of mean annual precipitation and mean altitude or on differentiation values of mean annual runoff. In these two cases all differences between the four identified regional types in terms of regional *L*-Cv values are statistically significant and regional types are mutually heterogeneous. In case of using cluster analysis (group average algorithm and K-means method) and logical division based on differentiation values of mean altitude and annual precipitation there are no significant differences in terms of regional *L*-Cv values between 3 and 4 regional types. Finally, by using the hierarchic clustering with average linkage algorithm, heterogeneity of regional types is identified only between the first and the fourth regional types. Regional types identified by the method of logical division on the basis of three differentiation values of the mean annual runoff were

also tested from the point of view of homogeneity of the at site *L*-Cv values. The result of the test showed their inner homogeneity.
The ungauged basins is possibly to classify into four heterogeneous regional types on the basis of their values of mean annual precipitation total and mean altitude or according the values of mean annual runoff, which are estimated by regression equation

ACKNOWLEDGEMENT

This research is a part of grant project 2/7050/20 " Hydrogeographical regional type of Slovakia – problem of extrapolation of hydrological values and rational exploiting of water resources", which is supported by VEGA agency. Author wish to express thank to Slovak Hydrometeorological Institute for supplying discharge and precipitation data used in this study.

REFERENCES

Acreman, M. C., Sinclair, C. D. (1986): Clasification of drainage basins according to their physical characteristics; an application for flood frequency analysis in Scotland. Journal of Hydrology, 84, 365-380. Elsevier. Amsterdam.

Acreman, M. C., Wiltshire, S. E. (1987): The regions are dead; long live the regions. Methods of identifying and dispensing with regions for flood frequency analysis. IAHS Publication, No.187, 175-188. Wallingford.

Andeberg, M. R. (1972): Cluster analysis for application. NTIS. New Mexico.

Armand, D. L. (1972): Nauka o landšafte. *Mysľ*. Moskva.

Bezák, A. (1996): Regional taxonomy: A review of problems and method. Acta Facultatis Rerum Naturalium Universitatis Comenanae, Geographica, 28, 43-59. Bratislava.

Burn, D. H. (1990): Evaluation of Regional Flood Frequency Analysis With a Region of Influence Approach. Water Resources Research, 26, 2257-2265. AGU. Washington.

Burn, D. H., Goel, N. K. (2000): The formation of groups for regional flood frequency analysis. Hydrological Sciences-Journal, 45, 97-112. IAHS. Wallingford.

Chowdhury, J. D. et al. (1991): Goodness-of-Fit Tests for Regional Generalized Extreme Value Flood Distributions. Water Resources Research, 27, 1765-1776. AGU. Washington.

Dalrymle, T. (1960): Flood frequency analyses .Water Supply Paper 1543-A, U.S. Geological Survey, Reston, Va.

Cunnane, C. (1988): Method and merits of regional flood frequency analysis. Journal of Hydrology, 100, 269-290. Elsevier. Amsterdam.

Faško, P. (1998): Map of isolines of mean annual precipitation 1976-1995 (manuscript). Slovak Hydrometeorological Institute. Bratislava.

Feranec, J. et al. (1996): Krajinná pokrývka Slovenska. Identifikovaná metódou Corine land cover. Geographia Slovaca, 11. Bratislava.

Fischer, M. (1987): Some fundamental problems in homogeneous and functional regional taxonomy. Bremer Beiträge zur Geographie und Raumplanung, 11, 267-282. Bremen.

Gordon, A. D. (1981): Classification. Chapman and Hall. London.

Greis, N. P., Wood, E. F. (1981): Regional flood frequency estimation and network design. Water resorces research, 17, 1167-1177. AGU. Washington.

Grigg, D. (1969): The logic of regional systems. Annals of the Association of American Geographers, 55, 465-491. Blackwell. Malden.

Hosking, J. R. M., Wallis, J. R. (1997): Regional frequency annalysis. An approach based on L-moments. Cambridge University Press. Cambridge.

Lettenmaier, D. P., Potter, K.W. (1985): Testing flood frequency estimation methods using a regional flood generation model. Water resources research, 21, 1903-1914. AGU. Washington.

Lettenmaier, D. P. et al. (1987): Efect of regional heterogeneity on flood frequency estimation. Water resources research, 23, 313-323. AGU. Washington.

Mosley, M. P. (1981): Delimitation of New Zealand hydrological regions. Journal of Hydrology, 49, 173-192. Elsevier. Amsterdam.

Neter, J. et al. (1985): Applied linear statistical models. Home Wood. Illinois.

Paar, W. C. (1983): A note on the jacknife, the bootstrap and delta method estimators of bias and variance. Biometrika, 70, 719-722. London.

Porubský, A. (1980): Hydrogeology. In: Mazúr, E. (ed). Atlas SSR, Geografický ústav SAV, Slovenský úrad geodézie a kartografie, 34-35. Bratislava.

Rosbjerg, D., Madsen, H. (1995): Uncertainty measures of regional flood frequency estimators. Journal of Hydrology, 165, 209-224. Elsevier. Amsterdam.

Solín, Ľ., Grešková, A. (1999): Malé povodia Slovenska - základné priestorové jednotky pre jeho hydrogeografické regionálne členenie. *Geografický časopis, 51, 77-96.* Bratislava.

Solín, Ľ. et al. (2000): Small basins of Slovakia and their physical characteristics. Institute of Geography and Slovak Committee for Hydrology, Bratislava.

Šúri, M. et al. (1997): Tvorba digitálneho modelu reliéfu Slovenskej republiky. Geodetický a kartografický obzor, 43, 257-262. Bratislava.

Wiltshire, S. E. (1986a): Identification of homogeneous regions for flood frequency analysis. Journal of hydrology, 84, 287-302. Elsevier. Amsterdam.

Wiltshire, S. E. (1986b): Regional flood frequency analysis I: homogeneity statistics. Hydrological Sciences Journal, 31, 321-333. IAHS. Wallingford.

Wiltshire, S. E. (1986c): Regional flood frequency analysis II: multivariate classification of drainage basins in Britain. Hydrological Sciences Journal, 31, 335-372. IAHS. Wallingford.

OUTSTANDING FLOODS IN EUROPE; A REGIONALIZATION AND COMPARISON

Viorel Alexandru Stanescu

National Institute of Meteorology and Hydrology, Hydrology Division, Sos. Bucuresti-Ploiesti 97, Bucharest 71552, Romania, stanescu@meteo.inmh.ro

SUMMARY

More than 600 historical, outstanding floods that occurred across Europe are considered in the work. From different published sources a catalogue of the very large floods of Europe has been compiled. The catchment areas of the selected stations (or river cross sections) range between a couple of square kilometres to more than hundred thousands. The main historical floods in Europe and their characteristic features are considered both regarding the flash floods and the lent floods. Then, regionalization relationships between specific peak discharges and the basin areas belonging to "macroscale" river flow regimes are drawn. The envelope curves of the regionalization relationships show the differences in the flood potential for the main river flow regimes. Some examples of outstanding historical rainstorms, which generate flash floods, are presented.
Concerning the flood potential a comparison between floods (flash and lent ones) that occurred across different areas within Europe has been carried out. The upper envelope curves of the specific peak discharge against the basin area are those occurred in Mediterranean regions of France and Italy.
In the second part of the work, for some climatic regions in Europe, a more detailed regionalization at "macroscale" as resulted from the physiographical peculiarities of the river catchment is considered.

Keywords: rainstorm, rain intensity, peak discharge, flash floods,

1 INTRODUCTION

The cognizance of very large floods offers to the hydrologists as well to the water policy and decision makers very valuable information enabling (i) identification of the zones of hazards and the estimation of the hazard, (ii) the achievement of a spatial-temporal analysis of the vulnerability to floods and the assessment of the flood risk, (iii) the design and establishment of monitoring warning and forecasting systems, (iv) the planning and the building of the preparedness and prevention measures for flood effect mitigation, (v) the education of the people that is jeopardised by the floods on the perception and correct understanding at risk and (vi) the development of the research in the domain of the natural sciences, of psychology of the communities coping with the flood danger as well as with the effect on the society and ecology.
The transfer between countries of knowledge concerning recorded and/or reconstructed outstanding floods enables better understanding of causes and processes of flood potential, flood formation and a more accurate estimation of the synthetic statistical characteristics.

2 DATA SOURCES

The assessment of the flood peak discharges produced in old historical times is very difficult to be achieved and there is only little information on such data. Some information concerning the reconstructed maximum discharges of outstanding floods is available for Main River (Germany) in 1342, 1451, 1546, 1682 and 1784 (Schiller, 1987) for Isère River (France) in 1651, 1740 and 1800, for Seine River (France) in 1658 (Rodier, Roche, 1984) and the Mulde River (Germany) in 1573.
More and reliable information on very large floods in Europe has been available since the nineteen century. Selected data concerning outstanding floods produced before XX-th century are presented in Table 2-1.
This study of the outstanding floods in Europe is based upon (i) the old historical data on maximum discharges and on the flood peak discharges and rainstorms causing floods that have been published in the international catalogues (Kikkawa, Stanescu,1976), (Rodier, Roche, 1982), (ii) the hydrological monographs (Wien-Hydrograph. Central Bureau, 1898), (Suisse-Insp. Federale, 1958), (Pardé, 1961), (Stanescu, 1967), (UNESCO-IHP-reg. cooperation, 1986), (Spreafico, Stadler, 1988), (Spreafico, Aschwanden, 1991), (Engel, 1996), (iii) the hydrological yearbooks of Romania, Austria, Yugoslavia and Hungary. Also, more than 40 scientific papers containing information and description of the characteristics, causes and the flood formation processes of outstanding floods occurred in the XXth century in Europe were used.

Table 2-1: Outstanding floods in Europe before XX-th Century.

Country	*Basin*	*River*	*Station*	*Basin area [km²]*	*Q_{max} [m³/s]*	*Date*
Austria	Danube	Danube	Wien	101700	14000	.08.1501
					11800	01.11.1787
		Inn	Innsbruck	5794	1350	17.06.1855
					1210	19.06.1871
		Traun	Wells	3499	1660	13.09.1899
Czech Rep.	Elbe	Elbe	Decin	51100	5600	30.03.1845
Germany	Rhine	Rhine	Maxau	50196	4620	28.12.1882
		Nekar	Heidelberg	13809	7400	01.05.1883
					4000	30.10.1824
					3000	28.12.1882
		Mosel	Cochem	27100	3640	28.11.1882
		Main	Wűrzburg	14031	3300	22.07.1342
	Wesser	Wesser	Intschede	37790	4650	21.01.1841
	Elbe	Elbe	Dresden	53100	4350	06.09.1890
		Mulde	Golzeen	5440	2200	14.08.1573
	Danube	Danube	Hofkirchen	47496	4470	31.03.1845
France	Rhone	Rhone	Lyon	20300	4500	31.05.1856
			Beaucaire	96500	10000	31.05.1856
		Drome	Livron	1640	1300	.09.1842
		Durance	Pont.	11900	5100	25.10.1882
		Isère	Grenoble	5720	2500	11.11.1651
					2000	20.12.1740
	Loire	Loire	Gien	35900	8500	02.06.1856
		Allier	Moulin	13000	7000	.11.1790
	Garonne	Garonne	Agen	34900	8500	.06.1875
Italy	Adige	Adige	Trento	9770	2500	17.09.1882
	Po	Ticino	Miorina	6600	5000	02.10.1868
Portugal	Tejo	Tejo	Vila Velha	59170	12000	07.12.1876
Romania	Danube	Danube	Orsova	575000	15900	17.04.1895
					15400	07.06.1897
Russia	Neman	Neman	Smolnikai	81200	6820	30.04.1829
Spain	Guandiana	Guandiana	Badajos	48515	10000	07.12.1877
	Ebro	Ebro	Zaragoza	40430	3800	18.12.1889
Sweden	Dalaven	Dalaven	Norslund	25300	2640	01.06.1860
Switzerland	Rhine	Rhine	Basel	35925	5700	13.06.1876
	Po	Ticino	Belinzona	1515	2500	28.09.1868
United Kingdom	Dee	Dee	Cairnton	1370	1900	.08.1829
	Thyne	Thyne	Hexam	3900	1970	.1771
Yugoslavia	Sava	Drina	Visegrad	11000	10000	.1896

More than 600 historical, outstanding flood peak discharges that occurred across Europe have been considered and a computer file of a catalogue has been compiled. That contains name of the country, river, hydrological station (or location), basin area, peak discharge and citation of the documentation source. Besides, the computed maximum specific discharge (l/skm^2) has been added. The catchment areas of the selected stations (locations) range between a couple of square kilometres and more than hundred thousand, as shown in Table 2-2.

Table 2-2: Distribution of basin areas corresponding to the selected basin locations.

Area [km^2]	*<10*	*10÷50*	*51÷100*	*101÷500*	*501÷2000*	*2001÷5000*	*5001÷10000*	*>10000*
Number of locations	14	53	50	153	127	81	52	74

The distribution of the number of inventoried locations with data on large floods is given in Table 2-3.

Table 2-3: Distribution of the stations (locations) in the European countries.

Country	*Number of selected stations (locations)*	*Country*	*Number of selected stations (locations)*	*Country*	*Number of selected stations (locations)*
Albania	5	Greece	1	Slovakia	12
Austria	17	Hungary	20	Slovenia	5
Bosnia-Herzegovina	8	Italy	46	Spain	50
Bulgaria	8	Moldavia	1	Switzerland	47
Croatia	5	Netherlands	7	Ukraine	13
Czech Republic	31	Poland	8	United Kingdom	64
France	117	Portugal	7	Yugoslavia	24
Germany	51	Romania	57		

Many of the maximum discharges contained in the catalogue have return periods that exceed 80 - 100 years and there are many events of flood having a regional development across large areas.
Among the outstanding floods that occurred across large basins the following ones have to be mentioned:

- The Rhine River floods occurred in December 1925, December 1993-January 1994 and January 1995 in Germany and Netherland. In many points the return period exceeded 50-100 years (Engel et al., 1994), (Ebel, Engel, 1995), (Ebel, Engel, 1996).
- The Danube River basin floods occurred in March-April 1988 occurred in Germany, April 1895 in Yugoslavia, Hungary and Romania and June 1897 occurred in Austria, Hungary, Yugoslavia and Romania. The return period of these floods was comprised between 80-100 years. (Stanescu, 1967)
- The Elbe and Wistla river basins flood occurred in July 1997 in Germany, Czech Republic and Poland. This flood has a return period of 50-100 years and more (Kubat, Vrabec, 1999), (Kindler, 1998).
- Among the most severe floods that occurred in medium size basins the following are worth to be mentioned:
- The flood of 10-15 May, 1970 in the river basins of Transylvania – Romania (Stanescu, 2000) that has a return period ranging between 70-200 years.
- The flood of 4-5 November 1994 in the Po river basin (Italy) having a return period in the upper part of 80-100 years (Marchi et al., 1995).
- The flood of 4 November 1966 in Toscana region – Arno river basin (Italy); in the majority of area the return period exceeded 100 years (Bendini, 1967).
- The flood of 17 January 1993 in the Tay river basin (United Kingdom) that has at the outlet a frequency of 1/70-1/80 years (Black, Anderson, 1994).
- The flood of 10-12 December 1994 in the Strathclyde region (United Kingdom) as well as the greatest historical floods in August 1970 in Findhorm and 1771 flood in Tyne River, respectively Black, Benett, 1995).
- The flood of 5-7 November 1994 in the Alpes-Côtes d'Azur region (France) that has a frequency estimated at the outlet of Var river at 1/100 years (Diren, 1995)

The main criteria for selecting the outstanding floods was their as great as possible return period of the maximum discharge, where the frequency estimation was available and / or the exceptional values of the flood peaks that have been recorded or reconstructed.

In Figure 2-1 the specific recorded/reconstructed flood peak discharges $q_{\max}(l/skm^2)$ against the specific maximum annual discharges of 1% probability of exceedance $q_{\max}^{(1\%)}(l/skm^2)$ as a function of the basin area $F(km^2)$ are comparatively presented. The upper envelope of the specific flood peak discharges $q_{\max}$ is found in the domain of the specific annual discharges of 1% probability of exceedance $q_{\max}^{(1\%)}$. It means that in selecting the recorded floods the outstanding ones were deemed.

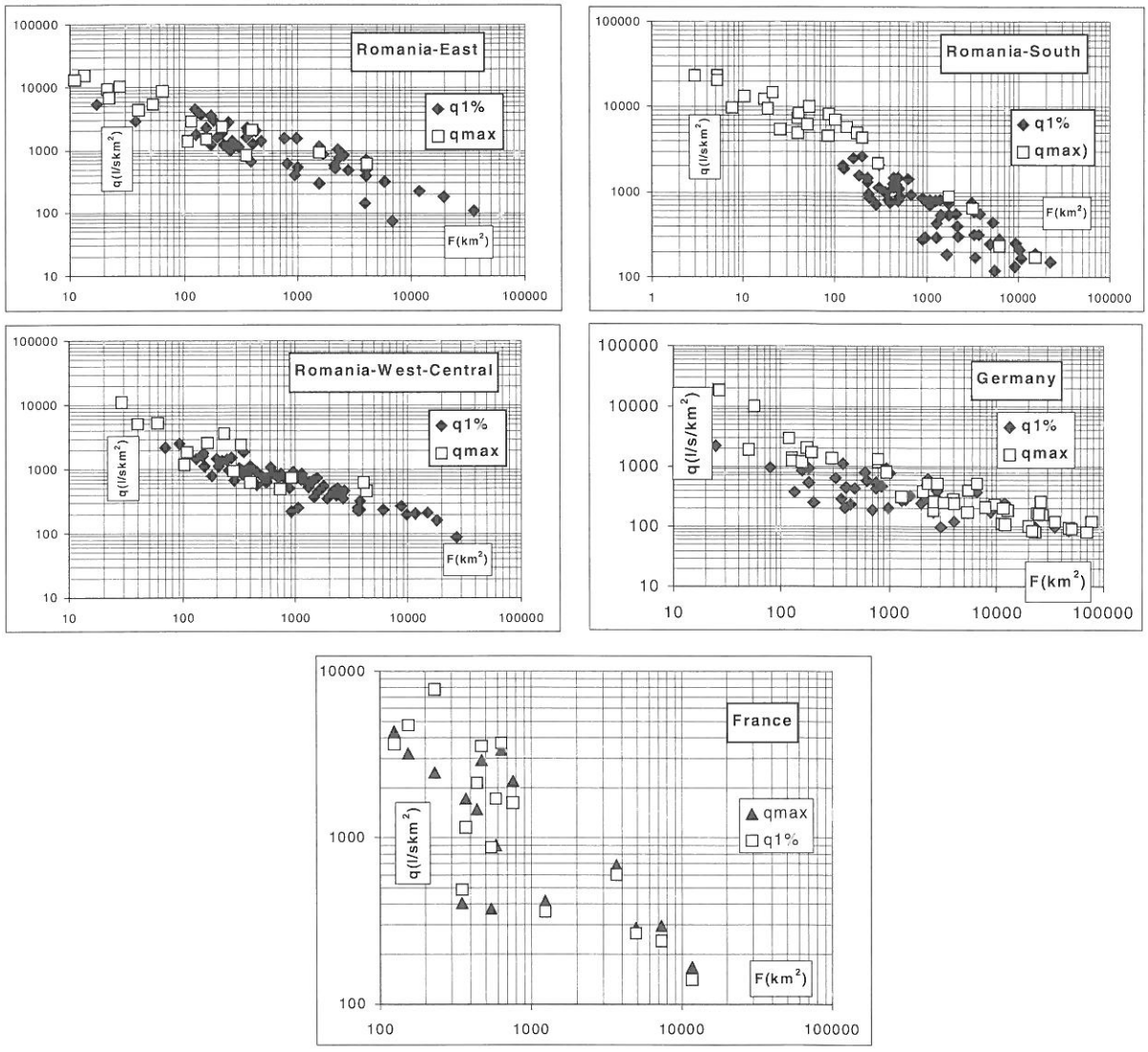

Figure 2-1: Specific recorded/reconstructed flood peak discharges and the specific maximum annual discharges of 1% probability of exceedance as a function of the basin area.

The flash floods having remarkable magnitudes have been also inventoried. The most severe ones in terms of maximum discharges (Q_{max}), generating rainstorms (P) and their duration (D), as well as the return period (T), are presented in Table 2-4.

Table 2-4: Selected outstanding flash floods in Europe.

Country	River	Station (location)	Basin area [km^2]	Q_{max} [m^3/s]	Date	P [mm]	Rainstorm duration	T [years]
France	Cadereaux	Nimes	42	1600	03.10.88	300	6h	200
	Ouvèze	Vaison la Romaine	580	1000	22.09.92	140	2h	1000
	Tech	Ceret	483	3500	17.10.40	360	6h	100
	Reart	Mas Palegry	137	1100	26.09.92	216	4h	100
	Solenzara	Canniciu	99.7	1575	31.10.93	794	24h	200
	Fiumicicoli	Outlet	97	1300	31.10.93	794	24h	300
Germany	Wolf	Outlet	14	225	03.08.51			
	Muglitz	Outlet	26.3	500	08.07.27	100	25'	-
	Gottleuba	Outlet	26.3	500	08.07.27	100	25'	-
United Kingdom	Farley	Lynmouth	17	286	15.08.52			
Italy	Orba	Orticlieto	141	2200	13.08.35	389	8h	-
	Ambra	Montorzi	158	726	04.11.66	437	24h	100
	Farma	Torniella	70	464	04.11.66	339	24h	100
	Magra	Calamazza	939	3480	15.10.60	205	24h	
	Oreto	Parco	75.6	352	26.10.51	147	6h	30-40
Romania	Cobia	Raciu	19	180	26.06.79	200	2h	200
	Potop	G.Foii	196	875	26.06.79	250	4h	200
	Mazgana	Outlet	17	209	03.07.75	150	4h	100
	V.Tatarani	Tatarani	3.0	70	21.06.80			200
	Hauzeasca	Hauzeasca	29.0	320	29.07.80	230	2h	200
	R. Mare	Gura Apelor Dam	234	850	12.07.99	250	2-3h	200

3 REGIONALISATION OF THE OUTSTANDING FLOODS IN EUROPE

Based on the estimates of the flood peak discharges $Q_{\max}$ comprised in the catalogue and the corresponding areas of the catchments, the specific maximum recorded/reconstructed discharges $q_{\max}$ have been computed. Then, the regionalization relationships of $q_{\max}$ with the area of the basins belonging to each country have been drawn. Some countries having similar features of the climate regime and somehow comparable aspect of the relief have been clustered into the same category of region. Thus, Romania, Bulgaria, Slovakia, Yugoslavia, Bosnia-Herzegovina, Croatia (Sava basin), Ukraine (Carpathian region) have been bunched together in the same category, likewise Spain and Portugal and Austria and upper mountains of Slovenia. The regional curves $q_{\max} = f(F)$ are presented in Figure 3-1. The upper envelope curves are those that produced in Italy and Mediterranean regions of France. This is the first group of $q_{\max} = f(F)$ curves. The second distinct group is formed of Germany, United Kingdom, Spain-Portugal as well as the countries belonging to the Carpathian and Balkan Mountains (Romania (RO), Bulgaria (BG), Yugoslavia (YU), Bosnia-Herzegovina (BO), Croatia (CR) - Sava basin, Ukraine (UK) and Hungary (West Carpathian Rivers)). The curves vary in a range of about 20-30% up to the discharges corresponding to the areas less than 200-300 km^2. The third grouping is formed of Austria-Switzerland (Rhone and Rhine basins) and the countries of the middle Europe (Czech Republic, Slovakia and Poland). The specific discharges vary in the range of 6000-9000 l/skm^2 for basin area of 10 km^2 and 3500-5000 l/skm^2 for basins having 100 km^2. The estimates of specific discharge became closer at 1000 km^2. Then, for basin area greater than 1000 km^2 the maximum discharges of the group Czech Republic, Slovakia and Poland become lesser than those of the Austria-Slovenia and Switzerland.
The fourth group formed of Sweden and Russia (European part except mountainous basin of Dnister River that becomes to the curve valid for Ukraine). The fifth group belongs to the plain areas of European countries among which Hungary (except the rivers coming from Carpathian Mountains).

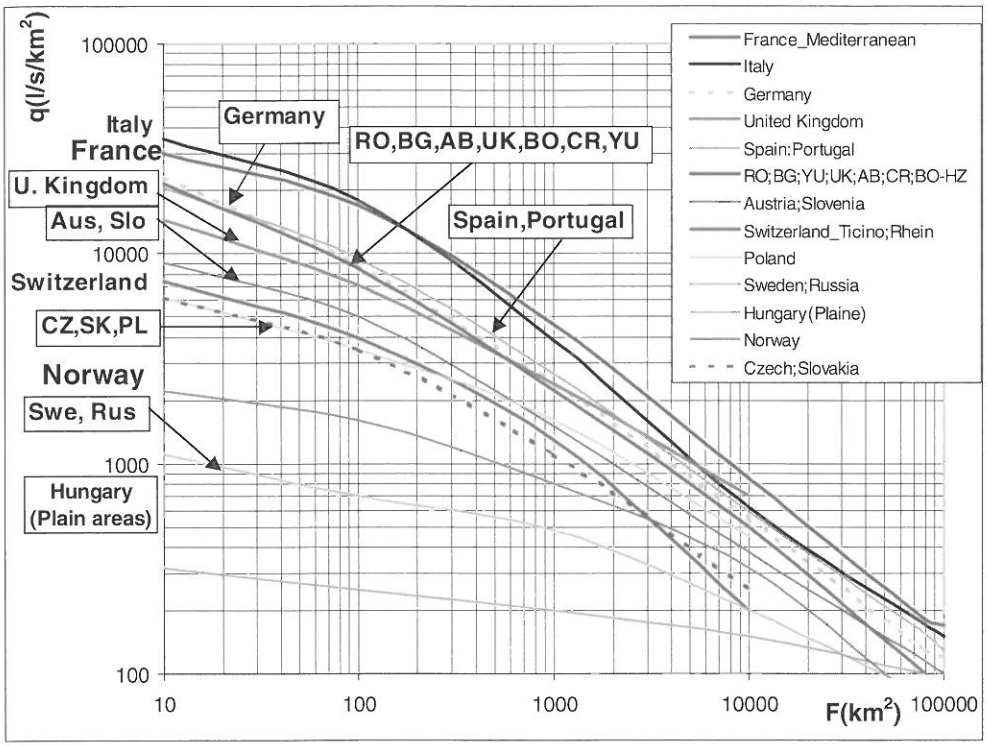

Figure 3-1: Regional curves of the maximum specific discharges of outstanding floods in Europe.

Mention is made that this regionalization has a "macro" character and the grouping that has been made is explainable rather by the different general climate features than by the relief characteristics. Some peculiarities of the morphological and especially of the precipitation regime might be considered for a somehow more detailed regionalization of the maximum specific discharge depending on the basin area. Such a more detailed regionalization could be achieved for the countries provided that the data on the flood peak discharges were both sufficient and representative from morphological features of the catchments point of view. As sufficient amount of data and representative ones as well have been collected for France (117 locations), Romania (180 locations) and Switzerland (47 locations) and the detailed regional $q_{\max} = f(F)$ only for these countries the regional detailed curves have been drawn (Figures 3-2, 3-3 and 3-4).
The distinct envelope curves in France are due to both the rainfall regime and the relief energy of the catchments that are found in each distinct group of regions. The high estimates of the specific peak discharges in the basins belonging to the côte Mediterannée are the result of the severe rainstorms in the area and the significant basin slopes both in Rhone-Alpes and in Mediterranean region.

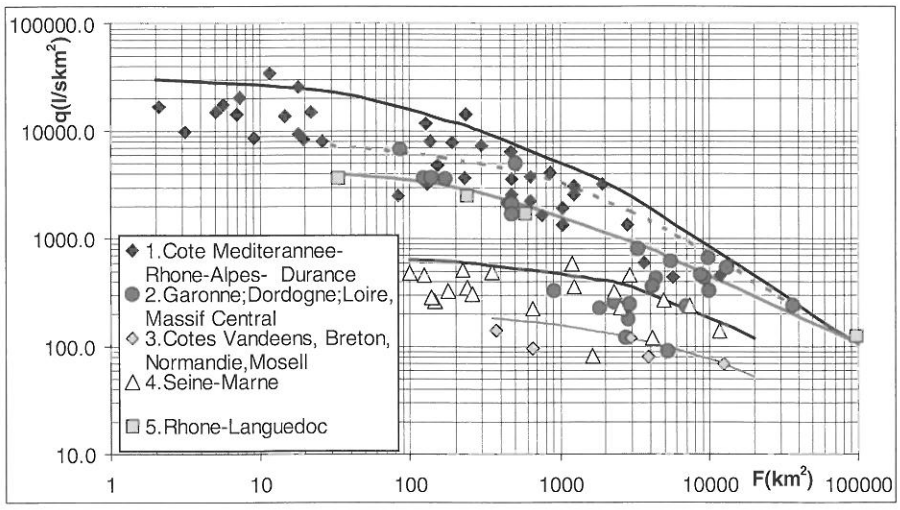

Figure 3-2: Regionalization of maximum specific discharge of outstanding floods in France.

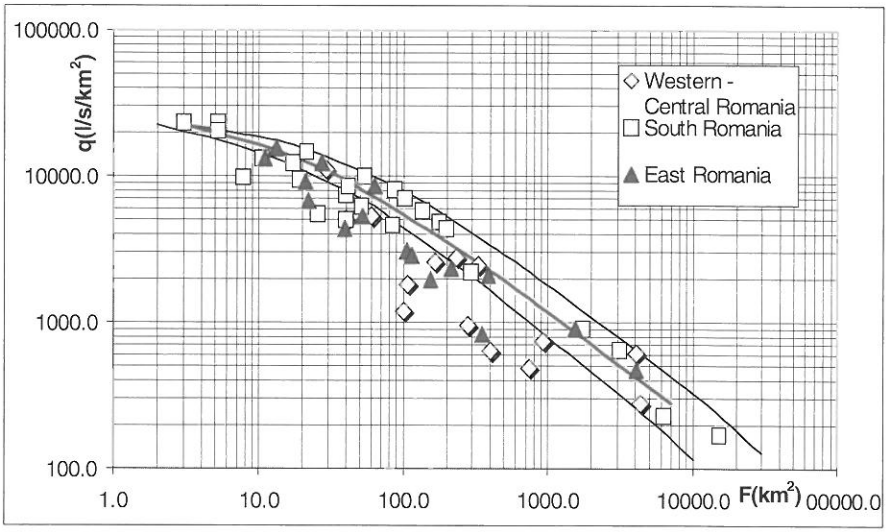

Figure 3-3: Regionalization of maximum specific discharge of outstanding floods in Romania.

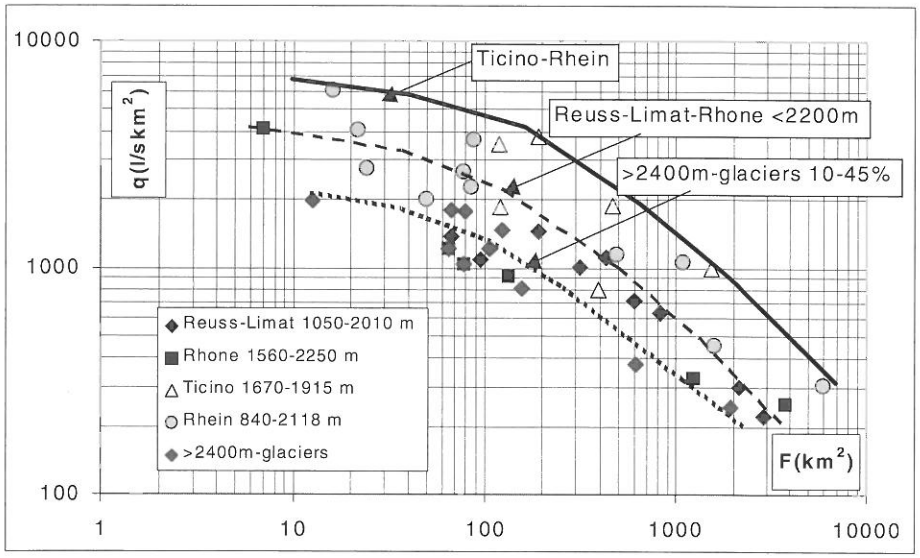

Figure 3-4: Regionalization of maximum specific discharge of outstanding floods in Switzerland.

The three curves that characterise the maximum runoff of Romania are explained by the differences in the precipitation regime but also in the peculiarities of the relief. The southern part of Romania is found in the influence of Mediterranean circulation that brings about intense rainfalls that have both a local character but also a regional one. This results in severe floods over medium size and somehow large size basins.
The envelope curves in Switzerland are differentiated due to the effect of the elevation and the existence of the glaciers at high altitudes. The lower envelope curve is valid for all the basins having elevations higher than 2400 m. The points representing Rhine basin are very scattered in the field of the graph because there is a large variation of the mean elevation of the considered sub-basins.
This type of regionalization is a detailed representation of the former one. In fact, the hydrological regionalization is as more significant as the space scale becomes greater. More than 300 hydrological stations were used In Romania to determine the quantiles of the maximum annual discharges and regional relationships between the quantiles of maximum specific discharge and morphological parameters of the catchment have been carried out.

In Figure 3-5 the morphologic parameter used for regionalization has been $\overline{H}/\sqrt{F}$, where $\overline{H}$ (m) is the mean altitude of the river basin and F (km^2) is the area of the catchment. This type of regionalization that is based on a great amount of data concerning the maximum runoff allows for assessing the design flood with a good accuracy.

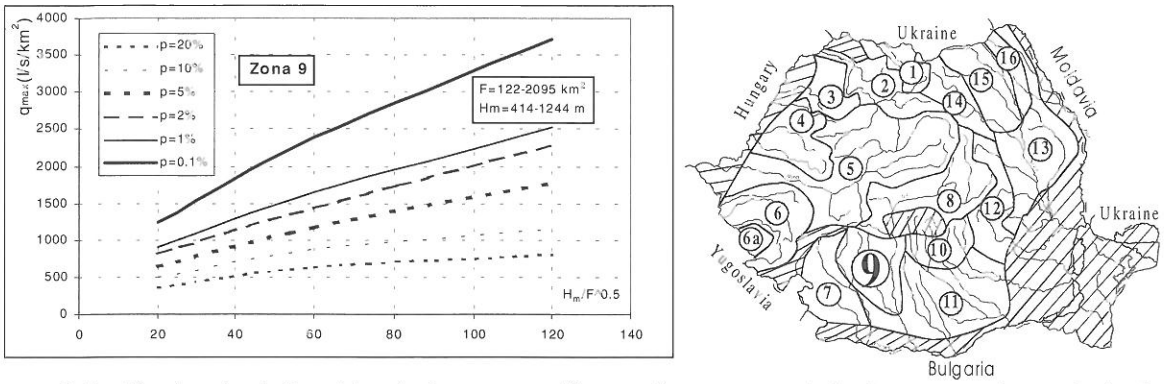

Figure 3-5: Regional relationships between specific maximum annual discharges and morphological parameter $\overline{H}/\sqrt{F}$.

The flash flood potential has been also considered in this study. The maximum specific discharges of the flash floods considered for the basin area less than 500 km^2 are presented in Figure 3-6.

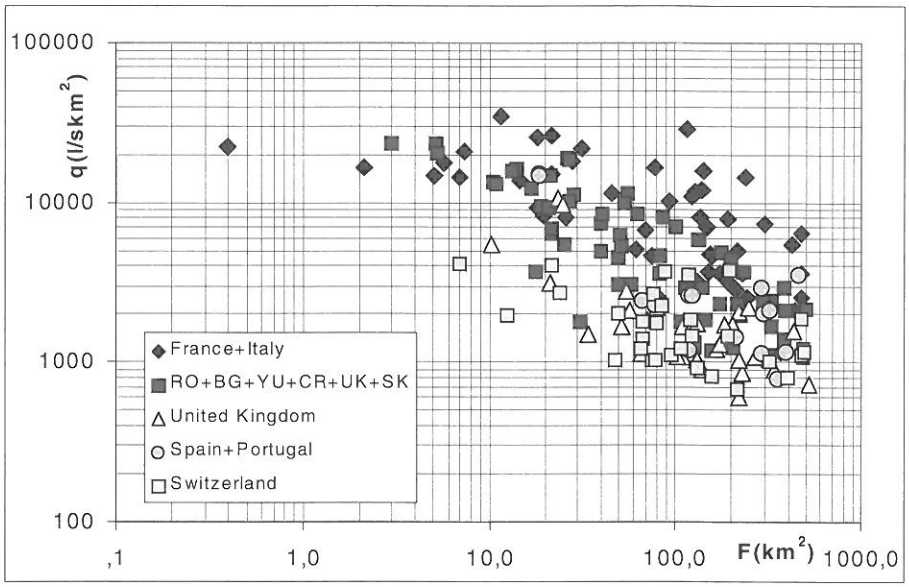

Figure 3-6: Comparison of the flash floods potential among some countries in Europe.

Again the upper envelope belongs to the points representing Italy and France (Mediterranean Zone) (Cosandey, 1999). For areas less than 100 km^2 the grouping of the points representing Romania, Bulgaria, Yugoslavia, Ukraine (Carpathian region), and Slovakia (Tatra Mountains) has an envelope that is lower with 50-70% than that representing France and Italy. Further, in the domain of basin areas comprising between 100-500 km^2 the flash floods are about half part of those of France and Italy. For basins smaller than about 100 km^2 the potential of rainfalls having duration that corresponds in average to the concentration time of such basins does not substantially differ from the Mediterranean zone to the mountainous area of the group of above-mentioned countries. Consequently, the differences in flash flood peak do not exceed 50-70% and as it can observe in the Figure 3-6, for very small basins the envelopes of the two groupings of considered countries tend asymptotically to a value of 25000 – 30000 l/skm^2. For basins larger than 100 km^2 the rainfall duration has to increase in order to "cover" a greater concentration time and the Mediterranean circulation is more capable to better feed with humid air the contiguous areas (France-southern part and Italy) than the inner ones. Consequently the potential of the flash floods diminishes with a half from that of Italy and southern France. The flash floods of Spain are comparable with those that occurred in the southeastern zone of Europe but it is expected that in Andalusia, Levante and especially in Catalonia the peak discharges of the flash floods would be much greater than those have been available in this study. (Llasat et al., 1999). With few exceptions the flash floods produced in United Kingdom and Switzerland are considerably lower than the others.

4 CONCLUSION

The inventoried outstanding floods occurred in Europe allowed the drawing of curves of the specific flood peak discharges against the basin area. This "macro-regionalization" provides an overall knowledge of the space distribution of the flood potential across Europe. Significant differentiation between countries has been found due to especially the differences in the climate features. Inputs of warm air masses, mainly of tropical origin coming across the Mediterranean Sea has a considerable effect on the increasing of the atmosphere humidity and produce a pronounced thermodynamic instability character of the atmosphere. As a result, the vertical ascendant movement of the air mass leads to the condensation of "cumulus" type followed by intense rainstorms. These processes are manifested across the "direct influenced countries" as France (Southern region) and Italy that show the highest potential of floods, both concerning the "lent" and the "flash" floods.
The countries located in the central and southeastern zone of Europe are under the influence of both the Mediterranean Sea and the cold fronts originating from the Atlantic Ocean. The latter transform the southern circulation into a western one, producing abundant rainfalls but less intense than those occurred in Italy and south of France. Therefore in this region of Europe the flood potential is less than that found in France (south) and Italy. In other countries with pronounced orography as Switzerland, southern Germany, Austria, and Slovenia the relief has an impact that overwhelms the differences in the climate features.
The flash floods originate either in the meteorological context of wet air advection where the vertical motion and the "cumulus effect" are very intensive or in the context of instability at the local scale. These circumstances are strongly manifested in the Mediterranean regions but equally in the central and south-eastern countries where the presence of mountains chains having steep slopes in the small basins associated with heavy rains result in a comparable flash flood potential with that of the Mediterranean countries. The comparable estimates of the flash flood potential become more evident for basin areas smaller than 10 km^2.
A "more detailed regionalization" has been performed for some countries where sufficient and representative data are available (France, Switzerland, Romania). These regional curves of the flood potential show significant differences both due to the climate characteristics and the relief features and they give more comprehensive information on the space variability of the flood potential across the deemed area.
A regionalization of the maximum runoff based on the relationships between the specific discharges and the more or less complex physiographical parameters of the river basin to which a "zonation" of the relations across the considered area is added might provide comprehensive information. Such achievement might be performed provided that a large quantity of data and representative ones is available. An international co-operation aiming to achieve a larger database of the outstanding floods is therefore desirable.

REFERENCES

Bendini, C. (1967): La grand crue de 4 novembre 1966. In: Proceedings of the Leningrad Symposium on Floods and Their Computation, ` vol. 2. Saint Petersburg

Black, A. R., Anderson, J. L. (1995): The Great Tay Flood of January 1993. 1993 Yearbook Hydrological Data UK Series, Institute of Hydrology. Wallingford. UK

Black, A. R., Benett, A. M. (1995): Regional Flooding in Strathclyde in December 1994. Hydrological Data UK: 1994 Yearbook, Institute of Hydrology. Wallingford. UK

Cosandey, C. (1999): Flood Generation Conditions In Mediterranean Middle Mountains. In: Proceedings of the joint FRIEND-AMHY Session. Istanbul Technical University, 16 October 1998. Topic: Heavy Rains and Flash Floods. Group for Prevention from Hydrogeological Desasters, Publ. no. 2049. Benvenuto Publ. House. Cosenza.Italy

Diren (Direction Générale de l'Environement) (1995): Les crues du 5 au 7 Novembre 1994 en Provence Alpes Côte d'Azur. Diren Report. France

Ebel, U., Engel, H. (1995): The "Christmas Floods in Germany 1993/1994. Bayerische Rüch, Special Issue 16. München

Ebel, U., Engel, H. (1996): ... 13 month later. The January 1995 floods. Bayerische Rüch, Special Issue 17. München

Engel, H. et al. (1994): The 1993/1994 flood in the Rhine Basin. BfG Publ.Report no. 0833. Koblenz

Engel, H. (1996): The Flood Events 993/1994 and 1995 in the Rhine River Basin. ASCE Congress. Anaheim. California. USA

Ferrari, E., Versace, P. (1999): Heavy rainfall in small Basins: the flooding of Crotone (October 1996, Italy). In: Proceedings of the joint FRIEND Session UNESCO – IHP Project – V 1.1 Topic: Heavy Rains and Flash Floods" Group for Prevention from Hydrogeological Desasters, Publ. no. 2049. Cosenza. Italy

Hydrograph. Central Bureau (1898): Die Hochwasserkatastrophe des Jahres 1897 in Österreichs. Hydrographischen Central Bureau. Wien

Kindler, J. (1998): 1997 Flood Emergency in Poland. A Lesson for Education and Training Program. In: Environment – Water, General Report for the Second Year of Activity 1997-1998, Vrije Universitet Brussel. First Edition

Kikkawa, H., Stanescu, V., Al. (1976): World Catalogue of Very Large Floods. Studies and Reports in Hydrology. The UNESCO Press. Paris

Kubat, J., Vrabec M. (1999): Flood Forecasting in the Czech Republic. In: National Weather Service. River Forecast System Workshop. Silver Spring Ma. USA

Llasat, M. C. et al. (1999): Flash Floods in the Northwest of the Mediterranean area: the 27^{th}-28^{th} September 1992 event.). In: Proceedings of the joint FRIEND Session UNESCO – IHP Project – V 1.1 Topic: Heavy Rains and Flash Floods" Group for Prevention from Hydrogeological Desasters, Publ. no. 2049. Cosenza. Italy

Marchi, E. et al. (1995): The November 1994 Flood Event on the Po River. Structural and Non-Structural Protection against the Inundation. Report of the Hydraulic Institute of University of Genoa. Genoa

Pardé, M. (1961): Sur la puissance des crues en diverses parties du monde. Geographica, Numero Monografico, Departement de Geografia Aplicada del Instituto Elcano. AnõVIII, Enero-Diciembre. Zaragoza

Rodier, I., Roche, M. (1984): World Catalogue of the Maximum Observed Floods. IASH Publication no. 143. Paris

Schiller, H. (1987): Ermittlung von Hochwasserwahrscheinlichkeiten *am schiffbaren Main und űber*-regionaler Vergleich der Ergebnisse. Beiträge zur Hydrologie. München

Spreafico, M., Stadler, K. (1988): Débits des crue dans les courses d'eau suisses. Vol. II, Publ. Service hydrologique et géologique national, Communication no.8. Berne

Spreafico, M., Aschwanden, H. (1991): Débits des crue dans les courses d'eau suisses. Vol. III et IV. Publ. Service hydrologique et géologique national, Communication no. 16 and no. 1. Berne

Stanescu, V. Al. (1967): Danube between Bazias and Ceatal Izmail (In Romanian). Hydrological Monograph, ISCH Press. Bucharest

Stanescu, V. Al., Matreata, M. (1997): Large Floods in Europe. FRIEND Third Report: 1994-1997. Cemagref Editions. Antony, France

Stanescu, V. Al. (2000): Outstanding Floods in Romania - a Comparison with Those Occurred in the Mediterranean Regions. In: Proceedings of the International Conference "Hydrology of the Mediterranean Regions" Montpellier. France

Suisse-Insp. Federale (1958): Les débits maximums des cours d'eau Suisses observés jusqu'en 1956. Publications de l'Inspection fédérale des travaux publics. Berne

UNESCO-IHP- reg. cooperation (1986): Die Donau und ihr Einzugsgebiet. Eine Hydrologische Monographie. UNESCO Regionale Zuzammenarbeit der Donauländer, vol. 1-3. München

REGIONALIZATION OF THE PEAK DISCHARGES IN THE DANUBE BASIN

Viorel Alexandru Stanescu[1], Valentina Ungureanu[1], Miklos Domokos[2]

[1] National Institute of Meteorology and Hydrology, Hydrology Division, Sos. Bucuresti-Ploiesti 97, Bucharest 71552, Romania, stanescu@ meteo.inmh.ro

[2] Water Resources Research Centre, H-1453 Budapest, Pf. 27, Hungary

SUMMARY

In 1986 The Hydrological Monograph of the Danube and its catchment was published in Munich, as a result of the 15 years long cooperation of the Danube Countries. Since that time, the Danube Countries have continued the cooperation in the frame of IHP-UNESCO. Its main purpose is to compile follow-up volumes to the Danube Monograph on selected topics of common interest. One of these projects has dealt with the analysis of annual maximum discharges observed in the Danube Catchment. The present paper offers a survey of the results of the project obtained by common efforts under Romanian coordination.
The first part of the study ("macro-regionalization") for the 176 gauging stations distributed across the Danube Basin the empirical distribution functions of the maximum discharge modulus coefficients were drawn. Then, the relationships between the coefficient of variation C_v and the maximum discharge modulus coefficient $K_p = ((Q_i / \overline{Q}) - 1) / C_v$ ($\overline{Q}$ stands for the mean and p for the probability of exceedance) are assessed. On the basis of a hydrological flood formation -criteria and physiographical considerations clustering of these relationships has been performed and five regions in the Danube Basin have been found. For each region the graphs of $K_p = f(C_v)$ are displayed and the quantiles of the modulus coefficients of annual peak discharge have been determined.
In the second part ("micro-regionalization") regression relationships were carried out for the five cvasi-homogeneous regions of Romania, between the specific maximum annual discharge and various physiographic characteristics of the catchments. The correlation $q_p = f(A, \overline{H}, B / L)$ proved to be the closest for the most catchments of the five regions (A is the basin area [km^2], $\overline{H}$ is the mean elevation of the basin [m], B its average width [km] and L the length of the main watercourse [km].
The regression relationships determined as a result of the micro-regionalization allow for determining the specific yields in ungauged river sections, for which the basin morphometric characteristics $A, \overline{H}, B$ and L are known.

Keywords: probability distribution function, annual maximum discharges, regionalization, basin physiographical characteristics

1 INTRODUCTION

The master plans for an integrated and complex water management imply good knowledge of the hydrological parameters in the basins lying above more points than where the data are recorded. An approach towards the knowledge of the laws that govern the manner of existence of the hydrological parameters over a territory is the regional analysis. While estimating the quantiles of the maximum discharge the first issue refers to the selection of the probability distribution function (**pdf**). In the Danubian countries a great diversity of pdf is used: Gumbel, Pearson III, Kritzky-Menkel, GEV, etc., fact which results in significant differences between the quantiles of the maximum discharge in the domain of rare and extreme frequencies (1/1000 to 1/10000). An attempt to determine regional probability curves valid for several zones which has to be established is made in this work.
Another issue of the hydrological regionalization refer to the manner in which the transfer of data to the ungauged basins or to deficient data sites is carried out. There are two main procedures to perform this transfer (Stanescu, 1992). The first one consists in finding out some relationships aiming to the spatial interpolation of the principal statistics of the probability curves, namely the mean and the variation. The mean may be correlated with the basin characteristics with acceptable results at a significance level of 95% (Roald, 1989), (Acreman, Wiltshire, 1989).

The second procedure consists in finding out several statistical distribution curves of standardised annual maximum discharge. Standardisation is achieved by dividing the maximum discharges quantiles by their average magnitude $\overline{Q}$. The mean value $\overline{Q}$ may be regionalized through correlating it with the physiographic characteristics of the basin (NERC, 1975), (Acreman, Wiltshire, 1989), (Roald, 1989). To apply the second procedure it is necessary to establish, both the regions to which several growth curves are assigned and correlation between $\overline{Q}$ and basin characteristics. One of the procedures to decide whether a group of catchments may form a region is the split-sample method (Acreman, Wiltshire, 1989). Another method of grouping consists in producing groups of basins where their physiographic characteristics present maximum similarity using a multivariate normal distribution to which the set of characteristics of each group considered "a priori" is fitted. A last procedure consists in allocating to an ungauged basin of weights of membership to a set of zones in order to take into account the discontinuities at their borders. (Acreman, Wiltshire, 1987). Only 176 series of maximum annual discharges have been available for this study. These restrictions concerning the availability of representative and large amount of data for the Danube Basin did not allow to apply these methods of grouping the basins within regions or to establish relations between maximum discharges and the basin physiographical characteristics. That is why a regionalization of the annual maximum discharges based upon the relationships with the physiographic factors has been performed only on a limited area, where sufficient data are available, namely over the territory of Romania. Taking into account the above-mentioned considerations on the theoretical and informational bases of the hydrological regionalization, the aims of this paper are:

- The first task is to carry out a regionalization of the probability curves across the Danube Basin. The quantiles of the maximum discharges are then computed making use of the regional **pdf** for a specific zone that has been determined by this "macro-regionalization" provided that the statistical parameters (mean and the variance) are available. They might be determined either at a given point on the base of the recorded series or by a "micro-regionalization" of the statistical parameters based on sufficient number of series recorded at the gauging stations.
- The second task is to apply a regionalization procedure to assess the maximum discharge quantiles for a partial area of Danube Basin (micro regionalization). This procedure has become applicable since a significant supplementary data recorded at more than 150 stations over the Romanian territory have been used. The quantiles of the maximum discharge have been computed making use of the regional probability curves as determined by the above-mentioned procedure for the entire area of the Danube River Basin.

2 DATA COLLECTION AND DATA BASE

The present work has been carried out as a result of the regional co-operation of the Danubian countries in the framework of IHP program. The database consists in:

- Location and recording periods of the selected hydrological stations.
- Some physiographic characteristics of the catchments.
- The series of the annual maximum discharges recorded at the selected stations.

Table 2-1: Length of the series of the recorded data (years).

Country	*Ranges*							
	30÷40	*40÷50*	*50÷60*	*60÷80*	*80÷100*	*100÷120*	*>120*	*Total*
Germany	1	5	9	23	7	1	-	**46**
Austria	-	15	-	-	-	1	-	**16**
Czech R.	-	-	-	4	-	-	-	**4**
Slovakia	4	3	3	8	-	-	-	**18**
Hungary	31	-	-	-	-	-	-	**31**
Ukraine	-	4	1	-	-	-	-	**5**
Slovenia	6	-	-	-	-	-	1	**7**
Croatia	3	-	-	2	-	-	-	**5**
Yugoslavia	-	13	-	-	-	-	-	**13**
Romania	1	11	3	3	3	4	1	**28**
Bulgaria	-	-	3	-	-	-	-	**3**
Moldavia	-	2	-	-	-	-	-	**2**
Total	48	60	28	41	10	5	3	**176**

3 METHODOLOGY OF REGIONALIZATION USED IN THE STUDY

3.1 Method of regionalization of the probability distribution curves

For each point observation the series Q_i of the maximum discharges is considered.
The values of the empirical probability (expressed as percents) are obtained by the formula:

(1) $$p = \frac{m}{n+1}$$

where p is the probability of exceedance of a sample occupying in decreasing order the m^{th} place in a series of n members.
For each series, the reduced variable K_i (modulus coefficient) has been computed as follows:

(2) $$K_i = \frac{\frac{Q_i}{\overline{Q}} - 1}{C_v}$$

where: $\overline{Q}$ is the mean value of the series and C_v is the coefficient of variation.
Then, the empirical distribution curves of the probability of exceedance of K_i were plotted on probability graphs. From (2) there results the value of the maximum discharge of a given probability of exceedance Q_p as follows:

(3) $$Q_p = \overline{Q} \cdot \left(C_v \cdot K_p + 1\right)$$

The next step is to draw the correlation between the variable K_p on the one hand and the coefficient of variation C_v and the probability of exceedance p on the other.
Thus the relationships $K_i=f(C_v,p)$ and then the regional probability curve belonging to a specific zone were determined. Relied on this curve, for a certain established zone, the maximum discharge of a certain probability of exceedance may be estimated according to the relation (6) provided that the parameters C_v and $\overline{Q}$ are known.
The skewness C_s of the distribution curves are implicitly considered in the relationship $K_i=f(C_v,p)$ as a linear function of C_v. One considers that the ratio C_s/C_v is constant across a certain region and this fact is reflected in the differentiation of the relationships $K_i=f(C_v,p)$ from one zone to the other. Anyhow, this procedure of "averaging" the K_p over a relative homogeneous zone is more correct than the on-site computation for estimating of the skewness coefficient C_s. The punctual computation of C_s is subjected to important errors of it unlike the number of terms of a series are great (100÷150 years).

3.2 Procedure for regionalization of the annual maximum discharge quantiles

This procedure consists in the determination of the relationships between each standard quantile of the maximum specific discharge ($q_p=Q_p/AREA$) and a set of basin physiographic characteristics. This approach leads to an analytical model, which reveals the manner in which each set of characteristics has a different influence on each quantile.
Denote $y=\log q_p$ and $x_i = \log X_i$, X_i being the value of a basin characteristic. Then, the linear regression relation is assumed:

(4) $$y = \log a_0 + \sum_{i=1}^{n} a_i x_i$$

where: n is the number of the characteristics considered in the set, a_i are the corresponding coefficients and a_0 is a constant.

From (4) one can write the equation:

(5) $$q_p = a_0 X_1^{a_1} X_2^{a_2} \ldots X_n^{a_n}$$

Each relationship of type (5) is then assigned to a region across which there is a cvasi-homogeneity of the physiographic and climatic characteristics.

4 DESCRIPTION OF THE WORK AND RESULTS

4.1 Regionalization of the probability distribution curves

Relied on the methodology described before, and in compliance with some considerations concerning the philosophy of the regionalization procedures and the availability of data, the following works were carried out:

- For each series of annual maximum discharge the statistical parameters $\overline{Q}$ and C_v have been derived and further on each series of annual maximum discharge has been transformed in a series of modulus coefficients according to the relation (2).
- The empirical curves of the probability of exceedance of K_i were drawn after putting in a decreasing order the terms of the series K_i to which the probability p computed by relation (1) has been assigned.
- The next step was to make a visual "on-trend" extrapolation on the empirical probability curves up to 1%.
- From the extrapolated empirical curves the estimates of the modulus coefficient K_p for all standard probability values p (1%; 5%; 10%; 20%; 50%; 80%; 90% and 95%) have been derived.
- For each of standard value of p the relationships between the coefficients K_p and the coefficient of variation C_v have been derived. While drawing up the correlation K_p - C_v the points were grouped so that on the one hand, their deviations from a regression curve should be minimised and simultaneously, they should be gathered as representing contiguous basins in an "a priori" selected zone, on the other hand. The membership of the points K_p - C_v to a specific zone has been justified by the cvasi-homogeneous characteristics of the relief and the climate (UNESCO-IHP-reg. cooperation, 1986), (Stancik, Jovanovic, 1988), (Stanescu, 1967). After some iteration a final gathering of points K_p - C_v and thus a "zonation" of the Danube Basin (Figure 4-1) has been achieved.

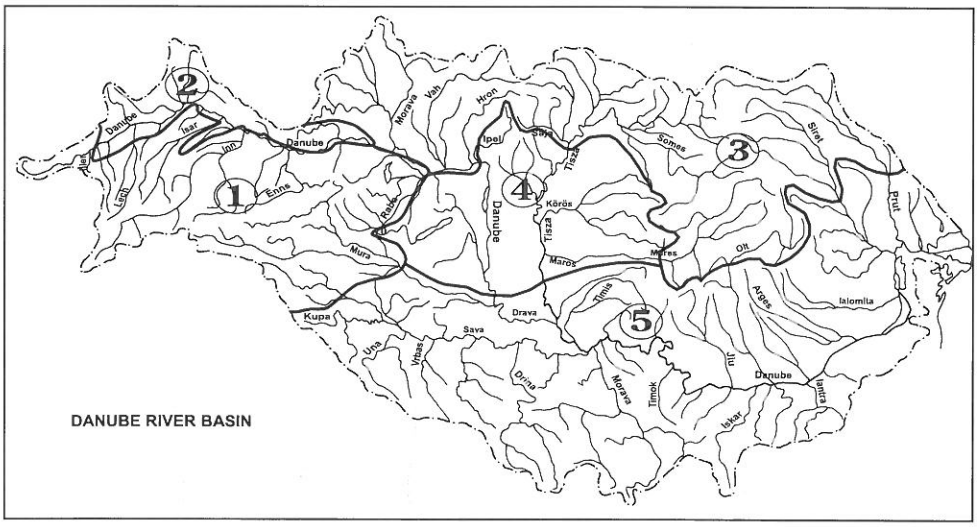

Figure 4-1: Zonation of the probability curves of the modulus coefficients of maximum discharges.

It is noteworthy to point out the facts, that the zonation has a "macro character" having in view the number of series used in the study, especially for the areas where the density of the stations is somehow limited. The correlation K_p-C_V grouped on the five specific zones is presented in Figure 4-2 and the analytical equations of their regression curves have been derived.
Besides their similar characteristics of the climate and the relief, the regions have been chosen so that there were a differentiation between the curves K_p-C_V . For 1% probability the relationships K_p-C_V valid for all five regions are superimposed plotted in Figure 4-3.

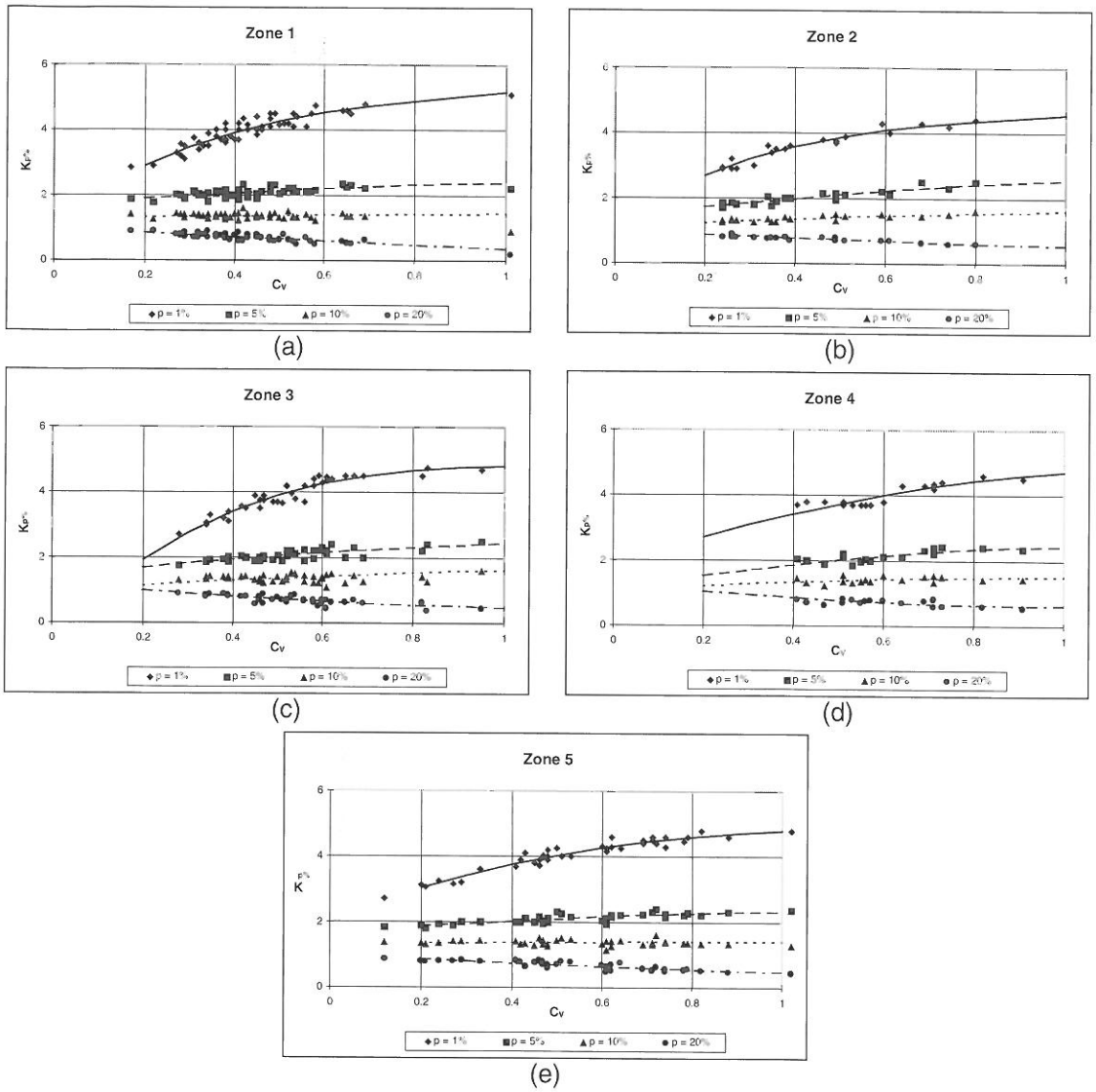

Figure 4-2: Relationships $K_{p\%}$ function of C_v and the probability of exceedance of 1%, 5%, 10%, 20% corresponding to the zone 1 (a), zone 2 (b), zone 3 (c), zone 4 (d) and zone 5 (e).

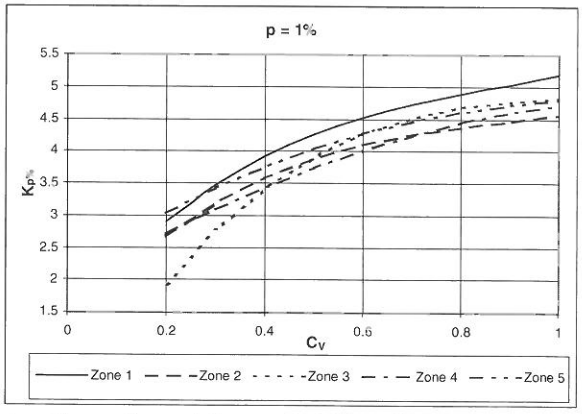

Figure 4-3: Relationships $K_{p\%}$ - C_v and the probability of exceedance of 1% for all five zones.

An analysis of the deviations of the regional probability curves from the probability distributions functions (**pdf**), the most commonly used in hydrology was carried out.
The Pearson III distribution curve shows the smallest deviations from the regional curves for any zone and any probability. As the regional curves have not been determined for the domain of rare and extreme frequencies the extrapolation starting from 1% quantile $Q_R^{1\%}$ is recommended to be made according to Pearson III distribution curve which, as determined by (Domokos et al.,1999) has shown the smallest deviation from the regional curve.
In Table 4.1 the deviations between the maximum discharges computed on the basis of the regional curves and some usual theoretical probability distribution curves (Pearson III-**PS**, Kritzky-Menkel-**KM**, Log-normal-**LN**) function of the probability and C_v are presented.

Table 4.1: Relative deviations $\varepsilon_{Q_{p\%}}$ of the regional probability curves from the pdf ones.

Zone	p	C_v = 0.4			C_v = 0.6			C_v = 0.8		
	(%)	PS	KM	LN	PS	KM	LN	PS	KM	LN
1	1	0.097	0.113	0.127	0.114	0.140	0.156	0.107	0.162	0.165
	5	0.018	0.037	0.040	0.044	0.078	0.073	0.121	0.156	0.148
2	1	0.030	0.048	0.063	0.067	0.094	0.111	0.068	0.125	0.129
	5	-0.023	-0.002	0.000	0.044	0.078	0.073	0.108	0.144	0.136
3	1	0.018	0.037	0.052	0.095	0.121	0.138	0.099	0.155	0.158
	5	0.013	0.033	0.035	0.047	0.081	0.075	0.101	0.137	0.129
4	1	-0.003	0.015	0.031	0.035	0.064	0.081	0.055	0.113	0.116
	5	0.002	0.022	0.025	0.021	0.056	0.051	0.113	0.149	0.141
5	1	0.065	0.083	0.097	0.087	0.114	0.131	0.092	0.147	0.151
	5	0.000	0.020	0.022	0.044	0.078	0.073	0.083	0.120	0.111

From Table 4.1 one can observe that the Pearson III distribution curve shows the smallest deviations from the regional curves for any zone and any given probability.
Taking into account that for the coefficients of variation which do not exceed 0.5 the deviations are below 5%, one admits that under these circumstances the Pearson III distribution curve is the closest one to the regionalization curves.
The regional probability curve extrapolation starts from the estimate of modulus coefficient of the regional probability curve ($K_R^{1\%}$) and the Pearson III frequency factor ($K_P^{(p)}$) as follows:

(6) $$Q_R^{(p)} = Q_R^{1\%} \frac{C_V \times K_P^{(p)} + 1}{C_V \times K_P^{1\%} + 1}$$

Then any quantile of maximum discharge of certain probability p in the domain of rare and extreme frequencies (p<1%) is computed making use of relation (6) and the modulus coefficient $K_R^{(p)}$ is derived as:

(7) $$K_R^{(p)} = \frac{K_R^{1\%}\left(C_V \times K_P^{(p)} + 1\right) + K_P^{p\%} - K_P^{1\%}}{C_V \times K_P^{1\%} + 1}$$

The regional probability curve specific to a certain zone of the Danube river basin may be used in two ways:

- Either in the considered point there are observations on the maximum annual discharges over a relative short period (20-25 years) which nevertheless allows to have good enough estimates of C_v and $\overline{Q}$. Then, one adopts the regional probability curve belonging to the zone where the basin is located;
- Or, in the considered area a relationship between the statistical parameters $\overline{Q}$ and C_v or the maximum discharge quantiles on the one hand and some characteristic feature of the basin, on the other, might be found.

4.2 Regionalization of the maximum annual quantiles in a limited area

Relied on a great number of hydrological stations from Romania where reliable estimates of maximum discharge quantiles are assessed, the procedure described before was applied.

The following set of physiographic parameters were considered: (H, F); ($H/\sqrt{F}$); (F, H, I_b); (F, H, B/L) where H, F, I_b, and B stands for the mean altitude, area, mean slope and width of the basin, respectively and L is the length of the main course of the catchment.

The quantiles of the specific maximum discharge were correlated with each set of the above-mentioned variables. By means of the analysis of the deviations of the quantiles as resulted from the regression (denoted q'_p) and those that were directly assessed at stations (q_p), five zones were established (Figure 4-4).

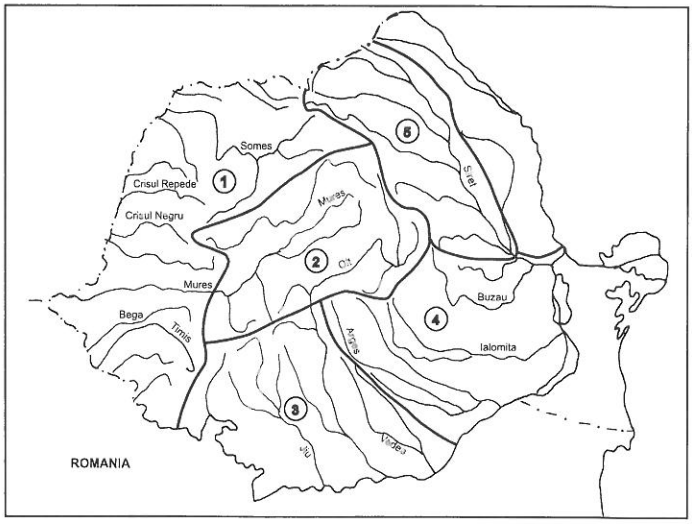

Figure 4-4: Zonation of the regression coefficients

For each region, the combination of basin characteristics that resulted in the best estimation of 1% quantile was chosen. The best result is given by the relation of the 1% quantile with the set (F, H, B/L). Further on, considering the set (F, H, B/L) the regression coefficients of all standard quantiles (0.1%, 0.5%, 1%, 2%, 5%, 10%) have been determined in the Table 4.2 according to the relation (4)

Table 4.2: Regression coefficients - variables: F, H, B/L.

Zone	p (%)	Regression coefficients of the morphometric characteristics F, H, B/L			
		F	H	B/L	Constant
Zone 1	0.1	-0.4645	0.5578	0.0487	755.24
	0.5	-0.4483	0.5624	0.0507	500.62
	1.0	-0.4362	0.5641	0.0558	394.95
	2.0	-0.4231	0.5599	0.0613	315.51
	5.0	-0.3965	0.5596	0.0656	201.68
	10.0	-0.3710	0.5589	0.0791	133.19
Zone 2	0.1	-0.5065	0.6583	0.0098	326.53
	0.5	-0.4805	0.6658	0.0170	200.76
	1.0	-0.4622	0.6559	0.0243	171.63
	2.0	-0.4421	0.6754	0.0511	112.94
	5.0	-0.4026	0.7196	0.0967	50.16
	10.0	-0.3719	0.7613	0.1298	24.02
Zone 3	0.1	-0.4739	0.2842	0.0010	5150.62
	0.5	-0.4560	0.2944	0.0015	3164.32
	1.0	-0.4441	0.3019	0.0057	2364.78

	2.0	-0.4282	0.3116	0.0082	1655.62
	5.0	-0.4000	0.3202	0.0093	957.06
	10.0	-0.3774	0.3351	0.0103	554.50
Zone 4	0.1	-0.5419	0.6060	0.1887	1724.76
	0.5	-0.5320	0.6144	0.1423	1038.00
	1.0	-0.5274	0.6190	0.1347	816.00
	2.0	-0.5204	0.6155	0.1240	643.61
	5.0	-0.5171	0.6213	0.0995	428.53
	10.0	-0.5122	0.6208	0.0766	295.23
Zone 5	0.1	-0.5368	0.0030	0.1197	8518.18
	0.5	-0.5151	0.0066	0.1279	5299.11
	1.0	-0.5053	0.0140	0.1248	3917.65
	2.0	-0.4819	0.0235	0.1127	2494.82
	5.0	-0.4569	0.0262	0.1308	1477.79
	10.0	-0.4231	0.0289	0.1364	756.48

The distribution of the errors defined by ($E_r=(q'_p - q_p)/q_p$) is presented by ranges in Table 4-3.

Table 4-3: Errors - variables: F, H, B/L.

Zone	p (%)	Errors				
		$E_r>25$	$20<E_r<25$	$10<E_r<20$	$5<E_r<10$	$E_r<5$
Zone 1	0.1	0	3	18	10	17
	1.0	0	4	14	11	19
	10.0	2	7	18	13	8
Zone 2	0.1	1	2	11	6	14
	1.0	1	0	13	9	11
	10.0	2	4	8	10	10
Zone 3	0.1	0	5	13	3	6
	1.0	1	2	12	6	6
	10.0	5	1	10	3	8
Zone 4	0.1	0	1	9	3	7
	1.0	0	1	9	3	7
	10.0	0	2	4	5	9
Zone 5	0.1	0	4	2	2	9
	1.0	0	4	2	4	7
	10.0	1	1	4	4	7

5 CONCLUSIONS

- This study is based on an important volume of data concerning the annual maximum discharges recorded at 176 stations located within the Danube basin.
- The length of the records is considered sufficient to accurately estimate the statistical parameters of the series. An important number of series provided by the Danube countries show records, which exceed 80 years.
- The spatial distribution analysis of the reduced variable K_i shows a regional grouping of it. Five specific zones valid for several relationships $K_p = f(C_V, p)$ were established.
- The limited number of series does not allow performing a regionalization of the distribution curve parameters. This can be achieved for limited, areas by the use of much greater number of hydrological rows of annual discharges.
- Since comparative analysis of the deviations of the regional curves from some usual theoretical distribution ones (Pearson III, Lognormal, Kritzky-Menkel) reveals that the Pearson III distribution curve shows the smallest deviations against the regional curves. for the extrapolation of the regional

curves in the domain of rare and extreme frequencies (0.01% and 0.1%) the use of Pearson III curve is recommended.

- Relied on a great number of hydrological stations from Romania where reliable estimates of maximum discharge quantiles are assessed a regression procedure was applied. Thus the relationships between the quantiles of several probability of exceedance and a combination of physiographical characteristics of the basins regionalized over five zones have been achieved. The best result is obtained by use of the relation of quantile with the set (F, H, B/L).

REFERENCES

Acreman, M. C., Wiltshire, S. E. (1989): The Regions are dead: Long Live the Regions. Methods of Identifying and Dispensing with Regions for Flood Frequency Analysis. IAHS Publ. No 187. IAHS Press. Wallingford. UK

Acreman, M. C., Wiltshire, S. E. (1987): Identification of Regions for Regional Flood Frequency Analysis. EOS, 68, 44, 1262

Domokos, M. et al. (1999): Analyse der jährlichen Hochwasser im Donauraum als Beitrag zum Hochwasserschutz und der Regionalisierung hydrologischer Daten. Sonderdruck aus Hydrologie und Wasserbewirtschaftung. 43. H6. München.

NERC (Natural Environmental Reasearch Council) (1975): Flood Studies Report. London

Roald, L. A. (1989): Application of Regional Frequency Analysis to Basins in Northwestern Europe. FRIENDS in Hydrology, IAHS Publ. No 187. IAHS Press. Wallingford. UK

Stancik, A., Jovanovic, S. (1988): Hydrology of the river Danube. Publishing House Priroda. Bratislava

Stanescu, V., Al. (1967): Danube between Bazias and Ceatal Izmail. I.S.C.H. Bucharest

Stanescu, V. Al. (1992): A spatio-temporal analysis for the assessment of the maximum discharges for project (in Romanian). Hidrotehnica No. 6-8. Bucharest

UNESCO-IHP-regional cooperation (1986): Die Donau und ihr Einzugsgebiet. Eine Hydrologische Monographie. UNESCO Regionale Zuzammenarbeit der Donauländer, vol. 1-3. München

REGIONAL FLOOD FREQUENCY IN NORTH BASINS OF IRAN

Abdoulrasoul Telvari[1], Alireza Islami[2]

[1] Soil Conservation and Watershed Management Research Center.13445-1136 Tehran, Iran, telvari@scwmrc.com

[2] Soil Conservation and Watershed Management Research Center Center.13445-1136 Tehran, Iran, islami@scwmrc.com

SUMMARY

Some relations for flood estimating in sub-catchments in the north basin of Iran, called Khazer basin, are established using multiple regression and index flood method. There are 31 sub-catchments in east part and 22 in west part of this area as gauged catchments. Flood frequency analysis shown that the three parameters log normal distribution is as dominant frequency distribution in this area.
Factor analysis approach has realized that amongst several factors affecting on instantaneous peak discharge, area of watershed, length of main channel, mean slope of watershed, mean annual precipitation, drainage density and compactness coefficient have the largest effects, thus they are used in regional flood estimation analysis.
Four homogenous groups of catchments are classified for each part of whole area and also entire area as one group using cluster analysis, Andrews' curves and discrimination test.
Some relations have been established for each of these groups and also for entire area of both part of Khazer basin using flood index method as well as multiple regression analysis. The results are successful in comparison with previous works that have been done by others in this area.

Keywords: Khazer basin, Flood estimation methods, Instantaneous peak discharge

1 INTRODUCTION

The accurate estimation of the flood magnitude associated with the recurrence interval T year flood is a task in water resource planning and management, designing river engineering and flood control works, soil and water conservation and watershed management.
In the area of flood estimation, complete data sets are required on stream flow. Unfortunately, records of such hydrological process are usually short and often have missing observations. Regional flood frequency analysis can be used to improve the estimation of extreme flow quantiles at sites that the data record lengths are short relative to the return period of interest. Either gauged or ungauged catchments can be analyzed. For an ungauged catchment, data from hydrologically similar gauged locations is used to characterize the extreme flow regime for the ungauged catchments.
Early methods of frequency analysis (Fuller, Foster, Hazen, Slade, Gumbel, Matalas and Benson, Bobee, and Kite, quoted in Stedinger,1992) were confined to fitting a statistical distribution to flood data of a single site. Assumptions were made of the population events and the statistical parameters of the distribution calculated from the sample data. The introduction of computers has extended these techniques to the development of regional flood frequency analysis based on available data of a region. Regional frequency analysis is preferable to single site frequency for tow reasons: (1) Because of short records at individual stations, frequency analysis at a single site is subjected to large error. (2) Regional frequency analysis has an added advantage in that estimation of flood frequency information at ungauged catchments within region can be made. Various regional flood estimation methods have been curried out in all over the world. Index flood method (Dalrymple, 1960), multiple regressions (Benson, 1962), square grid method (Solomon et al., 1968) standard frequency distribution (NERC, 1975), regional record maximum method (Conover and Benson, 1963); region of influences method (Zrinji and Burn, 1996), Wakeby regional distribution (Houghton,1978) Hybrid method(Johnson and Ayyub, 1992), are some of these methods.
The classical approach to regional flood frequency analysis involves the identification of fixed regions for the area under study and selection of appropriate frequency distributions for the identified regions. Regions are defined as subsets of the entire collection of sites for which extreme flow data is available or required. There are several characteristics that regions should posses (Burn and Goel, 2000). The first one is that the collection of catchments be hydrologically, homogeneous, the second requirement is that the region be identifiable, and third one is that the region be sufficient large.

Generally, most flood studies are analyzed through the use of univariate distributions. In flood frequency analysis, flood associated with different recurrence interval are estimated from annual flood series using various theoretical distribution. There are several complicating factors in selection of the frequency distribution (Potter and Lettenmaier, 1990). These can be summarized such as: unknown underlying distribution, exceeding of the return period of interest flood risk than the available record length, and the differences of physical flood generation mechanism in different locations. Several efforts have been made to provide physical and statistical basis for selecting the type of probability distribution function that best fits the frequency distribution of the actual data.
Most of the points mentioned above show that the flood frequency analysis should be made in a hydrologically homogenous region including enough recorded flood series at a relatively large area.
In the present study, efforts have done to identify homogenous regions and to apply two methods of regional flood estimation in north of Iran.

2 THE STUDY AREA

According to water resources national studies in Iran, the study area called Khazer basin that is located in north of the country between Alborz Chain Mountain and Caspian Sea. This area is bounded by latitude **35°, 36' N and 36°, 54'E**; and longitude **48° 32' E and 56° 26' E** as shown in Figure 2-1. In the present work this area has been divided into the east and the west parts as Alikhani (1997) has recommended. The humidity is high and it decreases from west to east as the amount of annual rainfall decrease from 1850 mm (in Bander Anzeli) to 630 mm (in Gorgan). There are two maximum rainfall regimes, which occurred in winter and autumn. The source of humid air in this area is Caspian Sea, however the Mediterranean air mass is found as another resource of rain. Mean annual rainfall in the west and the east part are 1261 mm and 539 mm respectively and the most part of these amounts rainfall are in autumn and winter. In the mountainous areas, the gradient of rainfall with height is inverse that means the rainfall at the lowland and close to the sea is much more than the high lands.
The catchments in the mountainous areas are covered with relative high dense forest trees up to height of 2000 m above sea level. The lowland areas have relatively gentle slope and they mostly have been used as agriculture areas. Rivers are generally located in deep valleys and they have steep slope beds.
In topographic point of view, the area can be divided into 3 groups of catchments. First, catchments, which entire or mostly are located in mountainous area and faced to the sea and the average height is 500 to 1000m above sea level. Second, catchments that just some parts are faced to the sea and the most parts are located in height of 1600 to 2000 m. The density of trees coverage is much less than the first group. The third group of catchments is located in very high lands and the average height is more than 1600m in the east Khazer and about more than 2000m for the west Khazer.
The geological formations are various and they appear from oldest Precambrian to Neocene layers.

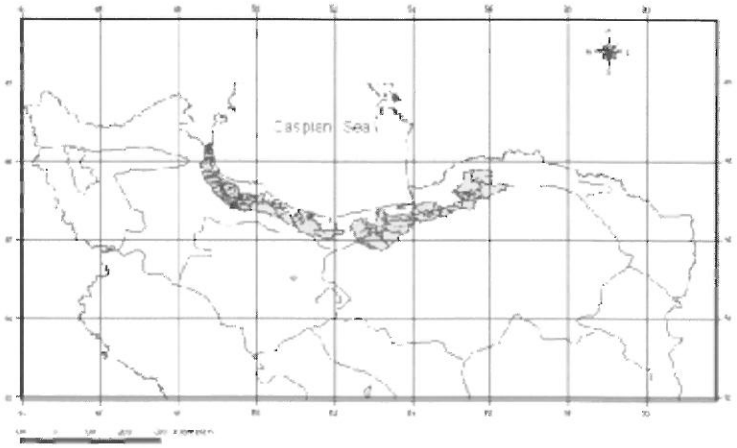

Figure 2-1: Location of the study area.

3 DATA USED IN STUDY

Annual maximum flood (AMF) and instantaneous maximum flood (IMF) data of 53-gauged stations with average record length of 27years (1968-1995) were selected in this area. The size of selected catchments ranged from 21.5 to 5439 Km^2. The IMF data were used for most of catchments, however, for those catchments where IMF data were not available, such a regression equation was developed relating IMF values with AMF for each catchment. The correlation of flows between stations may result when neighboring stations are subjected to the same meteorological event. Regression between the two stations, which are significantly correlated, is selected to estimate missing data.
In order to drive the catchment characteristics, topographic map with scale of 1:50000 are provided. The catchments boundaries were identified up to the hydrometrics location. Hydrological data was obtained from annual reports of Iran water resources organization. There are many gauged stations in the study area. 31 gauging stations located in the east Khazer and 22 gauged stations in the west Khazer.

4 OVERVIEW OF METHODOLOGY

The overall methodology was used to identify a set of homogeneous regions and to develop the regional equations are summarized as following steps.

4.1 Single site flood frequency analysis

The assumption of homogeneity of the stations data used in this study was based upon the criteria of unregulated stream flows. The record of annual peaks of gauging catchments is assumed independent because of insignificant influence between annual peaks. A series of annual peaks for each single station has been analyzed using HYFA software (Kite, 1999). The goodness of fit test has been done for all selected gauged catchments in both the east and the west part of area

4.2 Catchments characteristics

Catchments characteristics are derived for each area bonded by gauging site based on digital topographic map of 1:50000 scale. ILWIS software was used as a geographic information system (GIS). Geometric information such as area, perimeter, mean weighted slope of land and channels, mean height of area, length of mainstream, drainage density and shape coefficient are derived.

4.3 Factor analysis for independent variables of catchments characteristics

In order to select the independent variables that affect on instantaneous peak discharge, the factor analysis has been carried out for several catchments characteristics for selected locations. Kaiser-Meyer-Olkin Measure, eigen values, partial and simple correlation coefficient were used as criterion to identify the independent variables.

4.4 Test of homogeneity

Cluster analysis as well as test of Andrews' curves has been carried out using the independent variable to identify groups of catchments. The resulted groups as hydrological homogenous areas have been tested by discriminate analysis.

4.5 Flood index method

A simple regression was developed between area and mean annual discharge for each group as well as for both the west and the east part of Khazer basin. The ratios of IMF/Q were calculated based on derived various recurrences interval T year instantaneous flood (IMF) in single site analysis and annual discharge (Q) for each gauged catchments. Then, for each group a relation curve has been developed between the ratios and frequency upon the dominant distribution of three parameters lognormal as the regional frequency.

4.6 Multiple regression method

Using SPSS software and backward approach, multiple regression equation was analyzed between IMF and some catchments characteristics as independent variables for each cases that mentioned above. The criteria residual mean square error (RMSE) was applied for testing of goodness of the best fit.

(1) $$RMSE = \frac{1}{n}\left[\sum_{i=1}^{n}(Qto - Qte)^2\right]^{0.5}$$

Where Q_{to} and Q_{te} are flood flow as observed and estimated values respectively and n is the number of pair of data.

4.7 Comparison the results

In order to compare the results of different methods, RMSE has been calculated between the result of each method and the derived IMF from single site analysis. Two catchments within the east Khazer basin that have not contributed in both flood estimation methods were selected. Various recurrences interval T year instantaneous flood (IMF) were estimated for the above catchments using the resulted equations of the two methods for corresponding hydrologic homogenous group, and then compared with the result of single site analysis.

5 RESULTS AND DISCUSSION

The results of single site flood frequency analysis show that the three parameters lognormal distribution is the dominant frequency distribution in this area. Therefore, various recurrences interval T year instantaneous flood peaks (IMF) are derived for single site station based on the dominant distribution.
Several physical catchments variables considered to be useful either in the estimation of flood flows or testing of homogeneity were identified and derived from topographic map of 1:50000. These data are area, perimeter, length of main channel, drainage density, mean weighted slope of land, mean height of catchment and shape coefficient. Mean annual rainfall for a length of 27 years records (1968 – 1995) was calculated and summarized in table 5-1.

Table 5-1: Mean annual rainfall (mm) in the east and the west area (1968-1995).

The East area	Code	12001	12005	12007	12009	12011	12013	12015	12017	12019	12021	12023
	Rain(mm)	447.9	483.3	760.6	804.0	519.3	595.3	795.0	481.5	569.4	760.6	528.9
	Code	12033	12043	12045	12053	12065	12085	12097	13005	13006	13013	13019
	Rain(mm)	754.4	763.3	744.9	539.4	481.2	774.0	628.3	540	559.5	558.7	541.6
	Code	13023	13025	13029	14001	14003	14005	14007	14011	14017		
	Rain(mm)	498.3	570.3	532.7	509.1	725.1	608.1	509.1	689.9	675.7		
The West area	Code	14017	15015	16003	16007	16011	16035	16041	16049	16051	16059	16063
	Rain(mm)	675.7	446.4	599.0	884.0	768.4	1134.5	670.2	699.4	1018.	1206	1387
	Code	16089	17045	17051	17055	18019	18021	18023	18025	18035	18047	18055
	Rain(mm)	936.0	633.0	1330.0	1492.7	1224.0	986.0	807.8	1129.0	1097.0	1116.0	1181.8

Factor analysis for catchment characteristics and mean annual rainfall versus specific discharge of 2 years recurrence interval shows that area, mean weighted height of catchment, drainage density, mean weighted of catchment slope and mean annual rainfall are the independent variables. It must be mentioned that the area of catchment is the major independent variable whose effect can cover other independent variables. It means that in absence of this variable the other variables mentioned can be assumed as the independent variables.
Although homogenous regions may be found for any set of variables, in this study, it was desired to regionalize in two cases, first based on area and second by using the independent variables as being potentially useful in the estimation of flood peaks. The variables in the east part of Khazer basin are area, length of main channel, mean weighted slope of catchment, compactness coefficient and mean annual rainfall. In the west part, area, mean weighted slope of catchment, drainage density, mean height of catchment and mean annual rainfall are as independent variables. Results of cluster analysis, Andrews' curves method and discriminate analysis using the above variables show 4 homogenous

groups in both the west and the east part of Khazer basin. The group 2 in the east Khazer and the groups 2 and 4 in the west area are omitted because the numbers of gauged catchments within them are not enough to analyze. Same homogeneous grouping based on catchments' area resulted in 3 groups for each area. The group 2 in the east and the groups 2 and 3 in the west are neglected because of less number of data, thus in the west area the whole area is selected as a homogeneous area.
Index flood method was applied for the whole catchments as a region and the homogenous groups in both the east and the west part of Khazer basin in two cases of grouping. Hence there are 5 acceptable homogenous groups in the east Khazer basin. The catchments listed in each group and for the whole area were considered to be from 6 regions. Trail and error approach has been done to establish a regional Q (mean discharge) equation for each region using data of the groups and the whole catchments.
Several forms of equations between Q and either area (grouping case 1) or independent variables (in case 2 of grouping) were tested and 5 equations were developed as presented in table 5-2 and 5-3.
In the west area, there are only 2 acceptable homogenous groups (1, 3) with relative enough number of catchments for establishing regional Q equation, thus trail and error approach also has been done for data listed in these groups. In the west Khazer basin 3 regional Q equations have been developed which are shown in tables 5-2 and 5-3.

Table 5-2: Regional Q equations in the east and the west Khazer basin based on independent variables (a)

Main region	Region	The regional Q equation	Det. Coeff (R^2)	Stan. Error (S.E)	Level of Sig.(%)
The east part of Khazer	Group 1	$\log Q_2 = 0.704 \log A + 3.65 \log P + 2.437 \log H - 18.34$	0.96	0.07	0.001
	Group 2	------	------	------	------
	Group 3	$\log Q_2 = 0.489 \log A + 9.132 \log P - 2.654 \log S - 22.09$	0.98	0.17	0. 3
	Group 4	$\log Q_2 = 1.0256 \log A - 2.872 \log H + 7.824$	0.87	0.2	0.07
The west part of Khazer	Group 1	$\log Q_2 = 1.0978 \log A - 0.81 \log Lr + 2.65 \log P - 0.773 \log S - 6.42$	0.98	0.07	0.01
	Group 2	------	------	------	------
	Group 3	$\log Q_2 = 2.802 \log A - 4.368 \log Lr + 0.908 \log D + 8.015 \log S + 1.31 \log C - 9.26$	0.99	0.003	0.7
	Group 4	------	------	------	-----

Q in M^3/s and A in Km^2

Table 5-3: Regional Q equations in the east and in the west Khazer basin based on area (b).

Areas	Region	The regional Q equation	Cor. Coeff (R)	Stan. Error (S.E)	Level of Sig.(%)
The east	Group 1	$Q = 0.086A^{0.8407}$	0.84	0.25	0.001
	Group3	$Q = 0.1528A + 12.63$	0.98	16.6	0.001
	Whole Area.	$Q = 0.0184A + 20.87$	0.68	34.4	0.001
The west	Group 1	$Q = 4.73A^{0.378}$	0.61	0.22	Non. Sig.
	Whole Area.	$Q = 5.19A^{0.373}$	0.75	0.28	0.08

Q in M^3/s and A in Km^2

The median values of IMF/Q ratios were calculated using derived recurrences interval ***T*** year instantaneous flood peaks (IMF) from single site analysis that are shown in table 5-4. The corresponding regional frequencies of the median ratios for 4 cases are illustrated in Figure 5-1.
Trail and error approach has been done to correlate multi-regressions equations between recurrences interval ***T*** year instantaneous flood peaks and independent variables for each group and the whole

area in both the east and the west Khazer basin, which are summarized in table 5-5 and 5-6. It was not developed any equation for the whole area of the west Khazer basin.
Residual mean square of errors was calculated for results of equations (Q_{te}) comparing with those derived from single site frequency (Q_{to}) in the east area, which is shown in table 5-7. In the east Khazer basin, two gauged catchments named Zaringol and Darabcola, with 24 and 22 length of record, are selected for evaluation the two methods. A discriminating analysis shows that Zaringol catchment is located within group 4(a), with 99.9% of probability, and Darabcola, with 54% probability, belongs to group 1(a) as well as with 46% probability belongs to group 3(b). Various recurrences interval ***T*** year IMF were estimated by using regional equations of two methods and using catchment characteristics as independent variables for these catchments. Single site frequency analysis for both catchments has been done based on lognormal distribution and 2, 5, 10, 20, 25 50, 100 and 200 recurrences interval instantaneous flood peaks (IMF) were derived. Then, this pair series was compared that some of them are illustrated in Figure 5-2.

Table 5-4: The median ratios for various recurrence intervals in Khazer basin.

T	The east Khazer basin					The west Khazer basin		
Year	Whole area	Group1(b)	Group3(b)	Group4(a)	Group 1(a)	Whole area	Group 1(a)	Group 3(a)
2	1	1	1	1	1	1	1	1
5	1.807	2.156	1.808	2.297	1.789	1.702	1.664	1.922
10	2.297	3.298	2.483	3.697	2.497	2.22	2.158	2.592
20	3.361	4.719	3.21	5.458	3.304	2.775	2.67	3.274
25	3.663	5.243	3.458	6.119	3.589	2.961	2.839	3.499
50	4.707	7.101	4.282	8.5	4.559	3.566	3.385	4.215
100	11.673	9.347	5.188	11.443	5.667	4.213	3.962	4.963
200	15.035	12.033	6.184	15.035	6.928	4.908	4.561	5.748

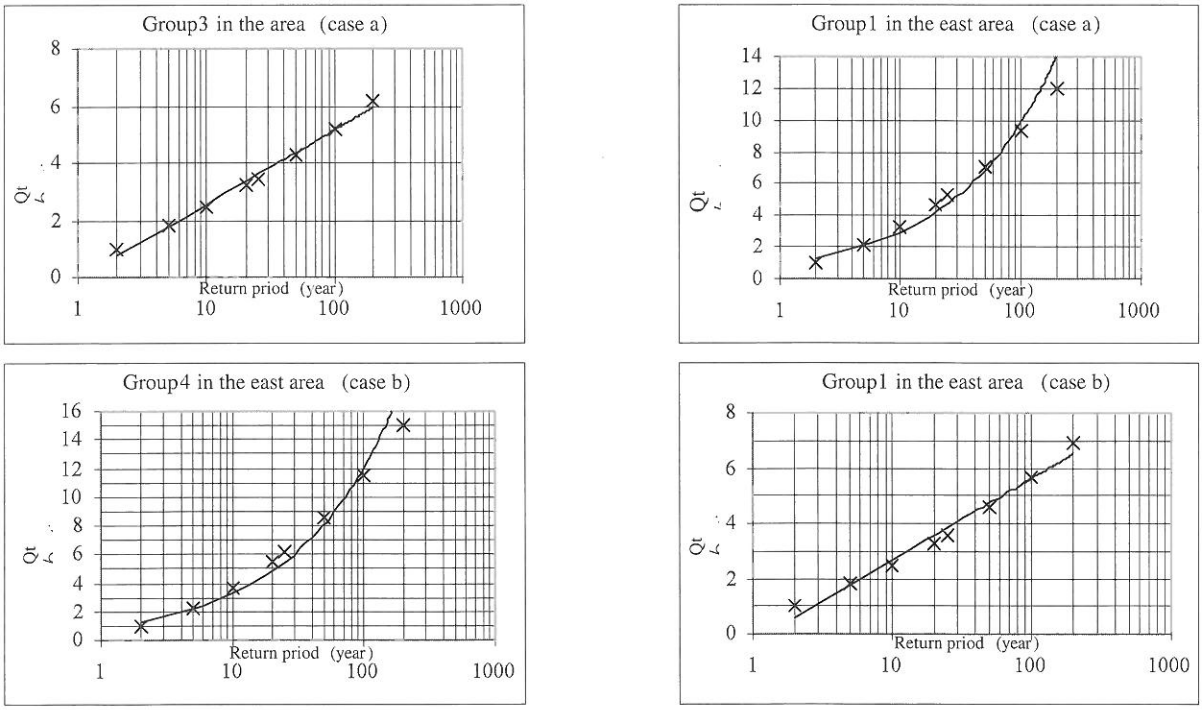

Figure 5-1: Regianal flood (Qt/Qratio) frequency for different homogenous groups.

Table 5-5: Multiple regression equations in the west Khazer basin.

Regression equation for group 1	R^2	S.E
$\log Q_2 = 1.0978\log A - 0.81\log Lr + 2.65\log P - 0.773\log S - 6.42$	0.97	0.07
$\log Q_5 = 1.1292\log A - 1.1247\log Lr + 2.1836\log P - 0.7921\log S - 4.35$	0.97	0.61
$\log Q10 = 1.1165\log A - 1.1654\log Lr + 1.8923\log P - 0.7665\log S - 3.3$	0.96	0.06
$\log Q25 = 1.297\log A - 1.534\log Lr + 1.512\log P - 0.798\log S + 0.22\log D - 1.79$	0.98	0.05
$\log Q50 = 1.293\log A - 1.548\log Lr + 1.289\log P - 0.776\log S + 0.24\log D - 1.04$	0.98	0.04
$\log Q100 = 1.284\log A - 1.545\log Lr + 1.086\log P - 0.754\log S + 0.26\log D - 0.36$	0.98	0.04
Regression equation for group 3	R^2	S.E
$\log Q_2 = 2.802\log A - 4.368\log Lr + 0.908\log D + 8.015\log S + 1.31\log C - 9.26$	0.99	0.03
$\log Q_5 = 1.778\log A - 3.401\log Lr + 0.875\log D + 5.898\log S - 6.12$	0.99	0.03
$\log Q10 = 1.041\log A - 0.875\log Lr + 0.369\log D + 1.45\log P - 3.34$	0.99	0.03
$\log Q25 = 1.271\log A - 1.411\log Lr + 0.474\log D + 0.828\log P - 1.09$	0.99	0.03
$\log Q50 = 1.797\log A + 1.995\log P - 4.773\log S + 1.675\log C + 1.15$	0.99	0.02
$\log Q100 = 1.878\log A + 1.81\log P - 5.552\log S + 1.722\log C + 2.83$	1.0	0.07

Table 5-6: Multiple regression equations in the east Khazer basin.

Group	Regression equation for group 1	R^2	S.E
1	$\log Q_2 = 0.704\log A + 3.65\log P + 2.437\log H - 18.34$	0.96	0.07
	$\log Q_5 = 0.664\log A + 2.696\log P + 2.119\log H - 14.59$	0.94	0.08
	$\log Q10 = 0.644\log A + 2.085\log P + 2.065\log H - 12.29$	0.93	0.09
	$\log Q25 = 0.426\log A + 1.508\log H - 0.81\log D - 4.59$	0.92	0.09
	$\log Q50 = 0.445\log A + 1.356\log H - 0.876\log D - 4.1$	0.94	0.08
	$\log Q100 = 0.462 ogA + 1.222\log H - 0.937\log D - 3.67$	0.95	0.07
3	$\log Q_2 = 0.489\log A + 9.132\log P - 2.654\log S - 22.09$	0.98	0.17
	$\log Q5 = 0.666\log A + 4.469\log P - 12.23$	0.98	0.08
	$\log Q10 = 0.796\log A + 2.475\log P + +0.848\log H + 1.36\log D - 8.58$	0.99	0.008
	$\log Q25 = 0.859\log A + 0.397\log H + 1.925\log D + 0.428\log S - 0.56$	0.99	0.003
	$\log Q50 = 0.9\log A - 1.664\log P + 2.244\log D + 0.763\log S + 5.01$	0.99	0.008
	$\log Q100 = 0.943\log A - 3.05\log P + 2.703\log D + 0.93\log S + 8.91$	0.99	0.02
4	$\log Q2 = 1.0526\log A - 2.872\log H + 7.82$	0.87	0.2
	$\log Q5 = 0.981\log A - 2.733\log H + 7.84$	0.92	0.14
	$\log Q10 = 0.980\log A - 2.611\log H + 7.66$	0.94	0.11
	$\log Q25 = 0.991\log A - 2.458\log H + 7.37$	0.96	0.09
	$\log Q50 = 1.0032\log A - 2.349\log H + 7.139$	0.95	0.1
	$\log Q100 = 1.0166\log A - 2.245\log H + 6.91$	0.93	0.12
Whole area (a)	$\log Q2 = 0.7487\log A + 3.9942\log P - 11.59$	0.76	0.22
	$\log Q5 = 0.7001\log A + 2.425\log P + 0.788\log S - 0.597\log H - 5.9$	0.86	0.14
	$\log Q10 = 0.63\log A + 1.655\log P + 0.91\log S - 0.793\log H - 2.95$	0.86	0.13
	$\log Q25 = 0.5228\log A + 1.218\log S - 1.113\log H + 2.722$	0.79	0.14
	$\log Q50 = 0.4934\log A + 1.1717\log S - 1.112\log H + 2.971$	0.76	0.14
	$\log Q100 = 0.4675\log A + 1.1309\log S - 1.1086\log H + 3.186$	0.7	0.16

Table 5-7: Residual mean square of errors resulted of equations in the east Khazer basin.

Return period (year)	Index flood method in case (a)	Index flood method in case (b)	Multi-regression method
2	53	41.68	41.68
5	76.6	61.66	51.21
10	91.76	78.82	61.27
25	118.42	108.38	81.51
50	149.98	145.33	102.02
100	199.25	205	139.28

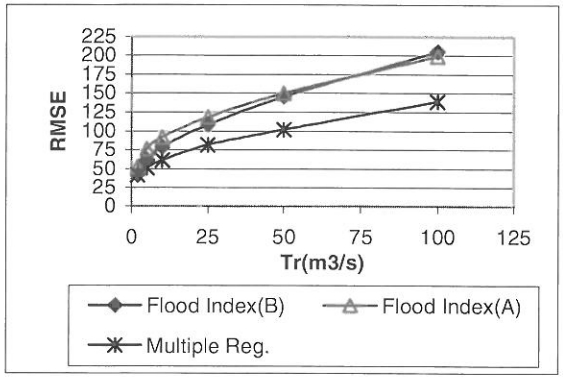

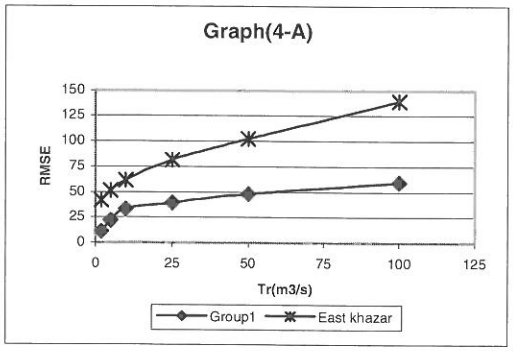

Figure 5-2: Comparison of index flood and multiple regressions in the east area.

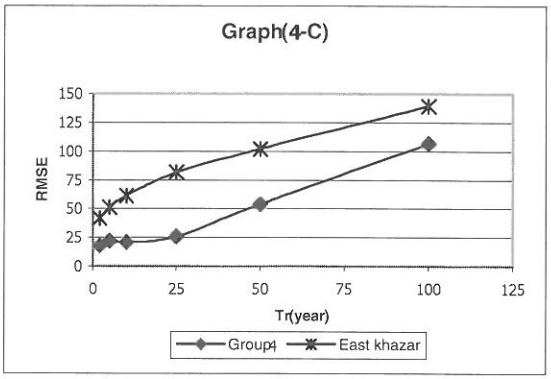

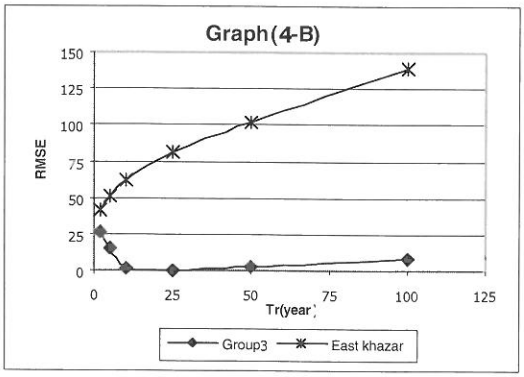

Figure 5-3: Comparison of RSME for regression in different groups in the cast area.

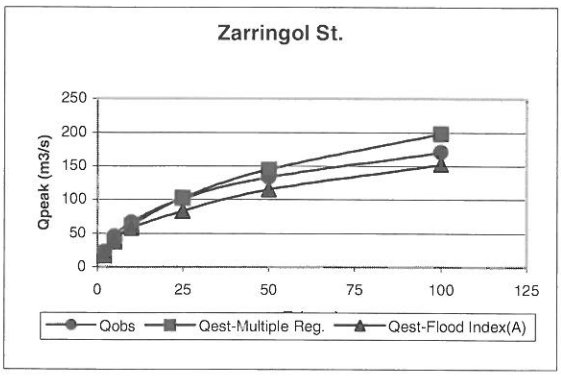

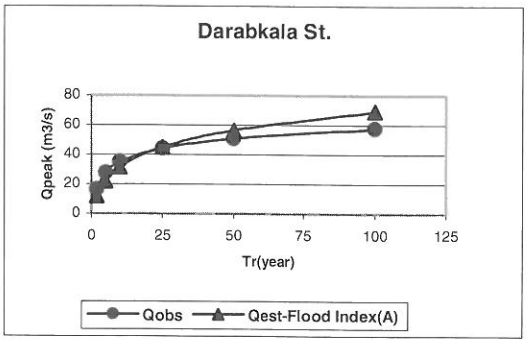

Figure 5-4: Observed and estimeted values of flood in Zarringol and Darabcola catchments.

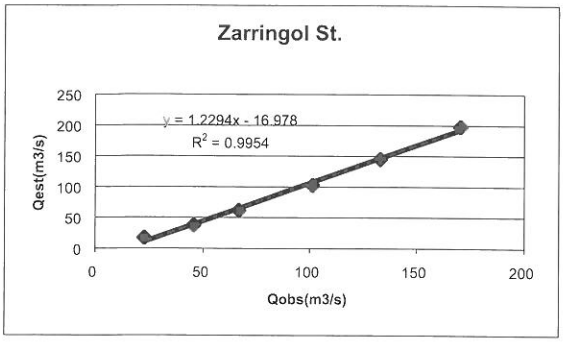

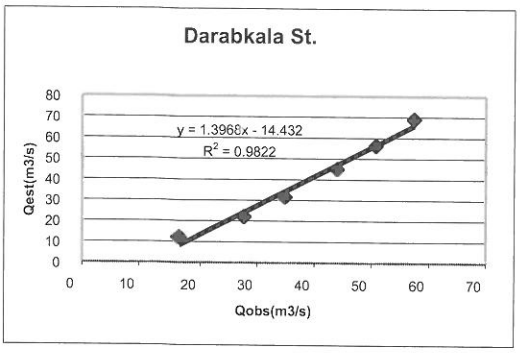

Figure 5-5: Estimated values of flood versus observed values in Zarringol and Darabcola catchment.

6 CONCLUSION

This study as many works done either in the world or Iran shows that the catchment area is the main factor that can be used as an independent variable for estimating flood magnitude. The result of this study is the same as works carried out by Daghestani (1997) and Ghiassi (1998) in a portion of this area. They determined that area, mean annual rainfall, and height of catchment are the major factors that affect on estimating of instantaneous peak flood.

In the east area, multiple regression analysis in region or homogenous group shows that in addition to the catchment area, factors such as annual rainfall, drainage density, mean weighted slope of land and mean height of area have important roles in flood estimation. Whereas in the west area, in addition to factors mentioned above, length of main channel is also an effective parameter because the shorter length of channel, the less travel time to reach to the catchment outlet in this area. It should be mentioned that the condition of forest trees in the east is much better than the west area.

Three parameters lognormal distribution is a dominant distribution for regional flood frequency in the north basins of Iran as quoted by other workers (Daghestani, 1997 and Ghiassi, 1998).

The comparison of results derived from multiple regression analysis and flood index methods shows that the first method using the homogeneous regions data is suitable for this area. Davoodirad (1999) also stated that multiple regression method estimates reasonable results compare to the flood index method for catchments located within middle part of Iran named Dariacheh Namak (salty lake). He also mentioned that homogenous grouping develops more accurate equations in both methods compare with equations have been resulted for the whole area as a region. His conclusion is similar to the results of present study. It was impossible to develop a regional Q equation for some groups. The reason can be related to the forestry condition of the considered catchments.

It is clear that the effect of forest on rainfall-runoff process is very important and It seems that it is necessary to group the catchments based on some criterion of vegetation condition such as coverage density and type of vegetation as Telvari et all (1997) applied in west of Iran.

Finely, it is recommended to apply the equations developed in the present study based on grouping and selecting the corresponding regression equations, which can estimate more reliable than the flood index method.

REFERENCES

Alikhani, B. (1997): Climatologic condition of Iran, University of Piamenoor (in Farsi).

Benson, M. A. (1962): Evolution of methods for evaluating the occurrence of floods, US Geological Survey, Water Supply Paper 1580-A.

Burn, D. H., Geol, N. K. (2000): The formation of groups for regional flood frequency analysis. Hydrological Sciences Journal No. 45(1).

Conover, W. J., Benson, M. A. (1963): Long-term flood frequencies based on extremes of short-term records, USGS Professional paper No. 450-E:159-160.

Daghestani, P. (1997): Effects of Physiographic and hydrologic factors affecting on maximum flood flows in Gilan and Mazenderan Proveniences (north of Iran), MSC. thesis. Faculty of agriculture, Tehran University (in Farsi).

Dalrymple, T. (1964): Flood characteristics and flow determination, in handbook of applied hydrology, Editor in chief V. T. Chow, McGraw Hill.

Davoodirad, A. (1999): Relationships between catchment morph metric factors and flood flows in central part of Iran, MSC. Thesis. Faculty of natural resources, Tehran University (in Farsi).

Ghiassi, N. (1998): Study of catchment geometric factors affecting on annual maximum flows using different derivation of catchment characteristics, Watershed management r annual research report, Soil Conservation and Watershed Management research Center, Ministry of Jihde-Sazendegy, Iran (in Farsi).

Houghton, J. C. (1978). Birth of a parent: The Wakeby distribution for modeling flood flows, Water Resource Research. vol. 14, No. 6:1105-1109.

Johnson, P. A., Ayyub, B. M. (1992): Assessing time-variant bridge reliability due to pier score, Jour. of Hydraulic Eng. Vol. 118, No. 6:887-914.

Kite, G. W. (1977): Frequency and risk analysis in hydrology. Fort Collins, Colorado: Water resources publication.

Nathan, R. J., McMahan, T. A. (1990): Identification of Homogeneous Regions for the Purposes of Regionalization, Jour. of Hydrology, 121:217-238.

Natural Environmental Resources Conservation (NERC) (1975): Flood studies report, vol. 1, Hydrological studies, London.

Potter, K. W., Lettenmaier, D. P. (1990): A comparison of regional flood frequency estimation methods using a resampling method., Wat. Resour. Res. Vol, 26, No.3:415-424.

Solomon, S. I. et al. (1968): the use of a square-grid system for computer estimation of precipitation, Temperature and runoff in sparsely gauged area, Wat. Resour. Res. Vol. 4, No. 5:919-930.

Stedinger, J. R. et al. (1992): Frequency analysis of extreme events, Chap. 18. In D. R. Maidment Editor in chief. Handbook of hydrology, McGraw-Hill, INC.

Telvari, A. (1997): Calibration of some experiences formula for flood estimating in Karkheh river basin in west of Iran, Watershed management r annual research report, Soil Conservation and Watershed Management research Center, Ministry of Jihde-Sazendegy, Iran,(in Farsi).

Zrinji, Z., Burn, B. H. (1996): Flood frequency analysis for ungauged sites using a region of influence approach, Jour. of Hydrology, Amsterdam, The Netherlands, 153: 1-21.

TOPKAPI: A PHYSICALLY BASED RAINFALL-RUNOFF MODEL

Ezio Todini, Zhiyu Liu

Department of Earth and Geo-Environmental Sciences, University of Bologna, Italy, todini@tin.it

SUMMARY

This paper introduces TOPKAPI (**TOP**ographic **K**inematic **AP**proximation and **I**ntegration), a new physically based distributed rainfall-runoff model deriving from the integration in space of the non-linear kinematic wave model. The TOPKAPI approach transforms the rainfall runoff and runoff routing processes into three non-linear reservoir differential equations. The first represents the drainage in the soil, the second represents the overland flow on saturated or impervious soil, and the last represents the channel flow along the drainage network. The geometry of the catchment is described by a lattice of cells (the pixels of a DEM and their slope) over which the equations are integrated to lead to a cascade of non-linear reservoir. The parameter values of the TOPKAPI model are shown to be scale independent and obtainable from digital elevation maps (e.g. DTM, DEM), soil maps and vegetation or land use maps in terms of slope, soil permeability, roughness, topology. It can be shown, under simplifying assumption, that the non-linear cascade aggregates into a unique non-linear reservoir at the sub-basin or basin level, which parameter values can be directly estimated from the small scale ones. The distributed version of TOPKAPI allows for its calibration on the basis of physical considerations and in particular its extension to un-gauged catchments. The lumped version of TOPKAPI allows for the extensive simulations needed, in combination with a stochastic rainfall generator, for deriving through simulation extreme discharges and flood wave volumes.

Keywords: Physically based rainfall runoff model, kinematic wave, non-linear reservoir.

1 INTRODUCTION

On the basis of a critical analysis of two well known and widely used hydrological rainfall runoff models, namely the ARNO (Todini, 1996) and the TOPMODEL (Beven and Kirby, 1979; Beven et al., 1984; Sivapalan et al., 1987), the authors recently proposed TOPKAPI (**TOP**ographic **K**inematic **AP**proximation and **I**ntegration) approach (Todini, 1995; Todini and Ciarapica, 2001; Liu, 2002). The ARNO model is a variable contributing area semi-distributed conceptual model driven by the total soil moisture storage, widely used for real-time flood forecasting. The major disadvantage of the ARNO model is the lack of physical grounds for establishing some of the parameters, which reduces its possible extension to ungauged catchments. The TOPMODEL is a variable contributing area model in which the predominant factors determining the formation of runoff are represented by the topography, the transmissivity of the soil and its vertical delay. However, it has been shown that the model preserves its physical meaning only at the hillslope scale (Franchini et al.,1996), while degrades into a conceptual model at larger scales, with the same problems mentioned for the ARNO model.
On the contrary, the TOPKAPI model is based on the lumping of a kinematic wave assumption in the soil, on the surface and in the drainage network, and leads to transform the rainfall runoff and runoff routing processes into three non-linear reservoir differential equations. The geometry of the catchment is described by a lattice of cells over which the equations are integrated to lead to a cascade of non-linear reservoir. The parameter values of the TOPKAPI model are shown to be scale independent and obtainable from digital elevation map, soil map and vegetation or land use map in terms of slope, soil permeability, roughness, topology. It can be shown, under simplifying assumption, that the non-linear cascade aggregates into a unique non-linear reservoir at the sub-basin or basin level, which parameter values can be directly estimated from the small scale ones.

2 STRUCTURE AND METHODOLOGY OF THE TOPKAPI MODEL

The TOPKAPI is a comprehensive distributed-lumped approach. The distributed TOPKAPI model is used to identify the mechanism governing the dynamics of the saturated area contributing to the surface runoff as a function of the total water storage, thus obtaining a law underpinning the development of the lumped model.

The model is based on the idea of combining the kinematic approach with the topography of the basin; a Digital Elevation Model (DEM), whose grid size generally increases with the overall dimensions, describes the latter. Each grid cell of the DEM is assigned a value for each of the physical characteristics represented in the model. The flow paths and slopes are evaluated starting from the DEM, according to a neighbourhood relationship based on the principle of the minimum energy cost (Band, 1986).
The integration in space of the non-linear kinematic wave equations results in three 'structurally-similar' zero-dimensional non-linear reservoir equations describing different hydrological and hydraulic processes. This lumping is performed on the individual cell of the DEM in the distributed model, while in the lumped model it is performed at the basin level. The equations obtained for the local scale and for the lumped scale are structurally similar; what distinguishes them are the coefficients, which in one case have local significance and, in the other, summarise the local properties in a global manner.
The present TOPKAPI model is structured around five modules that represent, namely the evapotranspiration, snowmelt, soil water, surface water and channel water component, respectively. As concerns the deep aquifer flow, the response time caused by the vertical transport of water through the thick soil above this aquifer is so large that we can speak of an almost constant horizontal flow in the aquifer with no significant response on one specific storm event in a catchment (Todini, 1995). For this reason, at the initial stage the model does not account for water percolation towards the deeper soil layers and for their contribution to the discharges; this is going to be introduced as an additional model layer soon.
The soil water component is affected by subsurface flow (or interflow) in a horizontal direction defined as drainage; drainage occurs in a surface soil layer, of limited thickness and with high hydraulic conductivity due to its macro-porosity. The drainage mechanism plays a fundamental role in the model both as a direct contribution to the flow in the drainage network, and most of all as a factor regulating the soil's water balance, particularly with regard to activating the production of overland flow. The soil water component is the most characterising aspect of the model because it regulates the functioning of the contributing saturated areas. The surface water component is activated on the basis of this mechanism. Lastly, both components contribute to feed the drainage network.
The most complex and physically realistic model for estimating actual evapotranspiration is the Penman-Montieth equation, which has been widely used in many distributed models, e.g. SHE (Abbott et al., 1986a,b), DHSVM (Wigmostra et al., 1994). However, for a practical utilisation a simplified approach is generally necessary due to the shortage of data and its accumulative nature of the evapotranspiration. In the present TOPKAPI model, evapotranspiration can be either directly introduced as an input to the model or computed externally or estimated internally as a function of the air temperature. A simplified radiation method (Doorembos et al., 1984) used to calculate the evapotranspiration starting from the temperature and from other topographic, geographic and climatic information is borrowed from the ARNO model. Again, for reasons of limited data availability, the snow accumulation and melting (snowmelt) component is driven by a radiation estimate based upon the air temperature measurements, which is also borrowed from the ARNO model.

3 THE DISTRIBUTED TOPKAPI MODEL

3.1 The soil water component

3.1.1 Kinematic wave formulation for sub-surface flow

In the TOPKAPI model, the horizontal sub-surface flow was thus calculated by means of the approximated formula (1) (Benning,1994; Todini and Ciarapica, 2001):

(1) $$q = \tan(\beta) k_s L \tilde{\Theta}^{\alpha}$$

where β is the slope, k_s is the saturated hydraulic conductivity, L is the thickness of the surface soil layer, $\tilde{\vartheta} = \frac{\vartheta - \vartheta_r}{\vartheta_s - \vartheta_r}$ is the reduced soil moisture content, ϑ_r is the residual soil moisture content, ϑ_s is the saturated soil moisture content, ϑ is the water content in the soil, $\tilde{\Theta} = \frac{1}{L}\int_0^L \tilde{\vartheta}(z)dz$ is the mean value along the vertical profile of the reduced soil moisture content and α is a parameter which depends on the soil characteristics (Benning, 1994; Todini, 1995).

Adding the flow Equation (1) to the continuity of mass equation, one obtains the following system:

$$\begin{cases} (\vartheta_s - \vartheta_r)L\dfrac{\partial\tilde{\Theta}}{\partial t} + \dfrac{\partial q}{\partial x} = p \\ q = \tan(\beta)k_s L\tilde{\Theta}^{\alpha} \end{cases} \tag{2}$$

where x is the main direction of flow along a cell, t is the time, q is the flow in the soil due to drainage, corresponding to a discharge per unit of width, and p is the intensity of precipitation. The model is written in just one direction since it is assumed that the flow along the slopes is characterised by a preferential direction, which can be described as the direction of maximum slope.
From the combination of the two equations (2), rewriting the problem in terms of actual total water content in the soil, $\eta = (\vartheta_s - \vartheta_r)L\tilde{\Theta}$, along the vertical profile, and making the following substitution:

$$C = \frac{Lk_s \tan(\beta)}{(\vartheta_s - \vartheta_r)^{\alpha} L^{\alpha}} \tag{3}$$

we get the following kinematic equation:

$$\frac{\partial\eta}{\partial t} = p - \frac{\partial q}{\partial x} = p - \frac{\partial\left(C\eta^{\alpha}\right)}{\partial x} \tag{4}$$

where the term C represents in physical terms a *local conductivity coefficient*, since it depends on soil parameters for a particular position or a particular cell, which encompasses the effects of hydraulic conductivity and slope, to which it is directly proportionate, and storage capacity, to which it is inversely proportionate.

3.1.2 Non-linear reservoir model for the soil water in a generic cell

Integrating Equation (3-4) in the soil over the i^{th} gird cell which space dimension is X, it gives:

$$\frac{\partial v_{s_i}}{\partial t} = pX - \left(C_{s_i}\eta_{s_i}^{\alpha_s} - C_{s_{i-1}}\eta_{s_{i-1}}^{\alpha_s}\right) \tag{5}$$

where v_{s_i} is the volume per unit of width stored in the i^{th} cell, while the last term in Equation (5) represents the inflow and outflow balance. Footer s is introduced to distinguish this soil water equation from the ones relevant to the overland and the drainage network flows.
Assuming that in each cell the variation of the vertical water content η_{s_i} along the cell is negligible, the volume of water stored into each cell can be related to the total water content η_{s_i}, that is equivalent to the free water volume in depth, by means of the following simple expression:

$$v_{s_i} = X\eta_{s_i} \tag{6}$$

Substituting for η_{s_i} in Equation (6) and writing it for the "source" cells namely the uppermost cells in each branch, the following non-linear reservoir equation is obtained, which solution can be obtained analytically based on an appropriate approximation (Liu, 2002):

$$\frac{\partial V_{s_i}}{\partial t} = p_i X^2 - \frac{C_{s_i} X}{X^{2\alpha_s}} V_{s_i}^{\alpha_s} \tag{7}$$

Similarly a non-linear reservoir equation can be written for a generic cell, given the total inflow to the cell:

$$\frac{\partial V_{s_i}}{\partial t} = \left(p_i X^2 + Q_{o_i}^u + Q_{s_i}^u\right) - \frac{C_{s_i} X}{X^{2\alpha_s}} V_{s_i}^{\alpha_s} \tag{8}$$

where V_{s_i} is the volume stored in the i^{th} cell in m^3, $Q_{o_i}^u$ is the discharge entering the active cell i as overland flow from the upstream contributing area (m^3/s), and $Q_{s_i}^u$ is the discharge entering the active cell as subsurface flow from the upstream contributing area in m^3/s.

3.1.3 Soil moisture accounting in a grid cell

For a generic i^{th} cell, at each time step the soil water balance calculation can be done by equations (9~11) as follows:

$$Q_{s_i}^d = (p_i X^2 + Q_{o_i}^u + Q_{s_i}^u) - \frac{V_{s_i}'(t_0 + T) - V_{s_i}'(t_0)}{T} \tag{9}$$

$$e_{o_i} = \max\left\{\left[V_{s_i}'(t_0 + T) - \min\left(V_{s_i}'(t_0 + T), V_{s_i}\right)\right], 0\right\} \tag{10}$$

$$V_{s_i}(t_0 + T) = \min\left[V_{s_i}'(t_0 + T), V_{sm_i}\right] - E_a X^2 \tag{11}$$

where T is the computational time interval, t_0 is the initial time of the computation step, $V_{s_i}'(t_0 + T)$ is the solution of Equation (9) at the time $t_0 + T$ in m^3, $Q_{s_i}^d$ is the outflow discharge from the i^{th} cell during the time $t_0 \sim t_0 + T$ in m^3/s, e_{o_i} is the saturation excess volume the i^{th} cell in m^3, V_{sm_i} is the saturated soil water in the i^{th} cell in m^3, E_a is the actural evapotranspiration within T calculated by the evapotranspiration model in m, and $V_{s_i}(t_0 + T)$ is the water volume stored in the soil in the i^{th} cell at the time $t_0 + T$.

Up to this point it was implicitly assumed that the entire outflow from a cell flows into the downstream cell immediately. However this is not entirely true; in fact the cells can be divided into two groups on the basis of the minimum drained area (threshold) suggested by O'Callaghan and Mark (1984). For the cells in the channel network the outflow is still evaluated by means of the Equation (9), but it is then partitioned between the channel and the downstream cell according to a gradient based upon the average slope of the four surrounding cells. This allows determining the amount of subsurface flow feeding the drainage channel network. This operation of flow partition is also performed for the overland flow.

3.2 The surface water and channel water components

The input to the surface water model is the *precipitation excess* resulting from the saturation of the soil layer. In addition, the flow in the soil can exfiltrate on the surface as return flow, thus also feeds the overland flow. The sub-surface flow and the overland flow together feed to the channel along the drainage network.

3.2.1 Non-linear reservoir model for overland flow and channel flow in a grid cell

Overland flow routings is described similarly to the soil component, according to the kinematic approach (Wooding, 1965), in which the momentum equation is approximated by means of the Manning's formula. The kinematic wave approximation of overland is described in Equations (12).

(12)
$$\begin{cases} \dfrac{\partial h_o}{\partial t} = r_o - \dfrac{\partial q_o}{\partial x} \\ q_o = \dfrac{1}{n_o}(\tan\beta)^{\frac{1}{2}} h_o^{\frac{5}{3}} = C_o h_o^{\alpha_o} \end{cases}$$

where h_o is the water depth over ground surface in *m*, r_o is the saturation excess resulting from the solution of the soil water balance equation (11), either as the precipitation excess or the ex-filtration from the soil in absence of rainfall, in *m/s*, n_o is the Manning friction coefficients for the surface roughness in $m^{-1/3}s^{-1}$, $C_o = (\tan\beta)^{1/2}/n_o$ is the coefficient relevant to the Manning formula for overland flow, $\alpha_o = 5/3$ is the exponent which derives from using Manning formula.

In analogy to what was done for the soil, by assuming that the water depth is constant over a cell and integrating the kinematic equation over the longitudinal dimension, it gives the non-linear reservoir model for the overland flow, as in Equation (13).

(13)
$$\frac{\partial V_{o_i}}{\partial t} = r_{o_i} X^2 - \frac{C_{o_i} X}{X^{2\alpha_o}} V_{o_i}^{\alpha_o}$$

where the footer *i* denotes the ith cell, V_{o_i} is the volume of the water on the surface in the cell in m^2.

Similar considerations also apply to the channel network, which is assumed to be tree shaped with reaches of wide rectangular cross sections. In this case the surface width is not constant but it is assumed to be increasing towards the catchment outlet. Under these assumptions, the following expression of non-linear reservoir model can be written for a generic reach:

(14)
$$\frac{\partial V_{c_i}}{\partial t} = \left(r_{c_i} X W_i + Q_{c_i}^u\right) - \frac{C_{c\,i} W_i}{(X W_i)^{\alpha_c}} V_{c_i}^{\alpha_c}$$

where V_{c_i} is the volume of water stored in the i^{th} channel reach in m^3, W_i is the width of the i^{th} rectangular channel reach, which is taken to increase as a function of the area drained by the ith cell on the basis of the geo-morphological considerations, $Q_{c_i}^u$ is the inflow discharge from the upstream reaches in m^3/s, r_c is the lateral drainage input, including the overland runoff reaching the channel reach and the soil drainage reaching the channel reach in *m/s*, s_0 is the bed slope, assumed to be equal to the ground surface slope, n_c is the Manning friction coefficients for the channel roughness in $m^{-1/3}s^{-1}$, $C_c = s_0^{1/2}/n_c$ is the coefficient relevant to the Manning formula for channel flow, $\alpha_c = 5/3$ is the exponent which derives from using Manning formula.

3.3 Philosophy of application of the distributed TOPKAPI model

3.3.1 Data requirements and parameters

The required data for the TOPKAPI model include watershed terrain data (e.g., DTM or DEM data, land survey data), soil survey data, and vegetation or land use data, geographical co-ordinates, precipitation data, evapotranspiration or air temperature data.

As far as the parameters are concerned, there are seven classes of parameters in the TOPKAPI model, namely *L* (thickness of the surface soil layer in *m*), k_s (saturated hydraulic conductivity in *m/s*), ϑ_r (residual soil moisture content), ϑ_s (saturated soil moisture content), α_s (exponent of the trasmissivity law for the soil component, assumed to be constant for all the cells), n_o (surface roughness in $m^{-1/3}s^{-1}$), and n_c (roughness for the channel in $m^{-1/3}s^{-1}$). Among them, five parameters (*L*,

k_s, ϑ_r, ϑ_s and α_s) are interested at the soil level, and control the runoff formulation, while the other two parameters (n_o, n_c) are deemed as routing parameters.

3.3.2 Model calibration

Although the TOPKAPI model is physically based, the model still needs a calibration procedure because of the uncertainty of the information on the topography, soil characteristics and land cover. Nonetheless the calibration of the TOPKAPI parameters is more an adjustment rather than a conventional calibration and is carried out by means of simple trial-and-error method.
Model parameter values are assigned according to the type of soil, land cover and channel order by the method of Strahler (1957). The initial parameter values can be taken from the literature, e.g. the values of the soil parameters k_s, ϑ_r and ϑ_s can be taken from the USDA parameter for the infiltration model of Green-Ampt. The initial values of parameters n_o and n_c can be guessed by referring to the Tabs. 5.5 and 5.6 in the book on *Open Channel Hydraulics* by Chow (1959) and a report on *Roughness Characteristics of Natural Channel* by Harry. H. Barnes (1967), while α_s usually varies 2.0 ~ 4.0 based on the soil property. In general, the model parameter values range: *L=0.10 ~2.00 m, = 10^{-6} ~ 10^{-3} m/s, ϑ_s = 0.25~0.70, ϑ_r = 0.01~0.10, n_o = 0.05~0.20, n_c =0.02~0.08.*

4 THE LUMPED TOPKAPI MODEL

As mentioned before, the TOPKAPI approach is a comprehensive distributed-lumped approach. Theoretically it proves the lumped version of the TOPKAPI model can be derived directly from the distributed version and does not require additional calibration (Todini and Ciarapica, 2001). The distributed TOPKAPI model is used to identify the mechanism governing the dynamics of the saturated area contributing to the surface runoff as a function of the total water storage, similarly to what is done in the Xinanjiang (Zhao, 1977) and in the ARNO (Todini, 1996). The relationship between the extent of saturated areas and the volume stored in the catchment can be approximated by a Beta-distribution function curve. The ex-filtration process identified in the distributed model is also represented in the lumped TOPKAPI model by means of relating the return flow discharge with the water storage in the river basin (Liu, 2002).

4.1 Structure of the lumped TOPKAPI model

In order to obtain the lumped version of the TOPKAPI, the basic kinematic wave equation must be integrated over the entire system of cells describing the basin. This is done first by computing the total volume stored in the soil, on the surface or in the channel network by adding up the single cell volumes as a function of the geo-morphology and topology of the catchment. Taking account of this aggregation and integrating the kinematic wave equation over the whole basin, under a simplifying assumption that the variation over time in the water content during the transient phase is not ignored as done in TOPMODEL but assumed to be constant in space, a zero-dimensional non-linear reservoir equation (Liu, 2002) as Equation (4-1) can be obtained for representing the basin as a whole.

(15)
$$\frac{\partial V_{s_T}}{\partial t} = RA - \left(\frac{\alpha_s + 1}{\alpha_s X^2} \frac{1}{\left[\sum_{l=1}^{N-1} \left(\prod_{m=l}^{N-1} f_m \right) + 1 \right]} \right)^{\alpha_s} X \overline{C}_{s_T} V_{s_T}^{\alpha_s} \quad \text{with}$$

$$\frac{1}{\overline{C}_{s_T}} = \left\{ \sum_{i=1}^{N} \left\{ \left[\frac{1 + \sum_{l=1}^{j-1} \left(\prod_{m=l}^{j-1} f_m \right)}{\sum_{l=1}^{N-1} \left(\prod_{m=l}^{N-1} f_m \right) + 1} \right]^{\frac{\alpha_s + 1}{\alpha_s}} - \left[\frac{\sum_{l=1}^{j-1} \left(\prod_{m=l}^{j-1} f_m \right)}{\sum_{l=1}^{N-1} \left(\prod_{m=l}^{N-1} f_m \right) + 1} \right]^{\frac{\alpha_s + 1}{\alpha_s}} \right\} \Big/ C_{s_i}^{1/\alpha_s} \right\}^{\alpha_s}$$

where i is the index of a generic cell; j is the of cells drained by the i^{th} cell; N is the total number of cells in the upstream contributing area, V_{s_T} is the water storage in the catchment, R is the infiltration rate; A is the catchment area; f_m represents the fraction of the total outflow from the m^{th} cell which flows towards the downstream cell, and α_s is a soil model parameter assumed constant in the catchment, Footer s and T denote 'soil' and 'total', respectively.
Equation (4-1) corresponds to a non-linear reservoir model and represents the lumped dynamics of the water stored in the soil. The same type of equation can be written for the overland flow and for the drainage network, thus transforming the distributed TOPKAPI model into a lumped model characterised by three 'structurally similar' non-linear reservoirs, namely 'soil reservoir', 'surface reservoir' and 'channel reservoir'.
In the lumped TOPKAPI model, on the basis of the soil condition and actual evapotranspiration the precipitation in the catchment is partitioned into the direct runoff and the infiltration by using the Beta-distribution curve that reflects the non-linear relationship between the soil water storage and the saturated contributing area in the basin. The infiltration and the surface runoff are input into the soil reservoir and the surface reservoir, respectively. The outflows from the two reservoirs in the terms of the interflow and the overland flow are then drained into the channel reservoir to form the channel flow.

5 APPLICATIONS

Since the advent of the TOPKAPI in 1995, the model has already been applied to several catchments for different uses. The model has been applied at least to the upper Reno River basin (1051 km^2) and the Arno River basin (8135 km^2) for flood forecasting and applied to Magra catchment (1682 km^2) for extreme flood analysis. The DEM grid size usually increasing with the catchment size ranges from 200 m to 1km in the three examples.

5.1 Results of model application in upper Reno River catchment

The upper Reno River catchment is enclosed at Casalecchio, covers an area of approximately 1,051 km^2 and comprises primarily clayey and marly soil, as well as alluvial deposits in its terminal section. The data available for this basin are the hourly rainfall, temperature and water level values over the whole year of 1990, and the soil map as well as the DEM with a grid size of 400 m.
Discharges were computed from hourly levels by means of a well-verified rating curve available at Casalecchio. The areal rainfall distribution was estimation based on the Thiessen Polygon method. The calibration of the TOPKAPI model was performed at a 1-hour time step using the hydrological data available over the period of Jan.~May 1990, and the validation test was performed using the rest data. Figs. 5.1~5.2 show the sequences of simulated and historical discharged values by using the model.

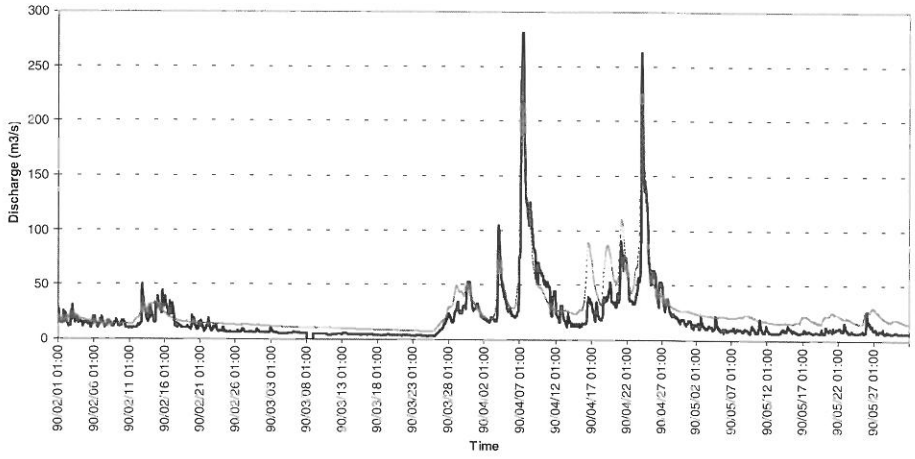

Figure 5.1: Upper Reno River basin: the TOPKAPI model calibration results. Reference period: Jan.– May 1990. Continuous line, observed discharges; dashed line, simulated discharges.

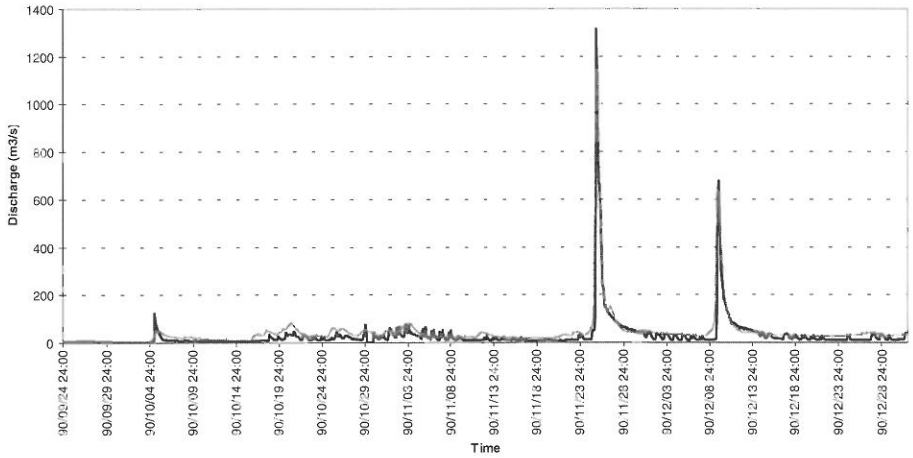

Figure 5.2: Upper Reno River basin: the TOPKAPI model verification results. Reference period: 1 June – 31 Dec. 1990. Continuous line, observed discharges; dashed line, simulated discharges.

The TOPKAPI model efficiency in terms of the explained variance coefficient *EV*, the determination coefficient *DC* and the correlation coefficient *CC* is shown in Table 5.1, and the calibrated model parameter values are shown in Table 5.2.

Table 5.1: The model efficiency of the TOPKAPI model in upper Reno River catchment.

EV		DC		CC	
Calibration	Validation	Calibration	Validation	Calibration	Validation
0.8497	0.8867	0.8426	0.8735	0.9179	0.9346

Table 5.2: Calibrated model parameter values of the TOPKAPI model.

Catchment	Area (km^2)	Grid size (m)	K_S (m/s)	θ_s-θ_r	α_s	n_o	n_c
Upper Reno River	1051	400	9e-4~1.4e-3	0.15~0.32	2.5	0.085~0.090	0.035 ~0.045

5.2 Results of model application in Magra catchment

The distributed version of TOPKAPI allows for its calibration on the basis of physical considerations and in particular its extension to ungauged catchments. The distributed TOPKAPI model was used for the extreme flood frequency analysis study in an Italian river basin, namely Magra catchment with the area of 1682 km^2, in which the hydrological data is not sufficient. The target outputs are required to include the extreme discharge values at the key control hydrological measurement points of both the main tributaries and the main stream under the given conditions of the preset return periods of 10, 20, 30, 50, 100, 200, 500 years (Liu and Todini, 2000).
This study comprises two phases: estimation of extreme rainfall values by undertaking the regional analysis of extreme precipitation, and evaluation of extreme flood discharge values by means of TOPKAPI model under various assumed initial saturated soil condition with the preset duration and return periods. FigURE 5.3 shows the extreme flood values at the catchment outlet in response to the storm events of 12-hour duration for the return periods of 10, 20, 30, 50, 100, 200, 500 years.
More reasonably, the extreme flood peak [$Q_m(T,d)$] of a return period T corresponding to a rainfall event of d-hour duration should be calculated in the following expression.

(16) $$Q_m(T,d) = \int Q(T,d,S_{ini}) f(S_{ini}) dS_{ini}$$

where $Q(T,d,S_{ini})$ is the flood peak of a return period T at a soil initial saturated percentage S_{ini}.Let us assume that the initial soil moisture saturated condition, specified in the TOPKAPI model with the initial soil saturated percentage S_{ini}, is a random variable with a probability distribution $f(S_{ini})$.

In connection to this need of obtaining the probability distribution of the initial soil saturation, the lumped version of TOPKAPI can be used for the extensive simulations, in combination with a stochastic rainfall generator, for deriving through simulation extreme discharges and flood wave volumes.

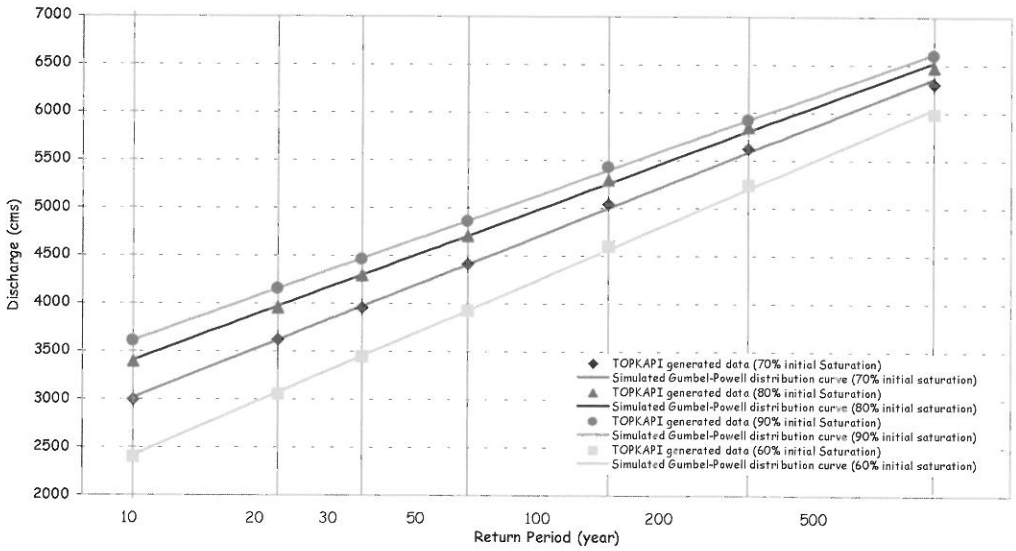

Figure 5.3: Gumbel-Powell probability distribution of extreme flood discharge peaks in Magra catchment under the different assumed initial soil conditions (60%, 70%, 80%, 90%).

6 CONCLUSIONS

A correct integration of the differential equations from the point to the finite dimension of a pixel, and from the pixel to larger scales, can actually generate relatively scale independent models, which preserve the physical meaning (although as averages) of the model parameters. This consideration is reflected in the TOPKAPI approach. The TOPKAPI model couples the kinematic approach with the topography of the catchment and transfers the rainfall-runoff processes into three 'structurally-similar' zero-dimensional non-linear reservoir equations describing different hydrological and hydraulic processes. The parameter values of the TOPKAPI model are shown to be scale independent and obtainable from digital elevation maps (e.g. DTM, DEM), soil maps and vegetation or land use maps in terms of slopes, soil permeability, roughness, topology.

The TOPKAPI approach is a comprehensive distributed-lumped one. The distributed TOPKAPI is used to identify the mechanism governing the dynamics of the saturated area contributing to the surface runoff as a function of the total water storage. Theoretically it proves the lumped version of the TOPKAPI model can be derived directly from the distributed version and does not require additional calibration.

With the advantage of being a physically based model with simple and parsimonious parameterisation, the TOPKAPI model can have numerous applications ranging from flood forecasting, the extreme flood, predicting hydrological response under the changed landscape conditions caused by human activities. Last but not least an appealing possibility exists in the future of deriving model representations from the available world 1x1 km^2 carthography (such as for instance GOTOPO30 produced by the USGS) to be lumped at the 50x50 or 20x20 km^2 meshes of the Mesoscale or Limited Area Meteorological (LAM) Models in order to better reproduce the soil atmosphere exchanges.

The distributed version of TOPKAPI allows for its calibration on the basis of physical considerations and in particular its extension to ungauged catchments. The lumped version of TOPKAPI allows for the extensive simulations needed, in combination with a stochastic rainfall generator, for deriving through simulation extreme discharges and flood wave volumes.

As far as the further development of the TOPKAPI model is concerned, at least a percolation and groundwater model and a new approach for considering the lakes and the reservoirs should be included in the new TOPKAPI model.

REFERNCES

Abbott, M. et al. (1986a): An introduction to the European Hydrological System – Système Hydrologique Européen, SHE; 1. History and philosophy of a physically based distributed modelling system, Journal of Hydrology, Vol. 87, 45-59. 2. Structure of a physically based, distributed modelling.

Abbott, M. et al. (1986b): Physically-based distributed modelling of an upland catchment using the Système Hydrologique Européen . Journal of Hydrology, Vol. 87: 79-102.

Band, L.E. (1986): Topographic partition of watersheds with digital elevation models. Water Resour. Res., 22(1): 15-24.

Benning R.G. (1994): Towards a new lumped parameterization at catchment scale. Doctoral thesis.

Beven K.J. (1981): Kinematic subsurface stormflow. Water Resour. Res., 17(5): 1419-1424.

Beven K.J., Kirkby M.J. (1979): A physically based, variable contributing area model of basin hydrology. Hydrological Sciences – Bulletin des Sciences Hydrologiques, 24, 1-3.

Beven K.J., Kirkby M.J., Schofield, N. and Tagg, A.F. (1984): Testing a physically-based flood forecasting model (TOPMODEL) for three U.K. catchments, J. Hydrology, 69: 119-143.

Cash, J.R., and Karp, A. H. (1990): A variable order Runge-Kutta method for initial value problems with rapidly varying right hand sides. ACM Transactions on Mathematical Software, 16(3): 201-222.

Chow V. T. (1959): Open-Channel Hydraulics. International student edition, McGraw-Hill Book Company, Inc.

Chow, V. T., Maidment, D.R., and Mays, L.W. (1988): Applied Hydrology. McGraw-Hill Book Company.

de Marsily, Ghislain (1986): Quantitative hydrology: Groundwater Hydrology for Engineers. Chapter 11: Geostatistic and stochastic approach in hydrogeology. Academic Press, Inc., California, p286-329

Dunne T. (1978): Field studies of hillslope flow process. In M.J. Kirkby (Ed.), Hillslope Hydrology. Wiley, New York:227-293.

Franchini M., Helmlinger K. R., E. Foufoula-Georgiou, Todini E. (1996): Stochastic storm transposition coupled with rainfall-runoff modelling for estimation of exceedance probabilities of design floods. Journal of Hydrology, 175: 511-532.

Harry H. Barnes, Jr. (1967): Roughness Characteristics of Natural Channels. Geological Survey Water –Supply Paper 1849. United States Government Printing Office, Washington.

Henderson F.M., Wooding R.A. (1964): Overland flow and groundwater flow from a steady rainfall of finite duration. J. Geophys. Res., 69(6): 1531-1540.

Liu, Z. (2002): Toward A Comprehensive Distributed/Lumped Rainfall-Runoff Model: Analysis of Available Physically Based Models and Proposal of a New TOPKAPI Model. PhD dissertation, the University of Bologna.

Liu, Z., Todini, E. (2000): Application of TOPKAPI Model for Extreme Flood Frequency Analysis Study in Magra Catchment. Proceedings of the International IDNDR Symposium held in Perugia in July. Volume entitiled 'Hydro-Geological Disasters Reduction: Recent Developments And Perspectives'.

Matheron, G. (1970): La théorie des variables regionaliséés et ses applications, Cah. Cent. Morphol. Math., 5.

O'Callaghan, J.F., Mark, D.M. (1984): The extraction of drainage networks from digital elevation data. Computer Vision, Graphics, and Image Processing, 28: 323-344.

Sivapalan, M., Beven, K.J. and Wood, E.F. (1987): On hydrological similarity 2. A scaled model of storm runoff production. Water Resour. Res. ,23(12), pp. 2266-2278.

Strahler, A. N. (1957): Quantitative analysis of watershed geomorphology. Transactions of the American Geophysical Union 38: 913-920.

Todini E. (1995): New trends in modelling soil processes from hill-slope to GCMS Scales - The role of water and the hydrological cycle in global change, edited by H. R. Oliver, S. A. Oliver, NATO ASI Series I: Global Environmental Change, 31: 317-347.

Todini. E. (1996): The ARNO rainfall-runoff model. J. Hydrology ,175, p339-382.

Todini, E., Ciarapica L. (2001): The TOPKAPI model. Mathematical Models of Large Watershed Hydrology, Chapter 12, edited by Singh. V.P. et al., Water Resources Publications, Littleton, Colorado.

Wigmosta M.S., Vail, L.W. and Lettenmier, D.P. (1994): A distributed hydrology-vegetation model for complex terrain. Water Resources Research, Vol. 30, No. 6: 1165-1679.

Zhao R.J. (1977): Flood forecasting method for humid regions of China. East China College of Hydraulic Engineering, Nanjing.

CLARK-WSL – A METHOD FOR THE ESTIMATION OF FLOOD HYDROGRAPHS IN SMALL TORRENTIAL CATCHMENTS

Stephan Vogt, Felix Forster, Christoph Hegg

WSL Swiss Federal Research Institute, Zürcherstrasse 111, 8903 Birmensdorf, Switzerland,
stephan.vogt@wsl.ch, christoph.hegg@wsl.ch

SUMMARY

The procedure proposed in this paper allows the determination of the peak flow and the corresponding hydrograph of an event for a given return period in small torrential catchments (< 5 km^2). The necessary catchment parameters are objectively determined during a field inspection.
Clark-WSL is based on the conceptual rainfall-runoff model of Clark which combines the concepts of linear storage and linear translation. The return period of the flood event is matched to the one of the initiating storm rainfall which is derived from the respective maps in the Hydrological Atlas of Switzerland. Its duration is given by the time of concentration which is calculated with a GIS-approach, using flow velocities of overland and channel flow. The volume runoff coefficient Ψ is assumed to depend on the event rainfall and the water storage capacity which is to be determined in the field according to a decision scheme.
The method has been applied in 10 small catchments in Switzerland where discharge time series exist. Events with return periods of 20 and 100 years have been estimated and compared with extrapolated measured flood data of the same return period. Clark-WSL leads to satisfying results with a slight tendency to underestimate the statistical values. Verification of the total discharge volume provided by the hydrograph has only been carried out for the Erlenbach catchment. There, Clark-WSL leads to realistic results compared with statistical values.
Since no estimation method is suitable for the entire spectrum of catchments, Clark-WSL makes part of a multi-method approach.

Keywords: hydrology, natural hazard, rainfall-runoff relationship, total discharge, peak flow

1 INTRODUCTION

Flood events in small torrential catchments in Switzerland result in costs of some 35 – 70 Mio € *every* year. This loss potential stands in contrast to the lack of longterm time series in small torrential catchments. Thus, engineers can use neither extreme value statistics nor complex hydrological models for design problems. In practice, estimation methods are therefore still the most common tools in hydrological design.
What are the demands on a modern flood estimation method for small torrential catchments?

- In practice, numerous estimation methods are popular. Most of the methods have been developed for mesoscale and large scale catchments. Applicability in small catchments has not always been tested systematically.
- Older methods are often developed to estimate the peakflow with a return period of 100 years (HQ_{100}) or the maximal possible peak flow (HQ_{max}). Today the choice of a return period depends on the protection goal. Therefore, an estimation method has to provide a flexible choice of the return period.
- Flood events combined with bedload transport processes are causing more damage than pure flood events. For the calculation of bedload transport not only a peak flow, but also the respective hydrograph is needed.
- Time exposure for the application of an estimation should not exceed a few days including field work.
- Parameters should be determined in an objective way. Different users should get similar results.

Taking these points into account, a method has been developed to estimate the peak flow and the respective hydrograph of rare flood events in small torrential catchments using the rainfall-runoff model of Clark (Clark, 1945). Up to now, this model has been known as a conceptual model to calculate past flood events. In this paper, the effort to use this model as a flood estimation method is presented. The paper bases mostly on an internal report (Vogt, Forster, 1999) and on a diploma thesis (Vogt, 2001).

In a first chapter the principles of Clark-WSL are shortly introduced. A second chapter will focus on the determination of the parameters. The following chapter will show the application and validation of the model in several small torrential catchments in Switzerland.
Investigations in several small catchments have shown that a single estimation method cannot cover the entire spectrum of small torrential catchment. It is strongly recommended to apply Clark-WSL as a part of a multi-method approach as presented in Forster and Hegg (2002).

1.1 Description of the model

The estimation method Clark-WSL combines the concepts of linear storage and linear translation. This linkage has been described by Clark (1945). In this approach, the linear storage is considered to be at the outlet of the catchment and is supplied with net rainfall. The temporal distribution of the inflow is calculated with the concept of linear translation.
The equation (1) for the **linear storage** shows that the outflow of the storage Q [m^3/s] is connected to the content of the storage S [m^3] via the storage constant K [s]:

(1) $$S = K \cdot Q$$

The storage constant K is representing the storage features of the linear storage and in the broader and more applied sense the response of the hydrological catchment to a rainfall event. An increasing value for K is characteristical for a delayed response of the catchment and vice versa.
Considering the continuity condition

(2) $$P = Q + \frac{dS}{dt}$$

where P [m^3/s] is the inflow to the storage, we can write the differential equation

(3) $$P = Q + K \cdot \frac{dQ}{dt}$$

With the condition $Q = 0$ for $t \leq 0$ the solution of equation (3) is

(4) $$Q(t) = \int_0^t P(t) \frac{1}{K} e^{-(t-\tau)/K} d\tau$$

This expression is equal to the convolution integral for linear time-invariant systems. The pulse response $h(t)$ is given by the mentioned convolution integral:

(5) $$h(t) = \frac{1}{K} e^{-t/K}$$

The second basic element of Clark-WSL is the concept of **linear translation** of discharge in the stretches of stream. This means that the inflow P into a system leaves with the same temporal distribution as it enters it (Formula 6):

(6) $$Q(t) = P(t - \tau)$$

The assumption of linear translation is warrantable due to short and steep flow paths in most of the small torrential catchments. Linear translation is comprised with an area-time diagram. The area-time diagram can be understood as a parallel connection of linear stretches of a stream.
For numerical treatment of the problem, Clark used the Muskingum model with pure storage. It can be written as

(7) $$Q_t = c_1 \cdot W_t + c_2 \cdot W_{t-\Delta t} + c_3 \cdot Q_{t-\Delta t}$$

where c_1, c_2 and c_3 are constants depending from the chosen time step and the storage constant K, and W is the input function (Net rainfall per time step and area section).

2 DETERMINATION OF MODEL PARAMETERS

2.1 Initiating rainfall

Short-time rainfall with high intensities is the most important trigger for extreme flood events in small torrential catchments. For past flood events, there is only a weak correlation between the return period of the initiating rainfall and the return period of the resulting peak flow. The most important reason are variable preconditions in the catchment. It is too complex for an estimation method to take antecedent moisture conditions into account. Assuming that the catchment can be characterised with medium preconditions, Clark-WSL matches the return period of the peak flow with the one of the initiating storm rainfall. The intensity of the storm rainfall is derived from the respective maps 2.4 and 2.4[2] in the Hydrological Atlas of Switzerland. The two versions of extreme point rainfall maps differ from the interpolation method used. With these maps, the intensity for any given duration and return period can be derived. The return period is chosen according to the protection goal, the duration is given by the time of concentration.
In consideration of a margin of safety in design problems, the maps resulting in the higher rainfall intensity have to be chosen unless swiss record values are exceeded (Forster, Baumgartner, 1999).
If available, own statistical analysis of rainfall data can be used to determine the rainfall.

2.2 Runoff Coefficient

Since Clark-WSL is calculating not only the peak flow of a flood event but also the respective hydrograph, a volume runoff coefficient is needed. Total flood discharge is given by the net rainfall which results from the following formula:

(8) $$N_{eff} = \frac{(N - 0.2 \cdot WSV)^2}{N + 0.8 \cdot WSV}$$

where N_{eff} [mm] is the net rainfall, N [mm] is the initiating rainfall as specified above and WSV is the water storage capacity [mm].
The water storage capacity WSV is defined as the storage capacity which can be mobilised for a short timeframe during a storm rainfall.
This definition is based on two publications:

- Ogrosky and Mockus (1964) are using a potential infiltration to deduce the SCS-CN method for the determination of net rainfall. The potential infiltration is corresponding in its formal meaning with the water storage capacity WSV.
- Kölla (1986) is describing the wetting volume as the rain volume the soil is able to take up until saturated overland flow will occur.

The scope of the values for the water storage capacity is similar to the one published by Kölla (1986). It must be pointed out that Kölla specifies the area of a small catchments with less than 100 km^2, while in this context an upper limit of 5 km^2 is used. In addition, the wetting volume in Kölla is determined as a lumped value for the entire catchment whereas the water storage capacity WSV is determined spatially distributed. In consequence, the scope of values has been extended in order to cover a wide range of different catchments.
A field inspection is absolutely necessary for the estimation of the water storage capacity WSV. Basing only on mapped information is inadequate for flood estimation in small torrential catchments. Mapped spatial information (i.e. soil maps) normally have a too rough resolution for direct application, but can be used as a first overlook and working hypothesis for field work.
The criteria for the estimation of the water storage capacity WSV have been established by Rickli and Forster (1997) (Figure 1). Two main aspects have to be investigated: infiltration conditions with soil compaction and waterlogging as indicators on the one hand and water absorption capacity with

waterlogging, content of soil skeleton, occurrence of macro pores, thickness of the hydrologically relevant soil layer and thickness of a possibly existing humus layer on the other hand.

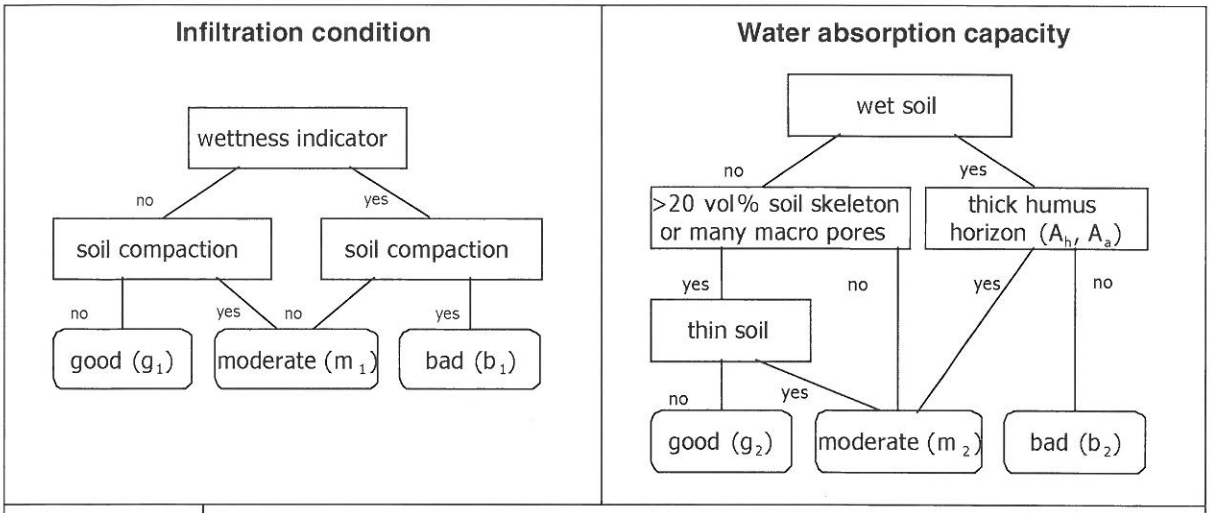

	water storage capacity [mm]				
	g_1g_2	g_1m_2, m_1g_2	m_1m_2	m_1b_2, b_1m_2	b_1b_2
Forest	40	30	25	20	10
Openland with vegetation	35	25	20	15	5

Figure 2-1: Decision scheme for an objective and spatially distributed determination of the water storage capacity WSV for a time of concentration of 60 minutes. Modified after Rickli, Forster (1997).

The water storage capacity is regarded to be dependent from the time of concentration. The values quoted in the decision scheme are valid for a time of concentration of 60 minutes. The adjustment of a value for any other time of concentration is given by the empirical formula

$$WSV_{cor} = WSV_{60\,\mathrm{min}} \cdot \left(\frac{1}{2} + \frac{t_c}{120} \right) \tag{9}$$

where WSV_{60min} [mm] is the water storage capacity estimated with the decision scheme (Figure 2-1), t_c [min] is the time of concentration and WSV_{cor} [mm] is the corrected value for the water storage capacity.
Once *WSV* is determined and corrected with regard to the time of concentration, net rainfall and consequentially the amount of infiltration can be calculated with formula (10). The time-dependent behavior of infiltration is considered with a simplified Hortonian infiltration model. For discrete time-steps cumulative infiltration can be calculated with

$$F(t) = f_c \cdot t + \left((f_0 - f_c)/r \right)\left(1 - e^{-rt}\right) \tag{10}$$

where f_0 is the initial infiltration rate, f_c is the saturated infiltration rate and k is the recession constant. Recommended values are given in Table 2-1.

Table 2-1: Parameters for the estimation of the temporal distribution of infiltration.

WSV_{60min} [mm]	f_0/f_c [-]	r [-]
≥ 30	1	-
25 – 30	2	0.02
20 – 25	5	0.04
≤ 20	8	0.06

2.3 Storage constant *K*

Originally, the model of Clark was applied to calculate past flood events. The storage constant *K* has been derived from measured flood hydrographs. Since the new method Clark-WSL is intended for flood estimation in small catchments without gauging, no hydrographs are available. It could be shown that the storage constant *K* can be parameterised with catchment parameters. Flood events of 9 small catchments with gauging stations have been evaluated. In every catchment the storage constant of 3 hydrographs with a peak flow close to a HQ_{20} has been determined. The average of these three values has been plotted against the water storage capacity (Figure 2-2), resulting in the regression equation

(11) $$K = 2.25 \cdot WSV_{60\,\mathrm{min}} \cdot 18.5$$

Due to the small sample, the significance of this regression has to be rated carefully. The data base will improve, when discharge time series in further small catchments reach a reasonable length for statistical extrapolation.

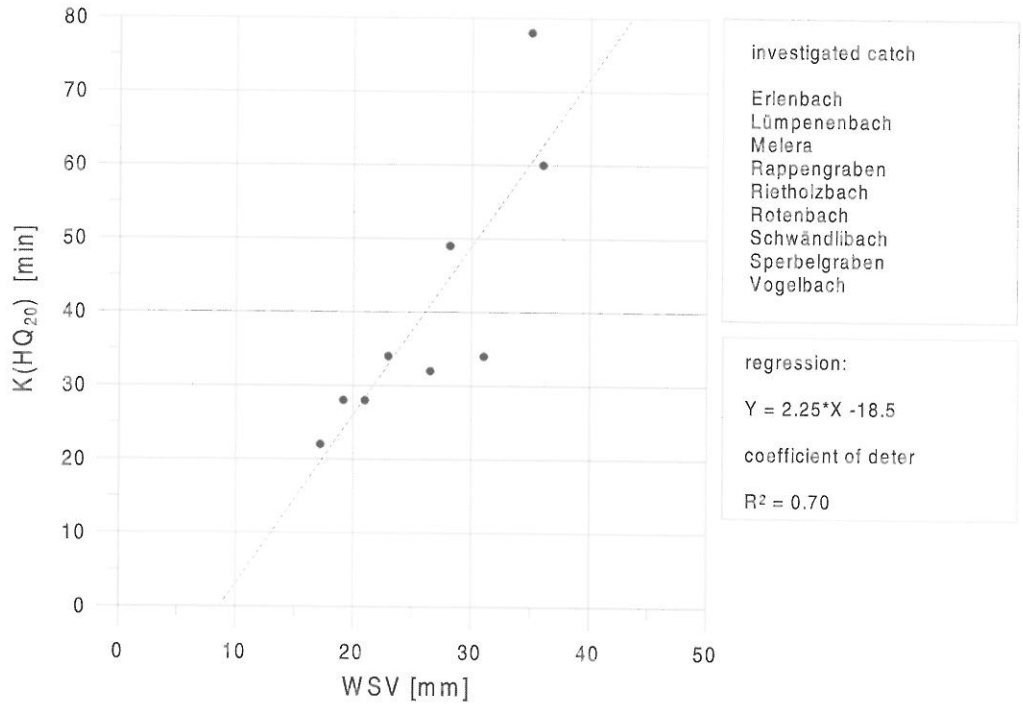

Figure 2-2: Plot of water storage capacity *WSV* and storage constant *K* in 10 small catchments.

2.4 Time of concentration

Peak flow is considered to be maximal if the complete catchment is contributing to discharge. For the model Clark-WSL not only a time of concentration but also an area-time diagram is needed. Both parameters are calculated with a grid-based GIS approach.
It is assumed that rainfall will be reduced by infiltration just after impinging on the terrain. The remaining net rainfall will reach the next channel as overland flow with the velocity $v_{overland}$. There, the water will travel as channel flow to the outlet of the catchment with the velocity $v_{channel}$. The flow path for every grid cell and consequently the flow length to the outlet of the catchment is calculated using a high-resolution digital terrain model. Having flow length and flow velocity, the flow time can easily be calculated for each cell. Time of concentration is given by the cell with maximum flow time.
Overland flow velocity is calculated with an approach using the Manning formula and roughness coefficients depending from land use. Velocity of channel flow is calculated with a formula published by Rickenmann (1996):

(12) $$v_{channel} = \frac{0.37 \cdot g^{0.33} \cdot Q^{0.34} \cdot J^{0.20}}{d_{90}^{0.33}}$$

where g [m/s^2] is the acceleration due to gravity, Q discharge in [m^3/s], J is the slope in [%] and d_{90} is the diameter of the grainsize in [m], whereas 90% of the bed material is smaller than d_{90}. This formula is applied at the outlet of the catchment and the result is valid for this point. It could be shown that multiplication with the factor 0.7 is a useful estimation for the mean channel flow velocity within the entire catchment.
The main problem of the application of formula 12 is the dependency on the discharge Q which represents the target variable of Clark-WSL. Since it is recommended to use not only one method for the estimation of extreme floods (Forster, Hegg, 2002), the result of another estimation method can be used as input. It has retained to use a modified version of the rational formula, presented in Baumann et al. (1992). It could be shown that the results of Clark-WSL are not very sensitive concerning the variation of Q in equation (12).
An example of an area-time diagram is shown in Figure 2-3.

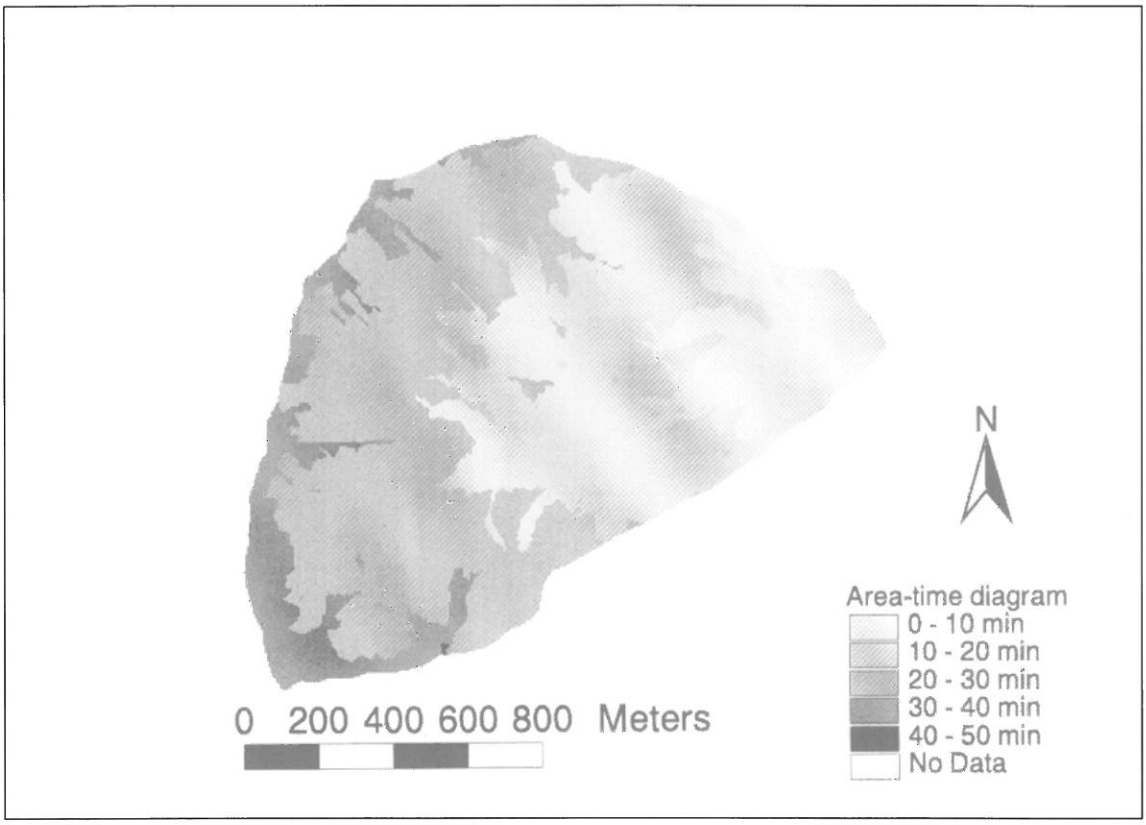

Figure 2-3: Example of an area-time diagram for the Vogelbach catchment.

3 APPLICATION AND VALIDATION

Clark-WSL has been applicated in 10 small catchments in Switzerland for a return period of 20 and 100 years and compared with extrapolated statistical values. As shown in Figure 3-1 and 3-2, Clark-WSL has a tendency to overestimate the statistical values for a return period of 20 years and to underestimate the statistical values for a return period of 100 years.
The HQ_{20} estimated with Clark-WSL has a variation of less than 25% compared with statistical values in 6 out of 10 catchments (Figure 3-1). In the Vogelbach, the Schwändlibach and the Wilenbergbach catchment the estimation value exceeds the statistical value more than 33%. In the Mülibach catchment the peak flow estimated with Clark-WSL is almost 50% lower than the statistical value.
For a return period of 100 years, Clark-WSL has a tendency to underestimate the statistical values (Figure 3-2). 7 out of 10 catchments show a variation of less than 25% compared with the statistical values. Again, estimation values of the Schwändlibach and the Vogelbach catchment exceeds the sta-

tistical values more than 33%. The Rietholzbach and the Mülibach catchment is underestimated by Clark-WSL with more than 30%.
Verification of the total discharge volume provided by the hydrograph has only been carried out for the Erlenbach catchment. Measured flood events have been evaluated regarding total discharge volume by means of extreme value statistics. Clark-WSL calculates a total discharge volume of 25000 m^3 for a HQ_{20} and 35000 m^3 for a HQ_{100}. Statistical values feature 50000 m^3 for a HQ_{20} and 100000 m^3 for HQ_{100}.

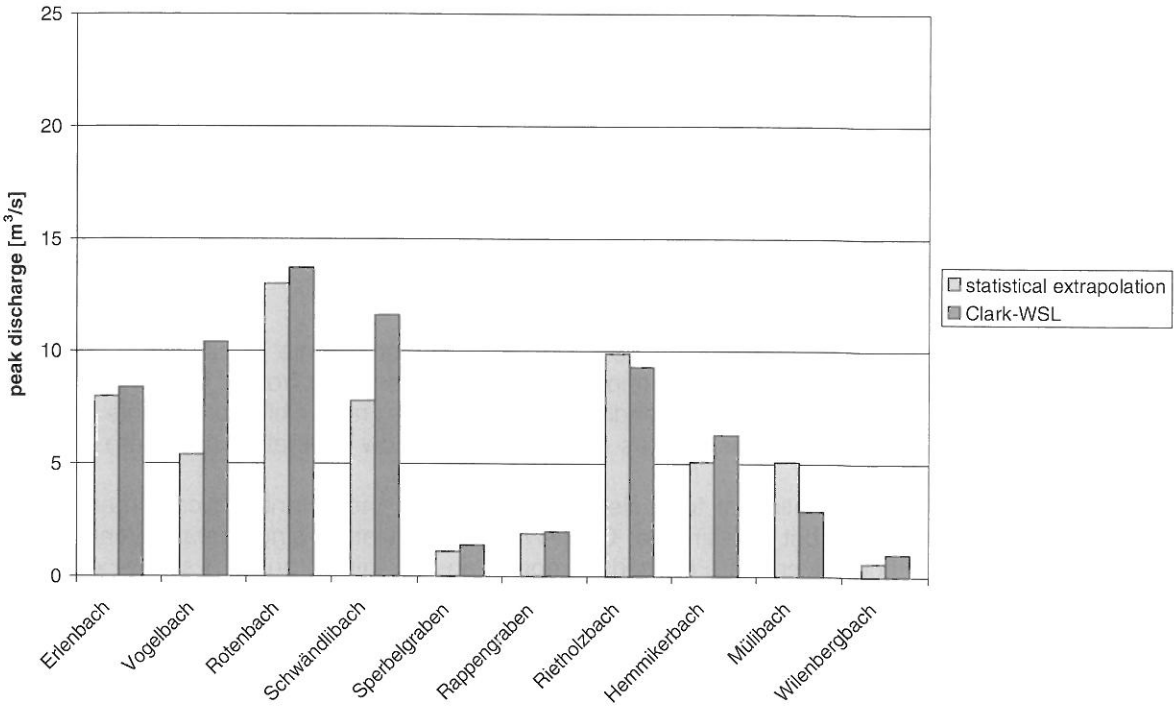

Figure 3-1: Estimation results and statistical values for a return period of 20 years.

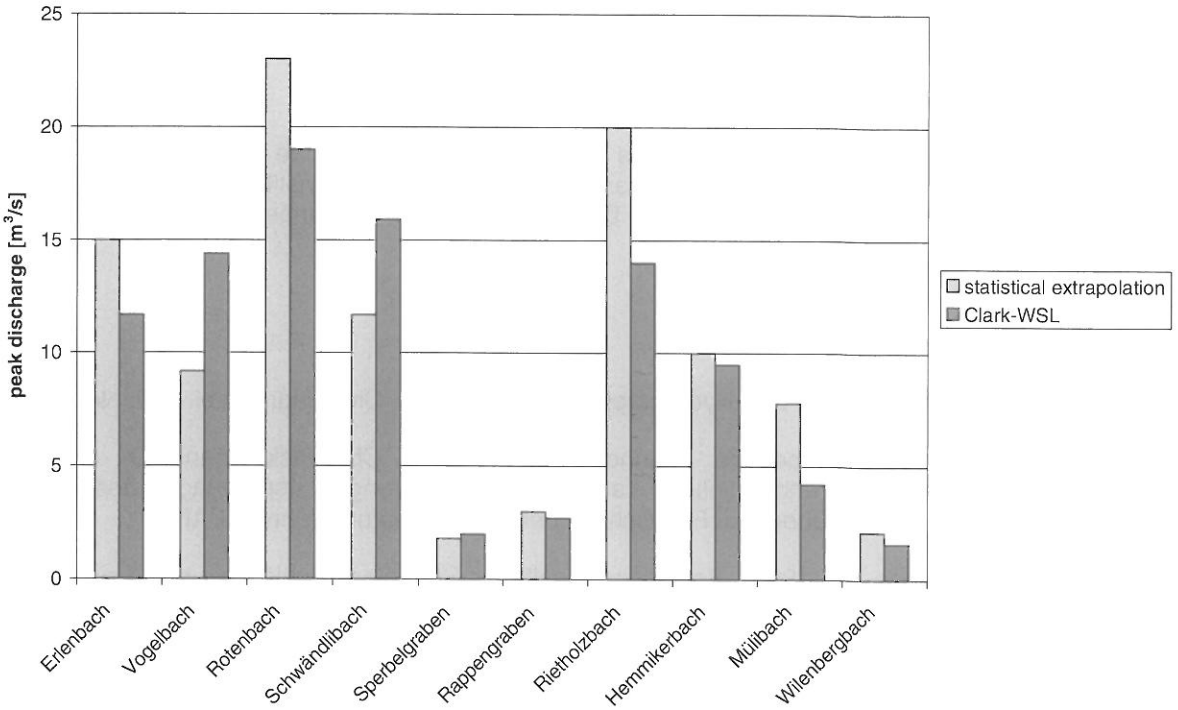

Figure 3-2: Estimation results and statistical values for a return period of 100 years.

4 DISCUSSION

The estimation of extreme peak flow with Clark-WSL leads to satisfying results. All results are within the confidence interval of the statistical extrapolation. For a return period of 20 years the results have a tendency to overestimate the statistical values in most of the catchments. Regarding design problems, estimation results provided by Clark-WSL are conservative. For a return period of 100 years Clark-WSL has a tendency to underestimate the statistical values.
A part of the variance can be explained with the following points:

- The main problem for the validation of the estimation with extrapolation of the measured values by means of extreme value statistics is the rather poor data base. 6 out of 10 catchments have time series of less than 30 years. Extrapolations to a return period of 100 years have to be rated very carefully. In at least three catchments (Erlenbach, Rotenbach, Hemmikerbach) extreme flood events occurred which are very unlikely to occur in the given measuring period. The statistical extrapolations based on time series containing outliers is afflicted with strong uncertainties.
- The measurement of dischare during extreme flood events has to be rated carefully. Several gauging stations are outlayed for the purpose of research on the water balance. If so, the gauging profile cannot take all the discharge in case of an event with high return period.

In general, Clark-WSL has difficulties with the estimation of flood events in catchments with high specific peak discharge (Erlenbach and Rotenbach catchment) resulting from a combination of high rainfall intensities and adverse catchment conditions. Furthermore, rather big catchments (according our definition of small catchments) as well as catchments with low inclination slope are more problematic for the estimation.
Differences between the estimation of total discharge volume in the Erlenbach catchment and the statistical values are notable but explainable. Clark-WSL is calculating single-peak events while in nature most of extreme flood events are caused by more than one rainfall pulse. If single-peak events are derived out of an entire event, total discharge volume is comparable to the estimation result.
Comparison with other estimation methods shows that Clark-WSL has a good performance; the variability of the results is similar or smaller.
As every flood estimation method Clark-WSL has its assets and drawbacks. In order to improve confidence in flood estimation not only one single method should be used. Forster and Hegg (2002) present an approach using five different methods including Clark-WSL. For every method it is recommended to vary essential parameters such as rainfall or water storage capacity using values at the upper and the lower limit and the most likely value to derive uncertainty related with all estimation methods.

ACKNOWLEDGEMENTS

A part of the presented work in this paper was financially supported by the Federal Office for Water and Geology. Rainfall and hydrological data has been provided by the Institute for Atmospheric and Climate Science, ETH Zürich and the Cantonal Departments for Civil Engineering, Cantons of Aargau, Luzern and Basel Landschaft.

REFERENCES

Clark, C. O. (1945): Storage and Unit Hydrograph. Trans. Am. Soc. Civil Engrs., Vol. 110. New York

Baumann, P., Forster, F., Gerber, W., Kienholz, H., Lehmann, Ch., Rickenmann, D., Rickli, Ch. (1992): Naturgefahren: Gefahrenbeurteilung, Landschaftsveränderung. Kursunterlagen des Weiterbildungskurses 1992 im Berner Oberland. Forstliche Arbeitsgruppe Naturgefahren (FAN).

Forster, F., Baumgartner, W. (1999): Bestimmung seltener Starkniederschläge kurzer Dauer – Fallbeispiele im Vergleich mit den schweizerischen Starkniederschlagskarten. Schweiz. Z. Forstw. 150 Jg. Nr. 6. pp. 209 – 218. Zürich

Forster, F., Hegg, Ch. (2002): A suggestion for the estimation of flood peak discharge in small torrential catchments. Proc. ICFE 2002. Bern

Hydrologischer Atlas der Schweiz (1992): Blatt 2.4: Extreme Punktregen unterschiedlicher Dauer und Wiederkehrperioden 1901 – 1970. Bern

Köhler, G. (1976): Niederschlag-Abfluss-Modelle für kleine Einzugsgebiete. Parey. Hamburg, Berlin

Kölla, E. (1986): Zur Abschätzung von Hochwassern in Fliessgewässern an Stellen ohne Direktmessungen. Mitteilungen der Versuchsanstalt für Wasserbau, Hydrologie und Glaziologie, Nr. 87. Zürich

Rickenmann, D. (1996): Fliessgeschwindigkeit in Wildbächen und Gebirgsflüssen. Wasser, Energie, Luft. 88 Jg. Heft 11/12. pp. 298-304. Baden

Rickli, Ch. and Forster, F. (1997): Einfluss verschiedener Standortseigenschaften auf die Schätzung von Hochwasserabflüssen in kleinen Einzugsgebieten. Schweiz. Zeitschr. Forstwesen. 148 Jg. Nr. 5. pp. 367-385. Zürich

Ogrosky, I. H. O., Mockus, V. (1964): Hydrology of Agricultural Lands. In: Chow, V. T. (Ed.): Handbook of Applied Hydrology. pp. 21-28 – 21-32. New York

Vogt, S., Forster, F. (1999): Hochwasserabschätzung in kleinen Einzugsgebieten. Ein Abschätzverfahren nach Clark zur Bestimmung einer Hochwasser-Bemessungsganglinie. Eidgenössische Forschungsanstalt für Wald, Schnee und Landschaft. Unveröffentlichter Praktikumsbericht. Birmensdorf

Vogt, S. (2001): Zur Abschätzung von Hochwasser in kleinen Wildbacheinzugsgebieten. Diplomarbeit. WSL/Institut für Klimaforschung der ETH. Zürich

MAXIMUM ANNUAL DISCHARGES IN OVERGROWN CROATIAN KARST

Ranko Žugaj

University of Zagreb, Faculty of Mining, Geology and Petroleum Engineering, Pierottijeva 6, 10000 Zagreb, Croatia, rzugaj@rgn.hr

SUMMARY

In the paper the results of the regional hydrological analysis for the region of overgrown karst in Croatia are presented. For the series of maximum annual discharges from 35 hydrological stations the homogeneity and the occurrence of trends were investigated. On the basis of the correlation analysis for the characteristic parameters of maximum annual discharges the 10 biparameter mathematical formulas were defined, in which the coefficients of correlation were $r > 0.80$. The maximum specific inflows recorded in the basin areas analysed are graphically presented. They were compared with the maximum recorded specific inflows of other basin areas in the Dinaric karst, with Creager's 10 and 20-years maximal envelop curves, with the envelope curve of the highest values for the basins of Danube and large European rivers and with the envelope curve of the highest values for the basin areas of Slovenia, Croatia, Bosnia and Herzegovina.

Keywords: Karst hydrology, regional hydrological analysis, discharge, hydrological parameter, Kupa basin, Croatia

1 INTRODUCTION

The upstream part of Kupa basin and the basins of its tributaries: Gornja and Donja Dobra, Mrežnica and Korana is a karst area with similar main characteristics of runoff, and thus for that particular basin area a regional hydrological analysis can be carried out. The basin area analysed belongs to the Dinaric karst (Figure 1-1), which comprises Slovenia, southern part of Croatia, Bosnia and Herzegovina and Monte Negro. It spreads parallel with the Adriatic Coast along a 50 to 150 km wide and about 700 km long belt. The total area of the Dinaric karst is about 57,000 km^2 (Herak, Stringfield, 1972).

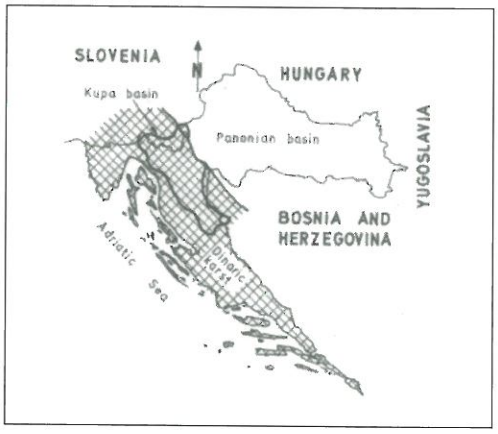

Figure 1-1: The region of the Dinaric karst in Croatia (according to Biondić et al., 1998).

The influential basin area of the Kupa river in the upper karstified part and of its main tributaries Dobra, Mrežnica and Korana is about 5,000 km^2 large (Figure 1-2), and the total mean inflows of water from that region is about 150 m^3/s - which corresponds with the average specific inflow of 30 l/s/km^2. Hence, the significant quantities of water are in question, with the main characteristic, in the terms of space and time, of being unevenly distributed.
The characteristic parameters describing the water runoff were treated regionally and in this paper the results relating to the relations of maximal runoff are presented.

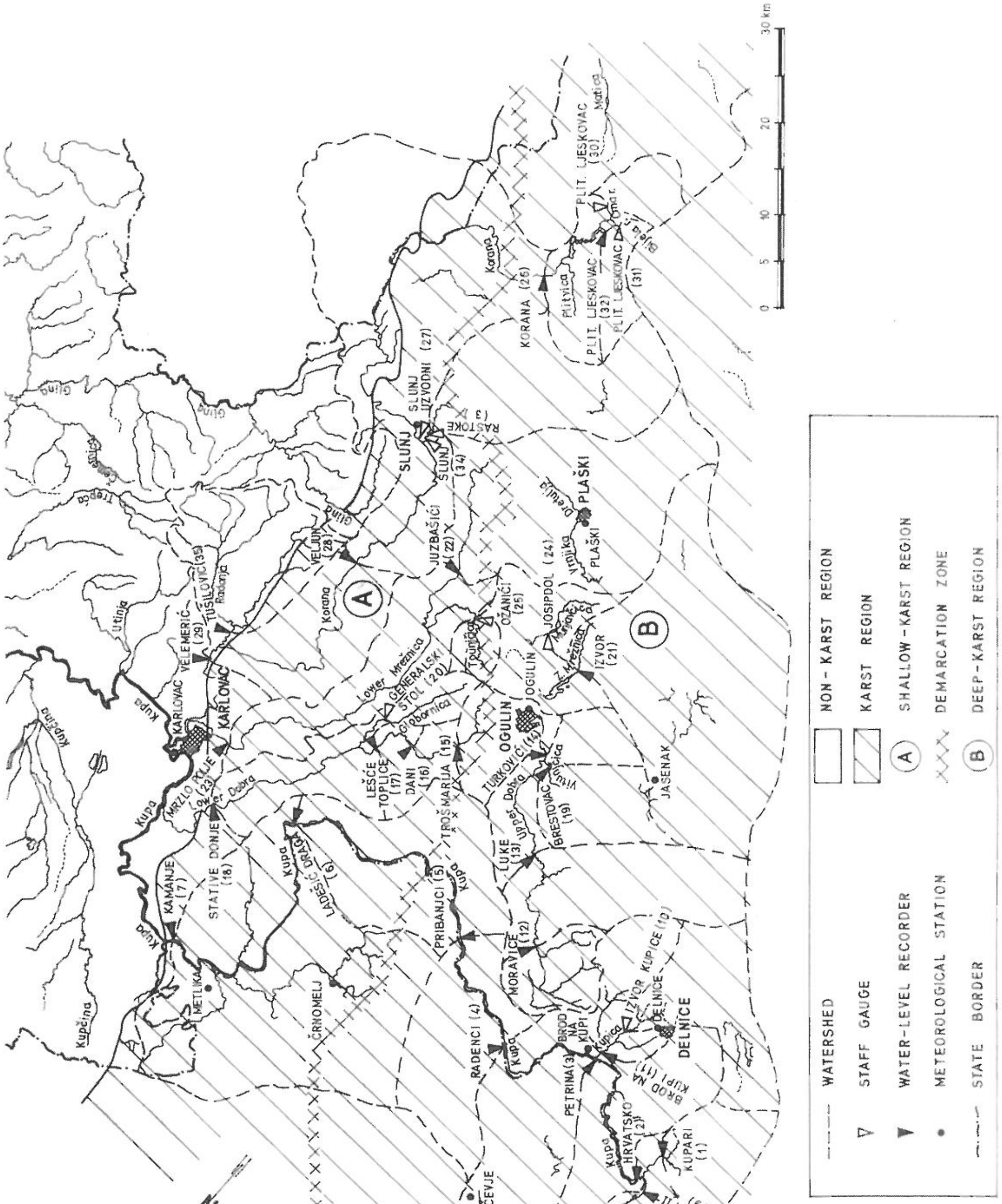

Figure 1-2: Basins of Kupa, Dobra, Mrežnica and Korana in karst (according to Jurak, 1983).

For the regional hydrological analysis of the water runoff from the basin areas of Kupa under karst, as well as Dobra, Korana and Mrežnica, the available data of observations and measurements of hydrological parameters collected from 35 hydrological stations from 18 watercourses were used. The data analysed are from the period from 1951 to 1995. These data are for the most part limnographic and for that reason more reliable than predominantly staff gauge data from the earlier period (before 1951).
For the regions of karst the so-called karst forms are characteristic, most often being presented with many cracks, passages, galleries, caves and underground paths and water reservoirs, respectively. Such characteristics are the main problem in determining the drainage divides, so very often it is impossible to determine the basin area of a particular spring precisely. Depending on the development of underground water paths, a topographic and a hydrogeologic drainage divide can differ a lot, so to some particular springs water from the regions topographically belonging to other basins can flow in. There are also cases when a drainage divide can be defined only approximately, because it depends on the conditions in the underground. At the same time that is the main difference between the karst and non-karst basin regions (where topographic and hydrogeological drainage divides overlap or differ *only slightly) (Stepinac, 1969; Jurak, 1983; Bonacci, 1987; Plantić, 1995).*
For the karst basins the differences in their largeness according to different analyses are not unusual. In this analysis the results of the recent available hydrogeological investigations were used and according to them the situation of the basin in Figure 1-2 finalized. Despite that, all the questions on the position of the drainage divide have not yet been solved, so field and study hydrogeological investigations should at any rate be continued.
The results of this regional analysis are interesting for practical use, since on the streamflows analysed even 27 multipurpose impounded lakes can be realized. The analyses described were carried out in the context of the three-annual scientific project of the Ministry of Technology and Science of the Republic of Croatia (Žugaj et al., 2000).

2 RESULTS OF THE INVESTIGATION

Out of 35 hydrological stations analysed, the data on maximum annual discharges in only one station (Kupa, Radenci) were not acceptable for a regional hydrological analysis. Hence, the data from 34 hydrological stations were treated regionally. During the period of the analysis of 45 years, from 1951 to 1995, the hydrological series analysed had averagely 31 data within the limits from 7 to 45.
Special attention was paid to the tests of the quality of the input calculated data, so homogeneity and the trends of series of annual discharges were particularly analysed. The incidence of a dry period after 1980 was established, which had an effect on the homogeneity of the most series of mean discharges and minimum annual discharges, and had practically no influence to the homogeneity of the series of maximum annual discharges. Out of the total of 34 series of maximum annual discharges analysed, the applied non-parameter Wilcox's test of homogeneity showed the occurrence of unhomogeneity in only two of them.
The investigation of the trends of the most series of mean and minimum annual discharges showed declining trends, and the series of maximum annual discharges manifested increasing trends. The comparisons of the series of maximum annual discharges with the series of mean and minimum annual discharges showed that in general the quantity of runoff after 1980 was averagely smaller than before 1980, but that the extreme values in the period after 1980 were more expressed than in the earlier period. A characteristic example for the hydrological profile Mrzlo Polje (or literally translated to English: Cold Field) on the river Donja Mrežnica is given in Figure 2-1.
Some of the interesting essential features of the characteristic parameters analysed are shown in the histograms in Figure 2-2.
The area of the basins up to the particular hydrological profiles range from A = 8.9 km^2 (the basin of Bijela *Rijeka to the profile of Plitvički Ljeskovac) to A = 2,337 km^2* (the basin of Kupa to the profile of Kamanje). The most frequent basins - in 47 percent of cases - are those with an area from 100 to 500 km^2.
Most often - in 47 percent of cases - the maximal registered specific inflows q_M are lower than 0.4 $m^3/s/km^2$, the coefficients of variation of maximum annual discharges most often - in 80 percent of cases - range between c_{vM} = 0.10 and c_{vM} = 0.30 and in 47 percent of cases the coefficients of skewness of maximum annual discharges range from zero to c_{sM} = 0.50.

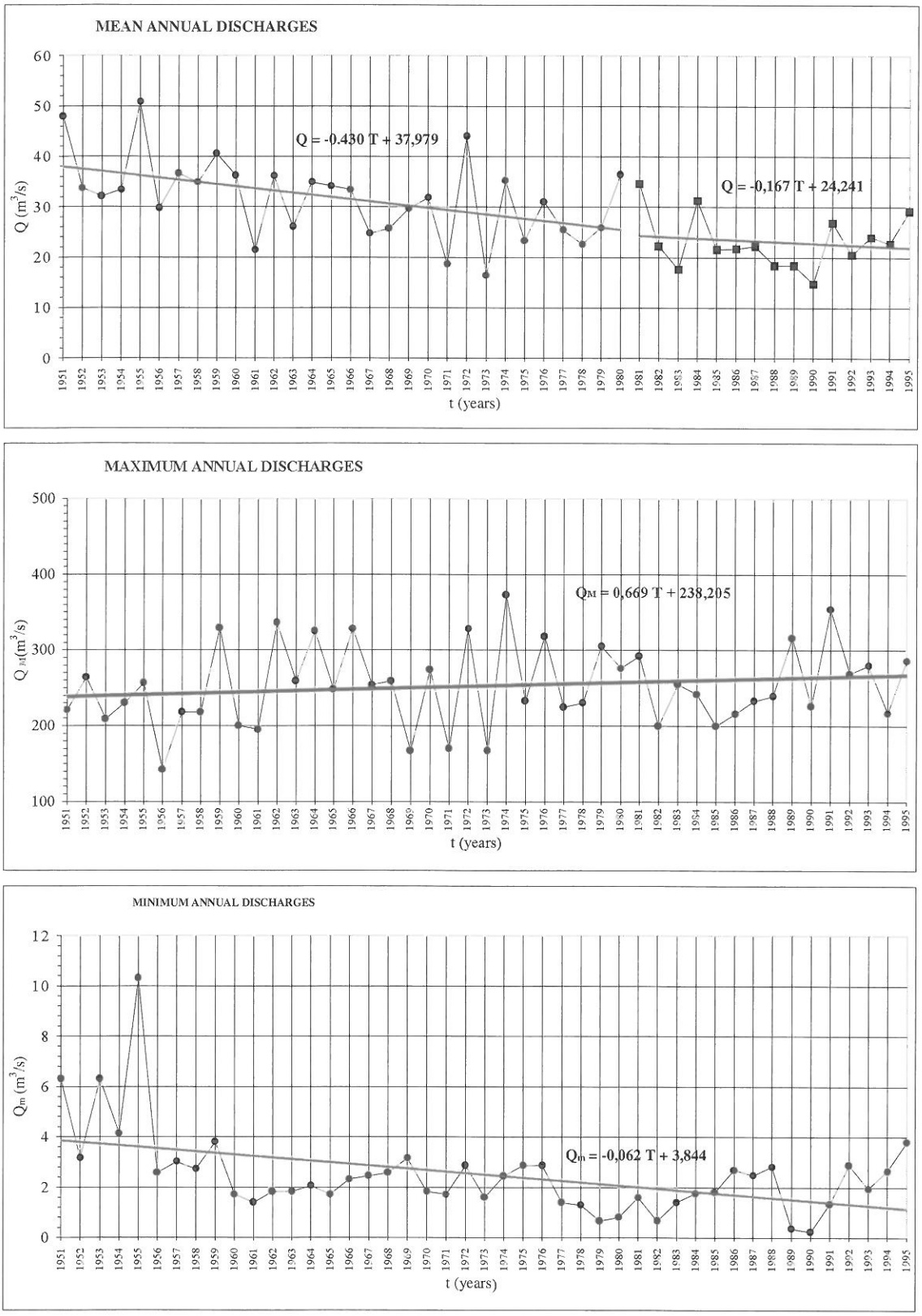

Figure 2-1: Series of mean Q, maximum Q_M and minimum Q_m annual discharges for Donja Mrežnica in the profile of Mrzlo Polje (the profile no. 24 in Figure 1-2).

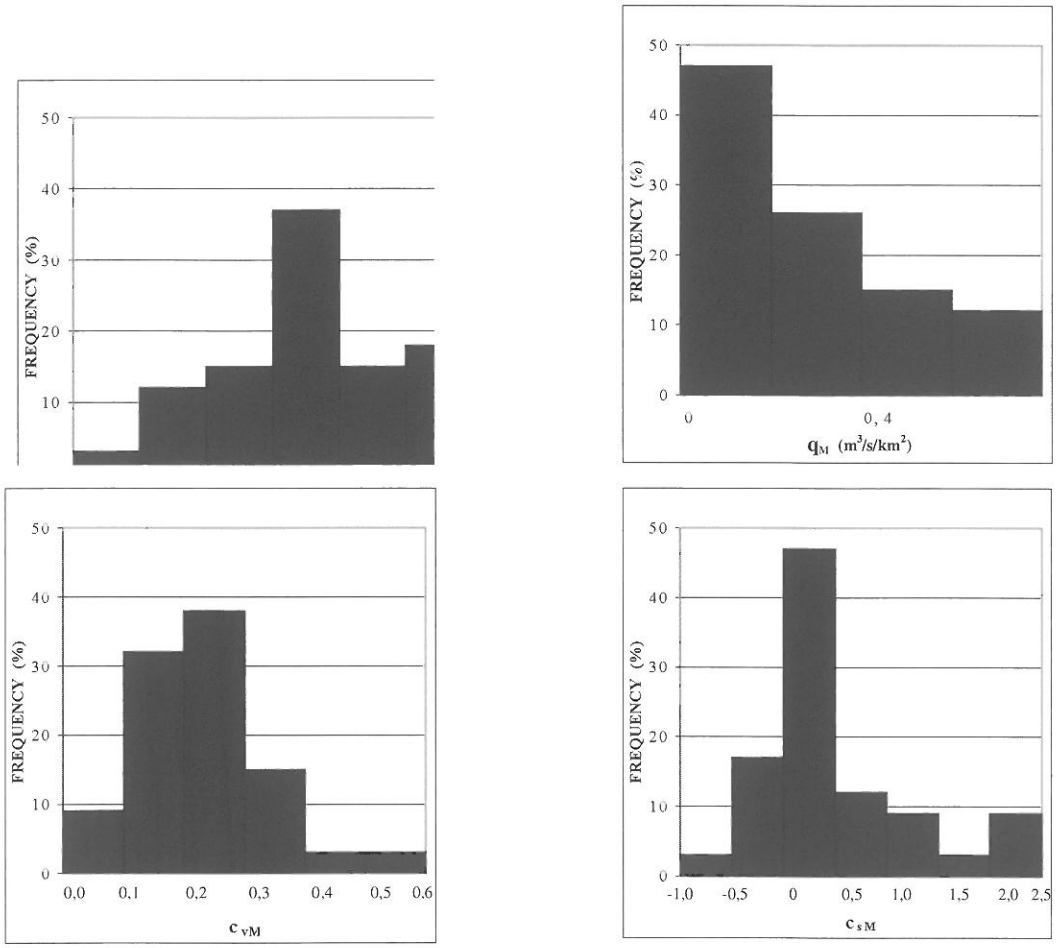

Figure 2-2: Histograms of the areas of the basins A, maximal recorded specific inflows q_M, coefficients of variation of maximum annual discharges c_{vM} and the coefficients of skewness of maximum annual discharges c_{sM}.

Table 2-1: The relations of characteristic parameters of maximum annual discharges.

Relation no.	Relation	Number of the data calculated	Coefficient of correlation	Number of figures	Probable deviation σ_p (%)
(1)	$Q_M = 0.445A+35.26$	34	0.88	2-3	±719.1
(2)	$Q_M = 0.662A^{0.939}$	34	0.91	2-4	±155.6
(3)	$Q_M = 14.567Q+20.12$	25*	0.95	-	±163.1
(4)	$Q_M = 20.721Q^{0.9005}$	25	0.96	2-5	± 83.8
(5)	$Q_M = 1.445Q^*_M+11.167$	34	0.99	2-6	±217.4
(6)	$Q_M = 1.657Q^{*0.983}_M$	34	0.99	-	±104.6
(7)	$Q^*_M = 11.047Q^{0.961}$	25	0.96	-	± 86.6
(8)	$\sigma_M = 0.129Q_M^{1.019}$	34	0.99	-	± 58.4
(9)	$\sigma_M = 0.225Q^{*0.992}_M$	34	0.96	-	±100.5
(10)	$Q_M/Q^*_M = 4.532c_{vM}+0.547$	34	0.84	2-7	± 27.3

*n = 25 since only homogenous series of mean annual discharges were analysed.

On the basis of the regional analysis carried out, 10 biparameter mathematical formulas were defined for the characteristic parameters of maximum annual discharges (Table 2-1), out of which five relations were picked out for graphical presentations together with the calculated data (Figures from 2-3 to 2-7). The important characteristic of the relations derived is that their coefficients of correlation are very high - in 80 percent of cases higher than r = 0.90, but probable deviations (within which there are 95 percent of cases) higher than ±100 percent are rather frequent.

Linear relation $Q_M = f(A)$ defined by formula (1) and presented in Figure 2-3 has a very large probable *deviation from the input calculated data:* $\sigma_p = \pm 719.1\%$. Non-linear relation $Q_M = f(A)$ defined by formula (2) and graphically presented in Figure 2-4 has also a very large probable deviation from the *input calculated data:* $\sigma_p = \pm 155.6\%$.

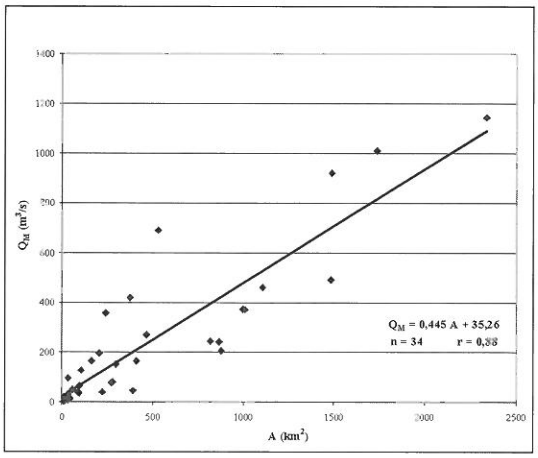

Figure 2-3: Maximum recorded discharges Q_M and basin areas A - linear dependence.

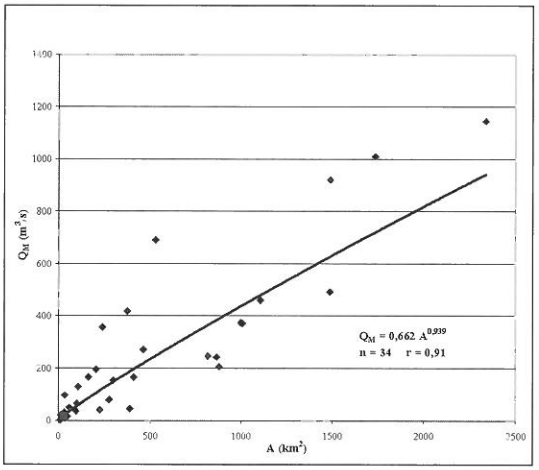

Figure 2-4: Maximum recorded discharges Q_M and basin areas A - non-linear dependence.

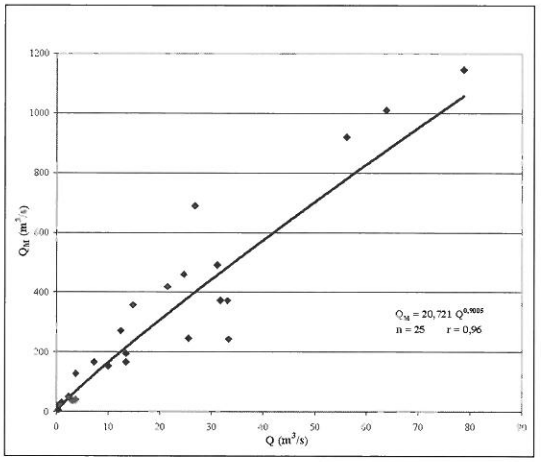

Figure 2-5: Maximum recorded discharges Q_M and mean discharges Q.

The relation of maximum recorded discharges and average annual discharges $Q_M = f(Q)$ defined by *formula (4) is presented in Figure 2-5 and has a probable deviation* $\sigma_p = \pm 83.8\%$. Both relations $Q_M = f(Q^*_M)$ have a high coefficient of correlation: r = 0.99. The linear relation (5) is presented in Figure 2-6. *The probable deviation from the input calculated data is* $\sigma_p = \pm 217.4\%$ *for a linear relation (5) and* $\sigma_p = \pm 104.6\%$ for a non-linear one (6).
From the rest of the relations from Table 2-1, the relation between the maximum recorded discharges in modal coefficients and the coefficients of variation of maximum annual discharges $Q_M/Q^*_M = f(c_{vM})$ defined by formula (10) was picked out as an interesting one. This relation is presented in Figure 2-7, *and the probable deviation is* $\sigma_p = \pm 27.3\%$.

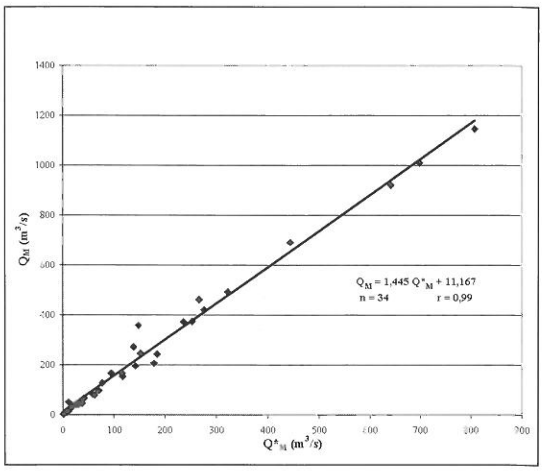

Figure 2-6: Maximum recorded discharges Q_M and average maximum annual discharges Q^*_M.

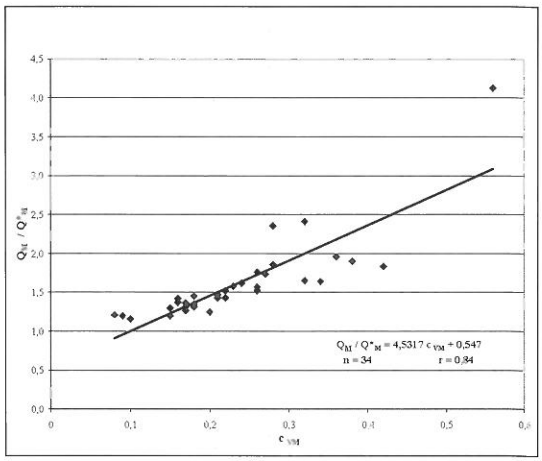

Figure 2-7: Maximum recorded discharges in modal coefficients Q_M/Q^*_M and coefficients of variation c_{vM} of maximum annual discharges.

Finally, all maximum specific inflows recorded in the basin areas analysed and in the other basin areas of the Dinaric karst in Croatia (Žugaj, 1995) were graphically presented in Figure 2-8. The corresponding envelope curves of the highest values were given and compared with Creager's 10- and 20-years envelope curves, the envelope curve of the highest values for the basin areas of the Danube *and large European rivers (Jovanović, Radić, 1985) and with the envelope curve of the highest values for the basin areas of Slovenia, Croatia, Bosnia and Herzegovina (Srebrenović, 1970).*
In the maximum specific inflows recorded the upper envelopes are particularly interesting and they are presented graphically in Figure 2-8. The envelope derived in the regional analysis of Croatian karst from 1995 for the basin areas larger than 36 km^2 was corrected by the envelope line defined in this particular analysis. Such an envelope gives lower values of maximum specific inflows comparing to the envelope for the Danube and larger European rivers, and in relation to the envelope derived for the inflows from the basin areas of Croatia, Bosnia and Herzegovina and Slovenia for the basins of up to 760 km^2 it gives higher values, and for the basins larger than 760 km^2 it gives lower values.

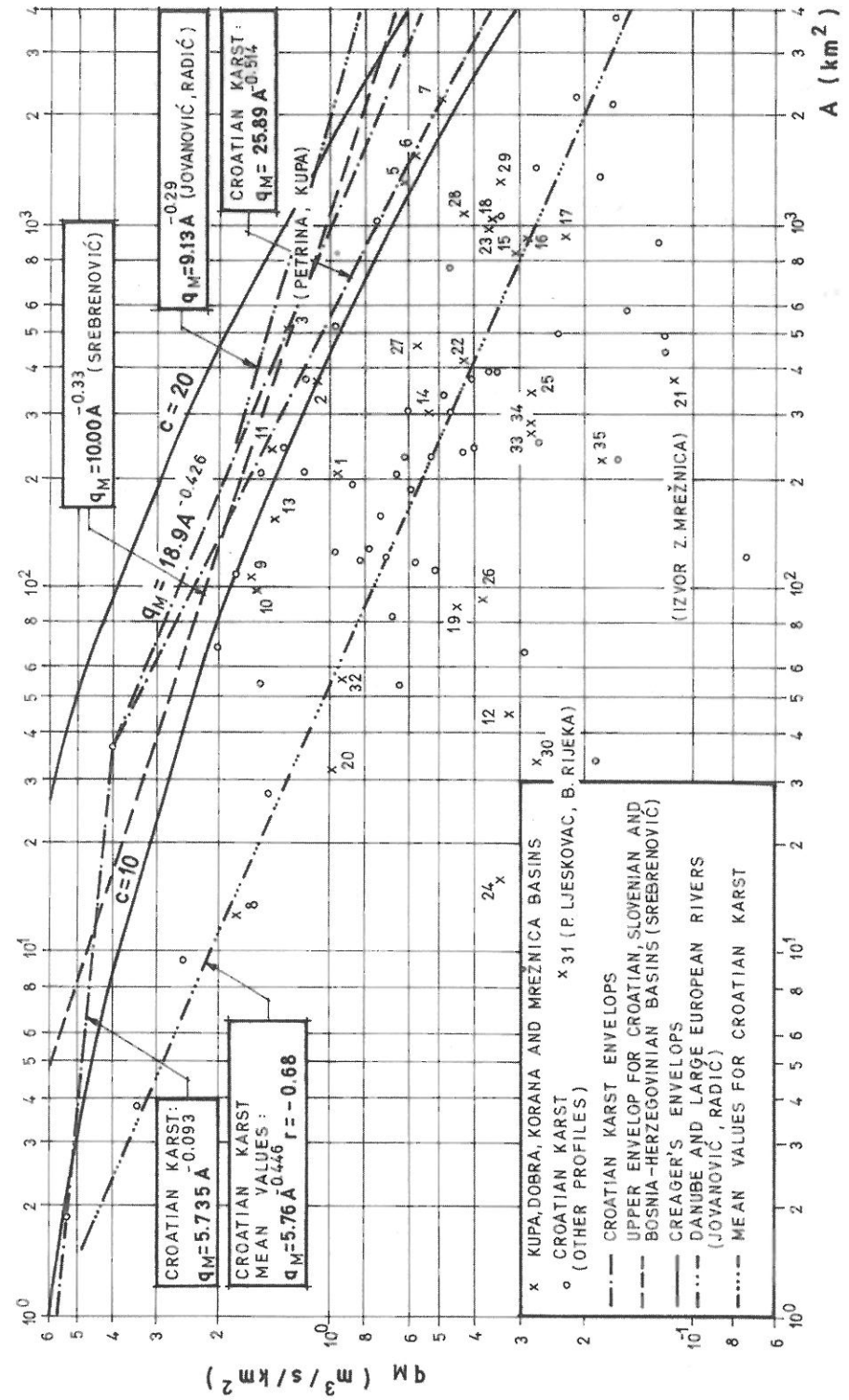

Figure 2-8: Maximal recorded specific inflows q_M and basin areas A (the numbers of hydrological profiles are indicated on situation in Figure 1-2).

3 CONCLUSION

On the basis of the material presented it can be concluded that in the analysed relations for the characteristic parameters of the series of maximum annual discharges the coefficients of correlation are high, but in most relations the probable deviations are very large (Table 2-1, Figure from 2-3 to 2-7). For that reason the formulas from Table 2-1 should be used in practice very carefully.
Due to the low value of the coefficient of correlation (r = 0.43), there is no point in defining the relation $q_M = f(A)$ for the maximum specific inflows, but there is a point in presenting their upper envelopes and in comparing them with the envelopes derived for other, regionally treated areas (Figure 2-8).

REFERENCES

*Biondić, B. et al. (1998): Protection of Karst Aquifers in the Dinarides in Croatia, Environmental Geo*logy, Springer-Verlag, Heidelberg, Vol. 34 (4), 309-319

Bonacci, O. (1987): Karst Hydrology, Springer-Verlag, Heidelberg

Herak, M., Stringfield, V. T. (1972): Karst - Important Karst Regions in the Northern Hemisphere, Elsevier, Amsterdam

Jovanović, S., Radić, Z. M. (1985): Regional Analysis of Hydrological Parameters, Water Resources Management, Belgrade, 17/93, 3-12

Jurak, V. (1983): Comparative Analysis of Hydrologic Regimes of the Rivers Glina, Korana and D. Mrežnica from the Aspects of the Hydrogeologic Characteristics of the River-Basins, Faculty of Mining and Geology, Belgrade

Plantić, K. (1995): Modeling the Runoff by Application of Mathematical Model in the Karst Region, 1st Croatian Geological Congress, Opatija, Vol. 2, 453-457

Srebrenović, D. (1970): Problems of Floods, Technical Book, Zagreb

Stepinac, A. (1969): Runoff in the Dinaric Karst, Yugoslav Academy of Arts and Sciences, Zagreb, 207-235

Žugaj, R. (1995): Regional Hydrological Analysis in the Karst of Croatia, Croatian Hydrological Society, Zagreb

Žugaj, R. et al. (2000): Regional Analysis of the Basin Areas of Kupa and the Tributaries in Karst, University of Zagreb, Faculty of Mining, Geology and Petroleum Engineering, Zagreb